METABOLIC REWIRING DRIVES DRUG RESISTANCE IN ACUTE LEUKEMIA

A THESIS PRESENTED BY

NITHYA.B

DEPARTMENT OF HAEMATOLOGY

CHRISTIAN MEDICAL COLLEGE,

VELLORE

TO

SREE CHITRA TIRUNAL INSTITUTE

FOR

MEDICAL SCIENCES AND TECHNOLOGY,
TRIVANDRUM

Thiruvananthapuram

IN PARTIAL FULFILMENT OF THE REQUIREMENTS

FOR THE AWARD OF

DOCTOR OF PHILOSOPHY

Declaration by student

I Nithya.B, hereby certify that I had personally carried out the work depicted in the thesis entitled "Metabolic rewiring drives drug resistance in acute leukemia". No part of the thesis has been submitted for the award of any other degree or diploma to this date.

Signature

Name of the candidate: Nithya.B

Reg.No: 2015/PhD (CMC)/05

Date:01.07.2020

DEPARTMENT OF HAEMATOLOGY
CHRISTIAN MEDICAL COLLEGE
IDA SCUDDER ROAD, VELLORE - 632 004, INDIA.

CERTIFICATE BY GUIDE

Dr. Vikram Mathews MD, DM, FASc
Associate Director
Professor
Department of Haematology
Christian Medical College,
Vellore - 632004
Tamil Nadu, India

This is to certify that Miss.Nithya B, in the Department of Haematology, Christian Medical college, Vellore has fulfilled the requirements prescribed for the Ph.D. degree of the Sree Chitra Tirunal Institute for Medical Sciences and Technology, Trivandrum.

The thesis entitled, "Metabolic rewiring drives drug resistance in acute leukemia" was carried out under my direct supervision. No part of the thesis was submitted for the award of any degree or diploma prior to this date.

Clearance was obtained from the Institutional Ethics committee and Institutional Animal Ethics for carrying out the study.

Signature:

Date: 1/7/2020

Dr. VIKRAM MATHEWS, MD., DM.,
Professor, Reg. No. 49804
Department of Haematology,
Christian Medical College,
VELLORE - 632 004 T. N. INDIA.

TEL : 0416 - 2282352 / 3072352 / 4212352
INTERNATIONAL : + 91 - 416 - 2282352 / 3072352 / 4212352
FAX : 0416 - 2226449 / 2232035
INTERNATIONAL : + 91 - 416 - 2226449 / 2232035
e-mail : haemat@cmcvellore.ac.in

Approval of thesis

Metabolic rewiring drives drug resistance in acute leukemia

Submitted by

Nithya B

For the degree of

Doctor of Philosophy

Of

SREE CHITRA TIRUNAL INSTITUTE

FOR

MEDICAL SCIENCES AND TECHNOLOGY, TRIVANDRUM

Thiruvananthapuram

Is evaluate and approved by

Dr. Vikram Mathews
(Name & signature of the guide)

MANJU SENGA

Name & Signature of the External
Examiner

ACKNOWLEDGMENTS

This dissertation is the end of the venture in obtaining my Ph.D. It would not have been possible without the guidance, help, support, and encouragement of several individuals who contributed and extended their valuable assistance in one way or another. It has been a great privilege to convey my sincere feelings, pay heartfelt homage and express my thanks to all those with whom I shared several vital years, which are true, a part of an unforgettable experience for me in my life.

To Dr. Vikram Mathews: When I started in your lab, I was so inexperienced, and now, after eight years, I feel like I have grown so much, both as a person and as a researcher. I am grateful for your insightful ideas, intellectual leadership, dynamic supervision, and continuous support. I always appreciated the freedom you have given me in the lab; it has not always been positive and has cost me some nights of sleep, but in the end, it helped me to become a more independent researcher. A person who believes that "whatever it is data is data" and giving importance to even smaller observation and make it worthwhile with a translational approach of what can we do with it in the clinic.

To my Doctoral Advisory committee: Dr. Poonkuzhali Balasubramanian and Dr. Eunice Sindhuvi: I thank both of you for the valuable input and comments during the doctoral advisory committee seminar and progress report meeting and made sure that finish the reports and exams without delay.

To Dr. Sanjeev Krishna and Dr. Yolanda Augustin, SGUL, London, UK: I am thankful for your valuable insights into my project and happy that I received the

opportunity to work with you. I admire you a lot and was amazed by your passion for science. You are one of the most inspiring people whom I look forward to working with in the future.

Yolanda, always a smiling face - thank you for all your help and welcoming into the lab and making me feel like I belong there. Thank you for showing me the shopping streets of London, gifts, Museums, and the dental clinic. I am happy that I get to work with you all during my Ph.D. period. Hope to see you all soon.

I owe you a lot for the technical skills (both in-vitro and in vivo) to **Dr. Saravanan Ganesan**, which I have gained in the initial years of my Ph.D. I appreciate all the time you spent with me and all the teachings, in and out of the lab. Your twisted mind certainly made me a better and more open-minded person. It was great working with you.

To Hamenth Kumar Palani: Thank you or all the help through the last eight years, as a friend and as a colleague, also, for being with me since day 1 in CMC and until the end. A humble and flexible person I ever met.

To Arvind Venkatraman: Thank you for being there for me as a sounding board when needed and the person who made me feel that I am getting older, and the years are passing by. I am thankful for taking care of my work when I was not around and staying up in the lab until late at night to drop me off.

Dr. Sachin David and Dr.Ansu Abu Alex: The seniors who made me feel younger in the lab and was there for me when I had doubts about performing the molecular and flow cytometry experiments. I am thankful for their wisdom of handling the Ph.D. life.

To Dr. Ezhilarasi Chendamarai: Though I did not have a chance to work with you, I am grateful for your work in the laboratory, which is the foundation for my Ph.D. work.

To the members of our past and present technical staff: I thank ***Miss. Diya Anna Thomas*** (Project student – VIT University) joined our lab during my thesis writing time and helped me to complete a few of the last-minute experiments.

I am thankful to *Mrs.* ***Ambika and Mrs. Shruthi,*** our laboratory technician, for their technical skills and for helping me with sample collection and molecular work.

To The Flowcytometry laboratory team – ***Mrs.Faranaz Khamruddin, Miss. Merlin Priyanka, Miss. Gayathri, Mr.Ramesh Shankar, Mr. Mohammed Aakif, Mr.Hari Krishnan, Ms.Raghavi, Mrs. Kotteswari, and Miss. Divya:*** I am happy and grateful that I had met you all and being there for me in my life. The people who helped me to learn the basic instrumentation to complex minimal residual disease monitoring panel and analysis. I enjoyed the coffee breaks, late evening snacks, and sharing your lunch boxes with me.

To the Clinical faculty, Clinicians and Nurses: ***Dr.Alok Srivastava, Dr.Biju George, Dr. Aby Abhraham, Dr.Uday Kulkarni, Dr.Anu Korula, Dr. Anup J Devasia, and Dr.Sushil Selvarajan, Nursing staff, and the patients:*** I sincerely thank all of you for the help during my study. I owe my heartfelt thanks to all the nursing staff in the department, without whom the samples for this study would not have been collected. I am grateful for the patients who consented and provided samples for the study.

To the laboratory faculty: ***Dr.Shaji Velayudham, Dr. Arun Kumar, and Dr.Nancy Beryl Janet :*** Thank you for all your comments and constructive critiques during the department seminar, journal club, and work in progress, which I have helped me improvise my presentation skills and public speaking.

To the Laboratory Technical staff: Mr.Neelagandan, Mr.Rajkumar, Mr.Gopi, Mr.Senthil, Mrs.Sumithra, Mrs.Eswari, Mrs.Sathya, Mrs.Selvi, Mrs.Hema Malini, Miss. Sherin and Mr.Rajesh: Thank you for making the working environment friendly to survive for long this year, from sharing foods to thoughts of the day.

I thank ***Mr. Sam, Ms.Rekha Singh, Ms.Revathi, Mr.Christopher, and Mr.Rajkumar*** from the administrative section of our department whose efficiency and the response to the need of the hour was always commendable.

To my other fellow labmates: ***Ms.Bharathi, Mr.Balaji, Ms.Esther Sathyabama, Mr.Gaurav Joshi, Mr.Ashwin Anand Pai, Ms.Rosy, Ms.Deborah, Ms.Aruna Barade, and Ms.Sreenithi.*** Thank you for making the working space amiable and friendly.

I also acknowledge my former seniors ***Dr.Ajay, Dr.Sreeja, Dr.Savitha and Dr.Ezhil Pavai*** for their good wishes

To the National Center for Biotechnology, Bengaluru: ***Prof. Mitradas Panicker and Prof. Krishna Murthy and Dr.Ashaq Hussain:*** I am grateful for accommodating me and providing the technical guidance working space for performing the Seahorse

extracellular flux analyzer and confocal imaging. Hussain, a warmly and friendly person, thank you very much for helping me with the laboratory's seahorse experiments.

To, Dr.Ganesh Kadsoor, National Manager, Olympus Medical systems: I sincerely thank you for guiding and helping me to capture the mitochondria images at IITM and NCBS.

To the Department of Biotechnology, Anna university: *Dr.TamilSelvan and Ms.Sudharsana:* Thank you for accommodating me and providing me the workspace to perform the seahorse experiments. Sudarshana, I owe you big time and lunch for staying up late in the lab until I completed my experiments.

To the British Council- Newton Fellowship and Department of Biotechnology: I am thankful to the British Council for providing me the Newton- Ph.D. fellowship to undergo training at St. the George's University of London for six months; DBT for providing the travel grant to attend the international conference; and Wellcome DBT for funding the study.

To the Molecular and Medical Parasitology group, at St. Georges University of London (SGUL), UK: *Dr.David Clark, Dr. Henry Staines Ms. Joana Benecke, Dr.Kameljit Kalsi, Mr.Greg, Mr.Benedict Davies, Dr.Cathy Moore, and Ms. Hajnalka Kovacsevics:* A special thanks to David for helping me a lot in terms of establishing the Cell culture facility, ordering reagents, and warm cups of coffee. Henry, for your valuable inputs in terms of iron measurement and providing access to the laboratory facility. Henny, thank you for all your timely help in terms of

accommodation and funding. I greatly appreciate and acknowledge the support received from you all.

I am grateful for SGUL and Richard Burchmore, Glasgow University, for funding me to travel and the data analysis workshop at the University of Glasgow.

To Dr. Santhosh Kumar and office staffs of SCTIMST,

Thank you for all the support to complete the degree in terms of meeting the deadlines and processing the documents without due. Also, for the kind and prompt responses.

To Stallon Ilangeswaran: Thank you for being there for me whenever I needed a venting space. A confidant, during the bumpy days of my life, who was there for me to lift my spirits.

To Daniel Zachariah Paul and Henna: A person whom I could count on and helped me during the troubled times with the laundries and a big smile. I envy his calmness during the pressure.

To Mubarak and Gauthaman: Lamest and the best friends of mine outside the lab who lives in different time zones. Especially Mubarak, thank you for being my go-to go person for all the amazing to worst thing of my life. Gauthaman, whom I met in London. Thank you for showing me around the Piccadilly circus, the theatre plays, and for a pleasant stay at Milton Keynes.

To my uncle Saravanan: I owe him a lot for helping me to come this far. Without him, I could not have joined higher studies nor a Ph.D. Being the first-generation learner in my family there were times where it was difficult to make my parents

understand my desire to pursue a Ph.D. He was there to convince them and helped me to continue what I wanted. I am grateful and indebted for his effort.

To My family, ***Mr.Balasundaram, Mrs.Tamil Selvi, Ms. Nirmala, Mr.Shanmugam, Mrs.Chandra, Mrs.Tamil Arasu, Mr.Badri and Ms.Porthika :*** My grandparents, Parents and Sister have always been a constant and perpetual source of motivation, inspiration, and encouragement throughout my studies and personal life. It is a matter of great honour, privilege, and pleasure to express a deep sense of gratitude for my respected and beloved grandparents and parents. I thank my cousins for bringing the joy when I was feeling low and for making mythe dark days lighthearted. I owe all of them my achievements till today for their profound devotion, unconditional love, and endless faith they have in me.

This doctorate thesis is as much an achievement of theirs as it is mine. I am highly indebted to them for their strong affection towards me and their earnest attachments to my career goals.

Synopsis

Background:

Leukemia is a heterogeneous and frequently an oligo-clonal disorder of hematopoietic progenitor cells resulting from arrested differentiation and uncontrolled proliferation of immature precursors compromising the normal function of the hematopoietic system. The net effect is an expansion of immature cells at the expense of the normal hematopoietic compartment, often rapidly leading to death. There have been significant advances in the treatment of acute leukemia in the last few decades. From an invariably fatal disease, a significant proportion of cases can be cured with current chemotherapy schedules. However, it is also important to recognize that the majority of patients with acute leukemia, more so in adults, are destined to have disease recurrence after treatment, and this remains the major cause of mortality. The major focus of research and explanation of relapse in leukemia has been on either acquired somatic genetic mutations that confer resistance within a sub-clone against chemotherapy and the presence of a leukemia-initiating compartment/leukemia stem cell population that is inherently resistant to chemotherapy and persists as minimal residual disease and eventually leads to disease recurrence. However, it is increasingly recognized that there are additional biological processes that can contribute to recurrence of leukemia after conventional chemotherapy.

Metabolic reprogramming of cancer cells is one of the hallmarks of cancer and increasing evidences suggests that metabolic plasticity of the cancer cells drives drug resistance in solid tumors. There are several studies supporting the concept that the

bone marrow microenvironment can induce resistance to chemotherapy in leukemic cells that reside in proximity/niches in this microenvironment. There are preliminary data to suggest that this is, at least in part, mediated by adaptive metabolic alterations in the leukemic cells that are induced by the microenvironment. It is potentially possible to target these metabolic alterations that favor survival to overcome drug resistance. The extent to which mitochondrial respiration / alterations occurs within malignant cells and the extent to which this is further altered in the micro-environment is debated but clearly appears to vary with the type of malignancy. It is important to dissect the metabolic dependency of the tumor cells and potential to overcome the innate and acquired drug resistance by incorporating a metabolic disruptor in the treatment either alone or in combination with standard therapy. The anti–diabetic drug metformin has stirred the field of drug repositioning when large epidemiological data provided the data of anti-cancer property of metformin. More recently large studies screening small molecule that inhibit metabolic pathways in cancer has gained attention as they have reported the ability of some of these molecules to selectively inhibit metabolism in cancer cells while sparing the normal counterpart. In epithelial cancer it has been shown that bedaquiline which is an anti-microbial agent approved by the FDA for the treatment of multi-drug resistant pulmonary tuberculosis (TB) has a potential anti-cancer property and could also potentially eradicate cancer stem cells. It is important to note that several similar observations of targeting the metabolic variations on cancer cells have already been translated into the clinic. Phase I clinical trials are in progress evaluating the mitochondrial inhibition using Tigecycline a widely used antibiotic as a single agent in the treatment of acute myeloid leukemia and

chronic myeloid leukemia. The importance of the metabolic adaptations in drug resistance has not been extensively evaluated in acute leukemia.

Objectives:

1. To study the metabolic perturbations in leukemic cells and its impact on innate and bone marrow micro-environment mediated drug resistance.
2. Evaluate the metabolic changes in relapsed and refractory leukemia in comparison to newly diagnosed leukemia.
3. To screen and evaluate molecules that can disrupt adaptive metabolic changes in leukemic cells and induce selective leukemic cell death.
4. To evaluate the potential synergy between such molecules and conventional chemotherapeutic agents used in the treatment of acute leukemia.

Materials and Methods:

Assays for viability: 5×10^5 cells were treated with different drugs and inhibitors and incubated for 48 hours at 37 °C CO2 incubator. After the incubation period the cells were collected and the viability was assessed using Annexin V/7-aminoactinomycin D (7AAD) apoptosis assay kit (BD Pharmingen, San Diego, CA, USA) as per the manufacturer's protocol. In vitro cytotoxicity of drugs was determined by MTT assay (Sigma, St. Louis, MO, USA). 105 cells were treated with increasing concentration of drugs and at the end of 48 hours treatment period MTT reagent was added followed by 10 % SDS after hours. The absorbance of MTT was read at 570nm with reference wavelength of 630nm Spectramax M4 (Molecular Devices, Sunnyvale, CA, USA).

The half-maximal inhibitory concentration (IC50) values were generated using Graph Pad Prism5 software (La Jolla, CA, USA).

Semi-quantitative real time PCR: Total RNA was extracted using Trizol reagent (Invitrogen Carlsbad, CA, USA). 500ng of the extracted RNA was converted into cDNA using superscript II cDNA kit (Invitrogen Carlsbad, CA, USA). The expression of genes was studied using SYBR green method (Finnzymes F410L, Thermo scientific, Rockford, IL, USA). The Ct values were normalized with ACTB and the fold differences were calculated using 2-ΔΔCt method.

Immunoblot: Cells homogenates were obtained by cell lysis in RIPA buffer (Sigma, St. Louis, MO, USA), with complete protease inhibitors (Roche, Basel, Switzerland).The lysates and elutes were analyzed in SDS–PAGE. After protein transfer to nitrocellulose membrane, membranes were blocked with non-fat dry milk (5%, 2 hours) followed by incubation with primary antibodies overnight. The protein bands were detected by standard chemiluminescence method (Thermo Pierce Femto, Rockford, IL, USA).

Seahorse Metabolic flux analysis: Extracellular flux assay kits XF24 (Agilent Technologies, CA, USA) were used to measure oxygen consumption and glycolytic flux. $5x10^5$ cells were plated in an XF24 cell culture microplate. Briefly, three replicate wells of 5×10^5 cell per well were seeded in a retronectin (Takara Bio Inc, JPY) coated 24-well XF24 plate. At 30 min prior to analysis, the medium was replaced with Seahorse XF media (Agilent Technologies, CA, USA) and the plate was incubated at 37 °C. Analyses were performed both at basal conditions and after injection of

oligomycin, FCCP, antimycin A, and rotenone for Mitochondrial function and glucose, oligomycin and 2-deoxy glucose for glycolytic function.

Mitochondrial morphology using Confocal -laser scanning microscopy: MitoTracker™ Red CM-H2Xros (Thermo Scientific) was added into culture media at a final concentration of 100nM to label the mitochondria of leukemic cells for 30 minutes in 37o C 5%CO2 incubator before harvesting cells for confocal studies. To prepare slides, labeled cells were washed 2 times with ice cold PBS and resuspended at a final concentration of 500K cells /ml in ice cold PBS. 150 ul of cell suspension (75K cells) was used for cytospin at 400rpm for 5 minutes at room temperature. The slides were air-dried in dark box at room temperature for 5 minutes before fixed in -20 º C 100% methanol for 10 minutes. The slides were then air-dried in dark box at room temperature for 10 minutes and mounted in Vectashield DAPI Mountant before confocal imaging. The stained slides were imaged on the Olympus FV3000 confocal microscope using its High sensitivity detectors excite the DAPI and its 633nm laser to excite the MitoTracker-Red. Z stacks were captured and the images were deconvoluted using Olympus Fluo view and the morphological analysis were carried out.

Mouse Model and Drug treatments: The animal study designs were approved by the institutional animal ethics committee (IAEC approval number (2/2018). APL cells from the spleen of MRP8-PML-RARA transgenic mice were harvested and cryo preserved (a kind gift from Dr. Scott Kogan). APL cells were injected intravenously via tail vein into the genetically compatible FVBN recipients. Treatment schedules were started on day post injection of leukemic cells.

Major Findings:

Leukemic cells from the different subtypes of acute leukemia differs significantly in their utilization of energy producing metabolic pathways (glycolysis and oxidative phosphorylation). We screened for FDA compounds which could selectively promote cell death in the leukemic cells in combination with arsenic trioxide (ATO). We observed that artesunate (ART) an antimalarial agent had a significant profound effect on the different subtypes of leukemia with minimal by stander effect on the normal cells even in combination with ATO. ART treatment resulted in dysfunction of mitochondria (fragmented) only in the leukemic cells and not in the normal cells. ART requires iron for its activity, and we observed that the malignant cells had increased levels of transferrin receptor expression (major iron importer). ART and ATO significantly affected the surface expression of transferrin but not the other conventional chemotherapeutic agents. Intra cellular iron enhancing agents significantly increased the cytotoxic activity of ATO and ART. Leukemic cells cleared the damaged mitochondria via mitophagy pathway and survived the cytotoxic effects of ART alone. Our in vivo experiments validated our in vitro findings that the combinations significantly increased the survival rate of the leukemic mice. ART and ATO synergized with the existing conventional chemotherapeutic agents such as cytosine arabinoside, daunorubicin hydrochloride and azacytidine used in the management of acute myeloid leukemia. ART in combination with the conventional chemotherapeutics agents significantly prolonged the survival of the leukemic mice.

Significance of the findings:

We have demonstrated the existence of metabolic heterogeneity of the acute myeloid leukemia cells. Targeting the oxidative phosphorylation is effective in different subtypes of leukemia in combination with ATO. Existing therapy in the management of leukemia is highly myelotoxic and not affordable by most of the patients who gets diagnosed in our center. The combination of ATO and ART significantly promoted cell death across the subtypes of leukemia with minimal bystander effect on the normal peripheral blood mono nuclear cells and hematopoietic stem cells. The combination synergized with the existing treatment care for leukemia and could possibly offer an alternative low-cost effective treatment strategy.

The thesis is dedicated to those who did not lose hope facing research frustrations and failures and keep seeking the objective truth with passion and a creative soul.

Ever tried. Ever failed. No matter. Try again. Fail again. Fail better.

- Samuel Beckett

1.0 Introduction

Curiosity has its own reason for existence- ***Albert Einstein***

The first descriptions of signs that can be retrospectively interpreted as cancer date as far back as 3000 BC. Ancient Egyptian writings called the Edwin Smith Papyrus to say about the disease, 'There is no treatment' (Marasca et al., 1999, Breasted, 1918). It was only in the early 19th century, European physicians identified patients with uncommon alteration of the blood - findings then interpreted as inflammation. David Craigie, a physician at the Royal Infirmary of Edinburgh, began to question the interpretation of such peculiar findings on a patient admitted and later died in his ward in 1841. A young Pathologist, John Hughes Bennet, who performed the autopsy on this patient and published the findings, concluded that the alteration of blood was independent of inflammation and that the pathology involved the whole-blood system. Shortly after, Rudolf Virchow described the case of a woman with a distended abdomen and increased circulating white blood cells – findings that can be interpreted in retrospect as chronic leukemia (Piller, 2001). Virchow called it 'Weisses Blut (White blood) and later used the term 'Leukemia' (Roehrl and Dzik, 2008).

Aging is associated with an increase in the incidence of solid and hematological malignancies. A rare subset of cells, the hematopoietic stem cells (HSCs), which reside in specific niches in the bone marrow, are responsible for the blood cell production. This process requires strict control of proliferation, differentiation, and apoptosis to maintain a steady equilibrium of cells throughout the lifespan of an organism (Groarke and Young, 2019).

Aged HSCs preferentially produces an increased number of myeloid cells and loss of lymphoid potential (Figure1). It is thought that the myeloid skewing observed with HSC aging may contribute to the increased incidence of myeloid malignancies with age (Figure 2) (Lopez-Otin et al., 2013).

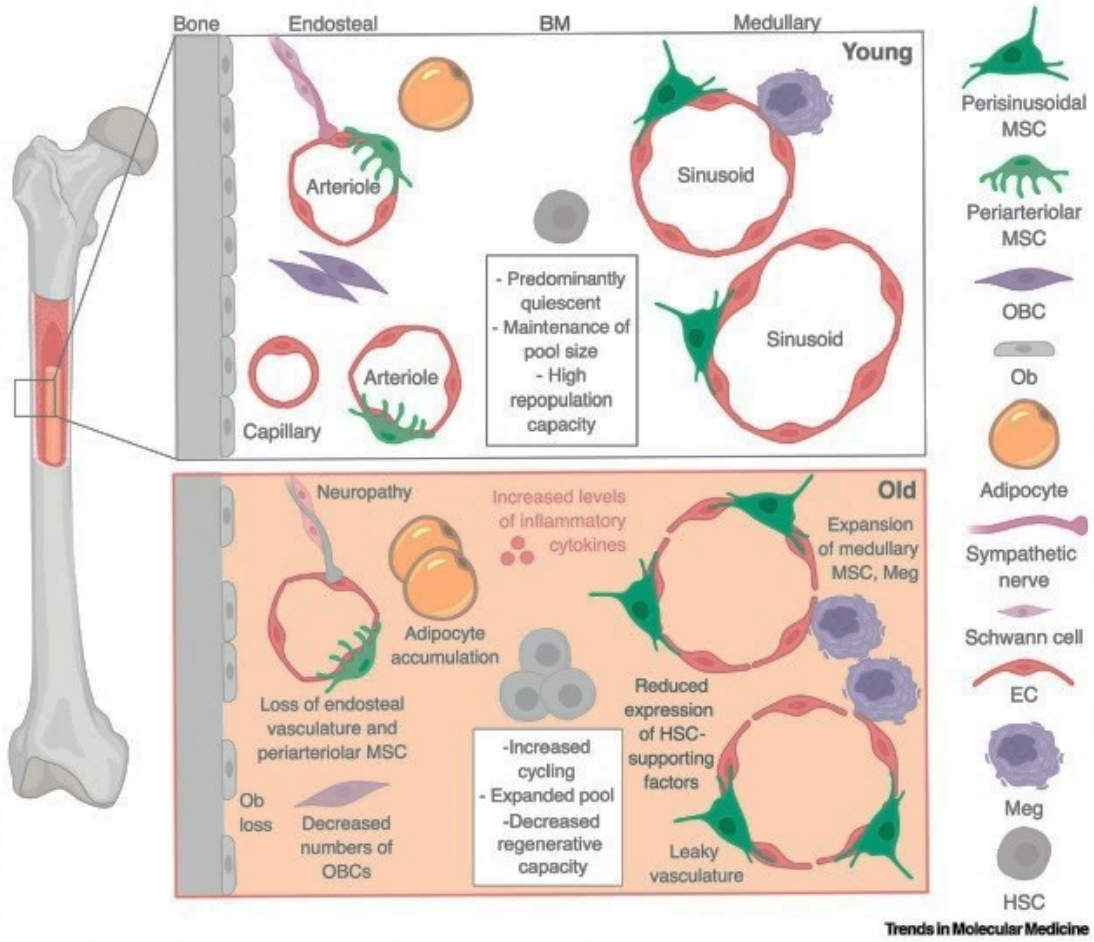

Figure 1: Changes in the hematopoietic stem cells and the bone marrow microenvironment to aging. (Verovskaya et al., 2019)

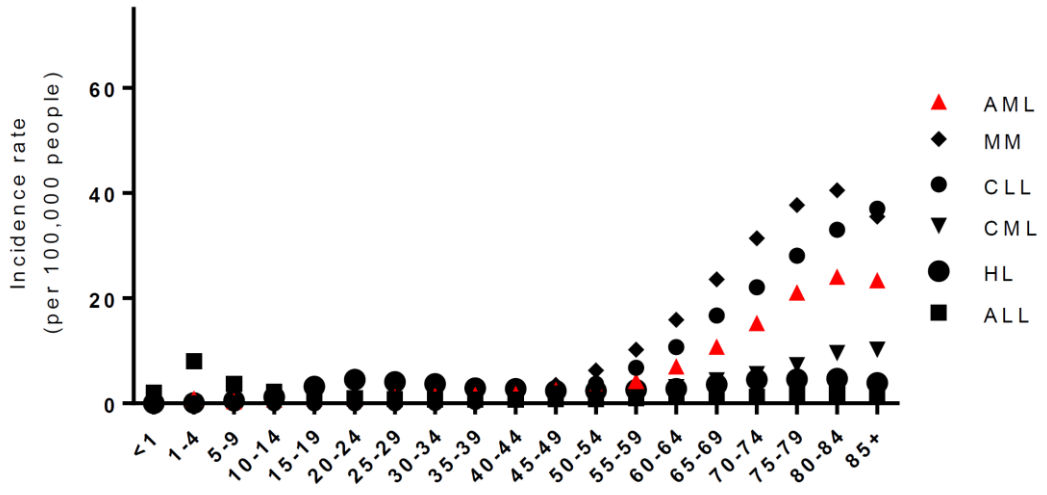

Figure 2: The incidence of hematological cancers increases with age. There is an increase in the incidence of hematological malignancies with age (multiple myeloma (MM), chronic lymphocytic leukemia (CLL), acute myeloid leukemia (AML), chronic myeloid leukemia (CML), Hodgkin's lymphoma (HL) and acute lymphocytic leukemia (ALL)) (Source: SEER.cancer.gov; Incidence datasets April 2019)

Leukemia, the cancer of blood and bone, can be classified into four main groups according to cell type and rate of progression: acute lymphocytic (ALL), chronic lymphocytic (CLL), acute myeloid (AML), and chronic myeloid leukemia (CML). Leukemia is now recognized to be a disease arising from both genetic and metabolic abnormalities (Kouchkovsky and Abdul-Hay, 2016). In spite of significant advances in the treatment of leukemia over the past few decades, apart from pediatric ALL and CML (after the advent of Imatinib), the outcomes remain poor for most other subtypes. AML is the commonest form of acute leukemia in adults, which accounts for the largest number of annual deaths from leukemia.

The standard of care for 90 % of acute myeloid leukemia (AML) cases is the cytotoxic chemotherapy, which is in use for the past forty years: combination treatment with the nucleoside analog cytarabine (ARA-C) and a topoisomerase inhibitor such as daunorubicin (DNR). Such treatment prevents successful DNA replication and is toxic to all rapidly proliferating cells in addition to the tumor itself. In contrast, in acute promyelocytic leukemia (AML-M3; APL) a subtype of AML, therapy has evolved into one where conventional myelosuppressive therapy is no longer required (Coombs et al., 2015), instead of combination therapy of all-trans retinoic acid (ATRA) and arsenic trioxide (ATO) that together induces differentiation of the malignant cell population along with relatively specific apoptosis of the malignant cell population. The combination of ATO and ATRA in APL treatment reduces the conventional side effects of chemotherapy, such as recurrent cytopenia, alopecia, and mucositis. The current anticipated cure rates in APL with this non-myelosuppressive regimens exceed 90% in most studies (Coombs et al., 2015a). In AML (non-AML-M3), on the other hand, in spite of intensive myelotoxic therapy, the majority of patients, more so in adults, are destined to have disease recurrence after treatment, and this remains the major cause of mortality.

The major focus and explanation of relapse in leukemia has been on either acquired somatic genetic and epigenetic mutation that confers resistance within a sub-clone against chemotherapeutic agents or the presence of leukemia-initiating compartment/leukemia stem cell population/that is inherently resistant to chemotherapy and persists as a minimal residual disease. However, it is increasingly recognized that additional biological processes can contribute to the recurrence of

leukemia after conventional chemotherapy. Recognizing these novel mechanisms of resistance can lead to the recognition of novel therapeutic targets. There is an increasing need to identify the compound(s) or combination of therapeutic agents specific for the malignant cell with reduced off-target side effects, which can be used in the treatment of AML.

Metabolic reprogramming of cancer cells is one of cancer's hallmarks, and increasing evidence suggests that metabolic plasticity of the cancer cells drives drug resistance in solid tumors (Hanahan and Weinberg, 2011). The malignant cells are reported to be relying on glycolysis for their cell survival and proliferation, which is a less energy-producing pathway in comparison to mitochondrial respiration. This phenomenon of the cancer cells is called the Warburg effect –aerobic glycolysis, where the cancer cells undergo glycolysis even in the presence of an ample amount of oxygen(Warburg, 1956c). The malignant cells resistant to the conventional agents are observed to be utilizing mitochondrial respiration for survival and agents that disrupt the metabolic adaptation and have been reported to overcome resistance when combined with conventional agents (Fiorillo et al., 2016, Kasznicki et al., 2014).

The energy metabolism reprogramming has been considered for decades as synonymous with the "Warburg effect" (Warburg, 1956b, Warburg, 1956a). This phenomenon, also known as "aerobic glycolysis," was described by the German biochemist Otto Heinrich Warburg as the impaired cell metabolism in the origin of cancer, due to mitochondrial respiration defects. Moreover, the theory proposed that the increased glycolytic flux as a compensatory mechanism of energy production

required to maintain the viability of cancer cells. In the following decades, both biochemists and oncologists criticized the Warburg theory for being too simplistic, not consistent with the evidence of apparent normal respiratory function in some tumor cells. Furthermore, Warburg did not consider the role of tumor-associated mutation. Therefore, the view of cancer as a metabolic disease was gradually replaced with the one of cancer as a genetic disease involving nuclear mutations in oncogenes and tumor suppressor genes (Hanahan and Weinberg, 2011). Numerous experimental evidences are still keeping alive to resolve "the chicken and the egg" dilemma about mitochondrial dysfunction and tumor formation. Specifically, two distinct hypotheses about the mitochondrial role in tumorigenesis keep the question still a debatable one, on the one hand, the mitochondrial dysfunction considered as a primary cause of tumorigenesis, on the other as a "second hit" in the process of cancer metabolic transformation, a consequence of accelerated glycolysis (Frezza and Gottlieb, 2009). Specifically, this event may be caused by the loss of tumor suppressors or the activation of oncogenes. The preference of aerobic glycolysis is currently recognized as one of the numerous ways malignant cells undergo metabolic reprogramming to survive and proliferate during tumor initiation, progression, and metastasis (Koppenol et al., 2011). These pathways, such as mitochondrial metabolism, oxidative phosphorylation, or redox balance, are usually pre-existing in normal cells, and they are still functional in malignant ones. Among reprogrammed activities, some mechanisms allow tumor cells to take up abundant nutrients to produce ATP (Adenosine triphosphate), generate biosynthetic precursors and macromolecules, tolerate malignancy-associated stress (redox stress and hypoxia), allow cancer cells to

tolerate nutrient depletion by catabolizing cellular or extracellular macromolecules through autophagy, micropinocytosis, or lipid scavenging (Commisso et al., 2013). The induction of these activities is regulated by signaling pathways commonly perturbed in cancer cells. Notably, even though the broad genetic heterogeneity of tumors, malignant cells share the induction of pathways related to anabolism, catabolism, and redox balance (Cantor and Sabatini, 2012). The resulting alterations in metabolite levels, in turn, induce post-translational modifications (PMTs) – such as acetylation, methylation, and thiol oxidation – that influence cellular signaling, epigenetics, and gene expression. However, the Warburg effect's acceptance as the main consequence of genomic instability selected during tumor progression (Kim and Dang, 2006), renewed the interest in the energy metabolism of cancer cells. Consequently, a new view of cancer cell homeostasis is emerging, related to the balance between newly acquired oncogenic and typical normal cell features (DeBerardinis and Chandel, 2016; Cairns et al., 2011). Importantly, the biological functions of normal cells are strongly required for the acquisition of malignant phenotype, and they are ensured by the proper preservation of key mitochondrial functions (Wallace, 2012; Weinberg and Chandel, 2015; Zong et al., 2016).

It is important to dissect the metabolic dependency of the tumor cells and the potential to overcome the innate and acquired drug resistance by incorporating a metabolic disruptor in the treatment alone or combination with standard therapy. The anti-diabetic drug metformin had stirred the field of drug repositioning when large epidemiological data provided the anti-cancer property of metformin (Kasznicki et al., 2014, Owen et al., 2000). More recently, large studies screening small molecules that

inhibit metabolic pathways in cancer has gained attention as they have reported the ability of some of these molecules to selectively inhibit metabolism in cancer cells while sparing the normal counterparts (Gohil et al., 2010a).

1.1 Rationale of the study:

While recent advances in the treatment of some hematological malignancies, the therapy for AML remains a clinical challenge. For patients diagnosed older than 60, the prognosis is particularly poor, with a 2-year survival probability of less than 10 percent (Löwenberg et al., 1998).

Our institutional data, as a tertiary care center, stresses the lack of financial support for patients who get diagnosed to have acute myeloid leukemia. In a two-year prospective study at our center, there were 380 newly diagnosed AML, 81 % of the patients opted for not to have treatment due to lack of financial constraint. Of the treated patients, around 25 % of them were induction deaths, and the major reason was observed to be due to bacterial sepsis and fungal infections. (Philip et al., 2015).

One approach to the development of more effective therapies for AML is to identify agents able to induce the death of proliferating leukemic and leukemia stem cells (LSCs). LSC's represent a rare subset of cells in the clone that share many properties with normal hematopoietic stem cells, including an extensive self-renewal ability, a slow turnover, and resistance to many standard chemotherapeutic drugs. As a result, LSCs are often not targeted by the available treatments, leading to eventual disease relapse (Dick, 1996, Hope et al., 2004). Thus, it is crucial to develop

therapeutic agents that can effectively target LSCs in AML. Recent evidence supports the existence of a metabolic difference between the normal and leukemic stem cells and how it could exploit as a therapeutic target (Schepers et al., 2015).

Novel strategies, targets, and targeted therapy that do not involve much toxicity and expense are urgently needed in the management of acute myeloid leukemia, especially in developing and under-developing countries.

1.2 Objectives and aims of the study

Objectives:

5. To study the metabolic perturbations in leukemic cells and its impact on innate and bone marrow micro-environment mediated drug resistance.
6. Evaluate the metabolic changes in relapsed and refractory leukemia in comparison to newly diagnosed leukemia.
7. To screen and evaluate molecules that can disrupt adaptive metabolic changes in leukemic cells and induce selective leukemic cell death.
8. Evaluate the potential synergy between such molecules and conventional chemotherapeutic agents used in the treatment of acute leukemia.

1.3 Brief overview of chapters

1.3.1 Literature review

Following the introduction, rationale, and objectives of the current study, the next major chapter in this thesis is the literature review, which elaborates on the disease model in this study, its pathologic and molecular mechanisms, and the standard of care. The mechanism of action each drug used was also described in this section. The central focus was on drug resistance with specific context on the metabolism of the leukemic cells and how it could be modulated to enhance the efficacy of the exiting chemotherapeutic agents described in the literature.

1.3.2 Materials and Methods

Different strategies for studying the metabolism and mitochondria were described in detail in the methodology section. The study design was outlined, and the various techniques and methods used for conducting experiments and analyzing data were described. Gene expression, assays, protein, and mRNA expression techniques were also described in this section. The establishment of leukemic mice models, seahorse extracellular flux analysis, 3D cultures, and various drug treatment protocols were also described in this section.

1.3.3 Results

ATO resistant and sensitive cell line was characterized using gene expression profiling, and whole-exome sequencing analysis is described in detail here. The role of glycolytic and mitochondrial metabolism in the leukemic cells and in the presence

of stromal cells is evaluated in detail. Screening of potential drugs to overcome metabolic adaptations and its mechanisms of synergy with ATO is also described in this part. The last major part involves evaluating the efficacy of artesunate (one of the screened drugs) and ATO and Aza in a transplantable mouse model of leukemia, which can be translated into phase I/II of the clinical trial.

1.3.4. Discussion

The significance of the major results obtained in this study has been described in detail in this section. The results obtained in this study have been discussed with the existing scientific data with implications to the clinic.

1.3.5 Summary and Conclusion

The key observations from this doctoral work have been summarized in this chapter, and the scope to take up this work forward has been suggested. A comprehensive figure of the findings from this was made and discussed in this section. The references cited in the text were listed in the bibliography.

Review of Literature

Character cannot be developed in ease and quiet. Only through experience of trial and suffering can the soul be strengthened, ambition inspired, and success achieved.

- Helen Keller

2.0 Review of the literature:

2..1 Hematopoiesis and leukemia:

Hematopoiesis is a process in which the cellular constituents of blood are continually replenished throughout the lifetime of an organism(de Haan and Lazare, 2018). The hematopoietic system consists of various populations of highly specialized cells with unique functions, such as oxygen transport and immune defense. It is estimated that an adult human generates ~4–5×10^{11} hematopoietic cells per day. The continuous production of many blood cell types requires a highly regulated yet highly responsive system. In the mammalian hematopoietic organization, hematopoietic stem cells (HSCs) sit at the top of the hierarchy. In adults, HSCs are found primarily in the bone marrow (BM). They are characterized by their ability to self-renew and produce various progenitors that proliferate and differentiate into mature blood cells (Pinho and Frenette, 2019). Committed progenitors have limited self-renewal ability, exhibit restricted lineage differentiation potential and exhaust within a few weeks after transplantation. At a steady-state, most HSCs are quiescent, which protects them from genotoxic insults, whereas the bulk of hematopoiesis is ensured by downstream progenitors. Several studies using single-cell transplantation and in vitro differentiation have challenged the classical hierarchical differentiation tree of hematopoietic progenitors, instead of revealing lineage-restricted progenitors (restricted to one or two lineages) that may bypass multipotent progenitors and are generated directly from HSCs. To ensure hematopoietic homeostasis throughout life, the balance between differentiation and self-renewal needs to be tightly regulated: excessive differentiation or insufficient self-renewal depletes the HSC pool, whereas

insufficient differentiation or unrestrained self-renewal can lead to myeloproliferative diseases or leukemia. HSC activity is regulated by an intricate interplay of cell-intrinsic factors, such as transcriptional and epigenetic regulators and metabolic pathways, and cell-extrinsic cues, including long-range humoral and neural signals or local cues from the BM microenvironment, which is referred to as the 'stem cell niche' (McKerrell and Vassiliou, 2015, Chambers et al., 2007).

Acute myeloid leukemia (AML) is a heterogeneous, oligoclonal disorder affecting both adult and pediatric patients in which variable genetic aberrations lead to the expansion of undifferentiated myeloid cells at the expense of the hematopoietic system. It is the most common form of acute leukemia in adults, accounting for ~80 percent of cases in this group (Figure 3).

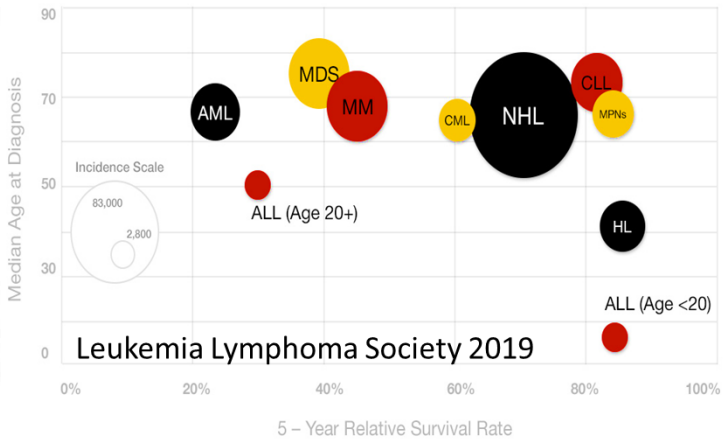

Figure 3: Five-Year Survival Rates of Blood Cancers: Incidence of myeloid malignancy is strongly related to age and is found to increase with age. Bubble size represents the proportion of the malignancy. AML survival lags other types of blood cancer. Leukemia and Lymphoma Society 2019.

2.2 Classification of acute myeloid leukemia:

Classification of leukemia can be done by the French American-British (FAB) system and the World Health Organization (WHO) system (Bennett et al., 1976, Arber et al., 2016).

2.2.1 French American-British classification:

The FAB system was the first to attempt to distinguish the various types and sub-types of leukemia based on morphology and cytochemistry.

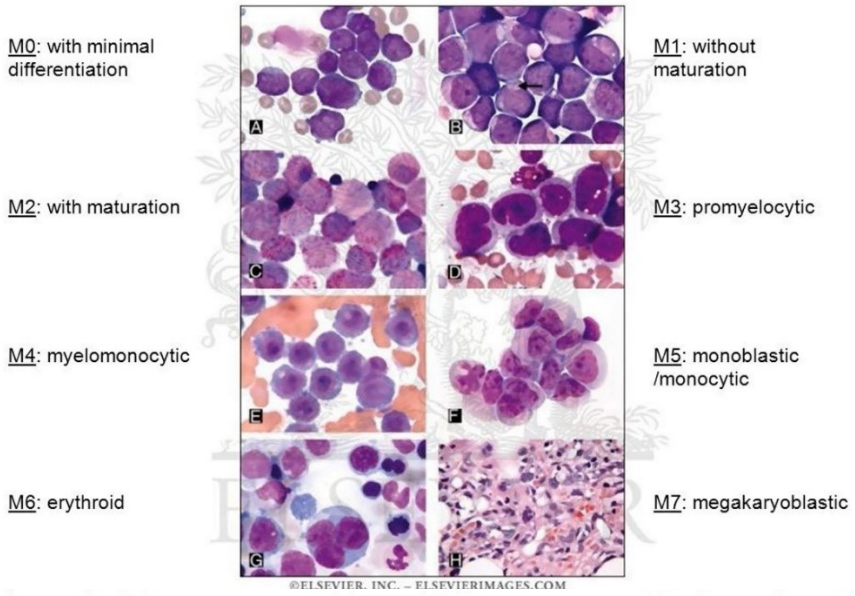

Figure 4: FAB classification of acute myeloid leukemia and shows the morphology of AML together with microscope images. Images from the History of Medicine, Bethesda, US.

Subtype	Name
M1	Myeloblasts without maturation
M2	Myeloblasts with maturation (best AML prognosis)
M3	Hyper granular promyelocytic leukemia (faggot cells)
	M3V - Variant, microgranular promyelocytic leukemia
M4	Myelomonocytic leukocytes
M5	Monocytic, subtype a. Poorly differentiated monocytic leukemia b. Well differentiated monocytic leukemia
M6	Erythroleukemia/DiGuglielmo syndrome
M7	Megakaryocytic leukemia Pleomorphic undifferentiated cells with cytoplasmic blebs; myelofibrosis or ↑ BM reticulin; positive for platelet peroxidase antifactor VIII

Table 1: French American British classification of AML. (Bennett et al., 1976)

2.2.2 World Health Organization (WHO) classification:

The World Health Organization (WHO) integrated new developments in the classification system in 2001, which was first revised in 2008 and later in 2016 (Vardiman et al., 2009, Arber et al., 2016). The WHO classification combined the cytogenetic/ genetic data that help to define biologically homogenous entities with prognostic and therapeutic relevance.

AML with recurrent genetic abnormalities
AML with t(8;21)(q22;q22.1); *RUNX1-RUNX1T1*
AML with inv(16)(p13.1q22) or t(16;16)(p13.1;q22); *CBFB-MYH11*
APL with *PML-RARA*
AML with t(9;11)(p21.3;q23.3); *MLLT3-KMT2A*
AML with t(6;9)(p23;q34.1); *DEK-NUP214*
AML with inv(3)(q21.3q26.2) or t(3;3)(q21.3;q26.2); *GATA2, MECOM*
AML (megakaryoblastic) with t(1;22)(p13.3;q13.3); *RBM15-MKL1*
Provisional entity: AML with *BCR-ABL1*
AML with mutated *NPM1*
AML with biallelic mutations of *CEBPA*
Provisional entity: AML with mutated *RUNX1*
AML with myelodysplasia-related changes
Therapy-related myeloid neoplasms
AML, NOS
AML with minimal differentiation
AML without maturation
AML with maturation
Acute myelomonocytic leukemia
Acute monoblastic/monocytic leukemia
Pure erythroid leukemia
Acute megakaryoblastic leukemia
Acute basophilic leukemia
Acute panmyelosis with myelofibrosis
Myeloid sarcoma
Myeloid proliferations related to Down syndrome
Transient abnormal myelopoiesis
Myeloid leukemia associated with Down syndrome

Table 2: List of the major subgroups of myeloid neoplasms and acute leukemia in the WHO classification 2016, and the specific entities of which they are composed (Table modified form Arber et al, Blood 2016)

2.3 Prognostic factors and risk stratification in the management of AML:

Over the years, prognostic factors in AML have remarkably evolved. Several clinical and biological features have been identified to predict the probability that a patient will achieve remission and eventually cure in response to treatment. Patient-related, as well as disease-related factors, influence the prognosis of AML.

Age remains as an independent prognostic factor in the management of AML due to the presentation with additional co-morbidities, which limits the use of conventional chemotherapy. In addition to age, the European Leukemia Network (ELN) classification scheme was created by incorporating chromosomal and molecular aberrations into prognostication (figure 5).

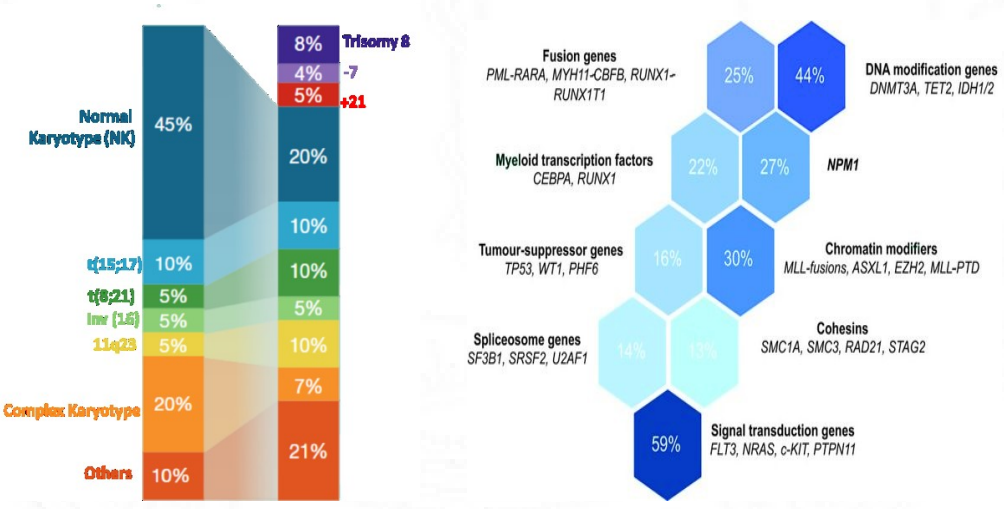

Figure 5: Represents the proportion of cytogenetic and molecular aberrations used in the prognosis of acute myeloid leukemia.(Grove and Vassiliou, 2014)

Prognostic category	Favorable risk (5 yr OS: 45%-80%)		Intermediate risk (5 yr OS: 20%-40%)		Adverse risk (5 yr OS: 5%-20%)	
	40%-45% of AML cases		25%-35% of AML cases		25%-30% of AML cases	
	Aberration	Frequency (%)	Aberration	Frequency (%)	Aberration	Frequency (%)
	• t(15:17)	7-12	• NK with *FLT3*-ITD	15-20	• 11q23,	3-5
	• t(8:21)	5-8	• NK with NPM^{WT} & no *FLT3*-ITD	10-17	• inv(3)/t(3;3)/*EVI-1*	~1
	• inv(16)	5-8	• t(9:11)	2-3	• t(6;9)/*DEK-NUP214*	~1
	• NK with NPM^{mut} & no *FLT3*-ITD	18-25	• Other cytogenetic abnormalities not included elsewhere	5-8	• -7/7q-	3-5
	• NK with biallelic $CEBPA^{mut}$	6-12			• -5/5q-	2-3
					• 17p deletions	~2
					• CK	10-12

Table 3: *Represents the ELN 2016 classification of AML with risk group and their genetic abnormality (Table modified from (Arber et al., 2016).*

Based on the retrospective analysis of data from large co-operative group studies, 40-50% of patients with de novo AML have a normal karyotype, which is associated with an intermediate risk in terms of survival outcomes (Table 3). Advances in molecular biology resulted in identifying mutations at the molecular level, which carry prognostic impact in AML. Therefore, by adding newly identified molecular markers to already existing cytogenetic risk groups helped in refining prognostics groups, particularly in patients with normal karyotype AML (Table 4).

	Gene	Frequency (in NK-AML) and comments
Signalling	*FLT3*-ITD	20%-25% (28%-35%); High blast count; Poor prognosis especially in cases with high mutant to WT allelic ratio
	FLT3-TKD	5%-7% (10%-14%); Prognostic impact remains controversial
	NRAS	10% (9%-14%); Enriched in CBF AML; Prognosis unknown
	C-KIT	<5% (<5%); 25-30% in CBF leukaemia
	PTEN	<2% (2%); Prognosis unknown
Transcription factors (TF)	*NPM1*	25%-30% (40%-65%); M4 blast morphology lacks CD34 expression; Hox gene upregulation; Favorable prognosis in the presence of $FLT3^{WT}$; Female preponderance
	CEBPA	5%-10% (10-19%); Favorable prognosis if biallelic mutation
	RUNX1	5%-13% (6-25%); Enriched in trisomy 13 and FAB M0; Poor prognosis
	WT1	10% (10%-13%); Associated with M0 FAB type; Poor prognosis
	TP53	2%-4% (<2%); Predominantly in CK-AML; Very poor prognosis
Epigenetic modifiers	*DNMT3A*	20%-25% (32%-35%); Heterozygous R882 mutations account for 40%-60% of mutations; Poor prognosis in NK-AML
	IDH1/IDH2	12%-22% (25%-30%); Mutant *IDH1 & 2* are mutually exclusive; *IDH1* mutations enriched in patients with $NPM1^{mut}$; IDH1 is localized in cytoplasm and peroxisomes
	TET2	7%-15% (15%-23%); Mutually exclusive to *IDH1/2* mutations; More prevalent in secondary AML especially MPN
	ASXL1	3% (3%-5%); Poor prognosis
	EZH2	<2% (<1%); Enriched in MDS/MPN; Prognosis unknown
	MLL-PTD	<2% (2%-5%); Enriched in trisomy 11
Overexpressed	*EVI-1*	Deregulated in inv(3)(q21q26); Poor prognosis
	MN1	Poor response to chemotherapy; Correlated with NPM^{WT} and high BAALC expression
	BAALC	High expression in NK and +8; Poor prognosis
	ERG	Poor prognosis in CK and NK AML
	miR-181	Increased in FAB M1/M2, $CEBPA^{mut}$; Favorable prognosis

Table 4: Frequency of mutation in the normal karyotype (NK-AML) and their class and prognosis. (Table modified from (Arber et al., 2016).

2.4 Current treatment strategies for AML:

The standard of care in AML (excluding APL) has remained largely unchanged for the past three decades and can be divided into induction and consolidation. Standard induction therapy consists of a combination treatment of the nucleoside analog cytarabine (Ara C) and an anthracycline such as daunorubicin to induce remission. The standard 7+3 regimen consists of 7- day continuous infusion of cytarabine at 100 or 200mg/m^2 daily on days 1 to 7 and daunorubicin at 60 mg/m2 on days 1-3 (Dombret and Gardi2.4.1n, 2016). The goal of induction therapy is to deplete the bone marrow of both malignant and benign cells (< 5% blast count), allowing hematopoiesis, to repopulate the marrow with normal cells and lead to remission. Once remission is observed, additional treatments are required to target undetectable leukemic cells and lead to a long-term cure.

Consolidation therapy includes additional chemotherapy treatment or allogeneic hematopoietic stem cell transplantation of the bone marrow. However, this technique carries a high morbidity risk due to chronic graft-versus-host diseases (Bonawitz et al., 2006). Consequently, allogeneic HSCT is applied based on risk-benefit ratio and considered standard care in patients with intermediate II-risk and adverse-risk AML after first complete remission. However, it is not advised for favorable-risk AML (figure 6).

APL has been improved from dismal to the curable subtype of acute myeloid leukemia (AML) after the introduction of all-trans retinoic acid (ATRA) and arsenic trioxide (ATO)(Mathews et al., 2006, Lo-Coco et al., 2013, Niu et al., 1999). ATO as a single agent or in combination with ATRA has improved the survival outcome

significantly with minimal toxicity in comparison to conventional chemotherapy in the management of newly diagnosed APL(Coombs et al., 2015a). In our center, we have been using single-agent ATO for the treatment of APL from 1998. Arsenic trioxide (ATO), in a dose-dependent manner, can induce differentiation and cause apoptosis of promyelocytes in APL(Chen et al., 1997). ATO, as a single agent, is effective in inducing remission in patients with relapsed APL (Shen et al., 1997, Soignet et al., 2001). It is equally effective in inducing remission in newly diagnosed cases of APL (Sun HD, 1992, Mathews et al., 2002). At the doses used to induce remission in APL, ATO is not associated with toxicities commonly seen with chemotherapy. We have used an ATO based regimen in India. It has special relevance to us in view of the low cost of this regimen ($1/4^{th}$ that of standard therapy) compared to conventional ATRA and chemotherapy-based regimens (Mathews et al., 2006). In low-risk patients defined based on the WBC count at diagnosis, this agent is very effective, while among high-risk cases, the clinical outcome is inferior to conventional therapy. From the available data single agent, ATO is a low-cost, effective regimen for patients in our country. However, for high-risk patients, more needs to be done to reduce the risk of relapse (figure 7).

However, treatment often fails for a majority of patients due to relapse from complete remission instead of primary resistance to therapy or treatment-related mortality.

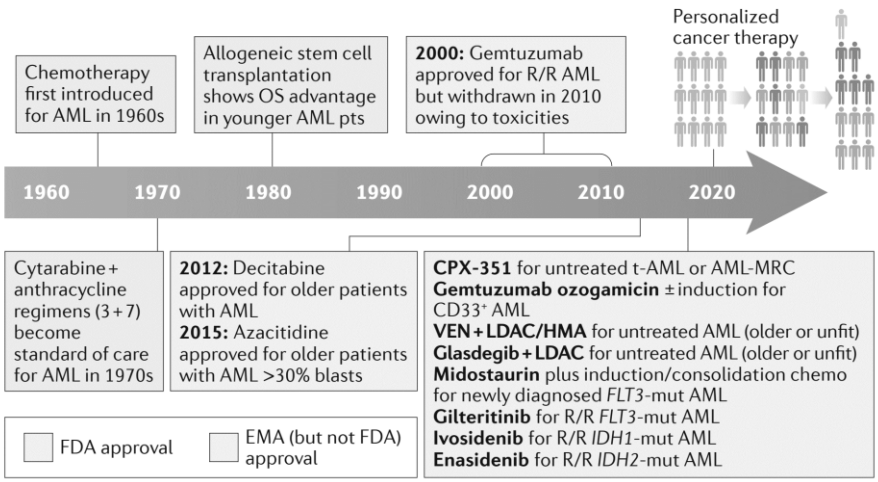

Figure 6: Developments in the treatment of acute myeloid leukemia. (DiNardo and Perl, 2019)

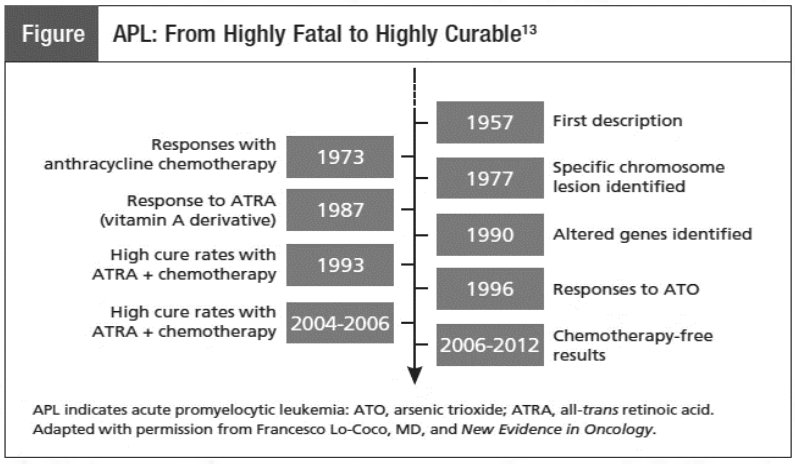

Figure 7: Developments in the treatment of acute promyelocytic leukemia. The transition from highly fatal to the curable subtype of acute myeloid leukemia. (Coombs et al., 2015b)

2.4.1. Cytosine arabinoside:

Naturally occurring arabinoside containing nucleosides were initially isolated in the early 1950s from a marine sponge *Cryptotethya crypta.* In 1959, Richard Walwick, Walden Roberts, and Charles Decker from the University of California, Berkeley, reported the preparations of 3-β-D arabinofuranosylcytosine, a synthetic pyrimidine nucleoside differing in its sugar moiety from the normal metabolite's cytidine and deoxycytidine.

It enters the cell using the same highly conserved dNTP Salvage Pathway used by the cell to recover normal cytidines from its surroundings (Toy et al., 2010). The addition of three phosphates metabolically activates Ara-C. The first phosphate is added by deoxycytidine kinase (DCK), which is also the rate-limiting enzyme in the dNTP Salvage Pathway. Ara-C is incorporated into the DNA during the S phase and interferes with replication by inhibiting polymerase and topoisomerase activity. As an independent molecule, Ara-C is quickly deaminated into a nontoxic uracil derivative and has a half-life of less than an hour. However, once incorporated into DNA, it can still be detected after 24 hours (Grem et al., 1995). As a result, Ara-C is more toxic to fast-growing cancer cells than to slow-growing cells, and to be an effective treatment for AML. It must be given intravenously in a continuous manner over a period of 7 days. Ara-C has been found to be particularly effective when combined with an anthracycline. However, this course of treatment is highly myelotoxic and is not always a viable option for older patients (Michaelis, 2019).

2.4.2. Anthracycline:

Anthracyclines are a class of drug extracted from the Streptomyces bacterium. Daunorubicin /daunomycin is naturally produced red-pigmented drug by Streptomyces *peucetius*, a species of actinobacteria, discovered in the early 1960s by Di Marco and co-workers.

Daunorubicin gets intercalated with DNA and interferes with DNA and RNA metabolism. Cytotoxicity effect of daunorubicin is mainly due to inhibition of the topoisomerase II enzyme, which is important for the religation of the DNA break. The basic structure of anthracyclines is of a tetracyclic molecule with an anthraquinone backbone connected to a sugar moiety by a glycosidic linkage. When taken up by a cell, the four-ring structure intercalates between DNA bases pairs while the sugar moiety occupies the minor groove and interacts with adjacent base pairs.

2.4.3. All-Trans Retinoic acid (ATRA):

In 1985, ATRA was introduced in the clinic and opened a new era in the management of APL (Wang and Chen, 2008). ATRA induces differentiation of malignant promyelocytes into mature granulocytes, leading to its evaluation either as a single agent or in combination with chemotherapy, first in relapsed/refractory disease and then in newly diagnosed patients (Tallman et al., 1997, Chen et al., 1991, Castaigne et al., 1990).

Pharmacological concentration (10^6-10^7M) of ATRA causes a configuration change of PML-RARα. Retinoic acid-induced APL differentiation is enhanced by cAMP signaling which activates protein kinase A (PKA), which dissociates RARα from SMRT co-repressor, allowing transcriptional activation through RXRα, whereas

a coactivator complex composed of proteins with histone acetylase (HAT) activity is recruited, opening the chromatin structure and relieving transcriptional repression and induce its degradation (Dilworth and Chambon, 2001) (Figure 8).

2.4.4. Arsenic trioxide (ATO):

Arsenical compounds are regarded as a potent toxin and carcinogen; they also have been medically used for over 2000 years and are still used in the treatment of leukemia, solid cancers, and trypanosomiasis. Potential mechanisms of action of ATO on the malignant promyelocytes are multifactorial. Some of the notable events are direct binding of ATO on the B2 domain of the fusion protein and bringing out the post-translational modifications such as sumoylation and ubiquitination marking them for degradation via proteasomal degradation pathway(Zhang et al., 2010) (figure 7). The indirect actions include increasing the cellular oxidative damage by ROS, up-regulation of pro-apoptotic factors (JNK, p38 signaling) and downregulation of the anti-apoptotic factors (BCL-2, Mcl-1) (Chen et al., 1997, Eguchi et al., 2011, Davison et al., 2004, Jing et al., 1999). Recent observations and studies report the novel mechanisms of action of ATO such as inhibition of glycolysis (Zhang et al., 2015) and promotion of ETosis (a novel form of cell death) in a dose-dependent manner(Li et al., 2018) which implies that ATO mechanism of action is indeed multifactorial.

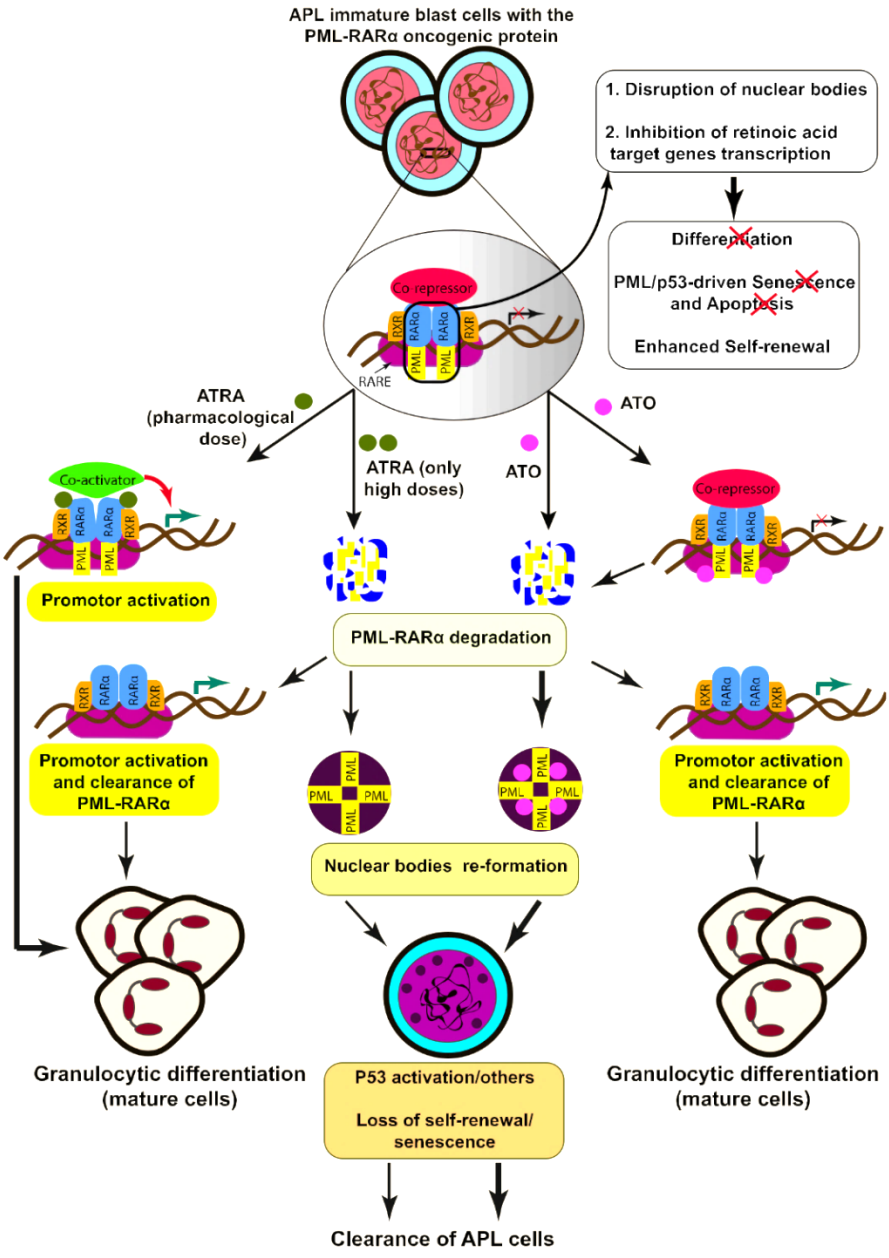

Figure 8: Mechanisms action of ATRA and ATO in acute promyelocytic leukemia. (adapted from (Moosavi and Djavaheri-Mergny, 2019))

Recent insights into the distinguishable metabolic features of the cancer cells have shed lights onto the novel mechanisms of action of anti-cancer agents such as arsenic trioxide (ATO), and Imatinib, which in addition to their conventional effects

can also act as glycolytic inhibitors(Gottschalk et al., 2004, Zhang et al., 2015) and this effect can be exploited in combination therapies to treat cancers that have not been conventionally treated with these agents

2.5 Treatment options in older patients with acute myeloid leukemia:

Non-intensive therapies such as hypomethylating agents, like decitabine or azacytidine (Deschler and Lübbert 2006), are given to older patients unable to withstand intensive treatments. In comparison to the best supportive care, superior survival and quality-of-life were seen in patients treated with these hypomethylating agents (Dombret, Seymour, et al. 2015).

2.5.1 Hypomethylating agents:

Hypomethylating agents are a class of drug that inhibits DNA methylation. In the 1960s, 5-Azacytidine (Aza) and 5-Aza-2′-deoxycytidine (decitabine) were synthesized as an analog of cytosine (like cytarabine) for the management of AML. Although these drugs showed anti-cancer properties, they were extremely toxic at high doses. Recent interest in Azacytidine and decitabine is not for their original discovery but their hypomethylating properties. The DNA hypomethylating property of Azacytidine and decitabine was traced to their ability to incorporate into DNA, trap DNA methyltransferases (DNMTs) and target these enzymes for degradation. Unlike the other structurally very similar analog, decitabine, 5-Azacytidine can be incorporated into both nucleic acids.

Aza-AML-001 (NCT01074047; registered: February 2010) trial is phase III, multicenter randomized controlled trial comparing Azacytidine and conventional care

regimen (CCR) in patients with newly diagnosed AML. That study included elderly AML patients (>65years) with > 30% blasts in the bone marrow. In total, 445 elderly patients were randomized to receive either azacytidine or conventional therapy. Post hoc analysis revealed that those receiving Azacytidine experienced improved median overall survival (OS; 10.4 vs. 6.5 months) and improved 1-year survival rates (46.5 vs. 34.2%)

In comparison to the patients treated with conventional therapy, azacytidine group had a significantly higher median survival of 24.5 months compared to 16 months for patients treated with conventional therapy(Maurillo et al., 2018, Dombret et al., 2015).

2.6. Mechanisms of relapse:

Although disease-specific factors can predict the probability of therapeutic resistance and AML relapse, the mechanism by which cancer cells can resist current therapies and propagate to relapse is still up for debate.

Significant advances have been made in the management of leukemia over the last decade. However, resistance to therapy and relapses remains the major obstacle to cure. The major reason for disease recurrence is due to the presence of a small population of quiescent leukemic stem cells (LSC) which are not affected by the drugs or due to the acquisition of genetic mutations that gives a clonal advantage and to escape the effect of therapy (Wang et al., 2016, Ning et al., 2016, Glasspool et al., 2006) (figure 9). Emerging evidence suggests that epigenetic and non-genetic factors

are also contributing to drug resistance and therapy failure (Raha et al., 2014, Gorre et al., 2001).

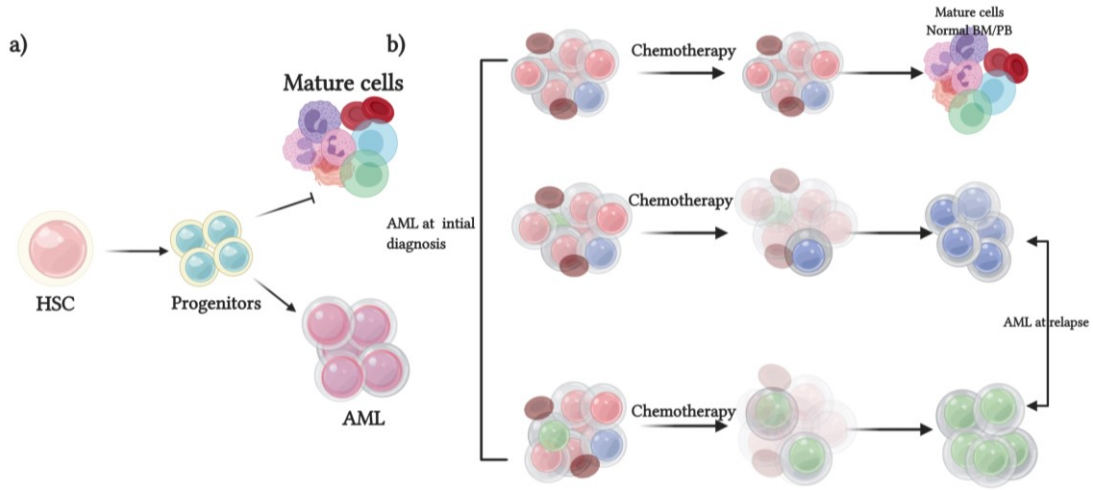

Figure 9: Representation of AML initiation and relapse. (A) Malignant transformation of hematopoietic stem/progenitor cells results in a block in differentiation capacity and gain in uncontrolled proliferation, leading to the accumulation of immature malignant cells in the bone marrow and peripheral blood. (B) Efficient eradication of AML cells results in the normal bone marrow and peripheral blood. However, inadequate removal of AML cells results in the recurrence of AML (relapse). This could be due to small subpopulations present at initial diagnosis, which are or become chemotherapy-resistant, or most cells might be more resistant to chemotherapy treatment.

Leukemic cells evade the strenuous effects of the chemotherapeutic agents and the immune system in a multifactorial manner, which are not only confined to clonal evolution and leukemic stem cells.

2.6.1. Clonal architecture, patterns of relapse, and the existence of preleukemic stem cells:

Frequent genetic evolution underlies the phenotypic evolution of the diagnostic clone. Initial studies highlighted the potential role of chemotherapy in promoting genetic diversification in the relapsed samples (figure 10).

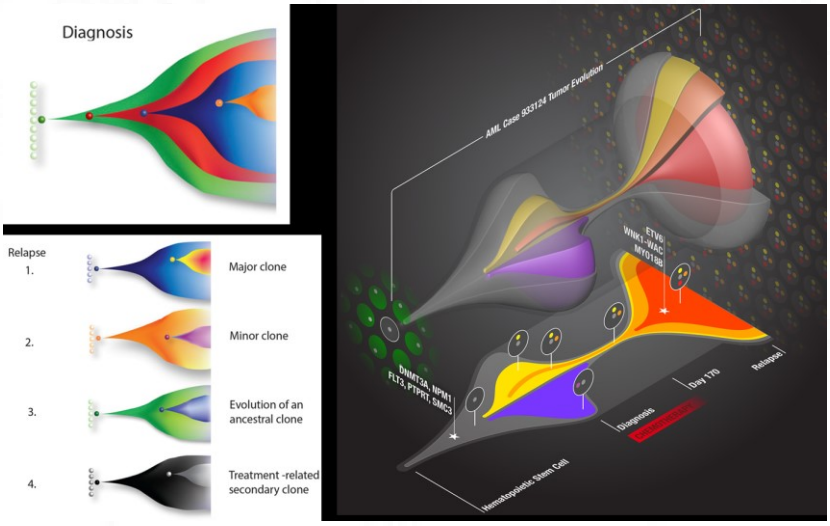

Figure 10: Clonal pattern of relapse in AML. Potential patterns of relapse from the hypothetical diagnosis clone. Fish plots representing the possibilities of clonal evolution of the diagnostic clone to the multiple patterns of relapse clone. 1- relapse of the dominant clone; 2, relapse of a subclone present at diagnosis; 3, relapse from an ancestrally related clone; 4, "apparent relapse," where the new tumor is not clonally related to initial leukemia, such as might happen in therapy-related AML. (adapted from (Grimwade et al., 2016))

2.6.2. Mutations in *PML-RARA* gene:

In acute promyelocytic leukemia, the available therapies are focused on the clearance of the PML-RARA fusion protein. However, Goto et al. in 2011 had reported that 2 of 15 patients with refractory/relapsed APL treated with ATO were clinically ATO-resistant. Leukemia cells from those two patients harbored missense mutations in promyelocytic leukemia gene-retinoic acid receptor-α gene (PML-RARA) transcripts, resulting in amino acid substitutions of A216V and L218P in the PML B2 domain (Goto et al., 2011). In another study done by Zhu HH et al. in 2014 had reported, of the 35 patients analyzed, 13 patients had ATO resistance, of which nine patients had *PML* mutations, seven patients had both *PML* and *RARA* mutations (Zhu et al., 2014) (figure 10). The mutations had been reported so far in the *PML-RARA* gene is mentioned in figure 16. However, reports from The' et al. (Lehmann-Che et al., 2014) had observed that mutation (A216V) in the wild-type *PML* but not in *the PML-RARA* gene had clonally evolved and caused therapy resistance (figure 11).

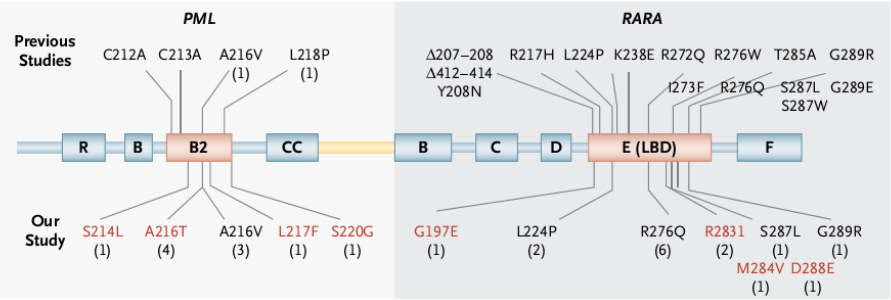

Figure 11: Mutations reported in PML-RARA gene and its involvement in therapy resistance (Zhu et al., 2014).

2.7. Metabolic adaptation of malignant cells: To survive the change

Tumor cell metabolism was actively explored in the pre-genomics era; the discovery of tumor suppressor genes and oncogenes dampened interest in metabolism as a potential way to identified cancer cell potential particularities and related therapeutic targets. In 2011, Hanahan and Weinberg identified reprogramming energy metabolism as an emerging hallmark of cancer, showing that scientists are rediscovering cancer metabolism to target cancer (Gogvadze et al., 2010).

Non-malignant, resting cells convert the highly abundant nutrient glucose during glycolysis to pyruvate. Pyruvate subsequently enters the tricarboxylic acid (TCA) cycle and mitochondrial oxidative phosphorylation to generate 36 mol adenosine triphosphate (ATP) per mole glucose that is consumed by the cell. In the absence of oxygen, cells convert glucose into pyruvate, which is fermented into lactate, generating 2 mol ATP per mole glucose (figure 12).

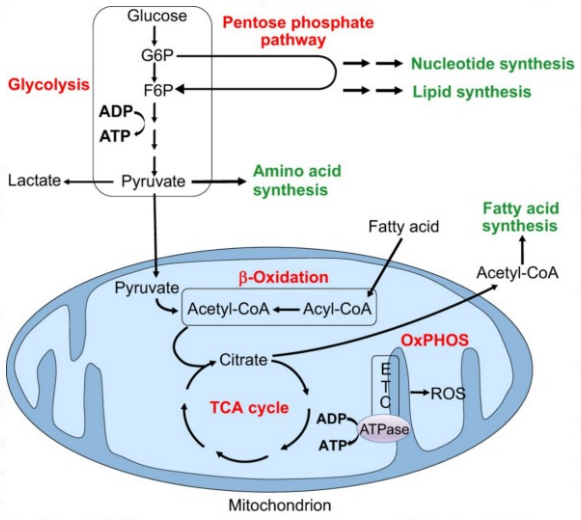

Figure 12: Energy metabolism of normal cells. (Mathieu and Ruohola-Baker, 2017)

2.7.1. Hematopoietic stem cells and metabolism:

The cellular features of HSC dysfunction in aging primarily manifest as a failure to maintain appropriate mitochondrial and metabolic regulation(Takubo et al., 2013). At a steady-state, HSCs utilize glycolysis and actively suppress mitochondrial respiration. This metabolic state appears to be transcriptionally hardwired and may be supported by the low oxygen tension of the BM niche as a result of increased activity of hypoxia-inducible factor 1 alpha (HIF1α). HIF1α is thought to promote glycolysis in HSCs by upregulating pyruvate dehydrogenase kinase (PDK) and lactate dehydrogenase A (LDHA), thereby limiting mitochondrial pyruvate import and flux through the tricarboxylic acid (TCA) cycle and thus favoring anaerobic catabolism to lactate(Takubo et al., 2010, Suda et al., 2011, Simsek et al., 2010).

During activation and differentiation, HSCs undergo a metabolic switch to oxidative phosphorylation (OXPHOS) and produce elevated levels of ATP and ROS to enter the cell cycle(Ho et al., 2017). Genetic knockout of the PDK enzymes that block pyruvate transit into the TCA cycle, as well as aberrant OXPHOS activation via deletion of the negative regulator mitochondrial carrier homolog 2 (MTCH2), prevent the maintenance of HSC quiescence and promote stem cell exhaustion mimicking aging phenotypes(Maryanovich et al., 2015). Complete inhibition of OXPHOS conversely leads to the accumulation of dysfunctional HSCs incapable of differentiation. Low levels of basal respiration also appear to possess important roles in HSC quiescence(Ansó et al., 2017, Maryanovich et al., 2015) (figure 13).

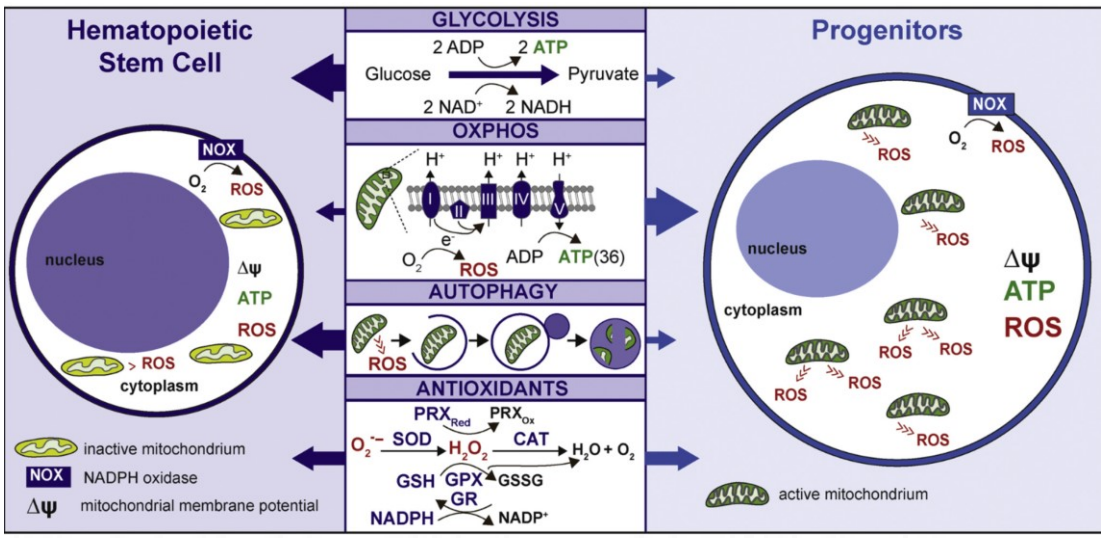

Figure 13: Represents the metabolic transition and reliance of normal hematopoietic stem cells and committed progenitors. HSCs are characteristically possessing low mitochondrial activity and low levels of reactive oxygen species (ROS), which are maintained by using glycolysis as their main energy source, removing damaged mitochondria (mitophagy) and neutralizing ROS by upregulating the anti-oxidative system. HSCs produce less ATP and have fewer active mitochondria compared to progenitors. The more differentiated progenitors characteristically have higher levels of mitochondrial activity and oxidative phosphorylation (OXPHOS), increased ATP production. (Mattes et al., 2019)

2.7.2. The Warburg Effect:

In 1924, Otto Warburg was the first scientist to observe that cancer cells perform glycolysis regardless of oxygen availability (Figure 13). Thus, this observation is also known as the Warburg effect or aerobic glycolysis. At first glance, this adaptation is counterintuitive since cancer cells require energy for their rapid proliferation and generate 9-fold less ATP during aerobic glycolysis (since mitochondria remain functional and oxidative phosphorylation occurs at low levels aerobic glycolysis generates ~4 mol ATP/mol glucose) (Koppenol et al., 2011, Warburg, 1956a). However, the rate of glycolysis is 10-100 times higher than the rate of oxidative phosphorylation, which compensates for the low ATP yield per mole glucose. The faster kinetics of glycolysis provides an advantage when cancer cells compete with surrounding stromal cells for glucose (Yu et al., 2017) (figure 14).

Another hypothesis for this metabolic adaptation is that intermediates, which are generated during glycolysis, serve as a starting material for e.g., nucleoside biosynthesis using the pentose-phosphate pathway and are therefore essential for DNA replication and division. Also, the need for reducing equivalents NADPH is much higher than ATP demand. NADPH is produced in high amounts through the pentose phosphate pathway, which is a pathway branch of glycolysis (Figure 14). Thus, until today the exact reason why cancer cells perform aerobic glycolysis remains controversial (Lunt and Vander Heiden, 2011).

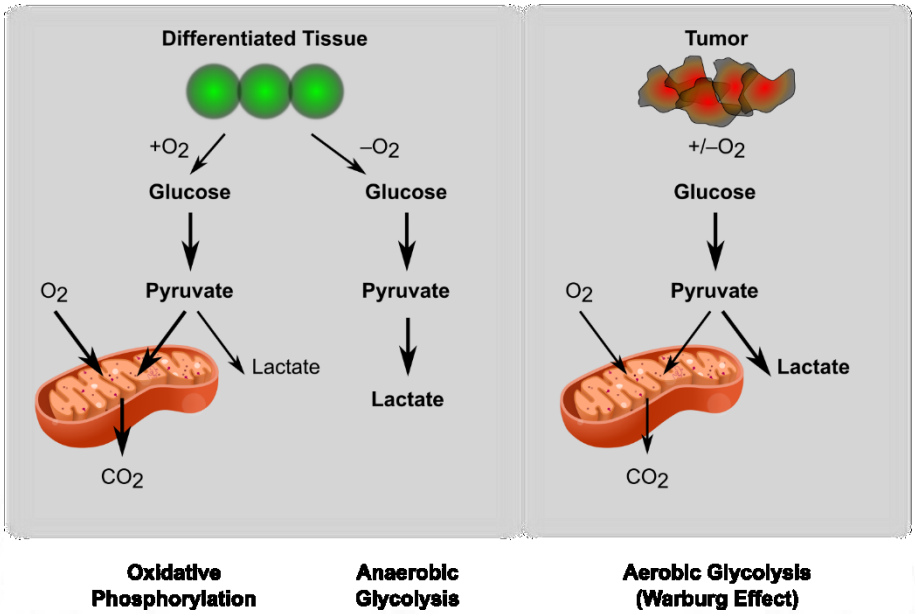

Figure 14: Differences in the metabolism of normal cells and cancer cells (adapted from Creative diagnostics)

2.7.3. Mitochondria:

Mitochondria are known as the powerhouses of the cell, but they are also crucial for normal cell function by regulating overall homeostasis. Cells have hundreds of mitochondria, which can be a mixture of wild-type and damaged organelles. Mitochondria have a 16Kb DNA genome (mtDNA) that encodes specific respiratory proteins. However, due to co-evolution, most mitochondrial proteins are nuclear-encoded. A relatively low mutation rate has been found in cancer mtDNA, indicating to a regulative mechanism involved in mitochondrial quality control to support cellular metabolism (Wallace, 2012).

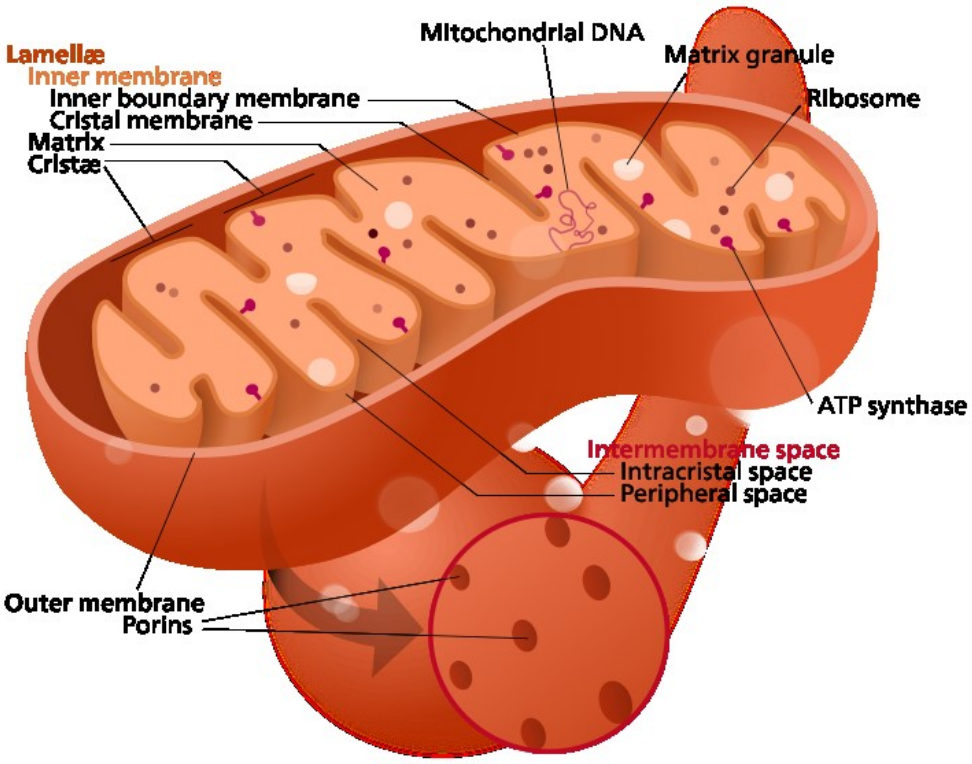

Figure 15: Cross-sectional view of the mitochondrion (adapted from Servier Medical Art -SMART)

Mitochondria is double-wall membrane organelles were the outer membrane that covers the organelle and the inner membrane folds and forms cristae, thus extending the surface and enabling numerous chemical reactions (figure 15). The enzymes of the tricarboxylic acid cycle (TCA, also called the citric acid cycle or Krebs cycle) are localized in the mitochondrial matrix. The prime function of the organelle is the oxidation of acetyl-CoA derived from carbohydrates, amino acids, and fatty acids (FAs), and it is the central pathway of metabolism. The TCA is structured into a supramolecular complex which enables its interaction with mitochondrial membranes and the electron transport chain (ETC) in OXPHOS. Stabilization of mitochondrial DNA (mtDNA), association with the translation of mitochondrial RNA (mtRNA),

oxidative stress, iron metabolism, and tumor suppression are few additional functions provided by the majority of the TCA enzymes (Vyas et al., 2016).

The ETC is localized in cristae, and it consists of five complexes with a supramolecular organization, where it generates a proton gradient due to the transport of protons by mitochondrial proton pumps (complexes I, III and IV) Electrons are transported to complex III. In the end, complex IV enables the conversion of O2 to H2O. The majority of the ATP synthesis arises from the electrochemical gradient that exists across the inner membranes of mitochondria by ATP synthase (complex V). The role of Co-Q cofactor includes transferring electrons from complexes I and II to complex III, and the second important cofactor is cytochrome c (Cyt c), which enables the transfer of electrons from complex III to complex IV(Zhao et al., 2019, Escoll et al., 2019) (figure 16).

2.7.4 Mitochondrial Respiratory complexes:

Complex I (NADH: ubiquinone oxidoreductase, NADH dehydrogenase, NADH-ubiquinone oxidoreductase) is a vital point of respiration. The oxidation of reduced nicotinamide adenine dinucleotide (NADH) is catalyzed by complex I thus, regenerating NAD+ for the TCA cycle and fatty acids (FAs) oxidation as well as reducing coenzyme Q10 (ubiquinone, CoQ) to ubiquinol. During electron passing through the complex I, four protons are pumped from the matrix into the intermembrane space. Complex-I is also considered a rate-limiting enzyme for the consumption of oxygen in the synapses.

Complex II (succinate: ubiquinone oxidoreductase, succinate dehydrogenase (ubiquinone)) is the acceptor of FADH molecules, which are the high energy intermediates produced during the TCA cycle. It is a membrane-bound lipoprotein consisting of 4sub units, which couples the oxidation of succinate to the reduction of Co-enzyme Q. It does not contribute to the proton gradient. The subunits of complex II are encoded only by nDNA. Hence, it is used to normalize the activity of OXPHOS in the presence of mitochondrial DNA defects.

Complex III (ubiquinol: ferricytochrome-c oxidoreductase, CoQ-cytochrome c reductase) comprises of two centers, Qi center that faces the matrix and Qo center which is oriented to the intermembrane space. It catalyzes the oxidation of one molecule of ubiquinol and the reduction of two molecules of cytochrome c. The reaction mechanism of complex III occurs in two stages known as the Q cycle in which four protons are released into the intermembrane space.

Complex IV (ferricytochrome-c: oxygen oxidoreductase, cytochrome c oxidase) allows the terminal reduction of O2 to H2O, thus retaining all partially reduced intermediates until complete reduction is achieved. It also mediates the pumping of 4 protons across the matrix to the intermembrane space.

Complex V (ATP synthase, FoF1-ATPase) made of two regions: The F1 portion is a soluble domain with three nucleotide-binding sites, and the Fo portion comprises three subunits which span the membrane from the inner to the outer side. The F1 portion is localized above the inner side of the membrane and stably connected with the Fo domain, while the Fo portion is a proton pore embedded in the membrane. A part of the Fo rotates as the protons pass through the membrane and forces F1 as a motor to

synthesize ATP, thus enabling the conversion of electrochemical potential energy to chemical energy (DeBalsi et al., 2016).

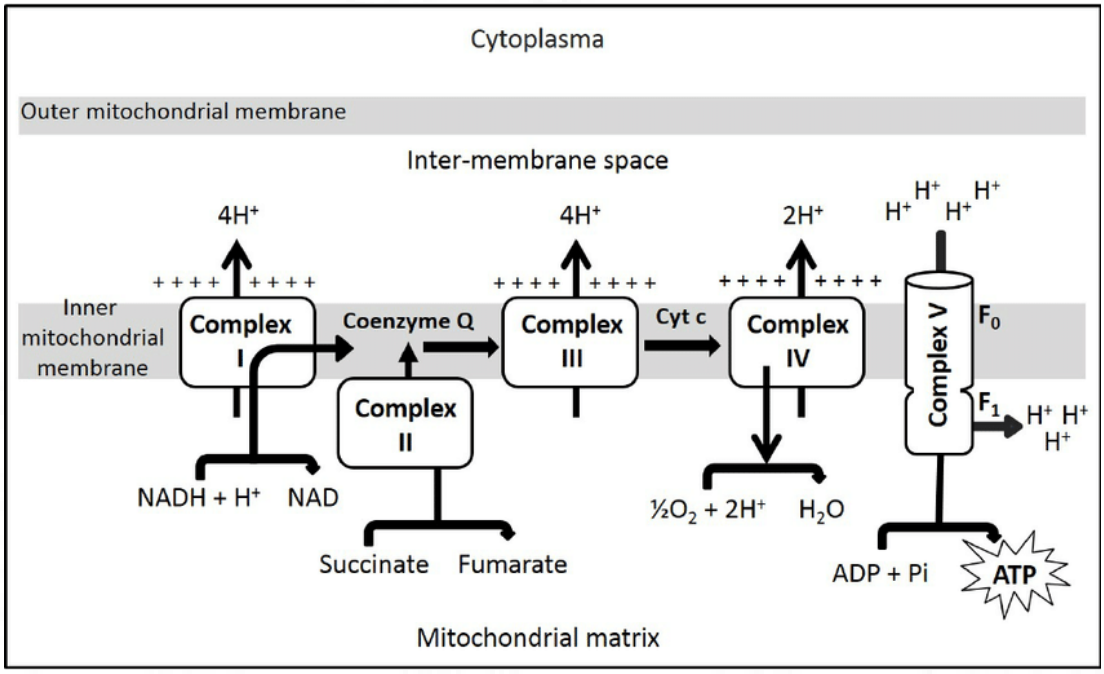

Figure 16: Summary of oxidative phosphorylation (OXPHOS) Thiago D Corrêa et al., 2015).

The first approved metabolic agents for the management of AML, ivosidenib, and enasidenib, inhibit mutant forms of isocitrate dehydrogenase 1 / 2 (IDH1/2), which converts αKG from the TCA cycle to the oncometabolite R-2-hydroxyglutarate. R-2-Hydroxyglutarate competitively inhibits αKG-dependent dioxygenases, resulting in aberrant epigenetic poising, thereby blocking differentiation and promoting self-renewal (Castro et al., 2019, Myers et al., 2018).

Leukemic stem cells were first described with an immunophenotype of CD34+/CD38− AML cells (Bonnet and Dick, 1997, Lapidot et al., 1994). The expression of CD34 in the AML patients shows a greater t inter- and intra-patient

heterogeneity. Hence, making use of CD34 as a sole marker for LSC isolation and characterization found to be a significant challenge. A better understanding of the intricate metabolic properties of the leukemic cells revealed that the LSC is enriched in a low metabolic state irrespective of the CD34 expression the cells had a greater self-renewal capacity(Lagadinou et al., 2013a, Jia and Gribben, 2014). From the existing literature, the metabolic phenotype of the LSC's are increased reliance on oxidative phosphorylation, BCL-2 dependency, and low reactive oxygen species(Sriskanthadevan et al., 2015). Targeting any of these metabolic properties in combination with the conventional chemotherapeutic agents was observed to enhance the treatment outcome. Venetoclax (VEN) – a BCL-2 inhibitor in combination with Azacytidine (Aza) has increased the treatment outcome of elderly patients significantly. The combination showed tolerable safety and favorable overall response rate (CR + CRi rate: 67%) in elderly patients with AML (DiNardo et al., 2019). The combination targeted the complex II of the electron transport chain – succinate dehydrogenase (SDH), thereby downregulating the levels of glutathione in the cells. This reduction in GSH levels was observed due to a block in amino acid uptake, with these results highlighting a connection with the increased amino acid dependency required for LSCs to use OXPHOS effectively.

LSCs that are resistant to venetoclax/5-Azacitidine combination therapy resulting in the amino acid deprivation was found to upregulate of fatty acid metabolism to rescue OXPHOS in LSCs (Jones et al., 2018). Hence, a combination of fatty acid inhibitor etomoxir is in evaluation with the VEN+Aza combination.

Dihydroorotate dehydrogenase (DHODH), an enzyme localized in the mitochondria, is crucial for the pyrimidine synthesis. This was also evaluated in the primary AML samples and found that the LSCs can be differentiated by forcing them to shift the metabolism (Sykes et al., 2016, Wu et al., 2018). The inhibition of the enzyme using brequinar (BRQ) or BAY 2402234 resulted in the differentiation of LSCs, thereby enhancing the efficacy of conventional chemotherapeutic agents (Christian et al., 2019).

These results highlight the metabolic adaptation of LSCs and the potential synergy of targeting multiple metabolic pathways.

2.7.5. Mitochondria – Role in cell survival and cell death:

Apoptosis comprises of the ordered and genetically programmed process that removes both the damaged cells and the cells that have become unessential to the functioning of the organism. It is critical to both the maintenance and development of cells and tissues. The BCL-2 family of proteins is one of the major regulators of the apoptotic process(Martinou and Youle, 2011) (figure 17).

Apoptosis occurs through two distinct but associated pathways: the intrinsic and the extrinsic pathway. The intrinsic pathway involves the conserved signaling proteins associated with mitochondria that lead to the formation of pores in the mitochondrial membrane leading to apoptosis. The extrinsic pathway transduces signaling from external apoptotic cues. Activation of the intrinsic pathway is controlled by the BCL2 family of proteins (Hata et al., 2015).

Cancer therapy thus deals with the challenges of finding approaches to induce apoptosis or to restore defective apoptosis. The apoptotic pathways can be thus therapeutically targeted at various levels, which can be classified into two main mechanisms: (i) induction of apoptosis (ii) restoration of downstream signaling cascades (Gross and Katz, 2017).

The pro-apoptotic members of the BCL-2 family have demonstrated tumor-suppression activity(Cory et al., 2016). However, over-expression of anti-apoptotic proteins in the BCL-2 family promotes tumorigenesis(Leibowitz and Yu, 2010). Several drugs that are currently available and used in the clinic function its therapeutic effects through the activation of the BCL-2-regulated apoptotic pathway. Nevertheless, studies showed that in this process, the initiators of this apoptotic pathway are mutated or silenced in the cancers, which makes the patients unable to get the full effect of treatment mechanism. 'BH3-mimetics' is another class of therapeutics developed to counter these resistance mechanisms. These drugs work by directly activating apoptosis by binding and inhibiting the anti-apoptotic BCL-2 family members.

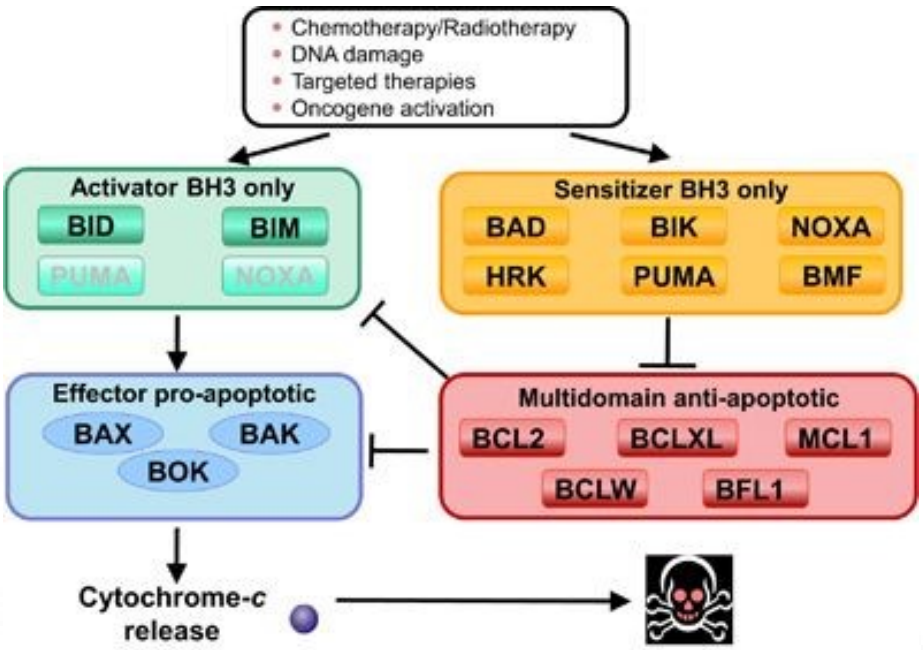

Figure 17: BCL-2 family of proteins. Anti-apoptotic proteins sequester activators or effector proteins to prevent apoptosis. Sensitizers act as selective antagonists of anti-apoptotic proteins. (Montero and Letai, 2018)

Mitochondrial priming determines the availability and readiness of a cell for apoptosis. A highly primed cell is more susceptible to apoptosis compared to an unprimed cell. In a primed state, the BCL2 or other anti-apoptotic family members have high levels of their pro-apoptotic counterparts to ensure the survival of a given cell(Hogdal, 2015, Leibowitz and Yu, 2010). BH3 profiling is an approach for determining which BCL2 family members a given cell population depends on for survival. Based on the pattern of mitochondrial sensitivity to a panel of BH3 peptides with known binding affinity profiles, the BCL2 family dependence profile of any cell population can be determined using this approach. This has led to the identification of several BCL2-dependent tumor types and has provided strong support for the mitochondrial-based, on-target mechanism of action of various BH3 mimetic drugs

developed. Recently, a novel technique described as Dynamic BH3 Profiling was described that could be used to expect the response of cancer cells to chemotherapeutic agents. It also identifies agents capable of inducing BCL2 priming. In this method, BH3 profiling is performed before and after treatment with a given agent to determine how a cell population's BCL2 family-dependence profile changes (Dai et al., 2016) (figure 18).

Anti-apoptotic proteins (BH3 family), which are localized in the mitochondria, have been reported to play an important role in predicting response to chemotherapy (Friedman et al., 2015). BH3 family profiling on the malignant cells, which are in the circulation and on the cells, which are localized in the stroma and lymph nodes in CLL, is reported to be distinct. The circulating CLL cells are reported to be highly primed (the pro-apoptotic proteins outnumber the anti-apoptotic proteins) Cells residing within lymph nodes upregulate anti-apoptotic BCL-XL and BCL2A1 (BFL-1) to reduce apoptotic priming, making them more likely to survive treatment and can lead to chemotherapy resistance in both solid and liquid tumors (Davids et al., 2013, Vogler et al., 2009)

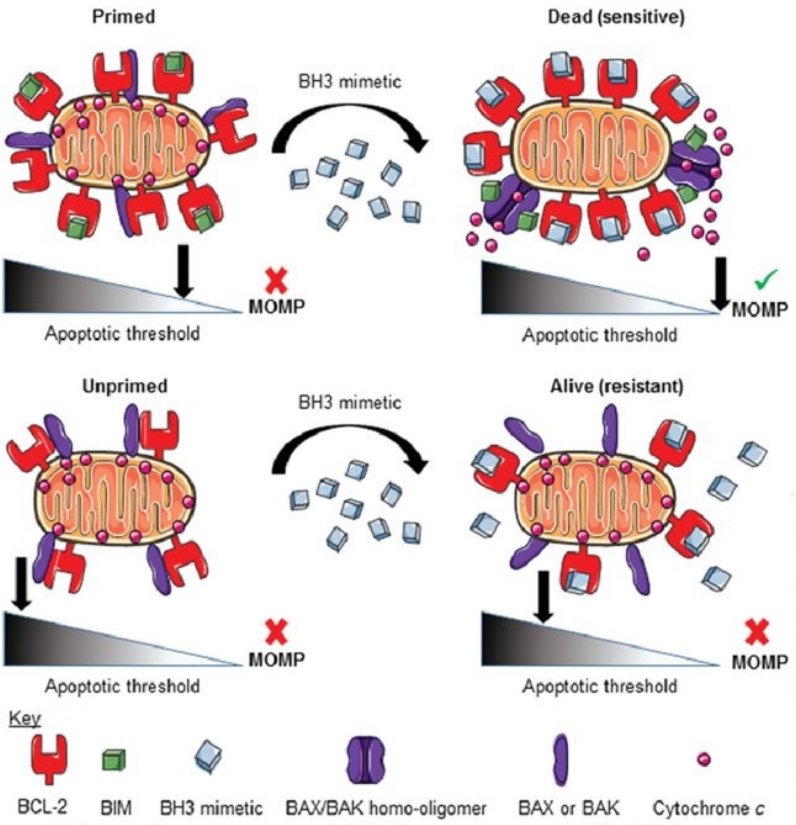

Figure 18: Priming of Mitochondria and drug resistance: Depicts the balance of anti-apoptotic and pro-apoptotic protein and how the proportion can be tuned to enhance the efficacy of the chemotherapeutic drugs. A primed cell has a relatively lower apoptotic threshold than an unprimed cell. Apoptotic stimuli such as treatment with a BH3 mimetic cause an imbalance in the pro and anti-apoptotic balance resulting in mitochondrial outer membrane permeabilization (MOMP) on a primed cell (Potter and Letai, 2016).

Understanding and identifying anti-apoptotic addictions of the different cell types are important for tailoring the use of specific BH3 mimetics, as well as prospectively identifying potential dose-limiting side effects on healthy tissue (Vo et al., 2012).

2.7.6. Mitochondria dynamics and quality control:

Mitochondria is a highly dynamic organelle that constantly undergoes fission and fusion to maintain a pool of healthy mitochondria (figure 19) (Youle and van der Bliek, 2012a).

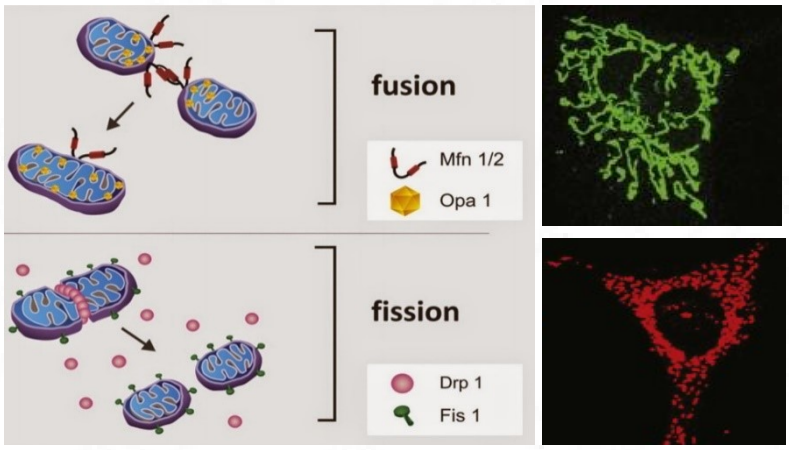

Figure 19: Mitochondrial dynamics. Changes in the mitochondria shapes – Fused Mitochondria (green) and fragmented Mitochondria (Red). (Wai and Langer, 2016)

Damaged mitochondria (defective OXPHOS), dissipation of transmembrane potential are the stimuli for the mitophagy process (Westermann, 2012). As mitochondria is a highly dynamic network, hence the dysfunctional mitochondria have to be separated from the healthy, requiring tight coordination between fusion, fission, and mitophagy machinery. The depolarized mitochondria, which are not able to fuse with the healthy mitochondria or isolated from the dynamic network by fission, mark them to be degraded via mitophagy(Evans and Holzbaur, 2020). Whereas the elongated mitochondria are spared from degradation and remain bio energetically functional. Damaged mitochondria are recognized by specific mitophagy receptors

whose identity depends on the particular trigger causing mitochondrial clearance, and which function as molecular bridges for the interaction with the autophagy machinery (Ding and Yin, 2012)

In acute myeloid leukemia, the ROS low LSC versus ROS high non-LSC population gene expression profile revealed that genes related to mitochondrial biology are upregulated in the ROS-low LSC population, which are involved in the mitochondrial dynamics. (Chen and Chan, 2017). The ROS low LSC had a distinct mitochondrial morphology - compact crescent-like localization pattern of mitochondria suggesting an asymmetrical division, an activity that has been observed in HSCs (Ito et al., 2012). ROS low LSC's had increased levels of Fis1 – a key regulatory gene in the mitochondrial fission pathway in comparison to the non-LSC ROS high population. Upon depletion of FIS1 in AML cells, there was a dramatic accumulation of mitochondria and more diffused, suggesting that mitochondrial fission is required to maintain the unique mitochondrial morphology seen in AML LSCs. Non-LSCs lack the mitophagy process; hence they undergo apoptosis, unlike the LSC, where they clear the damaged mitochondria (figure 20) (Pei et al., 2018).

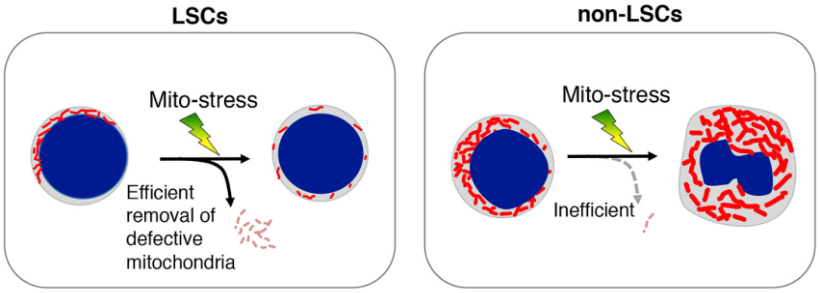

Figure 20: Quality control of mitochondria in AML: LSCs respond to mitocans with an efficient clearance of mitochondria, whereas non-LSCs accumulate damaged mitochondrial due to the lack of clearance pathway (Pei et al., 2018).

2.7.7 Lysosomes:

Lysosomes are called suicide bags of the cells. Cells depend on the lysosome for sequestration and degradation of macromolecules to maintain metabolic homeostasis. Lysosomes perform cellular degradation by utilizing more than 50 hydrolases, including proteases, glycosidases, lipases, and nucleases. Lysosomes can degrade all types of macromolecules. The hydrolases are active under acidic pH, which is maintained by the action of the vacuolar H+-ATPase. Depending on the organelles or material, the process is called selective autophagy (figure 21) (Zaffagnini and Martens, 2016).

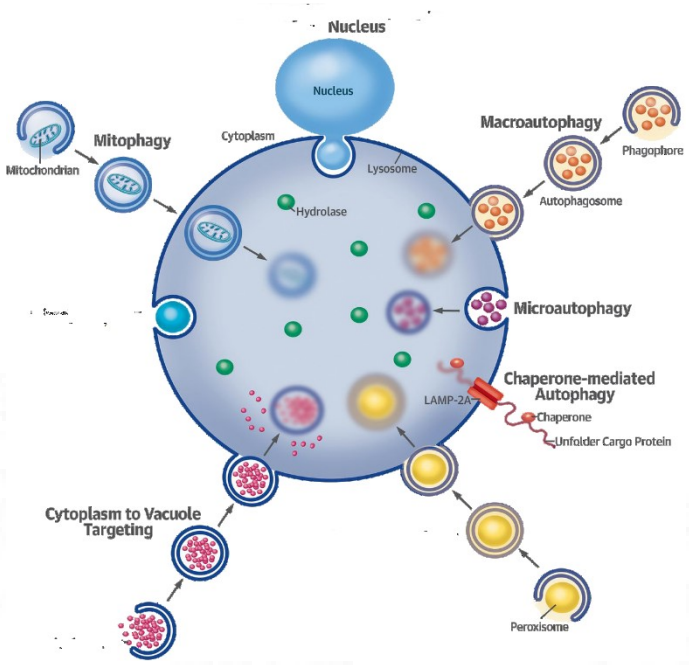

Figure 21: Lysosomes and selective and non-selective forms of autophagy.

Since many iron-containing macromolecules are degraded intra lysosomal, low mass iron is released inside the lysosomal compartment. Because the lysosomes also contain reducing agents, for example, glutathione, ascorbic acid, and the amino acid cysteine, low mass iron likely exists as Fe(II) with the capacity to generate highly reactive radicals if exposed to hydrogen peroxide (Kurz et al., 2008). As a result, lysosomes are very sensitive to oxidative stress, and their membranes easily peroxidized and permeabilized by the radicals that are formed secondary to Fenton-type reactions taking place in the lysosomes. The rupture of lysosomes with the relocation of the lytic enzymes results in apoptosis or necrosis, depending on the magnitude of this relocation (Guicciardi et al., 2004). Consequently, keeping the concentration of redox-active iron in lysosomes as low as possible is important for the survival of cells exposed to oxidative stress. The rapid transport of low mass iron from

lysosomes to the cytosol is thus important, as well as ways of temporarily binding iron in a non-redox-active form (Dielschneider et al., 2017)

Cancer cells have relatively large lysosomes, and these are thought to be more fragile than normal-sized lysosomes(Fennelly and Amaravadi, 2017). Moreover, cancer cells exhibit higher metabolic rates and an increased turnover of iron-containing proteins, leading to the lysosomal accumulation of iron, with consequent iron-mediated sensitization to reactive oxygen species (ROS)-induced lysosomal membrane permeabilization (LMP) (Fennelly and Amaravadi, 2017)

Iron is the essential function of lysosomes for cell proliferation under inhibition of lysosomal acidification. Lysosomal dysfunction, through iron depletion, resulted in a profound alteration in energy metabolism, including electron transport chain impairment, hypoxia, and also in central carbon metabolism.

A small-molecule screen on AML cells in in vitro and in vivo identified that lysosome disruption as a novel and promising therapeutic strategy for the management of AML. Mefloquine, an anti-malarial agent, has been reported to target the AML cells via disrupting the lysosomes. Selective specificity was identified to be due to the increased lysosomal size and biogenesis in the AML cells (Sukhai et al., 2013, Bernard et al., 2015).

2.7.8. Cellular iron metabolism:

Iron is a co-factor for several cellular processes such as oxidative phosphorylation, replication, and protein synthesis (Figure 22). Iron (Fe) exists in oxidized and reduced and involves in the various biological process by transitioning between the two different states (Wang et al., 2018).

The major cellular iron uptake is via transferrin (TF) receptor (TFR) and divalent metal iron transporter 1 (DMT1).

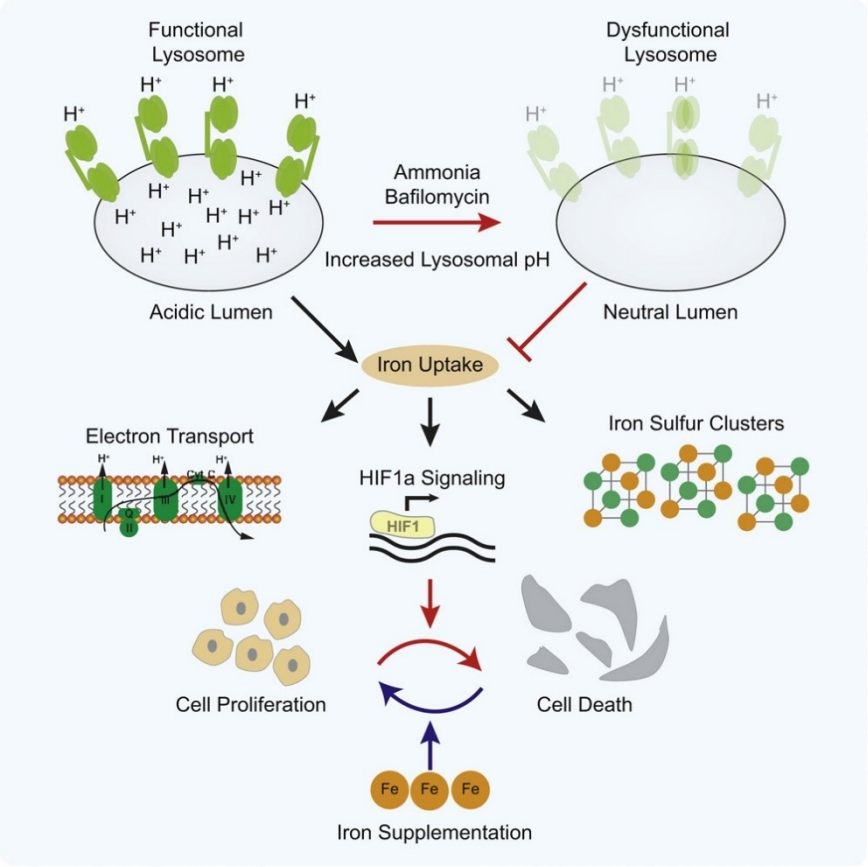

Figure 22: Interlink between Iron, lysosomes and mitochondria function (adapted from (Weber et al., 2020))

These two receptors are expressed on the surface of the cell membrane, and TFR carries iron in the form of Fe3+ and DMT1 as Fe2+. The TFR is endocytosed and fuses with the lysosomes to release iron (Fe3+), due to the acidic pH inside the lysosomes Fe3+ is converted into Fe2+ and released into the cytosol. The released iron contributes to the maintenance of the labile iron pool (LIP). LIP is directed to the different compartments of the cells for further biological functions such as heme synthesis, iron-sulfur clusters, and also as co-factor for biologicals enzymes. Excessive iron is either stored as ferritin (iron storage protein) or expelled out of the cells by ferroportin (FPN) (Stevens et al., 1988, Waldvogel-Abramowski et al., 2014).

Cancer cells have been discovered to have an addiction to Iron (Torti and Torti, 2013). It has been reported that the cancer cells require an increased amount of iron to support cell survival, proliferation (figure 23). Hence, treatments targeting iron metabolism in combination with the conventional chemotherapeutic agents are being evaluated and are also in clinical trials. FPN has been reported to be dysregulated in cancer, where more aggressive tumors of as prostate, ovarian, colorectal were low in FPN expression relative to the adjacent healthy tissue.

It has been reported in AML, that there is a significant dysregulation in iron metabolism(Callens et al., 2010). Leukemic cells had significantly low levels of FPN expression in comparison to normal stem cells. Increasing the intracellular iron content using an FDA approved iron-oxide nanoparticle ferumoxytol led to a significant increase in the intracellular iron content and decreased the cell survival of the leukemic cells. (Trujillo-Alonso et al., 2019).

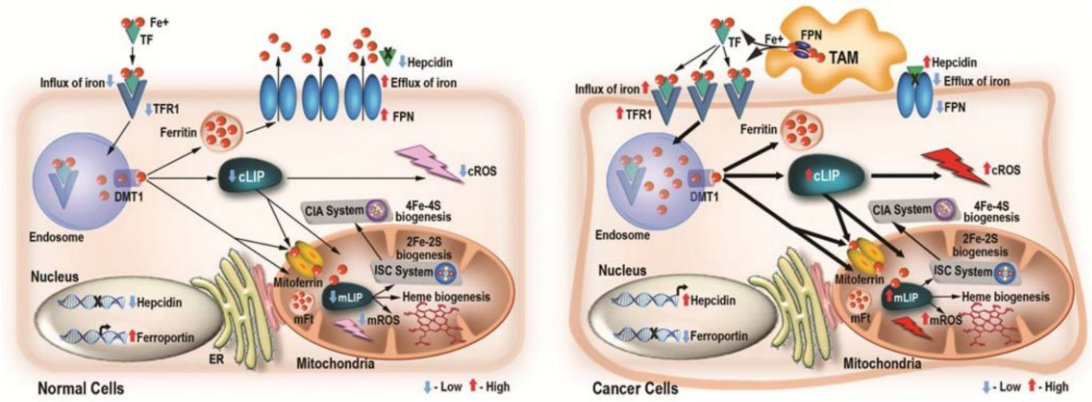

Figure 23: Iron-related cellular pathways of cancer cells relative to normal cells. The iron addiction phenotype of cancer cells is accompanied by alterations in several iron-related pathways (Mittler et al., 2018)

2.8. Bone marrow microenvironment induced metabolic changes in the malignant cells:

Although multiple leukemic intrinsic mechanisms of chemoresistance have been described, the microenvironment has recently attracted attention in protecting leukemic cells from chemotherapy. Early co-culture studies showed that cytarabine treatment of BMSCs interferes with apoptosis and enhances the survival of AML cells (Konopleva et al., 2002, Garrido et al., 2001). BMSC-derived TGF-b1 is a mediator of resistance during the Cytarabine treatment of AML (Tabe et al., 2013). Another key chemotherapy resistance-conferring pathway is CXCL12/CXCR4. Chemotherapy upregulates CXCR4 in AML cells, and Imatinib enhances CXCR4 expression in BCR-ABL1 cells, which results in increased CXCL12/CXCR4 survival signaling and lodgment into protective niches (Zeng et al., 2009, Zeng et al., 2006, Sison et al., 2013). Human AML cells preferentially home and engraft in the endosteal BM of

immunodeficient mice, where they remain more quiescent and protected from chemotherapy (Ishikawa et al., 2007).

Leukemic progenitors have been reported to be in close relationships with BM stromal cells directly and indirectly via secreted factors or tunneling nanotubes/ gap junctions. Intercellular communication with different cells of the microenvironment has been shown to affect the function of AML cells, reducing both their proliferation and apoptosis (Bendall et al., 1994)and increasing their drug resistance (Konopleva et al., 2008), thereby promoting AML relapse(Wang and Zhong, 2018, Wang et al., 2015).

Stromal cells support the survival of the leukemic cells by scavenging the oxidative stress using a gap junctions connexin 43 (Taniguchi Ishikawa et al., 2012) and also transfers mitochondria in a bidirectional manner to protect against the chemotherapeutic agents (Mistry et al., 2019, Moschoi et al., 2016).

Adipocytes in the bone marrow microenvironment have also been reported to protect the leukemic cells by providing free fatty acids (FFA), which are transferred to the AML blast via Fatty acid-binding protein 4 (FABP4) (Shafat et al., 2015). FFA enters the mitochondria, of BMSC origin, through carnitine palmitoyltransferase I (CPT1) to generate ATP through β-oxidation. CD36 – a glycoprotein receptor for free fatty acid has also used a marker for AML LSC's, and this is particularly up-regulated in the AML cells, which are the bone marrow microenvironment thereby helping to evade the apoptotic activity of conventional chemotherapeutic agents (Ye et al., 2016). It provides the fuel and the metabolic machinery for the AML cells to generate the energy required for survival and proliferation (figure 24).

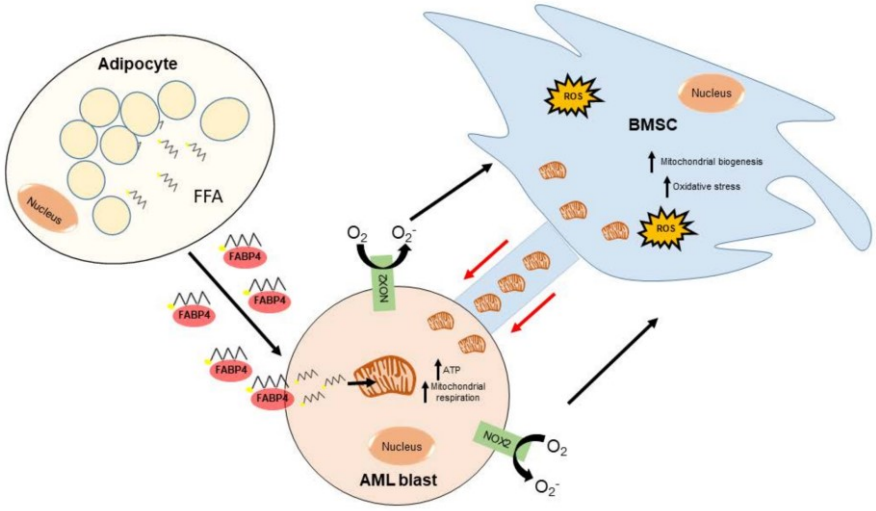

Figure 24: Cross-talk between the leukemic cells – adipocyte- stromal cells in the bone marrow microenvironment (adapted from (Marlein et al., 2017))

2.9. Metabolic alterations in the bone marrow microenvironment promote a permissive immune environment:

One of the hallmarks of the cancer cells is the evasion of immune cells (Hanahan and Weinberg, 2000, Hanahan and Weinberg). There have been increasing shreds of evidence to show that the AML LSC's evade immune recognition by expressing the self-antigens or excluding the expression of certain immune recognition ligands and receptors such as NKG2D. Increased levels of adenosine or increased levels of certain essential and non-essential amino acids, such as tryptophan, promote an immune permissive microenvironment.

Increased glycolytic activity, arginase II, and indoleamine-2,3-dioxygenase 1 (IDO1) in AML blasts result in depletion of glucose, tryptophan, and arginine which are required for proper T cell functionality (Brault et al., 2018, Brand et al., 2016).

Stromal cells also trigger these metabolic pathways. Aerobic glycolysis, NADPH-oxidase 2 (NOX2) activity, and IDO1 in AML blasts abundantly produce bioactive metabolites such as lactate, reactive oxygen species (ROS), and kynurenine which inhibits T cell responses. These metabolites enhance the survival and induction of regulatory T cells (Tregs) and myeloid-derived suppressor cells (MDSCs)(Cham et al., 2008), thereby promoting an immune suppressive microenvironment supporting the survival of leukemic cells. AML cells compete for the nutrients for cell survival, and the generated by-products promote an immunosuppressive/tolerogenic environment (figure 25).

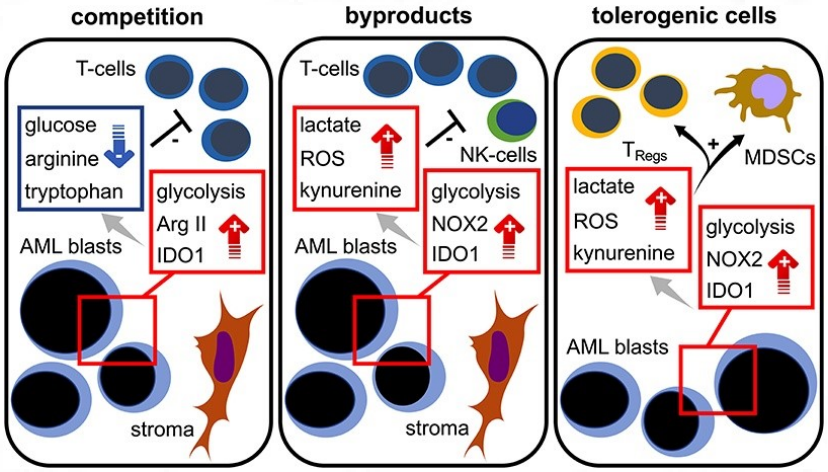

Figure 25: Metabolic alterations promoting an immune permissive microenvironment. (Mougiakakos, 2019)).

2.10. Drug repositioning - A strategy to rapidly advance novel therapeutic agents into clinical trials:

Drug repositioning or drug repurposing is a strategy to advance new therapeutic options into the clinical trials rapidly and has been shown to have clinical efficacy. The use of thalidomide as a therapeutic agent for the treatment of myeloma and myelodysplasia is one of the best-known examples of this strategy, but there have been multiple other successes. For example, The anti-diabetic drug metformin had stirred the field of drug repositioning when large epidemiological data provided the data of anti-cancer property of metformin(Kasznicki et al., 2014, Owen et al., 2000). More recently, large studies screening small molecules that inhibit metabolic pathways in cancer has gained attention as they have reported the ability of some of these molecules to selectively inhibit metabolism in cancer cells while sparing the normal counterparts (Gohil et al., 2010a). In epithelial cancer, it has been shown that bedaquiline, which is an anti-microbial agent approved by the FDA for the treatment of multi-drug resistant pulmonary tuberculosis (TB), has a potential anti-cancer property and could also potentially eradicate cancer stem cells(Fiorillo et al., 2016). Ribavirin, a broad spectrum anti-viral agent, was also evaluated in a phase I dose-escalation study in relapsed or refractory acute myeloid leukemia patients (Kentsis et al., 2004, Assouline et al., 2009)

It is important to note that several similar observations of targeting the metabolic variations on cancer cells have already been translated into the clinic. Phase I clinical trials are in progress evaluating the mitochondrial inhibition using Tigecycline, a widely used antibiotic as a single agent in the treatment of acute myeloid

leukemia and chronic myeloid leukemia (Reed et al., 2016). IACS-010759, a small molecule inhibitor of mitochondrial oxidative phosphorylation inhibitor, is also now being tested in phase I clinical trials (Clinical Trial ID: NCT02882321) (Yang et al., 2017).

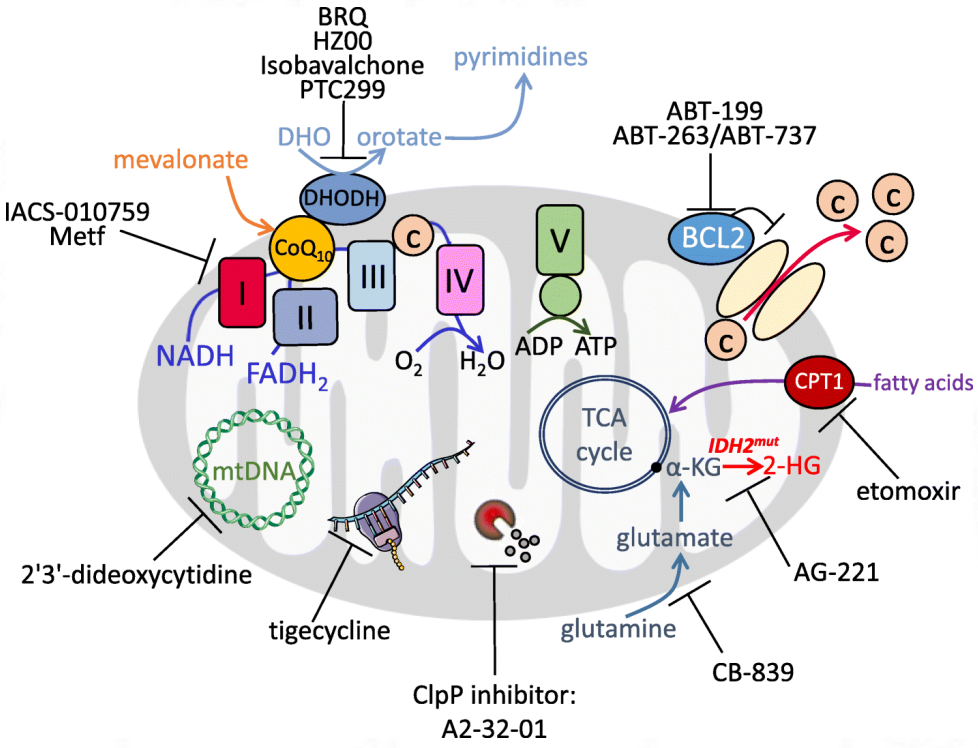

Figure 26: Currently available (approved and under clinical trial) mitochondrial inhibitors in the management of acute myeloid leukemia (adapted from (Stuani et al., 2019)).

Target protein or process	Pathway impacted	Drug	Patient group	Clinical trials
Hexokinases	Glycolysis	2-Deoxyglucose	AML	-
			AML with FTL3-ITD mutation	-
mTOR kinase	mTOR-dependent metabolic pathways	Sirolimus (rapamycin), temsirolimus, everolimus	AML/ CML	Phase I/II
Glutaminase	Glutaminolysis	CB839	AML	Phase I
			AML with IDH mutations	-
Asparagine glutamine availability	Amino acid metabolism	Erwinase alone L-asparaginase (encapsulated in red blood cells) + low-dose cytarabine	AML	Phase I/II
Arginine availability	Nucleotides polyamines biosynthesis	ADI-PEG20	AML	Phase I/II [30]
CKMT1	Creatine biosynthesis and OxPHOS	Cyclocreatine	AML with EVI1 aberrant expression	-
Mitochondrial protein translation	OxPHOS	Tigecycline	AML	Phase I
Mitochondrial protease ClpP	OxPHOS	A2-32-01	AML	-
mtDNA polymerase	OxPHOS	2'3'-Dideoxycytidine	AML	-
ETC complex I	OxPHOS	Metformin	AML	Phase I
		IACS-010759	AML	Phase I
DHODH	Nucleotides and OxPHOS	Brequinar sodium BRQ	AML	Phase I/II
		HZ00	CML	-
		Isobavalchone	AML	-
		PTC299	AML	Phase Ib
CPT1a	Fatty acid oxidation	Etomoxir	AML	-
		Avocatin B		-
		ST1326		-
Mitochondrial anti-apoptotic BCL2	OxPHOS and pyrimidine biosynthesis	Venetoclax ABT-199	AML/ CML	Phase I/II/III [50]
			AML with FTL3-ITD mutation	Phase I/II in combination with FLT3-ITD inhibitor
			AML with IDH1 mutation	Phase I/II in combination with IDH1 mutant inhibitor
Amino acid transporters	AA metabolism and OxPHOS	Venetoclax ABT-199 + azacitidine	AML	Phase I/II/III [50]
IDH2 mutant enzyme	2-HG production	Enasidenib AG-221	AML with IDH2 mutation	FDA approved phase I/III
IDH1 mutant enzyme	2-HG production	Ivosidenib AG-120	AML with IDH1 mutation	FDA approved phase I/III
		BAY1436032		Phase I
		IDH305		Phase I [61]
IDH1/IDH2 mutant enzyme	2-HG production	Vorasidenib AG-881	AML with IDH1 and/or IDH2 mutation	Phase I [62]
HMG-CoA reductase	Mevalonate biosynthesis	Statins: lovastatin, pravastatin	AML	Phase I/II [66, 67]
Stearoyl CoA desaturase 1	Lipid biosynthesis	BaP = combination of lipid-regulating bezafibrate and the sex hormone medroxyprogesterone acetate	AML	-

Table 5: Drugs targeting metabolic activities in myeloid leukemia and their current status of the clinical trials. adapted from (Stuani et al., 2019)

Despite the genetic and biological heterogeneity of acute myeloid leukemia, some common biological features remain accessible to selective targeting and potential therapeutic exploitation.

Material and Methods

3.0 Methods

3.1 Design of the study:

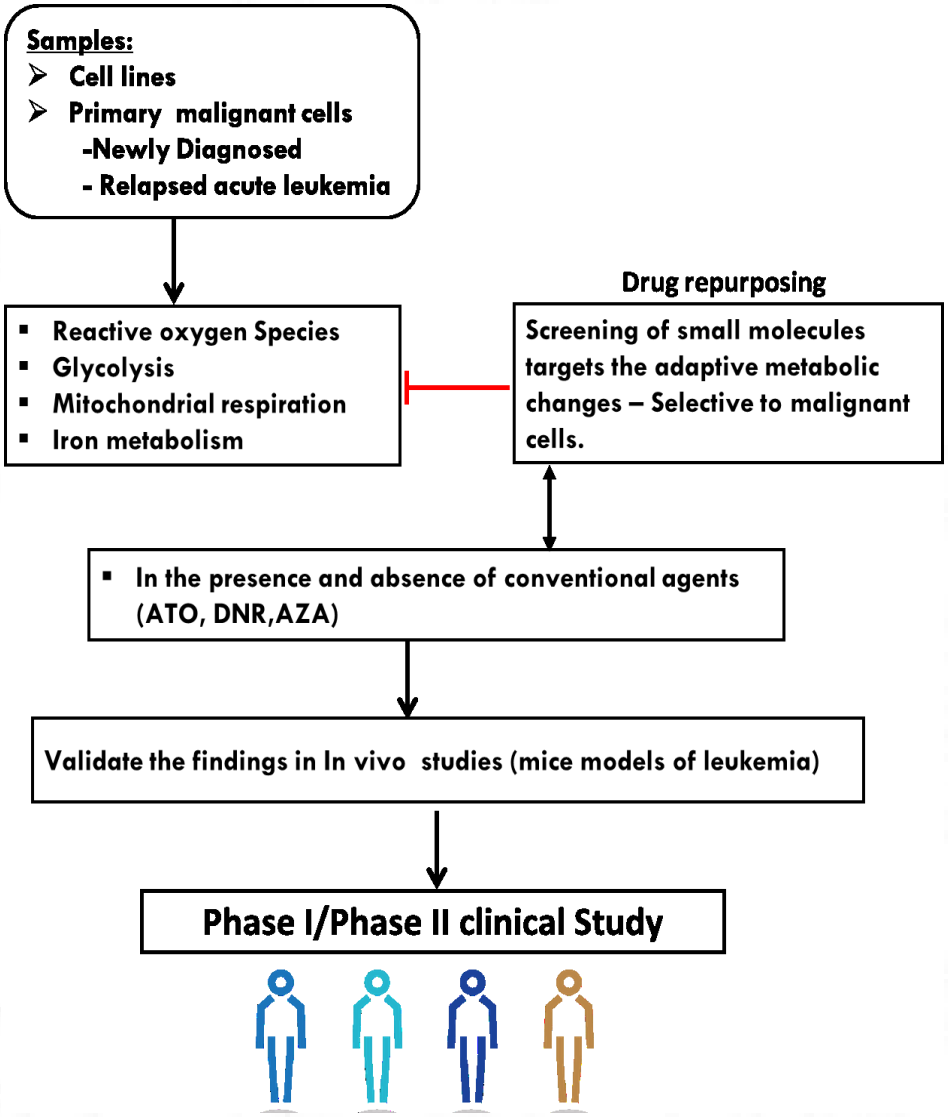

3.2 Samples:

3.2.1 Cell lines: The AML cell lines (HL60, K562, U937, Kasumi-1, THP-1, stromal cells (HS-5)) used for the study were obtained from ATCC (Manassas, US). The human APL cell line NB4 (Kind gift from Dr. Harry Iland, RPAH, Sydney, Australia with permission from Dr. Michel Lanotte). NB4 EV-AsR1, in-house generated ATO resistant, and UF1 APL cell line was also used in the study. In addition to HS-5, we also used HS-5 GFP cells for co-culture experiments. Cells were maintained in RPMI 1640 or DMEM media (Gibco, Thermo Fisher Scientific, Massachusetts, US) with 10% fetal bovine serum, 100 units/ml penicillin, and 100 µg/ml streptomycin (Gibco).

3.2.2 Mycoplasma testing: Mycoplasma detection PCR was done once in every six months as a quality control protocol to avoid mycoplasma contamination in cell lines. The Mycoplasma testing will be done using Mycoplasma detection kit (ATCC, Manassas, US)

3.2.3 Generation of arsenic trioxide resistant cell line:

ATO resistant cells were generated by exposing the naïve NB4 cell line to low concentrations of ATO (50nM) for about three months. Once the cells persisted and sustained the concentration of ATO was gradually increased to 1uM over one year. The cells which survived and proliferated at 1uM were termed as the "ATO tolerant persister cells" (ATO-TPs). The ATO-TPs were then subjected to serial limiting dilutions and single-cell colony-forming unit generation on methylcellulose to isolate clonal resistant populations. We isolated three different clones, expanded and named them NB4 EV-AsR1, NB4 EV-AsR2, NB4 EV-AsR3, respectively, based on the

published norms of NB4 resistant cell line nomenclature (Roussel and Lanotte, 2001). The IC50 for ATO was 3.25uM, 3.4 µM, and 2.88 µM, respectively, for NB4 EV-AsR1, NB4 EV-AsR2, and NB4 EV-AsR3 in contrast to naïve NB4, which was 0.9uM (figure 26a). The ATO resistant cell line was generated by Dr.Ezhilarasi Chendamarai (Figure 27).

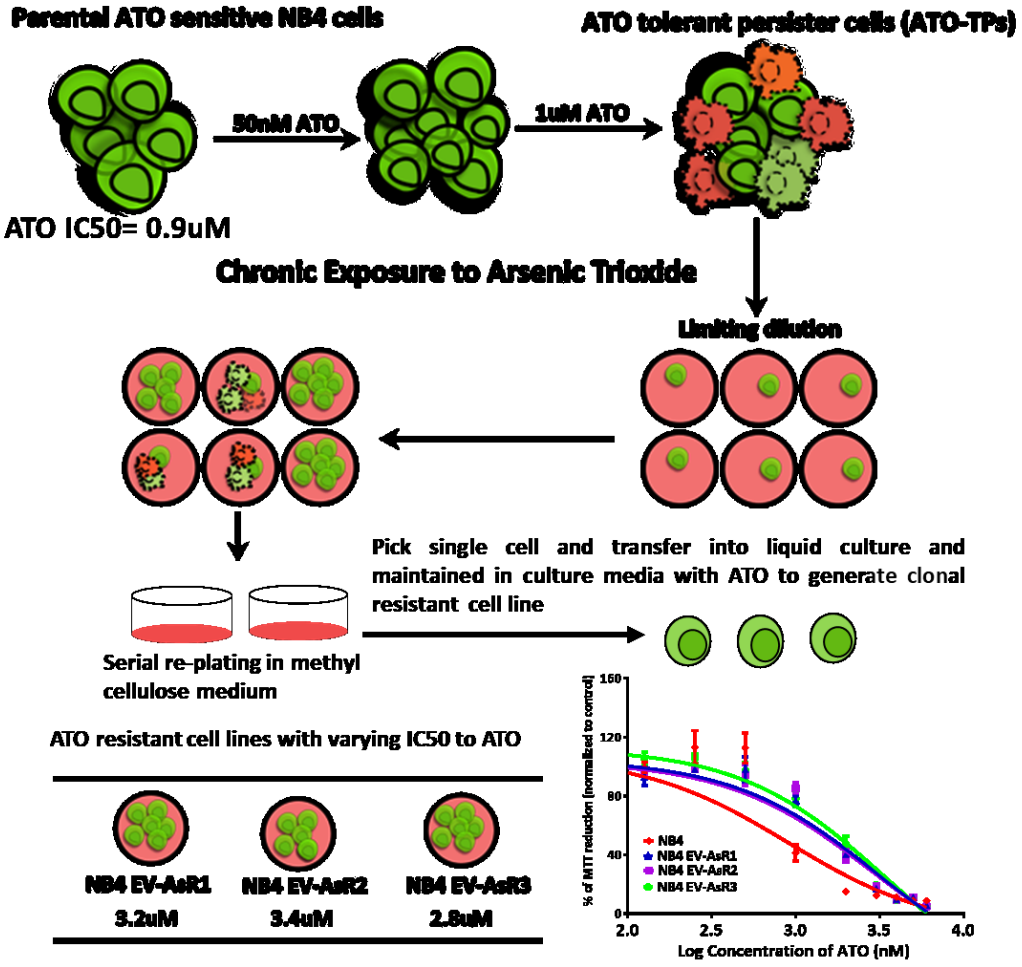

Figure 27: Generation of ATO resistant cell line: NB4 naive parental cell line was exposed to 50nM for three months and increased the concentration to 1uM ATO over the year for them to sustain and proliferate. Limiting dilutions and colony-forming units were performed to propagate the subclones of the resistant cell lines.

3.2.4 Primary cells

From July 2014 to January 2019, bone marrow and peripheral blood samples from AML patients were collected at diagnosis prior to treatment after getting written informed consent. The patient baseline clinical and demographic characteristics have been recorded regularly. The study was approved by the institutional review board (IRB Min. No. 8666 dated 19.02.2014).

The diagnosis of AML was made according to the WHO Classification of myeloid neoplasms and acute leukemia. The presence of ≥ 20% blasts was mandatory either in the peripheral blood or on the bone marrow. The presence of < 20 % blasts was acceptable only in those with recurrent genetic abnormalities. Conventional karyotyping and molecular markers as part of standard care has been done and documented for all patients who proceed to treatment. The details of the standard of care therapy and the patient's response to therapy, complications, the toxicity profile of chemotherapy agents, and long-term clinical outcome data have been recorded and maintained by an active data management program. We also validated our findings in APL (AML-M3) samples stored in our lab (IRB Min No. 7826 dated 18.04.2012) for a few experiments, as mentioned, respectively.

3.3 Isolation of mononuclear cells:

Mononuclear cells (MNCs) were separated using Ficoll-Paque Plus (GE Healthcare, Uppsala, Sweden). The bone marrow or the peripheral blood is carefully layered on to fill (1:2 ratio) and subjected to centrifugation at 400 g for 30 minutes with slow acceleration and deceleration. Post centrifugation, the mononuclear cells

were taken and subjected to RBC lysis and PBS wash. The cells were finally suspended in RPMI 1640 (Gibco, Thermo Fisher Scientific, Massachusetts, US) with 10% fetal bovine serum (Gibco) 100 units/ml penicillin and 100 ug/ml streptomycin (Gibco) and cultured in a humidified atmosphere with 5% CO2 incubator (Thermo Fisher Scientific).

3.4 Enrichment of CD34 positive cells:

CD34 positive stem cells are enriched using the Miltenyi microbead based kit. 10^8 allogeneic peripheral blood stem cells were incubated with 100ul of CD34 microbeads and 100ul of FCR blocking reagent and incubated at 4^o C for 30minutes. Then the cells are washed in the enrichment media (2% Fetal Bovine Serum, 2mM EDTA, and phosphate-buffered saline). The cells were resuspended in the enrichment media and passed through the Miltenyi MS column placed in the magnetic stand. The column was then washed thrice with enrichment media to collect the non-CD34 positive fraction. Then the column was displaced from the magnetic stand, and 1ml of enrichment media was added and flushed using the plunger provided with the kit. An aliquot of the sample was stained with a CD34fluorochrome-conjugated antibody to assess the enrichment.

3.5 In vitro cytotoxicity assay:

In vitro, cytotoxicity of drugs was determined using the MTT-assay as described previously (Pieters et al., 1990). Briefly, 2x 10^5 cells/well were seeded in 96 well plates followed by addition of increasing concentrations of drugs (incubated for 48 h with drugs at 37°C in humidified air containing 5% CO2, after which 10 µl of

MTT reagent was added, and the plates were incubated for an additional 4 hours. IC50 values were generated using Graph Pad Prism 8 software (La Jolla, CA, USA).

3.6 Assays for Apoptosis:

Cell lines or Primary cells were added ($1x10^5$cells/well) on a layer of primary MSCs or HS-5 stromal cell line in 24 well plates or seeded in trans wells. The cells were incubated for 4 hours and then exposed to ATO with and without other drugs/ small molecules, as mentioned along with appropriate controls. After 48-hour incubation at 37^0C CO_2 incubator, the leukemic cells were carefully pipetted out, and their viability was measured using Annexin V/7AAD apoptosis assay kit (BD Pharmingen, San Diego, CA, USA) as per manufacturer's protocol. CD105 or CD45 was used to gate only leukemic cells and exclude stromal cells if present during acquisition and analysis. The flow data were analyzed using Cell Quest Pro software (BD Biosciences, San Jose, CA, USA).

3.7 In vitro 3D Co-cultures and apoptosis assay:

Gelatin dental gel foam pads were punched and seeded with $1x10^4$ HS-5 or MS-5 cells per gel punch and incubated in the hypoxia chamber for 4 days, and on fif^{th} day $1x\ 10^5$ NB4 cells were seeded on each scaffold. The cells were incubated for 24 hours followed by treatment with ATO (1 and 2 uM) and after 48 hours of incubation, the cells were stained for Annexin V, PI and CD73 to study the percentage of apoptosis in leukemic cells using flow cytometry (BD CantoII) and the data was analyzed using FACS Diva software.

3.8 RNA Extraction

Total RNA was extracted from PB/BM-MNCs/cell lines using TRI Reagent (Sigma, St. Louis, USA) as per the manufacturer's protocol. Briefly, 2 x 10^7 cells were lysed in 1ml of Trizol Reagent followed by the addition of 0.2ml of chloroform per 1ml of Tri Reagent and incubated for 8-10 minutes after which the mixture was centrifuged at 12,000g for 15 minutes (2-8^o C). The aqueous phase was transferred to a fresh tube and to which equal volume of isopropanol was added and incubated for 10 minutes, centrifuged for 5 minutes at 12,000g (2-8^0 C) so that RNA is precipitated. RNA pellet formed was gently washed with 75% ethanol (prepared using nuclease-free water) twice and centrifuged briefly at 12,000g (2-8^0 C). The RNA pellet was air-dried for 2-3 minutes and re-suspended in RNase free H2O and immediately stored at -80^0 C.

3.8.1 Assessing the quality and quantity of extracted RNA

The concentration of the extracted RNA was determined by NanoDrop®ND-1000 UV (Thermo Scientific, Massachusetts, USA), which measures the absorbance at 260 nm. Pure RNA has an A260/A280 of 2. RNA quality was assessed in all samples by running RNA samples in 1% non-denaturing agarose gel in TAE buffer. RNA should appear as two bright discrete bands representing the 28S and 18S ribosomal species. The 28S band should be brighter than the 18S band. Tailing of these major bands down the gel, or a background smear behind these bands indicate degradation of the RNA. Samples failing quality check are discarded and not considered for further experiments.

3.8.2 cDNA synthesis

cDNA synthesis was performed using 1µg of total RNA using a High capacity reverse transcription kit (Applied Biosystems, Foster City, CA, USA) following the manufacturer's instructions. PCR-based cDNA synthesis was performed for all samples following the manufacturer's instructions and is stored at -20°C for further downstream applications.

3.8.3 Quality control – post cDNA synthesis

To compensate for potential variability introduced in cDNA synthesis, the expression of housekeeping gene β-glucuronidase (GUS) was assessed by RT-PCR (Primer sequences, master mix, and conditions of PCR were given in table XXX). The RT-PCR products were analyzed in 2% Agarose (Figure XXX). GUS has been reported to have the lowest inter-sample variability. Proper amplification of ACTIN by RQ- PCR will also validate the quality of cDNA synthesis.

Table 6: Primer sequences for GUS gene to perform RT-PCR

Gene Name	***Primer sequence***	***Amplicon Size***
GUS	*Forward 5`-CCTGTGACCTTTGTGAGCAA -3`*	*600 bp*
	Reverse 5`- GTCTGCCGTGAACAGTCCA-3`	

Table 7: Master mix composition and PCR conditions to amplify GUS gene from the cDNA synthesized

S. No.	Reagents	Volume (µl)	S. No.	Temperature & Time	Cycles
1.	Red dye mastermix	12.5	1.	95^0C – 5 minutes	1
2.	Forward Primer	1	2.	94^0C – 30 Secs	35 Cycles
3.	Reverse Primer	1	3.	58^0C – 1 minute	
4.	Water	9.5	4.	72^0C – 1 minute	
5.	cDNA	1	5.	72^0C – 7 minutes	1
	Total volume	25	6.	4^0C - Hold	

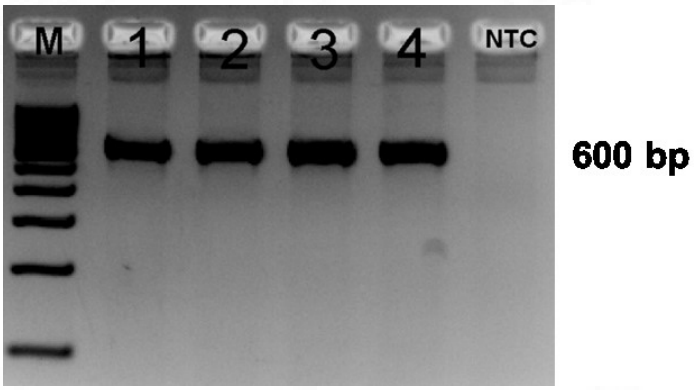

Figure 28: Agarose gel electrophoresis showing amplification of GUS from cDNA synthesized (Lane M: 100bp marker, Lane1-4: cDNA samples showing amplification of GUS gene, Lane NTC- Negative control).

3.9 Gene Expression array and Exome Sequencing:

Global gene expression array for differential gene expression in naïve NB4 cells and the ATO resistant NB4 primary resistant clone was performed. 2x107 cells (NB4 naïve, NB4 EV-AsR1, and UF1) were harvested and stored in RNA later solution. The extracted and labeled RNAs were hybridized to Agilent Human Whole Genome 8x60K Gene Expression Array (AMADID: 039494), and the Image analysis was done using Agilent Feature Extraction software Version 10.5.1.1 to obtain the raw data. Normalization and statistical analysis of the microarray data were done using GeneSpring GX (Agilent Technologies) using the 75th percentile shift and fold difference was calculated by comparing treated samples with control samples. Differentially regulated genes were clustered using hierarchical clustering to identify significant gene expression patterns Genes were classified based on functions and pathways using biological interpretation tool Biointerpreter (Genotypic Technology). The raw data have been deposited in NCBI's Gene Expression Omnibus, accessible through GEO Series accession number GSE115812 (https://www.ncbi.nlm.nih.gov/geo/).

Genomic DNA was isolated from the naïve NB4 cells and the ATO resistant NB4 197 subclones NB4-EVAsR1 and UF1 using Gentra pure gene blood kit (Qiagen, Hilden,198 Germany) and stored at 4°C. Library preparation and sequencing were performed at Genotypic Technology's Genomics facility, Bengaluru, following Ion TargetSeq™ 200 Exome Enrichment for the Ion Proton™ System. Sequencing was performed on Ion 201 Proton™ sequencer. The mutations were confirmed by Sanger sequencing.

3.10 Immunoblots:

Cell homogenates (with or without treatment) were obtained by cell lysis in RIPA buffer (Tris 20 mM, pH 8, NaCl 100 mM and glycerol 10%), with protease inhibitors (aprotinin 10 µg/mL, leupeptin 10 µg/mL, PMSF 1 mM) and Triton-100x 10%. After 20 min on ice, samples were centrifuged (13,000 rpm, 10 min), and supernatants were collected. The lysates and elutes were analyzed in SDS–PAGE. After protein transfer to a nitrocellulose membrane, membranes were blocked with non-fat milk (5%, 2 hours), blotted with the primary antibodies overnight. The blots were washed and probed with secondary antibodies conjugated with horseradish peroxidase - anti-mouse and anti-rabbit (Cell signaling, Massachusetts, US) for one hour, followed by washing in TBS-T thrice. The luminescence was obtained by membrane incubation with a chemiluminescence solution kit (Thermo pierce –Femto-Thermo Fisher Scientific, Massachusetts, US), and the images were captured using FluorChemQ system (Alpha Innotech, California, US) provided with Alpha View Q Software. Densitometric analysis was performed with ImageJ software (NIH, US).

3.11 Endogenous Reactive Oxygen Species (ROS) measurement

Intracellular Reactive Oxygen species was measured in cells by flow cytometry using CellROX Green (Life Technologies, NY, USA), which is a fluorogenic probe for measuring oxidative stress in live cells. Briefly, $5x10^5$ cells were treated with 2µl of CellROX Green reagent for 30 minutes at 37ºC followed by washing with PBS. The fluorescence intensity was measured in the Beckman Coulter Gallios flow cytometer (Becton Dickinson, Mansfield, MA, USA) with an excitation wavelength at 485nm and the data analyzed using Kaluza Analysis Software (Becton

Dickinson, Mansfield, MA, USA). The experiments were done in triplicates, and the results are expressed as average mean fluorescent intensity (MFI).

3.12 Measurement of Mitochondrial Membrane Potential:

The mitochondrial membrane potential ($\Delta\psi m$) (MMP) of the cells was measured using JC-1 dye (Life Technologies, Carlsbad, CA, USA), as previously reported. The fluorescence intensity was measured using Spectramax M4 (Molecular Devices, Sunnyvale, CA, USA) (green channel: excitation: 485 nm; emission: 530 nm; cut off 515 nm; red channel: excitation: 485 nm; emission: 590 nm; cut off 570 nm). The ratio of red to green fluorescence (590/530) was calculated, and the $\Delta\psi m$ of treated cells was compared with the untreated cells.

3.13 Mitochondrial morphology using Confocal -laser scanning microscopy:

MitoTracker™ Red CM-H2Xros (Thermo Scientific) was added into culture media at a final concentration of 200nM to label the mitochondria for 30 minutes in 37^{o} C 5% CO_2 incubator before harvesting cells for confocal studies. To prepare slides, labeled cells were washed two times with ice-cold PBS. 100 ul of cell suspension (10000 cells) was used for cytospin at 500rpm for 5 minutes at room temperature. The slides were air-dried in the dark box at room temperature for 5 minutes before fixed in -20^{o} C 100% methanol for 10 minutes. The slides were then air-dried in the dark box at room temperature for 10 minutes and mounted in Vectashield DAPI Mountant before confocal imaging. The stained slides were imaged on the Olympus FV3000 confocal microscope using its High sensitivity detectors excite the DAPI and its 633nm laser to excite the MitoTracker-Red. Z stacks were

captured, and the images were deconvoluted using Olympus Fluoview. Confocal images were captured at the nuclear imaging and flow cytometry facility of the National Centre for Biological Sciences (NCBS).

3.14 Seahorse metabolic flux analysis:

Extracellular flux assay kits XF24 (Agilent Technologies, CA, USA) was used to measure oxygen consumption and glycolytic flux. 5x105 cells were plated in an XF24 cell culture microplate. Oxygen consumption and glycolytic flux were measured according to the manufacturer's protocol and as previously described17. Briefly, three replicate wells of 5×10^4 cells per well were seeded in a retronectin (Takara Bio Inc, JPY) coated 24-well XF24 plate. At 30 min prior to analysis, the medium was replaced with Seahorse XF media (Agilent Technologies, CA, USA), and the plate was incubated at 37 °C. Analyses were performed both at basal conditions and after injection of oligomycin, FCCP, antimycin A, and rotenone for mitochondrial function(mito-stress) and glucose, oligomycin and 2-deoxy glucose for glycolytic function (Glyco-stress). Oxygen consumption rate (OCR) is indicating the mitochondrial function, and the extracellular acidification rate (ECAR) indicates glycolytic function. Seahorse extracellular flux analysis was carried out at the National Centre for Biological Sciences (NCBS, Bengaluru) and Department of Biotechnology, Anna University, Chennai.

3.15 Measurement of Compartmentalized and Labile iron pool:

The intracellular iron pool was measured using fluorescent iron sensor probes - Calcein-AM (Cytosolic) (Sigma, St. Louis, MO, USA) and Mito-Ferro Green

(Mitochondrial Iron) (Dojindo Molecular Technologies, Inc.) Briefly, $5x10^5$ cells were treated drugs, and after 6 hours, the cells were stained with 100nM of Calcein-AM or Mito Ferro green for 15 minutes in Phosphate buffered saline (PBS) at 37°C followed by washing with PBS. The fluorescence intensity was measured in FACS Calibur with an excitation wavelength at 485nm, and the data analyzed using Kaluza Analysis Software (Beckman Coulter, CA, USA). The experiments were performed in triplicates and were expressed as average mean fluorescent intensity (MFI).

3.16 Mouse model of leukemia:

All the experiments involving animals were performed according to the Institutional guidelines for animal care specified at Christian Medical College (Vellore, India), and the study design and euthanasia protocols were approved from Animal Ethics Committee IAEC (IAEC approval number: 04/2019). FVB/N mice strains were purchased from Jackson Laboratories (Bar Harbor, Maine, US). Mice of 6 to 8 weeks of age were used in all the experiments. Intraperitoneal, intravenous or sub-cutaneous interventions were done during the experimental procedures as per the animal facility rules. Retro-orbital blood samples were collected for experiments. At the end of the study, mice were euthanized by carbon dioxide (CO_2) inhalation.

3.16.1 Establishment of APL transplantable mouse model

Transgenic APL mice bearing the human PML-RARα cDNA (bcr1) with hMRP8 promoter were previously constructed in FVB/N inbred strain of mice, and a transplantable model was established in which 100% of the mice die of the disease. To allow reproducible APL development, mouse APL blasts were obtained as a kind gift

from Dr. Christine Chomienne and Dr. Rose-Ann Padua, Inserm UMR-S940 Institut Univérsitaire d'Hématologie, Hôpital Saint-Louis with the permission from Dr. Scott Kogan and Dr.Michael Bishop (University of California, US). 6- 8week old wild type FVB/N mice were injected intravenously in the tail with 5x 104 APL blasts without conditioning with either radiation or chemotherapy. After one week, leukemia was confirmed by the following parameters and thus re-established the APL mouse model at our center.

3.16.2 Confirmation of leukemia

a) Blood counts: White blood cell (WBC), hemoglobin, and platelet counts in peripheral blood (PB) were determined using an automated hematology analyzer (Horiba ABX ABC Vet automated veterinary analyzer, Kyoto, Japan).

b) RQ-PCR: The PML-RARA fusion gene transcript bcr1were quantified using real-time PCR. RNA from bone marrow and other organs were extracted using Tri reagent, cDNA was made as per the method described earlier. The human PML-RARA bcr1 transcript was quantified by normalizing it with mouse ABL; the normalized copy numbers were calculated using the formula mentioned before.

c) Immunophenotyping of immature CD117+ Gr1+ cells: Bone marrow cells were flushed from the murine long bones (tibias and femurs) or murine spleen cells and were harvested and disrupted in RPMI and filtered through a nylon cell strainer (70µm) to obtain a single-cell suspension. The peripheral blood samples were collected from retro-orbital plexus, and the whole-cell RBC lysis was done. After washing with PBS, Peripheral blood cells/bone marrow mononuclear cells/ spleen cells ($1x10^6$cells) were

incubated with Mac-1 (CD11b) antibody, c-Kit (CD117), CD45 and Gr-1 (myeloid differentiation antigen) antibodies (BioLegend, Calfornia, US) conjugated with FITC, PE, PerCP and APC respectively for 20 minutes followed by RBC lysis and PBS wash. At least 10,000 events were analyzed from each sample on Gallios flow cytometry and analyzed using Kaluza software (Beckman Coulter).

3.16.3 Harvesting of cells and cryopreservation from APL mice

After the confirmation of leukemia, the APL mice were sacrificed. Bone marrow and spleen cells were harvested (as explained above) and cryopreserved (90%FBS + 10% DMSO dimethyl sulfoxide) in liquid nitrogen for future experiments.

3.17 Statistical Analysis:

Data were represented as mean of values ± SEM (standard error mean) or as median values with the range as indicated in the figure legends of the results section. Two-tailed Student's t-test was used to compare mean values between two groups. One-way or two-way analysis of variance (ANOVA) was used to compare mean values between multiple groups. Statistical analysis was performed using Prism version 8.0 (GraphPad Software, La Jolla, CA). P values < 0.05 were considered as statistically significant. The probability of survival was estimated with the use of the product-limit method of Kaplan-Meier for overall survival (OS), and the log-rank test assessed the significance.

Results

The results discussed were published /under preparation as following papers.

- **Nithya Balasundaram,** Saravanan Ganesan, Ezhilarasi Chendamarai, Hamenth Kumar Palani, Arvind Venkatraman, Ansu Abu Alex, Sachin David1, Swathy Palani Kumar, Nair Reeshma Radhakrishnan, Mohammed Yasar, Sanjeev Krishna, Anu Korula, Uday Kulkarni, Nancy Beryl Janet, Poonkuzhali Balasubramanian,Vikram Mathews. Metabolic adaptation drives arsenic trioxide resistance in acute promyelocytic leukemia. Blood Advances, 2021
- Arsenic trioxide in combination with artemisinin's selectively disrupts cellular energetics of acute leukemia. **Nithya Balasundaram,** Yolanda Augustin, Arvind Venkatraman, Hamenth Kumar Palani, Sachin David, Uday P. Kulkarni, Biju George, Eunice Sindhuvi, Poonkuzhali Balasubramanian, Sanjeev Krishna, Vikram Mathews.

A little progress each day adds up to big results…

4.1 Characterization of inhouse generated ATO acute promyelocytic leukemia resistant cell line:

4.1.1.ATO resistant APL cell lines are resistant to other conventional drugs:

To characterize the in-house generated ATO resistant cell lines -NB4 EV-AsR1, NB4 EV-AsR2 in comparison to their sensitive parental cell line, we evaluated their sensitivity to other conventional chemotherapeutic agents which are used in the management of leukemia. We found that when the NB4 naïve and inhouse generated ATO resistant cell lines were treated with 2uM of ATO (physiologically achievable concentration) for 48 hours, the viability of the cell lines was significantly unaffected in comparison to the parental cell line (figure 29a).

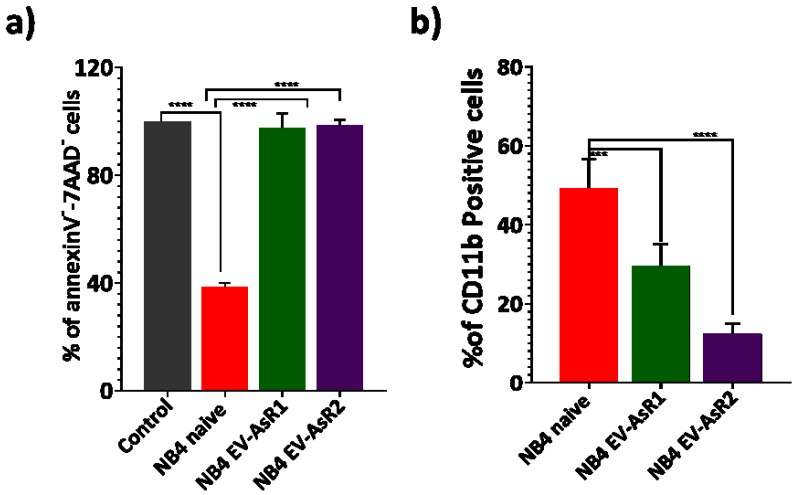

Figure 29: a) Percentage of viable cells post 48 hours of ATO treatment represented as % of annexin V⁻- 7AAD⁻ cells (n=5) b) percentage of cells positive for CD11b expression post 72hours of ATRA treatment (n=5). Error bars represent the mean± SEM of independent experiments (p<0.05, **p<0.01, ***p<0.001).*

The naïve and ATO resistant cell lines were treated with 1uM of ATRA for 72hrs and assed for their differentiation ability by the surface expression of CD11b. The resistant cell lines were observed to be less sensitive to the ATRA in comparison to the parental cell line (figure 29 b).

4.1.2 In-house generated ATO resistant cell lines displayed significant genetic heterogeneity:

On PML immunofluorescence studies, we noted nuclear body (NB) formation in the resistant cell lines, unlike the naive NB4 cells where these were completely absent, and the characteristic micro-speckled pattern was seen (figure 30a).

The ability to accumulate arsenic trioxide intracellularly was also found to be significantly less in the resistant cell lines in comparison to naïve NB4 cells (figure 30b). The PML-RARA transcripts and protein levels were also found to be significantly lower in the ATO resistant cell lines in comparison to the NB4 cell line (figure 30c and d).

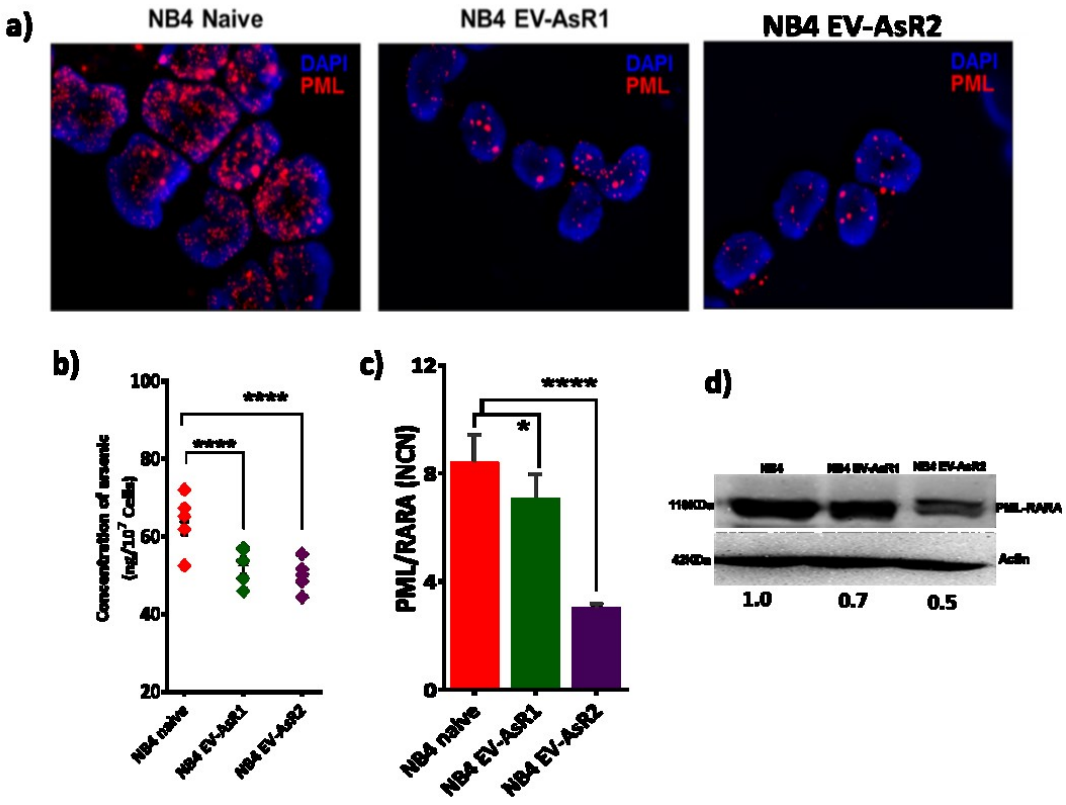

Figure 30: a) Immunofluorescent images of the PML stained NB4 and ATO resistant cell lines displaying nuclear body formation (right) and micro speckled pattern (left). (n=3) b) The intracellular level of ATO was significantly less in the resistant cell lines. c)Normalized copy number of PML-RARA transcripts in NB4 and ATO resistant cell lines (n=4). d)Immunoblots of cell lysates obtained from NB4 naïve and ATO resistant cell lines displaying the differential amount of PML-RARA fusion protein and quantification was performed using Image J software. Error bars represent the mean± SD of independent experiments (p<0.05, **p<0.01, ***p<0.001).*

4.1.3: ATO resistance is not exclusive to PML mutations:

As reports are implicating the emergence/existence of drug resistance-conferring (PML domain mutations) somatic mutations in APL cells against ATO, we performed whole-exome sequencing on our in-house generated ATO resistant cell line NB4 EV-AsR1(as a representative of other ATO resistant clones) in comparison to the parental cell line NB4 naïve and also on the UF1 (ATRA resistant cell line) found to be resistant to ATO.

Whole exome sequencing revealed that in comparison to NB4 naive, a significant number of genes were mutated in the NB4 EV-AsR1 and UF1 cell lines. Based on the mutation frequency, we observed that in comparison to the NB4 naïve majority of the mutated genes in NB4 EV-AsR1 belong to cell surface proteins, especially mucins (MUC6, MUC5B, MUC4, MUC3A, MUC16) and PRSS genes (PRSS1, PRSS3, PRSS3P2). In contrast, the UF1 cell line showed a higher frequency of mutations involving MUC16, ITGB4, PRSS1, CUL7, CDH23, LTBP3, OBSCN, STAB1 genes (figure 31a, and b).

While focusing on ATO resistance, we observed the presence of PML B2 domain ATO resistance-conferring mutation A216V in the NB4 EV-AsR1 and not in the UF1 cell line. Further comparison of mutated genes in the resistant cell lines with the commonly observed mutations in the TCGA dataset revealed that the resistant cell line had gained additional and novel mutations in them over and above those seen in the naïve NB4 cell line.

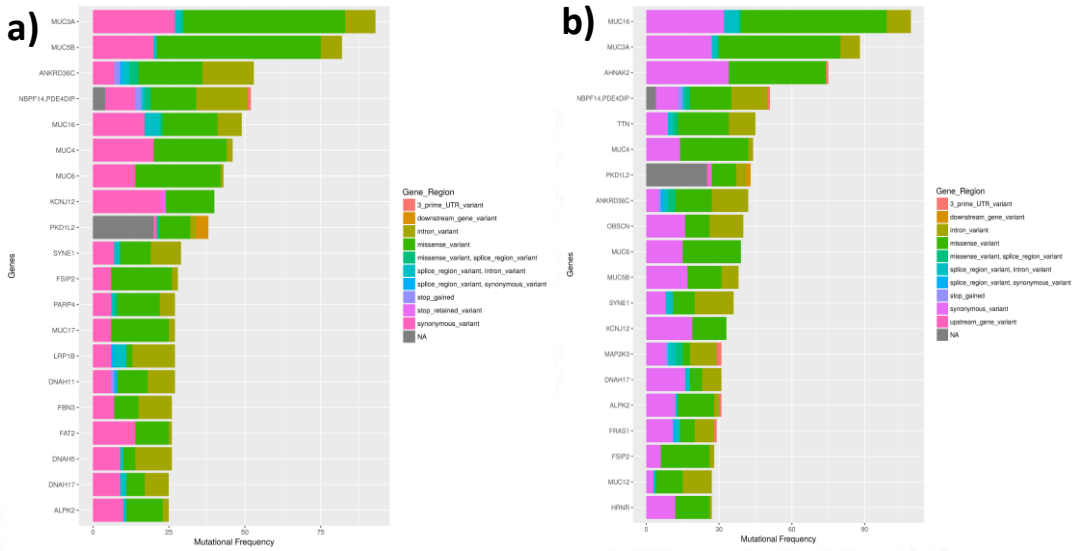

Figure 31: Genomic variations observed in the ATO resistant cell lines a) NB4 EV-AsR1 and b) UF1 cell line in comparison to NB4 naïve.

In NB4 EV-AsR1, except for the PML, we did not observe any additional mutation in the TCGA gene set. However, in UF1, there were additional novel mutations found in the DNMT3A, TP53, RUNX1, IDH2, SMC3, ARID1B, ARID1A, and PML genes addition to the known variations of AML TCGA gene set (figure 32a).

We validated the PML and p53 mutation using Sanger sequencing, where the ATO resistance-conferring mutation A216V was present in the in-house generated ATO resistant cell lines. UF1 had two intronic variations in the PML domain and was negative for A216V (figure 32b). We also noted that the existence of a p53 gain of function mutation (R248Q) in the in house generated ATO resistant cell line, which was also present in the parental naïve NB4 cell line. UF1 cell line had a point mutation (R196*) and a deletion of exon 10 of the p53 (Table 8), which are reported to be pathogenic.

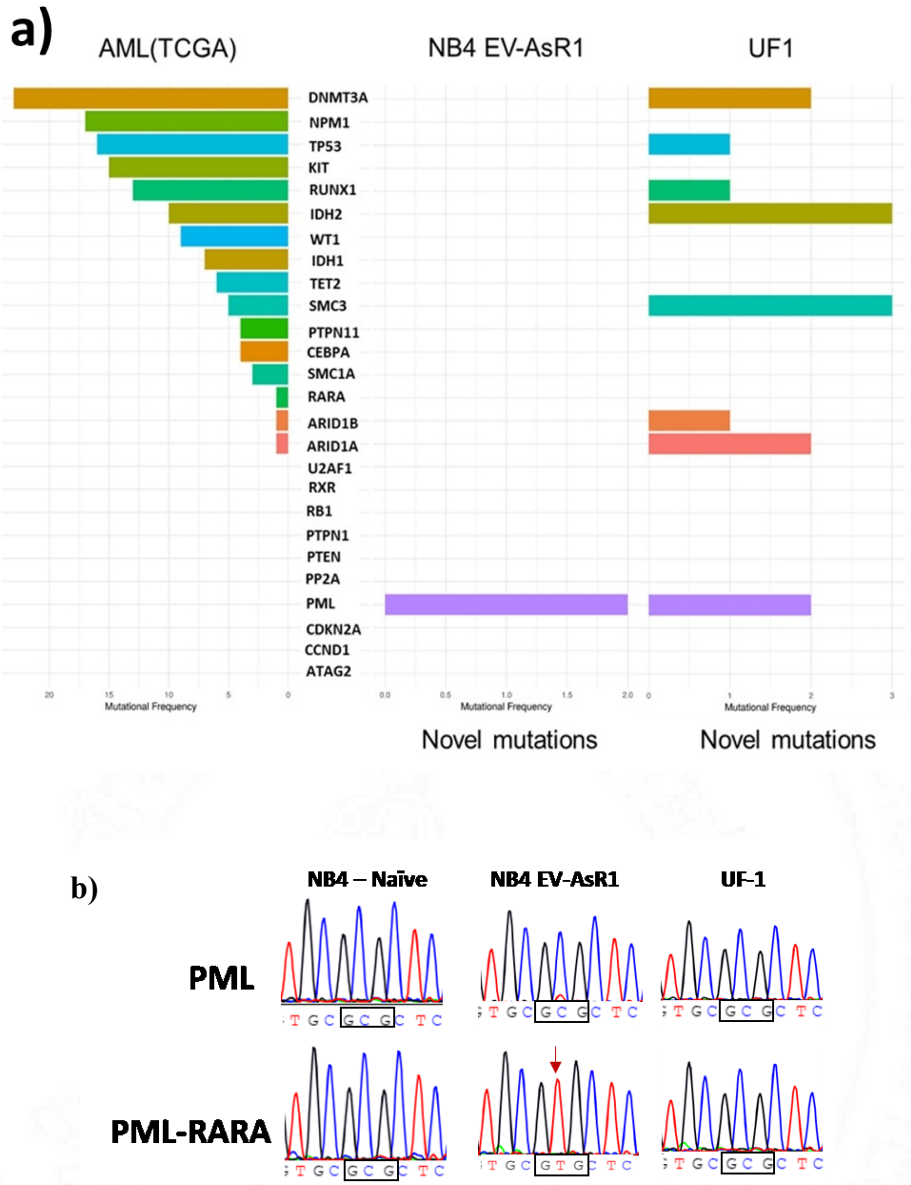

Figure 32: a) AML TCGA data set was compared with ASR1 and UF1, and the graph represents the known and novel mutations and their mutation frequency. b) Sanger sequencing showed the existence of PML – A216V in the inhouse generated ATO resistant cell line and not in the UF1, parental cell line NB4 naïve.

Cell line	Exon	TP53 mutation
NB4 naïve	7	c.743 G>A (R248Q)
NB4 EV-AsR1	7	c. 743 G>A (R248Q)
UF1	5	c.586 C>T (R196*)
	10	c.1083_1083 del (S362Afs*8)

Table 8: Mutations observed in the TP53 gene of ATO sensitive and ATO resistant cell lines.

We subjected NB4 naïve and one of the ATO resistant sub-clone (NB4 EV-AsR1) to gene expression profiling and UF1, observed that 1490 genes were differentially regulated (> 2-fold). Out of which 719 numbers were up-regulated, and 771 numbers were down-regulated. The pathways significantly enriched for differentially expressed genes were 'cell survival' 'cell cycle' 'immune regulation' ABC transporters, Glutathione metabolism, redox system, mitochondrial biogenesis, cellular respiration, and ubiquitin-proteasome degradation system (figure 33a).

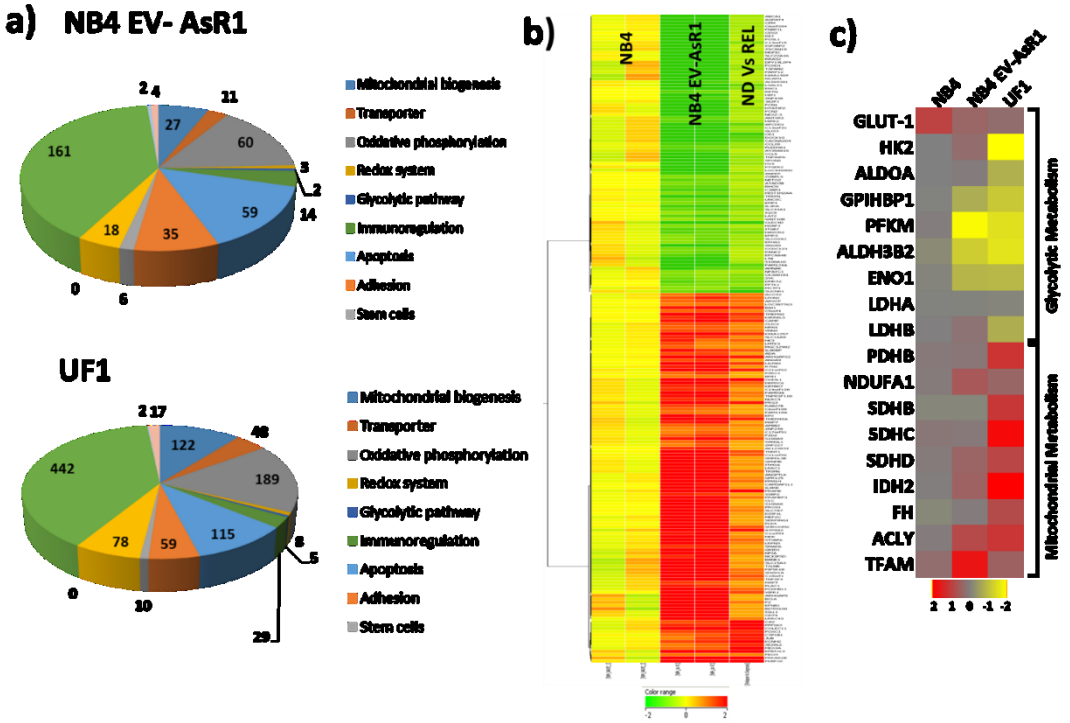

Figure 33: a) Pie chart representing the dysregulated genes in the inhouse generated ATO resistant cell line NB4 EV-AsR1 and UF1 in comparison to parental cell line NB4. b) Comparison of the GEP of NB4 EV-AsR1 and newly diagnosed and relapsed APL primary samples c) Heatmap representing the genes involved in the glycolytic and mitochondrial metabolism genes.

We also noted that the gene expression profile of the in-house generated ATO resistant cell line was similar to the gene expression profile of relapsed APL patients treated with front line ATO based regimens (figure 33b). Gene expression profiling revealed significant dysregulation of glycolytic and mitochondrial metabolism in the resistant cell line when compared to NB4 naïve (figure 33c).

4.2. ATO–resistant promyelocytic cells are metabolically distinct:

Baseline metabolic features, reactive oxygen species, glucose uptake, and the enzymes involved in the glycolytic pathway were found to be significantly down-regulated in the resistant cell lines (figure 34).

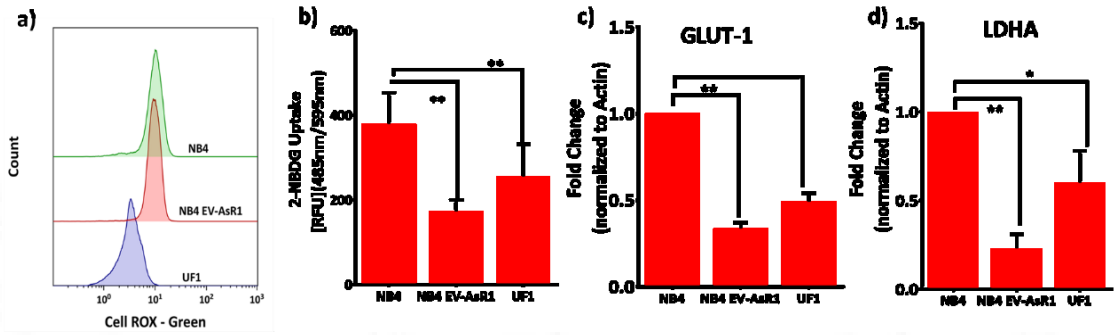

Figure 34: a) Baseline total reactive oxygen species were measured using redox-sensitive dye – cell ROX Green in the flow cytometry. b) Glucose uptake was measured using a fluorescent analog of 2- deoxy glucose and represented as relative mean fluorescence intensity. c) GLUT-1 and LDHA transcripts were significantly less in the resistant cell lines. Error bars represent the mean± SEM of 3 independent experiments ($p<0.05$, ** $p<0.01$, *** $p<0.001$).*

It is well known that the cancer cells rely on the Warburg effect (utilize glucose and undergoes aerobic glycolysis even in the presence of an ample amount of oxygen) and based on the basal metabolic differences in the resistant cell lines we performed metabolic flux analysis. Seahorse extracellular flux analysis revealed that the glycolytic capacity of the naïve NB4 cells is significantly higher in comparison to the resistant cell lines (figure 35).

a)

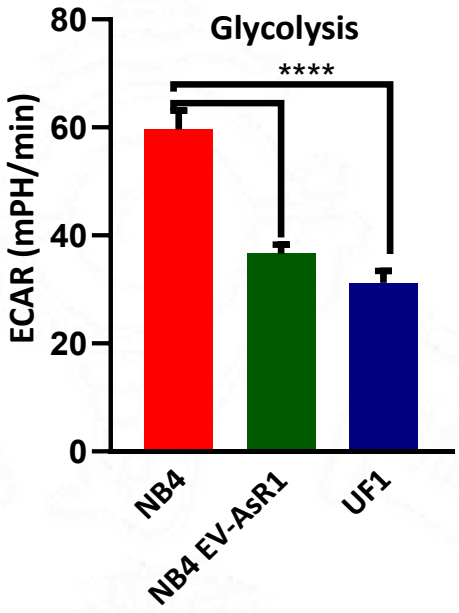

b)

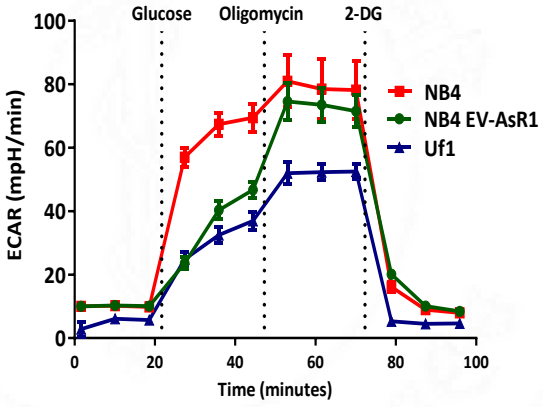

Figure 35: Representative result of the glyco-stress test on the NB4 naïve and ATO resistant cell lines shows an increased rate of glycolysis in the parental cell line. Error bars represent the mean± SD of independent experiments (p<0.05, **p<0.01, ***p<0.001).*

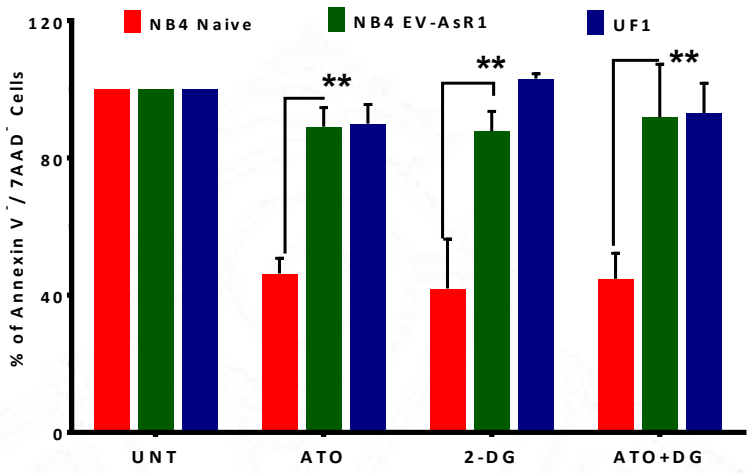

Figure 36: Viability of the sensitive and resistant cell lines post 48 hours glycolytic inhibitor ATO and 2-DG treatment. (ATO = 2uM; 2-DG= 5mM; n=6; viability was assessed using annexin-V- 7AAD). Error bars represent the mean± SEM of independent experiments (p<0.05, **p<0.01, ***p<0.001).*

To address the degree to which glycolysis is necessary, we treated the naïve NB4 and ATO resistant cell lines to 2-Deoxy glucose (2-DG), a glucose analog that inhibits glycolysis via its action on hexokinases. We noted that naïve NB4 cell line viability was significantly affected in the presence of a glycolytic inhibitor 2-Deoxy glucose (2-DG) equivalent to the effect seen with 2uM of ATO. There was no evidence of an additive effect when these two agents were combined (figure 36). In contrast, the viability of the resistant cell line was not significantly affected when the 2-DG was used alone at the same concentrations or when it was combined with ATO (figure 36). The data suggest that the ATO resistant cell lines were not relying on the Warburg effect, for their proliferation and survival.

As the glycolytic inhibition by 2-DG promoted apoptosis in NB4 cells as comparable to ATO. We performed in-vivo glycolytic inhibition to understand the physiological relevance of glycolytic inhibition in the ATO sensitive transplantable APL mouse model (figure 37a). We observed that 2-DG or ATO as single agents reduced the leukemic burden in the peripheral blood (PB) (figure 37b), bone marrow (BM) (figure 37c), and PML-RARA copy number in BM (figure 37d) at the end of 22 days to levels that were comparable and indistinguishable from each other.

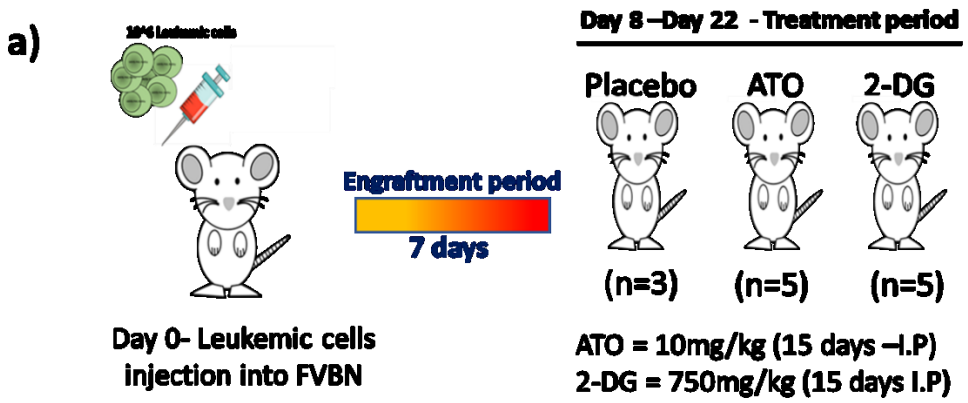

Figure 37: Reduction of the leukemic burden by glycolytic inhibition: a) Schematic representation of the in vivo APL mouse model experimental plan.

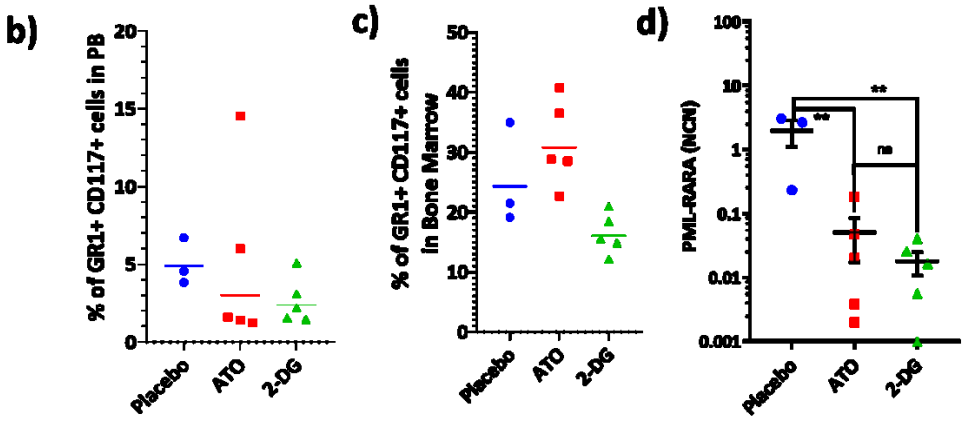

Figure 37: Reduction of the leukemic burden by glycolytic inhibition: Post 15 days of treatment with single agents of ATO (10mg/kg) and 2-DG (750mg/kg), the animals were sacrificed. The percentage of blasts (CD117+ and GR1+) were assessed in the b) peripheral blood (PB), c) bone marrow, and c) PML-RARA transcripts in the bone marrow.

We then further evaluated the effect of mitochondrial oxidative phosphorylation (OXPHOS) inhibitor on these cell lines. We anticipated that the resistant cell lines viability would be significantly affected by FCCP (an un-coupler of OXPHOS) treatment since they do not rely on the Warburg effect. However, we observed that the viability of the resistant cell lines remained unaffected when FCCP was used as a single agent, whereas when we combined it with ATO, the combination significantly reduced the viability. In ATO sensitive naïve NB4 cells, there was no significant additive effect of the combination of ATO+FCCP (figure 38).

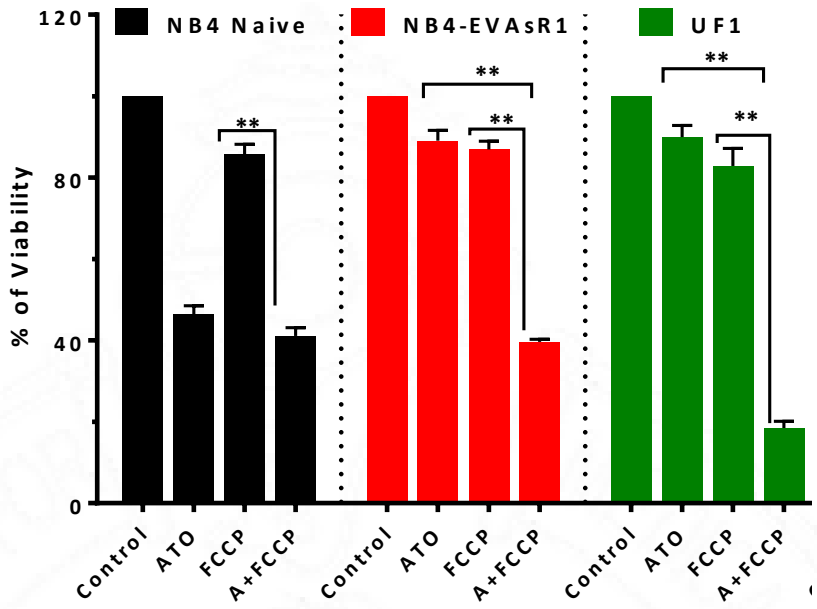

Figure 38: Viability of the sensitive and resistant cell lines when treated with OXPHOS uncoupler in combination with ATO. (ATO = 2uM; 2-DG= 5mM; FCCP =10uM; n=6; viability was assessed using annexin-V- 7AAD). Error bars represent the mean± SD of independent experiments (p<0.05, **p<0.01, ***p<0.001).*

4.3 Non-APL ATO resistant AML cells are also metabolically distinct:

As we observed that the ATO resistant APL cell line had a significant metabolic adaptaion to confer resistance to ATO, we extended evaluations of the metabolic properties of non-M3 AML cell lines. AML cell lines (U937, THP-1, and Kasumi-1) had significantly lower levels of glucose transporter (GLUT1) expression when compared to ATO sensitive APL cell line NB4 (figure 39a).

We also validated this observation on primary samples of APL, AML, ALL, and normal cells (MNC, CD34 positive cells, and Granulocytes (GRAN)) (figure 39b).

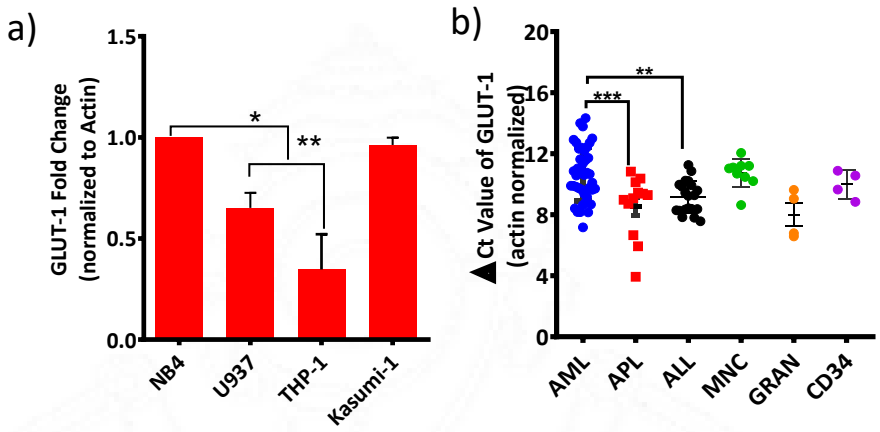

Figure 39: RQ-PCR analysis of GLUT-1 expression ATO sensitive APL cell line (NB4 naïve) and primary APL cells (n=12) in comparison to the AML cell lines and primary AML cells (n=42), primary ALL (n=20), and normal cells- MNC (n=10), GRAN (n=5), CD34 positive cells (n=4). (dCT value inversely proportional to the mRNA transcript levels) Error bars represent the mean± SEM of independent experiments (p<0.05, **p<0.01, ***p<0.001).*

To assess the reliance of the glycolytic pathway for survival, we treated the AML cell lines with glycolytic inhibitors, 2-Deoxy Glucose (2-DG) and arsenic trioxide (ATO). We observed that there was no significant reduction in the viability except in the APL cell line NB4 naïve (figure 40).

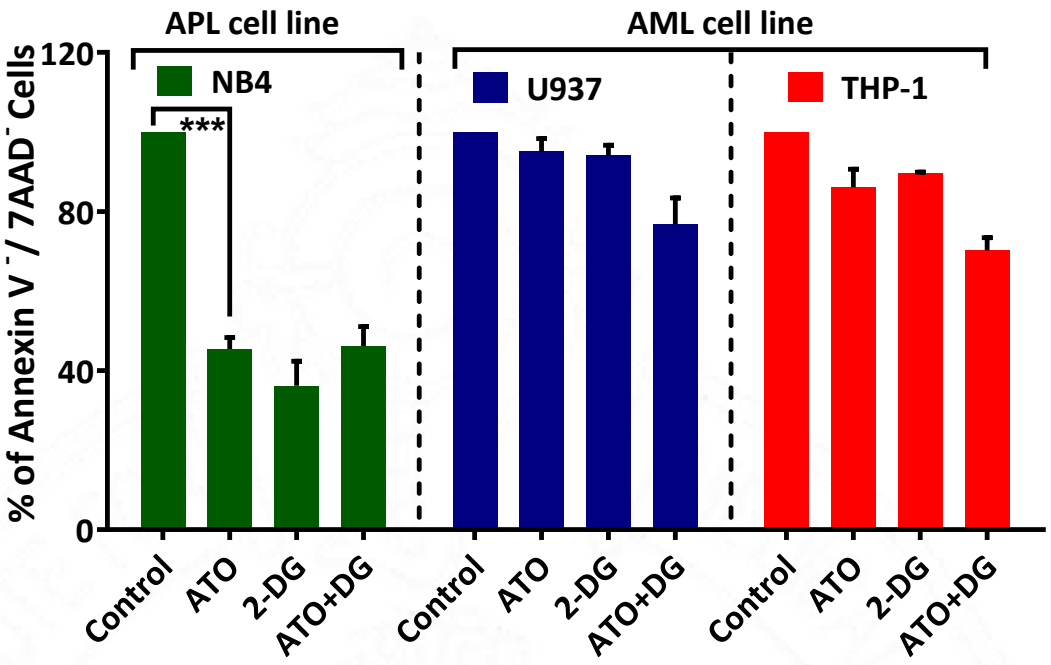

Figure 40: Viability of the ATO sensitive APL cell line and non-APL ATO resistant cell line post 48 hours of ATO with 2-deoxy glucose treatment (n=5; ATO=2uM; 2-DG = 5mM). Error bars represent the mean± SEM of independent experiments (p<0.05, **p<0.01, ***p<0.001).*

Whereas when the cells were treated FCCP (mitochondrial uncoupler) and ATO (glycolytic inhibitor), there was a significant reduction in the viability. However, the effect of this combination on the malignant cells was not specific, and we also noted that there was a significant bystander effect on the normal peripheral blood mononuclear cells (figure 41)

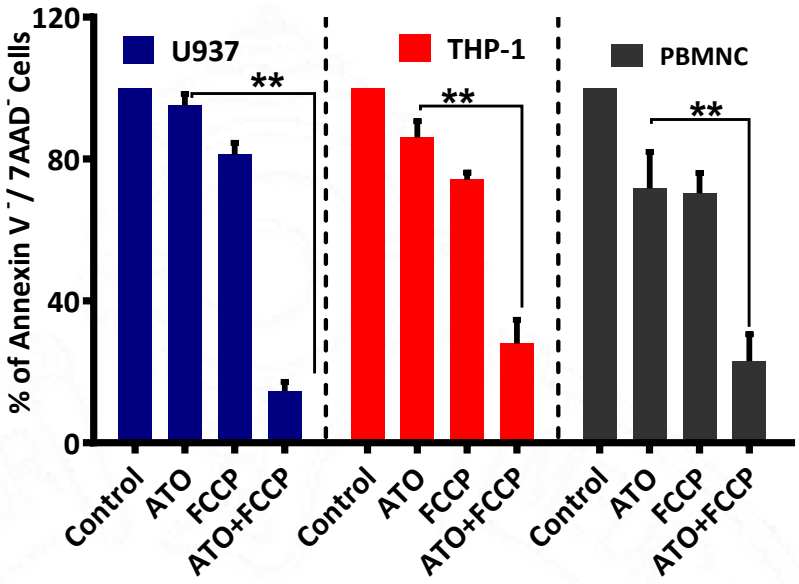

Figure 41: Viability of the non-APL ATO resistant cell lines and Healthy control - peripheral blood mononuclear cells post 48 hours of ATO with FCCP treatment (n=5; ATO=2uM; FCCP = 10uM). All error bars represent the mean± SEM of independent experiments (p<0.05, **p<0.01, ***p<0.001).*

4.4. Bone marrow microenvironment and metabolic adaptations

4.4.1 Bone marrow microenvironment protect leukemic cells from chemotherapeutic agents in a contact-dependent and independent system:

When the leukemic cells were co-cultured with the stromal cells in a contact-dependent and independent system, there was a significant protective effect given by the stromal cells to leukemic cells against the apoptotic action of the ATO and cytosine arabinoside (ARA-C) (figure 42).

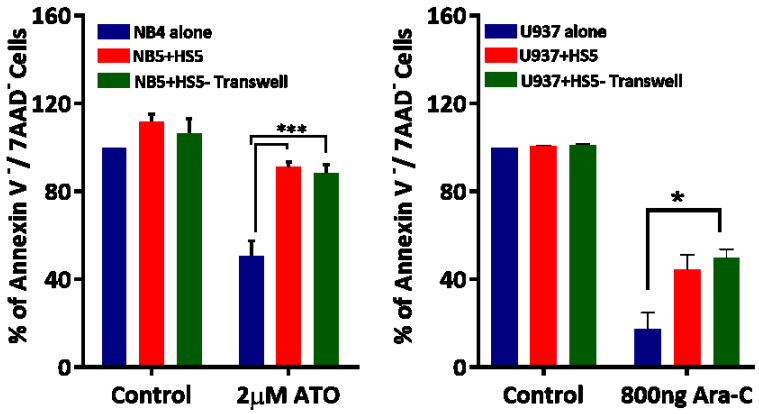

Figure 42: Viability of NB4(left) and U937 cells(right) cultured in a contact-dependent / independent system and treated with 2uM ATO (NB4) and 800ng of Ara-c (u937). Blue bars – leukemic cells alone, red bars – leukemic cells in contact with stromal cells HS5 and the green bars – leukemic cells cultured in trans well system). All error bars represent the mean± SEM of independent experiments (p<0.05, **p<0.01, ***p<0.001).*

We observed that when the NB4 are co-cultured with stromal cells there were significant changes in the metabolic features such as less proliferation rate, enrichment of G0/G1 population, increased levels of autophagy and a lower amount of reactive oxygen species even in the presence of chemotherapy as a protective mechanism (figure 43).

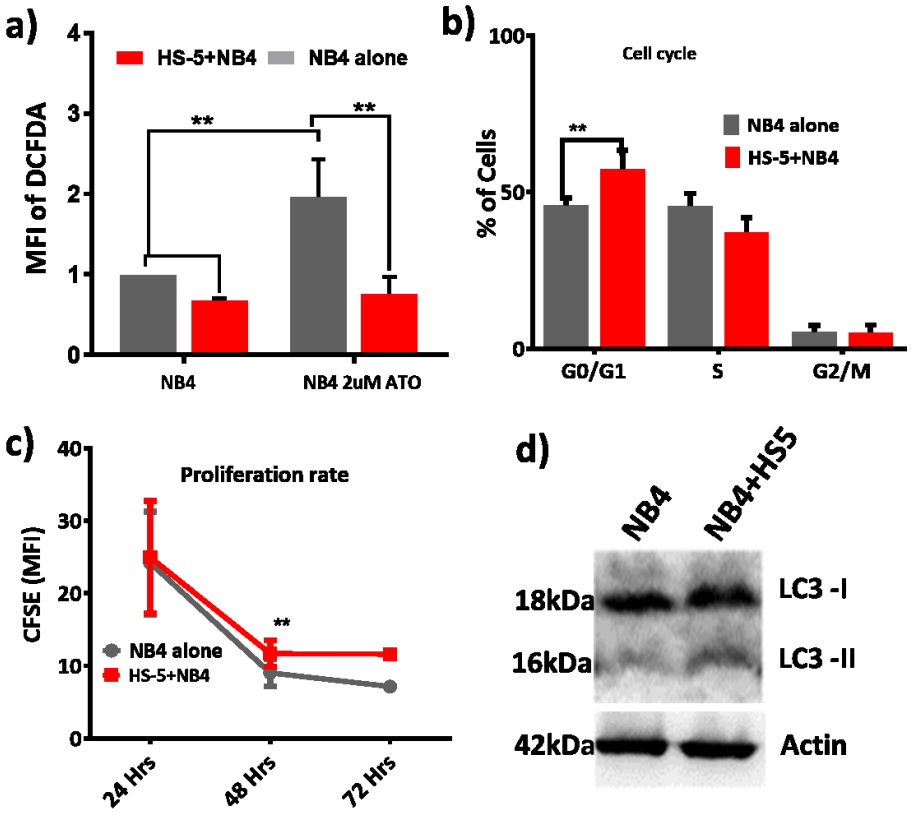

Figure 43: Baseline metabolic adaptations in the NB4 cell line in the presence of stromal cells. a) ROS levels b) cell cycle phase c) line graph representing the proliferation rate (CFSE staining) d) LC3- I to LC3-II conversion representing the basal autophagy levels. (n=3). Error bars represent the mean± SEM of independent experiments (p<0.05, **p<0.01, ***p<0.001).*

We also observed that when the leukemic cells are cultured in a contact-dependent system, there was a transfer of mitochondria from the stromal to the leukemic cells. The transfer was significantly increased in the presence of chemotherapeutic agents as a protective mechanism to maintain cell survival (figure 44).

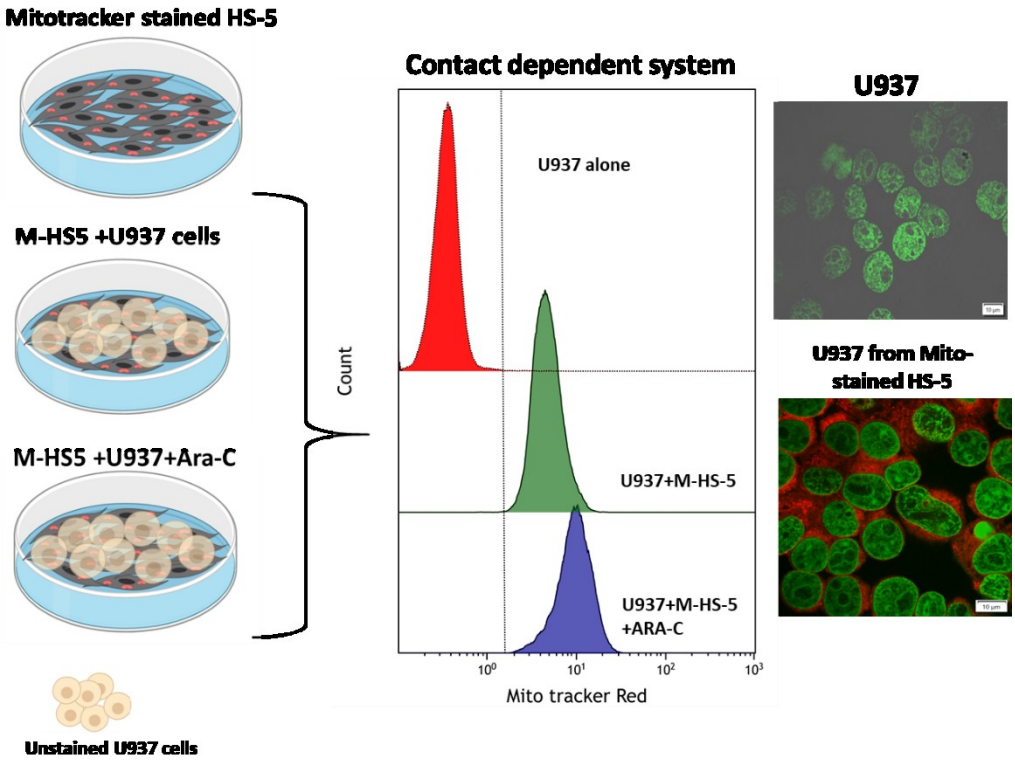

Figure 44: a) Experimental design of U937 cells were cultured onto the mitotracker red cmx-ROS stained stromal cells. Post 24 hours, U937 cells were collected from the contact system and assessed for the mito tracker staining. (n=3). b) Histograms in the change of intensity of the Mito-Tracker red in comparison to the cell alone. c) confocal images of the U937 cells, which are obtained after in contact with the mito-stained stromal cells. (n=3).

We also assessed whether this transfer requires direct contact as we observed a significant protective effect, even in the absence of direct contact system. Hence, we cultured the U937 cells with the supernatant harvested from the mito-tracker stained stromal cells post 24 hours treated with and without ara-c. We fractionated the supernatant into total and less than 0.2micron to assess the role of other cellular vesicles in carrying the mitochondria to the leukemic cells. We found

there were significant levels of transfer in both the total and 0.2micron filtered supernatant (figure 45).

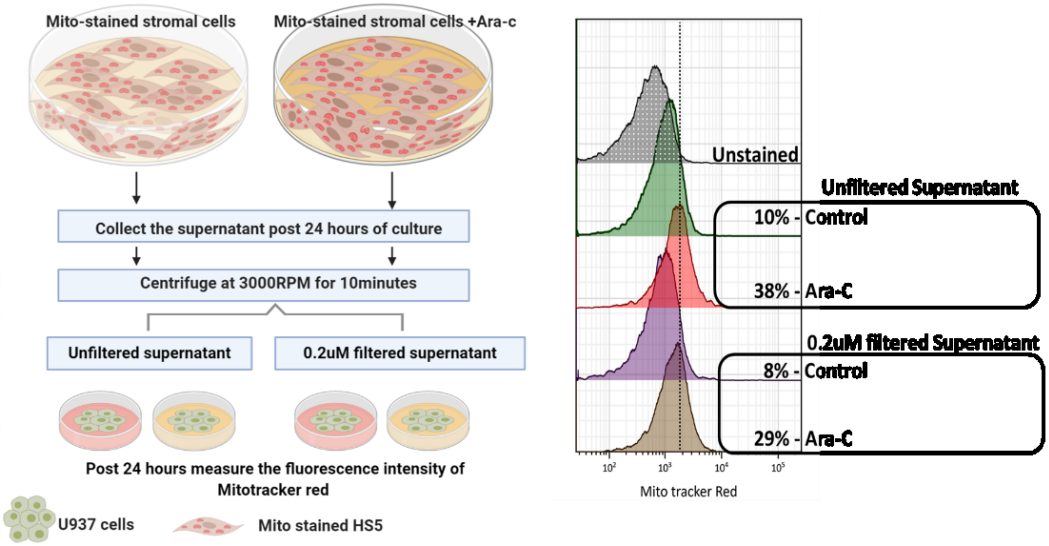

Figure 45: a) Experimental scheme to assess the contact-independent contact transfer of mitochondria from the stromal cells to leukemic cells. b) Histograms representing the gain of Mito-Tracker red fluorescence in the leukemic cells and also the percentage of cells positive for the stain are represented.

4.4.2. Metabolic inhibitors abrogate the protective effect provided by the stromal cells:

We have reported earlier that stromal cells protect the NB4 cells from ATO induced apoptosis. Based on the observation of significant metabolic changes of the leukemic cells in contact with stromal cells, we assessed the impact of metabolic disruptors in overcoming bone marrow microenvironment mediated drug resistance. When ATO was treated in combination with 2-Deoxy glucose and FCCP in a co-

culture system, the protective effect given by the stromal cells to leukemic cells against ATO was abrogated significantly (figure 46).

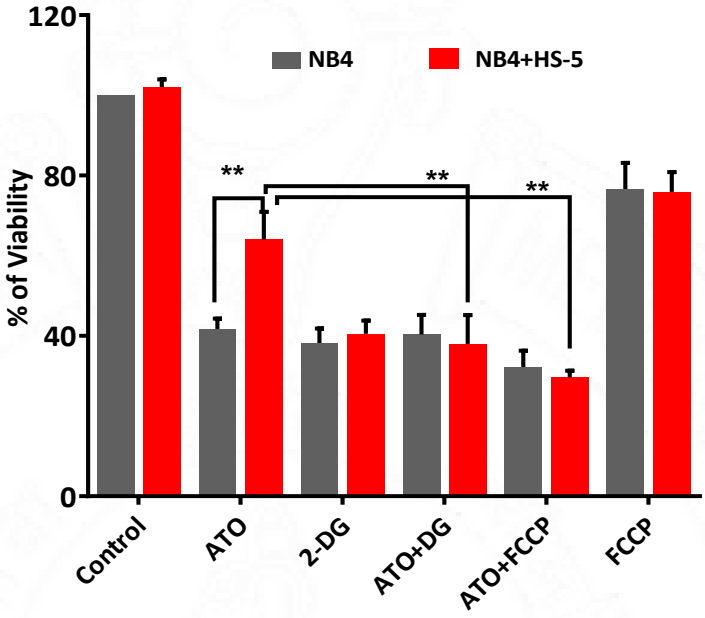

Figure 46: Viability of the NB4 cells in the presence and absence of stromal cells and the effect of metabolic inhibitors (2-DG, FCCP) in combination with ATO. (n=4; ATO=2uM; FCCP=10uM; 2-DG = 5mM; 48 hours). Error bars represent the mean± SEM of independent experiments (p<0.05, **p<0.01, ***p<0.001).*

4.5 Strategies to overcome the metabolic adaptation of the leukemic cells:

4.5.1 Drug repurposing approach to target the metabolic adaptations:

Our observations suggest that naïve ATO sensitive cells are dependent on the glycolytic pathway for survival. In contrast, ATO resistant cell lines (including AML cell lines) can switch between the two energy-producing pathways efficiently when one is inhibited.

Combined inhibition of these pathways by agents that have specificity towards the leukemia cells over normal cells could potentially be a strategy to address these adaptations. Hence, we employed the drug repurposing approach to target mitochondrial metabolism. FDA approved small molecule screening compounds were chosen based on the existing literature, and their effect of mitochondrial respiration focused on dissipating the mitochondrial membrane potential (Gohil et al., 2010b).

We performed the initial screening experiments in the U937 (AML M5 - monocytic) cell line. We treated the U937 cells with the intended screening compounds (targeting the mitochondrial respiration) for 48 hours, either alone or in combination with ATO. We found that the effect of the mitochondrial inhibitors as a single agent at a dose of 5uM did not significantly affect the survival of the leukemic cells, whereas, in combination with ATO, some of the mitochondrial inhibitors showed profound effect (figure 47).

Artesunate (ART), an anti-malarial drug sesquiterpene with anticancer properties, showed more significant synergy with ATO in comparison to other members of artemisinin family and metabolic inhibitors screened (figure 47).

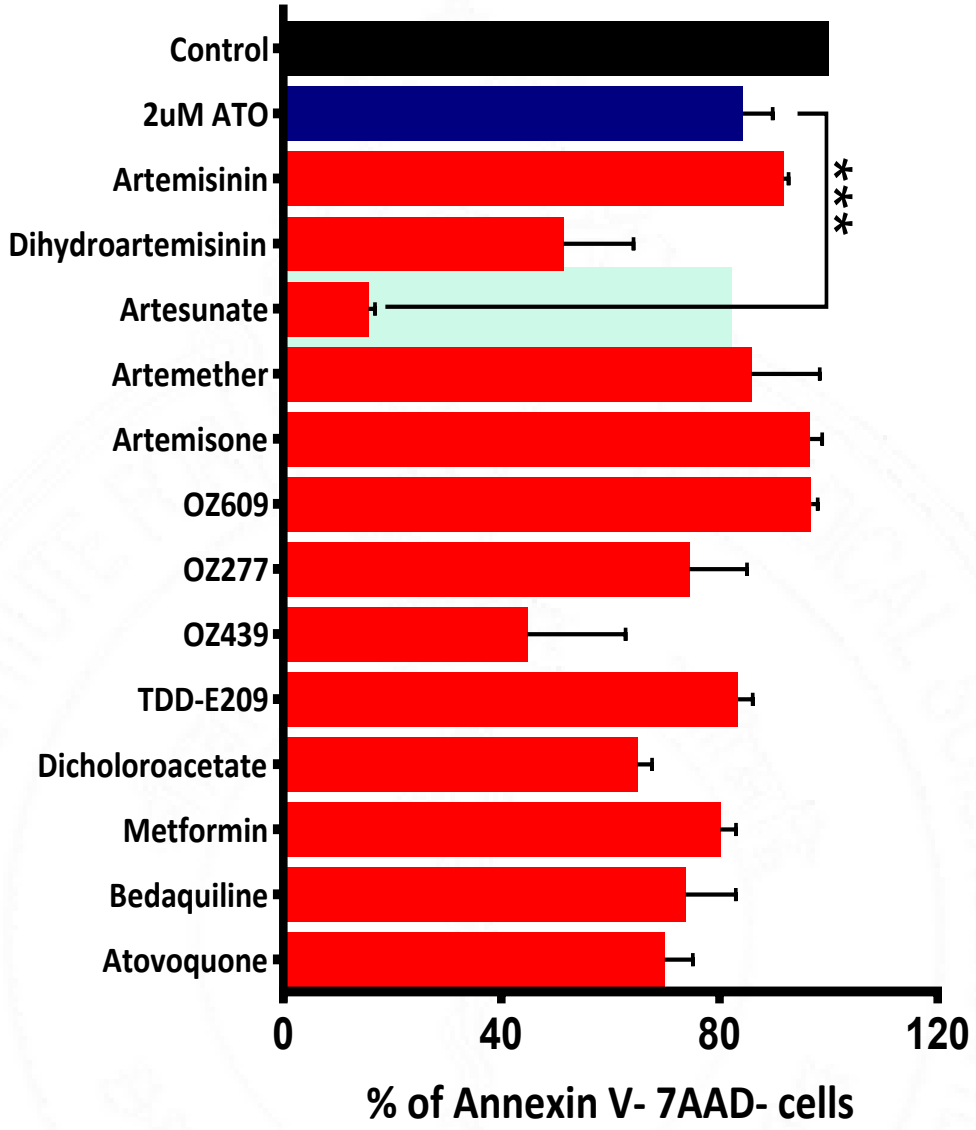

Figure 47: Screening of drugs targeting the mitochondrial OXPHOS in combination with 2uM ATO on U937 cells (ATO resistant AML cell line) (n= 4; 48hours; ATO =2uM and other drugs at 5uM). Blue bar represents ATO alone, and the red bars represent the viability of U937 cells in combination with mitochondrial inhibitors. All error bars represent the mean± SEM of independent experiments (p<0.05, **p<0.01, ***p<0.001).*

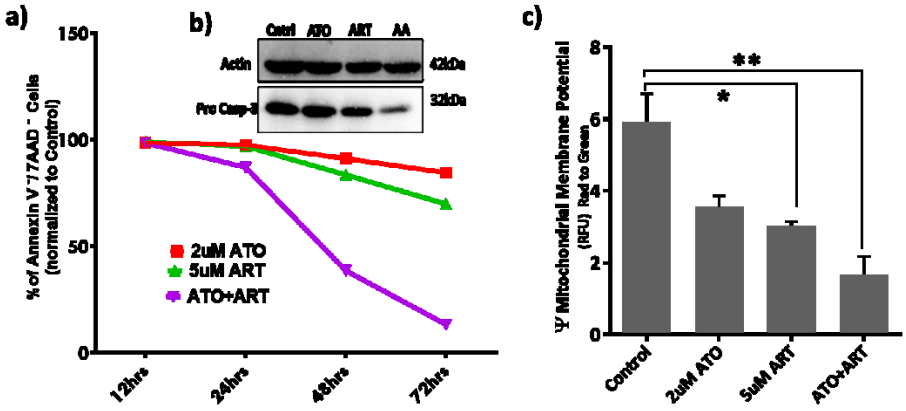

Figure 48: a) Viability of U937 cells treated with ATO, ART, and ATO+ART after 12hrs, 24hrs, 48hrs, and 72hrs. b) Immunoblot of U937 cells post 48 hours drug treatment probed for Pro-caspase-3 protein levels of U937 cells; actin was used as a loading control. c) Post 24 hours of drug treatment, mitochondrial membrane potential was assessed using JC-1 ratiometric dye. (n=3; ATO =2uM; ART = 5uM)

Time-course experiments revealed that the combination promotes time-dependent cell death in the U937 cells. Apoptosis is also validated by probing for pro-caspase-3 levels post-treatment with the combination (figure 48a and b). The mitochondrial membrane potential is also significantly reduced in the presence of ATO and ART, suggesting the decline in mitochondrial function (Figure 48c).

Seahorse extracellular flux analyzer mitochondrial stress test was also performed to assess the ART induced mitochondrial dysfunction (Figure 49a). We observed that ART-treated cells had a significant increase in the proton leak and a decline in the ATP production rate validating uncoupled respiration for cell survival in the ART alone treatment (figure 49b and c).

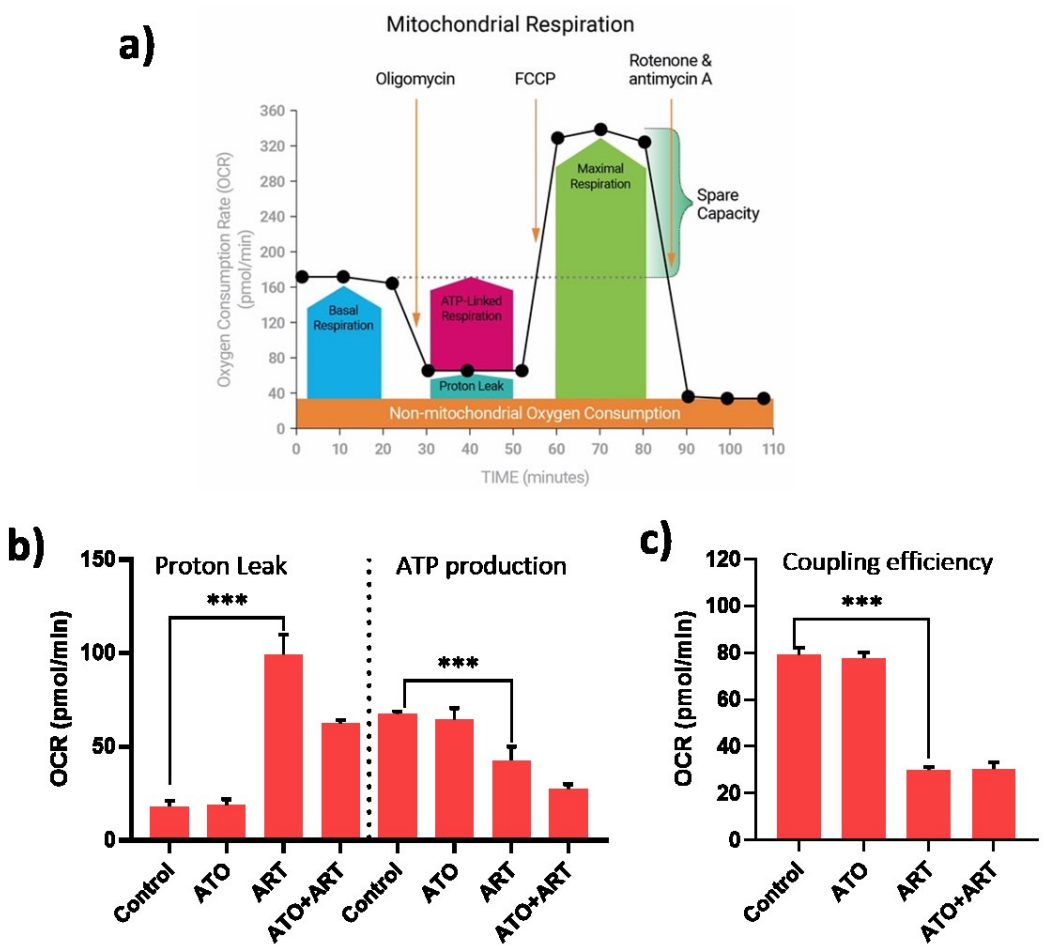

Figure 49: Mito-stress test of U937 cells treated with 2uM ATO, 5uM ART, and in combination for 6 hours. a) Overview of the mito-stress test. Post 6 hours of the treatment with ATO and ART, the cells were assessed for their mitochondrial function. b) proton leak and amount of ATP production c) coupling efficiency of the cells. Coupling efficiency is calculated by ATP production rate / Basal respiration X 100; Proton leak = minimum rate of OCR measurement after oligomycin injection – non-mitochondrial respiration). oxygen consumption rate-OCR. (n=3; ATO =2uM; ART = 5uM)

4.5.2 Arsenic trioxide and artesunate reduced the viability of different subtypes and types of acute leukemia cell lines:

ART is widely used in the treatment of complicated and uncomplicated malaria. ART is also is under Phase I clinical trial for the management of colorectal carcinoma (Krishna et al., 2014). Based on the existing literature, ART seems to have a low toxicity profile, greater bioavailability, routes of administration, and cost-effectiveness in comparison to the conventional chemotherapeutic agent used in the treatment of leukemia cytosine arabinoside (Ara-C) and daunorubicin (DNR) (7+3 induction therapy).

Hence, we evaluated the effect of ATO and ART combination on the other AML cell line, which are harboring different cytogenetic and molecular aberrations.

We observed that the combination significantly affected the viability of other subtypes of AML (Figure 50 -THP-1, Kasumi-1 and MV 4;11) and ALL cell lines (figure 51- SUP B-15, Jurkat E6.1, and MOLT-4). The combination had only a minimal bystander effect on the normal CD34 positive stem cell and peripheral blood cells (figure 52).

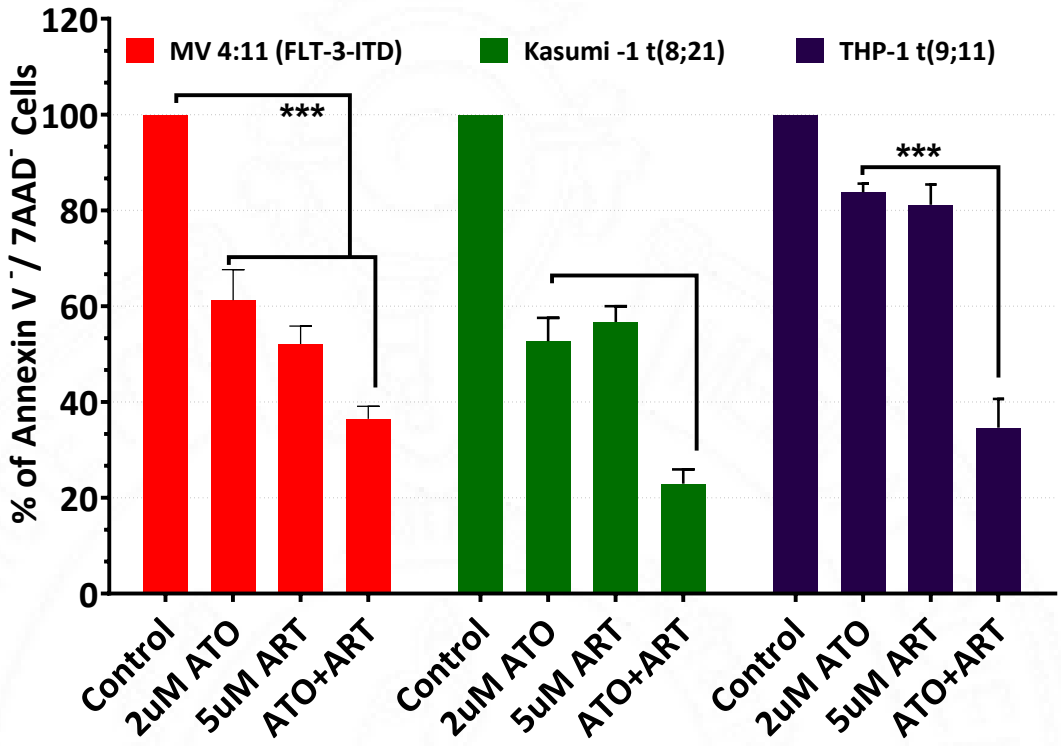

Figure 50: Viability of different AML cell lines harboring different molecular aberrations post 48 hours ATO and ART treatment (n=8; 2uM of ATO and 5uM of ART). All the error bars represent the mean± SEM of independent experiments (p<0.05, **p<0.01, ***p<0.001).*

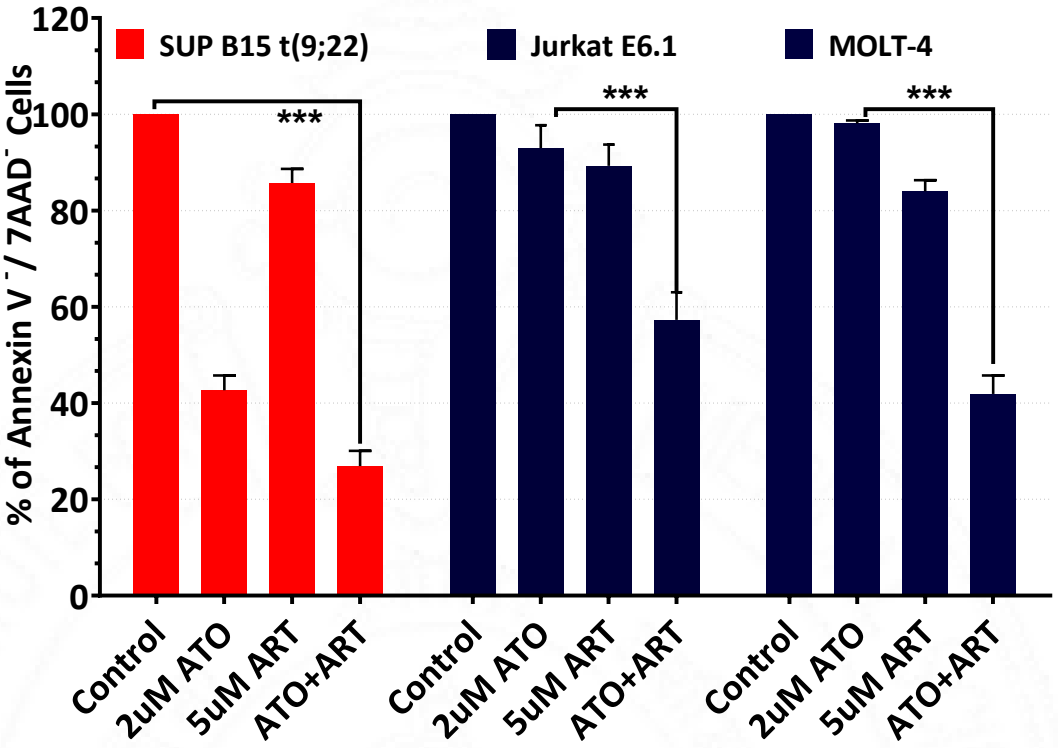

Figure 51: Viability of ALL cell lines harboring different molecular aberrations SUP B-15 (BCR-ABL1 translocation) and Jurkat E6.1 and MOLT-4 (T-cell ALL) post 48 hours ATO and ART treatment (n=8; 2uM of ATO and 5uM of ART). All the error bars represent the mean± SEM of independent experiments (p<0.05, **p<0.01, ***p<0.001).*

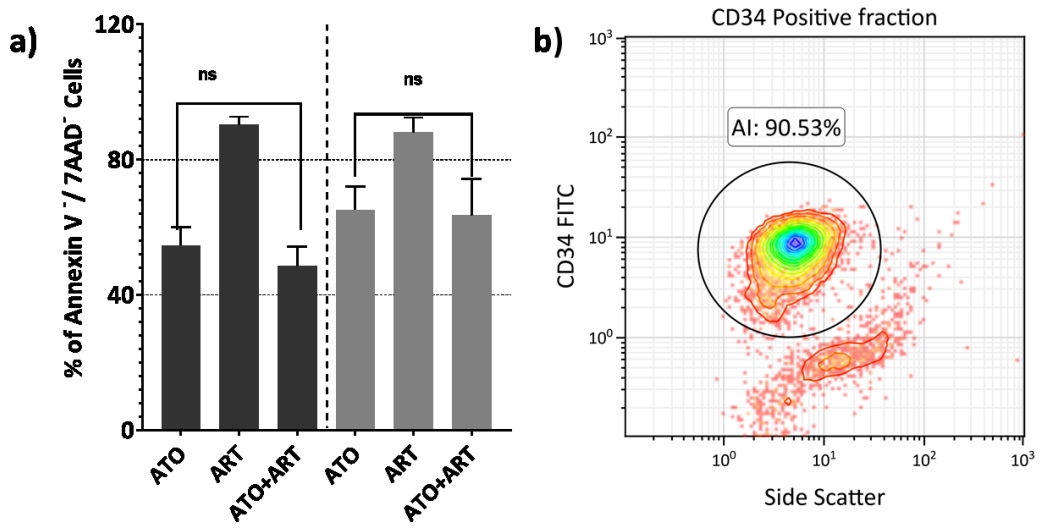

Figure 52: Viability of different healthy control peripheral blood (PB) and CD34 positive cells cell lines post 48 hours ATO and ART treatment (PB -n=8; CD34- n=3) 2uM of ATO and 5uM of ART). All the error bars represent the mean± SEM of independent experiments (p<0.05, **p<0.01, ***p<0.001). b) Representative dot plot represents the percentage of enriched CD34 positive cells used for the assay.*

4.5.3: ATO+ART affects the mitochondrial dynamics of the leukemic cells:

We assessed the effect of ATO and ART on the mitochondrial dynamics (fusion and fission), as the viability of the leukemic cells was unaffected by the treatment of ART alone or ATO alone.

We stained the U937 cells with Mito tracker -Red CMxROS dye post 24 hours of drug treatment with ATO and ART. We observed tubulated mitochondria in control, and ATO treated cells, whereas ART-treated cells showed fragmented

mitochondria, and the fragmentation was further enhanced in the combination treatment (figure 53a).

Studies suggest that in response to mitochondrial damage, the cells try to clear out the damaged mitochondria via the process of mitophagy (Youle and van der Bliek, 2012b, Anyasor et al., 2009). Fission and fusion are key steps of the mitophagic process. As ART induced mitochondrial damage, we measured the genes which are involved in fission and fusion of the mitochondria. We noted that the fission machinery of mitochondria - Fis1 and Drp1 were significantly up-regulated at the transcript level in comparison to the fusion machinery in the ART-treated U937 cells, and it was further enhanced in the combination. (figure 53b)

To assess the importance of mitochondrial fission and fusion process in ART and ATO induced apoptosis, we treated the leukemic cells with mitochondrial fission inhibitor mdivi-1 (Mitochondrial Division Inhibitor 1) alone and in combination with ART and ATO+ART. The combination of ART with mdivi -1 resulted in enhanced toxicity and not when combined with ATO. The addition of midivi-1 enhanced the cytotoxic effect of the combination ATO+ART (Figure 53c).

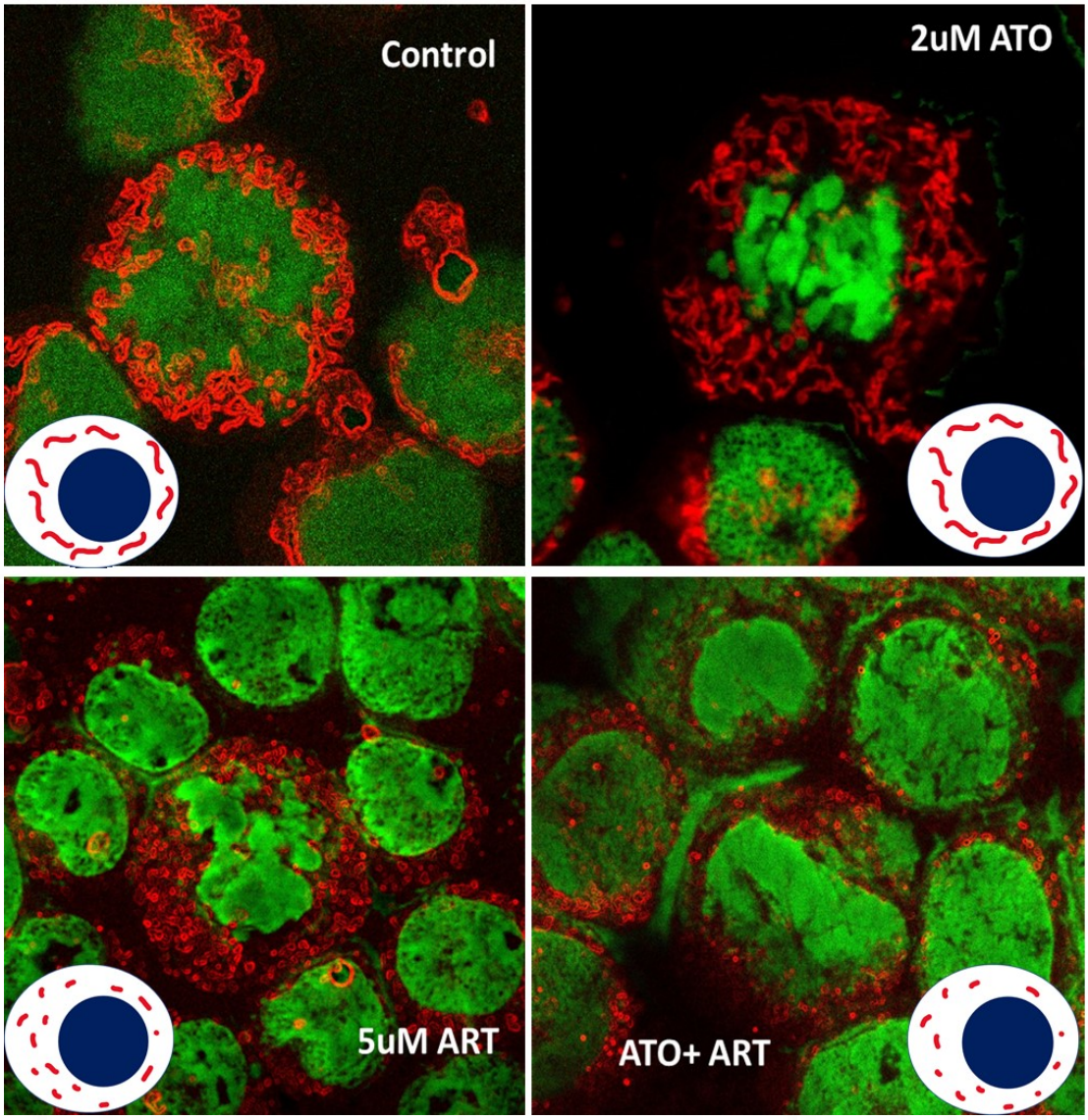

Figure 53: a) Mito tracker Red-CMxROS staining of U937 cells post 24 hours of drug treatment. Images were acquired in Olympus FV3000 using 60X objective oil immersion magnification. (n=3; ATO =2uM; ART = 5uM). Control and 2uM ATO treated cells showing tubulated forms of mitochondria, whereas in the ART and combination treatment showed a reduction in the mitochondria and also fragmentation.

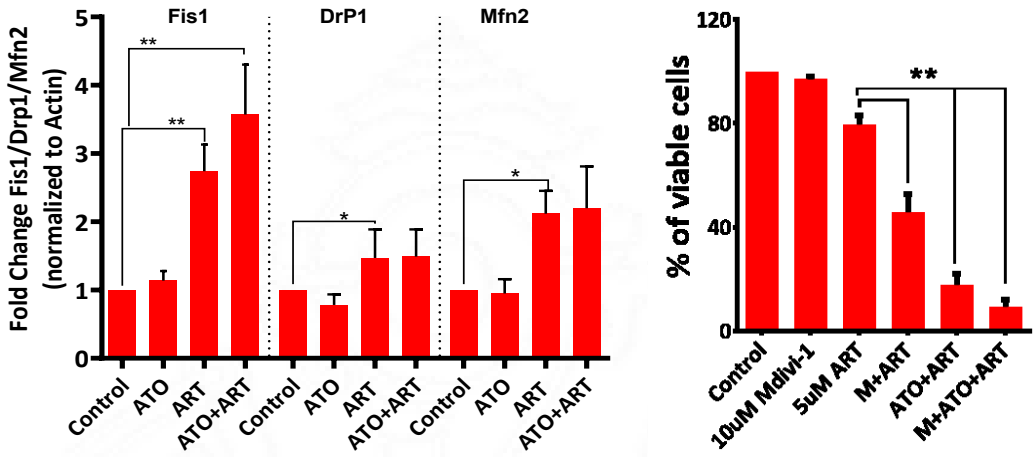

Figure 53: b) Transcript levels of mitochondrial fission (Fis1 and DrP1) and fusion gene (Mitofusin 2) were measured in the U937 cells post 24 hours of treatment (n=3; ATO=2uM; ART =5uM). c) Post 48 hours viability of U937 cells treated with 10uM of mdivi-1 in combination ART and ATO+ART. (n=6; ATO= 2uM; ART = 5uM). All the error bars represent the mean± SEM of independent experiments (p<0.05, **p<0.01, ***p<0.001).*

4.5.4 Artesunate positively affects compensatory metabolic pathways:

As the leukemic cells survived the mitochondrial inhibition alone (ART), we questioned whether it is due to the upregulation of other compensatory energy metabolism pathways. Hence, we assessed the effect of the artesunate on the other metabolic pathway such as glycolysis, glutamylosis, and fatty acid metabolism. GLUT-1 expression for glycolysis, glutaminase (GLS) expression for glutamine metabolism, and CD36 for fatty acid uptake was used as indicative of the different metabolic pathways. We observed that glutaminase and glut-1 transporters were

significantly up-regulated in the presence of ART as a compensatory survival mechanisms (figure 54).

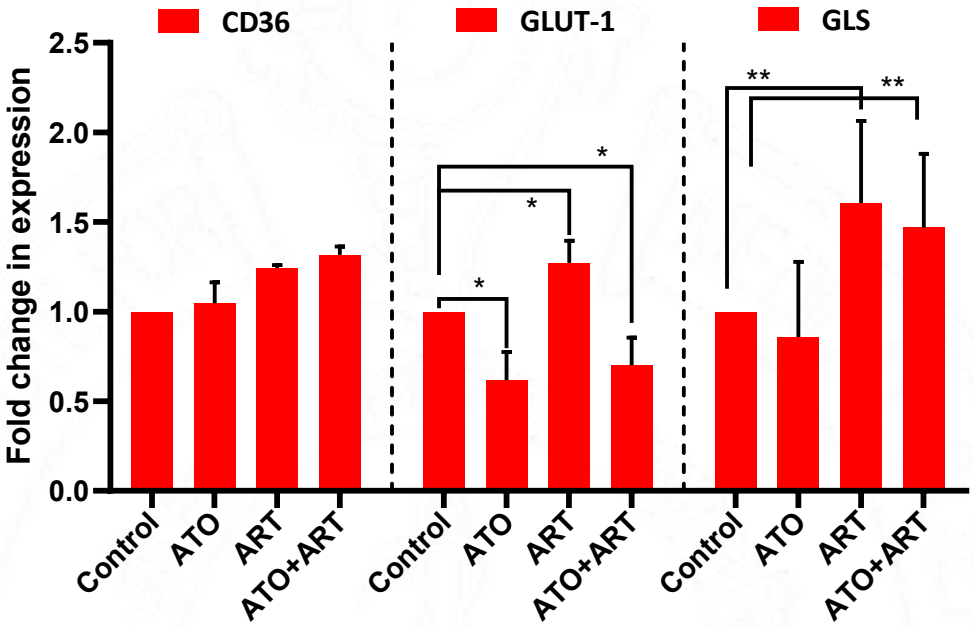

Figure 54: Cell surface expression of FA uptake transporter CD36 and transcript levels of GLUT-1 and GLS were measured post 24 hours treatment. (U937 cells ; n=3; ATO=2uM; ART= 5uM; time point 24 hours). All the error bars represent the mean± SEM of independent experiments (p<0.05, **p<0.01, ***p<0.001).*

This data further suggests that ATO is not affecting the mitochondrial or fatty acid metabolism (CD36 and GLS) only affecting the glycolytic pathway (GLUT-1).

4.5.5: Effect of ATO and ART on the anti-apoptotic proteins:

As the mitochondria are the central hub for the anti-apoptotic and apoptotic machinery, we also evaluated the impact of the combination and single agents on the anti-apoptotic protein machinery. We also assessed whether the combination effect was dependent on a cell anti-apoptotic protein dependency such as BCL-2, BCL-XL, and MCL-1. We observed that BCL-2 and BCL-XL expression is significantly increased in the presence of ART and down-regulated the MCL-1 anti-apoptotic protein (figure 55).

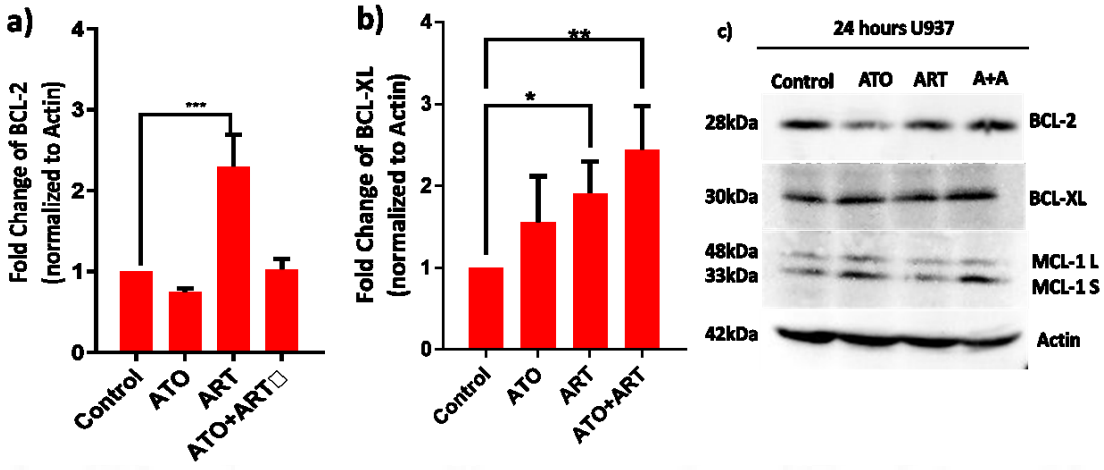

Figure 55: Transcript levels of BCL-2 (a) and BCL-XL (b) levels in U937 cells treated with ATO and ART for 24hours. (n=5; ATO=2uM; ART= 5uM; time point 24 hours). All the error bars represent the mean± SEM of independent experiments (p<0.05, **p<0.01, ***p<0.001). c) Immunoblots of the anti-apoptotic proteins post 24 hours of treatment BCL-2 and BCL-XL and MCl-1 anti-apoptotic protein levels of U937 cells treated with ATO and ART for 24 hours.*

4.6 Arsenic trioxide and artesunate show selective specificity towards malignant cells:

We also observed that ART treatment did not affect the mitochondrial staining of the normal cells (lymphocytes, monocytes, granulocytes, and CD34 positive cells) and showed greater specificity towards the malignant cells (figure 56).

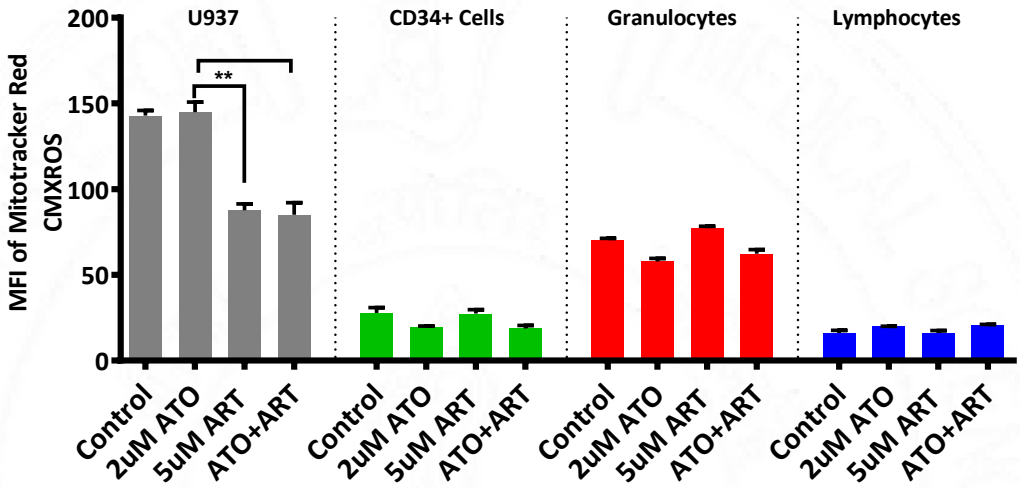

Figure 56: Post 24 hours of treatment, the leukemic cells (U937) and normal cells were stained with Mito-tracker red, and the fluorescence intensity was measured. (n=3; ATO=2uM; ART= 5uM; time point 24 hours). All the error bars represent the mean± SEM of independent experiments (p<0.05, **p<0.01, ***p<0.001).*

We observed that, when the malignant cells and normal cells were treated with ART, the malignant cells attained a fluorescence in the red channel (FL-2; filter 585/42), and this fluorescence phenomenon was not in the normal cells (figure 57).

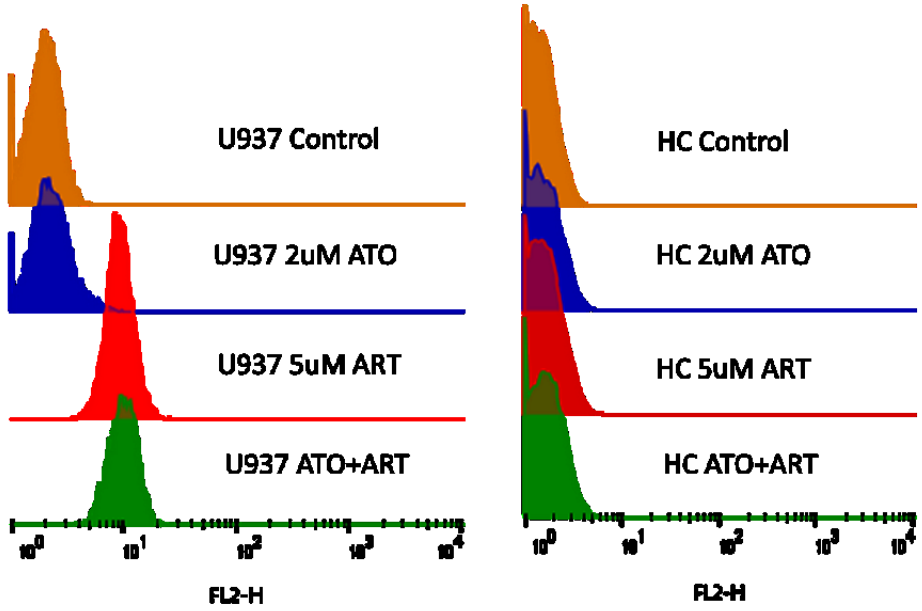

Figure 57: Autofluorescence property of the leukemic cells (U937- left) treated with ATO and ART alone and in combination, whereas healthy control (HC-right) did not gain any fluorescence property. (n=3; ATO=2uM; ART= 5uM; time point 24 hours).

Based on the existing literature on the mechanism of action of ART, the observed fluorescence of leukemic cells post ART treatment might be due to the effect of ART on haem biosynthesis and accumulation of protoporphyrin IX (Fluorophore). This phenomenon of fluorescence property is widely used in the solid tumor resection were the administration of 5-aminolaevulinic acid (ALA) -induced protoporphyrin-IX accumulation preferentially occurs in the cancer cells, and this

enhanced fluorescence has been employed in the detection and photodynamic treatment of solid tumors (McNicholas et al., 2019).

This data suggest the specificity of the artesunate in targeting the malignant cells and not the normal cells.

4.7 Intracellular iron determines the specificity and anti-leukemic activity of arsenic trioxide and artesunate:

4.7.1 Iron chelators antagonize the anti-leukemic activity of ATO and ART:

Iron plays an important role in the anti-malarial activity of artemisinins by catalysing the activation of the endoperoxide moiety. Deferoxamine (DFO) has been reported to abrogate the anti-malarial activity of artemisinins (Ismail et al., 2016, O'Neill et al., 2010). Hence to evaluate the importance of iron in the anti-leukemic activity of artesunate and arsenic trioxide, we used iron chelators such as deferiprone (DFP-Mitochondria and cytosol), DFO for lysosomes, and 2'2' Bipyridyl (BIP) (cytosolic) in combination with ATO and ART to assess the importance of subcellular compartments of iron in their anti-leukemic activity. DFO – a lysosomal iron chelator significantly abrogated the anti-leukemic activity of ATO+ART, whereas DFP and BIP did not (figure 58a and b).

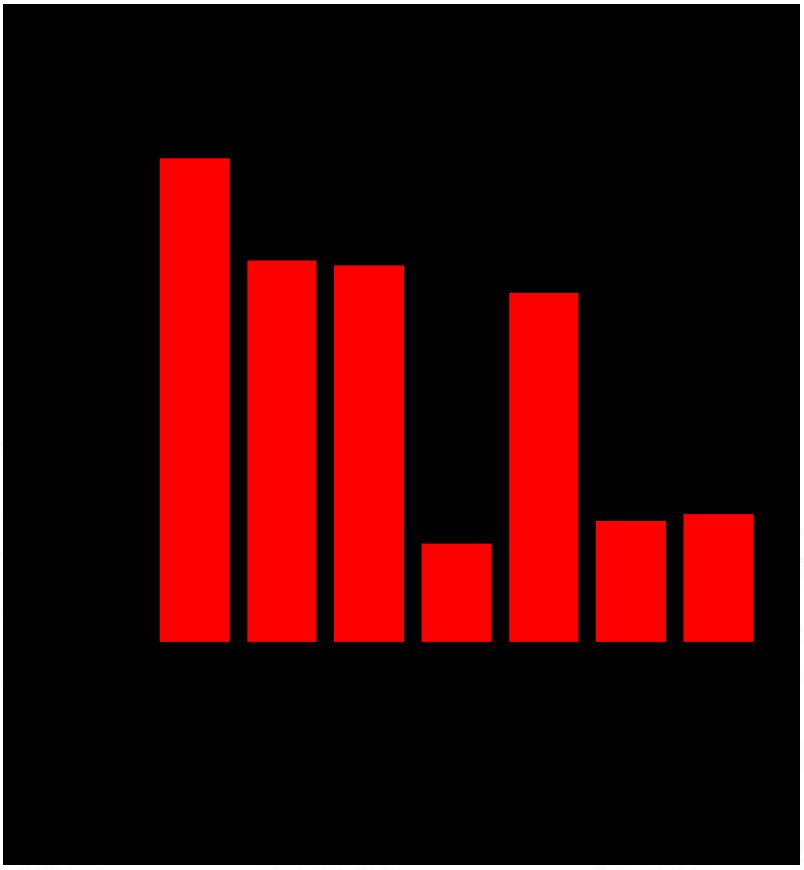

Figure 58: a) Post 48 hours viability of U937 cells treated with different compartments of iron chelator in combination with ATO and ART. (DFO -Deferoxamine; DFP – Deferiprone; BIP – 2'2' Bipyridyl used at a concentration of 20uM; ATO = 2uM and ART = 5uM; 48hours; n=5) All the error bars represent the mean± SEM of independent experiments (p<0.05, **p<0.01, ***p<0.001).*

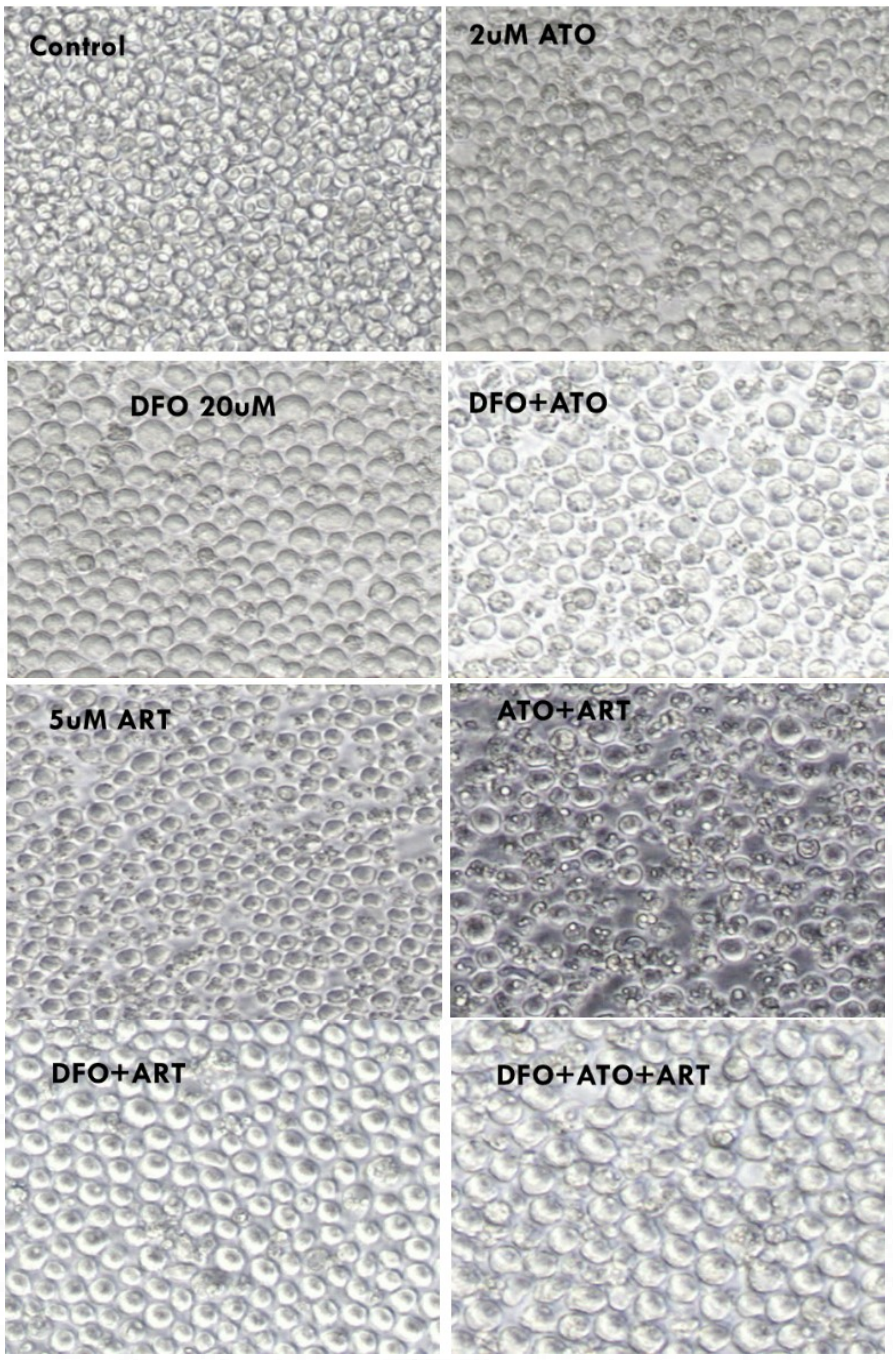

Figure 58: b) Phase-contrast images of U937 cells post 48 hours of drug treatment in combination with lysosomal iron chelator DFO. (n=3).

4.7.2 Leukemic cells possess higher levels of intracellular iron reserves

We measured the cell surface expression of transferrin receptor (TFRC) as TFRC mediated iron uptake is a major iron pathway in the cells. Transferrin bound iron (holo-transferrin) is taken up via receptor-mediated endocytotic pathway, and it fused with lysosomes releasing iron in the cytosol and recycling the receptor (apo-transferrin) to the cell surface. We observed that cell surface expression of TFRC was significantly higher in the leukemic cell lines and primary AML cells in comparison to their normal counterparts and normal CD34 positive cells (figure 59)

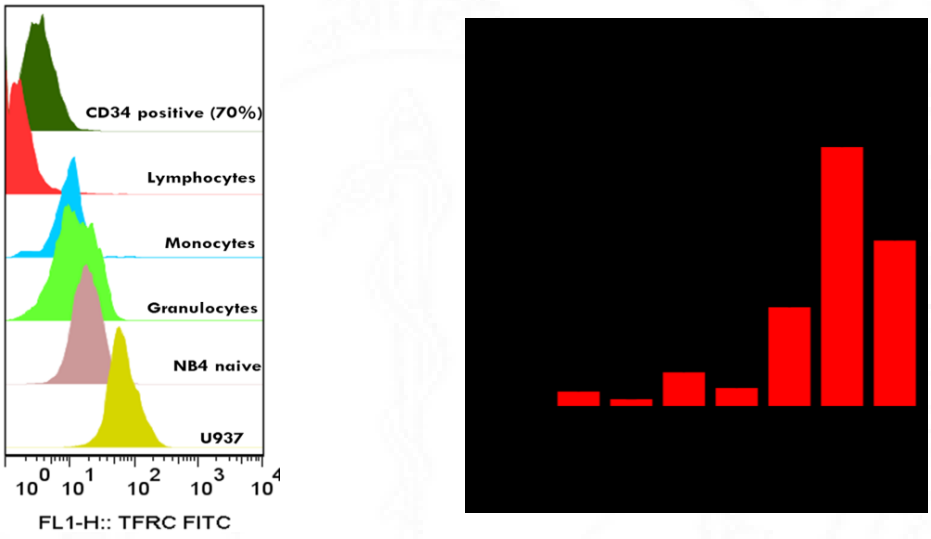

Figure 59: Cell surface expression of transferrin receptor (TFRC) a major regulator of iron uptake in the cells was measured using flow cytometry and found to be significantly higher in the leukemic cells in comparison to their normal counterparts. (Cell lines n=5; primary AML = 20) All the error bars represent the mean± SEM of independent experiments (p<0.05, **p<0.01, ***p<0.001)*

4.7.3. Artesunate quenches intracellular iron of the leukemic cells to promotes apoptosis:

We used different probes to measure the intracellular iron pool, as depicted in figure 60.

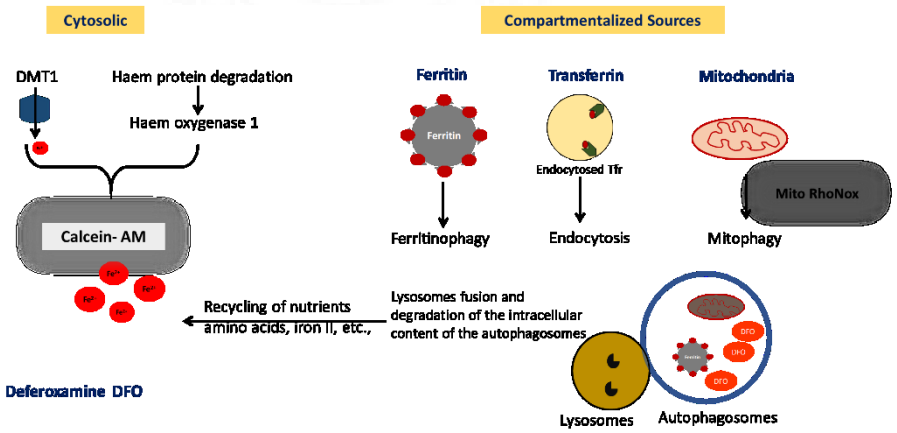

Figure 60: Illustrates the different sources and compartments of iron stores in the cell.

The cell surface expression of the TFRC was found to be significantly reduced when the leukemic cells are treated with ATO and ART. To address whether it is a specific event with these agents, we treated the leukemic cells with the conventional chemotherapeutic agent daunorubicin (DNR) or cytosine arabinoside (ARA-C). We found that the expression was not affected by conventional agents (figure 61).

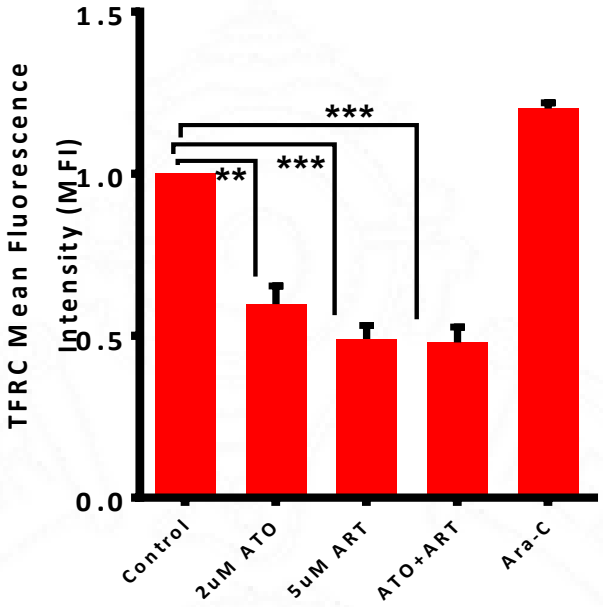

Figure 61: TFRC expression was significantly down-regulated when the U937 cells were treated with ART / ART+ATO, which was not observed with other conventional chemotherapeutic agents- Ara-C (cytosine arabinoside) (n=4). All the error bars represent the mean± SEM of independent experiments (p<0.05, **p<0.01, ***p<0.001).*

We also measured the intracellular labile iron pool using the fluorescent dyes specific for the different compartments. For cytosol using calcein-AM and for mitochondria, mito-Ferro green-1 was used. Calcein-AM fluorescent intensity is inversely proportional to the amount of labile iron pool in the cytosol of the cells. We observed that there was a significant reduction in the amount of cytosolic and mitochondrial labile iron pool content in the presence of ATO and ART (figure 62 and b), suggesting that ART quenched the iron for its activity.

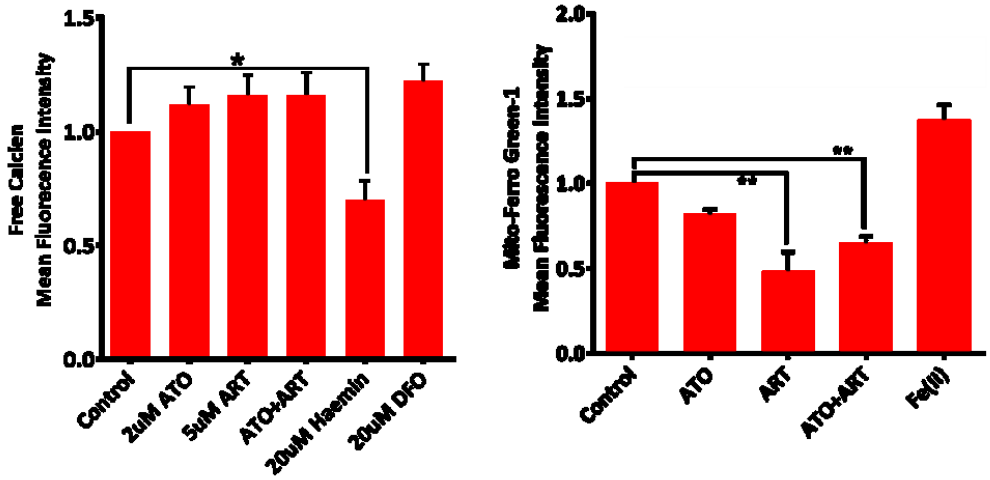

Figure 62: a) Cytosolic Iron was measured using Calcein-AM after 6 hours of treatment with ATO, ART, and ATO+ART on the U937 cell line. Hemin and DFO were used as internal controls (amount of free calcein-AM is inversely proportional to the intracellular labile iron pool). The fluorescence intensity was measured using flow cytometry (n=3). b) Mitochondrial labile iron (II) was measured after treating U937 cells with ATO, ART, and ATO+ART for 24 hours, followed by staining with Mito-ferrogreen-1 and fluorescence was measured using flow cytometry.10ug ammonium ferrous sulfate (Fe (II)) was used as a positive control (n=3).

The other contributors to cytosolic iron, such as haem protein degrading enzyme haem oxygenase-1 (HMOX1) and ferritin was also found to be significantly up-regulated in the ATO and ART treatment (Figure 62c). Ferritin, the cytosolic iron storage protein, is significantly downregulated in the ART treatment (Figure 62d). We observed a significant upregulation of Ferritin in the presence of ATO and reduction in the combination, suggesting that ATO is enhancing the cellular availability of ART.

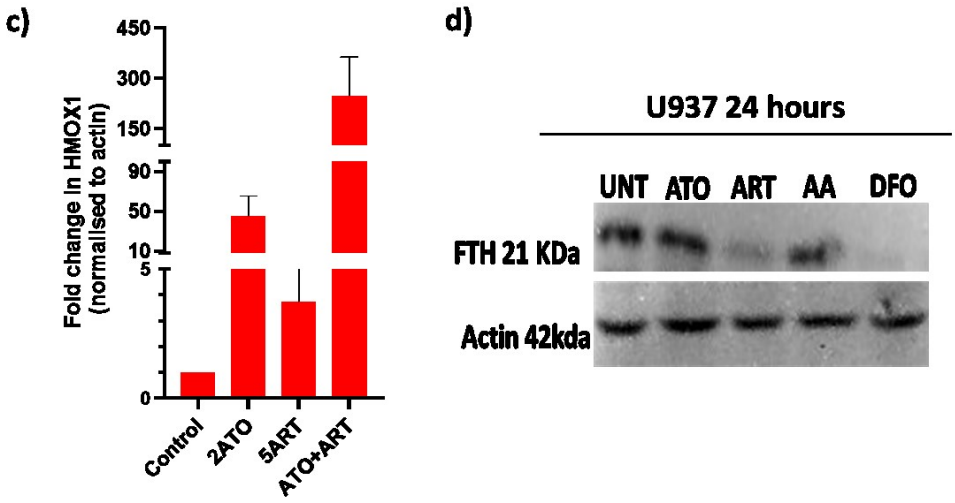

Figure 62: c) *Haem protein degrading enzymes haem oxygenase 1 (HMOX1) transcript levels and d) Immunoblots of Ferritin (FTH) post 24 hours of U937 cells treated with ATO and ART (n=3). DFO is used as a control for ferritin degradation. All the error bars represent the mean± SEM of independent experiments (* $p<0.05$, ** $p<0.01$, *** $p<0.001$).*

4.7.4 Iron in the form of haemin increases the efficacy of ATO+ART anti-leukemic activity:

To identify the source and form of iron required for the activity of ATO+ART, we treated the U937 cells with holo and apo transferrin, Iron II sucrose, hemin, and alpha-aminolaevulinic acid (ALA) in combination with ART and ATO+ART. Only the heme-based iron supplementation (hemin and ALA) showed significant synergy in enhancing the apoptotic activity of ATO+ART (figure 60). Primary AML cells were also found to be sensitive to the combination of ATO+ART, and the combination was

further enhanced when combined with hemin/ALA (figure 63). These data strongly suggest that heme bound iron plays an important role in the anti-leukemic activity of the combination.

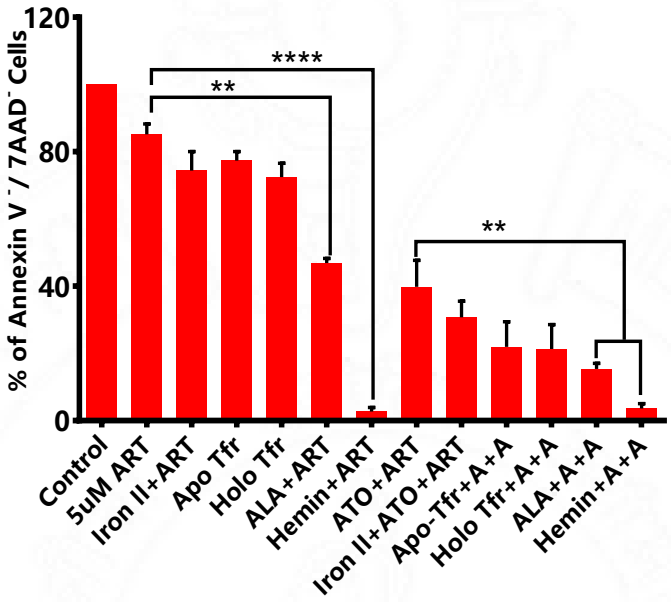

Figure 63: Viability of U937 cells treated with hemin (20uM), a-aminolevulinic acid (ALA)(1mM) as heme form of iron and holotransferrin (10ug/ml), apo transferrin (10ug/ml), Iron (II) sulfate as a non-heme source of iron in combination with ART and ATO+ART for 48hours (n=3). All the error bars represent the mean± SEM of independent experiments (p<0.05, **p<0.01, ***p<0.001).*

4.8: ATO requires iron for its anti-leukemic activity:

Iron chelation experiments revealed that ATO also significantly affected the cellular iron stores; hence we evaluated the importance of iron in ATO induced apoptosis in the sensitive cells line NB4 naive. Iron also plays an important role in oxidative stress by the formation of hydroxyl radical through Fenton reaction.

We treated NB4 naïve cell line with iron chelators (20uM) targeting the different intracellular compartments of iron distribution such as 2'2 Bipyridyl (BIP-cytosol). Post 48 hours of treatment DFO -lysosomal iron chelator alone significantly abrogated the ATO induced cell death while others failed to so. Increasing the intracellular iron levels by the treatment of hemin (20uM), in combination with ATO, significantly enhanced the amount of cell death. The rescue of viability by DFO was observed only with ATO and not with another conventional chemotherapeutic agent, daunorubicin (DNR) (Figure 64a), implying the role of iron in ATO induced cell death.

Immunoblots probed for procaspase-3 reduction as a marker for apoptosis showed a significant reduction in the procaspase-3 levels in ATO alone, whereas, in the combination of ATO and DFO, the levels were not affected significantly (figure 64b).

ATO treatment significantly downregulated the mRNA levels of iron import genes (TFR1 and DMT1). In contrast, it did not show any significant impact on the iron export gene ferroportin (FPN) (figure 64 c) in the NB4 cells. Hence, we measured the intracellular iron reserve in the NB4 cells treated with 2uM ATO and observed that there was a significant increase in the intracellular ferritin levels in comparison to the control cells and addition of DFO in combination with ATO reduced the Ferrtin level (figure 64d).

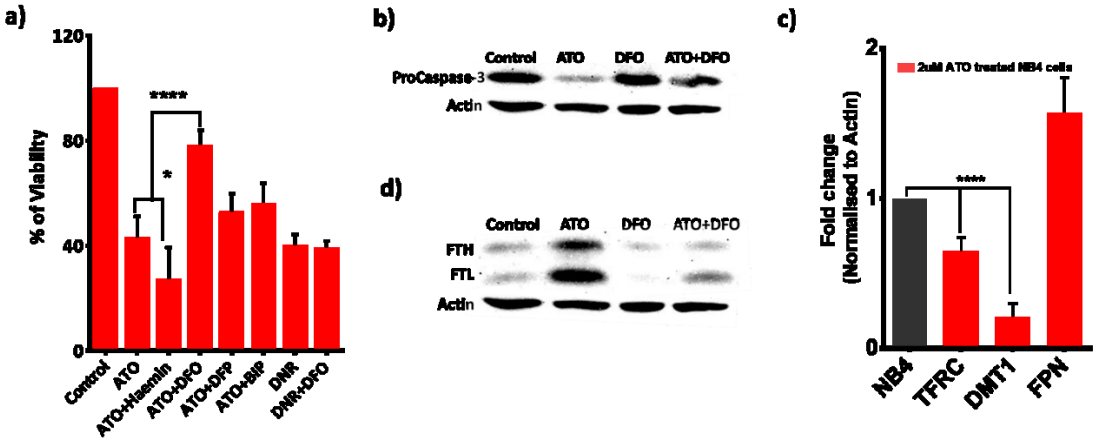

Figure 64: Viability of the NB4 cells treated with different compartment iron chelators in combination with ATO. (n=7) b) Immunoblots probed for Caspase -3 levels in the NB4 cells treated with ATO in combination with DFO (n=3). c) Iron import genes are significantly affected at the transcript levels when the NB4 cells were treated with ATO (n=3). d) Immunoblots probed for ferritin levels show increased accumulation in the ATO treated cells (n=3). (48hours; ATO=2uM; DFO/DFP/BIP/Hemin =20uM; DNR=40ng) All the error bars represent the mean± SEM of independent experiments (p<0.05, **p<0.01, ***p<0.001).*

4.9: ATO and ART showed a synergistic effect with the existing conventional chemotherapeutic agents:

We assessed the ability of the ATO and ART in combination with the conventional chemotherapeutics agents used in leukemia such as all-trans retinoic acid (ATRA), daunorubicin hydrochloride (DNR) and cytosine arabinoside (Ara-C).

We observed that ATO, in combination with DNR or ARA-C, is antagonistic in AML cell lines and not on the ATO sensitive APL cells. However, when ART was

treated with ATRA or DNR, even in the presence of ATO, there was synergistic activity on both APL and AML cell lines (ATO+DNR vs. DNR Vs. ATO+ART+DNR) (figure 65).

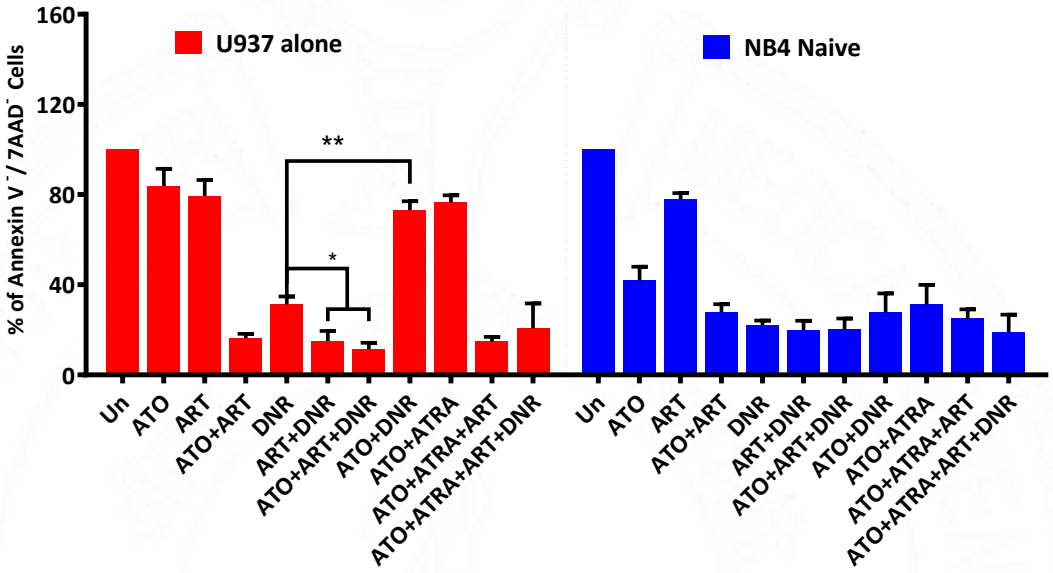

Figure 65: Post 48 hours viability of the ATO resistant AML cell line U937 and ATO sensitive APL cell line treated with a combination of chemotherapeutic agents along with ATO and ART. (n=3; 48 hours; ATO =2uM; ART =5uM; DNR; 80ng; ATRA-1uM). The viability was assessed by Annexin V 7AAD apoptosis assay by flow cytometry (p<0.05, **p<0.01, ***p<0.001).*

We also evaluated the ATO and ART activity in combination with azacytidine (Aza – used in the elderly AML patients). We observed that unlike the ATO+DNR, the combination of Aza with ATO and or ART had a synergistic activity in promoting apoptosis of the different subtypes of myeloid and lymphoid leukemic cells.

Venetoclax (VEN) – a BCL-2 inhibitor in combination with Azacytidine (Aza) has been reported to improve the treatment outcome of elderly patients significantly in a subset of AML. Hence, we compared the cytotoxic effect of ATO+ART, Aza+ART, and ATO+ART+Aza versus VEN+Aza. Unlike VEN+Aza, the combination of ATO, ART, and or Aza was observed to be effective against all the subtypes of myeloid and lymphoid leukemia (figure 66 and figure 67).

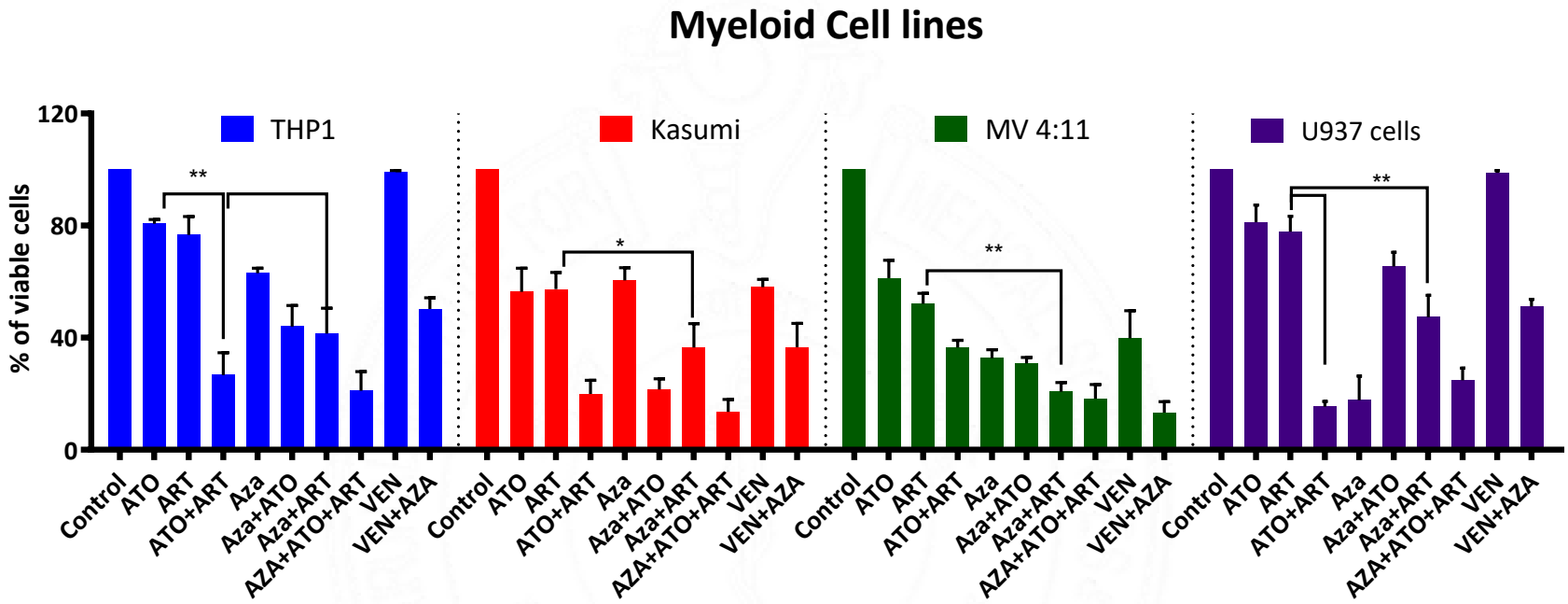

Figure 66: Post 48 hours viability of myeloid cell lines harboring different molecular aberrations and cytogenetics treated with Aza in combination with ART and or ATO. (n=4; ATO=2uM; ART =5uM; Aza=2.5uM; Venetoclax (VEN)= 500nM). The viability was assessed by Annexin V 7AAD apoptosis assay by flow cytometry (p<0.05, **p<0.01, ***p<0.001).*

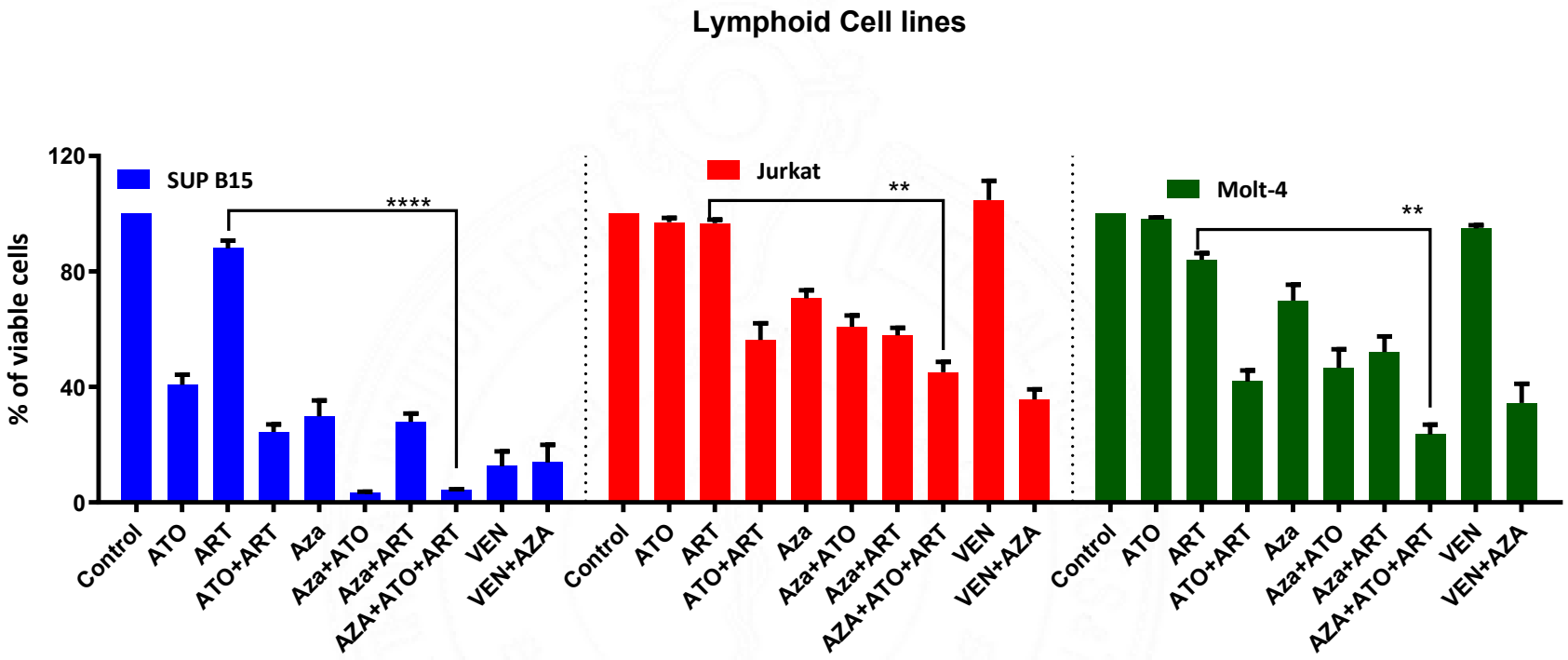

Figure 67: Post 48 hours viability of myeloid cell lines harboring different molecular aberrations and cytogenetics treated with Aza in combination with ART and or ATO. (n=4; ATO=2uM; ART =5uM; Aza=2.5uM; Venetoclax (VEN)= 500nM). The viability was assessed by Annexin V 7AAD apoptosis assay by flow cytometry (p<0.05, **p<0.01, ***p<0.001).*

4.9.1: Triple combination had a minimal cytotoxic effect on the normal cells:

To validate our cell line data, we assessed the effects of the triple combination comprising of ATO, ART, and Aza on the normal cells. We observed only a minimal bystander effect on the normal peripheral blood cells, unlike the effect on the leukemic cells(figure 68).

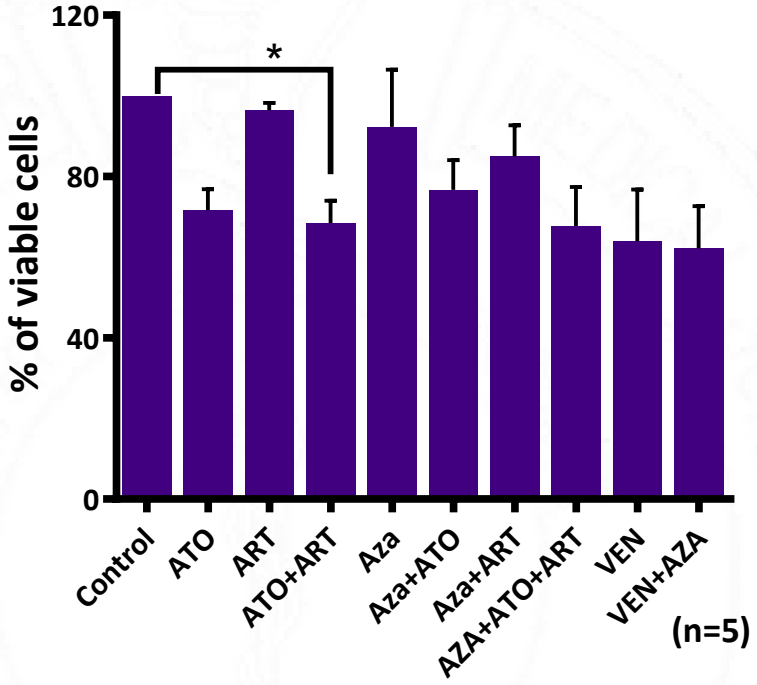

Figure 68: Post 48 hours viability of the normal peripheral blood cells treated with ATO, ART, and Aza as single agents and combinations. (ATO =2uM; ART=5uM, Aza = 2.5uM and VEN= 500nM) The viability was assessed by Annexin V 7AAD apoptosis assay by flow cytometry (p<0.05, **p<0.01, ***p<0.001).*

4.9.2: Effect of ATO+ART+Aza on primary leukemic cells:

We validated our cell line data on the primary bone marrow sample of acute myeloid leukemia with different cytogenetics and molecular aberrations collected at the time of diagnosis (figure 69 and figure 70). In comparison to existing VEN+AZA therapy in the management of elderly patients, the ATO +ART combination was also found to be effective.

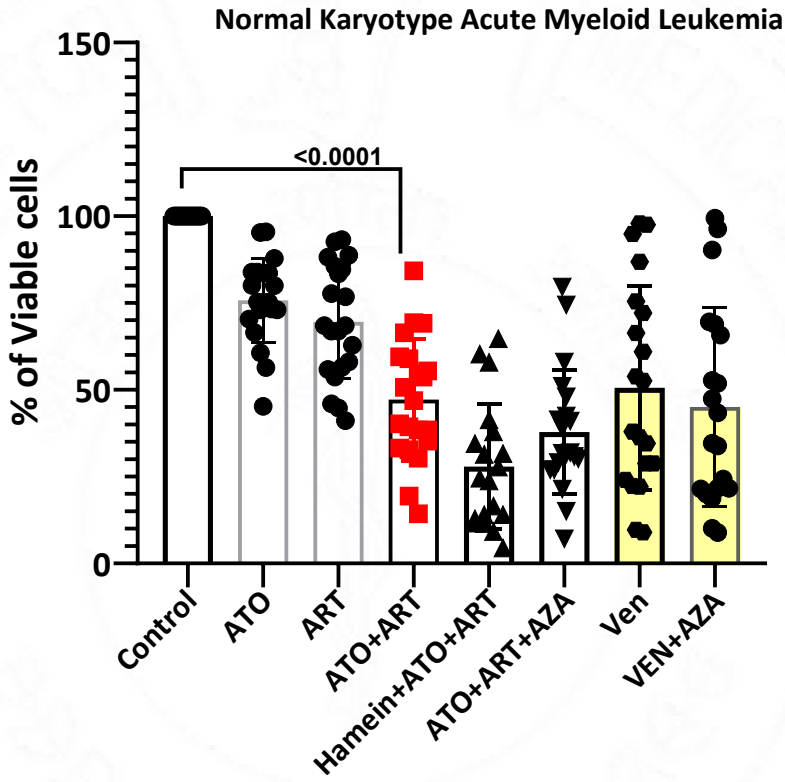

Figure 69: Viability of primary AML cells (normal karyotype AML) treated with ATO, ART in combination with Aza, haemin (iron enhancer) for 48 hours. The apoptotic activity of VEN+Aza is not significantly different when compared to ATO+ART. (n=24; ATO=2uM; ART = 20uM; Haemin = 20uM; Ven= 500nM and Aza =2.5uM). The viability was assessed by Annexin V 7AAD apoptosis assay by flow cytometry (p<0.05, **p<0.01, ***p<0.001).*

It has also been reported that VEN+AZA is not effective in monocytic AML patients (Pei et al., 2020). Hence, we assessed the effect of ATO+ART on the bone marrow leukemic cells of monocytic AML patients and observed that the combination is effective and targets different subtypes of leukemic cells unlike VEN+AZA.

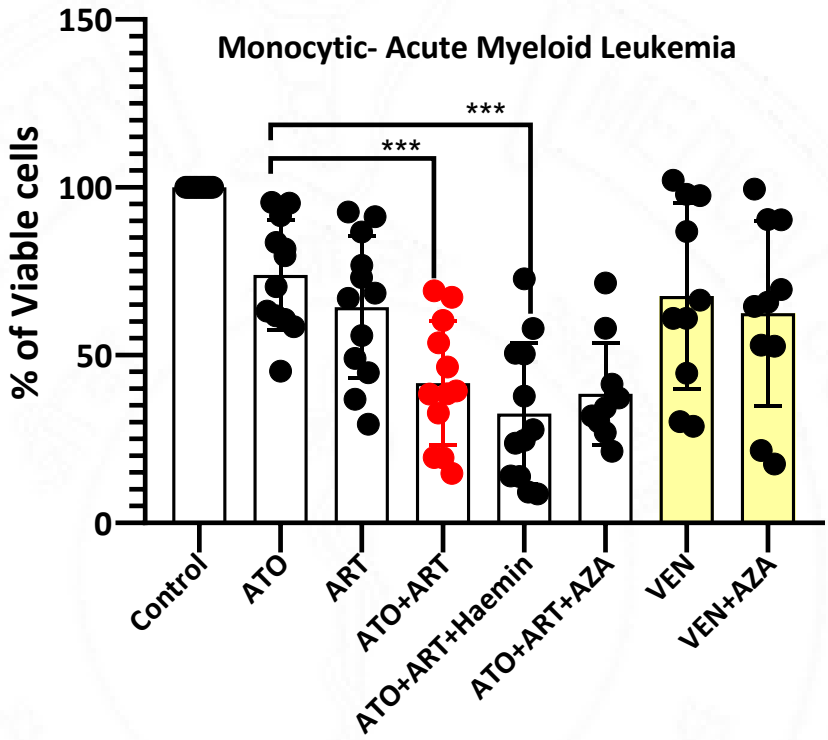

Figure 70: Viability of primary AML cells (monocytic AML) treated with ATO, ART in combination with Aza and haemin (iron enhancer) for 48 hours. The apoptotic activity of VEN+Aza is not significantly different when compared to ATO+ART. (n=12; ATO=2uM; ART = 20uM; Haemin = 20uM; Ven= 500nM and Aza =2.5uM). The viability was assessed by Annexin V 7AAD apoptosis assay by flow cytometry (p<0.05, **p<0.01, ***p<0.001).*

The combination was also found to be effective in primary bone marrow leukemic cells of acute promyelocytic leukemia and acute lymphoblastic leukemia patients (Figure 71)

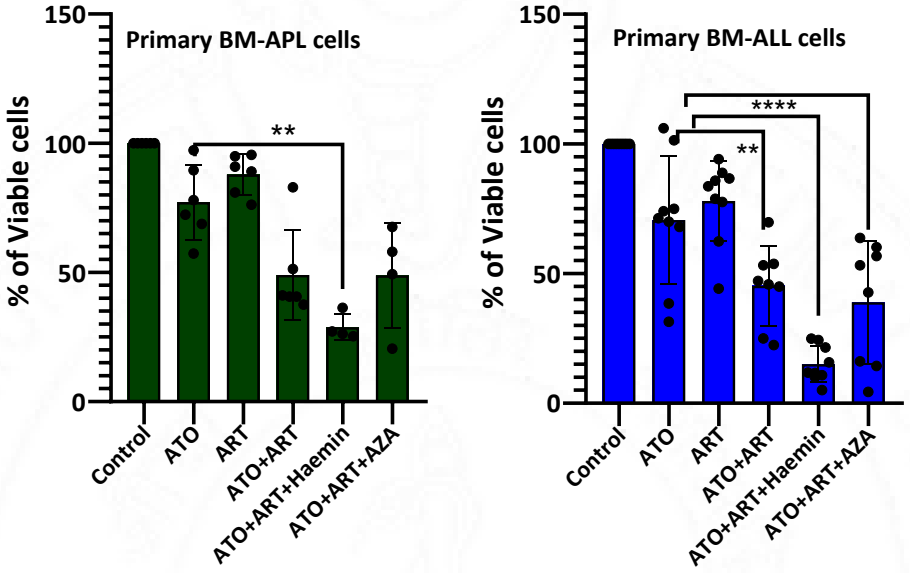

Figure 71: Viability of primary APL (left -green color) and ALL (right -blue color) bone marrow cells treated with ATO, ART in combination with Aza, haemin (iron enhancer). (APL n=6; ALL = n=10; ATO=2uM; ART = 20uM; Haemin = 20uM and Aza =2.5uM). The viability was assessed by Annexin V 7AAD apoptosis assay by flow cytometry (p<0.05, **p<0.01, ***p<0.001).*

4.10: Effect of ATO+ART combination in the presence of bone marrow microenvironment:

4.10.1: 2D -co-culture system:

We have reported earlier that there is a significant level of protective effect given by the stromal cells both in a contact-dependent and independent manner to the leukemia cells. We evaluated the effect of ATO and ART in the bone marrow microenvironment. We observed that the ATO and ART are effective in promoting apoptosis of the leukemic cells even in the presence of stromal cells. However, the stromal cells significantly reduced the efficacy of the combination in comparison to the effect of the combination on leukemic cells alone (figure 72).

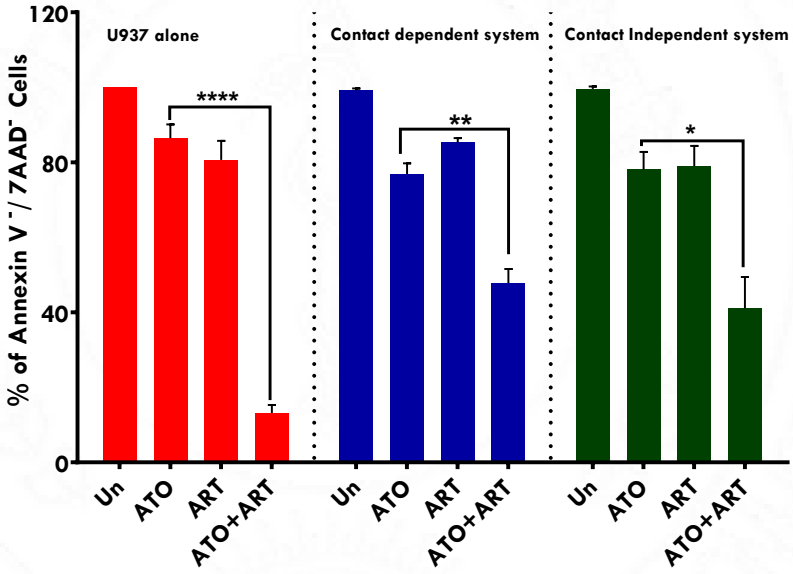

Figure 72: Post 48 hours viability of U937 cells alone (red), co-cultured with HS5 (blue), and the supernatant collected from the stromal cells (green) treated with ATO, ART and in combination. (ATO=2uM; ART = 5uM; 48hours; n=3) The viability was assessed by Annexin V 7AAD apoptosis assay by flow cytometry (p<0.05, **p<0.01, ***p<0.001).*

4.10.2: 3D co-culture system:

We have previously demonstrated the stroma mediated the protective effect of leukemic cells in 3D culture system using gelatin scaffolds; the workflow has been described in Figure70 a and Figure 70b represents the microscopic picture of leukemic cells and stromal cells in a 2D and 3D stromal cell co-culture system. The viability of leukemic cells showed a predominant protective effect of stromal cells in 3D culture system compared to 2D along with respective controls shown below (Figure 73)

The relevance of 3D co-culture:

Current in vitro drug testing models or experiments is based on 2-dimensional (2D) cell culture systems. Although widely used in pre-clinical testing, these in vitro models do not always predict in vivo responses, and it remains suboptimal with lack of correlation with clinical outcomes at the bedside. Therefore, we explored a 3-dimensional co-culture system to study the effects of drugs on leukemia cells in the presence of stroma in an environment more similar to that of human leukemia in the bone marrow micro-environment.

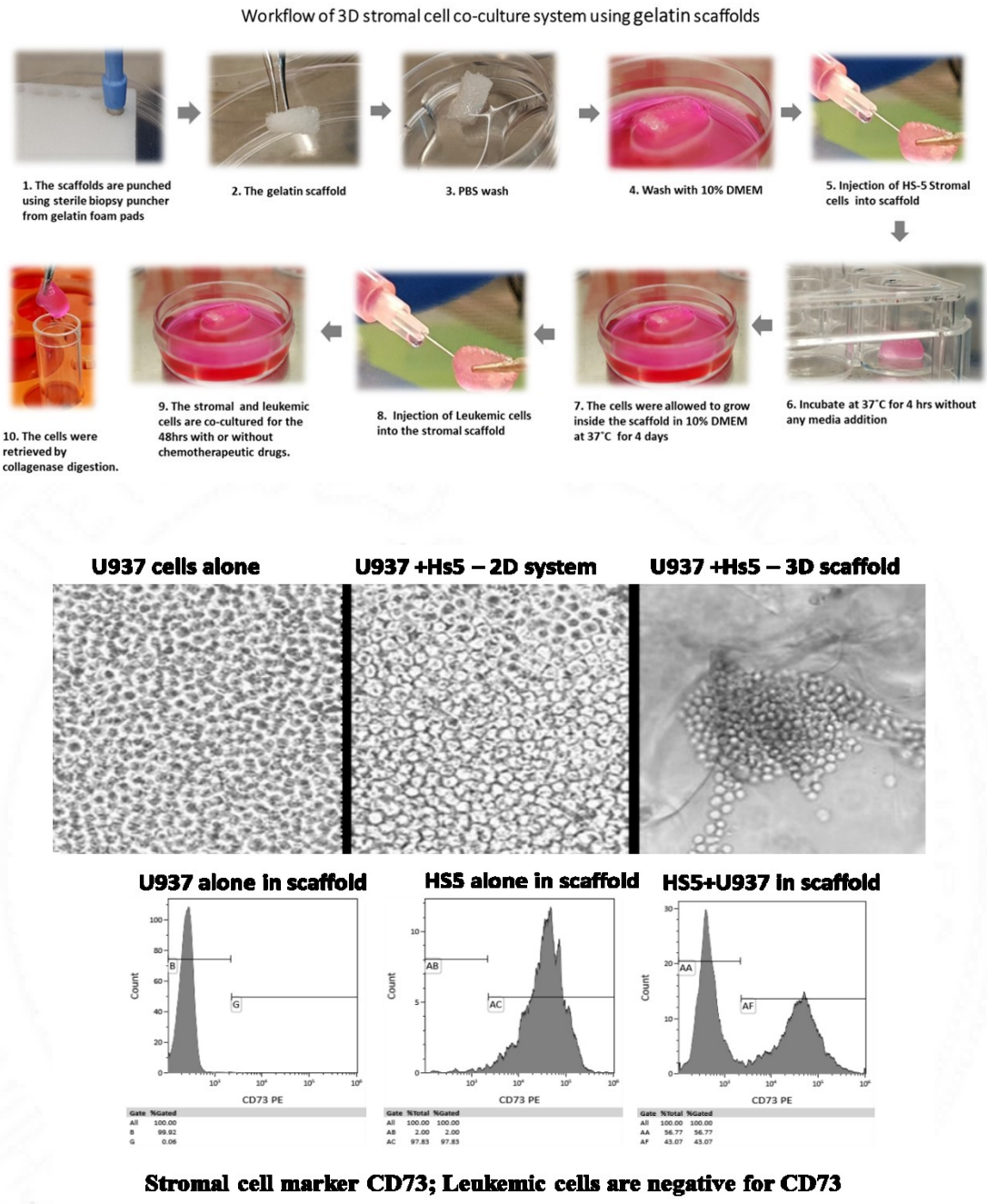

Figure 73: a. Pictures demonstrating the workflow of the 3D stromal cell co-culture system. Microscopic view of U937cells in 2D and 3D culture systems. Cells retrieved from the scaffold after collagenase treatment depicting the presence of both the cell types using CD73 as a marker for stromal cells.

We observed that even in the 3D culture system ATO, ART combination, along with Aza, was observed to be effective in promoting apoptosis (Figure 74).

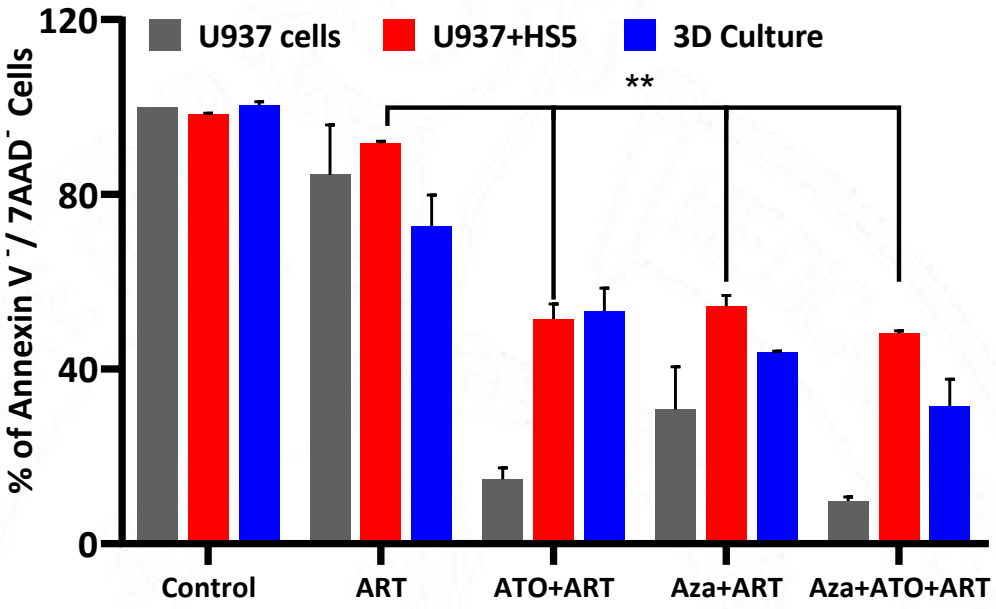

Figure 74: Viability of U937 cells cultured alone in the presence of HS5 and 3D scaffold system treated with ATO, ART, and in combination with Aza for 48 hours. (ATO=2uM; ART = 5uM; Aza = 2.5uM; 48hours; n=3) The viability was assessed by Annexin V 7AAD apoptosis assay by flow cytometry (p<0.05, **p<0.01, ***p<0.001).*

4.11: Combination of ATO and ART reduced leukemic burden and extended long time survival in an APL mouse model:

We next evaluated the combination's efficacy in an *in vivo setting* using a transplantable acute promyelocytic leukemia mouse model (figure 75a). The dual (ATO+ART and ART+AZA) and triple combination (ATO+ART+AZA and ATO+ART+Haemin) of treated mice showed a significant reduction in WBC counts and PML-RARA transcripts in comparison to ATO or placebo groups (Figure 75b and 75c).

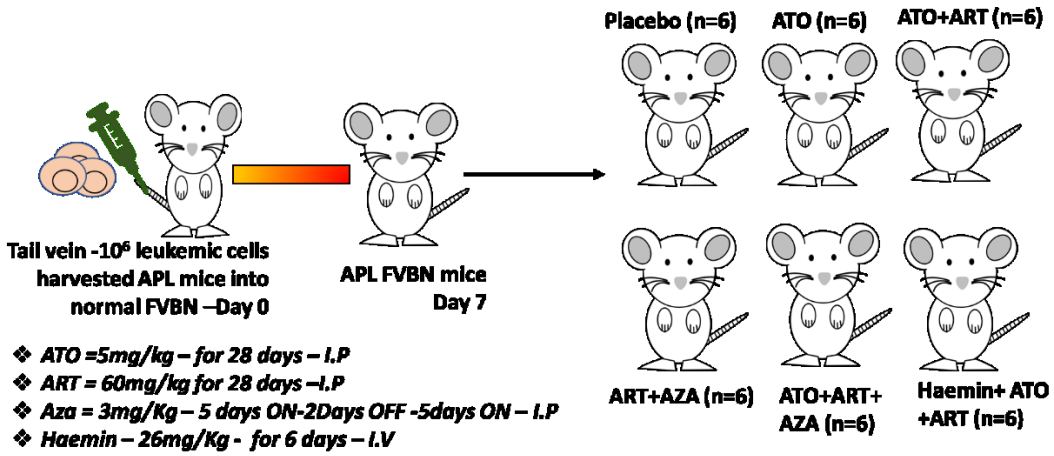

Figure 75: a) Schematic representation of the APL transplantable mice model and treatment plan.

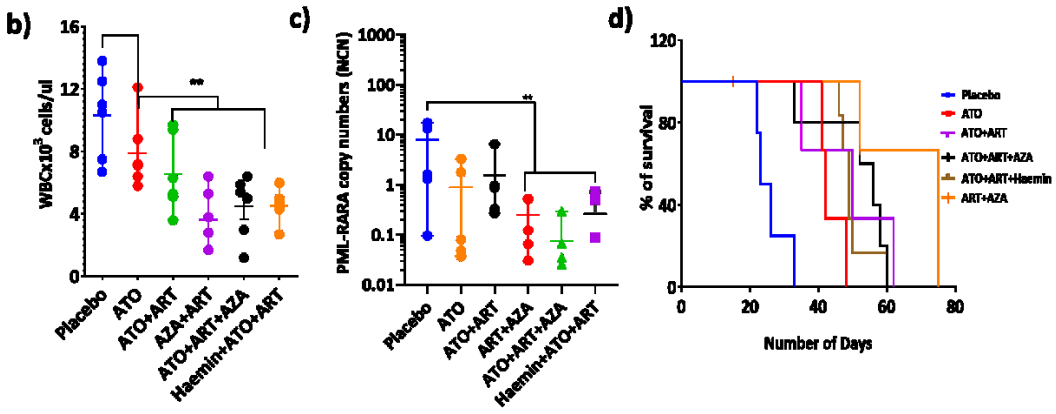

Figure 75: Leukemia burden was assessed by evaluating the WBC counts (B) PML RARA (copy number) (C) in the peripheral blood sample at day 20 assessed by Q PCR. (D) survival curve of mice n=6 each group.

Dual and triple combination therapy was able to prolong the survival of APL mice when compared to the mean survival of Placebo and ATO *(Figure 75d).*

Discussion

Everything Begins with An Idea.

-Earl Nightengale

5.0 Discussion

In recent years, metabolic adaptations have gained a significant spotlight in understanding the intricate biology of cancer. Malignant cells have been reported to rewire the metabolic pathways to feed anabolic cell growth. Oncogenic drivers directly or indirectly regulate the metabolic pathways, and aberrant metabolism is central not only for proliferation and survival but also mediating oncogene addiction with significant implications for the development of targeted therapies. In our present study, we evaluated the metabolic adaptations of leukemic cells and how it could be targeted to promote selective leukemic cell death.

5.1 ATO resistance in acute promyelocytic leukemia:

The combination of ATRA and ATO in the management of APL has improved the survival and treatment outcome of patients by replacing the myelotoxic conventional chemotherapy. However, a proportion of newly diagnosed (10-20%) and relapsed APL (40-50%) patients' relapse after standard of care. The resistance and therapy failure observed in the clinic against ATO has been focused on the presence/acquisition of *PML* B2 domain mutations (Tomita et al., 2013, Marasca et al., 1999). Our recent publication on the mutational spectrum of relapsed and newly diagnosed APL patients suggests the importance of additional genetic events (FLT3, KRAS, NRAS, ARID1B, p53, and WT1) during disease recurrence; however, it is also noted that mutations resulting in primary or secondary ATO resistance were extremely rare and could not explain the majority of disease relapses after treatment with ATO based regimens(Madan et al., 2016). Other mechanisms such as bone marrow

microenvironment mediated drug resistance, up-regulation of anti-apoptotic factors, modulation of cellular energy metabolism, and oxidative stress can contribute to therapy resistance.

In comparison to the existing ATO resistant cell lines (Lunghi et al., 2005, Gianni et al., 1998) our inhouse generated ATO resistant cell lines are stable, well-characterized at the genomic levels and also possess the well-known ATO resistance-conferring mutation A216V in the B2 domain of the PML-RARA oncoprotein.

In comparison to the naïve NB4, in house generated ATO resistant cell lines overexpressed ATO efflux transporters such as AQP9, MRP4, and ABCA7, which correlated with their inability to accumulate intracellular ATO. We did not observe this phenomenon in primary blasts from relapsed APL patients previously treated with ATO in comparison to newly diagnosed (Chendamarai et al., 2015).

We noted the presence of a genetic mutation in the B2 domain of the *PML* gene in our in-house generated ATO resistant cell line that has been reported to confer resistance. It is important to note that these mutations are acquired post ATO treatment, and none of the APL cell lines or relapsed APL patients prior to ATO therapy had the B2 domain mutation (Kulkarni et al.). ATO sensitivity has also been reported to be impacted by *p53*, which regulates the nuclear body formation and reactive oxygen species levels. We evaluated the p53 mutation and observed that the p53 mutation was present in the ATO resistant cell lines the same as the NB4 naive. Based on our data demonstrating nuclear body formation and the lower reactive oxygen species in ATO

resistant cell lines, the resistance to ATO is likely to be independent of p53 status in these cell lines.

5.2. ATO resistant APL cells are metabolically distinct:

We observed that the cellular redox system of the ATO resistant cell lines was significantly altered in these cell lines having lower reactive oxygen species, lower proliferative rate, and an increased antioxidant system favoring quiescence and stemness like properties (Lagadinou et al., 2013b) (figure 76).

ATO sensitive cell line NB4 naive was observed to be more reliant on the Warburg effect for their survival and proliferation, and it was significantly affected by a glycolytic inhibitor (2-DG). We also noted that in the in vivo APL mouse model, 2-DG significantly reduced the leukemic burden comparable to the standard of care (ATO). This further supports that the naïve ATO sensitive APL cells are affected by glycolytic inhibition in vivo validating our in-vitro findings.

The ATO resistant cell lines were observed to be dependent on OXPHOS for their survival and also could switch between two metabolic pathways when one is inhibited. A combination of ATO and mitocans (mitochondrial targeting drugs) significantly affected the survival of ATO resistant cell lines.

The observed metabolic plasticity of the ATO resistant cell lines is similar to the metabolic phenotype of non-APL AML (non-M3) cell lines and primary cells (Han et al., 2019).

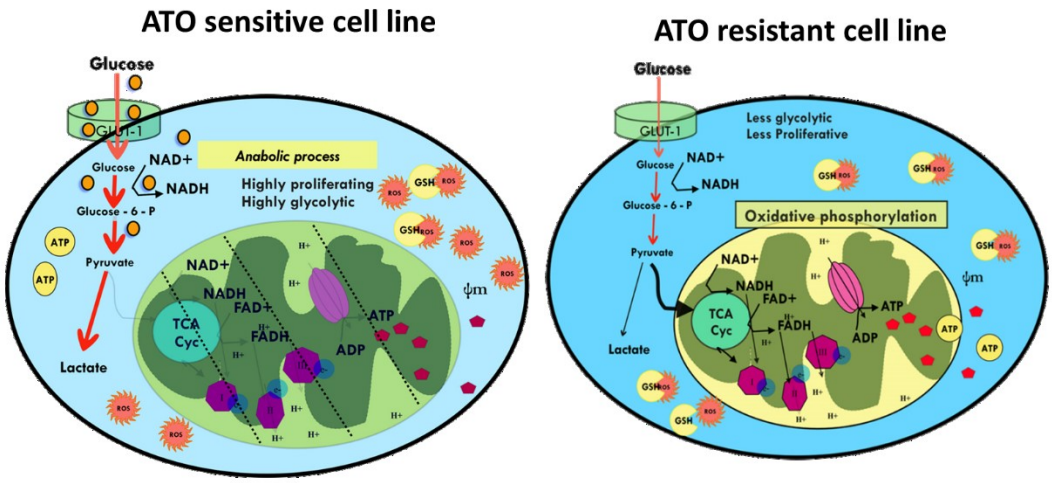

Figure 76: Illustrates the metabolic features of the ATO sensitive (NB4 naïve) and ATO resistant cell line (NB4 EV-AsR1 and UF1).

5.3 Metabolic disruptors overcome bone marrow microenvironment mediated drug resistance:

Previous work from our group reported that in acute promyelocytic leukemia (a most curable subtype of AML) that there is a significant microenvironment mediated resistance to ATO. In the present study, we observed that when the leukemic cells cultured in the presence of stromal cells, basal metabolic features of the leukemic cells are significantly altered, favoring quiescence, and drug resistance. The stromal cells significantly reduced the amount of ROS level and proliferation rate of the leukemic cells. The stromal cells contact enriched the leukemic cells in the G0/G1 phase of the cell cycle and increased the levels of autophagy as a means of favoring quiescence.

We have observed that the leukemic cells, which were sensitive to the chemotherapeutic agents, become resistant to them by the external cues of the bone marrow compartment. We found that combining metabolic inhibitor (2-DG / FCCP) with the conventional chemotherapeutic agents significantly affected the survival of the leukemic cells even when they are in contact with stromal cells. We also found there is the transfer of energy-producing organelle mitochondria from the stromal cells to leukemic cells as a means of protection from the cytotoxic insults both in direct contact and independent system (Figure 77).

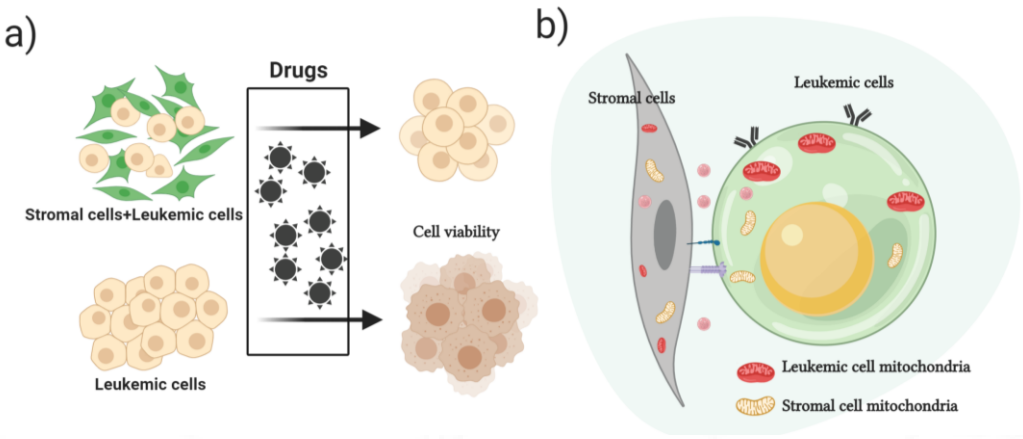

Figure 77: Bone marrow micro-environment mediated drug resistance. a) when the leukemic cells are in contact with stromal cells, their sensitivity to the chemotherapeutic agents is significantly less. b) Transfer of cellular contents (for recycling) of leukemic cells and stromal cells as a survival mechanism against chemotherapeutic agents.

5.4 Repurposing artesunate – as an anti-leukemic drug targeting the powerhouse of the cell:

Although the combination of ATO+FCCP was effective against the leukemic cells and in overcoming bone marrow microenvironment mediated drug resistance, there was a significant bystander effect on the healthy cells. Hence, we screened a small library of FDA-approved compounds reported to have similar effects as FCCP on mitochondrial respiration and found that only artesunate (ART) was very effective in combination with ATO to promote apoptosis in the leukemic cells. The combination of ATO+ART was observed to be significantly less cytotoxic to the normal peripheral blood and stem cells.

Seahorse extracellular analysis validated that ART had a significant effect on the mitochondrial respiration and promoted uncoupled respiration, which was evident by decreased coupling efficiency and ATP production. Cellular redox and mitochondrial membrane potential were also observed to be significantly low due to the uncoupled respiration of the leukemic cells in the presence of ART. Mitochondrial staining of the leukemic cells and normal cells treated with artesunate revealed that the mitochondrial staining was significantly affected only in the leukemic cells, not in the normal cells implicating the specificity of the combination. Confocal imaging of mitochondria revealed significant changes in the dynamics of the mitochondria, where ART-treated showed fragmented mitochondria in comparison to ATO and control, where it was tubulated structures.

When we treated the leukemic cells with a combination of ART and a mitochondrial fission inhibitor (mdivi-1) resulted in enhanced cell death due to inefficient clearance of damaged mitochdornia, mitochondrial fission inhibitor enhanced the anti-leukemic activity of the ATO and ART combination suggesting the critical of mitochondria.

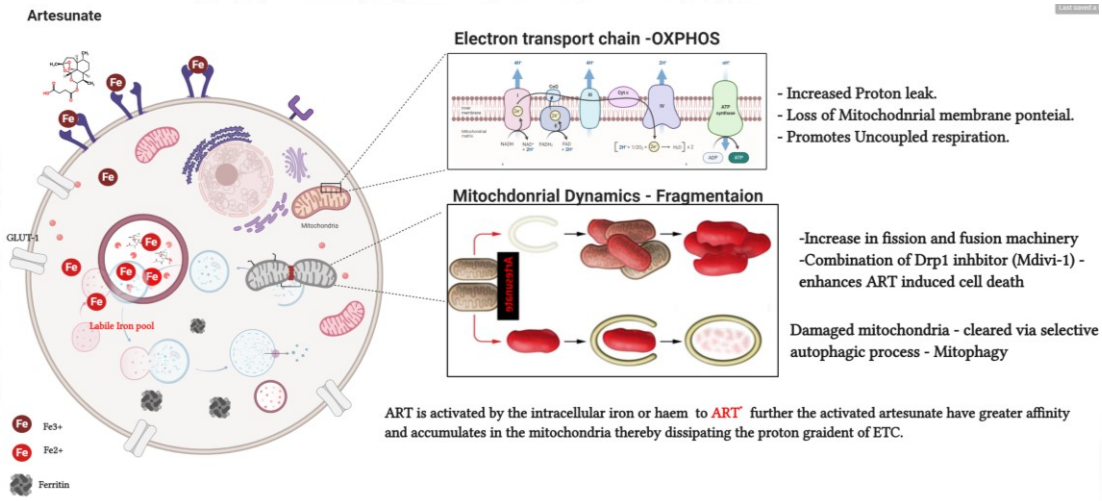

Figure 78: Illustration of ART activity in the leukemic cells

As we have observed selective specificity, we evaluated this combination on other myeloid and lymphoid leukemic cell lines harboring different molecular aberrations. The combination was found to be significantly targetting the different subtypes and types of acute leukemia.

5.5 Cellular iron reserve plays a critical role in selective specificity of ATO+ART combination:

We observed that leukemic cells had increased cellular iron in comparison to the normal cells. Interestingly, we noted that when the leukemic and normal cells were treated with artesunate, the leukemic cells gained a fluorescence property in contrast to the normal cells. Based on the existing literature about the mechanisms of action of artesunate, iron (II) / haem bound iron been reported to play a significant role in the oxidation of the endoperoxide ring of the ART and its functional activity. From these observations, we extrapolate that the fluorescence observed in the leukemic cells is due to the accumulation of protoporphyrin IX as the free iron is quenched by ART for its activity thereby hindering the haem biosynthetic process (takes places in mitochondria).

We noted that the major iron import gene- transferrin receptor (TFRC) is significantly up-regulated in the leukemic cells in comparison to normal peripheral blood and CD34 positive cells. Treatment of the leukemic cells with ATO and ART significantly downregulated the TFRC expression. The intracellular iron content highly regulates transferrin receptor surface expression. We validated the importance of iron and its compartment by treating the cells with different iron chelators targetting the different compartments in combination with ATO and ART. We found that only a lysosomal iron chelator (DFO) significantly abrogated the anti-leukemic activity of the combination. We also altered the intracellular iron content by using different forms of iron, such as transferrin-bound (apo and holo transferrin, free iron (II), haemin, and alpha aminolaevulinic acid (ALA- the precursor of heme biosynthesis) and found that

only hemin and ALA significantly enhanced the anti-leukemic activity of ART and ATO suggesting the importance of heme in ART activity.

5.6 Arsenic trioxide promotes iron-dependent cell death in APL:

We observed that the ATO sensitive leukemic cell viability was significantly restored with a lysosomal iron chelator (DFO). We noted that the rescue is only with ATO, and not with conventional chemotherapeutic agents DNR or ARA-C. This data strongly suggested that ATO requires iron for its activity; hence we increased the intracellular iron by hemin/ ALA and observed enhancement of the apoptotic activity of ATO activity in NB4 naïve cells. We also noted that ATO significantly increased the intracellular iron storage protein ferritin and downregulated the mRNA levels of iron import genes (TFRC and DMT1), suggesting that ATO promoting an intracellular iron-rich environment and regulating iron metabolism ina feedback loop mechanism. ROS levels were also significantly reduced in the presence of DFO and also when combined ATO, implying that chelating iron using DFO reduces the free iron availability for the Fenton reaction (ROS production). These results suggest that the mechanism of action of ATO in inducing cell death requires lysosomal iron for its activity and that ATO induced apoptosis can further be enhanced by increasing intracellular iron levels in acute promyelocytic leukemia.

5.7 ATO+ART anti-leukemic activity is as effective as the conventional myelotoxic chemotherapy with minimal bystander effect:

Artesunate significantly enhanced the cytotoxic effect of the conventional chemotherapeutic agents used in the management of acute myeloid leukemia such as daunorubicin and cytosine arabinoside. A combination of ATO and ART effect on the leukemic cells was observed to be as effective as the highly myelosuppressive chemotherapy. We also found that the combination of ATO and ART was effective across the subtypes of acute myeloid and lymphoid leukemia.

We also evaluated the combination of ATO and ART with azacytidine (used in older patients who are unable to withstand intensive 7+3 regimen). We found that a combination of Aza with ART and the triple combination is effective in promoting apoptosis in the leukemic cells with minimal cytotoxicity on the normal cells.

We compared the combination of ATO+ART and Aza+ART or the triple combination with the current standard of care VEN+Aza combination, which has gained significant importance in the management of elderly AML patients. We found that our combination either as the dual combination (ATO+ART or AZA+ART) or triple combination (ATO+ART+AZA) is effective across the different subtypes of AML, whereas VEN+Aza has been reported to be non-effective on the monocytic AML.

In our in vivo experiments, we have faced few challenges in terms of dosing and administration of AZA and hemin in combination with ATO and ART. Hemin administration via I.V was difficult in the initial stages; hence we admisitred hemin as

an intraperitoneal injection.Administration of AZA at a dose of 5mg/kg for five days, in combination with ATO+ART, showed a significant decline in the health of animals (diarrhea and weight loss). In contrast, the animals received AZA+ART were performed well. Hence, we reduced the concentration of AZA to 3mg/kg and increased the number of doses to two cycles of AZA at a dose of 3mg/kg of the animal (5days ON- 2Days OFF- 5days ON). The animals with this dosing performed well without any additional toxicity, which was observed earlier.

In the evolving armamentarium of AML therapy, the addition of ART with ATO or Aza has the potential to de-escalate the highly myelotoxic therapy in the management of acute myeloid leukemia.

Limitation of the study:

Our aim of the study was to evaluate the metabolic adaptations of the leukemic cells and how it could be exploited for therapeutic approaches. We have performed the seahorse extracellular flux analysis only on the leukemic cells and how the treatment of ATO and ART modulated it. Though we have shown that metabolic disruptors overcome environment mediated drug resistance, it would have been better if we were able to replicate the shift in the metabolism of leukemic cells when they are in contact with stromal cells and hypoxia.

We have demonstrated that the dual and triple combination was effective across the subtypes of acute myeloid leukemia (morphology and cytogenetics). It would be more interesting to categorize the primary samples based on mutations

reported in the ELN risk category and assess their response to conventional chemotherapeutic agents vs. the dual and triple combination.

We have shown that the combination was found to be effective in prolonging the survival of the acute promyelocytic leukemia mouse model; however, it would have been more interesting to evaluate the combination in non-M3 AML mouse models harboring different molecular aberrations.

Future directions:

- The chemical proteomics approach of ART to identify the key proteins involved in the selective specificity of the combination need to identify.
- Identify a biomarker to assess the response to ART based therapy, which could be employed in the clinic to monitor the patients.
- Study the impact of adipocytes, osteoblasts, and endothelial cells on the leukemic cell metabolism.
- Evaluate the impact of immune cells on leukemic cell metabolism in promoting immune-compromised microenvironment for their survival.

6.0. Summary and Conclusion:

Leukemic cells from the different subtypes of acute leukemia differ significantly in their utilization of energy-producing metabolic pathways (glycolysis and oxidative phosphorylation). We observed that ATO sensitive APL cells line NB4 naive to be highly sensitive to glycolytic inhibition, and this inhibition by 2-Deoxy glucose was found to be as effective as ATO in vitro and in vivo. We found that ATO resistant APL cell line and non-M3 AML cells are more reliant on OXPHOS and could switch between the two major energy-producing metabolic pathways for their survival. Based on the existing literature and our observation of ATO as a glycolytic inhibitor for glycolysis and to identify a mitochondrial targeting agent, we screened for FDA approved compounds known to have a significant effect on mitochondrial respiration in combination with ATO. Based on our screening criteria for mitochondrial targeting agents, we found that an anti-malarial agent artesunate to be a promising compound because of their synergism with ATO and limited off-target toxicity, bioavailability, affordability and the modes of administration.

We observed that the selective specificity of the combination of ATO +ART is because of the amount of intracellular iron content of the malignant cells where the leukemic cells had increased levels of iron in comparison to the normal cells.

ART quenched the intracellular iron from different cellular compartments, especially mitochondria, for its activation. We also noted that ART significantly affected the mitochondrial dynamics, and the leukemic cells survived the ART

treatment by clearing the damaged mitochondria via mitophagy and upregulating glycolysis for survival.

The combination of ATO and ART synergized well with the conventional chemotherapeutic agents used in the management of AML. We observed that ART synergized with azacytidine (AZA) in inducing selective leukemic cell death. It is interesting to note that the apoptotic effect observed with the ATO+ART combination is comparable to existing standards of care (7+3 ARA-C and DNR; VEN+AZA).

Our in vivo experiments with the leukemic mice model strengthened our in-vitro findings that a dual combination of ATO+ ART or ART+AZA is more effective in reducing the leukemic burden. The triple combination of ATO+ART+AZA was also found to be effective in promoting selective leukemic cell death, in reducing the leukemic burden and prolonging the survival of leukemic mice

The study lays a foundation for evaluating the clinical efficacy of the dual and triple combination in phase I/II clinical trial in patients with acute myeloid leukemia.

Major findings of the study:

- There is a significant level of metabolic heterogeneity in the acute myeloid leukemia cells.
- APL cells are highly glycolytic in comparison to the other subtypes of AML.
- In vivo, glycolytic inhibition reduces the leukemic burden in the APL mouse model.
- ATO resistant cells rely on mitochondrial respiration for their survival

- Targeting the mitochondrial respiration in combination with ATO is effective in different subtypes of leukemia.
- The combination of ATO and ART significantly promoted cell death across the subtypes of leukemia with minimal bystander effect on the normal peripheral blood mononuclear cells and hematopoietic stem cells.
- Intracellular iron content plays a significant role in the selective specificity of the combination ATO+ART on leukemic cells.
- ATO promoted an iron-rich environment, blocked glycolysis, thereby enhancing the anti-leukemic activity of ART.
- Existing therapy in the management of leukemia is highly myelotoxic and not affordable by most of the patients who get diagnosed in our center.
- The combination synergized well with the existing standard of care for leukemia, and it could offer an alternative, low-cost, effective treatment strategy.
- A dual combination of ATO and ART or ART and AZA or triple combination of these drugs could de-escalate the intensive therapy required for the management of AML.
- This could potentially lead to affordable care, especially in the low-middle income countries like us.

Bibliography

ANSÓ, E., WEINBERG, S. E., DIEBOLD, L. P., THOMPSON, B. J., MALINGE, S., SCHUMACKER, P. T., LIU, X., ZHANG, Y., SHAO, Z., STEADMAN, M., MARSH, K. M., XU, J., CRISPINO, J. D. & CHANDEL, N. S. 2017. The mitochondrial respiratory chain is essential for haematopoietic stem cell function. *Nature cell biology,* 19**,** 614-625.

ANYASOR, G., AJAYI, E. I. O., SALIU, J., AJAGBONNA, O. & OLORUNSOGO, O. 2009. Artesunate opens mitochondrial membrane permeability transition pore. *Annals of Tropical Medicine and Public Health,* 2**,** 37-41.

ARBER, D. A., ORAZI, A., HASSERJIAN, R., THIELE, J., BOROWITZ, M. J., LE BEAU, M. M., BLOOMFIELD, C. D., CAZZOLA, M. & VARDIMAN, J. W. 2016. The 2016 revision to the World Health Organization classification of myeloid neoplasms and acute leukemia. *Blood,* 127**,** 2391-2405.

ASSOULINE, S., CULJKOVIC, B., COCOLAKIS, E., ROUSSEAU, C., BESLU, N., AMRI, A., CAPLAN, S., LEBER, B., ROY, D. C., MILLER, W. H., JR. & BORDEN, K. L. 2009. Molecular targeting of the oncogene eIF4E in acute myeloid leukemia (AML): a proof-of-principle clinical trial with ribavirin. *Blood,* 114**,** 257-60.

BENDALL, L. J., DANIEL, A., KORTLEPEL, K. & GOTTLIEB, D. J. 1994. Bone marrow adherent layers inhibit apoptosis of acute myeloid leukemia cells. *Exp Hematol,* 22.

BENNETT, J. M., CATOVSKY, D., DANIEL, M. T., FLANDRIN, G., GALTON, D. A., GRALNICK, H. R. & SULTAN, C. 1976. Proposals for the classification of the acute leukaemias. French-American-British (FAB) co-operative group. *Br J Haematol,* 33**,** 451-8.

BERNARD, D., GEBBIA, M., PRABHA, S., GRONDA, M., MACLEAN, N., WANG, X., HURREN, R., SUKHAI, M. A., CHO, E. E., MANOLSON, M. F., DATTI, A., WRANA, J., MINDEN, M. D., AL-AWAR, R., AMAN, A., NISLOW, C., GIAEVER, G. & SCHIMMER, A. D. 2015. Select microtubule inhibitors increase lysosome acidity and promote lysosomal disruption in acute myeloid leukemia (AML) cells. *Apoptosis,* 20**,** 948-959.

BRAND, A., SINGER, K., KOEHL, G. E., KOLITZUS, M., SCHOENHAMMER, G., THIEL, A., MATOS, C., BRUSS, C., KLOBUCH, S., PETER, K., KASTENBERGER, M., BOGDAN, C., SCHLEICHER, U., MACKENSEN, A., ULLRICH, E., FICHTNER-FEIGL, S., KESSELRING, R., MACK, M., RITTER, U., SCHMID, M., BLANK, C., DETTMER, K., OEFNER, P. J., HOFFMANN, P., WALENTA, S., GEISSLER, E. K., POUYSSEGUR, J., VILLUNGER, A., STEVEN, A., SELIGER, B., SCHREML, S., HAFERKAMP, S., KOHL, E., KARRER, S., BERNEBURG, M., HERR, W., MUELLER-KLIESER, W., RENNER, K. & KREUTZ, M. 2016. LDHA-Associated Lactic Acid Production Blunts Tumor Immunosurveillance by T and NK Cells. *Cell Metab,* 24**,** 657-671.

BRAULT, C., ZERBIB, Y., DELETTE, C., MARC, J., GRUSON, B., MAROLLEAU, J. P. & MAIZEL, J. 2018. The Warburg Effect as a Type B Lactic Acidosis in a Patient With Acute Myeloid Leukemia: A Diagnostic Challenge for Clinicians. *Front Oncol,* 8**,** 232.

BREASTED, J. H. 1918. Ancient Times: A History of the Early World. By J. H. Breasted, Professor in the University of Chicago. 1 vol. 8vo. Pp. 742. Numerous maps and illustrations. Ginn and Co. 6s. 6d. net. *The Classical Review,* 32**,** 44-44.

CALLENS, C., COULON, S., NAUDIN, J., RADFORD-WEISS, I., BOISSEL, N., RAFFOUX, E., WANG, P. H., AGARWAL, S., TAMOUZA, H., PAUBELLE, E., ASNAFI, V., RIBEIL, J. A., DESSEN, P., CANIONI, D., CHANDESRIS, O., RUBIO, M. T., BEAUMONT, C., BENHAMOU, M., DOMBRET, H., MACINTYRE, E., MONTEIRO, R. C., MOURA, I. C. & HERMINE, O. 2010. Targeting iron homeostasis induces cellular differentiation and synergizes with differentiating agents in acute myeloid leukemia. *J Exp Med,* 207**,** 731-50.

CANTOR, J. R. & SABATINI, D. M. 2012. Cancer cell metabolism: one hallmark, many faces. *Cancer Discov,* 2**,** 881-98.

CASTRO, I., SAMPAIO-MARQUES, B. & LUDOVICO, P. 2019. Targeting Metabolic Reprogramming in Acute Myeloid Leukemia. *Cells,* 8**,** 967.

CHAM, C. M., DRIESSENS, G., O'KEEFE, J. P. & GAJEWSKI, T. F. 2008. Glucose deprivation inhibits multiple key gene expression events and effector functions in CD8+ T cells. *Eur J Immunol,* 38**,** 2438-50.

CHAMBERS, S. M., SHAW, C. A., GATZA, C., FISK, C. J., DONEHOWER, L. A. & GOODELL, M. A. 2007. Aging hematopoietic stem cells decline in function and exhibit epigenetic dysregulation. *PLoS biology,* 5.

CHEN, G. Q., SHI, X. G., TANG, W., XIONG, S. M., ZHU, J., CAI, X., HAN, Z. G., NI, J. H., SHI, G. Y., JIA, P. M., LIU, M. M., HE, K. L., NIU, C., MA, J., ZHANG, P., ZHANG, T. D., PAUL, P., NAOE, T., KITAMURA, K., MILLER, W., WAXMAN, S., WANG, Z. Y., DE THE, H., CHEN, S. J. & CHEN, Z. 1997. Use of arsenic trioxide (As2O3) in the treatment of acute promyelocytic leukemia (APL): I. As2O3 exerts dose-dependent dual effects on APL cells. *Blood,* 89**,** 3345-53.

CHENDAMARAI, E., GANESAN, S., ALEX, A. A., KAMATH, V., NAIR, S. C., NELLICKAL, A. J., JANET, N. B., SRIVASTAVA, V., LAKSHMI, K. M., VISWABANDYA, A., ABRAHAM, A., AIYAZ, M., MULLAPUDI, N., MUGASIMANGALAM, R., PADUA, R. A., CHOMIENNE, C., CHANDY, M., SRIVASTAVA, A., GEORGE, B., BALASUBRAMANIAN, P. & MATHEWS, V. 2015. Comparison of newly diagnosed and relapsed patients with acute promyelocytic leukemia treated with arsenic trioxide: insight into mechanisms of resistance. *PloS one,* 10**,** e0121912-e0121912.

CHRISTIAN, S., MERZ, C., EVANS, L., GRADL, S., SEIDEL, H., FRIBERG, A., EHEIM, A., LEJEUNE, P., BRZEZINKA, K., ZIMMERMANN, K., FERRARA, S., MEYER, H., LESCHE, R., STOECKIGT, D., BAUSER, M., HAEGEBARTH, A., SYKES, D. B., SCADDEN, D. T., LOSMAN, J.-A. & JANZER, A. 2019. The novel dihydroorotate dehydrogenase (DHODH) inhibitor BAY 2402234 triggers differentiation and is effective in the treatment of myeloid malignancies. *Leukemia,* 33**,** 2403-2415.

COMMISSO, C., DAVIDSON, S. M., SOYDANER-AZELOGLU, R. G., PARKER, S. J., KAMPHORST, J. J., HACKETT, S., GRABOCKA, E., NOFAL, M., DREBIN, J. A., THOMPSON, C. B., RABINOWITZ, J. D., METALLO, C. M., VANDER HEIDEN, M. G. & BAR-SAGI, D. 2013. Macropinocytosis of protein is an amino acid supply route in Ras-transformed cells. *Nature,* 497**,** 633-637.

COOMBS, C. C., TAVAKKOLI, M. & TALLMAN, M. S. 2015a. Acute promyelocytic leukemia: where did we start, where are we now, and the future. *Blood Cancer Journal,* 5**,** e304.

COOMBS, C. C., TAVAKKOLI, M. & TALLMAN, M. S. 2015b. Acute promyelocytic leukemia: where did we start, where are we now, and the future. *Blood cancer journal,* 5**,** e304-e304.

CORY, S., ROBERTS, A. W., COLMAN, P. M. & ADAMS, J. M. 2016. Targeting BCL-2-like proteins to kill cancer cells. *Trends in cancer,* 2**,** 443-460.

DAI, H., MENG, X. W. & KAUFMANN, S. H. 2016. Mitochondrial apoptosis and BH3 mimetics [version 1; referees.

DAVIDS, M. S., LETAI, A. & BROWN, J. R. 2013. Overcoming stroma-mediated treatment resistance in chronic lymphocytic leukemia through BCL-2 inhibition. *Leukemia & lymphoma,* 54**,** 1823-1825.

DAVISON, K., MANN, K. K., WAXMAN, S. & MILLER, W. H., JR. 2004. JNK activation is a mediator of arsenic trioxide-induced apoptosis in acute promyelocytic leukemia cells. *Blood,* 103**,** 3496-502.

DE HAAN, G. & LAZARE, S. S. 2018. Aging of hematopoietic stem cells. *Blood,* 131**,** 479-487.

DEBALSI, K., HOFF, K. & COPELAND, W. 2016. Role of the mitochondrial DNA replication machinery in mitochondrial DNA mutagenesis, aging and age-related diseases. *Ageing Research Reviews,* 33.

DICK, J. E. Normal and leukemic human stem cells assayed in SCID mice. Seminars in immunology, 1996. Elsevier, 197-206.

DIELSCHNEIDER, R. F., HENSON, E. S. & GIBSON, S. B. 2017. Lysosomes as Oxidative Targets for Cancer Therapy. *Oxidative Medicine and Cellular Longevity,* 2017**,** 3749157.

DINARDO, C. D. & PERL, A. E. 2019. Advances in patient care through increasingly individualized therapy. *Nature Reviews Clinical Oncology,* 16**,** 73-74.

DINARDO, C. D., PRATZ, K., PULLARKAT, V., JONAS, B. A., ARELLANO, M., BECKER, P. S., FRANKFURT, O., KONOPLEVA, M., WEI, A. H., KANTARJIAN, H. M., XU, T., HONG, W.-J., CHYLA, B., POTLURI, J., POLLYEA, D. A. & LETAI, A. 2019. Venetoclax combined with decitabine or azacitidine in treatment-naive, elderly patients with acute myeloid leukemia. *Blood,* 133**,** 7-17.

DING, W.-X. & YIN, X.-M. 2012. Mitophagy: mechanisms, pathophysiological roles, and analysis. *Biological chemistry,* 393**,** 547-564.

DOMBRET, H., SEYMOUR, J. F., BUTRYM, A., WIERZBOWSKA, A., SELLESLAG, D., JANG, J. H., KUMAR, R., CAVENAGH, J., SCHUH, A. C., CANDONI, A., RÉCHER, C., SANDHU, I., BERNAL DEL CASTILLO, T., AL-ALI, H. K., MARTINELLI, G., FALANTES, J., NOPPENEY, R., STONE, R. M., MINDEN, M. D., MCINTYRE, H., SONGER, S., LUCY, L. M., BEACH, C. L. & DÖHNER, H. 2015. International phase 3 study of azacitidine vs conventional care regimens in older patients with newly diagnosed AML with >30% blasts. *Blood,* 126**,** 291-299.

EGUCHI, R., FUJIMORI, Y., TAKEDA, H., TABATA, C., OHTA, T., KURIBAYASHI, K., FUKUOKA, K. & NAKANO, T. 2011. Arsenic trioxide induces apoptosis through JNK and ERK in human mesothelioma cells. *J Cell Physiol,* 226**,** 762-8.

ESCOLL, P., PLATON, L. & BUCHRIESER, C. 2019. Roles of Mitochondrial Respiratory Complexes during Infection.

EVANS, C. S. & HOLZBAUR, E. L. F. 2020. Degradation of engulfed mitochondria is rate-limiting in Optineurin-mediated mitophagy in neurons. *eLife,* 9**,** e50260.

FENNELLY, C. & AMARAVADI, R. K. 2017. Lysosomal Biology in Cancer. *Methods in molecular biology (Clifton, N.J.),* 1594**,** 293-308.

FIORILLO, M., LAMB, R., TANOWITZ, H. B., CAPPELLO, A. R., MARTINEZ-OUTSCHOORN, U. E., SOTGIA, F. & LISANTI, M. P. 2016. Bedaquiline, an FDA-approved antibiotic, inhibits mitochondrial function and potently blocks the proliferative expansion of stem-like cancer cells (CSCs). *Aging (Albany NY),* 8**,** 1593-1606.

FREZZA, C. & GOTTLIEB, E. 2009. Mitochondria in cancer: not just innocent bystanders. *Semin Cancer Biol,* 19**,** 4-11.

FRIEDMAN, A. A., LETAI, A., FISHER, D. E. & FLAHERTY, K. T. 2015. Precision medicine for cancer with next-generation functional diagnostics. *Nat Rev Cancer,* 15**,** 747-756.

GARRIDO, S. M., APPELBAUM, F. R., WILLMAN, C. L. & BANKER, D. E. 2001. Acute myeloid leukemia cells are protected from spontaneous and drug-induced apoptosis by direct contact with a human bone marrow stromal cell line (HS-5). *Exp Hematol,* 29**,** 448-57.

GIANNI, M., KOKEN, M. H. M., CHELBI-ALIX, M. K., BENOIT, G., LANOTTE, M. & CHEN, Z. 1998. Combined arsenic and retinoic acid treatment enhances differentiation and apoptosis in arsenic-resistant NB4 cells. *Blood,* 91.

GLASSPOOL, R. M., TEODORIDIS, J. M. & BROWN, R. 2006. Epigenetics as a mechanism driving polygenic clinical drug resistance. *British Journal Of Cancer,* 94**,** 1087.

GOGVADZE, V., ZHIVOTOVSKY, B. & ORRENIUS, S. 2010. The Warburg effect and mitochondrial stability in cancer cells. *Mol Aspects Med,* 31**,** 60-74.

GOHIL, V. M., SHETH, S. A., NILSSON, R., WOJTOVICH, A. P., LEE, J. H., PEROCCHI, F., CHEN, W., CLISH, C. B., AYATA, C., BROOKES, P. S. & MOOTHA, V. K. 2010a. Discovery and therapeutic potential of drugs that shift energy metabolism from mitochondrial respiration to glycolysis. *Nature biotechnology,* 28**,** 249-255.

GOHIL, V. M., SHETH, S. A., NILSSON, R., WOJTOVICH, A. P., LEE, J. H., PEROCCHI, F., CHEN, W., CLISH, C. B., AYATA, C., BROOKES, P. S. & MOOTHA, V. K. 2010b. Nutrient-sensitized screening for drugs that shift energy metabolism from mitochondrial respiration to glycolysis. *Nature biotechnology,* 28**,** 249-255.

GORRE, M. E., MOHAMMED, M., ELLWOOD, K., HSU, N., PAQUETTE, R., RAO, P. N. & SAWYERS, C. L. 2001. Clinical Resistance to STI-571 Cancer Therapy Caused by BCR-ABL Gene Mutation or Amplification. *Science,* 293**,** 876.

GOTO, E., TOMITA, A., HAYAKAWA, F., ATSUMI, A., KIYOI, H. & NAOE, T. 2011. Missense mutations in PML-RARA are critical for the lack of responsiveness to arsenic trioxide treatment. *Blood,* 118**,** 1600-9.

GOTTSCHALK, S., ANDERSON, N., HAINZ, C., ECKHARDT, S. G. & SERKOVA, N. J. 2004. Imatinib (STI571)-mediated changes in glucose metabolism in human leukemia BCR-ABL-positive cells. *Clin Cancer Res,* 10**,** 6661-8.

GRIMWADE, D., IVEY, A. & HUNTLY, B. J. 2016. Molecular landscape of acute myeloid leukemia in younger adults and its clinical relevance. *Blood,* 127**,** 29-41.

GROARKE, E. M. & YOUNG, N. S. 2019. Aging and Hematopoiesis. *Clin Geriatr Med,* 35**,** 285-293.

GROSS, A. & KATZ, S. G. 2017. Non-apoptotic functions of BCL-2 family proteins. *Cell death and differentiation,* 24**,** 1348.

GROVE, C. S. & VASSILIOU, G. S. 2014. Acute myeloid leukaemia: a paradigm for the clonal evolution of cancer? *Disease Models & Mechanisms,* 7**,** 941.

GUICCIARDI, M. E., LEIST, M. & GORES, G. J. 2004. Lysosomes in cell death. *Oncogene,* 23**,** 2881-2890.

HAN, L., CAVAZOS, A., BARAN, N., ZHANG, Q., KURUVILLA, V. M., GAY, J. P., FENG, N., BATTULA, V. L., KANTARJIAN, H. M., DAVER, N. G., MARSZALEK, J. R., ANDREEFF, M. & KONOPLEVA, M. Y. 2019. Mitochondrial Oxphos As Survival Mechanism of Minimal Residual AML Cells after Induction Chemotherapy : Survival Benefit By Complex I Inhibition with Iacs-010759. *Blood,* 134**,** 5161-5161.

HANAHAN, D. & WEINBERG, ROBERT A. Hallmarks of Cancer: The Next Generation. *Cell,* 144**,** 646-674.

HANAHAN, D. & WEINBERG, R. A. 2000. The hallmarks of cancer. *Cell,* 100**,** 57-70.

HANAHAN, D. & WEINBERG, R. A. 2011. Hallmarks of cancer: the next generation. *Cell,* 144**,** 646-74.

HATA, A. N., ENGELMAN, J. A. & FABER, A. C. 2015. The BCL2 family: key mediators of the apoptotic response to targeted anticancer therapeutics. *Cancer discovery,* 5**,** 475-487.

HO, T. T., WARR, M. R., ADELMAN, E. R., LANSINGER, O. M., FLACH, J., VEROVSKAYA, E. V., FIGUEROA, M. E. & PASSEGUÉ, E. 2017. Autophagy maintains the metabolism and function of young and old stem cells. *Nature,* 543**,** 205-210.

HOGDAL, L. J. 2015. *Mitochondrial Priming and Anti-Apoptotic Dependencies in Aging and Diseased Bone Marrow.*

HOPE, K. J., JIN, L. & DICK, J. E. 2004. Acute myeloid leukemia originates from a hierarchy of leukemic stem cell classes that differ in self-renewal capacity. *Nature immunology,* 5**,** 738-743.

ISHIKAWA, F., YOSHIDA, S., SAITO, Y., HIJIKATA, A., KITAMURA, H., TANAKA, S., NAKAMURA, R., TANAKA, T., TOMIYAMA, H., SAITO, N., FUKATA, M., MIYAMOTO, T., LYONS, B., OHSHIMA, K., UCHIDA, N., TANIGUCHI, S., OHARA, O., AKASHI, K., HARADA, M. & SHULTZ, L. D. 2007. Chemotherapy-resistant human AML stem cells home to and engraft within the bone-marrow endosteal region. *Nat Biotech,* 25**,** 1315-1321.

ISMAIL, H. M., BARTON, V., PHANCHANA, M., CHAROENSUTTHIVARAKUL, S., WONG, M. H. L., HEMINGWAY, J., BIAGINI, G. A., O'NEILL, P. M. & WARD, S. A. 2016. Artemisinin activity-based probes identify multiple molecular targets within the asexual stage of the malaria parasites Plasmodium falciparum 3D7. *Proceedings of the National Academy of Sciences of the United States of America,* 113**,** 2080-2085.

JIA, L. & GRIBBEN, J. G. 2014. Dangerous power: mitochondria in CLL cells. *Blood,* 123.

JING, Y., DAI, J., CHALMERS-REDMAN, R. M. E., TATTON, W. G. & WAXMAN, S. 1999. Arsenic Trioxide Selectively Induces Acute Promyelocytic Leukemia Cell Apoptosis Via a Hydrogen Peroxide-Dependent Pathway. *Blood,* 94**,** 2102.

JONES, C. L., STEVENS, B. M., D'ALESSANDRO, A., REISZ, J. A., CULP-HILL, R., NEMKOV, T., PEI, S., KHAN, N., ADANE, B., YE, H., KRUG, A., REINHOLD, D., SMITH, C., DEGREGORI, J., POLLYEA, D. A. & JORDAN, C. T. 2018. Inhibition of Amino Acid Metabolism Selectively Targets Human Leukemia Stem Cells. *Cancer Cell,* 34**,** 724-740 e4.

KASZNICKI, J., SLIWINSKA, A. & DRZEWOSKI, J. 2014. Metformin in cancer prevention and therapy. *Annals of Translational Medicine,* 2**,** 57.

KENTSIS, A., TOPISIROVIC, I., CULJKOVIC, B., SHAO, L. & BORDEN, K. L. 2004. Ribavirin suppresses eIF4E-mediated oncogenic transformation by physical mimicry of the 7-methyl guanosine mRNA cap. *Proc Natl Acad Sci U S A,* 101**,** 18105-10.

KIM, J. W. & DANG, C. V. 2006. Cancer's molecular sweet tooth and the Warburg effect. *Cancer Res,* 66**,** 8927-30.

KONOPLEVA, M., KONOPLEV, S., HU, W., ZARITSKEY, A. Y., AFANASIEV, B. V. & ANDREEFF, M. 2002. Stromal cells prevent apoptosis of AML cells by up-regulation of anti-apoptotic proteins. *Leukemia,* 16**,** 1713-24.

KONOPLEVA, M., WATT, J., CONTRACTOR, R., TSAO, T., HARRIS, D., ESTROV, Z., BORNMANN, W., KANTARJIAN, H., VIALLET, J., SAMUDIO, I. & ANDREEFF, M. 2008. Mechanisms of antileukemic activity of the novel Bcl-2 homology domain-3 mimetic GX15-070 (obatoclax). *Cancer Res,* 68**,** 3413-20.

KOPPENOL, W. H., BOUNDS, P. L. & DANG, C. V. 2011. Otto Warburg's contributions to current concepts of cancer metabolism. *Nat Rev Cancer,* 11**,** 325-37.

KOUCHKOVSKY, I. & ABDUL-HAY, M. 2016. 'Acute myeloid leukemia: A comprehensive review and 2016 update'. *Blood cancer journal,* 6**,** e441.

KRISHNA, S., GANAPATHI, S., STER, I. C., SAEED, M. E. M., COWAN, M., FINLAYSON, C., KOVACSEVICS, H., JANSEN, H., KREMSNER, P. G., EFFERTH, T. & KUMAR, D. 2014. A Randomised, Double Blind, Placebo-Controlled Pilot Study of Oral Artesunate Therapy for Colorectal Cancer. *EBioMedicine,* 2**,** 82-90.

KULKARNI, U., GANESAN, S., ALEX, A. A., PALANI, H., DAVID, S., BALASUNDARAM, N., VENKATRAMAN, A., THENMOZHI, M., JEYASEELAN, L., KORULA, A., DEVASIA, A., ABRAHAM, A., JANET, N. B., BALASUBRAMANIAN, P., GEORGE, B. & MATHEWS, V. A

phase II study evaluating the role of bortezomib in the management of relapsed acute promyelocytic leukemia treated upfront with arsenic trioxide. *Cancer Medicine,* n/a.

KURZ, T., TERMAN, A., GUSTAFSSON, B. & BRUNK, U. T. 2008. Lysosomes in iron metabolism, ageing and apoptosis. *Histochemistry and cell biology,* 129**,** 389-406.

LAGADINOU, E. D., SACH, A., CALLAHAN, K., ROSSI, R. M., NEERING, S. J. & MINHAJUDDIN, M. 2013a. BCL-2 inhibition targets oxidative phosphorylation and selectively eradicates quiescent human leukemia stem cells. *Cell Stem Cell,* 12.

LAGADINOU, E. D., SACH, A., CALLAHAN, K., ROSSI, R. M., NEERING, S. J., MINHAJUDDIN, M., ASHTON, J. M., PEI, S., GROSE, V., O'DWYER, K. M., LIESVELD, J. L., BROOKES, P. S., BECKER, M. W. & JORDAN, C. T. 2013b. BCL-2 inhibition targets oxidative phosphorylation and selectively eradicates quiescent human leukemia stem cells. *Cell Stem Cell,* 12**,** 329-41.

LEHMANN-CHE, J., BALLY, C. & DE THE, H. 2014. Resistance to therapy in acute promyelocytic leukemia. *N Engl J Med,* 371**,** 1170-2.

LEIBOWITZ, B. & YU, J. 2010. Mitochondrial signaling in cell death via the Bcl-2 family. *Cancer biology & therapy,* 9**,** 417-422.

LI, T., MA, R., ZHANG, Y., MO, H., YANG, X., HU, S., WANG, L., NOVAKOVIC, V. A., CHEN, H., KOU, J., BI, Y., YU, B., FANG, S., WANG, J., ZHOU, J. & SHI, J. 2018. Arsenic trioxide promoting ETosis in acute promyelocytic leukemia through mTOR-regulated autophagy. *Cell Death & Disease,* 9**,** 75.

LO-COCO, F., AVVISATI, G., VIGNETTI, M., THIEDE, C., ORLANDO, S. M., IACOBELLI, S., FERRARA, F., FAZI, P., CICCONI, L., DI BONA, E., SPECCHIA, G., SICA, S., DIVONA, M., LEVIS, A., FIEDLER, W., CERQUI, E., BRECCIA, M., FIORITONI, G., SALIH, H. R., CAZZOLA, M., MELILLO, L., CARELLA, A. M., BRANDTS, C. H., MORRA, E., VON LILIENFELD-TOAL, M., HERTENSTEIN, B., WATTAD, M., LUBBERT, M., HANEL, M., SCHMITZ, N., LINK, H., KROPP, M. G., RAMBALDI, A., LA NASA, G., LUPPI, M., CICERI, F., FINIZIO, O., VENDITTI, A., FABBIANO, F., DOHNER, K., SAUER, M., GANSER, A., AMADORI, S., MANDELLI, F., DOHNER, H., EHNINGER, G., SCHLENK, R. F. & PLATZBECKER, U. 2013. Retinoic acid and arsenic trioxide for acute promyelocytic leukemia. *N Engl J Med,* 369**,** 111-21.

LOPEZ-OTIN, C., BLASCO, M. A., PARTRIDGE, L., SERRANO, M. & KROEMER, G. 2013. The hallmarks of aging. *Cell,* 153**,** 1194-217.

LÖWENBERG, B., SUCIU, S., ARCHIMBAUD, E., HAAK, H., STRYCKMANS, P., DE CATALDO, R., DEKKER, A., BERNEMAN, Z., THYSS, A. & VAN DER LELIE, J. 1998. Mitoxantrone Versus Daunorubicin in Induction-Consolidation Chemotherapy-The Value of Low-Dose Cytarabine for Maintenance of Remission, and an Assessment of Prognostic Factors in Acute Myeloid Leukemia in the Elderly: Final Report of the Leukemia Cooperative Group of the European Organization for the Research and Treatment of Cancer and th Dutch-Belgian Hemato-Oncology Cooperative Hovon Group Randomized Phase III Study AML-9. *Journal of Clinical Oncology,* 16**,** 872-881.

LUNGHI, P., TABILIO, A., LO-COCO, F., PELICCI, P. G. & BONATI, A. 2005. Arsenic trioxide (ATO) and MEK1 inhibition synergize to induce apoptosis in acute promyelocytic leukemia cells. *Leukemia,* 19**,** 234-44.

LUNT, S. Y. & VANDER HEIDEN, M. G. 2011. Aerobic glycolysis: meeting the metabolic requirements of cell proliferation. *Annu Rev Cell Dev Biol,* 27**,** 441-64.

MADAN, V., SHYAMSUNDER, P., HAN, L., MAYAKONDA, A., NAGATA, Y., SUNDARESAN, J., KANOJIA, D., YOSHIDA, K., GANESAN, S., HATTORI, N., FULTON, N., TAN, K. T.,

ALPERMANN, T., KUO, M. C., ROSTAMI, S., MATTHEWS, J., SANADA, M., LIU, L. Z., SHIRAISHI, Y., MIYANO, S., CHENDAMARAI, E., HOU, H. A., MALNASSY, G., MA, T., GARG, M., DING, L. W., SUN, Q. Y., CHIEN, W., IKEZOE, T., LILL, M., BIONDI, A., LARSON, R. A., POWELL, B. L., LUBBERT, M., CHNG, W. J., TIEN, H. F., HEUSER, M., GANSER, A., KOREN-MICHOWITZ, M., KORNBLAU, S. M., KANTARJIAN, H. M., NOWAK, D., HOFMANN, W. K., YANG, H., STOCK, W., GHAVAMZADEH, A., ALIMOGHADDAM, K., HAFERLACH, T., OGAWA, S., SHIH, L. Y., MATHEWS, V. & KOEFFLER, H. P. 2016. Comprehensive mutational analysis of primary and relapse acute promyelocytic leukemia. *Leukemia,* 30**,** 1672-81.

MARASCA, R., ZUCCHINI, P., GALIMBERTI, S., LEONARDI, G., VACCARI, P., DONELLI, A., LUPPI, M., PETRINI, M. & TORELLI, G. 1999. Missense mutations in the PML/RARalpha ligand binding domain in ATRA-resistant As(2)O(3) sensitive relapsed acute promyelocytic leukemia. *Haematologica,* 84**,** 963-8.

MARLEIN, C. R., ZAITSEVA, L. & RUSHWORTH, S. A. 2017. Pulling the plug - halting cancer's theft of mitochondria. *Oncoscience,* 4**,** 173-174.

MARTINOU, J.-C. & YOULE, R. J. 2011. Mitochondria in apoptosis: Bcl-2 family members and mitochondrial dynamics. *Developmental cell,* 21**,** 92-101.

MARYANOVICH, M., ZALTSMAN, Y., RUGGIERO, A., GOLDMAN, A., SHACHNAI, L., ZAIDMAN, S. L., PORAT, Z., GOLAN, K., LAPIDOT, T. & GROSS, A. 2015. An MTCH2 pathway repressing mitochondria metabolism regulates haematopoietic stem cell fate. *Nat Commun,* 6**,** 7901.

MATHEWS, V., BALASUBRAMANIAN, P., SHAJI, R. V., GEORGE, B., CHANDY, M. & SRIVASTAVA, A. 2002. Arsenic trioxide in the treatment of newly diagnosed acute promyelocytic leukemia: a single center experience. *Am J Hematol,* 70**,** 292-9.

MATHEWS, V., GEORGE, B., LAKSHMI, K. M., VISWABANDYA, A., BAJEL, A., BALASUBRAMANIAN, P., SHAJI, R. V., SRIVASTAVA, V. M., SRIVASTAVA, A. & CHANDY, M. 2006. Single-agent arsenic trioxide in the treatment of newly diagnosed acute promyelocytic leukemia: durable remissions with minimal toxicity. *Blood,* 107**,** 2627-32.

MATHIEU, J. & RUOHOLA-BAKER, H. 2017. Metabolic remodeling during the loss and acquisition of pluripotency. *Development,* 144**,** 541 - 551.

MATTES, K., VELLENGA, E. & SCHEPERS, H. 2019. Differential redox-regulation and mitochondrial dynamics in normal and leukemic hematopoietic stem cells: A potential window for leukemia therapy. *Critical Reviews in Oncology/Hematology,* 144**,** 102814.

MAURILLO, L., BUCCISANO, F., SPAGNOLI, A., VOSO, M. T., FIANCHI, L., PAPAYANNIDIS, C., GAIDANO, G. L., BRECCIA, M., MUSTO, P., DE BELLIS, E., DEL PRINCIPE, M. I., LUNGHI, M., LESSI, F., MARTINELLI, G. & VENDITTI, A. 2018. Comparative analysis of azacitidine and intensive chemotherapy as front-line treatment of elderly patients with acute myeloid leukemia. *Ann Hematol,* 97**,** 1767-1774.

MCKERRELL, T. & VASSILIOU, G. S. 2015. Aging as a driver of leukemogenesis. *Science translational medicine,* 7**,** 306fs38-306fs38.

MCNICHOLAS, K., MACGREGOR, M. N. & GLEADLE, J. M. 2019. In order for the light to shine so brightly, the darkness must be present—why do cancers fluoresce with 5-aminolaevulinic acid? *British Journal of Cancer,* 121**,** 631-639.

MICHAELIS, L. C. 2019. Venetoclax in AML: aiming for “just right”. *Blood,* 133**,** 3-4.

MISTRY, J. J., MARLEIN, C. R., MOORE, J. A., HELLMICH, C., WOJTOWICZ, E. E., SMITH, J. G. W., MACAULAY, I., SUN, Y., MORFAKIS, A., PATTERSON, A., HORTON, R. H., DIVEKAR,

D., MORRIS, C. J., HAESTIER, A., DI PALMA, F., BERAZA, N., BOWLES, K. M. & RUSHWORTH, S. A. 2019. ROS-mediated PI3K activation drives mitochondrial transfer from stromal cells to hematopoietic stem cells in response to infection. *Proceedings of the National Academy of Sciences,* 116**,** 24610.

MITTLER, R., DARASH-YAHANA, M., SOHN, Y. S., BAI, F., SONG, L., CABANTCHIK, I. Z., JENNINGS, P. A., ONUCHIC, J. N. & NECHUSHTAI, R. 2018. NEET Proteins: A New Link Between Iron Metabolism, Reactive Oxygen Species, and Cancer. *Antioxidants & Redox Signaling,* 30**,** 1083-1095.

MONTERO, J. & LETAI, A. 2018. Why do BCL-2 inhibitors work and where should we use them in the clinic? *Cell Death & Differentiation,* 25**,** 56-64.

MOOSAVI, M. A. & DJAVAHERI-MERGNY, M. 2019. Autophagy: New Insights into Mechanisms of Action and Resistance of Treatment in Acute Promyelocytic leukemia. *International Journal of Molecular Sciences,* 20**,** 3559.

MOSCHOI, R., IMBERT, V., NEBOUT, M., CHICHE, J., MARY, D., PREBET, T., SALAND, E., CASTELLANO, R., POUYET, L., COLLETTE, Y., VEY, N., CHABANNON, C., RECHER, C., SARRY, J.-E., ALCOR, D., PEYRON, J.-F. & GRIESSINGER, E. 2016. Protective mitochondrial transfer from bone marrow stromal cells to acute myeloid leukemic cells during chemotherapy. *Blood,* 128**,** 253-264.

MOUGIAKAKOS, D. 2019. The Induction of a Permissive Environment to Promote T Cell Immune Evasion in Acute Myeloid Leukemia: The Metabolic Perspective. *Frontiers in Oncology,* 9.

MYERS, R. A., WIRTH, S., WILLIAMS, S. & KIEL, P. J. 2018. Enasidenib: An Oral IDH2 Inhibitor for the Treatment of Acute Myeloid Leukemia. *Journal of the advanced practitioner in oncology,* 9**,** 435-440.

NING, X., DU, Y., BEN, Q., HUANG, L., HE, X., GONG, Y., GAO, J., WU, H., MAN, X., JIN, J., XU, M. & LI, Z. 2016. Bulk pancreatic cancer cells can convert into cancer stem cells(CSCs) in vitro and 2 compounds can target these CSCs. *Cell Cycle,* 15**,** 403-412.

NIU, C., YAN, H., YU, T., SUN, H. P., LIU, J. X., LI, X. S., WU, W., ZHANG, F. Q., CHEN, Y., ZHOU, L., LI, J. M., ZENG, X. Y., YANG, R. R., YUAN, M. M., REN, M. Y., GU, F. Y., CAO, Q., GU, B. W., SU, X. Y., CHEN, G. Q., XIONG, S. M., ZHANG, T. D., WAXMAN, S., WANG, Z. Y., CHEN, Z., HU, J., SHEN, Z. X. & CHEN, S. J. 1999. Studies on treatment of acute promyelocytic leukemia with arsenic trioxide: remission induction, follow-up, and molecular monitoring in 11 newly diagnosed and 47 relapsed acute promyelocytic leukemia patients. *Blood,* 94**,** 3315-24.

O'NEILL, P. M., BARTON, V. E. & WARD, S. A. 2010. The Molecular Mechanism of Action of Artemisinin—The Debate Continues. *Molecules,* 15**,** 1705-1721.

OWEN, M. R., DORAN, E. & HALESTRAP, A. P. 2000. Evidence that metformin exerts its anti-diabetic effects through inhibition of complex 1 of the mitochondrial respiratory chain. *Biochem. J.,* 348**,** 607-614.

PEI, S., MINHAJUDDIN, M., ADANE, B., KHAN, N., STEVENS, B. M., MACK, S. C., LAI, S., RICH, J. N., INGUVA, A., SHANNON, K. M., KIM, H., TAN, A.-C., MYERS, J. R., ASHTON, J. M., NEFF, T., POLLYEA, D. A., SMITH, C. A. & JORDAN, C. T. 2018. AMPK/FIS1-Mediated Mitophagy Is Required for Self-Renewal of Human AML Stem Cells. *Cell Stem Cell,* 23**,** 86-100.e6.

PEI, S., POLLYEA, D. A., GUSTAFSON, A., STEVENS, B. M., MINHAJUDDIN, M., FU, R., RIEMONDY, K. A., GILLEN, A. E., SHERIDAN, R. M., KIM, J., COSTELLO, J. C., AMAYA, M. L., INGUVA, A., WINTERS, A., YE, H., KRUG, A., JONES, C. L., ADANE, B., KHAN, N., PONDER, J., SCHOWINSKY, J., ABBOTT, D., HAMMES, A., MYERS, J. R., ASHTON, J. M.,

NEMKOV, T., D'ALESSANDRO, A., GUTMAN, J. A., RAMSEY, H. E., SAVONA, M. R., SMITH, C. A. & JORDAN, C. T. 2020. Monocytic Subclones Confer Resistance to Venetoclax-Based Therapy in Acute Myeloid Leukemia Patients. *Cancer Discovery*, CD-19-0710.

PHILIP, C., GEORGE, B., GANAPULE, A., KORULA, A., JAIN, P., ALEX, A. A., LAKSHMI, K. M., SITARAM, U., ABUBACKER, F. N., ABRAHAM, A., VISWABANDYA, A., SRIVASTAVA, V. M., SRIVASTAVA, A., BALASUBRAMANIAN, P. & MATHEWS, V. 2015. Acute myeloid leukaemia: challenges and real world data from India. *British journal of haematology,* 170**,** 110-117.

PIETERS, R., LOONEN, A. H., HUISMANS, D. R., BROEKEMA, G. J., DIRVEN, M. W., HEYENBROK, M. W., HAHLEN, K. & VEERMAN, A. J. 1990. In vitro drug sensitivity of cells from children with leukemia using the MTT assay with improved culture conditions. *Blood,* 76**,** 2327-36.

PILLER, G. 2001. Leukaemia - a brief historical review from ancient times to 1950. *Br J Haematol,* 112**,** 282-92.

PINHO, S. & FRENETTE, P. S. 2019. Haematopoietic stem cell activity and interactions with the niche. *Nature Reviews Molecular Cell Biology,* 20**,** 303-320.

POTTER, D. & LETAI, A. 2016. To Prime, or Not to Prime: That Is the Question. *Cold Spring Harbor Symposia on Quantitative Biology,* 81**,** 030841.

RAHA, D., WILSON, T. R., PENG, J., PETERSON, D., YUE, P., EVANGELISTA, M., WILSON, C., MERCHANT, M. & SETTLEMAN, J. 2014. The Cancer Stem Cell Marker Aldehyde Dehydrogenase Is Required to Maintain a Drug-Tolerant Tumor Cell Subpopulation. *Cancer Research,* 74**,** 3579.

REED, G. A., SCHILLER, G. J., KAMBHAMPATI, S., TALLMAN, M. S., DOUER, D., MINDEN, M. D., YEE, K. W., GUPTA, V., BRANDWEIN, J., JITKOVA, Y., GRONDA, M., HURREN, R., SHAMAS-DIN, A., SCHUH, A. C. & SCHIMMER, A. D. 2016. A Phase 1 study of intravenous infusions of tigecycline in patients with acute myeloid leukemia. *Cancer Medicine,* 5**,** 3031-3040.

ROEHRL, M. H. & DZIK, W. S. 2008. Weisses Blut--Leukapheresis in acute leukemia. *Am J Hematol,* 83**,** 254-5.

ROUSSEL, M. J. S. & LANOTTE, M. 2001. Maturation sensitive and resistant t(15;17) NB4 cell lines as tools for APL physiopathology: nomenclature of cells and repertory of their known genetic alterations and phenotypes. *Oncogene,* 20**,** 7287-7291.

SCHEPERS, K., CAMPBELL, T. B. & PASSEGUÉ, E. 2015. Normal and leukemic stem cell niches: insights and therapeutic opportunities. *Cell stem cell,* 16**,** 254-267.

SHAFAT, M. S., FENECH, M. E., ABDUL-AZIZ, A. M., TURNER, J., BOWLES, K. M. & RUSHWORTH, S. A. 2015. FABP4 Regulates Fatty Acid Transfer from Bone Marrow Adipocytes to Acute Myeloid Leukemia Blasts. *Blood,* 126**,** 3065-3065.

SHEN, Z. X., CHEN, G. Q., NI, J. H., LI, X. S., XIONG, S. M., QIU, Q. Y., ZHU, J., TANG, W., SUN, G. L., YANG, K. Q., CHEN, Y., ZHOU, L., FANG, Z. W., WANG, Y. T., MA, J., ZHANG, P., ZHANG, T. D., CHEN, S. J., CHEN, Z. & WANG, Z. Y. 1997. Use of arsenic trioxide (As2O3) in the treatment of acute promyelocytic leukemia (APL): II. Clinical efficacy and pharmacokinetics in relapsed patients. *Blood,* 89**,** 3354-60.

SIMSEK, T., KOCABAS, F., ZHENG, J., DEBERARDINIS, R. J., MAHMOUD, A. I., OLSON, E. N., SCHNEIDER, J. W., ZHANG, C. C. & SADEK, H. A. 2010. The distinct metabolic profile of hematopoietic stem cells reflects their location in a hypoxic niche. *Cell stem cell,* 7**,** 380-390.

SISON, E. A., MCINTYRE, E., MAGOON, D. & BROWN, P. 2013. Dynamic chemotherapy-induced upregulation of CXCR4 expression: a mechanism of therapeutic resistance in pediatric AML. *Mol Cancer Res,* 11**,** 1004-16.

SOIGNET, S. L., FRANKEL, S. R., DOUER, D., TALLMAN, M. S., KANTARJIAN, H., CALLEJA, E., STONE, R. M., KALAYCIO, M., SCHEINBERG, D. A., STEINHERZ, P., SIEVERS, E. L., COUTRE, S., DAHLBERG, S., ELLISON, R. & WARRELL, R. P., JR. 2001. United States multicenter study of arsenic trioxide in relapsed acute promyelocytic leukemia. *J Clin Oncol,* 19**,** 3852-60.

SRISKANTHADEVAN, S., JEYARAJU, D. V., CHUNG, T. E., PRABHA, S., XU, W., SKRTIC, M., JHAS, B., HURREN, R., GRONDA, M., WANG, X., JITKOVA, Y., SUKHAI, M. A., LIN, F.-H., MACLEAN, N., LAISTER, R., GOARD, C. A., MULLEN, P. J., XIE, S., PENN, L. Z., ROGERS, I. M., DICK, J. E., MINDEN, M. D. & SCHIMMER, A. D. 2015. AML cells have low spare reserve capacity in their respiratory chain that renders them susceptible to oxidative metabolic stress. *Blood,* 125**,** 2120-2130.

STEVENS, R. G., JONES, D. Y., MICOZZI, M. S. & TAYLOR, P. R. 1988. Body iron stores and the risk of cancer. *N Engl J Med,* 319**,** 1047-52.

STUANI, L., SABATIER, M. & SARRY, J.-E. 2019. Exploiting metabolic vulnerabilities for personalized therapy in acute myeloid leukemia. *BMC Biology,* 17**,** 57.

SUDA, T., TAKUBO, K. & SEMENZA, G. L. 2011. Metabolic regulation of hematopoietic stem cells in the hypoxic niche. *Cell stem cell,* 9**,** 298-310.

SUKHAI, M. A., PRABHA, S., HURREN, R., RUTLEDGE, A. C., LEE, A. Y., SRISKANTHADEVAN, S., SUN, H., WANG, X., SKRTIC, M., SENEVIRATNE, A., CUSIMANO, M., JHAS, B., GRONDA, M., MACLEAN, N., CHO, E. E., SPAGNUOLO, P. A., SHARMEEN, S., GEBBIA, M., URBANUS, M., EPPERT, K., DISSANAYAKE, D., JONET, A., DASSONVILLE-KLIMPT, A., LI, X., DATTI, A., OHASHI, P. S., WRANA, J., ROGERS, I., SONNET, P., ELLIS, W. Y., COREY, S. J., EAVES, C., MINDEN, M. D., WANG, J. C., DICK, J. E., NISLOW, C., GIAEVER, G. & SCHIMMER, A. D. 2013. Lysosomal disruption preferentially targets acute myeloid leukemia cells and progenitors. *J Clin Invest,* 123**,** 315-28.

SUN HD, M. L., HU XC, ZHANG TD 1992. Ai-Lin I treated 32 cases of acute promyelocytic leukemia. *Chin J Integrat Chin & West Med,* 12**,** 170.

SYKES, D. B., KFOURY, Y. S., MERCIER, F. E., WAWER, M. J., LAW, J. M. & HAYNES, M. K. 2016. Inhibition of dihydroorotate dehydrogenase overcomes differentiation blockade in acute myeloid leukemia. *Cell.,* 167.

TABE, Y., SHI, Y. X., ZENG, Z., JIN, L., SHIKAMI, M., HATANAKA, Y., MIIDA, T., HSU, F. J., ANDREEFF, M. & KONOPLEVA, M. 2013. TGF-beta-Neutralizing Antibody 1D11 Enhances Cytarabine-Induced Apoptosis in AML Cells in the Bone Marrow Microenvironment. *PLoS One,* 8**,** e62785.

TAKUBO, K., GODA, N., YAMADA, W., IRIUCHISHIMA, H., IKEDA, E., KUBOTA, Y., SHIMA, H., JOHNSON, R. S., HIRAO, A. & SUEMATSU, M. 2010. Regulation of the HIF-1α level is essential for hematopoietic stem cells. *Cell stem cell,* 7**,** 391-402.

TAKUBO, K., NAGAMATSU, G., KOBAYASHI, C. I., NAKAMURA-ISHIZU, A., KOBAYASHI, H., IKEDA, E., GODA, N., RAHIMI, Y., JOHNSON, R. S. & SOGA, T. 2013. Regulation of glycolysis by Pdk functions as a metabolic checkpoint for cell cycle quiescence in hematopoietic stem cells. *Cell stem cell,* 12**,** 49-61.

TANIGUCHI ISHIKAWA, E., GONZALEZ-NIETO, D., GHIAUR, G., DUNN, S. K., FICKER, A. M. & MURALI, B. 2012. Connexin-43 prevents hematopoietic stem cell senescence through transfer of reactive oxygen species to bone marrow stromal cells. *Proc Natl Acad Sci USA,* 109.

TOMITA, A., KIYOI, H. & NAOE, T. 2013. Mechanisms of action and resistance to all-trans retinoic acid (ATRA) and arsenic trioxide (As2O 3) in acute promyelocytic leukemia. *Int J Hematol,* 97**,** 717-25.

TORTI, S. V. & TORTI, F. M. 2013. Iron and cancer: more ore to be mined. *Nature reviews. Cancer,* 13**,** 342-355.

TRUJILLO-ALONSO, V., PRATT, E. C., ZONG, H., LARA-MARTINEZ, A., KAITTANIS, C., RABIE, M. O., LONGO, V., BECKER, M. W., ROBOZ, G. J., GRIMM, J. & GUZMAN, M. L. 2019. FDA-approved ferumoxytol displays anti-leukaemia efficacy against cells with low ferroportin levels. *Nature nanotechnology,* 14**,** 616-622.

VARDIMAN, J. W., THIELE, J., ARBER, D. A., BRUNNING, R. D., BOROWITZ, M. J., PORWIT, A., HARRIS, N. L., LE BEAU, M. M., HELLSTROM-LINDBERG, E., TEFFERI, A. & BLOOMFIELD, C. D. 2009. The 2008 revision of the World Health Organization (WHO) classification of myeloid neoplasms and acute leukemia: rationale and important changes. *Blood,* 114**,** 937-51.

VEROVSKAYA, E. V., DELLORUSSO, P. V. & PASSEGUÉ, E. 2019. Losing Sense of Self and Surroundings: Hematopoietic Stem Cell Aging and Leukemic Transformation. *Trends in Molecular Medicine,* 25**,** 494-515.

VO, T.-T., RYAN, J., CARRASCO, R., NEUBERG, D., ROSSI, DERRICK J., STONE, RICHARD M., DEANGELO, DANIEL J., FRATTINI, MARK G. & LETAI, A. 2012. Relative Mitochondrial Priming of Myeloblasts and Normal HSCs Determines Chemotherapeutic Success in AML. *Cell,* 151**,** 344-355.

VOGLER, M., BUTTERWORTH, M., MAJID, A., WALEWSKA, R. J., SUN, X. M., DYER, M. J. & COHEN, G. M. 2009. Concurrent up-regulation of BCL-XL and BCL2A1 induces approximately 1000-fold resistance to ABT-737 in chronic lymphocytic leukemia. *Blood,* 113**,** 4403-13.

VYAS, S., ZAGANJOR, E. & HAIGIS, M. 2016. Mitochondria and Cancer. *Cell,* 166**,** 555-566.

WAI, T. & LANGER, T. 2016. Mitochondrial Dynamics and Metabolic Regulation. *Trends in Endocrinology & Metabolism,* 27**,** 105-117.

WALDVOGEL-ABRAMOWSKI, S., WAEBER, G., GASSNER, C., BUSER, A., FREY, B. M., FAVRAT, B. & TISSOT, J. D. 2014. Physiology of iron metabolism. *Transfus Med Hemother,* 41**,** 213-21.

WALLACE, D. C. 2012. Mitochondria and cancer. *Nature reviews. Cancer,* 12**,** 685-698.

WANG, A. & ZHONG, H. 2018. Roles of the bone marrow niche in hematopoiesis, leukemogenesis, and chemotherapy resistance in acute myeloid leukemia. *Hematology,* 23.

WANG, T., NARAYANASWAMY, R., REN, H. & TORCHILIN, V. P. 2016. Combination therapy targeting both cancer stem-like cells and bulk tumor cells for improved efficacy of breast cancer treatment. *Cancer Biology & Therapy,* 17**,** 698-707.

WANG, W., CORRIGAN-CUMMINS, M., BARBER, E. A., SALEH, L. M., ZINGONE, A., GHAFOOR, A., COSTELLO, R., ZHANG, Y., KURLANDER, R. J., KORDE, N., ROCCARO, A. M., GHOBRIAL, I. M., LANDGREN, O. & CALVO, K. R. 2015. Aberrant Levels of miRNAs in Bone Marrow Microenvironment and Peripheral Blood of Myeloma Patients and Disease Progression. *J Mol Diagn,* 17**,** 669-78.

WANG, Y., YU, L., DING, J. & CHEN, Y. 2018. Iron Metabolism in Cancer. *Int J Mol Sci,* 20.

WARBURG, O. 1956a. On respiratory impairment in cancer cells. *Science,* 124**,** 269-70.

WARBURG, O. 1956b. On the origin of cancer cells. *Science,* 123**,** 309-14.

WARBURG, O. 1956c. On the Origin of Cancer Cells. *Science,* 123**,** 309.

WEBER, R. A., YEN, F. S., NICHOLSON, S. P. V., ALWASEEM, H., BAYRAKTAR, E. C., ALAM, M., TIMSON, R. C., LA, K., ABU-REMAILEH, M., MOLINA, H. & BIRSOY, K. 2020. Maintaining Iron Homeostasis Is the Key Role of Lysosomal Acidity for Cell Proliferation. *Molecular Cell,* 77**,** 645-655.e7.

WESTERMANN, B. 2012. Bioenergetic role of mitochondrial fusion and fission. *Biochimica et Biophysica Acta (BBA) - Bioenergetics,* 1817**,** 1833-1838.

WU, D., WANG, W., CHEN, W., LIAN, F., LANG, L. & HUANG, Y. 2018. Pharmacological inhibition of dihydroorotate dehydrogenase induces apoptosis and differentiation in acute myeloid leukemia cells. *Haematologica,* 103.

YANG, H., TABE, Y., SEKIHARA, K., SAITO, K., MA, H., RUVOLO, V., IMOTO, J., IKEO, K., MOGUSHI, K., HOSOYA, M., HAYASHIZAKI, Y., YAMANAKA, Y., MIIDA, T., ANDREEFF, M., MARSZALEK, J. R. & KONOPLEVA, M. 2017. Novel Oxidative Phosphorylation Inhibitor IACS-010759 Induces AMPK-Dependent Apoptosis of AML Cells. *Blood,* 130**,** 1245.

YE, H., ADANE, B., KHAN, N., SULLIVAN, T., MINHAJUDDIN, M., GASPARETTO, M., STEVENS, B., PEI, S., BALYS, M., ASHTON, J. M., KLEMM, D. J., WOOLTHUIS, C. M., STRANAHAN, A. W., PARK, C. Y. & JORDAN, C. T. 2016. Leukemic Stem Cells Evade Chemotherapy by Metabolic Adaptation to an Adipose Tissue Niche. *Cell stem cell,* 19**,** 23-37.

YOULE, R. J. & VAN DER BLIEK, A. M. 2012a. Mitochondrial fission, fusion, and stress. *Science (New York, N.Y.),* 337**,** 1062-1065.

YOULE, R. J. & VAN DER BLIEK, A. M. 2012b. Mitochondrial Fission, Fusion, and Stress. *Science,* 337**,** 1062-1065.

YU, L., CHEN, X., SUN, X., WANG, L. & CHEN, S. 2017. The Glycolytic Switch in Tumors: How Many Players Are Involved? *Journal of Cancer,* 8**,** 3430-3440.

ZAFFAGNINI, G. & MARTENS, S. 2016. Mechanisms of Selective Autophagy. *Journal of molecular biology,* 428**,** 1714-1724.

ZENG, Z., SAMUDIO, I. J., MUNSELL, M., AN, J., HUANG, Z., ESTEY, E., ANDREEFF, M. & KONOPLEVA, M. 2006. Inhibition of CXCR4 with the novel RCP168 peptide overcomes stroma-mediated chemoresistance in chronic and acute leukemias. *Mol Cancer Ther,* 5**,** 3113-21.

ZENG, Z., SHI, Y. X., SAMUDIO, I. J., WANG, R. Y., LING, X., FROLOVA, O., LEVIS, M., RUBIN, J. B., NEGRIN, R. R., ESTEY, E. H., KONOPLEV, S., ANDREEFF, M. & KONOPLEVA, M. 2009. Targeting the leukemia microenvironment by CXCR4 inhibition overcomes resistance to kinase inhibitors and chemotherapy in AML. *Blood,* 113**,** 6215-24.

ZHANG, H.-N., YANG, L., LING, J.-Y., CZAJKOWSKY, D. M., WANG, J.-F., ZHANG, X.-W., ZHOU, Y.-M., GE, F., YANG, M.-K., XIONG, Q., GUO, S.-J., LE, H.-Y., WU, S.-F., YAN, W., LIU, B., ZHU, H., CHEN, Z. & TAO, S.-C. 2015. Systematic identification of arsenic-binding proteins reveals that hexokinase-2 is inhibited by arsenic. *Proceedings of the National Academy of Sciences of the United States of America,* 112**,** 15084-15089.

ZHANG, X.-W., YAN, X.-J., ZHOU, Z.-R., YANG, F.-F., WU, Z.-Y., SUN, H.-B., LIANG, W.-X., SONG, A.-X., LALLEMAND-BREITENBACH, V., JEANNE, M., ZHANG, Q.-Y., YANG, H.-Y., HUANG, Q.-H., ZHOU, G.-B., TONG, J.-H., ZHANG, Y., WU, J.-H., HU, H.-Y., DE THÉ, H., CHEN, S.-J. & CHEN, Z. 2010. Arsenic Trioxide Controls the Fate of the PML-RARα Oncoprotein by Directly Binding PML. *Science,* 328**,** 240.

ZHAO, R. Z., JIANG, S., ZHANG, L. & YU, Z. B. 2019. Mitochondrial electron transport chain, ROS generation and uncoupling (Review). *Int J Mol Med,* 44**,** 3-15.

ZHU, H. H., QIN, Y. Z. & HUANG, X. J. 2014. Resistance to arsenic therapy in acute promyelocytic leukemia. *N Engl J Med,* 370**,** 1864-6.

Annexures

blood advances

American Society of Hematology
2021 L Street NW, Suite 900,
Washington, DC 20036
Phone: 202-776-0544 | Fax 202-776-0545
bloodadvances@hematology.org

Metabolic adaptation drives arsenic trioxide resistance in acute promyelocytic leukemia

Tracking no: ADV-2021-005300R1

Nithya Balasundaram (Christian Medical College, India) Saravanan Ganesan (Inserm UMR-S1131, Université de Paris, IRSL, Hôpital Saint-Louis, France) Ezhilarasi Chendamarai (Christian Medical College, India) Hamenth Palani (Christian Medical College, India) Arvind Venkatraman (Christian Medical College, India) Ansu Abu Alex (Christian Medical College,) Sachin David (Christian Medical College, Vellore - 632004, India) Swathy Palanikumar (Christian Medical College, India) Nair Reeshma Radhakrishnan (Christian Medical College, India) Mohammed Yasar M (Christian Medical College, India) Sanjeev Krishna (St.George's University of London, United Kingdom) Anu Korula (CHRISTIAN MEDICAL COLLEGE AND HOSPITAL VELLORE, India) Uday Kulkarni (Christian Medical College, India) Nancy Janet (Christian Medical College, India) Poonkuzhali Balasubramanian (Christian Medical College, India) Vikram Mathews (Christian Medical College, India)

Abstract:
Acquired genetic mutations can confer resistance to arsenic trioxide (ATO) in the treatment of acute promyelocytic leukemia (APL). However, such resistance-conferring mutations are rare and do not explain most disease recurrence seen in the clinic. We have generated stable ATO-resistant promyelocytic cell lines that are also less sensitive to ATRA and the combination of ATO and ATRA compared to the sensitive cell line. Characterization of these in-house generated resistant cell lines showed significant differences in immunophenotype, drug transporter expression, anti-apoptotic protein dependence, and PML-RARA mutation. Gene expression profiling revealed prominent dysregulation of the cellular metabolic pathways in these ATO resistant APL cell lines. Glycolytic inhibition by 2-DG was sufficient and comparable to the standard of care (ATO) in targeting the sensitive APL cell line. 2-DG was also effective in the in vivo transplantable APL mouse model; however, it did not affect the ATO resistant cell lines. In contrast, the resistant cell lines were significantly affected by compounds targeting the mitochondrial respiration when combined with ATO, irrespective of the ATO resistance-conferring genetic mutations or the pattern of their anti-apoptotic protein dependency. Our data demonstrate that the addition of mitocans in combination with ATO can overcome ATO resistance. We further show that this combination has the potential in the treatment of non-M3 AML and relapsed APL. The translation of this approach in the clinic needs to be explored further.

Conflict of interest: No COI declared

COI notes:

Preprint server: Yes; bioRxiv 10.1101/2020.06.21.154633

Author contributions and disclosures: NB: performed research, involved in designing the study, performed molecular tests, and analyzed data and written the paper. SG: performed research, performed molecular tests, and analyzed data. EC: performed research, performed molecular tests, and analyzed data. HKP: performed research, performed molecular tests, and analyzed data AV: performed research, performed molecular tests, and analyzed data AAA: performed research, performed molecular tests, and analyzed data. SD: performed research, performed molecular tests, and analyzed data. SPK: performed research, performed molecular tests, and analyzed data. NRR: performed research, performed molecular tests, and analyzed data. MY: performed research, performed karyotyping tests, and analyzed data. AK: performed research and analyzed data. UK: performed research and analyzed data. NBJ: performed research, performed karyotyping tests, and analyzed data. SK: performed research and analyzed data. PB: performed research and analyzed data. VM: performed research, designed study, analyzed data, and written the paper.

Non-author contributions and disclosures: No;

Agreement to Share Publication-Related Data and Data Sharing Statement: The datasets discussed in this manuscript have been deposited in the NCBI under the following accession number 1.GSE115812 - Gene expression data of NB4 naïve, NB4 EV-AsR1 and UF-1 2.GSE42030 - Gene expression data of Newly diagnosed and relapsed APL samples. 3.Whole exome sequencing and Chip Sequencing data deposition has been initiated and the SRA numbers will be updated. The datasets will also be shared upon an email request to Dr.Vikram Mathews (vikram@cmcvellore.ac.in).

Clinical trial registration information (if any):

Metabolic adaptation drives arsenic trioxide resistance in acute promyelocytic leukemia

Nithya Balasundaram[1], Saravanan Ganesan[1], Ezhilarasi Chendamarai[1], Hamenth Kumar Palani[1], Arvind Venkatraman[1], Ansu Abu Alex[1], Sachin David[1], Swathy Palani Kumar[1], Nair Reeshma Radhakrishnan[1], Mohammed Yasar[1], Sanjeev Krishna[2], Anu Korula[1], Uday Kulkarni[1], Nancy Beryl Janet[1], Poonkuzhali Balasubramanian[1], Vikram Mathews[1].

[1]Department of Haematology, Christian Medical College, Vellore, India.
[2]Institute for Infection and Immunity, St George's University of London, London, United Kingdom.

Running title: ATO resistance in acute promyelocytic leukemia

Keywords: acute promyelocytic leukemia, arsenic trioxide, drug resistance, metabolism.

Abstract word count:	227
Manuscript word count:	3991
Number of figures:	7
Number of tables:	0
References:	28

Correspondence:
Vikram Mathews
Department of Haematology
Christian Medical College
Vellore - 632004
Tamil Nadu, India.
Telephone No: 91-416-2282891
Fax No: 91-416-2226449
E-mail: vikram@cmcvellore.ac.in

Key points:

- Metabolic rewiring promotes ATO resistance in APL, independent of PML mutation status.
- Inhibiting mitochondrial respiration in combination with ATO can be used as a potential therapeutic option for relapsed APL and non-M3 AML.

Abstract:

Acquired genetic mutations can confer resistance to arsenic trioxide (ATO) in the treatment of acute promyelocytic leukemia (APL). However, such resistance-conferring mutations are rare and do not explain most disease recurrence seen in the clinic. We have generated stable ATO-resistant promyelocytic cell lines that are also less sensitive to ATRA and the combination of ATO and ATRA compared to the sensitive cell line. Characterization of these in-house generated resistant cell lines showed significant differences in immunophenotype, drug transporter expression, anti-apoptotic protein dependence, and PML-RARA mutation. Gene expression profiling revealed prominent dysregulation of the cellular metabolic pathways in these ATO resistant APL cell lines. Glycolytic inhibition by 2-DG was sufficient and comparable to the standard of care (ATO) in targeting the sensitive APL cell line. 2-DG was also effective in the in vivo transplantable APL mouse model; however, it did not affect the ATO resistant cell lines. In contrast, the resistant cell lines were significantly affected by compounds targeting the mitochondrial respiration when combined with ATO, irrespective of the ATO resistance-conferring genetic mutations or the pattern of their anti-apoptotic protein dependency. Our data demonstrate that the addition of mitocans in combination with ATO can overcome ATO resistance. We further show that this combination has the potential in the treatment of non-M3 AML and relapsed APL. The translation of this approach in the clinic needs to be explored further.

Introduction:

Acute promyelocytic leukemia (APL) is a subtype of acute myeloid leukemia (AML) characterized by the presence of reciprocal translocation between the PML gene on chromosome 15 and the retinoic acid receptor α (RARα) gene on chromosome 17 [t(15;17)], resulting in the production of a chimeric and novel PML-RARα fusion oncoprotein that leads to the differentiation block of promyelocytes to mature granulocytes[1]. Combination therapy of arsenic trioxide (ATO) and all-trans-retinoic acid (ATRA)[2-4] in the management of APL has significantly improved survival rates compared to either administered as single agents or a combination of ATRA with chemotherapy[5-7].

We recently reported on the mutational spectrum of relapsed and newly diagnosed APL patients and demonstrated the importance of additional genetic events (FLT3, KRAS, NRAS, ARID1B, p53, and WT1) during disease recurrence. However, it was also noted that mutations resulting in primary or secondary ATO resistance are extremely rare and could not explain the majority of disease relapses[8]. Other mechanisms such as bone marrow microenvironment mediated drug resistance, up-regulation of anti-apoptotic factors, modulation of cellular energy metabolism, and oxidative stress could potentially contribute to therapy resistance.

Existing literature on ATO resistance in APL has focused on the presence / acquisition of *PML* B2 domain mutations, with evidence supporting the presence of genetic mutations in the *PML* B2 domain (C212-S220; A216V) conferring resistance to ATO in APL. These mutations alter or inhibit ATO binding to the B2 domain of the PML component of the PML-RARA oncoprotein[9-13]. However, such acquired somatic mutations are rarely seen in the clinic and cannot explain the relapses that occur in patients treated with ATO based regimens. Additionally, in APL, unlike the other subtypes of AML, there is little evidence to suggest the existence of a leukemic stem cell population to explain disease recurrence[14].

Recent observations and studies report the novel mechanism of action of ATO such as promotion of non-classical apoptosis (ETosis: extracellular DNA traps) in a dose dependent manner[15] and inhibition of glycolysis. ATO directly binds to the Cys256

and Cys704 residues in hexokinase 2 (HK2) and pyruvate kinase (PKM2) reducing the enzymatic activity of these proteins and acts as glycolytic inhibitor[16]. It has further been demonstrated that this glycolytic inhibition is an important mechanism by which it promotes apoptosis in cancer cells and over expression of HK2 significantly rescued the cells from ATO induced apoptosis[16-18]. These observations further illustrate that the mechanisms of action of ATO are complex and multi-factorial, suggesting that mechanisms of resistance are also likely to be varied.

To further interrogate the mechanisms of ATO resistance we generated and characterized a stable ATO resistant cell line with the objective of finding potentially druggable targets that could be used to overcome ATO resistance in APL.

Methods:

Cell lines and chemicals:

The human APL cell line NB4 was a kind gift from Dr. Harry Iland, RPAH, Sydney, Australia, with permission from Dr. Michel Lanotte. In addition to the in house generated ATO resistant cell lines, we also used an ATRA resistant APL cell line UF1 (a kind gift from Dr. Christine Chomienne, Hôpital Saint Louis, Paris). The cell lines were free from mycoplasma contamination (Universal Mycoplasma Detection Kit, ATCC Manassas, VA, USA). Primary cells were obtained after getting written and informed consent (IRB No: 5884). Arsenic trioxide was a kind gift from INTAS Pharmaceuticals, Ahmedabad, India. 2-NBDG – fluorescent analog of D-Glucose, JC-1 and 2- Deoxy Glucose (2-DG), Carbonyl cyanide 4-(trifluoromethoxy) phenylhydrazone - FCCP were purchased from Sigma Aldrich (Sigma Aldrich, St Louis, MO, USA).

Exome sequencing:

Genomic DNA was isolated from the naïve NB4 cells and the ATO resistant NB4 sub clones NB4-EVAsR1 and UF1 using Gentra puregene blood kit (Qiagen, Hilden, Germany) and stored at 4°C. Library preparation and sequencing were performed at Genotypic Technology's Genomics facility, Bengaluru, following Ion TargetSeq™

Exome Enrichment for the Ion Proton™ System, sequencing was performed on Ion Proton™ sequencer. The mutations were confirmed by Sanger sequencing.

Chromatin-immunoprecipitation sequencing (ChiP-Seq):

H3K27ace pull down was performed using simpleChIP® Enzymatic Chromatin IP Kit as per the manufacturers protocol (Cell signaling Technology, MA, USA). ChIP-Seq data was generated from two independent experimental replicates. Total genomic DNA (input) derived from formaldehyde cross-linked samples was used as control during peak calling. Raw sequence reads that passed quality control were aligned to the human reference genome (available from the UCSC genome browser, http://genome.ucsc.edu/). Peak calling on all ChIP-Seq data was performed using MACS v2.1.

Gene expression array and analysis:

A global gene expression array for differential gene expression in naïve NB4 cells and the ATO resistant NB4 primary resistant clone was performed. $2x10^7$ cells (NB4 naïve, NB4EV-AsR1, and UF1) were harvested and stored in RNA later solution. The extracted labeled RNAs were hybridized to Agilent Human Whole Genome 8x60K Gene Expression Array (AMADID: 039494), and the Image analysis was done using Agilent Feature Extraction software Version 10.5.1.1 to obtain the raw data. Normalization and statistical analysis of the microarray data were done using GeneSpring GX (Agilent Technologies, CA, USA). Differentially regulated genes were clustered using hierarchical clustering to identify significant gene expression patterns Genes were classified based on functions and pathways using biological interpretation tool Biointerpreter (Genotypic Technology, Bangalore).

Seahorse extracellular flux analysis:

Extracellular flux assay kit XF24 (Agilent Technologies, CA, USA) was used to measure oxygen consumption rate and glycolytic flux. Briefly, three replicate wells of 5×10^4 cells per well were seeded in a retronectin (Takara Bio Inc, JPY) coated 24-well XF24 plate. At 30 min before analysis, the medium was replaced with Seahorse XF

media (Agilent Technologies, CA, USA), and the plate was incubated at 37 °C. Analyses were performed both at basal conditions and after injection of glucose, oligomycin, and 2-deoxy glucose for glycolytic function.

Mouse model and drug treatments:

FVB/N mice were obtained from Jackson Laboratory (Bar Harbor, ME, USA). Mice at 6 to 8 weeks of age were used in all the experiments. The animal study design and euthanasia protocols were approved by the institutional animal ethics committee (IAEC approval number 04/2019). APL cells from the spleen of MRP8-PML-RAR transgenic mice (FVB/N) were harvested and cryopreserved (a kind gift from Dr. Scott Kogan, UCSF, USA). APL cells (10^6 cells/mouse) were injected intravenously via the tail vein into genetically compatible FVB/N recipients, without conditioning. After the leukemic cell engraftment period (day 8), intraperitoneal injection of ATO (10mg/Kg) and 2-DG (750mg/Kg) was administered for 15 days.

Intracellular BH3 (iBH3) profiling:

10^6 cells/mL were suspended in BH3 profiling buffer, digitonin permeabilized and exposed to pro-apoptotic peptides at a concentration of 20µM (Bim, BAD, HRK and MS-1, GenScript, New Jersey, United States) for 90minutes. We then proceeded according to the standardized protocol from the Anthony Letai laboratory (http://letailab.dana-farber.org/bh3-profiling.html) to measure intracellular retention of cytochrome c. After an overnight incubation with anti-Cytochrome-c (6H2.B4)-FITC antibody (BioLegend, CA, USA) the cells were acquired on a flow cytometer (Beckman Coulter Navios, Brea, CA, USA). Loss of cytochrome-c is proportional to the priming status of the mitochondria and its anti-apoptotic dependency by their peptide specificity.

Statistical Analysis:

All statistical analyses were carried out using GraphPad Prism 7.0 (GraphPad Software, La Jolla, CA). All data points are represented as means ± SEM. Two-tailed Student’s t-test was used to compare mean values between two groups. For

experiments where multiple groups are compared with control, one-way ANOVA was used. P values < 0.05 were considered as statistically significant.

For further details and other methods, see supplemental methods.

Results:

Generation of arsenic trioxide resistant cell line:

ATO resistant cells were generated by exposing the naïve NB4 cell line to low concentrations of ATO (50nM) for about 3 months. The concentration of ATO was gradually increased to 1μM over one year. The cells which survived and proliferated were termed as the “ATO tolerant persister cells” (ATO-TPs). The ATO-TPs were then subjected serially to limiting dilutions and single cell colony-forming unit formation on methylcellulose to isolate monoclonal resistant populations. We isolated three different clones, expanded and named them NB4EV-AsR1, NB4EV-AsR2, NB4EV-AsR3 respectively based on the published norms of NB4 resistant cell line nomenclature[19]. The IC50 for ATO in these cell lines was 3.25μM, 3.4μM, and 2.88μM for NB4EV-AsR1, NB4EV-AsR2, and NB4EV-AsR3 respectively in contrast to naïve NB4 which was 0.9μM (figure 1a). The viability of the in-house generated ATO resistant cell lines were not significantly affected by exposure to 2μM ATO in comparison to the sensitive cell line NB4 (figure 1b). The in-house generated ATO resistant cell lines were also significantly less sensitive to differentiation-inducing agent ATRA, similar to UF1 a known ATRA resistant cell line. Even the combination of ATO and ATRA (0.5uM and 1uM respectively) did not induce a significant differentiation or cell death in the in-house generated ATO resistant cell lines when compared to naive NB4 cells (Figure 1c). Post exposure to ATRA(1uM) the induction of downstream targets of the RAR like TGM2, RARβ and RARα transcripts were also found to be significantly less in the in-house generated ATO resistant cell lines in comparison to NB4 naive (supplementary figure 1).

The doubling time of parental cell line NB4 was 28 hours, whereas for NB4EV-AsR1 and NB4EV-AsR2 clones, it was 46 and 48 hours, respectively. Long term withdrawal of ATO for 3 months from the culture system did not result in the

reacquisition of ATO sensitivity (supplementary figure 2). Currently, the resistant cell lines have a stable resistant phenotype when grown with or without ATO. We have also observed that the ATRA resistant UF1 cell line is also cross-resistant to ATO with an IC-50 of 4.9μM, an observation that has not been previously reported (Supplementary figure 3).

ATO-resistant cell lines exhibit distinct cell surface markers and transporters:

The ATO resistant cell lines were abnormal promyelocytes where the cell surface expression of the typical myeloid markers CD13 and CD33 was significantly reduced in comparison to the parental naïve cell line (figure 2a and Supplementary figure 4). The ATO efflux transporters such as AQP9, MRP4, ABCB6, and ABCA7 were significantly upregulated in the ATO resistant cell lines which mirrored in the reduced concentration of intracellular ATO (figure 2b and 2c).

Since ATO induces the degradation of PML-RARA protein, we examined the sub cellular localization, transcript, and protein levels of PML / PML-RARA in the resistant cells in comparison to sensitive cell line NB4. In the immunofluorescence assay, we observed that the PML localized in the nucleus in a typical APL specific micro-speckled pattern in the NB4 cells whereas in the resistant cell lines we observed a similar micro-speckled pattern but a decrease in the amount of nuclear PML (Figure 2d). There was also significant reduction in the levels of PML-RARA both at the transcript and protein levels in the resistant cell lines (figure 2e and 2f).

In-house generated ATO resistant cell lines harbor additional cytogenetic and molecular aberrations:

Cytogenetic analysis of both cell lines showed triploidy as well as the t(15;17). However, the NB4 EV-AsR1 showed additional cytogenetic abnormalities such as the deletion 5q, gain of chromosome 4 and loss of chromosome 22. The loss of the X chromosome as well as absence of the derivative chromosome 21 and the addition 16q which was seen in NB4 naïve was not observed in NB4 EV-AsR1 (supplementary table 1).

As there are reports implicating the emergence of drug resistance-conferring somatic PML domain mutations in APL cells against ATO, we performed whole-exome sequencing on our in-house generated ATO resistant cell line NB4EV-AsR1 (as a representative of other ATO resistant clones) in comparison to the parental cell line NB4 naïve and also on the UF1 cell line that was found to be resistant to ATO.

Whole exome sequencing revealed that in comparison to NB4 naïve, a significant number of genes were mutated in the NB4EV-AsR1 and UF1 cell lines. Based on the mutation frequency, we observed that in comparison to the NB4 naïve majority of the mutated genes in NB4EV-AsR1 belong to cell surface proteins especially mucins (MUC6, MUC5B, MUC4, MUC3A, MUC16), serine protease genes (PRSS1, PRSS3, PRSS3P2) and the ATO resistance-conferring PML B2 domain mutation (A216V). In contrast, the UF1 cell line showed a higher frequency of mutations involving MUC16, ITGB4, PRSS1, CUL7, CDH23, LTBP3, OBSCN, STAB1 genes (supplementary figure 5) and did not have a PML B2 domain mutation. Further comparison of mutated genes in the resistant cell lines with the commonly observed mutations in the AML TCGA dataset revealed that in NB4EV-AsR1 with the exception of the PML B2 domain mutation, we did not observe any additional novel mutations over and above those described in the AML TCGA gene set. However, in UF1, there were additional novel mutations found in DNMT3A, TP53, RUNX1, IDH2, SMC3, ARID1B, ARID1A, and PML genes in addition to the known mutations in the AML TCGA gene set (figure 3a and supplementary file 1).

Validation of PML and p53 mutation using sanger sequencing confirmed the existence of previously reported ATO resistance-conferring mutation A216V[10] in the in-house generated ATO resistant cell lines (including NB4EV-AsR2 and EV-AsR3). UF1 had two intronic variations in the PML domain and was negative for A216V (figure 3b). We also noted that the existence of a p53 gain of function mutation (R248Q) in the in house generated ATO resistant cell line, which was also present in the parental naïve NB4 cell line. UF1 cell line had a point mutation (R196*) and a deletion of exon 10 of the p53 (figure 3c), which are reported to be pathogenic[20].

Heterogeneity in ATO resistant cell lines:

As evident from drug withdrawal conditions and exome sequencing analysis, the observed ATO resistance was not explained by either a transient epigenetic poising or presence of a known acquired genetic mutation in the *PML-B2* domain (absence of *PML-B2* domain mutation in UF1). We next subjected NB4 naïve, NB4 EV-AsR1 and UF1 to gene expression profiling. We observed that 1717 genes in NB4 EV-AsR1 and 6149 genes in UF1 were significantly upregulated (> 2-fold) in comparison to NB4 naïve. The pathways significantly enriched for differentially expressed genes were cell survival, cell cycle, immune regulation, ABC transporters, glutathione metabolism, redox system, mitochondrial cellular respiration, and ubiquitin-proteasome degradation system (figure 4a). We also noted that the gene expression profile of the in-house generated ATO resistant cell line was similar to that of the relapsed APL patient's gene profile (8 unmatched newly diagnosed and relapsed APL) treated with front line ATO based regimens and previously reported by us[21] (Figure 4b). Gene expression profiling revealed significant dysregulation of glycolytic and mitochondrial metabolism in the resistant cell line when compared to NB4 naïve (figure 4c).

We also carried out a limited analysis of epigenetic modifications using chromatin immunoprecipitation combined with high-throughput sequencing (ChIP-Seq) for the H3k27ace, as an epigenetic marker of active enhancers and promoters and, H3k27me3 as a marker for gene repression. In the in-house generated resistant cell line NB4EV-AsR1 gene ontology enrichment on the H3k27ace mark of promoter regions showed significant enrichment for DNA damage, mitochondria, cell cycle and mRNA splicing clusters in comparison to the naïve NB4 cell line (supplementary file 2).

We validated the finding by measuring the basal metabolic properties such as reactive oxygen species (ROS), antioxidant level, glucose uptake, and mitochondrial membrane potential (MMP), which are reported to be key factors in the mechanisms of action of ATO. We observed that in comparison to naïve NB4 cells, ATO resistant cell lines (NB4EV-AsR1 and UF1) had low levels of basal ROS (Figure 5a), lower mitochondrial membrane potential (MMP) and low glucose uptake capacity (2-NBDG uptake, GLUT-1 and LDHA, both at transcript and protein level) in comparison to the naïve NB4 cells (figure 5c, d, and e). As expected, GSH levels were elevated in NB4EV-AsR1 in comparison to naïve NB4 though it remained low in UF1 (figure 5b). In patients,

consistent with the above observation in comparison to newly diagnosed primary APL samples we observed significant downregulation of GLUT-1 and LDHA transcript levels in the relapsed APL samples (supplementary figure 6).

ATO resistant APL cell lines are metabolically distinct in comparison to ATO sensitive cell line:

Glyco stress test revealed that the naïve NB4 cells had increased glycolysis where the basal extracellular acidification rate (ECAR) was significantly higher (figure 6a) with increased oxygen consumption rate (OCR) (supplementary figure 7) in comparison to ATO resistant cell lines.

To address the degree to which glycolysis is necessary for cell survival, we treated the naïve NB4 and ATO resistant cell lines with 2-Deoxy glucose (2-DG), a glucose analog that inhibits glycolysis via its action on hexokinases. We noted that naïve NB4 cell line viability was significantly affected in the presence of 2-DG, equivalent to the effect seen with 2μM of ATO. There was no evidence of an additive effect when these agents were combined (figure 6b). In contrast, the viability of the APL resistant cell lines and AML cell lines (U937 and THP-1; data not shown) was not significantly affected when 2-DG was used alone or in combination with ATO (figure 6b).

Having noted that glycolytic inhibition by 2-DG promoted apoptosis in NB4 cells comparable to that seen with ATO, we performed in-vivo glycolytic inhibition to understand the physiological relevance of glycolytic inhibition in the ATO sensitive transplantable APL mouse model. We observed that 2-DG or ATO as single agents reduced the leukemic burden in the peripheral blood (PB) and PML-RARA copy number at the end of 22 days to levels that were comparable and indistinguishable from each other (figure 6c).

Heterogeneity of anti-apoptotic protein dependency of ATO resistant APL cell lines:

We next assessed the mitochondria priming status of the ATO resistant cell lines by employing iBH3 profiling and their sensitivity to the BH3 mimetics. We observed a significant difference between the in-house ATO resistant cell lines and the parental cell line (independent of A216V). Neither a BCL-2 inhibitor (ABT-199 -Venetoclax-VEN) nor a BCL-XL inhibitor (A1331852) promoted apoptosis as a single agent in the parental and resistant cell lines whereas MCL-1 inhibitor (S63845) promoted apoptosis only in parental NB4 naïve and NB4EV-AsR2 (figure 7a). The sensitivity to the BH3 mimetics correlated with their basal BH3 profiling (figure 7b).

Combination of glycolytic inhibitor (ATO) and mitocans promoted apoptosis in the ATO resistant cell lines:

We then evaluated the effect of mitochondrial OXPHOS uncoupler on the ATO resistant promyelocytic and non-promyelocytic AML cell lines. The viability of ATO resistant cell lines was not affected significantly when treated with the mitochondrial OXPHOS un-coupler FCCP as a single agent, whereas in combination with ATO, the viability was significantly reduced in NB4EV-AsR1(harbors A216V mutation; resistant to BCL-2 and MCL-1 inhibition); NB4EV-AsR2 (harbors A216V mutation, and sensitive to MCL-1inhbition), UF1 cell line (A216V negative, sensitive to BCL-2 and MCL-1 inhibition) (Figure 7c). A similar effect was observed in non-M3 AML cell lines, U937 and THP-1 (resistant to BCL-2 inhibition and ATO whereas sensitive to MCL-1; Supplementary figure 8). We observed that the ATO resistant APL and AML cell lines, were significantly different in their metabolic preferences for their survival from the ATO sensitive NB4 naïve cell line and by targeting this difference we were able to overcome the resistance independent of the existence of the *PML-B2* domain mutation and their anti-apoptotic protein dependency. Blocking mitochondrial respiration in combination with ATO therefore can enhance cell death in ATO and ATRA resistant APL cell lines and non-M3 AML cell lines. However, this combination had significant off target effects on the normal peripheral blood mononuclear cells and further evaluation for compounds that selectively target the leukemic cell's mitochondrial respiration is needed for these observations to be translated to the clinic.

Discussion:

The study highlights that in comparison to the existing ATO resistant APL cell lines[22,23] our in-house generated ATO resistant cell lines are stable, well-characterized at the genomic levels and they also possess the well-known ATO resistance-conferring mutation A216V in the B2 domain of the PML-RARA oncoprotein. These ATO resistant cell lines are observed to be less sensitive to differentiation with ATRA and to the combination therapy of ATO and ATRA and are hence an excellent tool to evaluate additional mechanisms that could contribute to drug resistance. We also noted that the UF1 APL cell line was resistant to ATO (not been previously reported) but did not have the well-defined PML-RARA B2 domain mutation giving us an opportunity to study ATO resistance with and without PML-RARA B2 domain mutations.

In comparison to the naïve NB4, in house generated ATO resistant cell lines overexpressed ATO efflux transporters such as AQP9, MRP4, and ABCA7, which correlated with their inability to accumulate intracellular ATO. This phenomenon was not observed in primary blasts from relapsed APL patients previously treated with ATO in comparison to newly diagnosed[21]. The possibility of efflux transporters as a protective mechanism of ATO resistance cannot be excluded in the clinic and needs further evaluation.

We noted the presence of a somatic mutation in the B2 domain of the *PML* gene in our in-house generated ATO resistant cell line that has been reported to confer resistance to ATO. It is important to note that these mutations are acquired post ATO treatment, and none of the APL cell lines or relapsed APL patients prior to ATO therapy had the B2 domain mutation[24]. The in-house resistant cell lines did not acquire additional mutations in p53 gene which has been reported to be critical for the regulation of NB formation and ROS generation. The observation suggests that the reduction in the PML micro-speckled pattern formation and low ROS levels are independent of p53 status in these cell lines. The cellular redox system of the resistant cell lines was found to be significantly altered in these cell lines having lower ROS levels, lower proliferative rate, and an increased antioxidant system favoring quiescence

and stemness like properties[25]. This was further corroborated by the observation of low ECAR and OCR status of the resistant cell lines [26].

ATO sensitive cell line NB4 naïve was observed to be more reliant on the Warburg effect for their survival and proliferation, and their viability was significantly affected by a glycolytic inhibitor (2-DG). In an in-vivo APL model, 2-DG significantly reduced the leukemic burden comparable to the standard of care (ATO). This further supports our observation that the naïve ATO sensitive APL cells survival could be targeted by glycolytic inhibition. Based on the recognized inhibitory effect of ATO on the glycolytic pathway[17] this could also be an important mechanism by which ATO induces apoptosis in malignant promyelocytes. In contrast, the ATO resistant APL and AML cell lines were mainly dependent on OXPHOS for their survival. However, unlike NB4 naïve cells the ATO resistant and AML cell lines had greater metabolic plasticity to switch between glycolysis and the OXPHOS when one is inhibited but were susceptible to a combination of ATO and mitocans, this susceptibility was independent of their PML B2 domain mutation status and their anti-apoptotic protein dependency. It is well known that A216V mutation alters the ATO binding on the B2 domain of the PML-RARA oncoprotein, the observed combinatorial effect of ATO in combination with mitocan on the resistant cell lines is hence likely to be due to the inhibitory effect of ATO on the glycolytic pathway[13,27].

Taken together, our work demonstrates that ATO resistance is multi-factorial and is not limited to presence or absence of either PML or p53 mutations. The in-house generated ATO resistant cell line would be a useful model to further evaluate mechanisms of resistance in leukemia. Targeting the metabolic adaptations seen in ATO resistant cell lines has the potential to overcome such resistance. Inhibiting mitochondrial respiration in combination with ATO could overcome ATO resistance and translating this approach to the clinic both in relapsed APL and in the treatment of newly diagnosed AML needs to be explored further. While the combination of ATO and FCCP was observed to be non-selective, there are a number of FDA approved drugs used in the clinic that have the property to selectively inhibit mitochondrial respiration in cancer cells, these could potentially be evaluated for their synergistic activity with ATO in

leukemia[28]. Our data also draws attention to possible severe off target toxicity of such combinations which may be inadvertently used in the clinic.

Data Sharing Statement:

The datasets discussed in this manuscript have been deposited in the NCBI under the following accession numbers: 1) GSE115812 [GEO] - Gene expression data of NB4 naïve, NB4 EV-AsR1 and UF-1. 2) GSE42030 [GEO] - Gene expression data of Newly diagnosed and relapsed APL samples. 3) PRJNA758248 [BioProject] - Comparison of epigenetic variations in ATO sensitive and Resistant APL cell lines. 4) PRJNA643016 [BioProject] - Comparing Genomic variations of ATO sensitive and Resistant cell lines. The datasets will also be shared upon an email request to Dr. Vikram Mathews (vikram@cmcvellore.ac.in).

Acknowledgments:

This study is supported by India Alliance Wellcome-DBT research grant (IA/CPHS/18/1/503930), DBT-COE grant (BT/COE/34/SP13432/2015) and DST-SERB (CRG/2019/001214), New Delhi, India. VM is supported by the senior fellowship program of India Alliance Wellcome-DBT (IA/CPHS/18/1/503930), New Delhi, India. SG, HKP, SD were supported by a senior research fellowship from the Council for Scientific and Industrial Research (CSIR), New Delhi, India. AV is supported by junior research fellowship from Department of Biotechnology (DBT), Government of India. We acknowledge Intas Pharmaceutical Ltd, India, and NATCO pharmaceutical Ltd, India, for kindly providing us API of pharmaceutical drugs for this study. We acknowledge

Prof. Mitradas Panicker, National Center for Biological Sciences, Bengaluru, and Prof. Tamil Selvan, Department of Biotechnology, Anna University, Chennai, for providing access to the seahorse extracellular flux analyzer. Seahorse facility at Anna University is funded by Department of Science and Technology; Fund for Improvement of S&T Infrastructure (DST-FIST) (SR/FST/LSI-649/2015)

Author contribution:

NB: performed research, involved in designing the study, performed molecular tests, and analyzed data and written the paper.
SG: performed research, performed molecular tests, and analyzed data.
EC: performed research, performed molecular tests, and analyzed data.
HKP: performed research, performed molecular tests, and analyzed data
AV: performed research, performed molecular tests, and analyzed data
AAA: performed research, performed molecular tests, and analyzed data.
SD: performed research, performed molecular tests, and analyzed data.
SPK: performed research, performed molecular tests, and analyzed data.
NRR: performed research, performed molecular tests, and analyzed data.
MY: performed research, performed karyotyping tests, and analyzed data.
AK: performed research and analyzed data.
UK: performed research and analyzed data.
NBJ: performed research, performed karyotyping tests, and analyzed data.
SK: performed research and analyzed data.
PB: performed research and analyzed data.
VM: performed research, designed study, analyzed data, and written the paper.

Conflict of interest: No conflict of interest

References:

1. Wang Z-Y, Chen Z. Acute promyelocytic leukemia: from highly fatal to highly curable. *Blood*. 2008;111(5):2505-2515.
2. Mathews V, George B, Lakshmi KM, et al. Single-agent arsenic trioxide in the treatment of newly diagnosed acute promyelocytic leukemia: durable remissions with minimal toxicity. *Blood*. 2006;107(7):2627-2632.
3. Lo-Coco F, Avvisati G, Vignetti M, et al. Retinoic acid and arsenic trioxide for acute promyelocytic leukemia. *N Engl J Med*. 2013;369(2):111-121.
4. Niu C, Yan H, Yu T, et al. Studies on treatment of acute promyelocytic leukemia with arsenic trioxide: remission induction, follow-up, and molecular monitoring in 11 newly diagnosed and 47 relapsed acute promyelocytic leukemia patients. *Blood*. 1999;94(10):3315-3324.
5. Coombs CC, Tavakkoli M, Tallman MS. Acute promyelocytic leukemia: where did we start, where are we now, and the future. *Blood Cancer Journal*. 2015;5:e304.
6. Sanz MA, Fenaux P, Tallman MS, et al. Management of acute promyelocytic leukemia: updated recommendations from an expert panel of the European LeukemiaNet. *Blood*. 2019;133(15):1630-1643.
7. Lengfelder E, Hofmann WK, Nowak D. Impact of arsenic trioxide in the treatment of acute promyelocytic leukemia. *Leukemia*. 2012;26(3):433-442.
8. Madan V, Shyamsunder P, Han L, et al. Comprehensive mutational analysis of primary and relapse acute promyelocytic leukemia. *Leukemia*. 2016;30(8):1672-1681.
9. Goto E, Tomita A, Hayakawa F, Atsumi A, Kiyoi H, Naoe T. Missense mutations in PML-RARA are critical for the lack of responsiveness to arsenic trioxide treatment. *Blood*. 2011;118(6):1600-1609.
10. Zhu H-H, Qin Y-Z, Huang X-J. Resistance to Arsenic Therapy in Acute Promyelocytic Leukemia. *New England Journal of Medicine*. 2014;370(19):1864-1866.
11. Lou Y, Ma Y, Sun J, et al. Evaluating frequency of PML-RARA mutations and conferring resistance to arsenic trioxide-based therapy in relapsed acute promyelocytic leukemia patients. *Ann Hematol*. 2015;94(11):1829-1837.
12. Kawakita M, Ferhi O, Soilihi H, Le Bras M, Lallemand-Breitenbach V, Thé H. PML is a ROS sensor activating p53 upon oxidative stress. *The Journal of Experimental Medicine*. 2017;214:jem.20160301.
13. Liu J, Zhu H-H, Jiang H, Jiang Q, Huang X-J. Varying responses of PML-RARA with different genetic mutations to arsenic trioxide. *Blood*. 2016;127(2):243-250.
14. Ablain J, Rice K, Soilihi H, de Reynies A, Minucci S, de The H. Activation of a promyelocytic leukemia-tumor protein 53 axis underlies acute promyelocytic leukemia cure. *Nat Med*. 2014;20(2):167-174.
15. Li T, Ma R, Zhang Y, et al. Arsenic trioxide promoting ETosis in acute promyelocytic leukemia through mTOR-regulated autophagy. *Cell Death & Disease*. 2018;9(2):75.
16. Zhang HN, Yang L, Ling JY, et al. Systematic identification of arsenic-binding proteins reveals that hexokinase-2 is inhibited by arsenic. *Proc Natl Acad Sci U S A*. 2015;112(49):15084-15089.
17. Zhang T, Lu H, Li W, Hu R, Chen Z. Identification of Arsenic Direct-Binding Proteins in Acute Promyelocytic Leukaemia Cells. *Int J Mol Sci*. 2015;16(11):26871-26879.
18. Zhang X, Yang F, Shim J-Y, Kirk KL, Anderson DE, Chen X. Identification of arsenic-binding proteins in human breast cancer cells. *Cancer letters*. 2007;255(1):95-106.
19. Roussel MJS, Lanotte M. Maturation sensitive and resistant t(15;17) NB4 cell lines as tools for APL physiopathology: nomenclature of cells and repertory of their known genetic alterations and phenotypes. *Oncogene*. 2001;20(49):7287-7291.

20. Bouaoun L, Sonkin D, Ardin M, et al. TP53 Variations in Human Cancers: New Lessons from the IARC TP53 Database and Genomics Data. *Hum Mutat*. 2016;37(9):865-876.
21. Chendamarai E, Ganesan S, Alex AA, et al. Comparison of newly diagnosed and relapsed patients with acute promyelocytic leukemia treated with arsenic trioxide: insight into mechanisms of resistance. *PloS one*. 2015;10(3):e0121912-e0121912.
22. Lunghi P, Tabilio A, Lo-Coco F, Pelicci PG, Bonati A. Arsenic trioxide (ATO) and MEK1 inhibition synergize to induce apoptosis in acute promyelocytic leukemia cells. *Leukemia*. 2005;19(2):234-244.
23. Gianni M, Koken MHM, Chelbi-Alix MK, Benoit G, Lanotte M, Chen Z. Combined arsenic and retinoic acid treatment enhances differentiation and apoptosis in arsenic-resistant NB4 cells. *Blood*. 1998;91.
24. Kulkarni U, Ganesan S, Alex AA, et al. A phase II study evaluating the role of bortezomib in the management of relapsed acute promyelocytic leukemia treated upfront with arsenic trioxide. *Cancer Med*. 2020;9(8):2603-2610.
25. Lagadinou ED, Sach A, Callahan K, et al. BCL-2 inhibition targets oxidative phosphorylation and selectively eradicates quiescent human leukemia stem cells. *Cell Stem Cell*. 2013;12(3):329-341.
26. Hlozkova K, Pecinova A, Alquezar-Artieda N, et al. Metabolic profile of leukemia cells i nfluences treatment efficacy of L-asparaginase. *BMC Cancer*. 2020;20(1):526.
27. Tomita A, Kiyoi H, Naoe T. Mechanisms of action and resistance to all-trans retinoic acid (ATRA) and arsenic trioxide (As2O3) in acute promyelocytic leukemia. *International Journal of Hematology*. 2013;97(6):717-725.
28. Gohil VM, Sheth SA, Nilsson R, et al. Discovery and therapeutic potential of drugs that shift energy metabolism from mitochondrial respiration to glycolysis. *Nature biotechnology*. 2010;28(3):249-255.

Figure Legends:

Figure 1: Generation of ATO resistant cell lines. a) NB4 naïve parental cell line was exposed to 50nM of ATO for three months, and the concentration was gradually increased to 1µM ATO over a period of one year until they sustained and proliferated. Limiting dilutions and colony-forming unit assay were performed to generate mono clones of the resistant cell lines. b) The bar graph represents the percentage of viable cells post 48 hours of 2µM ATO. c) Representative dot plots and stacked bars (summarizes the dot plots results) NB4 and resistant cell lines were treated with 0.5µM and 1uM of ATRA for 72hrs as single agents and in combination with 2uM ATO, and the percentage of differentiation was measured by the surface expression of CD11b and dead cells were measured by 7AAD. Graphs and statistical parameters were generated from three independent experiments. *p≤0.05; **p≤0.01; ***p≤0.001; ***p≤0.0001.

Figure 2: Heterogeneity in the cell surface marker and transporters expression of the ATO resistant cell line in comparison to parental cell line: a) CD13 and CD33 surface expression of ATO resistant cell lines in comparison to NB4 naïve. b) Relative mRNA levels of ATO influx gene (ABCA1) and efflux transporters genes (ABCA7, AQP9, MRP4, and ABCB6) in the in-house generated ATO resistant cell lines compared to NB4 naïve which is normalized to one. c) Intracellular ATO levels in NB4 naïve and ATO resistant cell lines post 24 hours of 0.5µM ATO treatment. d)Fluorescent microscopic image of the PML (RED) in NB4 naïve and ATO resistant cell lines displaying nuclear body formation and micro speckled pattern (magnification 63x – oil immersion) e) PML-RARA transcripts in the NB4 naïve and in-house generated ATO resistant cell lines f) Immunoblots of the PML-RARA fusion protein levels in NB4 naïve and ATO resistant cell lines. All error bars represent the mean ± SEM of three independent experiments. *p≤0.05; **p≤0.01; ***p≤0.001; ***p≤0.0001.

Figure 3: Whole-exome sequencing reveals changes in the ATO resistant cell lines at the genomic level. a) AML TCGA data set was compared with novel mutations observed

in AsR1 and UF1, and the graph represents the novel mutations (only found in resistant cell lines) and their mutation frequency. B) Sanger sequencing showing the existence of PML – A216V in the in-house generated ATO resistant cell line and not in the UF1 and parental cell line NB4 naïve. c) Mutations observed in the p53 gene of ATO resistant and sensitive cell lines.

Figure 4: Gene expression analysis of the ATO resistant cell lines reveals dysregulation of cellular metabolism. a) Pie chart representing the dysregulated genes in the in-house generated ATO resistant cell line NB4 EV-AsR1 and UF1 in comparison to parental cell line NB4 naïve. b) Heatmap highlighting gene signature of NB4 naïve (duplicate) in-house generated ATO resistant cell line (duplicate) and the 8 unmatched newly diagnosed and relapsed APL samples (primary cells data previously reported and adapted from Ezhilarasi Chendamari., et.al., PloS one 2015). c) Heatmap representing NB4 naïve, ATO resistant cell line NB4 EV-AsR1 and UF1 cell lines genes involved in the glycolytic and mitochondrial metabolism.

Figure 5: ATO resistant cell lines are metabolically distinct. a) Baseline total reactive oxygen species were measured using redox-sensitive dye (cell ROX Green) by flow cytometry. b) Baseline protein thiols was measured as an indicative of antioxidant using OPT (Phthaldialdehyde) and median fluorescence intensity are represented as bar graphs. c) Mitochondria membrane potential of the resistant cell lines were measured using JC-1 d) Glucose uptake was measured using a fluorescent analogue of 2- deoxy glucose and represented as relative mean fluorescence intensity. GLUT-1 and LDHA transcripts (e) and protein (f) levels of NB4 naïve, NB4 EV-AsR1 and UF1 cell lines. All error bars represent the means ± SEM of three to four independent experiments. *p≤0.05; **p≤0.01; ***p≤0.001; ***p≤0.0001.

Figure 6: ATO resistant cells are metabolically heterogeneous and *in vivo* effect of glycolytic inhibition by 2-DG reduces leukemic burden in APL mouse model**.** a)

extracellular acidification rate (ECAR) and glycolytic potential of NB4 naïve, NB4 EV-AsR1 and UF1 cell lines were assessed in real time using seahorse extracellular flux analyzer. b) Viability of the sensitive and resistant cell lines post 48 hours of glycolytic inhibitor ATO and 2-DG (ATO = 2µM; 2-DG = 5mM; 48 hours; n=4). All error bars represent the means ± SEM of four independent experiments. *p≤0.05; **p≤0.01; ***p≤0.001; ***p≤0.0001. c) Schematic representation of the APL transplantable mouse model and treatment plan. Mice were euthanized on day 22 and examined for the presence of leukemic cells as CD117+Gr1+ cells in peripheral blood, and PML-RARA transcript levels in bone marrow.

Figure 7: Mitocans synergize with ATO to promote apoptosis in the ATO resistant cell lines. a) Viability of NB4 and in-house generated ATO resistant cell lines to BH3 mimetics (n=5). b) Intracellular BH3 profiling of ATO resistant and sensitive cells (n=3) measured using intracellular cytochrome-c retention. c) Viability of the sensitive and resistant APL and non-APL cell lines treated with OXPHOS uncoupler FCCP in combination with ATO. ATO = 2µM; FCCP =10µM and BH3 mimetics = 250nM; 48 hours. All error bars represent the means ± SEM of four independent experiments. *p≤0.05; **p≤0.01; ***p≤0.001; ***p≤0.0001. (ABT-199 – Venetoclax; S63845 - MCL-1 inhibitor; A1331852 – BCL-XL inhibitor; ALM – Alamethicin).

Figure 1

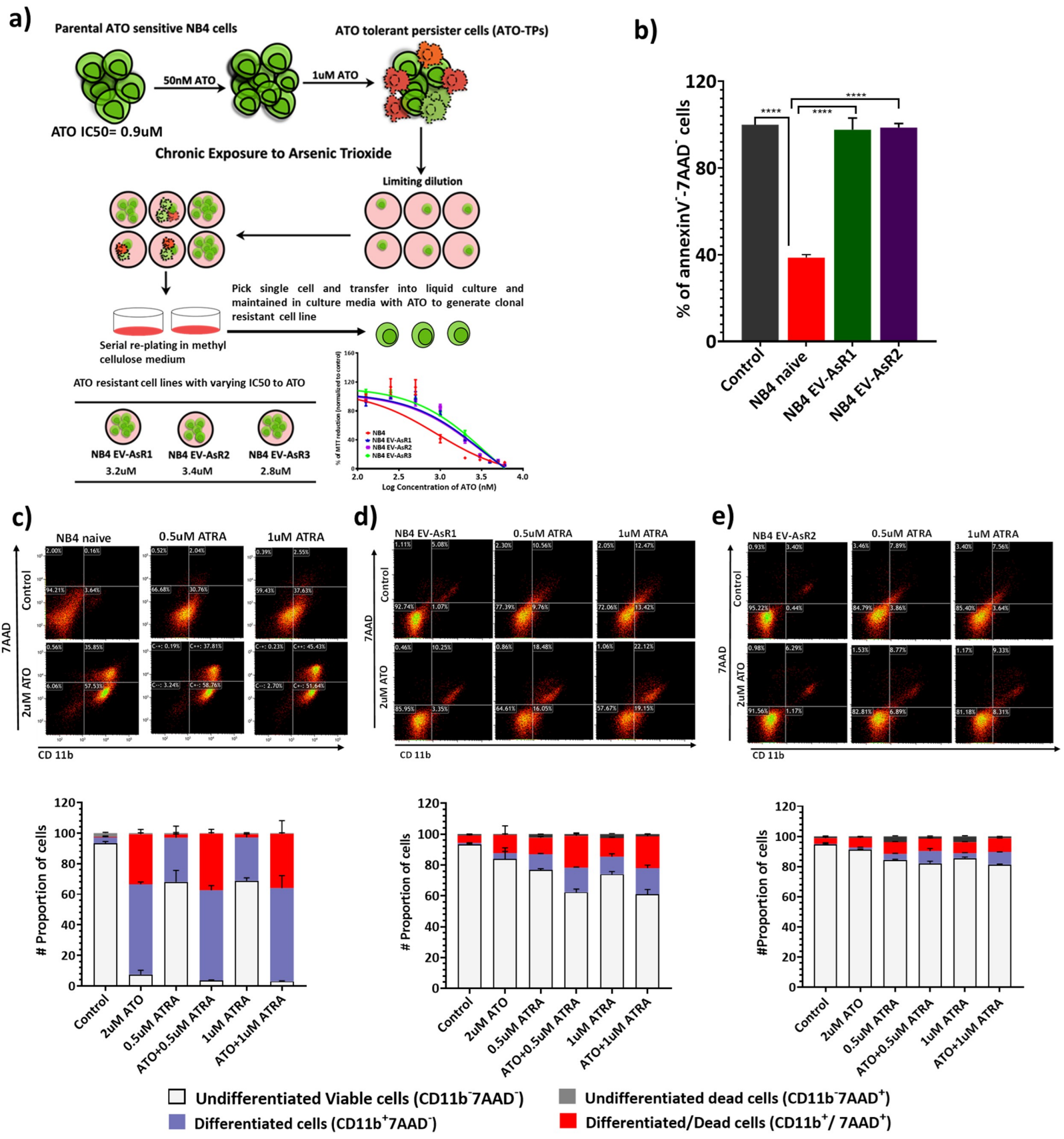
a)
Parental ATO sensitive NB4 cells
ATO tolerant persister cells (ATO-TPs)
50nM ATO
1uM ATO
ATO IC50= 0.9uM
Chronic Exposure to Arsenic Trioxide
Limiting dilution
Pick single cell and transfer into liquid culture and maintained in culture media with ATO to generate clonal resistant cell line
Serial re-plating in methyl cellulose medium
ATO resistant cell lines with varying IC50 to ATO
NB4 EV-AsR1
3.2uM
NB4 EV-AsR2
3.4uM
NB4 EV-AsR3
2.8uM
% of MTT reduction (normalized to control)
Log Concentration of ATO (nM)
NB4
NB4 EV-AsR1
NB4 EV-AsR2
NB4 EV-AsR3
b)
% of annexinV-7AAD- cells
Control
NB4 naive
NB4 EV-AsR1
NB4 EV-AsR2
c)
NB4 naive
0.5uM ATRA
1uM ATRA
Control
2uM ATO
7AAD
CD 11b
d)
NB4 EV-AsR1
e)
NB4 EV-AsR2
Proportion of cells
#Proportion of cells
Control
2uM ATO
0.5uM ATRA
ATO+0.5uM ATRA
1uM ATRA
ATO+1uM ATRA
Undifferentiated Viable cells (CD11b-7AAD-)
Undifferentiated dead cells (CD11b-7AAD+)
Differentiated cells (CD11b+7AAD-)
Differentiated/Dead cells (CD11b+/ 7AAD+)

Figure 2

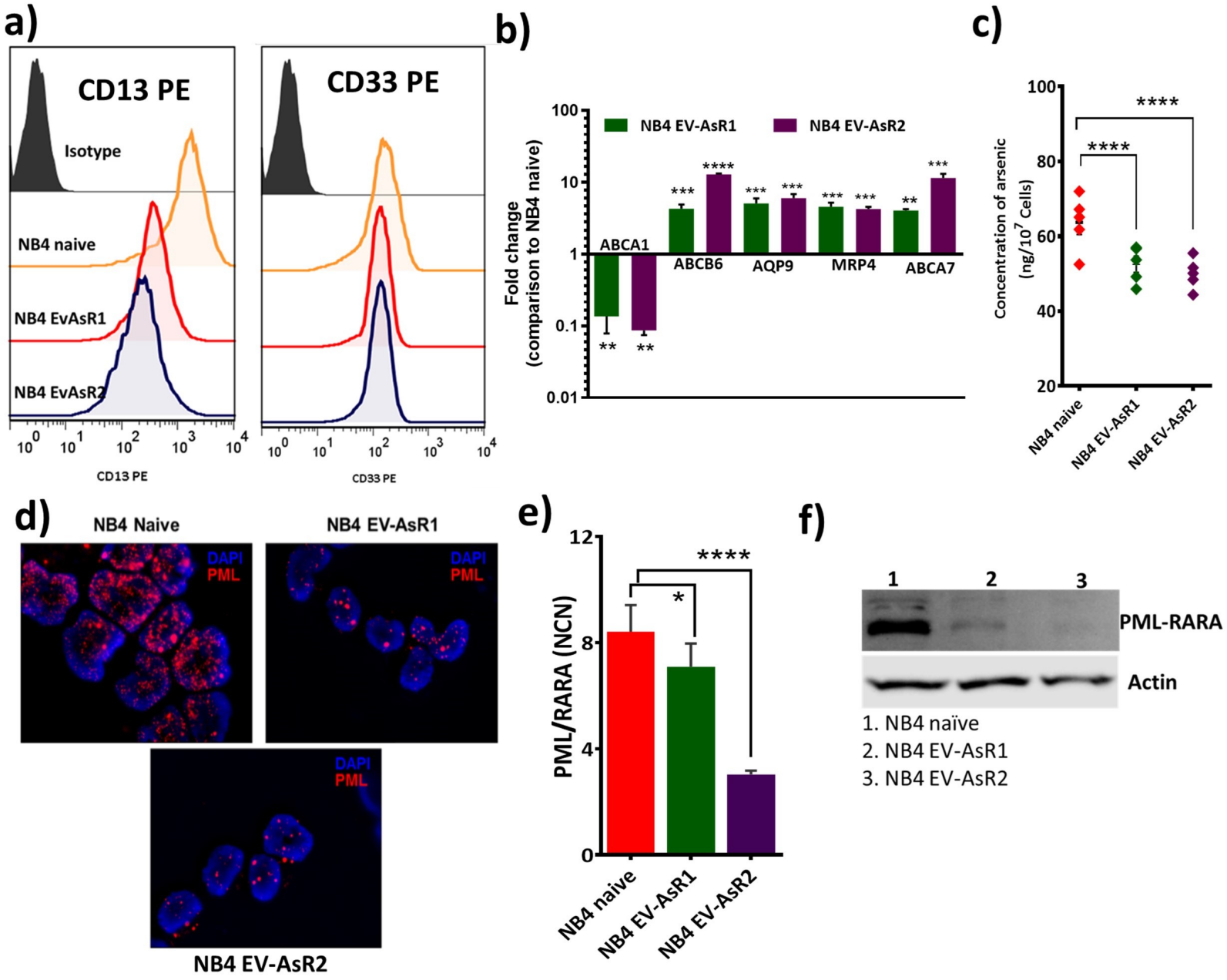
a)
CD13 PE
CD33 PE
Isotype
NB4 naive
NB4 EvAsR1
NB4 EvAsR2
CD13 PE
CD33 PE
b)
NB4 EV-AsR1
NB4 EV-AsR2
Fold change (comparison to NB4 naive)
ABCA1
ABCB6
AQP9
MRP4
ABCA7
c)
Concentration of arsenic (ng/10^7 Cells)
NB4 naive
NB4 EV-AsR1
NB4 EV-AsR2
d)
NB4 Naive
NB4 EV-AsR1
NB4 EV-AsR2
DAPI
PML
e)
PML/RARA (NCN)
NB4 naive
NB4 EV-AsR1
NB4 EV-AsR2
f)
PML-RARA
Actin
1. NB4 naïve
2. NB4 EV-AsR1
3. NB4 EV-AsR2

Figure 3

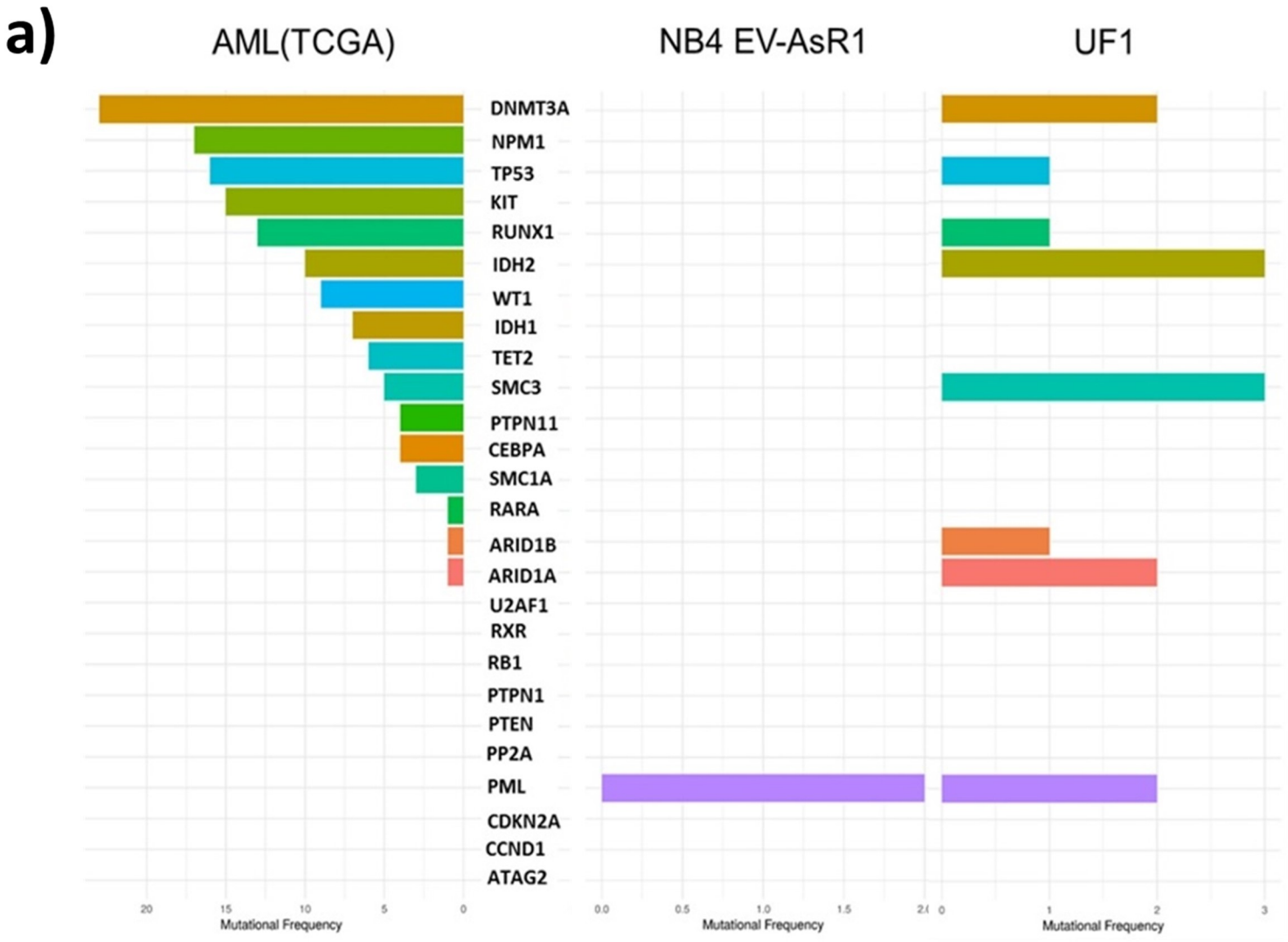

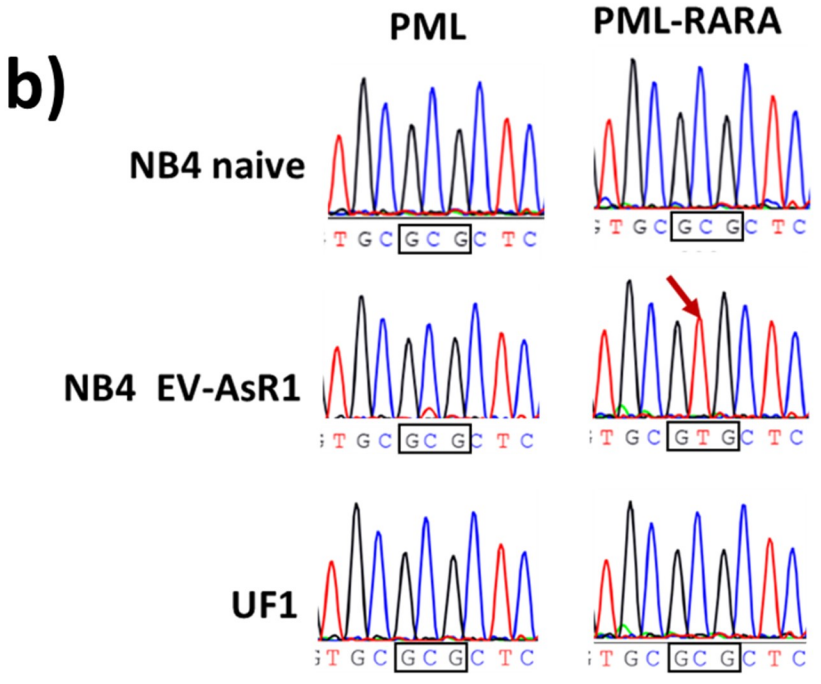

c)

Cell line	Exon	TP53 mutation
NB4 naïve	7	c.743 G>A (R248Q)
NB4 EV-AsR1	7	c. 743 G>A (R248Q)
UF1	5	c.586 C>T (R196*)
	10	c.1083_1083 del (S362Afs*8)

Figure 4

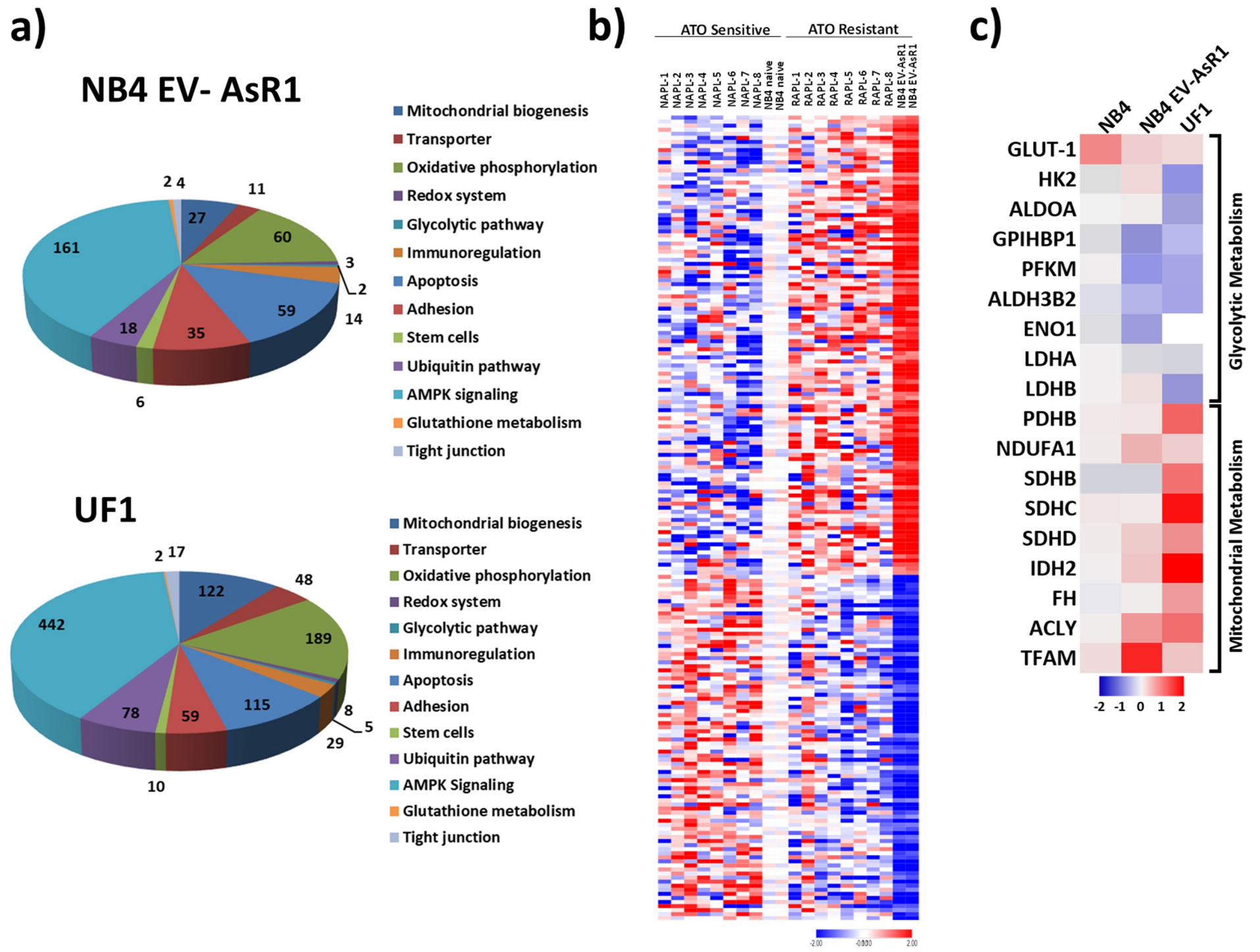
a)
NB4 EV- AsR1
2 4
11
27
60
161
3
2
59
14
18
35
6
Mitochondrial biogenesis
Transporter
Oxidative phosphorylation
Redox system
Glycolytic pathway
Immunoregulation
Apoptosis
Adhesion
Stem cells
Ubiquitin pathway
AMPK signaling
Glutathione metabolism
Tight junction
UF1
2 17
48
122
442
189
8
5
29
115
78
59
10
Mitochondrial biogenesis
Transporter
Oxidative phosphorylation
Redox system
Glycolytic pathway
Immunoregulation
Apoptosis
Adhesion
Stem cells
Ubiquitin pathway
AMPK Signaling
Glutathione metabolism
Tight junction
b)
ATO Sensitive
ATO Resistant
NAPL-1
NAPL-2
NAPL-3
NAPL-4
NAPL-5
NAPL-6
NAPL-7
NAPL-8
NB4 naive
NB4 naive
RAPL-1
RAPL-2
RAPL-3
RAPL-4
RAPL-5
RAPL-6
RAPL-7
RAPL-8
NB4 EV-AsR1
NB4 EV-AsR1
-2.00
-0.000
2.00
c)
NB4
NB4 EV-AsR1
UF1
GLUT-1
HK2
ALDOA
GPIHBP1
PFKM
ALDH3B2
ENO1
LDHA
LDHB
PDHB
NDUFA1
SDHB
SDHC
SDHD
IDH2
FH
ACLY
TFAM
Glycolytic Metabolism
Mitochondrial Metabolism
-2 -1 0 1 2

Figure 5

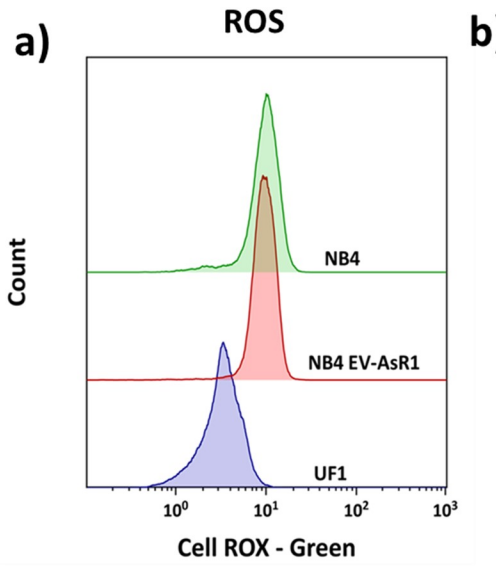
a)
ROS
Count
NB4
NB4 EV-AsR1
UF1
10^0
10^1
10^2
10^3
Cell ROX - Green

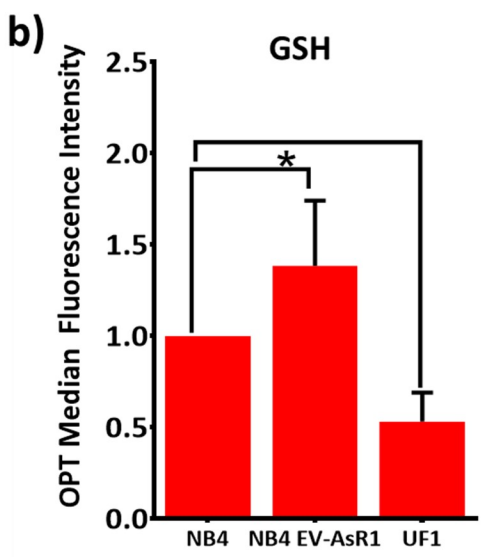
b)
GSH
OPT Median Fluorescence Intensity
2.5
2.0
1.5
1.0
0.5
0.0
*
NB4
NB4 EV-AsR1
UF1

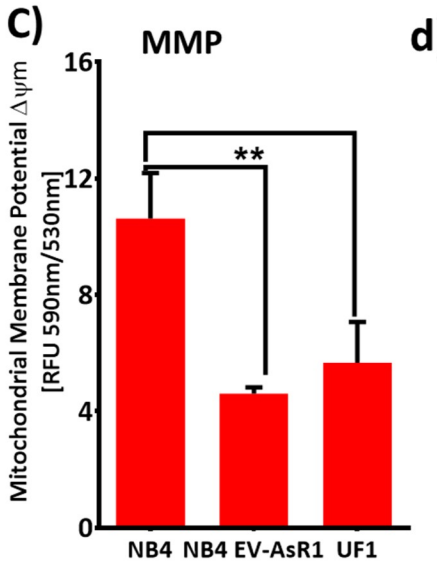
C)
MMP
Mitochondrial Membrane Potential Δψm
[RFU 590nm/530nm]
16
12
8
4
0
**
NB4
NB4 EV-AsR1
UF1

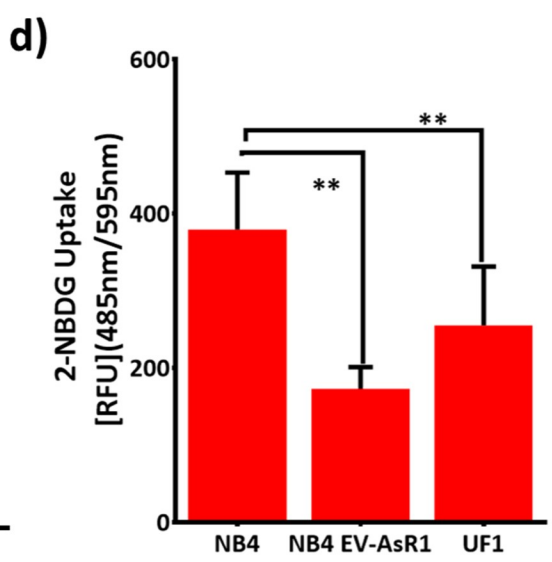
d)
2-NBDG Uptake
[RFU](485nm/595nm)
600
400
200
0
**
**
NB4
NB4 EV-AsR1
UF1

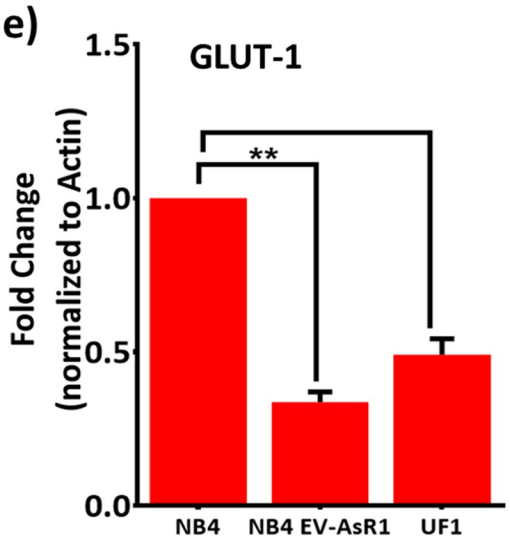
e)
GLUT-1
Fold Change
(normalized to Actin)
1.5
1.0
0.5
0.0
**
NB4
NB4 EV-AsR1
UF1

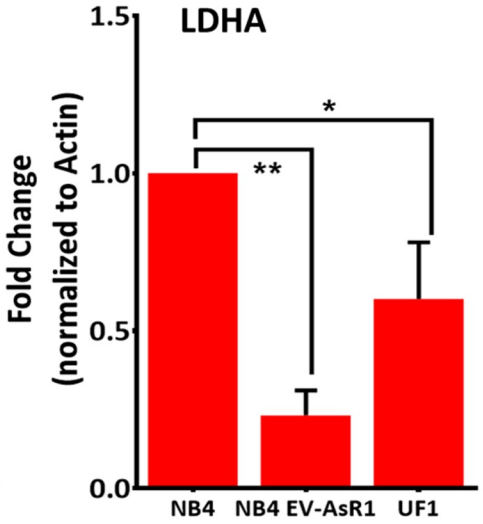
LDHA
Fold Change
(normalized to Actin)
1.5
1.0
0.5
0.0
*
**
NB4
NB4 EV-AsR1
UF1

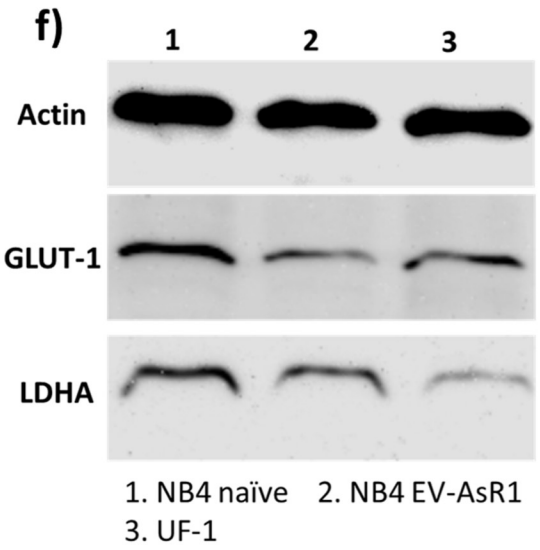
f)
1
2
3
Actin
GLUT-1
LDHA
1. NB4 naïve
2. NB4 EV-AsR1
3. UF-1

Figure 6

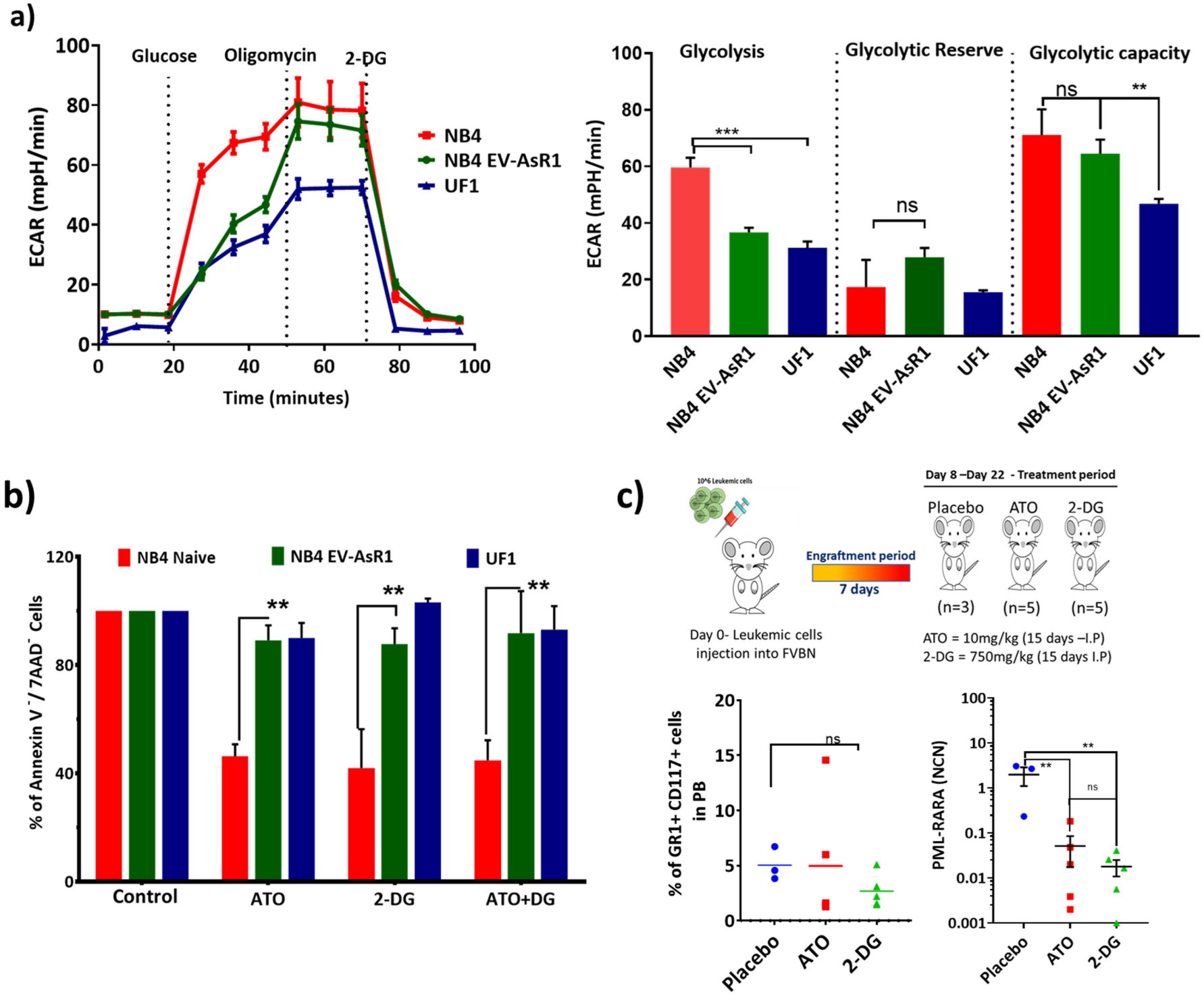
a)
Glucose
Oligomycin
2-DG
ECAR (mpH/min)
Time (minutes)
NB4
NB4 EV-AsR1
UF1
Glycolysis
Glycolytic Reserve
Glycolytic capacity
ECAR (mPH/min)
***
ns
**
b)
% of Annexin V⁻/ 7AAD⁻ Cells
NB4 Naive
NB4 EV-AsR1
UF1
Control
ATO
2-DG
ATO+DG
c)
10^6 Leukemic cells
Engraftment period
7 days
Day 0- Leukemic cells injection into FVBN
Day 8 –Day 22 - Treatment period
Placebo
ATO
2-DG
(n=3)
(n=5)
(n=5)
ATO = 10mg/kg (15 days –I.P)
2-DG = 750mg/kg (15 days I.P)
% of GR1+ CD117+ cells in PB
PML-RARA (NCN)

Figure 7

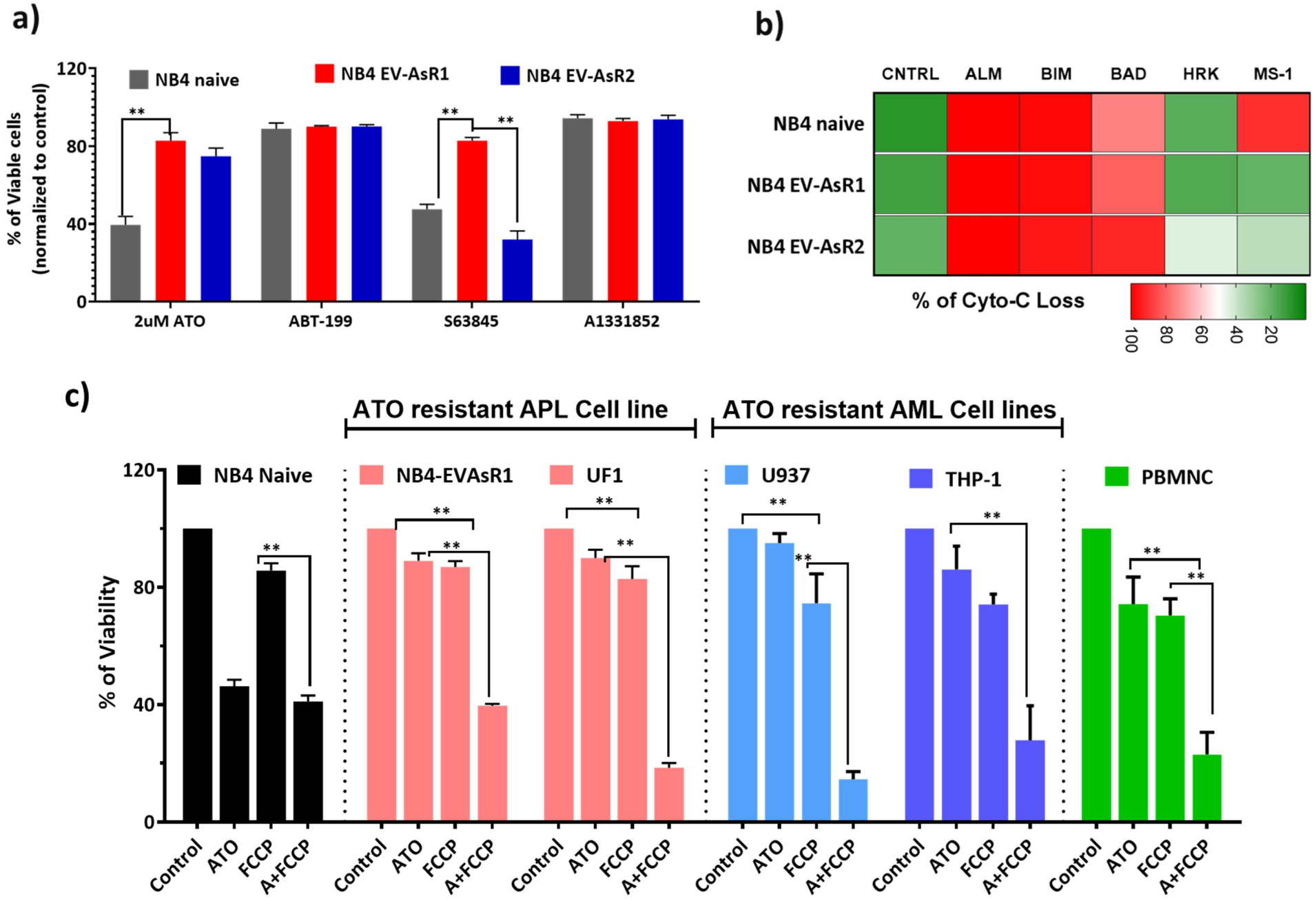
a)
NB4 naive
NB4 EV-AsR1
NB4 EV-AsR2
% of Viable cells (normalized to control)
120
80
40
0
**
2uM ATO
ABT-199
S63845
A1331852
b)
CNTRL
ALM
BIM
BAD
HRK
MS-1
NB4 naive
NB4 EV-AsR1
NB4 EV-AsR2
% of Cyto-C Loss
100
80
60
40
20
c)
ATO resistant APL Cell line
ATO resistant AML Cell lines
NB4 Naive
NB4-EVAsR1
UF1
U937
THP-1
PBMNC
% of Viability
120
80
40
0
Control
ATO
FCCP
A+FCCP

bjh research paper

Management of relapse in acute promyelocytic leukaemia treated with up-front arsenic trioxide-based regimens

N. A. Fouzia,[1] Vibhor Sharma,[1] Saravanan Ganesan,[1] Hamenth K. Palani,[1] Nithya Balasundaram,[1] Sachin David,[1] Uday P. Kulkarni,[1] Anu Korula,[1] Anup J. Devasia,[1] Sukesh C. Nair,[2] Nancy Beryl Janet,[1] Aby Abraham,[1] Thenmozhi Mani,[3] Jeyaseelan Lakshmanan,[3] Poonkuzhali Balasubramanian,[1] Biju George[1] and Vikram Mathews[1]

[1]*Department of Haematology, Christian Medical College, Vellore,* [2]*Department of Immunohaematology and Transfusion Medicine, Christian Medical College, Vellore, and* [3]*Department of Biostatistics, Christian Medical College, Vellore, India*

Received 12 July 2020; accepted for publication 29 September 2020

Correspondence: Vikram Mathews, Department of Haematology, Christian Medical College, Vellore 632004, India.
E-mail: vikram@cmcvellore.ac.in

Summary

The standard of care for patients with acute promyelocytic leukaemia (APL) relapsing after front-line treatment with arsenic trioxide (ATO)-based regimens remains to be defined. A total of 67 patients who relapsed after receiving ATO-based up-front therapy and were also salvaged using an ATO-based regimen were evaluated. The median (range) age of patients was 28 (4–54) years. While 63/67 (94%) achieved a second molecular remission (MR) after salvage therapy, three (4·5%) died during salvage therapy. An autologous stem cell transplant (auto-SCT) was offered to all patients who achieved MR, 35/63 (55·6%) opted for auto-SCT the rest were administered an ATO + all-*trans* retinoic acid maintenance regimen. The mean (SD) 5-year Kaplan–Meier estimate of overall survival and event-free survival of those who received auto-SCT *versus* those who did not was 90·3 (5·3)% *versus* 58·6 (10·4)% ($P = 0·004$), and 87·1 (6·0)% *versus* 47·7 (10·3)% ($P = 0·001$) respectively. On multivariate analysis, failure to consolidate MR with an auto-SCT was associated with a significantly increased risk of relapse [hazard ratio (HR) 4·91, 95% confidence interval (CI) 1·56–15·41; $P = 0·006$]. MR induction with ATO-based regimens followed by an auto-SCT in children and young adults with relapsed APL who were treated with front-line ATO-based regimens was associated with excellent long-term survival.

Keywords: relapse acute promyelocytic leukaemia, arsenic trioxide (ATO), post up-front ATO relapse, autologous stem cell transplant.

Introduction

Acute promyelocytic leukaemia (APL) is a relatively rare subtype of acute myelogenous leukaemia (AML) that occurs in 8–15% of all AMLs.[1] Facilitated by an increased understanding of the molecular mechanisms of the disease and resistance, significant advances have been made in the management of APL over the last two decades. There has been a steady transition over the years to a non-myelotoxic therapy consisting of arsenic trioxide (ATO) combined with all-*trans* retinoic acid (ATRA).[2] Optimal treatment of APL requires rapid initiation of ATO and/or ATRA therapy and intensive supportive care for APL-specific complications, including bleeding disorders and APL differentiation syndrome.[1] The widespread clinical employment of this combination of ATO + ATRA has reduced relapse from ~50% to <10% in adult patients with APL over the past two decades.[1]

Challenges remain in the management of patients with high-risk disease at presentation and those with relapsed APL. Salvage therapies with combined ATRA and arsenic compound-based regimens have been shown to induce a complete remission (CR) in 50–80% of patients with refractory or relapsed APL.[1,3] The available data for the management of relapsed APL are mostly in the context of relapse after conventional ATRA plus chemotherapy-based regimens and in this setting the existing data suggests that an autologous stem cell transplant (auto-SCT) in molecular remission (MR) is associated with better survival in comparison to ATO-based maintenance therapy.[1,4–8]

The standard of care for patients with APL relapsing after front-line treatment with ATO-based regimens remains to be defined. Reports on response and survival outcomes in patients who had received ATO as part of their up-front therapy suggest that there is a high incidence of resistance to

First published online 20 November 2020
doi: 10.1111/bjh.17221

ATO and ATRA resulting in inferior response and survival[9–12]; ~25% of relapsed APL treated with up-front ATO were noted to have promyelocytic leukaemia (*PML*) gene mutations, and survival in these patients was reported to be <30%, this is in contrast to experience at most other centres. In our single-centre experience, failure to achieve MR with ATO-based regimens in relapsed APL is very rare.[13] Further, in an international multicentre study that our institution was involved in, evaluating the mutational landscape of newly diagnosed and relapsed APL, it was noted that the occurrence of mutations that resulted in primary or secondary ATO resistance was also extremely rare.[14]

We present a retrospective analysis of our experience in the management of relapse in patients with APL treated up-front with ATO-based regimens.

Patients and methods

All consecutive patients with relapsed APL who received up-front ATO-based therapy, who were diagnosed and treated between January 1998 and December 2015, were included in the analysis. In addition to patients who were initially treated for a diagnosis of APL at our centre, we also included patients who were initially treated at other centres and referred to us at relapse provided adequate details of their initial treatment was available (summarised in Fig 1). Up-front therapy in these patients included single-agent ATO or a combination of ATO and ATRA with or without anthracycline in induction and consolidation administered in a risk-adjusted manner and was followed by ATO-based maintenance therapy. Until December 2014, we used the single-agent ATO-based regimen, the details of the protocol and the early and long-term data have been reported previously by our group.[15,16] From January 2015, a combined ATO and ATRA regimen was used along with anthracylines for high-risk APL (Figure S1 summarises the protocols that were used). Minimal residual disease (MRD) was monitored by qualitative peripheral blood reverse transcription polymerase chain reaction (RT-PCR), as previously reported by us.[17] In brief, RT-PCR analysis for *PML*-retinoic acid receptor alpha (*RARA*)_fusion transcripts with a sensitivity of 10^{-4} was done using Europe Against Cancer programme protocols, the assays were run on an ABI PRISM 7000 DNA Sequence Detection System (Thermo Fisher Scientific, Inc., Waltham, MA, USA). The MRD assay was done once every 3 months for 2 years and up to 5 years for high-risk cases. This retrospective study protocol was reviewed and approved by the Institutional Review Board (IRB 12120; dated 26 June 2019).

Treatment of relapsed APL

Salvage chemotherapy. All relapses were confirmed by morphology and molecular investigations. Only patients who were positive for t(15;17) by karyotyping, fluorescence *in situ* hybridisation (FISH), or RT-PCR were included in this analysis. A diagnostic lumbar puncture was done on all patients at the time of suspected relapse evaluation with adequate blood product cover as required. After the diagnosis of relapse, all patients received induction treatment with the ATO-based regimen, either alone or in combination with ATRA and anthracycline as per the treating physician's discretion.[13,16] ATO was adminsitered, as we always do, at a dose of 0·15 mg/kg for paediatric patients and those whose weight is <45 kg to a maximum dose of 10 mg/day. All adults and those weighing ≥45 kg received a fixed dose of 10 mg/day. Since 2013, patients who had relapsed APL after front-line exposure to ATO were enrolled in an ongoing clinical trial that added bortezomib to the salvage regimen.[18] Salvage therapy at relapse consisted of induction followed 4 weeks later by consolidation, usually with the same agents

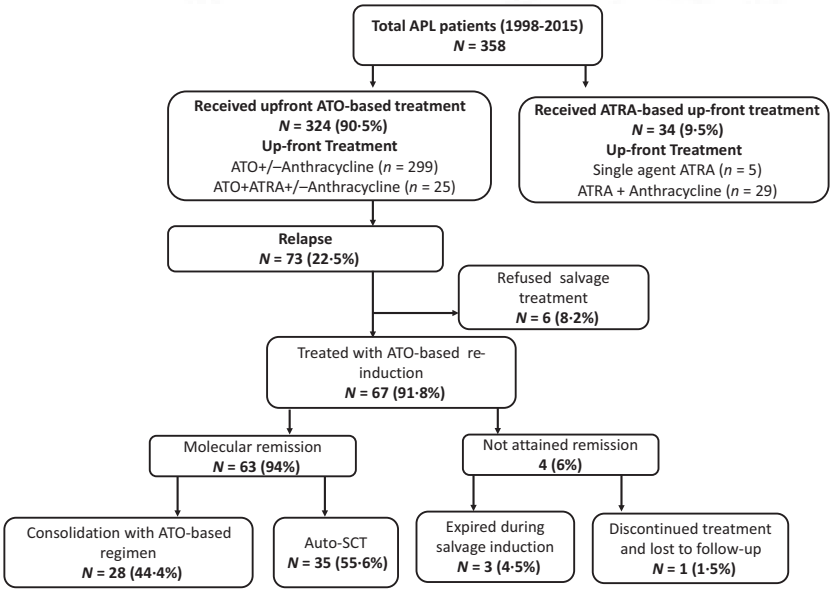

Fig 1. Flow chart of the patients treated. Of the 67 patients with relapsed acute promyelocytic leukaemia (APL) treated with arsenic trioxide (ATO)-based re-induction therapy, 63 (94%) achieved molecular remission; 35 (55·6%) underwent autologous stem cell transplantation (Auto-SCT) and 28 (44·4%) were consolidated with ATO-based maintenance chemotherapy. ATRA, all-*trans*retinoic acid.

used in induction (illustrated in Figure S2), all salvage regimens were centred on the use of ATO in combination with other drugs. Table I summarises the different types of salvage regimens that were utilised. All patients who achieved a MR at the end consolidation were offered an auto-SCT. Methods used for molecular monitoring were as reported previously by us.[17] For those who opted not to undergo an auto-SCT, usually due to financial constraints, a maintenance regimen of ATO- or ATO + ATRA-based regimens at standard doses were administered for 10 days a month for 6 months. Patients who had central nervous system (CNS) involvement at relapse also received triple intrathecal (2 doses/week × 6 doses) concomitant cranial radiotherapy (2.4 Gy), along with the salvage systemic therapy. For those with isolated CNS relapse post-remission induction, they received one more course of systemic consolidation therapy followed by maintenance therapy and they were not offered an auto-SCT.

Table I. Patients' baseline characteristics.

Variable	Value
Age, years, median (range)	28 (4–54)
≤12 years, *n* (%)	13 (19)
Gender, *n* (%)	
Male	44 (65·7)
Female	23 (34·3)
Time to relapse from diagnosis, months, median (range)	19·6 (5·9–128·4)
≤2 years, *n* (%)	41 (61)
>2 years, *n* (%)	26 (39)
Sites of relapse, *n* (%)	
Isolated molecular	1 (1·5)
Isolated CNS	6 (9·0)
Marrow + CNS	13 (19·4)
Isolated marrow	47 (70·1)
Salvage therapy at relapse, *n* (%)	
ATO	5 (7·5)
ATO + anthracycline	1 (1·5)
ATO + bortezomib	3 (4·5)
ATO + ATRA	10 (14·9)
ATO + ATRA + anthracycline	26 (38·8)
ATO + ATRA + anthracycline + bortezomib	22 (32·8)
Response to salvage therapy, *n* (%)	
Molecular remission	63 (94·0)
Discontinued treatment	1 (1·5)
Expired	3 (4·5)
Consolidation at CR2 (*n* = 63), *n* (%)	
Auto-SCT	35 (55·6)
ATO-based maintenance	28 (44·4)
Time to auto-SCT, months, median (range) (*n* = 35)	5·8 (3·8–32·2)
ATO-based maintenance (*n* = 28), *n* (%)	
ATO alone	6 (21·4)
ATO + ATRA	22 (78·6)
Status at last follow-up, *n* (%)	
Auto-SCT Group (*n* = 35)	
Continued in CR2	32 (91·4)
Second relapse and expired	2 (5·7)
in CR3	1 (2·9)
ATO-based maintenance Group (*n* = 28), *n* (%)	
Continued in CR2	17 (60·7)
Second relapse and expired	8 (28·6)
in CR3	3 (10·7)

ATO, arsenic trioxide; ATRA, all-*trans* retinoic acid; auto-SCT, autologous stem cell transplant; CNS, central nervous system; CR, complete remission.

Auto-SCT. All patients scheduled for auto-SCT underwent peripheral blood stem cell (PBSC) collection after chemomobilisation with granulocyte colony-stimulating factor (G-CSF) administered at a dose of 10 μg/kg/day for 4 days. The targeted CD34 stem cell dose was 5×10^6/kg, and a minimum dose of 2×10^6/kg was required to proceed with the transplant. The conditioning regimen consisted of oral busulfan (Bu) at a dose of 16 mg/kg administered over 4 days, followed by cyclophosphamide (Cy) administered intravenously at a dose of 120 mg/kg over 2 days. The mobilised and cryopreserved PBSC product was thawed and rapidly infused a day after the completion of the conditioning regimen. All patients were started on G-CSF (5 μg/kg/day) from day 7 of PBSC infusion and continued until neutrophil engraftment occurred. After auto-SCT, maintenance intrathecal methotrexate was administered once a month for 6 months.

Definition of outcomes

Achievement of CR required that a patient have no clinical evidence of APL, an absolute neutrophil count (ANC) of $>1{\cdot}0 \times 10^9$/l, and unsupported platelet count of $>100 \times 10^9$/l, as well as bone marrow (BM) showing normo-cellularity to moderate hypo-cellularity, with <5% blasts plus pro-myelocytes. An exception was made in patients with an ANC of $<1.0 \times 10^9$/l who achieved an unsupported platelet count of $>100 \times 10^9$/l for >2 weeks with no evidence of residual disease, as defined previously.[4,16] Molecular relapse was defined as two consecutive positive RT-PCRs obtained 1 month apart after achieving MR. Overall survival (OS) and event-free survival (EFS) were defined as the time from initiation of treatment to death due to any cause and the time from the start of treatment to relapse or death due to any reason respectively.

Statistical analysis

For descriptive statistics, the median and range were used as appropriate, while for categorical variables, number and proportion were used. For the association between two categorical variables, a chi-square test/Fisher's exact test was used. The cumulative probability of survival was estimated using the Kaplan–Meier method for OS and EFS, and a log-rank test was used to compare two or more survival curves. The study variables that were significant at <0·05 levels in a univariate analysis alone were included in a multivariate Cox

proportional hazards model. The model assumption was verified using log–log S (t) plots and Global test. A $P < 0{\cdot}05$ was considered as statistically significant. All statistical analyses were performed using the Statistical Package for the Social Sciences (SPSS®), version 21·0 (IBM Corp., Armonk, NY, USA).

Results

Baseline patient characteristics

Out of the total 358 patients diagnosed with APL during the study period, 104 (29%) patients relapsed; 73 (70%) had received up-front ATO-based treatment (70 had received up-front ATO ± anthracycline and three received up-front ATO + ATRA ± anthracyline), six (8·2%) of these patients abandoned further treatment, while the remaining 67 (91·8%) patients who received an ATO-based salvage regimen were included in this analysis (summarised in Fig 1). The six patients who abandoned therapy were all in poor general condition with sepsis at admission and they were discharged at request on supportive measures. None of them received any disease-specific treatment and on telephone follow-up they had all died over the next few days. During this period, there were a total of 1659 patients diagnosed to have AML other than APL at our centre. The median (range) age of the patients with APL and AML was 30 (3–75) and 36 (0–85) years respectively (Figure S3).

The baseline and treatment characteristics of the 67 patients analysed are summarised in Table I. The median (range) age of the patients was 28 (4–54) years, 13 (19%) were in the paediatric age group (≤12 years) and 44 (66%) were males. The median (range) time to relapse was 19·6 (5·9–128·4) months. The majority of patients (61%) relapsed within 2 years of initial diagnosis, 19 (28%) between 2 and 5 years, and four (6%) relapsed after 5 years of diagnosis and one of these (a 9-year-old child) had relapsed after 10 years. Except for one patient who only had evidence of a molecular relapse; the remaining patients had a morphologically documented relapse. The majority of the morphological relapses were in the BM 47 (70·1%). There were six (9%) isolated CNS relapses and 13 (19·4%) having both medullary and CNS disease at the time of diagnosis of relapse.

Post-relapse salvage therapy

The majority of patients (71·6%) received a combination of ATO + ATRA + anthracycline at relapse. One patient opted to discontinue treatment while on induction therapy and was discharged at request against medical advice. Three patients (4·5%) died during induction therapy (two had presented with severe neutropenic sepsis, and one at presentation had an intracranial bleed). The remaining 63 patients (94%) achieved haematological remission, and all these patients achieved MR, as previously defined by us,[17] after completion of their first consolidation therapy.

Auto-SCT

As per standard recommendations, all patients who achieved MR after salvage therapy were offered an auto-SCT; however, only 35 (56%) patients who had financial resources opted for an auto-SCT. The median (range) CD34 cell dose was 8·3 (2·5–24·3) × 10^6/kg; 13/35 (37·1%) required a second-day harvest to achieve target stem cell dose. The entire harvested cell product was infused after completion of the conditioning regimen. All the patients had documented neutrophil and platelet engraftment at a median (range) of 11 (9–13) and 17 (9–33) days respectively.

Although febrile neutropenia was documented in 88·6% of the patients, only six (17%) had documented bacteraemia. None of the patients developed a fungal infection after transplant. Mucositis was documented in 32 (91·4%) patients. Among the 35 patients who underwent auto-SCT, there was no transplant-related mortality. Maintenance intrathecal chemotherapy after auto-SCT (monthly methotrexate × 6 months) starting from 3 months after auto-SCT was offered to all; however, only 28 (80%) received intrathecal therapy as per the planned schedule. Three (8·6%) patients in the auto-SCT group had a second relapse at a median (range) of 10 (4·6–21·9) months after auto-SCT. One of these relapsed patients underwent allogeneic SCT and is in CR3 at the last follow up visit (>10 years from initial diagnosis and 82 months after the second relapse). The other two died of sepsis soon after the second relapse.

ATO-based maintenance therapy

Of the 63 patients in CR2, 28 (44%) opted against auto-SCT due to social and financial constraints and were given ATO-based maintenance therapy for 10 days a month × 6 months. Those with CNS involvement at relapse also received monthly intrathecal methotrexate for 6 months. The majority (78·6%) received an ATO + ATRA-based regimen as maintenance, while six patients received only ATO as maintenance therapy (four of them had isolated CNS relapse and two had isolated BM relapse). The maintenance regimen was administered on an outpatient basis, and the Eastern Cooperative Oncology Group (ECOG) Performance Score during this period was 0/1 in all cases. There was no evidence of significant toxicity that warranted discontinuation of maintenance in any patient, and all patients completed the scheduled maintenance regimen. Of the 28 patients on ATO-based maintenance therapy, 11 (39·3%) had a second relapse at a median (range) of 12·3 (5·4–16·2) months, and one died during follow up (cause unknown). Three of the 11 relapsed patients subsequently underwent auto-SCT after salvage therapy (ATO-based regimen) and achieved a MR and remain in continuous CR3 at the last follow-up visit (at 48, 55 and

67 months from initial diagnosis and 9, 21 and 30 months from the second relapse). Characteristics of patients who received an auto-SCT *versus* those that received maintenance with ATO-based therapy are compared in Table II.

Survival

With an actuarial median (range) follow up of 43 (0–220) months, the mean (SD) 5-year Kaplan–Meier estimates of OS and EFS of the whole cohort (Fig 2A, B) were 73·6 (5·7)% and 67 (6·1)% respectively. The mean (SD) 5-year Kaplan–Meier estimates of OS and EFS of those who underwent auto-SCT were 90·3 (5·3)% and 87·1 (6·0)% respectively. In comparison, similar estimates for those on ATO-based maintenance therapy were significantly lower at a mean (SD) of 58·6 (10·4)% and 47·4 (10·3)% respectively (Fig 2C, D). The survival analysis was repeated using a 'landmark method' from the time of SCT in one group and from starting maintenance therapy in the other, which were not significantly different in the two groups from the date of diagnosis of relapse. There was no significant variation from the survival data presented above nor did it change the data of the multivariate analysis signifcantly (Table SI), ruling out the effect of an immortal time bias in the analysis.

Impact on clinical outcome of additional factors

On analysing the factors impacting EFS using Cox regression analysis, those who received only ATO-based maintenance therapy instead of auto-SCT consolidation after having achieved MR had an increased risk of relapse, both on univariate and multivariate analysis [hazard ratio (HR) 5·73, 95% confidence interval (CI) 1·86–17·66, $P = 0·002$; and HR 4·91, 95% CI 1·56–15·41, P 0·006 respectively) compared to those that received auto-SCT (Table III). On univariate analyses, no significant impact of age, total white blood cell (WBC) count at relapse, site of relapse, early *versus* late relapse (≤2 vs. >2 years) or adult *versus* paediatric patients (≤12 vs. >12 years) on survival were noted on comparing these two groups (Table SII also shows the comparison between those aged ≤18 vs. >18 years). All the events in the group that did not undergo auto-SCT were due to relapses and there were no deaths due to regimen-related toxicity or inadequate medical support, reflecting the inadequacy of the consolidation therapy in these patients.

Mutation analysis was not done routinely as part of our clinical service. However, ~50% of the patients in this cohort had undergone *PML* mutation analysis as part of two previously reported studies,[13,14] and 15% of relapsed patients who were tested were noted to have *PML-B2* domain mutations. None of the mutations that we detected were associated with secondary ATO resistance, all those with mutations achieved MR, and none of our relapsed patients had the *PML-B2* A216V mutation.[14]

Discussion

The standard of care for managing patients with relapsed APL when ATO has been used as up-front therapy has not yet been established. In the recently published European

Table II. Comparison of patient characteristics assigned to auto-SCT *versus* ATO-based chemotherapy.

Variable	Auto-SCT ($n = 35$)	ATO-based chemotherapy ($n = 28$)	P
Age, years, median (range)	28 (4–53)	26 (6–54)	0·961
Gender, *n* (%)			
Male	26 (74·3)	15 (53·6)	0·087
Female	9 (25·7)	13 (46·4)	
Time to relapse from diagnosis, *n* (%)			
≤2 years	19 (54·3)	19 (67·9)	0·274
>2 years	16 (45·7)	9 (32·1)	
Sites of relapse, *n* (%)			
Marrow + CNS	7 (20)	5 (17·9)	0·017
Isolated marrow	27 (77·1)	17 (60·7)	
Isolated CNS	–	6 (21·4)	
Isolated molecular	1 (2·9)	0 (0)	
Salvage therapy at relapse, *n* (%)			
ATO based*	4 (5·7)	14 (28·6)	0·000
ATO + ATRA + anth ± bortezomib†	31 (94·3)	14 (71·4)	
Post-consolidation relapse, *n* (%)			
Yes	4 (11·4)	12 (42·9)	0·004
No	31 (88·6)	16 (57·1)	

anth, anthracycline; ATO, arsenic trioxide; ATRA, all-*trans* retinoic acid; CNS, central nervous system; auto-SCT, autologous stem cell transplant.
*ATO-based chemotherapy included ATO alone = 4, ATO + anthracycline = 1, ATO + bortezomib = 3, ATO + ATRA = 10.
†22 patients received bortezomib along with ATO + ATRA + anthracycline.

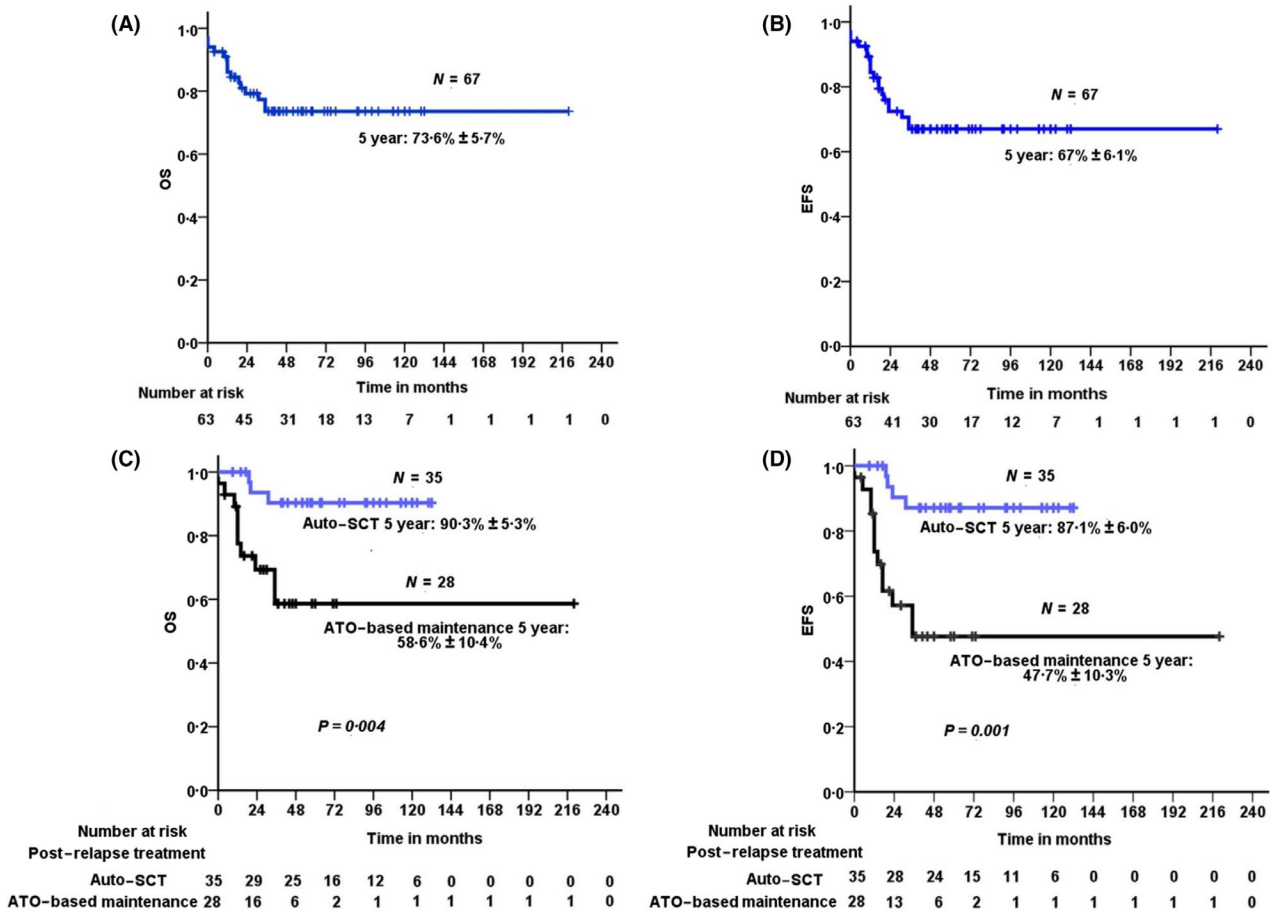

Fig 2. Kaplan–Meier estimate of overall survival (OS) and event-free survival (EFS) of patients with relapsed acute promyelocytic leukaemia treated with up-front arsenic trioxide (ATO)-based regimens. The mean (SD) 5-year (A) OS and (B) EFS for the whole cohort ($N = 67$) was 73·6 (5·7)% and 67 (6·1)% respectively. The mean (SD) 5-year (C) OS and (D) EFS of patients consolidated with autologous stem cell transplant (SCT) ($n = 35$) *versus* ATO-based chemotherapy maintenance ($n = 28$) was 90·3 (5·3)% *versus* 58·6 (10·4)% ($P = 0·004$) and 87·1 (6·0)% *versus* 47 ·4 (10·3)% ($P = 0·001$) respectively. Auto-SCT, autologous stem cell transplantation. [Colour figure can be viewed at wileyonlinelibrary.com]

Table III. Adjusted Cox regression analysis.

	Unadjusted analysis		Adjusted analysis	
Variable	HR (95% CI)	*P*	HR (95% CI)	*P*
Post-relapse treatment				
Auto-SCT	1·00		1·00	
ATO-based chemotherapy	5·73 (1·86–17·66)	0·002	4·91 (1·56–15·41)	0·006
Duration of CR1	0·998 (0·997–0·999)	0·025	0·999 (0·997–1·00)	0·070
Total WBC at relapse	1·01 (0·99–1·03)	0·162	–	–
Age	1·003 (0·97–1·04)	0·853	–	–
Salvage therapy at relapse*				
ATO based	1·00		–	–
ATRA + anth ± bortezomib	0·81 (0·30–2·18)	0·673	–	–

anth, anthracycline; ATO, arsenic trioxide; ATRA, all-*trans* retinoic acid; CNS, central nervous system; auto-SCT, autologous stem cell transplant. *There were 25 patients who received bortezomib (three along with ATO and 22 along with ATO + ATRA + anth) as part of salvage chemotherapy at relapse].

LeukemiaNet (ELN) guidelines, a new recommendation was to consider using an ATRA + chemotherapy-based regimen unless the relapse happened >2 years of CR1[1]; this was based on an expert consensus and not on any large dataset or clinical experience (Level IVC recommendation). We have previously reported that *PML-RARA* mutations that contribute to

secondary ATO resistance were infrequent and that with a rare exception, most patients achieve complete MR with an ATO-based re-induction for relapse and even after multiple relapses.[13,14] Considering the proven efficacy of ATO alone or combination with ATRA/chemotherapy in newly diagnosed APL, in relapsed APL post-ATRA plus chemotherapy regimens and based on our experience in relapsed APL treated with up-front ATO, it would be reasonable to consider ATO-based combination therapies for patients with relapsed APL treated with up-front ATO-based regimens as well.[18–20] Our present data do not suggest that either early or late relapses after up-front ATO-based therapy has an impact on the ability of repeat ATO-based regimens to induce remission or survival in these patients. The theoretical concerns of ATO resistance[10,11] in patients who relapse after up-front ATO-based regimens do not appear to be a relevant concern based on our present data and in communications with other centres in the clinic.

Although auto-SCT is offered to all patients with relapsed APL who achieve CR2 at our centre, due to financial constraints, only a proportion of these patients can afford this approach as previously reported by us[4]; hence, a substantial proportion of patients opt to continue ATO maintenance without an auto-SCT. As a result, we were in a unique position to do this retrospective comparative analysis of patients with relapsed APL who underwent consolidation therapy with either auto-SCT or a combination of ATO and ATRA maintenance therapy.

Our experience, as summarised in the present analysis, demonstrated that ATO-based combination therapy was as effective in re-inducing complete MR in patients with relapsed APL with previous exposure to ATO-based therapy in both the paediatric and the adult population, as well as in early (≤2 years of CR1) and late relapses. However, our present data would suggest that for sustained remission, these patients should be consolidated with an auto-SCT after they have achieved a MR. The clinical outcomes with this approach are associated with excellent results, as reported here [mean (SD) 5-year OS and EFS of 90·3 (5·3)% and 87·1 (6·0)% respectively], and is similar to the observation in patients with relapsed APL treated with up-front ATRA-based regimens.[4–7,20,21] While maintenance with an ATO-based regimen is well tolerated, the risk of subsequent relapse is very high (39·3%) compared to that seen in the group that received an auto-SCT consolidation (8·6%). Additionally, in our experience, cases that relapsed after ATO-based maintenance therapy were difficult to salvage, with a median time to death from such relapses of <1 month.

While the number of paediatric patients in the present study was small, the available data would suggest that the results of salvage with an ATO-based regimen followed by consolidation with auto-SCT are similar to those seen in adults and to several previous reports.[7] As observed in adults, there was no transplant-related mortality in children who underwent auto-SCT. Moreover, with a median (range) follow up of 43 (0–220) months, no long-term complications were observed in these children.

A limitation of the present study is the retrospective nature of the study and the relatively small numbers evaluated in a single institution setting. However, considering the relatively small number of relapses in patients with current treatment strategies of newly diagnosed APL, it is unlikely that a large Phase III trial would ever be done to address this question. The relatively younger population in the present study is not due to selection bias (all consecutive cases were included and accounted for), but a reflection of the population pyramid in low- and middle-income (LMIC) countries, such as ours, with a significantly lower median age of diagnosis of patients with APL and AML in LMIC tertiary centres as illustrated in Figure S2. Extrapolating, these data to older patients would be difficult due to the complete absence of cases aged >55 years in our present analysis.

Cumulatively, our observation is that in relapse after up-front ATO-based therapy in young adults and paediatric patients an ATO-based re-induction is appropriate, well-tolerated and associated with good response rates immaterial of whether the relapse happened early (<2 years) or late. Auto-SCT in this group of patients as consolidation has a clear survival advantage over ATO-based maintenance therapy alone and could be considered the standard of care in this group.

Acknowledgements

This study is supported by a Wellcome Department of Biotechnology (DBT) India Alliance research grant (IA/S/11/2500267) and the DBT-COE grant (BT/COE/34/SP13432/2015), New Delhi, India. Vikram Mathews is supported by the senior fellowship programme of the Wellcome DBT India Alliance (IA/CPHS/18/1/503930). Poonkuzhali Balasubramanian is supported by the senior fellowship programme of the Wellcome DBT India Alliance (IA/CPHS/18/1/503930) New Delhi, India. Uday P. Kulkarni is supported by an early career fellowship programme of the Wellcome DBT India Alliance (IA/CPHE/17/1/503351), New Delhi, India.

Conflict of interest

None.

Author contributions

N.A. Fouzia: performed research, designed study, analysed data and wrote the paper. V. Sharma, U.P. Kulkarni, A. Korula, A.J. Devasia, S.C. Nair, A. Abraham and B. George: performed research and analysed data. S. Ganesan, H.K. Palani, N. Balasundaram, S. David, N. Beryl Janet and P. Balasubramanian: performed research, performed molecular tests, and analysed data. T. Mani and J. Lakshmanan: statistical analysis of data. V. Mathews: performed research,

designed study, clinical data accrual, analysed data, and wrote the paper.

Supporting Information

Additional supporting information may be found online in the Supporting Information section at the end of the article.

Figure S1. Summary of up-front ATO-based regimens that were used.

Figure S2. Salvage chemotherapy protocol for relapsed APL.

Figure S3. Age distribution of patients with AML and APL diagnosed during the period of this study at our centre (1998–2015).

Table SI. Adjusted Cox regression analysis (done using date of SCT and date of starting maintenance therapy).

Table SII. Comparison of patient characteristics based on age ≤18 *versus* >18 years.

References

1. Sanz MA, Fenaux P, Tallman MS, Estey EH, Lowenberg B, Naoe T, et al. Management of acute promyelocytic leukemia: updated recommendations from an expert panel of the European LeukemiaNet. *Blood*. 2019;**133**:1630–43.
2. Lo-Coco F, Di Donato L, Gimema SR; German-Austrian Acute Myeloid Leukemia Study G, Study Alliance L. Targeted therapy alone for acute promyelocytic leukemia. *N Engl J Med*. 2016;**374**:1197–8.
3. Tallman MS. Treatment of relapsed or refractory acute promyelocytic leukemia. *Best Pract Res Clin Haematol*. 2007;**20**:57–65.
4. Thirugnanam R, George B, Chendamarai E, Lakshmi KM, Balasubramanian P, Viswabandya A, et al. Comparison of clinical outcomes of patients with relapsed acute promyelocytic leukemia induced with arsenic trioxide and consolidated with either an autologous stem cell transplant or an arsenic trioxide-based regimen. *Biol Blood Marrow Transplant*. 2009;**15**:1479–84.
5. Ganzel C, Mathews V, Alimoghaddam K, Ghavamzadeh A, Kuk D, Devlin S, et al. Autologous transplant remains the preferred therapy for relapsed APL in CR2. *Bone Marrow Transplant*. 2016;**51**:1180–3.
6. Yanada M, Yano S, Kanamori H, Gotoh M, Emi N, Watakabe K, et al. Autologous hematopoietic cell transplantation for acute promyelocytic leukemia in second complete remission: outcomes before and after the introduction of arsenic trioxide. *Leuk Lymphoma*. 2017;**58**:1061–7.
7. Abla O, Kutny MA, Testi AM, Feusner JH, Creutzig U, Gregory J Jr, et al. Management of relapsed and refractory childhood acute promyelocytic leukaemia: recommendations from an international expert panel. *Br J Haematol*. 2016;**175**:588–601.
8. Holter Chakrabarty JL, Rubinger M, Le-Rademacher J, Wang HL, Grigg A, Selby GB, et al. Autologous is superior to allogeneic hematopoietic cell transplantation for acute promyelocytic leukemia in second complete remission. *Biol Blood Marrow Transplant*. 2014;**20**:1021–5.
9. Lu J, Huang X, Bao L, Jiang H, Zhu H, Jiang B. Treatment outcomes in relapsed acute promyelocytic leukemia patients initially treated with all-trans retinoic acid and arsenic compound-based combined therapies. *Oncol Lett*. 2014;**7**:177–82.
10. Goto E, Tomita A, Hayakawa F, Atsumi A, Kiyoi H, Naoe T. Missense mutations in PML-RARA are critical for the lack of responsiveness to arsenic trioxide treatment. *Blood*. 2011;**118**:1600–9.
11. Zhu HH, Qin YZ, Huang XJ. Resistance to arsenic therapy in acute promyelocytic leukemia. *N Engl J Med*. 2014;**370**:1864–6.
12. Lehmann-Che J, Bally C, de Thé H. Resistance to therapy in acute promyelocytic leukemia. *N Engl J Med*. 2014;**371**:1170–2.
13. Chendamarai E, Ganesan S, Alex AA, Kamath V, Nair SC, Nellickal AJ, et al. Comparison of newly diagnosed and relapsed patients with acute promyelocytic leukemia treated with arsenic trioxide: insight into mechanisms of resistance. *PLoS One*. 2015;**10**:e0121912.
14. Madan V, Shyamsunder P, Han L, Mayakonda A, Nagata Y, Sundaresan J, et al. Comprehensive mutational analysis of primary and relapse acute promyelocytic leukemia. *Leukemia*. 2016;**30**:1672–81.
15. Mathews V, George B, Lakshmi KM, Viswabandya A, Bajel A, Balasubramanian P, et al. Single-agent arsenic trioxide in the treatment of newly diagnosed acute promyelocytic leukemia: durable remissions with minimal toxicity. *Blood*. 2006;**107**:2627–32.
16. Mathews V, George B, Chendamarai E, Lakshmi KM, Desire S, Balasubramanian P, et al. Single-agent arsenic trioxide in the treatment of newly diagnosed acute promyelocytic leukemia: long-term follow-up data. *J Clin Oncol*. 2010;**28**:3866–71.
17. Chendamarai E, Balasubramanian P, George B, Viswabandya A, Abraham A, Ahmed R, et al. Role of minimal residual disease monitoring in acute promyelocytic leukemia treated with arsenic trioxide in frontline therapy. *Blood*. 2012;**119**:3413–9.
18. Kulkarni U, Ganesan S, Alex AA, Palani H, David S, Balasundaram N, et al. A phase II study evaluating the role of bortezomib in the management of relapsed acute promyelocytic leukemia treated upfront with arsenic trioxide. *Cancer Med*. 2020;**9**:2603–10.
19. Soignet SL, Frankel SR, Douer D, Tallman MS, Kantarjian H, Calleja E, et al. United States multicenter study of arsenic trioxide in relapsed acute promyelocytic leukemia. *J Clin Oncol*. 2001;**19**:3852–60.
20. Yanada M, Tsuzuki M, Fujita H, Fujimaki K, Fujisawa S, Sunami K, et al. Phase 2 study of arsenic trioxide followed by autologous hematopoietic cell transplantation for relapsed acute promyelocytic leukemia. *Blood*. 2016;**121**:3095–102.
21. Pemmaraju N, Tanaka MF, Ravandi F, Lin H, Baladandayuthapani V, Rondon G, et al. Outcomes in patients with relapsed or refractory acute promyelocytic leukemia treated with or without autologous or allogeneic hematopoietic stem cell transplantation. *Clin Lymphoma Myeloma Leuk*. 2019;**13**:485–92.

Received: 29 August 2019 | Revised: 2 January 2020 | Accepted: 14 January 2020

DOI: 10.1002/cam4.2883

ORIGINAL RESEARCH

Cancer Medicine Open Access WILEY

A phase II study evaluating the role of bortezomib in the management of relapsed acute promyelocytic leukemia treated upfront with arsenic trioxide

Uday Kulkarni[1] | Saravanan Ganesan[1] | Ansu Abu Alex[1] | Hamenth Palani[1] | Sachin David[1] | Nithya Balasundaram[1] | Arvind Venkatraman[1] | Mani Thenmozhi[2] | Lakshmanan Jeyaseelan[2] | Anu Korula[1] | Anup Devasia[1] | Aby Abraham[1] | Nancy Beryl Janet[1] | Poonkuzhali Balasubramanian[1] | Biju George[1] | Vikram Mathews[1]

[1]Department of Haematology, Christian Medical College, Vellore, India

[2]Department of Biostatistics, Christian Medical College, Vellore, India

Correspondence
Vikram Mathews, Department of Haematology, Christian Medical College, Vellore 632004, India.
Email: vikram@cmcvellore.ac.in

Funding information
The Wellcome Trust DBT India Alliance, Grant/Award Number: IA/CPHE/17/1/503351, IA/S/11/2500267 and IA/S/15/1/501842; Department of Biotechnology , Ministry of Science and Technology, Grant/Award Number: BT/COE/34/SP13432/2015

Abstract

The standard-of-care for patients with acute promyelocytic leukemia (APL) relapsing after upfront arsenic trioxide (ATO) therapy is not defined. The present study was undertaken to evaluate the safety of addition of bortezomib to ATO in the treatment of relapsed APL based on our previously reported preclinical data demonstrating synergy between these agents. This was an open label, nonrandomized, phase II, single-center study. We enrolled 22 consecutive patients with relapsed APL. The median age was 26.5 years (interquartile range 17.5 to 41.5). The median time from initial diagnosis to relapse was 23.1 months (interquartile range 15.6 to 43.8). All patients achieved hematological remission at a median time of 45 days (range 40-63). Nineteen patients were in molecular remission at the end of induction. Grade 3 adverse events occurred in eight instances with one patient requiring discontinuation of therapy for grade 3 neuropathy. Twelve (54.5%) patients underwent autologous transplantation (auto-SCT) in molecular remission while the rest opted for maintenance therapy. The median follow-up was 48 months (range 28-56.3). Of the patients undergoing auto-SCT, all except one was alive and relapse free at last follow-up. Of the patients who opted for maintenance therapy, three developed a second relapse. For treatment of APL relapsing after upfront ATO therapy, addition of bortezomib to a standard ATO-based salvage regimen is safe and effective. This trial was registered at www.clinicaltrials.gov as NCT01950611.

KEYWORDS

arsenic trioxide, PML mutations, proteasome inhibitor, relapsed acute promyelocytic leukemia

1 | INTRODUCTION

Acute promyelocytic leukemia (APL) is a subtype of acute myeloid leukemia (AML) with distinct molecular and clinical features and characterized by the presence of a reciprocal translocation involving a portion of the retinoic acid receptor alpha gene (RARα) on chromosome 17 and a variable portion of a partner gene, which in 95% of cases is the PML gene on chromosome 15; t(15;17)(q22;q21).[1] This reciprocal translocation results in the production of a fusion onco-protein PML-RARA which is central to initiating and maintaining this subtype of leukemia.[2] Significant advances in the management of APL have resulted in this subset of leukemia having the highest cure rates.[3] Additionally, these advances have been brought about by the use of differentiating agents and a nonmyelotoxic approach.[4-6] The combination of all-trans retinoic acid (ATRA) and arsenic trioxide (ATO), a nonmyelotoxic approach, has been established as the standard of care based on a phase III randomized control trial for patients with low and intermediate risk APL that accounts for more than two-thirds of all APL patients.[4,5,7] The current understanding of the mechanism of action of ATO and its efficacy in clearing the leukemia initiating compartment is based on its ability to clear the PML-RARA onco-protein which in turn is dependent on an intact functional proteasome and proteasomal degradation of this onco-protein.[8,9] For high-risk disease, most protocols that are currently used would add an anthracycline or a combination chemotherapy schedule in induction and consolidation in addition to ATRA with or without ATO.[5,10-14] Despite these advances disease relapse remains a challenge especially in high-risk APL and about 10%-20% patients with APL treated upfront with ATRA and chemotherapy will relapse.[15] The current standard of care for patients who do relapse is to reinduce molecular remission with ATO either alone or in combination with other agents, such as gemtuzumab which is effective in this setting, and to follow this up with an autologous stem cell transplantation (auto-SCT) in second molecular remission.[16] It is anticipated that with this approach one could potentially cure 60%-70% of these patients.[16,17] However, it must be noted and recognized that the available data with management of relapsed APL are from the era where ATO was not used as upfront therapy. With ATO increasingly being used as part of upfront therapy the optimal approach to management of patients who have already been exposed to ATO has not been described. Available data on response and survival outcomes in patients who had received ATO as part of upfront therapy suggests that resistance to ATO can occur resulting in inferior response and inferior survival than seen in patients who had not received ATO as part of upfront therapy.[18,19] This has been attributed to mutations in the oncogenic PML-RARA gene following treatment with ATO which have been reported to occur in one-third of patients with relapsed APL and the clinical outcomes in this subset with mutations is poor.[19]

We had previously reported a comprehensive evaluation comparing newly diagnosed and relapsed APL patients who had received upfront treatment with ATO, we noted that reinduction with ATO at relapse is effective; however, in spite of achieving molecular remission in the majority of patients the risk of subsequent relapse is high especially in the absence of consolidation with autologous transplantation.[16,17] We also demonstrated that there was significant microenvironment-mediated drug resistance (EM-DR) to ATO, which is predominantly mediated by the upregulation of the NF- κB pathway and is more prominent in relapsed APL.[20] This EM-DR to ATO could be overcome by the use of proteasome inhibitors in-vitro and in a preclinical mouse model.[21] In contrast to expectations, based on the known mechanism of action of ATO, we were able to demonstrate that malignant promyelocytes were exquisitely sensitive to bortezomib a known proteasome inhibitor and demonstrated significant synergy on combining it with ATO both in an in-vitro system and in a mouse model of APL.[21] We further clarified the mechanism of PML-RARα onco-protein degradation on combining these two agents by a proteasome-independent pathway.[21] Based on our promising preclinical data we hypothesized that the combination of ATO and bortezomib would be clinically effective at APL relapse and could potentially obviate the need of an auto-SCT.

2 | MATERIALS AND METHODS

2.1 | Study design and patient eligibility

This was an open label, nonrandomized, phase II, single-center interventional trial with single group assignment to bortezomib in addition to conventional therapy. The trial was approved by the institutional ethics committee (IRB 8225 27/02/13) and was registered in the public domain (Clinical Trials.gov: NCT01950611 and CTRI No: REF/2014/08/007490). Any patient with hematological relapse of PML-RARA positive APL was eligible to be enrolled in this study. The detailed inclusion and exclusion criteria are provided in the supplementary methods. Some of the key exclusion criteria were intracranial bleeding at presentation, Eastern Co-operative Oncology Group (ECOG) performance score ≥ 3, severe uncontrolled infection, cardiac dysfunction and secondary APL. All patients were enrolled after getting written and informed IRB approved consent or assent form as appropriate.

2.2 | Study protocol

The treatment schema is summarized in Figure 1. Briefly, during induction therapy, enrolled patients received ATO 10 mg/day IV (or 0.15 mg/kg for patients weighing less than 45 kg) and ATRA 45 mg/m^2/day PO for a minimum duration of 42 days and a maximum duration of 60 days. Mitoxantrone 10mg/m^2/day IV for 2 days was given on the first 2 days of induction. Additionally, patients received two doses of bortezomib 1.4 mg/m^2/dose SC on days 2 and 5. Patients with central nervous system (CNS) involvement received twice weekly triple intrathecal injections (methotrexate 12.5 mg, hydrocortisone 50 mg, and cytosine 40 mg) till the cerebrospinal fluid cytology was negative along with 24 Gray of cranial radiation therapy. Consolidation therapy consisted of ATO and ATRA for 4 weeks along with two doses of bortezomib at the same dosages as used in induction. Patients who were in molecular remission postconsolidation were offered an auto-SCT. Patients in molecular remission who were unwilling for an auto-SCT were offered maintenance therapy with ATO and ATRA given for 10 days in a month for 6 months. These patients also received a dose of bortezomib during each month of maintenance. Post auto-SCT or during maintenance for those who did not undergo an auto-SCT, intrathecal methotrexate was administered once a month for 6 months.

2.3 | Quantification of PML-RARA copy numbers by RT-qPCR

The dynamics of molecular remission achieved was evaluated by analyzing the PML-RARA copy numbers using RT-qPCR. Peripheral blood was collected from patients every week till the end of induction therapy as described above. Quantification of the *PML-RARA* transcripts was done using Europe against Cancer (EAC) program protocols.[22] The RT-qPCR sensitivity was assessed in-house using methodology as reported previously.[23]

2.4 | PML-RARA sequencing by Illumina RNA fusion kit

Total RNA extracted from malignant promyelocytes was used to selectively enrich for 507 genes that have been reported to be associated with gene fusions in cancer using Illumina Trusight RNA Fusion Panel kit. The RNA was fragmented using divalent cations under high temperature and cDNA was generated from the cleaved RNA fragments using random priming during first and second strand synthesis. Then, sequencing adapters were ligated to the resulting double stranded cDNA fragments. The coding regions of expressed cancer associated genes were captured from this library using sequence specific probes to create the final library. Streptavidin magnetic beads were used to capture probes

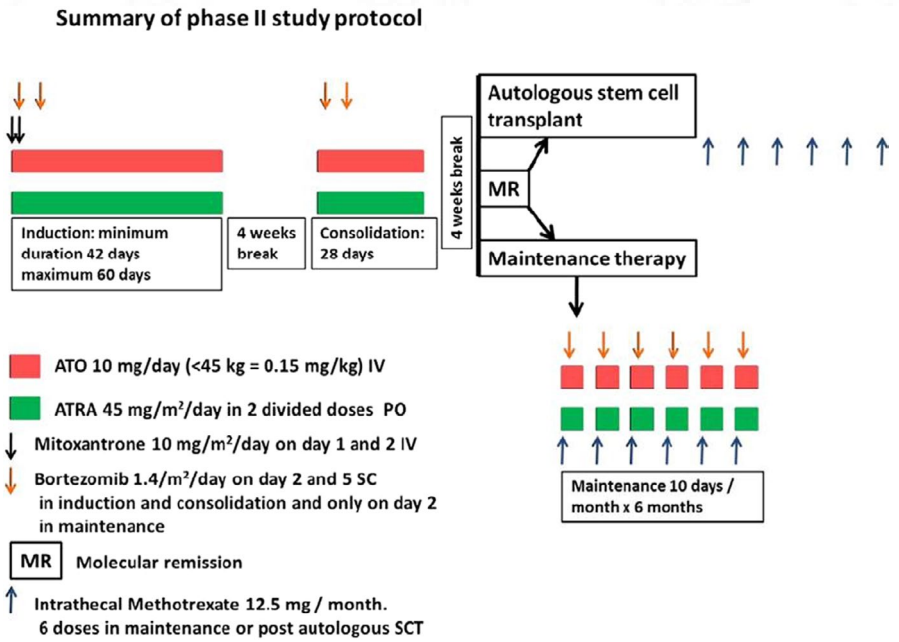

FIGURE 1 Overview of treatment schedule. ATO: Arsenic trioxide, ATRA: All trans-retinoic acid (ATRA). During induction therapy, enrolled patients received ATO and ATRA for a minimum duration of 42 d and a maximum duration of 60 d. Mitoxantrone for 2 d was given on the first 2 d of induction. Patients also received two doses of bortezomib 1.4 mg/m^2/dose SC on days 2 and 5. Consolidation therapy consisted of ATO and ATRA for 4 wks along with 2 doses of bortezomib. Patients who were in molecular remission post consolidation were offered SCT. Patients in molecular remission who due to various reasons could not proceed to a SCT were offered maintenance therapy with ATO and ATRA given for 10 d in a month for 6 mo. These patients also received one dose of bortezomib during each month of maintenance. Post auto-SCT or with each maintenance cycle, intrathecal methotrexate was administered once a month for 6 mo

hybridized to the targeted regions. Two rounds of hybridization ensure the high specificity of the captured regions of interest. The enriched libraries were then sequenced on the Illumina platform Hiseq4000 by 2x100 bp paired-end sequencing. Bio-informatics analysis was performed in collaboration with Medgenome Labs Pvt Ltd, Bengaluru, India. The details of bioinformatics analysis are provided in the supplementary methods section.

2.5 | Outcome variables

The primary outcome measure was safety graded according to the National Cancer Institute Common Terminology Criteria for Adverse Events (NCI CTCAE) version 4.0. The secondary outcome measure was efficacy measured as the proportion of patients achieving molecular remission at the end of induction therapy, event-free (EFS) and overall survival (OS) at follow-up. Molecular remission was defined as a negative qualitative RT-PCR reading with a sensitivity of 10^{-4}. For EFS, an event was defined as death or disease relapse at any time after enrolment. For OS, an event was defined as death due to any cause after enrolment.

2.6 | Statistical analysis and comparison with historical cohort

A comparison was done with an historical cohort of patients who were treated for relapsed APL with a combination therapy similar to the study with the exception of bortezomib. For baseline comparison between groups, Chi-square test or Fisher's exact test was used for nominal data, Mann-Whitney U test was used for ordinal and numerical data. For time to event analysis, the comparison of two cohorts was done using the Kaplan-Meier survival curve with logrank test (unadjusted analysis) for overall survival and event free survival. The variables that were significant at less than 0.05 level in logrank test were considered as potential variables for multivariable Cox-proportional hazards model (adjusted analysis). The model assumption was evaluated using log-log (S(t)) vs log time and global test. A value of $P < .05$ was considered as statistically significant. Statistical analysis was performed using SPSS version 21.0.

3 | RESULTS

3.1 | Patient characteristics

Between September 2013 and January 2017, 22 patients met the eligibility criteria and were enrolled in this study. The median age was 26.5 years (interquartile range 17.5-41.5). Fourteen (63.6%) were males. The time from initial diagnosis to relapse was 23.1 months (interquartile range 15.6-43.8). The *PML-RARA* transcript was bcr1 in 12 patients (54.5%), bcr2 in 1 patient (4.5%), and bcr3 in 9 patients (40.9%). Fourteen patients (63.6%) were clinically asymptomatic at relapse while others had symptoms like bleeding (four patients), headache (one patient), fever (one patient), and fatigue (two patients). Seven patients (31.8%) had concomitant CNS involvement. The summary of the baseline clinical and laboratory characteristics is provided in Table 1 while the Table S1 provides the data for individual patients.

3.2 | Treatment response

All patients enrolled in the study achieved hematological remission at the end of induction therapy. The median time to hematological remission was 45 days (range 40-63). Nineteen patients (90.5%; N = 21. one patient RT-PCR not sent postinduction) also achieved molecular remission postinduction therapy. All patients achieved molecular remission postconsolidation therapy. Of the 22 patients, 12 opted for autologous transplantation while the rest opted for maintenance therapy. Six patients (27.3%) did not require hospital admission during reinduction therapy. There was no induction death among the patients enrolled in the study.

3.3 | Safety

Table S2 summarizes the toxicity encountered in the patients on the present study. Grade 3 toxicity was seen in eight instances. Of these, one was motor and sensory neuropathy which required discontinuation of bortezomib. Others were all transient and were clinically managed with the standard of care along with temporary discontinuation of drugs in some cases (1—severe headache resolved after temporary discontinuation of ATRA, 1—eight episodes of loose stools in 1 day postbortezomib which did not recur subsequently, 2—febrile neutropenia requiring hospital admission, 1—oral ulcers causing dysphagia requiring hospital admission, 1—maculopapular rash over involving > 30% of the body surface area which resolved spontaneously, 1—severe backache secondary to bone marrow necrosis which resolved with steroids). Remaining toxicities were grade 1 or 2 and resolved completely with symptomatic management.

3.4 | Survival analysis

The 2-year overall survival and event-free survival were 95 ± 4.9% and 80.2 ± 8.9%, respectively (Figure 2A,B). At a

TABLE 1 Comparison of the clinical and laboratory parameters between the study cohort and the historical cohort

Characteristic	Bortezomib cohort (n = 22) N (%) Mean ± SD/ Median(IQR)	Historical cohort (n = 29) N (%) Mean ± SD/ Median(IQR)	*P* Value
Upfront therapy			
ATO based	21 (95.5)	24 (82.8)	0.218
ATRA based	1 (4.5)	5 (17.2)	
Use of anthracycline in upfront therapy	10 (45.5)	13 (44.8)	0.964
Time from initial diagnosis to relapse (in months)	23.1 (15.6 to 43.8)	20.6 (14.3 to 33.2)	0.481
Age (in years)	26.5 (17.5 to 41.5)	26 (8.0 to 43.0)	0.402
Gender: Male	14 (63.64)	22 (75.9)	0.343
Patients with promyelocytes and blasts in peripheral blood	6 (27.3)	21 (75.0)	**0.001**
Hemoglobin (g/dL)	12.7 (10.3 to 13.7)	11.6 (10.2 to 13.6)	0.430
White blood cell count (in 10^9/L)	2.65 (1.63 to 6.59)	3.45 (1.43 to 13.13)	0.417
Platelet count (in 10^9/L)	112 (37.8 to 154.3)	49 (19.5 to 76.8)	**0.010**
Serum creatinine (in mg/dL)	0.75 (0.65 to 0.85)	0.82 (0.64 to 1.00)	0.183
Prothrombin time (in s)	11.8 (11.15 to 13.75)	13.9 (13.0 to 15.5)	**0.002**
Activated partial thromboplastin time (in s)	31.7 (28.5 to 32.7)	30.0 (26.1 to 34.8)	0.441
Plasma fibrinogen (in mg%)	200.7 (102.5 to 249.5)	117.45 (82.4 to 158.5)	0.076
Percentage of bone marrow blasts and promyelocytes	64.0 (49.0 to 77.5)	75.5 (67.5 to 90.5)	0.059
Major bleeding at presentation	2 (9.1)	2 (7.4)	1.000
Major thrombosis at presentation	0 (0)	3 (11.5)	0.242
Transfusions during induction			
Packed red cell concentrates	1 (0 to 4)	1.5 (0 to 2.3)	0.691
Fresh frozen plasma	0 (0 to 5)	4 (1.5 to 16.3)	**0.015**
Cryoprecipitate	0 (0 to 8.5)	5.5 (0 to 9.0)	0.332
Platelet rich concentrate	10 (0 to 29.3)	11 (4.3 to 26.5)	0.690
Patients with molecular remission post induction	19 (90.5)	16 (69.6)	0.137
Duration of follow-up (in months)	48 (28 to 56.3)	69 (7 to 113.5)	0.361

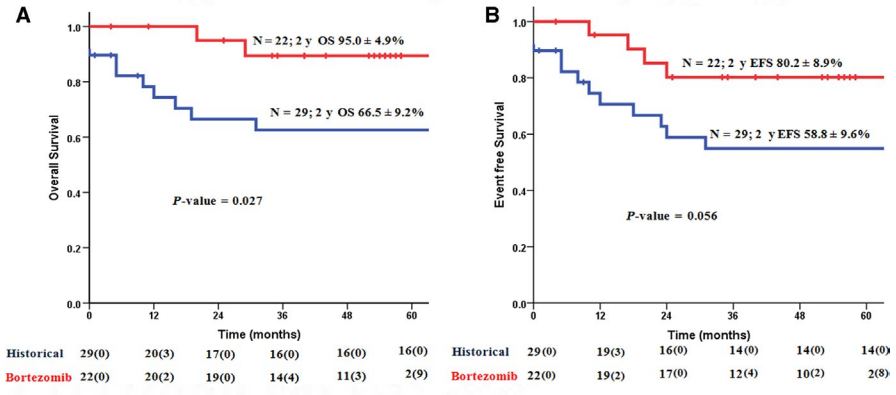

FIGURE 2 Overall survival (A) and event free survival (B) of the study cohort compared to a historical cohort

median follow-up of 48 months (range 28-56.3), 2 (9.1%) patients died (1—disease progression, 1—acute demyelination while in remission) while there were three (13.6%) relapses. All the three patients who relapsed had opted for maintenance therapy postconsolidation. All of them received salvage treatment (retreatment with the induction therapy of the same protocol). Of these, one patient died of disease progression. Of the remaining two patients, one achieved molecular remission after the second salvage treatment while another required additional gemtuzumab ogazamicin to achieve molecular remission. Subsequently both underwent autologous transplantation and are alive at last follow-up. Figure 2A,B show the overall and event-free survival of the study cohort alongside that of the historical cohort.

3.5 | Comparison with the historical cohort

Table 1 and Tables S3-S5 depict the comparison of the clinical and laboratory characteristics and the treatment outcomes between the study cohort and the historical cohort.

3.6 | PML-RARA mutation analysis and dynamics of molecular response

Out of 20 samples analyzed, we identified eight patients carrying mutations in either PML or RARA or both regions. Figure 3 shows the mutations identified in the PML-RARA fusion gene in patients in the study cohort. Of these mutations, we observed that the reported ATO resistance causing mutations[19] in the hot spot of the B2 domain of PML gene such as S214L and L217F as well as a novel L218F mutation (Figure 3) were identified in four patients. Similarly, we noted mutation in ligand binding domain of the RARA gene which may cause resistance to ATRA (Figure 3). However, none of these mutations were associated with secondary ATO resistance in these patients. Based on weekly RT-qPCR, we noted that most patients achieved complete molecular remission by week 4 of induction therapy as shown in Figure S1.

4 | DISCUSSION

The standard of care for the treatment of patients with acute promyelocytic leukemia relapsing after frontline treatment with arsenic trioxide is yet to be defined. In patients who have been previously treated with ATO, at relapse, about one-third harbor mutations in the PML-RARA fusion gene and the clinical outcomes in this subset are poor.[19] Besides the mutations in PML-RARA fusion gene, microenvironment-mediated drug resistance (EM-DR) to ATO mediated by the upregulation of the NF-κB pathway also contributes to drug resistance in relapsed APL.[20] Recently, in a mouse model experiment, we showed that this EM-DR could be overcome by proteasome inhibition.[21]

In the present phase II clinical trial, we showed that addition of bortezomib to the combination of ATO, ATRA, and anthracycline is safe. Although there were eight instances of grade 3 adverse events, only one required discontinuation of bortezomib. Thus the treatment regimen was well tolerated with a manageable toxicity profile. We also noted that five patients had mutations in the PML-RARA fusion gene (Figure 3). Despite this, we noted that with the addition of bortezomib, all patients were in molecular remission post-consolidation therapy. The RT-qPCR data (Figure S1) showed that the molecular response was attained by 5th week of induction therapy. As compared to the historical cohort treated without bortezomib, the overall survival of the study cohort was significantly better (Figure 2). All three relapses in the study cohort occurred in patients who did not opt for autologous transplantation. One patient died in remission more than a year after treatment was completed at a secondary hospital and the possibility of an acute demyelinating disease was considered based on the clinical assessment of the treating physician, unfortunately this was not corroborated with a tissue biopsy.

An inherent limitation of the present phase II nonrandomized single arm study was that the historical controls might not have been prognostically comparable to the accrued patients. On comparison of the baseline data of the study cohort with that of the historical cohort, we noted that the historical cohort had greater proportion of patients with peripheral blood blasts or promyelocytes. The patients in the historical cohort also had lower platelet counts and elevated prothrombin time at diagnosis of relapse as compared to the study cohort. Hence they also required more fresh frozen plasma transfusions than the study cohort. Another limitation of the study was that we did not have the mutation and RT-qPCR data for the historical cohort for comparison.

Despite these limitations, the present study shows that the addition of bortezomib to a combination of ATO,

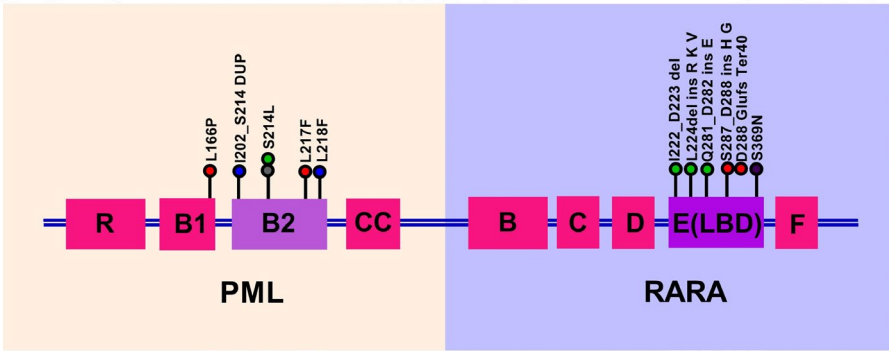

FIGURE 3 Illustration of mutations identified in PML-RARA gene using Illumina Trusight RNA Fusion Panel kit. Of the 20 samples analysed, we identified 5 patients carrying mutations in either PML or RARA or both regions. ATO resistance causing mutations such as S214L, L217F and L218F in the B2 domain of PML gene were seen in 4 patients. (Each colour represents one patient)

ATRA, and anthracycline is safe and effective. The efficacy needs to be validated in a randomized clinical trial, with an optimized dose and schedule of bortezomib (in the present study dosing of bortezomib was limited to two doses since the main end point was to address safety). If efficacy and safety are proven unequivocally, after optimized dose and scheduling, it may obviate the need for an autologous transplant in second molecular remission. This would be of relevance to patients with relapsed APL especially in developing countries.

ACKNOWLEDGMENT

This study is supported by a Wellcome DBT India Alliance research grant (IA/S/11/2500267). VM is supported by senior fellowship program of Wellcome DBT India Alliance (IA/S/11/2500267), New Delhi, India. UK is supported by an early career fellowship program of Wellcome DBT India Alliance (IA/CPHE/17/1/503351), New Delhi, India. PB is supported by a senior fellowship program of Wellcome DBT India Alliance (IA/S/15/1/501842). There was no role of the funding source in the study design; in the collection, analysis, and interpretation of data; in the writing of the report; and in the decision to submit the paper for publication.

AUTHOR CONTRIBUTION

UK performed research, clinical data accrual, analyzed data, and wrote paper. SG performed research, performed molecular tests, analyzed data, and wrote paper. AAA, HP, SD, NB, and AV performed research, performed molecular tests, flow cytometry tests, and analyzed data. MT and LJ performed statistical analysis. AK, AD, and AA performed research, clinical data accrual, and analysis. NBJ performed research and performed cytogenetic tests. BG performed research, clinical data accrual, and analysis. PB performed research, performed molecular tests, and analyzed data. VM performed research, designed study, clinical data accrual, analyzed data, and wrote paper.

ORCID

Uday Kulkarni https://orcid.org/0000-0003-2230-2424
Saravanan Ganesan https://orcid.org/0000-0002-5773-1715
Poonkuzhali Balasubramanian https://orcid.org/0000-0002-9443-439X
Vikram Mathews https://orcid.org/0000-0001-9417-2353

REFERENCES

1. Sirulnik A, Melnick A, Zelent A, Licht JD. Molecular pathogenesis of acute promyelocytic leukaemia and APL variants. *Best Pract Res Clin Haematol*. 2003;16(3):387-408.
2. Arber DA, Orazi A, Hasserjian R, et al. The 2016 revision to the World Health Organization classification of myeloid neoplasms and acute leukemia. *Blood*. 2016;127(20):2391-2405.
3. Avvisati G, Lo Coco F, Mandelli F. Acute promyelocytic leukemia: clinical and morphologic features and prognostic factors. *Semin Hematol*. 2001;38(1):4-12.
4. Lo-Coco F, Avvisati G, Vignetti M, et al. Retinoic acid and arsenic trioxide for acute promyelocytic leukemia. *N Engl J Med*. 2013;369(2):111-121.
5. Burnett AK, Russell NH, Hills RK, et al. Arsenic trioxide and all-trans retinoic acid treatment for acute promyelocytic leukaemia in all risk groups (AML17): results of a randomised, controlled, phase 3 trial. *Lancet Oncol*. 2015;16(13):1295-1305.
6. Abaza Y, Kantarjian H, Garcia-Manero G, et al. Long-term outcome of acute promyelocytic leukemia treated with all-trans-retinoic acid, arsenic trioxide, and gemtuzumab. *Blood*. 2017;129(10):1275-1283.
7. Sanz MA, Fenaux P, Tallman MS, et al. Management of acute promyelocytic leukemia: updated recommendations from an expert panel of the European LeukemiaNet. *Blood*. 2019;133(15):1630-1643.
8. Nasr R, Guillemin M-C, Ferhi O, et al. Eradication of acute promyelocytic leukemia-initiating cells through PML-RARA degradation. *Nat Med*. 2008;14(12):1333-1342.
9. Lallemand-Breitenbach V, Jeanne M, Benhenda S, et al. Arsenic degrades PML or PML-RARalpha through a SUMO-triggered RNF4/ubiquitin-mediated pathway. *Nat Cell Biol*. 2008;10(5):547-555.
10. Avvisati G, Lo-Coco F, Paoloni FP, et al. AIDA 0493 protocol for newly diagnosed acute promyelocytic leukemia: very long-term results and role of maintenance. *Blood*. 2011;117(18):4716-4725.
11. Iland HJ, Collins M, Bradstock K, et al. Use of arsenic trioxide in remission induction and consolidation therapy for acute promyelocytic leukaemia in the Australasian Leukaemia and Lymphoma Group (ALLG) APML4 study: a non-randomised phase 2 trial. *Lancet Haematol*. 2015;2(9):e357-366.
12. Sanz MA, Montesinos P, Rayón C, et al. Risk-adapted treatment of acute promyelocytic leukemia based on all-trans retinoic acid and anthracycline with addition of cytarabine in consolidation therapy for high-risk patients: further improvements in treatment outcome. *Blood*. 2016;115(25):5137-5146.
13. Lo-Coco F, Avvisati G, Vignetti M, et al. Front-line treatment of acute promyelocytic leukemia with AIDA induction followed by risk-adapted consolidation for adults younger than 61 years: results of the AIDA-2000 trial of the GIMEMA Group. *Blood*. 2010;116(17):3171-3179.
14. Ravandi F, Estey E, Jones D, et al. Effective treatment of acute promyelocytic leukemia with all-trans-retinoic acid, arsenic trioxide, and gemtuzumab ozogamicin. *J Clin Oncol*. 2009;27(4):504-510.
15. Adès L, Sanz MA, Chevret S, et al. Treatment of newly diagnosed acute promyelocytic leukemia (APL): a comparison of French-Belgian-Swiss and PETHEMA results. *Blood*. 2008;111(3):1078-1084.
16. Ganzel C, Mathews V, Alimoghaddam K, et al. Autologous transplant remains the preferred therapy for relapsed APL in CR2. *Bone Marrow Transplant*. 2016;51(9):1180-1183.
17. Thirugnanam R, George B, Chendamarai E, et al. Comparison of clinical outcomes of patients with relapsed acute promyelocytic leukemia induced with arsenic trioxide and consolidated with either an autologous stem cell transplant or an arsenic trioxide-based regimen. *Biol Blood Marrow Transplant*. 2009;15(11):1479-1484.

18. Liu J, Zhu HH, Jiang H, Jiang Q, Huang XJ. Varying responses of PML-RARA with different genetic mutations to arsenic trioxide. *Blood*. 2016;127(2):243-250.
19. Zhu HH, Qin YZ, Huang XJ. Resistance to arsenic therapy in acute promyelocytic leukemia. *N Engl J Med*. 2014;370(19):1864-1866.
20. Chendamarai E, Ganesan S, Alex AA, et al. Comparison of newly diagnosed and relapsed patients with acute promyelocytic leukemia treated with arsenic trioxide: insight into mechanisms of resistance. *PLoS ONE*. 2015;10(3):e0121912.
21. Ganesan S, Alex AA, Chendamarai E, et al. Rationale and efficacy of proteasome inhibitor combined with arsenic trioxide in the treatment of acute promyelocytic leukemia. *Leukemia*. 2016;30(11):2169-2178.
22. Gabert J, Beillard E, van der Velden VHJ, et al. Standardization and quality control studies of 'real-time' quantitative reverse transcriptase polymerase chain reaction of fusion gene transcripts for residual disease detection in leukemia - a Europe Against Cancer program. *Leukemia*. 2003;17(12):2318-2357.
23. Chendamarai E, Balasubramanian P, George B, et al. Role of minimal residual disease monitoring in acute promyelocytic leukemia treated with arsenic trioxide in frontline therapy. *Blood*. 2012;119(15):3413-3419.

SUPPORTING INFORMATION

Additional supporting information may be found online in the Supporting Information section.

How to cite this article: Kulkarni U, Ganesan S, Alex AA, et al. A phase II study evaluating the role of bortezomib in the management of relapsed acute promyelocytic leukemia treated upfront with arsenic trioxide. *Cancer Med*. 2020;9:2603–2610. https://doi.org/10.1002/cam4.2883

Published OnlineFirst January 8, 2020; DOI: 10.1158/1541-7786.MCR-19-0431

Combination Lenalidomide/Bortezomib Treatment Synergistically Induces Calpain-Dependent Ikaros Cleavage and Apoptosis in Myeloma Cells

Saravanan Ganesan, Hamenth Kumar Palani, Nithya Balasundaram, Sachin David, Anup J. Devasia, Biju George, and Vikram Mathews

ABSTRACT

Multiple myeloma had been successfully treated by combining lenalidomide and bortezomib with reports suggesting benefits of such a combination even in relapsed/refractory cases. Recently, it was demonstrated that Ikaros degradation by lenalidomide happens via proteasome-dependent pathway and this process is critical for the eradication of myeloma cells. On the basis of this, an antagonistic effect should be observed if a combination of both these agents were used, which however is not the observation seen in the clinical setting. Our study demonstrates that when these agents are combined they exhibit a synergistic activity against myeloma cells and degradation of Ikaros happens by a proteasome-independent calcium-induced calpain pathway. Our study identifies the crucial role of calcium-induced calpain pathway in inducing apoptosis of myeloma cells when this combination or lenalidomide and bortezomib is used. We also report that this combination enhanced the expression of CD38 compared with lenalidomide alone. Thus, data from our study would establish the rationale for the addition of daratumumab along with this combination to further enhance therapeutic activity against multiple myeloma.

Implications: Lenalidomide and bortezomib combination degrades IKZF1 in multiple myeloma through a calcium-dependent calpain and caspase pathway.

Visual Overview: http://mcr.aacrjournals.org/content/molcanres/18/4/529/F1.large.jpg.

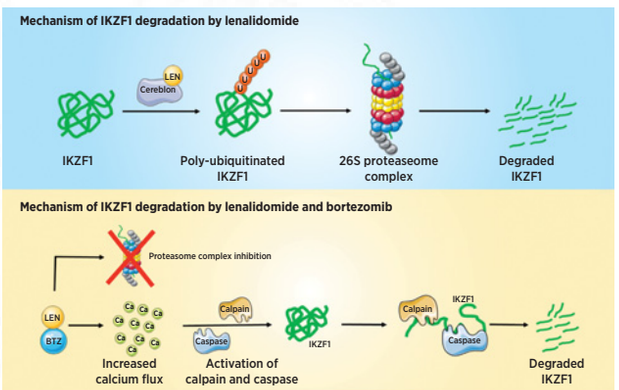

Introduction

Multiple myeloma represents a spectrum of B-cell–derived neoplasm that accounts for approximately 13% of all hematologic malignancies (1). In the younger patients, over the past 2 decades, high-dose chemotherapy along with autologous stem cell transplantation has been the standard of care (1, 2). In the past decade, introduction of immunomodulatory drugs (IMiD) and proteasome inhibitors along with dexamethasone have been shown to increase the rate of complete response without increased toxicity and were able to increase progression-free survival and overall survival in patients with newly diagnosed multiple myeloma (3), as well as improved partial response in two third of patients with relapsed/refractory multiple myeloma (4).

Recent evidences suggests that the mechanism of action of lenalidomide in multiple myeloma depends upon its ability to interact with cereblon E3 ubiquitin ligase to induce the degradation of IKZF1 and IKZF3 proteins via proteasome machinery (5, 6). It was also noted that this IKZF1 degradation axis remains central to the efficacy of lenalidomide in multiple myeloma. This degradation of IKZF1 and IKZF3 results in the downregulation of c-MYC and IRF4 and as a result the multiple myeloma cells undergo apoptosis (7). Recently, it was also shown that when multiple myeloma cells are treated with lenalidomide, it interfere with CD147 and MCT1 protein interaction by binding to cereblon, which acts as chaperon for CD147 maturation (8). Although inhibition of CD147–MCT1 complex induces cell death in multiple myeloma, the IKZF1 degradation by lenalidomide still remains central for disease clearance (9). Recently, it has been shown that IKZF1 can suppress the expression of CD38 antigen in myeloma cells and degradation of IKZF1 by IMiDs can induce CD38 expression (10) thereby facilitating daratumumab-mediated cytotoxicity. Furthermore, pretreating the cells with bortezomib a proteasome inhibitor, resulted in the accumulation of IKZF1, thereby reducing the efficacy of lenalidomide (9). However, even prior to this understanding of the mechanism of action of lenalidomide in the treatment of multiple myeloma, the combination of lenalidomide and bortezomib was routinely used in combination in the clinic with reported

Department of Haematology, Christian Medical College, Vellore, Tamil Nadu, India.

Note: Supplementary data for this article are available at Molecular Cancer Research Online (http://mcr.aacrjournals.org/).

S. Ganesan and H.K. Palani contributed equally as co-first authors to this article.

Corresponding Author: Vikram Mathews, Christian Medical College, Ida Scudder Road, Vellore, Tamil Nadu 632004, India. Phone: 416-228-2891; Fax: 416-222-6449; E-mail: vikram@cmcvellore.ac.in

Mol Cancer Res 2020;18:529–36

doi: 10.1158/1541-7786.MCR-19-0431

Published OnlineFirst January 8, 2020; DOI: 10.1158/1541-7786.MCR-19-0431

synergy on combining them (3, 4, 11). The mechanism of synergy and more importantly the fate of IKZF1 on combining these drugs are not well understood. In this article, we undertook a study to evaluate the fate of IKZF1 in multiple myeloma when a combination of lenalidomide and bortezomib was administered.

Materials and Methods

Cell lines

The human myeloma cell line MM.1S and U266 were obtained from the ATCC and were used in their early passages. The cell lines were periodically characterized phenotypically by flow cytometry. *Mycoplasma* detection was done once in every 6 months and the cell lines used were free from *Mycoplasma* contamination (Universal Mycoplasma detection Kit, ATCC).

Reagents and antibodies

Chemicals such as lenalidomide, bortezomib, MG132, bafilomycin A1, hydroxychloroquine, PD150606, Calpeptin, BAPTA, Ionomycin, E64, pepstatinA, and zVAD.fmk were obtained from Sigma and were used in this study. Antibodies against Actin, p62, IKZF1, BIM, Bcl2, cIAP2, and XIAP1 (Santa Cruz Biotechnology), LC3, Caspase-3, and PARP (Cell Signaling Technology), IRF4 and IKZF3 (Abcam), CD38 FITC conjugate (BD Biosciences), and anti-mouse and anti-rabbit secondary antibodies conjugated with horseradish peroxidase (Cell Signaling Technology), and with Alexa Fluor 594 (Invitrogen) were also used for Western blotting, immunofluorescence, and flow cytometry assays.

Assays for apoptosis

Myeloma cell lines were treated with drugs for indicated time. After incubation at 37°C in CO_2 incubator, the leukemic cells were carefully pipetted out and their viability was measured using Annexin V/7AAD Apoptosis Assay Kit (BD Pharmingen) as per the manufacturer's protocol. The flow data were analyzed using Kaluza Software (Beckman Coulter) and FlowJo v10 (FlowJo LLC).

In vitro cytotoxicity assay

In vitro cytotoxicity of drugs was determined using the MTT assay as described previously (12). Combination index between drugs was calculated using CalcuSyn Software (Biosoft).

qRT-PCR

Total RNA was extracted using TRizol Reagent (Invitrogen Carlsbad). Five-hundred nanogram of the extracted RNA was converted into cDNA using superscript II cDNA Kit (Invitrogen Carlsbad). The expression of genes was studied using SYBR green method (Finnzymes F410L, Thermo Fisher Scientific). The C_t values were normalized with ACTB and the fold differences were calculated using $2^{-\Delta\Delta Ct}$ method. Primer details are provided in **Table 1**.

Coimmunoprecipitation and immunoblots

Myeloma cells lines (MM.1S and U266) were treated with drugs for indicated time and the homogenates were obtained by cell lysis in RIPA Buffer (Sigma), with complete protease inhibitors (Roche). Coimmunoprecipitation was performed using Co-IP Kit (Thermo Pierce) according to the manufacturer's protocol. The lysates and elutes were analyzed in SDS-PAGE. After protein transfer to nitrocellulose membrane, membranes were blocked with BSA (5%, 2 hours) followed by incubation with primary antibodies overnight. The protein bands were detected by standard chemiluminescence method (Thermo Pierce Femto).

Table 1. Details of primers used.

S. No.	Primer	Sequence
1.	Actin forward	5′-CCTTCCTGGGCATGGAGTCCT-3′
2.	Actin reverse	5′-GGAGCAATGATCTTGATCTTC-3′
3.	IRF4 forward	5′-TTAATTCTCCAAGCGGATGC-3′
4.	IRF4 reverse	5′-AAGGAATGAGGAAGCCGTTC-3′

Immunofluorescence

This was done as previously reported by us (13). In summary, the myeloma cells were treated with drugs for 24 hours and cytospun slides were made. The cells were fixed in 4% paraformaldehyde followed by blocking using 5% goat serum. It was further incubated with primary antibodies such as IKZF1 (Santa Cruz Biotechnology) overnight at 4°C. The slides were rinsed with PBS thrice and incubated with secondary antibodies (anti-mouse) conjugated with Alexa Fluor 594, (Invitrogen) for 1 hour. The slides were again washed, air dried, and counterstained with DAPI containing mountant (Vectashield). The images were acquired in fluorescence microscope (Axioimager M1, Carl Zeiss) at 100 × with oil immersion and images were analyzed using ISIS Metasystem (Metasystems GmbH).

Autophagy assay

Induction of autophagy was assessed using CYTO-ID Autophagy Detection Kit (Enzo Life Sciences). The assays were carried out as per the manufacturer's instructions post 24 hours of drug treatments.

Calcium flux assay

Relative estimate of intracellular calcium was analyzed using Fura2-Am Reagent (Molecular Probes). Briefly, the cells were treated with drugs for 6 hours followed by incubation with Fura2-Am reagent (1 μmol/L) for 1 hour. The cells were washed and incubated further for 30 minutes. The fluorescence intensity was measured as ratio of values at an excitation at 340 nm and 380 nm with an emission at 510 nm, using Spectramax M4 (Molecular Devices).

Calpain activity assay

The cells were treated with different drugs for 24 hours and were resuspended in 100 μL extraction buffer and homogenized by pipetting. Protein concentration was determined by the Bradford assay. Calpain activity was measured using a kit from Abcam according to the manufacturer's instructions. The fluorescence intensity (calpain activity) was measured at an excitation at 400 nm and with an emission at 505 nm, using Spectramax M4 (Molecular Devices).

Statistical analysis

Statistical significance was calculated using Student *t* test (two tailed *t* test) or one sample *t* test. The values are denoted as mean ± SD. The *P* values are denoted as *, $P < 0.02$; **, $P = 0.001$; ***, $P = 0.0001$; NS, not significant.

Results

Lenalidomide and bortezomib combination induces apoptosis synergistically in multiple myeloma cell lines

We initially tested the efficacy of lenalidomide on two multiple myeloma cell lines (MM.1S and U266). We evaluated the viability on day 5 post-treatment of lenalidomide and found that MM.1S cell line is

Published OnlineFirst January 8, 2020; DOI: 10.1158/1541-7786.MCR-19-0431

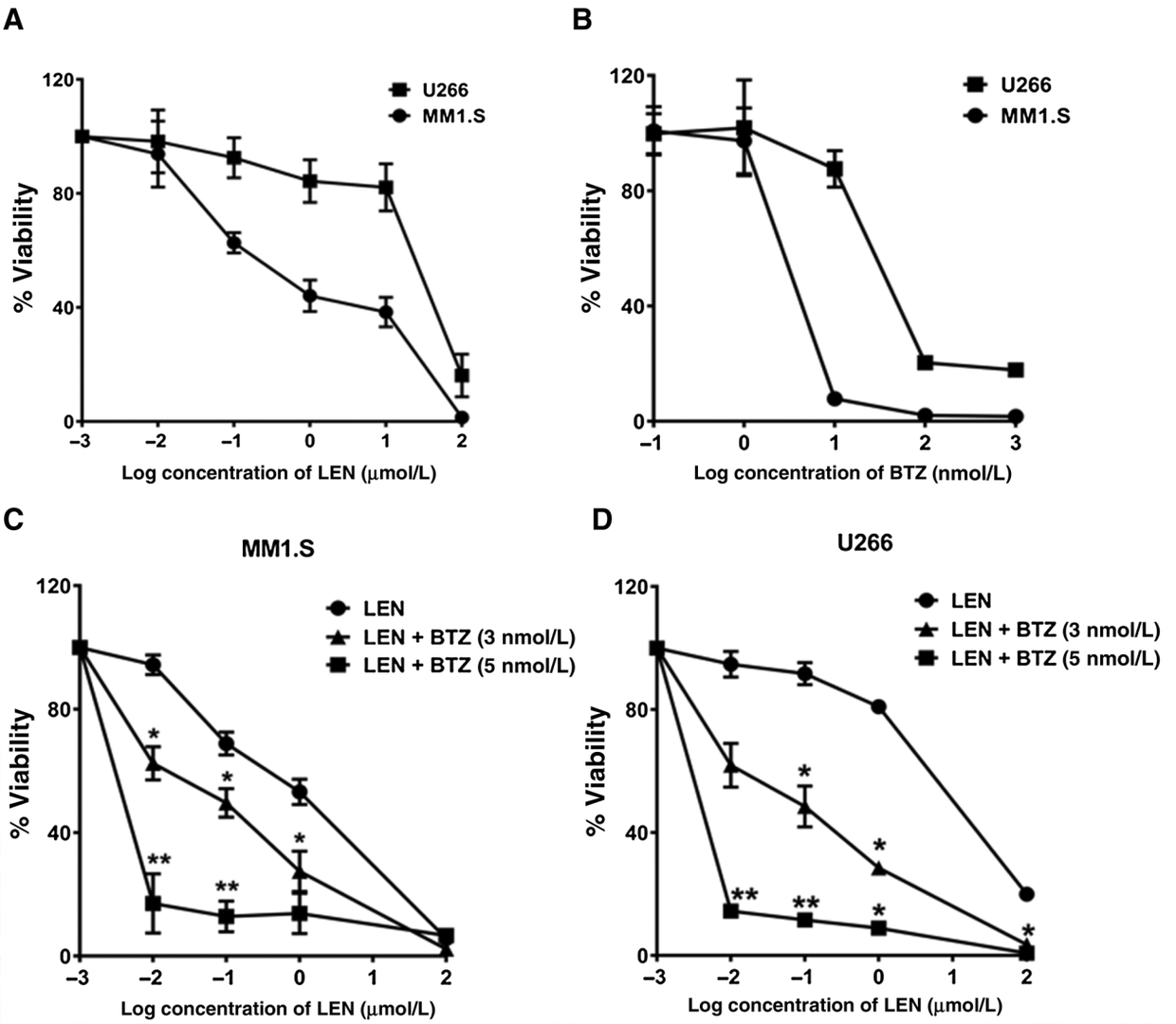

Figure 1.

Lenalidomide and bortezomib induces apoptosis synergistically in myeloma cell lines. **A,** Viability of myeloma cell lines (MM.1S and U266) upon treatment with lenalidomide on day 5 ($n = 3$). **B,** Viability of myeloma cell lines (MM.1S and U266) upon treatment with bortezomib at 48 hours ($n = 3$). Combination of lenalidomide (different concentration) and bortezomib (3 and 5 nmol/L) induces significant apoptosis in myeloma cell line with a combination index of 0.7 (MM.1S, **C**) and 0.5 (U266, **D**) compared with lenalidomide alone–treated cells ($n = 3$). All the assays were done at the end of 5 days (bortezomib was added at the end of day 4) using MTT assays. Statistical significance was calculated using Student *t* test (two tailed *t* test) and the values are denoted as mean ± SD (*, $P < 0.02$; **, $P = 0.001$).

comparatively more sensitive to lenalidomide compared with U266 (**Fig. 1A**). We also checked for the effect of bortezomib on these cell lines. Again we found that MM.1S cell lines were comparatively more sensitive to bortezomib compared with U266 (**Fig. 1B**). These results were consistent with previous reports (14). Next, we showed a significantly increased kill, when bortezomib was combined with increasing concentration of lenalidomide and vice versa (**Fig. 1C** and **D**; Supplementary Fig. S1). The synergism was well documented with a combination index of 0.5 for U266 and 0.7 for MM.1S. The induction of apoptosis was also confirmed by a Western blot where a decrease in antiapoptotic proteins and increase in apoptotic proteins were observed in MM.1S cell line (Supplementary Fig. S2). Next, we assessed the function of proteasome when lenalidomide was combined with bortezomib. We observed that combining these two agents does not interfere with bortezomib action in inhibiting proteasome complex (**Fig. 2A**). As a result of this proteasome inhibition, we also observed an accumulation of ubiquitinated proteins in the bortezomib- and lenalidomide + bortezomib–treated cells when compared with lenalidomide alone treated and control cells (**Fig. 2B**).

Combination of lenalidomide and bortezomib degrades IKZF1 through a proteasomal-independent pathway

Next, we looked for the fate of IKZF1 in myeloma cells treated with lenalidomide and bortezomib combination. We observed a degradation of IKZF1 in both MM.1S (**Fig. 2B** and **C**) and U266 cells

Published OnlineFirst January 8, 2020; DOI: 10.1158/1541-7786.MCR-19-0431

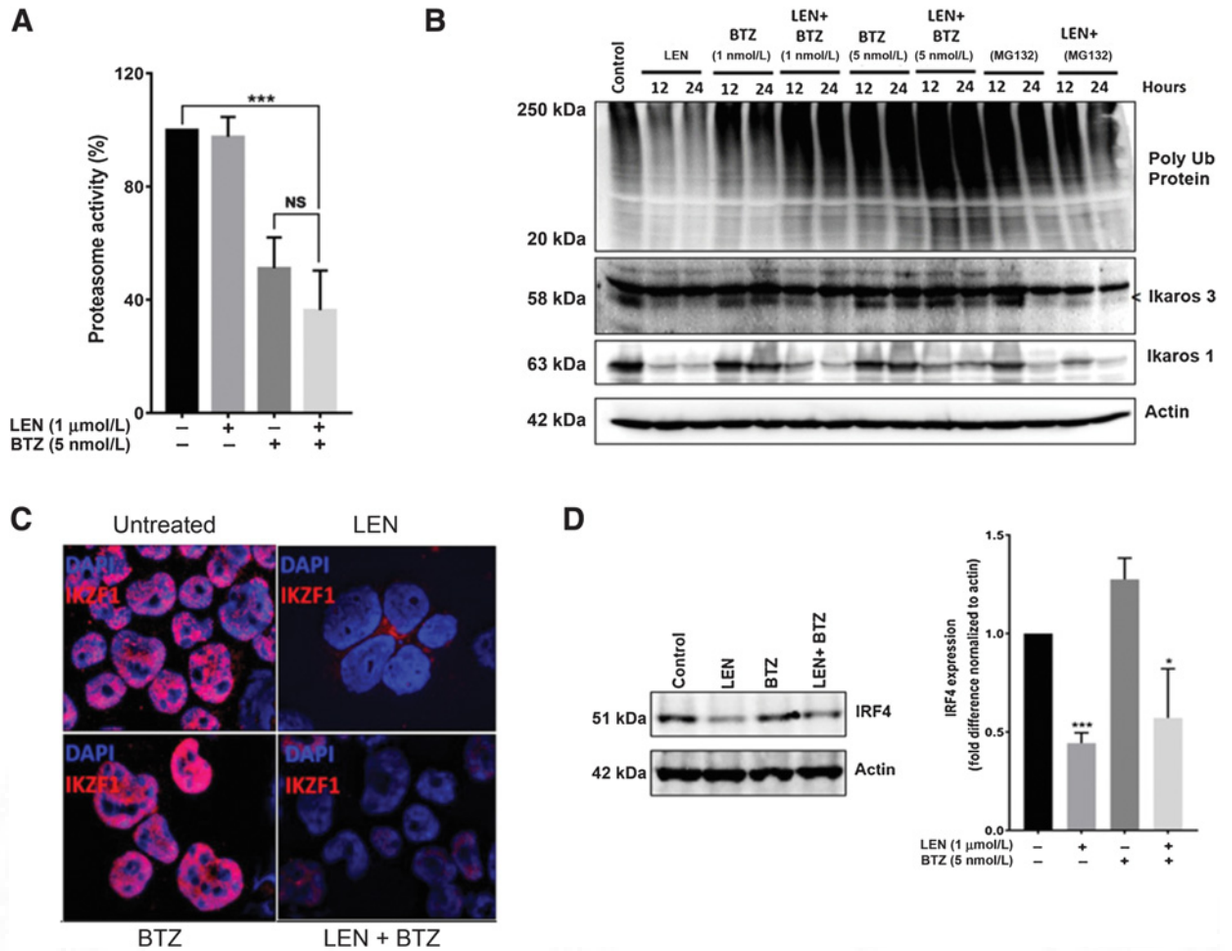

Figure 2.

Lenalidomide and bortezomib induces degradation of IKZF1 in myeloma cell lines. **A,** Addition of lenalidomide (LEN, 1 μmol/L) with bortezomib (BTZ, 5 nmol/L) does not interfere with bortezomib's activity on inhibiting proteasome complex ($n = 3$). Fluorescence-based spectrophotometry-based proteasome activity assay was done using proteasome substrate (Z-Gly-Gly-Leu-7-amido-4-methylcoumarin). **B,** Representative immunoblot showing accumulation of ubiquitinated proteins due to proteasome inhibition upon lenalidomide (1 μmol/L), bortezomib (1 and 5 nmol/L), MG132 (10 μmol/L), and combination treatment. This combination also degraded IKZF1 and IKZF3 in MM.1S cell line ($n = 3$). **C,** Representative immunofluorescence micrograph showing degradation of IKZF1 in MM.1S cell line upon treatment with lenalidomide and bortezomib ($n = 3$). **D,** Downregulation of *IRF4* regulated by IKZF1 was observed when a combination of lenalidomide and bortezomib was used. Assays were done using Western blot analysis (proteins) and real-time PCR (for transcript; $n = 3$) at the end of 24 hours post-drug treatments. Statistical significance was calculated using Student *t* test (two tailed *t* test) and one sample *t* test. The values are denoted as mean ± SD (*, $P = 0.02$; ***, $P = 0.0001$; NS, not significant).

(Supplementary Fig. S3A and S3B) in lenalidomide alone and lenalidomide + bortezomib–treated cells. This was further validated by downregulation of IRF4 (transcriptionally regulated by IKZF1) by Western blot analysis and qPCR in MM.1S cell line (**Fig. 2D**). We also noted that along with IKZF1, IKZF3 was also degraded in the combination-treated cells (**Fig. 2B**). We were able to demonstrate that before degradation, IKZF1 was ubiquitinated by an immunoprecipitation assay when a combination of lenalidomide + bortezomib was used (Supplementary Fig. S4). A similar effect of degrading IKZF1 and IKZF3 was observed when another irreversible proteasome inhibitor (MG132; **Fig. 2B**) was used along with lenalidomide. This suggested that the observed phenomenon is an after effect of proteasome inhibition. Taken together, we were able to show that in spite of significant proteasome complex inhibition IKZF1 was degraded, which suggested involvement of alternative pathway for its degradation.

IKZF1 is not degraded by autophagy pathway which is upregulated because of proteasome inhibition

From our previous article (15), it was evident that autophagy can act as an alternative pathway to degrade an onco-protein meant to be degraded via proteasome complex. We hypothesized, that autophagy pathway induced because of proteasome complex inhibition could degrade IKZF1 (ubiquitinated by lenalidomide). Hence, we looked for the expression of autophagy-associated proteins. As expected and as previously reported by us (15), we observed an induction of autophagy pathway, evidenced through increased generation of LC3II bands along with p62 and poly-ubiquitinated protein accumulation and degradation at time points (**Fig. 3A**), which correlated with time points at which there was an increased intensity of autophagosome staining measured by Cyto-ID (**Fig. 3B**). To support our hypothesis that IKZF1 is degraded by autophagy in the absence of proteasome complex, we pretreated myeloma cells with autophagy inhibitors

Published OnlineFirst January 8, 2020; DOI: 10.1158/1541-7786.MCR-19-0431

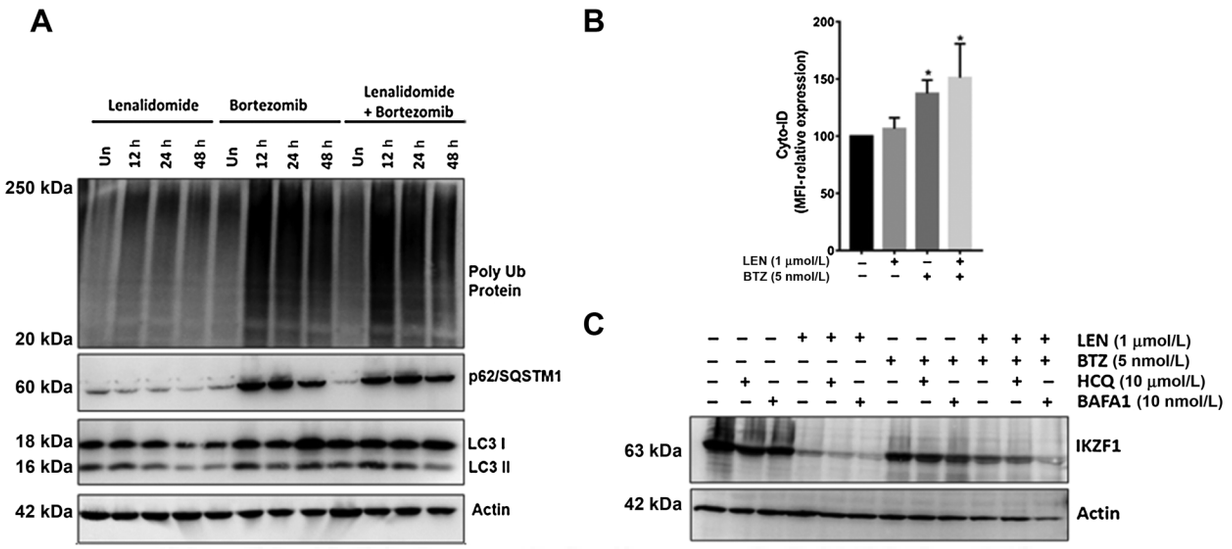

Figure 3.

Lenalidomide (LEN) and bortezomib (BTZ) induces autophagy but does not degrade IKZF1. **A,** Combination of lenalidomide and bortezomib induces autophagy in MM.1S cell line as a result of proteasome inhibition. Representative immunoblots showing timepoint accumulation and degradation of p62 and ubiquitinated proteins in myeloma cell line correlating with activation of LC3II bands at the same time ($n = 3$). **B,** Induction of autophagy as demonstrated by increase staining by Cyto-ID stain ($n = 3$). **C,** Immunoblots showing inhibition of autophagy by hydroxychloroquine (HCQ, 10 μmol/L) or bafilomycin A1 (BAFA1, 10 nmol/L) along with lenalidomide and bortezomib did not interfere in the degradation of IKZF1 ($n = 3$). Statistical significance was calculated using one sample *t* test and the values are denoted as mean ± SD (*, $P = 0.02$).

[hydroxychloroquine and bafilomycin (BAFA1), inhibition of autophagy was confirmed by cyto-ID and other autophagy markers; Supplementary Fig. S5] followed by treatment with lenalidomide and bortezomib. However, we did not observe an accumulation of IKZF1 proteins when autophagy was inhibited (**Fig. 3C**; Supplementary Fig. S6). Taken together, these data indicate that IKZF1 is degraded by an alternative pathway independent of the proteasome and autophagy pathways when lenalidomide and bortezomib are combined.

IKZF1 is degraded by calcium-dependent calpain and caspase pathway by the combination in multiple myeloma cells

Previous reports had demonstrated that inducing apoptosis by kinase inhibitors in myeloma cells can degrade IKZF1 (16). It was also well recognized that lenalidomide degrades IKZF1 in MDS cells through activation of calcium-activated calpain pathway (17) and bortezomib can also induce a transient calcium flux in cells (18, 19). We hypothesized, that when lenalidomide and bortezomib were combined, it induces an increased calcium flux followed by apoptosis where IKZF1 can be degraded via calpain (activated by calcium flux) and caspase-dependent pathways. Toward this, we measured the intracellular calcium levels of myeloma cell line using Fura2-Am post 6 hours of drug treatment. We noted that there was an increased calcium level in the myeloma cells when a combination of lenalidomide and bortezomib was used (**Fig. 4A**). We also noted an increased activity of calpain in cells treated with lenalidomide + bortezomib (**Fig. 4B**). Furthermore, chelating calcium by BAPTA or inhibiting calpain (calpastatin or PD150606) or caspase (zVAD.fmk) resulted in the accumulation of IKZF1 (**Fig. 4C** and **D**; Supplementary Fig. S7) in the presence of lenalidomide and bortezomib and no accumulation of IKZF1 was noted when other protease inhibitors (E64 and Pepstatin A) were used (data not shown). This suggested that specific protease system activated because of calcium flux in myeloma cells degrades IKZF1 protein in the absence of proteasome machinery. This inhibition of calpain or chelation of calcium also resulted in the rescue of myeloma cells from apoptosis induced by the combination drugs (**Fig. 4C–E**; Supplementary Fig. S8). Furthermore, modulation of calcium flux with ionomycin induced IKZF1 degradation in ionomycin alone or in combination with lenalidomide treatment (Supplementary Fig. S9). This suggests a crucial role of calcium flux which can activate calpain and caspase to degrade IKZF1 and induce apoptosis in myeloma cells by bortezomib and lenalidomide.

Combination of lenalidomide and bortezomib also induces CD38 expression in multiple myeloma cells

Finally, we also looked for the expression of CD38 in myeloma cells posttreatment with lenalidomide and bortezomib. Here, we used a lower concentration of bortezomib (1 nmol/L) because the other concentration used was shown to kill almost 90% of the myeloma cells by itself (Supplementary Fig. S10) and we had also demonstrated that at these lower concentrations, IKZF1 was still degraded (**Fig. 2B**). We noted that upon combination of these two agents, there was an increased expression of CD38 in MM.1S cells compared with either of the drug treated MM.1S cells (**Fig. 5**). This further validates our finding that IKZF1 is degraded by the combination and also suggests a rationale for using daratumumab along with lenalidomide and bortezomib to further enhance efficacy in multiple myeloma.

Discussion

Multiple myeloma had been treated successfully with lenalidomide and bortezomib along with dexamethasone, which had significantly improved the clinical outcomes even in older patients, not eligible for high-dose chemotherapy and autologous stem cell transplantation. Recently, it has been demonstrated that the mechanism of action of lenalidomide includes degradation of IKZF1 and IKZF3, which act as a central transcription factor regulating various genes involved in the

Published OnlineFirst January 8, 2020; DOI: 10.1158/1541-7786.MCR-19-0431

survival of myeloma cells. The degradation was brought by the activation of cereblon protein which can ubiquitinate the IKZF1 and IKZF3 proteins and makes them a substrate for proteasome complex. Hence, this proteasome complex–mediated degradation of IKZF1 and IKZF3 would appear to be central for the clearance of this disease. Previously it was also demonstrated that combining lenalidomide and proteasome inhibitor inhibited the degradation of IKZF1 (9). However, these experiments were done at short time points (3 hours and

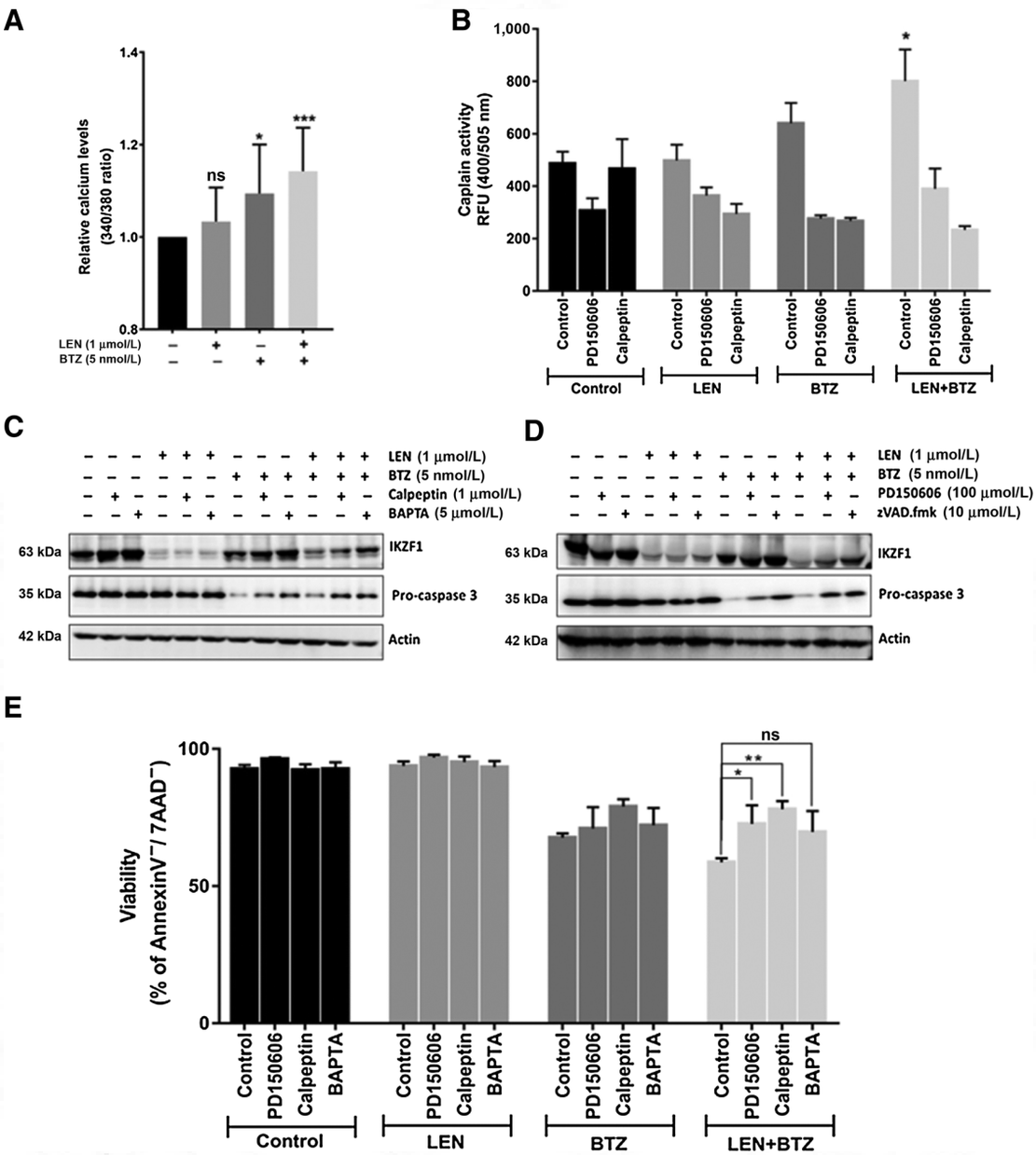

Figure 4.

Lenalidomide and bortezomib combination degrades IKZF1 through calpain and caspase pathway. **A,** Combination of lenalidomide and bortezomib induces significant intracellular calcium in MM.1S cell line compared with either of the drug alone treated cells ($n = 12$). Fluorescence-based spectrophotometer assays were performed using Fura2-AM (calcium sensor) at the end of 6 hours of drug treatment. The 340/380 ratio were calculated and the untreated controls were normalized to 1 and the test were compared with normalized controls. **B,** Calpain activity assay showing increased calpain activity in MM.1S cells treated with lenalidomide (LEN, 1 μmol/L) and bortezomib (BTZ, 5 nmol/L) for 24 hours ($n = 3$). **C,** Inhibition of calpain by calpeptin (1 μmol/L) or chelation of calcium by BAPTA (5 μmol/L) resulted in accumulation of IKZF1 in the presence of lenalidomide and bortezomib ($n = 3$) in MM.1S cell line. **D,** Inhibition of calpain and caspase using PD150606 (100 μmol/L) and zVAD.fmk (10 μmol/L), respectively, resulted in accumulation of IKZF1 in the presence of lenalidomide and bortezomib ($n = 3$) in MM.1S cell line, assays were analyzed by immunoblots where the lysates were collected at the end of 24 hours post-drug treatment. **E,** Reversal of apoptosis was observed in MM.1S cells when the cells were treated with calpain inhibitor or calcium chelator in the presence of lenalidomide and bortezomib for 24 hours. The assay was done using Annexin V/7AAD staining kit ($n = 3$). Statistical significance was calculated using Student t test (two tailed t test) and one sample t test. The values are denoted as mean ± SD (*, $P = 0.02$; **, $P = 0.001$; ***, $P = 0.0001$; ns, not significant).

Published OnlineFirst January 8, 2020; DOI: 10.1158/1541-7786.MCR-19-0431

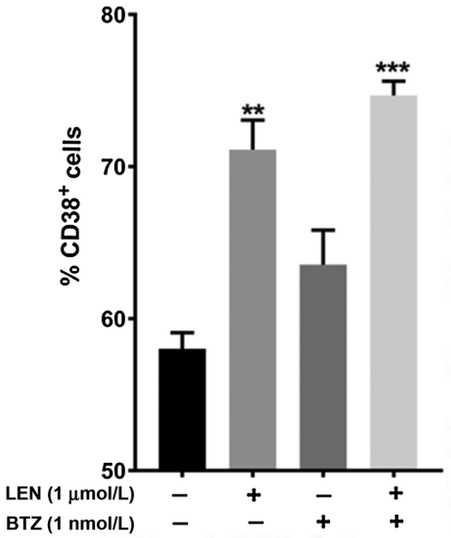

Figure 5.

Lenalidomide and bortezomib combination induces the expression of CD38 in multiple myeloma cells. Combination of lenalidomide (1 μmol/L) and bortezomib (1 nmol/L) increased the expression of CD38 antigen expression on MM.1S cell line. The assay was carried out using flow cytometer post 24 hours of drug treatment ($n = 3$). The statistical analysis were done using Student *t* test and the significance was calculated by comparing the test group with control and between lenalidomide- and lenalidomide combination–treated cells (**, $P = 0.001$; ***, $P = 0.0001$).

5 hours posttreatment), which may not be adequate for demonstration of biological activity. As seen in the clinic, we were able to demonstrate a synergistic activity of these two drugs on multiple myeloma cell lines. We were able to demonstrate that both IKZF1 and IKZF3 were degraded at 12 and 24 hours when these drugs were combined. We also checked for the induction of apoptosis and found there was an increase in the induction of apoptosis; however, we could not find a significant difference between Caspase-3 and BIM expression between bortezomib alone and in combination. Furthermore, we were able to demonstrate that this combination does not interfere with the degradation of IKZF1, in spite of significant proteasome inhibition. We also report that calcium-dependent calpain, as well as caspases activated during apoptosis of myeloma cells can act as an alternative pathway to proteasome machinery by which IKZF1 is degraded with this combination. We believe that the calpain activated upon the drug treatment can induce apoptosis by altering mitochondrial membrane potential of myeloma cells as demonstrated by decrease in BCL2 proteins and cleavage of autophagic proteins (20) induced during drug treatment. This in turn can induce apoptosis. To validate this, we had further showed that inhibiting calpain restored the viability (as shown by pro-caspase 3 levels and viability assay), which suggests that activation of calcium-induced calpain determines the efficacy of this combination in inducing apoptosis in multiple myeloma cells. These observations validate the existing report where it has been shown that the sensitivity of myeloma cells to lenalidomide relies on its ability to decompose H_2O_2 (21), which can generate reactive oxygen species which can also be the effect of increased calcium flux (22).

Thus, our results demonstrate a significant *in vitro* synergism between lenalidomide and bortezomib as seen in the clinic and mechanistically explain how IKZF1 degradation happens even in the presence of proteasome inhibitor. Furthermore, we also demonstrated that this combination enhanced the expression of CD38 in myeloma cells suggesting that a triple therapy combining daratumumab with lenalidomide and bortezomib would be rationale way to further enhance efficacy in multiple myeloma.

Disclosure of Potential Conflicts of Interest

No potential conflicts of interest were disclosed.

Authors' Contributions

Conception and design: S. Ganesan, H.K. Palani, V. Mathews
Development of methodology: S. Ganesan, H.K. Palani, N. Balasundaram, B. George, V. Mathews
Acquisition of data (provided animals, acquired and managed patients, provided facilities, etc.): S. Ganesan, H.K. Palani, N. Balasundaram, A.J. Devasia, B. George, V. Mathews
Analysis and interpretation of data (e.g., statistical analysis, biostatistics, computational analysis): S. Ganesan, H.K. Palani, N. Balasundaram, S. David, A.J. Devasia, V. Mathews
Writing, review, and/or revision of the manuscript: S. Ganesan, H.K. Palani, B. George, V. Mathews
Administrative, technical, or material support (i.e., reporting or organizing data, constructing databases): S. Ganesan, H.K. Palani, N. Balasundaram, S. David
Study supervision: V. Mathews

Acknowledgments

This study was supported by a Wellcome-DBT India Alliance research grant (IA/S/11/2500267) and DBT-COE grant (BT/COE/34/SP13432/2015). V. Mathews was supported by senior fellowship program of Wellcome-DBT India Alliance IA/S/11/2500267 and IA/CPHS/18/1/503930. S. Ganesan, H.K. Palani, and S. David were supported by senior research fellowship from Council for Scientific and Industrial Research. We acknowledge Intas Pharmaceutical Ltd, and NATCO Pharmaceutical Ltd, for kindly providing us API of pharmaceutic drugs for this study.

The costs of publication of this article were defrayed in part by the payment of page charges. This article must therefore be hereby marked *advertisement* in accordance with 18 U.S.C. Section 1734 solely to indicate this fact.

Received April 25, 2019; revised September 14, 2019; accepted December 23, 2019; published first January 8, 2020.

References

1. Moreau P, Attal M, Facon T. Frontline therapy of multiple myeloma. Blood 2015; 125:3076–84.
2. Child JA, Morgan GJ, Davies FE, Owen RG, Bell SE, Hawkins K, et al. High-dose chemotherapy with hematopoietic stem-cell rescue for multiple myeloma. N Engl J Med 2003;348:1875–83.
3. Richardson PG, Weller E, Lonial S, Jakubowiak AJ, Jagannath S, Raje NS, et al. Lenalidomide, bortezomib, and dexamethasone combination therapy in patients with newly diagnosed multiple myeloma. Blood 2010; 116:679–86.
4. Richardson PG, Xie W, Jagannath S, Jakubowiak A, Lonial S, Raje NS, et al. A phase 2 trial of lenalidomide, bortezomib, and dexamethasone in patients with relapsed and relapsed/refractory myeloma. Blood 2014;123:1461–9.
5. Lu G, Middleton RE, Sun H, Naniong M, Ott CJ, Mitsiades CS, et al. The myeloma drug lenalidomide promotes the cereblon-dependent destruction of Ikaros proteins. Science 2014;343:305–9.
6. Krönke J, Udeshi ND, Narla A, Grauman P, Hurst SN, McConkey M, et al. Lenalidomide causes selective degradation of IKZF1 and IKZF3 in multiple myeloma cells. Science 2014;343:301–5.

Published OnlineFirst January 8, 2020; DOI: 10.1158/1541-7786.MCR-19-0431

7. Bjorklund CC, Lu L, Kang J, Hagner PR, Havens CG, Amatangelo M, et al. Rate of CRL4CRBN substrate Ikaros and Aiolos degradation underlies differential activity of lenalidomide and pomalidomide in multiple myeloma cells by regulation of c-Myc and IRF4. Blood Cancer J 2015;5:e354.
8. Eichner R, Heider M, Fernández-Sáiz V, van Bebber F, Garz A-K, Lemeer S, et al. Immunomodulatory drugs disrupt the cereblon–CD147–MCT1 axis to exert antitumor activity and teratogenicity. Nat Med 2016;22:735.
9. Shi CX, Kortüm KM, Zhu YX, Jedlowski P, Bruins L, Braggio E, et al. Proteasome inhibitors block Ikaros degradation by lenalidomide in multiple myeloma. Haematologica 2015;100:e315–7.
10. Fedele PL, Willis SN, Liao Y, Low MS, Rautela J, Segal DH, et al. IMiDs prime myeloma cells for daratumumab-mediated cytotoxicity through loss of Ikaros and Aiolos. Blood 2018;132:2166–78.
11. Attal M, Lauwers-Cances V, Hulin C, Leleu X, Caillot D, Escoffre M, et al. Lenalidomide, bortezomib, and dexamethasone with transplantation for myeloma. N Engl J Med 2017;376:1311–20.
12. Pieters R, Loonen AH, Huismans DR, Broekema GJ, Dirven MW, Heyenbrok MW, et al. In vitro drug sensitivity of cells from children with leukemia using the MTT assay with improved culture conditions. Blood 1990;76:2327–36.
13. Ganesan S, Palani HK, Lakshmanan V, Balasundaram N, Alex AA, David S, et al. Stromal cells downregulate miR-23a-5p to activate protective autophagy in acute myeloid leukemia. Cell Death Dis 2019;10:736.
14. Hu X, Xuan H, Du H, Jiang H, Huang J. Down-regulation of CD9 by methylation decreased bortezomib sensitivity in multiple myeloma. PLoS One 2014;9:e95765.
15. Ganesan S, Alex AA, Chendamarai E, Balasundaram N, Palani HK, David S, et al. Rationale and efficacy of proteasome inhibitor combined with arsenic trioxide in the treatment of acute promyelocytic leukemia. Leukemia 2016;30:2169–78.
16. Liu Y, He X, Sui Y, Yu R, Xu G. Transcription factor IKZF1 is degraded during the apoptosis of multiple myeloma cells induced by kinase inhibition. FEBS Lett 2015;589:2233–40.
17. Fang J, Liu X, Bolanos L, Barker B, Rigolino C, Cortelezzi A, et al. A calcium- and calpain-dependent pathway determines the response to lenalidomide in myelodysplastic syndromes. Nat Med 2016;22:727.
18. Williams JA, Hou Y, Ni HM, Ding WX. Role of intracellular calcium in proteasome inhibitor-induced endoplasmic reticulum stress, autophagy, and cell death. Pharm Res 2013;30:2279–89.
19. Li C, Chen S, Yue P, Deng X, Lonial S, Khuri FR, et al. Proteasome inhibitor PS-341 (bortezomib) induces calpain-dependent IkappaB(alpha) degradation. J Biol Chem 2010;285:16096–104.
20. Zhu X, Messer J, Wang Y, Lin F, Cham C, Chang J, et al. Cytosolic HMGB1 controls the cellular autophagy/apoptosis checkpoint during inflammation. J Clin Invest 2015;125:1098–110.
21. Sebastian S, Zhu YX, Braggio E, Shi CX, Panchabhai SC, Van Wier SA, et al. Multiple myeloma cells' capacity to decompose H(2)O(2) determines lenalidomide sensitivity. Blood 2017;129:991–1007.
22. Görlach A, Bertram K, Hudecova S, Krizanova O. Calcium and ROS: a mutual interplay. Redox Biology 2015;6:260–71.

Published OnlineFirst January 8, 2020; DOI: 10.1158/1541-7786.MCR-19-0431

Molecular Cancer Research

Combination Lenalidomide/Bortezomib Treatment Synergistically Induces Calpain-Dependent Ikaros Cleavage and Apoptosis in Myeloma Cells

Saravanan Ganesan, Hamenth Kumar Palani, Nithya Balasundaram, et al.

Mol Cancer Res 2020;18:529-536. Published OnlineFirst January 8, 2020.

Ganesan et al. *Cell Death and Disease* (2019)10:736
https://doi.org/10.1038/s41419-019-1964-8

Cell Death & Disease

ARTICLE Open Access

Stromal cells downregulate *miR-23a-5p* to activate protective autophagy in acute myeloid leukemia

Saravanan Ganesan[1], Hamenth Kumar Palani[1], Vairavan Lakshmanan[2], Nithya Balasundaram[1], Ansu Abu Alex[1], Sachin David[1], Arvind Venkatraman[1], Anu Korula[1], Biju George[1], Poonkuzhali Balasubramanian[1], Dasaradhi Palakodeti[2], Neha Vyas[3] and Vikram Mathews[1]

Abstract

Complex molecular cross talk between stromal cells and the leukemic cells in bone marrow is known to contribute significantly towards drug-resistance. Here, we have identified the molecular events that lead to stromal cells mediated therapy-resistance in acute myeloid leukemia (AML). Our work demonstrates that stromal cells downregulate *miR-23a-5p* levels in leukemic cells to protect them from the chemotherapy induced apoptosis. Downregulation of *miR-23a-5p* in leukemic cells leads to upregulation of protective autophagy by targeting TLR2 expression. Further, autophagy inhibitors when used as adjuvants along with conventional drugs can improve drug sensitivity in vitro as well in vivo in a mouse model of leukemia. Our work also demonstrates that this mechanism of bone marrow stromal cell mediated regulation of *miR-23a-5p* levels and subsequent molecular events are relevant predominantly in myeloid leukemia. Our results illustrate the critical and dynamic role of the bone marrow microenvironment in modulating miRNA expression in leukemic cells which could contribute significantly to drug resistance and subsequent relapse, possibly through persistence of minimal residual disease in this environment.

Introduction

Bone-marrow microenvironment is known to be actively involved in an onco-protective role for metastatic cancer cells, as well as in leukemia[1,2]. Several studies have demonstrated that tumor-stroma cross talk can play a major role in drug resistance and cancer relapse by retaining minimal residual disease[3]. The molecular mechanism and molecular players involved in contributing towards minimal residual disease and drug resistance are highly dynamic. This can be achieved by stroma-derived secretory factors such as cytokines and chemokines, which help in homing, survival, and growth of the cancer cell in bone-marrow, as well as provide protection against drug toxicity[4]. Apart from several secretory factors, microenvironment mediated changes in micro-RNA (miRNA) expression in tumor cells for cancer progression, metastasis, and drug resistance has also been highlighted[5–8]. Microenvironment can influence miRNA mediated regulation of gene expression in cancer cells either by regulating their expression in tumor cells via modulating signaling networks or by direct miRNA transfer[9]. Identifying the molecular mechanisms and dynamics of microenvironment mediated response to therapy and cancer progression is therefore crucial to improve therapy and achieve prolonged disease free survival in cancer patients.

Acute myeloid leukemia involves abnormal proliferation and accumulation of immature myeloid cells. Currently, World Health Organization (WHO) had classified this disease based on its molecular pathology. Amongst the different AML subtypes, APL (AML-M3) is known to have best response to therapy when arsenic trioxide (ATO) based regimens are used. However, even in APL

Correspondence: Neha Vyas (neha.v@sjri.res.in) or Vikram Mathews (vikram@cmcvellore.ac.in)
[1]Department of Haematology, Christian Medical College, Vellore, India
[2]Institute for Stem Cell Biology and Regenerative Medicine (InStem), Bengaluru, India
Full list of author information is available at the end of the article.
These authors contributed equally: Saravanan Ganesan, Hamenth Kumar Palani
Edited by P. Agostinis

SPRINGER NATURE CDDpress

the relapse rate varies from 10–15% when ATO is used as a single agent. Unlike most cancers it has been noticed that primary resistance to ATO is almost never seen in patients both at initial diagnosis and at relapse[10,11]. This suggests that there could be other mechanisms by which the leukemic cells in APL evade drug toxicity rather than by clonal evolution or drug binding site mutations. Microenvironment-mediated drug resistance or adaptation of leukemic cells is one of the mechanisms where the relapse of the disease can occur through persistence of minimal residual disease. Previous reports, including data from our laboratory suggests that bone-marrow stromal cell mediated drug resistance, predominantly mediated by NF-kB signaling, is significant in APL and AML cell lines and primary cells[12,13].

In this study, we have uncovered the molecular mechanism of stroma mediated drug resistance via NF-kB signaling in APL. We find that stromal cells activate NF-kB signaling in leukemic cells which is directly responsible for downregulation of *miR-23a-5p*. Downregulation of *miR-23a-5p* in co-cultured leukemic cells results in upregulation of protective autophagy via TLR2, which protects the leukemic cells from chemotherapy induced apoptosis. Using GFP-based miRNA reporter constructs and *miR-23a-5p* mimic, we demonstrate that this miRNA plays a significant role in protection of leukemic cells against chemotherapy toxicity. We also demonstrate that this molecular mechanism of drug resistance identified in APL, is also relevant in some AML cell-lines and patient samples but not in acute lymphoid leukemia.

Results

Malignant promyelocytes upon interaction with bone-marrow stromal cells significantly downregulates miR-23a-5p

Leukemic cell-lines, as well as the primary blasts from APL patients demonstrate survival advantage against ATO when co-cultured with either primary stromal cells or stromal cell-lines[14]. This stroma-mediated protective effect against ATO is both contact dependent and independent (Fig. 1a and supplementary Fig. 1). Since miRNAs are known to be one of the major regulators of therapy-resistance in different cancers, we focused on deciphering if cellular miRNAs are differentially expressed in leukemic cells upon stromal co-culture to mediate this protective effect. Towards this, we analyzed the expression of miRNAs in leukemic cells with and without stromal co-culture. Several miRNAs were differentially expressed in leukemic cells after stromal co-culture (supplementary Table 1). miRNAs which have been validated for their role in inducing apoptosis[15–19] were downregulated; while the miRNAs known to be involved in anti-apoptosis mechanism[20–22] were upregulated in the co-cultured leukemic cells (Fig. 1b). Among these differentially regulated miRNAs, we found that *miR-23a-5p* was the most significantly downregulated and stood out even after employing stringent analysis parameters using Deseq (supplementary Fig. 2 and supplementary Table 1) and we could validated its downregulation by Q-PCR analysis (Fig. 1c). Moreover, *miR-23a-5p* can act as both oncogene and tumor suppressor[23,24], hence we selected *miR-23a-5p* to further evaluate its role in stromal cells-induced ATO-resistance.

Downregulation of miR-23a-5p in leukemic cells correlates with upregulation of NF-kB pathway

NF-kB pathway is known to play an important role in stromal cell mediated protective effect[12]. In our current experiments too we were able to confirm NF-kB upregulation in leukemic cells upon stromal co-culture (supplementary Figs. 3 and 4). To evaluate if *miR-23a-5p* expression could be regulated by NF-kB signaling or vice-a-versa, we took a variant of NB4 cell-line (NB4/GFP-MAD cells) where the NF-kB pathway was repressed by overexpressing a mutant IkB super-repressor (supplementary Fig. 5). We found that NB4/GFP-MAD cells showed no significant alteration in the levels of *miR-23a-5p* upon stromal co-culture (Fig. 1c). Expression of *miR-23a-5p* was also significantly higher in NB4/GFP-MAD compared to NB4 (Fig. 1c). This inverse correlation between NF-kB signaling and *miR-23a-5p* suggests that NF-kB pathway regulates *miR-23a-5p* expression. To further resolve the relationship between NF-kB and *miR-23a-5p*, we also inhibited NF-kB signaling using Bay11 or p65 esiRNA in NB4 cells, this again lead to upregulation of *miR-23a-5p* levels in leukemic cells (Fig. 1d). Our results thus suggests that the activation of NF-kB pathway via stromal interactions (contact dependent or independent) negatively regulates the expression of *miR-23a-5p* in leukemic cells. This inverse relationship between *miR-23a-5p* and NF-kB signaling was also evident in APL patient's samples, as assessed by NF-kB target gene expression (*CXCL2, CXCL10, IL6*) and *miR-23a-5p* expression (Fig. 1e).

Stroma-mediated downregulation of miR-23a-5p can drive drug-resistance and relapse in APL

Next, we analyzed the expression of miR-23a-5p in NB4 cells upon treatment with ATO and we noted that ATO significantly increased the expression of miR-23a-5p levels (Fig. 2a). Moreover, we noted a modest increase in the expression of this miRNA when the cells were in co-culture and treated with ATO compared to co-culture alone (Fig. 2a). Further, to investigate if downregulation of *miR-23a-5p* in leukemic cells during stromal co-culture was responsible for drug-resistance, we overexpressed *miR-23a-5*p in NB4 cells using mimics. Overexpression of *miR-23a-5p* mimics was confirmed by Q-PCR (Fig. 2a),

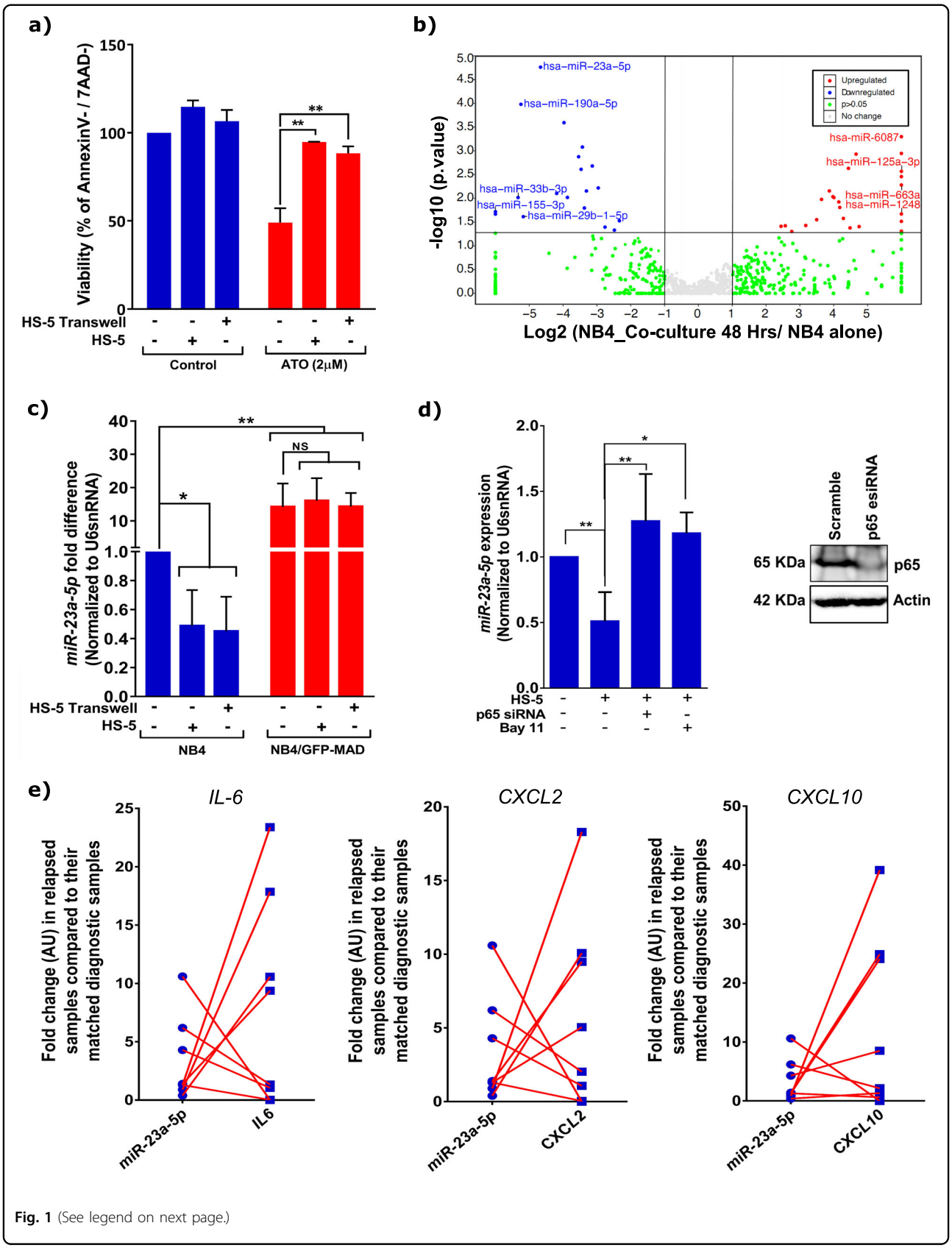

Fig. 1 (See legend on next page.)

(see figure on previous page)

Fig. 1 Bone-marrow stromal cells protects leukemic cells from chemotherapy induced apoptosis via NF-kB pathway mediated suppression of *miR-23a-5p* expression. a Stromal cells induces a protective effect against arsenic trioxide in malignant promyelocytes (NB4) in both contact dependent and independent systems ($n = 5$) Viability was assessed using Annexin V /AAD kit, post 48 h treatment with ATO, the viability of untreated cells were normalized to 100% and the treated cells viability were compared to normalized untreated cells. **b** Volcano Plot represents fold change in miRNA content in NB4 cells upon co-culture with stromal cells. Arrow represents the miRNA of interest which as changed to significant levels ($p < 0.05$). We plotted volcano plot using R ggplot2 package. **c** *miR-23a-5p* in leukemic cells (NB4) is downregulated upon co-culture (direct and transwell) with stromal cells and NB4/GFP-MAD cells showing high expression of *miR-23a-5p* compared to NB4 cells. Downregulation of *miR-23a-5p* was not observed in NB4/GFP-MAD cells even after co-culture with stromal cells NB4/GFP-MAD cells showing high expression of *miR-23a-5p* compared to NB4 cells ($n = 3$). **d** *miR-23a-5p* in leukemic cells is downregulated on co-culture with stromal cells and this effect is reversed on inhibiting the NF-kB pathway as demonstrated here by either knock down of p65 or by use of small molecule inhibitors of the NF-kB pathway (bay-11; 10 μM) ($n = 3$). **e** NF-kB target genes (*IL-6, CXCL2, CXCL10*) levels in the relapsed (compared to their matched diagnostic samples) inversely correlated with *miR-23a-5p* levels for the same samples at relapse. Statistical significance was calculated using Student's *t*-test (two tailed *t*-test) and the values are denoted as mean ± SD. The *P*-values are denoted as $*P = 0.02$, $**P = 0.005$, $****P < 0.0001$, NS Not significant

as well as using GFP-*miR-23a-5p*-reporter assay (supplementary Fig. 6). Overexpression of *miR-23a-5p* mimic, restored sensitivity to ATO (Fig. 2b and supplementary Fig. 7) and daunorubicin (DNR) (supplementary Fig. 8) in NB4 cells even in the presence of stromal co-culture. Also, NB4/GFP-MAD cells which show higher cellular *miR-23a-5p* levels were sensitive to ATO (Fig. 2b) and DNR even in presence of stroma cells (supplementary Fig. 8). We also analyzed the expression of *miR-23a-5p* in primary APL samples collected at the time of diagnosis and correlated with relapse. We observed a significantly lower expression of *miR-23a-5p* in 'at diagnosis' sample of patients who had relapsed subsequently (Fig. 2c) compared to patients who did not relapse upon ATO treatment. Together our results demonstrate that the restoration of cellular *miR-23a-5p* levels could overcome stroma-mediated protection against chemotherapeutics drugs in leukemic cells and downregulation of this miRNA can be correlated to relapse in APL.

miR-23a-5p targets TLR2 and modulates autophagic flux in leukemic cells

To get functional insights about the role of *miR-23a-5p* in mediating drug sensitivity, it becomes imperative to identify its targets. Using TargetScan-software the genes involved in autophagy and toll-like receptors (TLR) were identified as top five targets that could be potentially regulated by *miR-23a-5p* (supplementary Table 2). We observed that in co-cultured leukemic cells where *miR-23a-5p* is downregulated, there was increase in autophagy proteins, as well as TLR2 (Fig. 3a, b). To identify if TLR2, as well as autophagy proteins were direct targets of *miR-23a-5p*, we evaluated levels of TLR2 and autophagy genes in miRNA add-back conditions. We noted decreased expression of TLR2 protein, as well as TLR2 transcript (Fig. 3b and supplementary Fig. 9) and decreased autophagic flux (as measured through accumulation of cellular levels of p62/SQSTM1 protein and LC3-II conversion; Fig. 3c). However, the mRNA levels of autophagy genes remained unperturbed (supplementary Fig. 10). NB4/GFP-MAD cells, where *miR-23a-5p* levels are significantly higher, also demonstrated decreased expression of TLR2 (supplementary Fig. 11). To validate that TLR2 is a direct target of *miR-23a-5p* in leukemic cells, we generated a GFP-reporter by cloning 3′UTR of *TLR2* region (identified by TargetScan software as *miR-23a-5p* target) at 3′ end of GFP (Fig. 3d, top panel). *miR-23a-5p* mimic when overexpressed in leukemic cells could lead to decrease in the intensity of GFP-TLR2-reporter expressing cells unlike the control or the TLR2–3′UTR mutants (Fig. 3d). Overall our data suggests that TLR2 is the direct target of miR-23a-5p.

TLR2 expression regulates autophagy levels and induces ATO-resistance in APL

TLR2 is known to regulate autophagy[25,26]. We hence hypothesized that decrease in autophagic flux might be influenced by TLR2. To evaluate this, we transiently knocked-down *TLR2* in NB4 cells. Knock-down of *TLR2* resulted in decreased expression of autophagy proteins (LC3, ATG5–12, and Beclin1) (Fig. 4a), even in presence of stromal-cells (supplementary Fig. 12). Increased expression of TLR2 was also observed in co-cultured NB4 cells post ATO-exposure (Fig. 4b) suggesting that TLR2 could play an important role in drug-resistance. Further, the *TLR2*-knowdown NB4 cells were sensitized to ATO in the presence of stromal cells (Fig. 4c and supplementary Fig. 13). Further, a modestly upregulated expression of *TLR2* in APL patients at diagnosis was noted in those that subsequently relapsed (Fig. 4d). Altogether, we observed that stromal cells induced downregulation of *miR-23a-5p* in leukemic cells can increase TLR2 expression which in turn regulates autophagy pathway to induce drug-resistance.

miR-23a-5p also targets TLR2 and autophagy in other subtypes of acute myeloid leukemia

Stromal cell mediated drug-resistance has also been implicated in other subtypes of AML. We hence

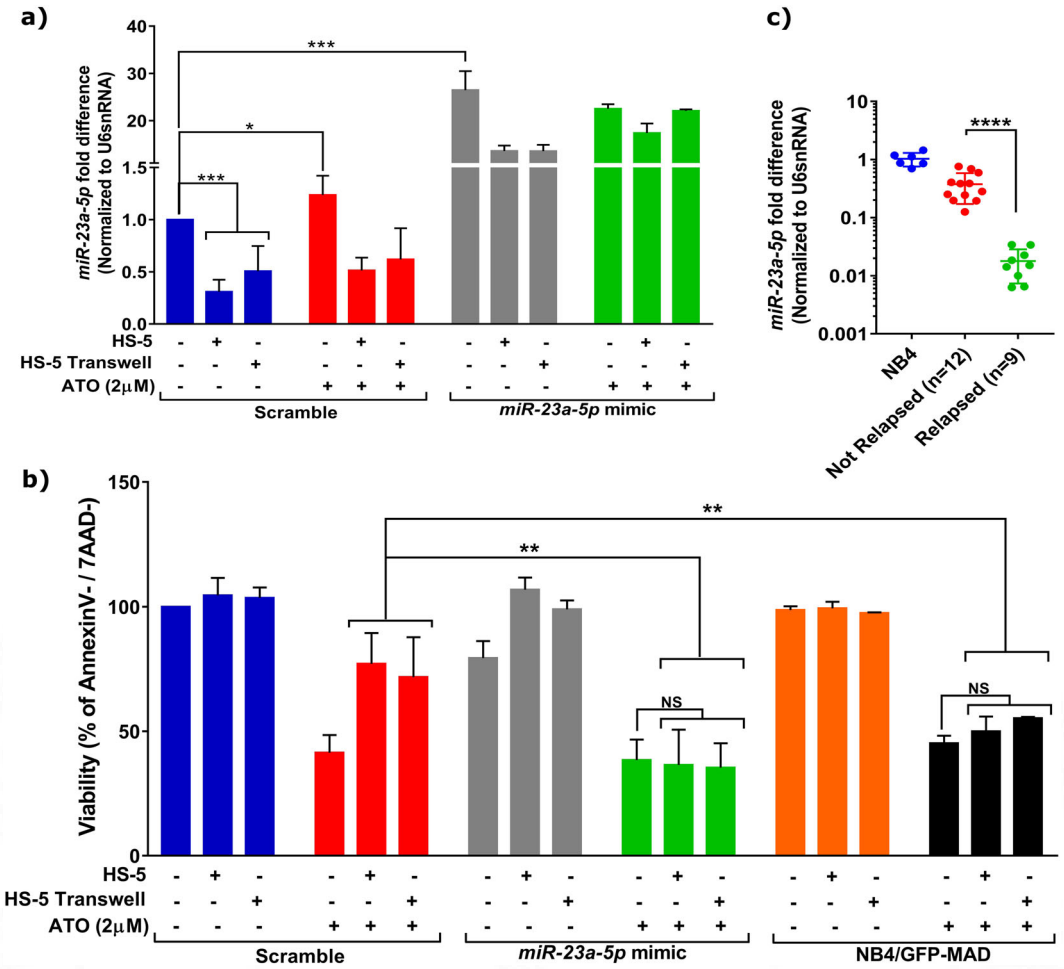

Fig. 2 Stromal cells mediated downregulation of *miR-23a-5p* is responsible for drug-resistance a Effect of ATO on *miR-23a-5p* expression in leukemic cells upon co-culture, as well as during mimic overexpression conditions ($n = 3$). **b** Re-introduction of *miR-23a-5p* mimic into NB4 cells restores sensitivity against ATO in the presence of stroma ($n = 3$) in both transwell and direct co-culture conditions, viability was measured using Annexin V/7AAD kit. NB4/GFP-MAD cells having high expression of miR-23a-5p did not show a protective effect against ATO in the presence of stroma. **c** Correlation of expression of *miR-23a-5p* in APL patients to relapse. Expression *miR-23a-5p* (normalized with U6snRNA-housekeeping) and compared to NB4 cell-line, suggesting higher expression of *miR-23a-5p* in patients who had not relapsed compared to patients who had relapsed. Statistical significance was calculated using Student's *t*-test (two tailed *t*-test) and the values are denoted as mean ± SD. The *P*-values are denoted as $^{**}P = 0.005$, $^{***}P < 0.001$, $^{****}P < 0.0001$, NS not significant

investigated if HS-5 cells could also protect different AML cell-lines against their respective chemotherapeutic agents. We observed significant protection in co-cultured AML cell-lines (U937, THP1, Kasumi-1) and primary AML cells against DNR or Cytarabine (Ara-C) (Fig. 5a and supplementary Fig. 14). Activation of NF-kB pathway was also observed in AML cells upon co-culture (supplementary Fig. 15). Further, compared to NB4 cells; NB4/GFP-MAD and Kasumi-1 cell-lines had higher expression of *miR-23a-5p* while myeloid leukemic cells such as U937, HEL, and THP1 cell-lines had lower expression of miR-23a-5p (supplementary Fig. 16). Interestingly, we noted that this miRNA was down-regulated even in NB4 EV-AsR1(supplementary Fig. 16; an in-house derived ATO resistant cell-line). Further we looked for the expression of *miR-23a-5p* in different AML cells upon co-culture. Downregulation of this miRNA upon stromal co-culture was seen with U937 and Kasumi-1 (AML cell-lines) but not in THP-1 (AML cell-line) or the Sup-B15 and Jurkat-E6.1 cell-lines (ALL cell-line; Fig. 5b). We identified that there was also significant difference in levels of *miR-23a-5p* between ALL, AML, and APL patients (Fig. 5c).

Similar to APL, we also noted an increase expression of this miRNA in U937 cells when exposed to daunorubicin (supplementary Fig. 17). Further, when the *miR-23a-5p* mimics were re-introduced in AML cells, there was a reversal of resistance in U937 cell-line but not in THP1

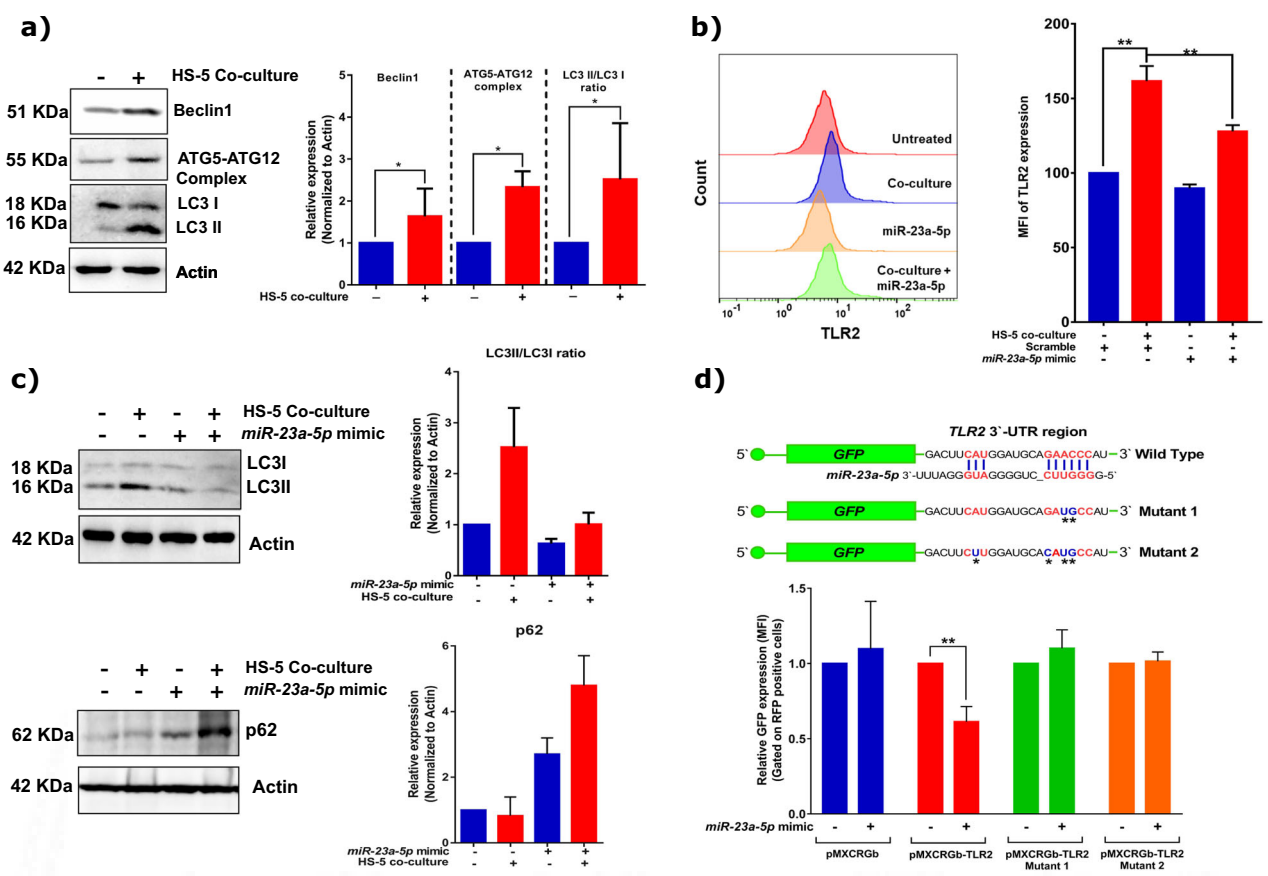

Fig. 3 Stromal cells mediated downregulation of *miR-23a-5p* induces drug-resistance by targeting TLR2 expression: a Autophagy is upregulated in malignant promyelocytes upon co-culture with stromal cells. Western blots showing the protein intensities were quantitated by densitometry and normalized to actin ($n = 3$). **b** Expression of TLR2 (protein) in leukemic cells upon co-culture and in the presence of *miR-23a-5p* mimic ($n = 3$) by a flow cytometry based assay. **c** Autophagic flux as measured by decrease levels in p62 levels and increase levels of LC3II is upregulated in malignant promyelocytes upon co-culture with stromal cells and *miR-23a-5p* targets autophagic flux as shown by accumulation of p62 in malignant promyelocytes upon co-culture ($n = 3$). Western blots showing the protein intensities were quantitated by densitometry and normalized to actin ($n = 3$). **d** Top panel-cartoon showing the 3′UTR region of *TLR2* mRNA where *miR-23a-5p* can bind as well the mutant showing the modified bases. Quantitation of GFP fluorescence (Mean Flourescent Intensity-MFI) when *miR-23a-5p* is re-introduced in NB4 cells which were made to transiently express GFP protein where the 3′UTR of GFP is replaced by TLR2 3′UTR (pMXCRGb-TLR2). This reduction in GFP intensity was not observed in control system having vector alone (pMXCRGb) or in the mutants generated ($n = 3$). Statistical significance was calculated using Student's *t*-test (two tailed *t*-test) and the values are denoted as mean ± SD. The *P*-values are denoted as $*P = 0.02$, $**P = 0.005$

cell-line against DNR (Fig. 5d and supplementary Fig. 18). Also, upregulation of *TLR2* upon stromal co-culture was observed only with U937 but not with THP-1 cells (supplementary Fig. 19). The difference in the regulation of TLR2-expression by *miR-23a-5p* overexpression suggests that while stroma-mediated protection is observed in most leukemic cells; the molecular mechanism of this protection is variable and needs to be identified in a context specific manner.

Further, to evaluate if the *miR-23a-5p*-TLR2-autophagy circuit can be used to predict the outcome in patients we correlated the expression of *miR-23a-5p* with prognosis (favorable risk, intermediate risk and adverse risk) in AML patients. Our preliminary results showed that, as observed in APL patient samples (Fig. 2b), high expression of *miR-23a-5p* correlated with favorable risk AML patients; while there were no differences in *miR-23a-5p* expression in intermediate and adverse risk patients (Fig. 5e). Once again, we also noticed a reduction in expression of *TLR2* and *BECN1* (autophagy gene) in favorable risk AML samples when compared to intermediate or adverse risk patient's samples (Fig. 5e).

Inhibition of autophagy can overcome stroma-mediated drug-resistance in vitro and modestly improve survival in an APL transplantable mouse model

Since we identified NF-kB-*miR-23a-5p*-TLR2-autophagy circuit can drive drug-resistance, we evaluated if inhibition of autophagy (activated due to low *miR-23a-5p* levels) is sufficient to overcome stroma-mediated

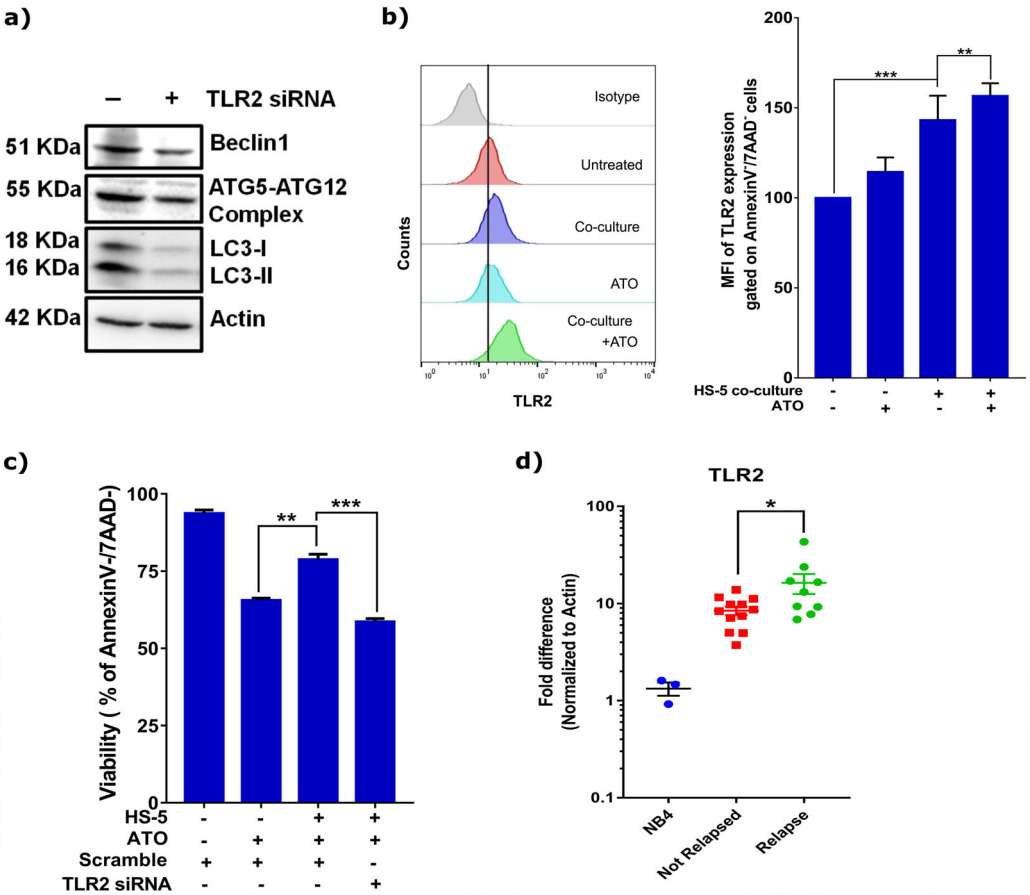

Fig. 4 m*iR-23a-5p* targets autophagic flux and autophagy inhibitors can overcome stroma mediated protection to ATO. a Autophagy is regulated by TLR2 – knock down of TLR2 gene in NB4 resulted in downregulation of genes (*LC3, Beclin1, ATG12*) involved in autophagy pathway ($n = 3$). **b** Expression (MFI) of TLR2 on NB4 cells which are surviving (Annexin V-/7AAD-) post ATO exposure (2 μM) in the presence of stromal cells shows increased expression of TLR2 (n = 3) compared to controls. **c** Transient knock down of TLR2 sensitized the NB4 cells to ATO even in the presence of stromal cells; viability assay was performed using AnnexinV and 7AAD ($n = 3$). **d** Correlation of expression of TLR2 in APL patients to relapse. Expression of TLR2 (normalized with actin-housekeeping) were compared to NB4 cell-line, suggesting higher expression of TLR2 in patients who had relapsed compared to patients who had not relapsed). Statistical significance was calculated using Student's *t*-test (two tailed *t*-test) and the values are denoted as mean ± SD. The *P*-values are denoted as $*P = 0.02$, $**P = 0.005$, $***P < 0.001$

protective effect. For this, we treated co-cultured cells with known autophagy inhibitors-Bafilomycin A1 and Hydroxychloroquine (HCQ) along with ATO. The ability of the autophagy inhibitor (at the concentrations used) to inhibit autophagy was verified (supplementary Fig. 20). As observed with *miR-23a-5p* mimic overexpression condition, autophagy inhibitors were also able to restore the sensitivity of ATO in APL, as well as to DNR in AML cells upon co-culture (Fig. 6a, b and supplementary Figs. 21 and 22). Taken together, our results demonstrates that the stroma mediated upregulation of protective-autophagy in leukemic cells, via downregulation of cellular *miR-23a-5p* levels, results in protection against conventional therapy in vitro. Finally, we evaluated the efficacy of HCQ along with ATO to improve the overall survival in an APL mouse model. Based on our previous experience[12], we used reduced dosage of ATO (from 10 mg/kg to 5 mg/kg) so that a synergy between ATO and HCQ, if any, could be observed. We find that when HCQ was combined with ATO, there was significant reduction of tumor burden in the APL mice (Fig. 6c, supplementary Fig. 23) in the peripheral blood of APL mice on day 20 compared to controls. Though, this combination showed a significant decrease in the leukemia burden, there was modest improvement in the survival of APL mice (median 52 days) when compared to placebo (median 27 days), ATO (median 45 days) or HCQ (median 27.5 days) arms (Fig. 6d). Our results here, using cell based assays, as well as APL mouse model, suggests that inhibiting protective autophagy can overcome the resistance induced by stroma in APL. Our data also suggests that, NF-kB-*miR-23a-5p*-TLR2-Autophagy axis is an important target to

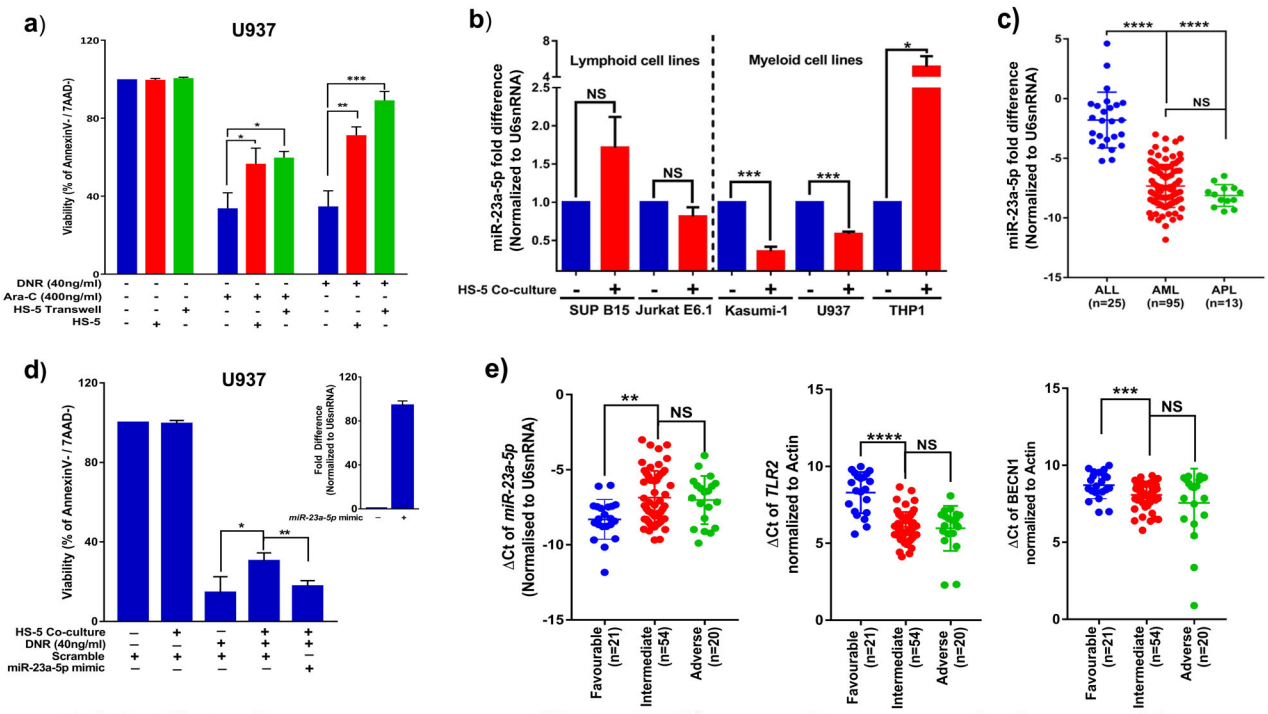

Fig. 5 m*iR-23a-5p* also targets TLR2 and autophagy flux in other subtypes of acute myeloid leukemia: a Stromal cells induces a protective effect against arsenic trioxide in AML cell-line (U937) in both contact dependent and independent systems ($n = 3$). Viability was assessed using Annexin V /AAD kit, post 48 h treatment with daunorubicin (DNR-40ng/ml) and cytarabine (Ara-C-400 ng/ml). The viability of untreated cells were normalized to 100% and the treated cells viability were compared to normalized untreated cells. **b** Expression of *miR-23a-5p* (2-ΔΔCt-fold difference) in various lymphoid and myeloid leukemic cells co-cultured with stromal cells (HS-5) ($n = 3$). **c** Expression (ΔCt) of *miR-23a-5p* in primary ALL ($n = 25$), AML ($n = 27$) and APL ($n = 15$) samples (ΔCt is inversely correlated to the expression). **d** Re-introduction of *miR-23a-5p* mimic into U937 cells restores sensitivity against DNR in the presence of stroma ($n = 3$), viability was measured using Annexin V/7AAD kit. Insert showing the efficacy of electroporation in U937 cells ($n = 3$). **e** Higher expression of *miR-23a-5p* and lower expression of *TLR2* and *BECN1* correlates with favorable risk prognosis ($n = 21$) in AML (including AML-M3; $n = 13$). Lower expression of *miR-23a-5p* and higher expression of *TLR2* and *BECN1* also correlated with intermediate ($n = 54$) and adverse risk ($n = 20$) AML patients. (ΔCt values are inversely proportional to the expression levels of genes). Statistical significance was calculated using Student's *t*-test (two tailed *t*-test) and the values are denoted as mean ± SD. The *P*-values are denoted as $***P = 0.0001$, $**P = 0.005$, $*P = 0.02$, NS not significant

overcome drug-resistance in APL and subtypes of AML (Fig. 6e).

Discussion

Accumulating evidence suggests that bone marrow stromal micro-environment act as sanctuary site for leukemic cells and affords protection from conventional chemotherapy agents. We had previously reported in APL that there was significant microenvironment-mediated ATO-resistance by upregulation of the NF-kB pathway[12]. In this manuscript we have addressed the molecular mechanism of NF-kB pathway mediated drug-resistance in AMLs. Here, using in vitro co-culture assays we try to mimic the intercellular cross talk conditions. To identify the secreted factor(s) involved in activation of NF-kB signaling, we performed cytokine array using conditioned medium from stromal cells line. Our results suggests that several cytokines, up to 43, were upregulated upon stromal co-cultures (data not shown), several of which could potentially activate NF-kB signaling. Apart from cytokines, exosomes derived from stromal cells are also known for their protective effect on the cancer cells via juxtacrine signaling or due to delivery of exosomal miRNAs or other regulatory factors ferried in the lumen of the exosomes[27,28]. Recently, even Wnt5 has also been identified as a ligand involved in activate NF-kB signaling[29]. Wnt proteins are also known to be ferried on exosomes[30]. Thus NF-kB signaling can be activated by several possible stroma-derived paracrine factors. Secreted cytokines and exosomes can act in additive or redundant manner to activate NF-kB signaling. A more detailed study needs to be initiated to understand if NF-kB activation or ATO resistance can be imparted by stromal cells in exosome dependent or independent manner and to nail the dominant player (if any) in activation of NF-kB signaling in leukemic cells upon stromal co-culture.

It has been reported that apart from upregulating cell proliferation and anti-apoptotic genes, NF-kB signaling is

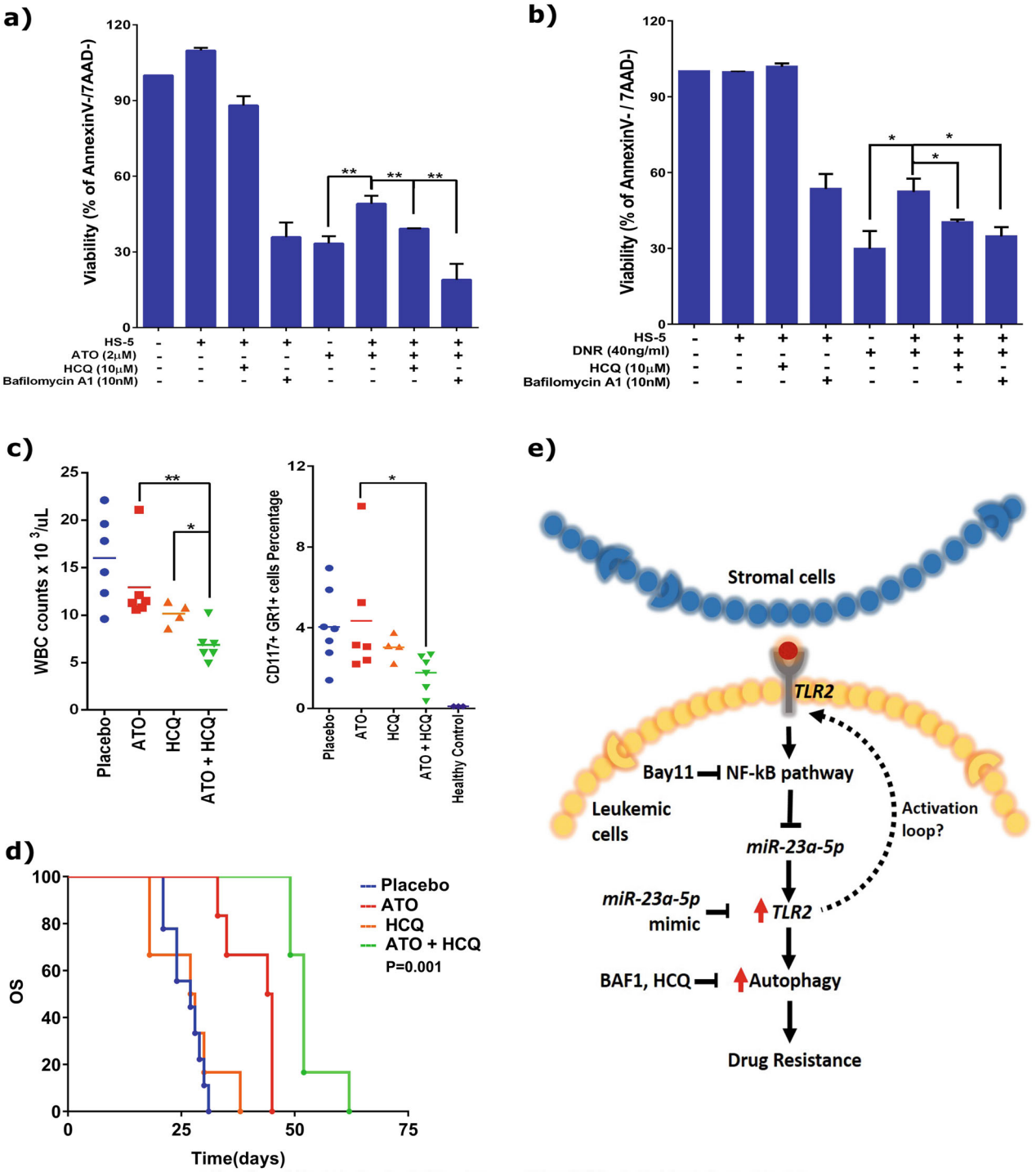

Fig. 6 Inhibition of autophagy restores sensitivity to chemotherapeutics drugs in acute myeloid leukemia a, b Inhibition of autophagy using autophagy inhibitors (bafilomycin A1–10 nM and hydroxychloroquine–10 μM) restores the sensitivity of ATO (2 μM) in NB4 cells (**a**) and DNR in U937 (**b**) in the presence of stroma ($n = 3$), assays were done at the end of 48 h using apoptosis assay (AnnexinV /7AAD kit). **c** ATO along with HCQ reduces tumor burden in APL mice on day 20 as evidenced through decreased WBC counts and decreased leukemic cells percentage in peripheral blood analyzed by flow cytometry. **d** ATO and HCQ prolongs the survival of APL mice as illustrated in the Kaplan–Meier plot. **e** Image representing the stromal cell mediated downregulation of *miR-23a-5p* and its effect on drug-resistance in leukemic cells. Statistical significance was calculated using Student's *t*-test (two tailed *t*-test) and the values are denoted as mean ± SD. The *P*-values are denoted as $^{**}P = 0.005$, $^{*}P = 0.02$, NS Not significant

also known to exhibit their pro-tumorigenic activity by regulating expression of specific miRNAs[31,32]. Here, using NGS based approach and stringent analysis parameters, we identify that *miR-23*a-5p is significantly downregulated among other miRNAs in co-cultured leukemic cells. Our data using NF-kB inhibitors, NF-kB signaling incompetent leukemic cells, as well as relapsed APL patient samples, strongly suggest that downregulation of *miR-23a-5p* is a result of upregulated NF-kB signaling upon stromal co-culture. This inverse relationship between *miR-23a-5p* and NF-kB identified in leukemic cells by our study is in agreement with a study done in Jurkat cells, where NF-kB has been shown to inversely regulate miR-23a-5p expression[33]; unlike HEK, K562 and HEL cells were NF-kB signaling upregulated expression of *miR23a-27a-24* cluster[34]. The observed difference in regulation of *miR-23a-5p* levels suggests role of other tissue specific regulators.

Further, *miR-23a-5p* overexpression experiments suggests that downregulation of this miRNA plays a significant role in protection of leukemic cells against chemotherapy toxicity. To the best of our knowledge this is the first time that *miR-23a-5p* has been implicated in leukemia drug-resistance in a NF-kB dependent manner. In order to understand the molecular mechanism of *miR-23a-5p* downregulation mediated drug-resistance in AML cells, we predicted the targets of *miR-23a-5p*. As reported for Mycobacterium infected macrophages[35], we were also able to validate *TLR2* as its direct target using GFP-reporter assays and *miR-23a-5p* mimics. Further knockdown of *TLR2* resulted in reversal of drug-resistance in leukemic cells even in the presence of stroma. Consistent with our findings, it has also been reported that increased expression of TLR2 in AML is associated with poor clinical outcomes[36].

Overexpressing *miR-23a-5p* in leukemic cells results in downregulation of cellular autophagic flux, estimated by accumulation of p62 [a well-established autophagy target[37]], as well as reduced the expression of autophagy proteins. Here, we conclude that this *miR-23a-5p*-mediated effect on autophagy pathway is via TLR2 since overexpression of *miR-23a-5p* mimics resulted in downregulation of *TLR2* transcripts but did not influence autophagy transcripts. Therefore, TLR2 may activate cellular autophagy probably via post translational modifications of autophagy genes[38]. Upregulation of autophagy and its association with drug-resistance identified here, is consistent with reported clinical studies in AML that have demonstrated an increased risk of relapse and decreased overall survival associated with an increased expression of autophagy related genes[39,40].

Further, we observed that both, HCQ or bafilomycin A1 when used in combination with DNR or ATO can reverse the stroma-mediated drug protection and can improve survival in APL mouse model. This suggests that autophagy inhibitors when used as adjuvants can overcome stroma-mediated protection to leukemic cells in vitro, as well as in vivo conditions (APL mouse model) for better treatment outcome. It must be noted that we had demonstrated previously that bortezomib when used in combination with ATO can improve therapy outcome by inducing cytotoxic-autophagy[12]. Whereas this study suggests that the stromal co-culture induces cytoprotective-autophagy in leukemic cells. It is well noted that autophagy is a 'double edged sword' and the threshold where the protective-autophagy can be converted into cytotoxic-autophagy is not known. However, nuclear accumulation of B-catenin is a known marker of cytotoxic-autophagy[41]; we found that the autophagy induced during drug treatment [based on our previous study[12]], indeed leads to nuclear accumulation of B-catenin unlike stromal co-cultures (supplementary Fig. 24). Based on these observations we conclude that, in contrast to bortezomib, stromal co-cultures activate protective-autophagy in these cells.

Further, in order to evaluate impact of our findings in other leukemia's, we attempted to validate if the *miR-23a-5p*-mediated protective influence is valid for myeloid (NB4, U937, Kasumi-1, THP-1) and lymphoid cells (Jurkat E6.1 and SUP B15). We were able to demonstrate a significant downregulation *of miR-23*a-5p in myeloid malignant cells (except THP1) but not in lymphoid cells upon co-culture. Data from primary cells suggested that at baseline APL cells had the highest expression *of miR-23*a-5p followed by AML (with variable expression levels) and ALL samples, respectively. Comparing the conventionally defined risk groups in AML, the favorable risk group patients had highest expression *of miR-23*a-5p compared to intermediate and adverse risk groups analyzed. The high expression of *miR-23a-5p* could be one of the reason why APL cells are most sensitive to ATO and anthracycline and being most curable leukemia, while other acute leukemia are not. Further, correlating relapse with *miR-23a-5p* expression, we identified that those who relapsed had a lower expression of *miR-23a-5p* in their malignant cells at diagnosis compared to those who did not relapse. We suspect that there will be a significant heterogeneity in the cellular levels of miR-23a-5p in AML patient samples and active regulation of miR-23a-5p-TLR2-Autophagy circuit which might be restricted to rather small subset of cells which are close to the bone-marrow stromal cells which would in turn contribute to disease relapse. While upregulation of autophagy in AML cells upon co-culture has been identified before[42,43], our work resolves the underlying molecular events, as well as their dynamic nature. It must be noted that, the illustrated stroma-mediated mechanism of protection against chemotherapeutic agents was predominantly seen

in myeloid leukemia it cannot be generalized to all myeloid leukemia's, as noted with exception seen with THP1 cell-line.

This study thus demonstrates that myeloid leukemia cells can adapt themselves to the drug-induced stress by interacting with stromal cells in bone-marrow niches. Identifying and targeting such molecular cross talks could potentially prove to be an effective strategy in treating high risk or relapsed patients.

Materials and methods

Cell-lines and patient samples

The human leukemic cell-line such as U937, Kasumi-1, THP-1, Jurkat E6.1, SUP B15 and stromal cell line HS-5 were obtained from ATCC, USA, NB4 was a kind gift from Dr. Harry Iland, RPAH, Sydney, Australia (with permission from Dr. Michel Lanotte), NB4/GFP and NB4/GFP-MAD cells (Kind gift from Dr. Christine Chomienne, Hôpital St. Louis, Paris, France with permission form Dr. F. Besancon) were used in this study. Mycoplasma detection was done once in every 6 months and all the cell-lines used were free from Mycoplasma. The study was approved by the institute review board (IRB Min. No. 7826 dated 18.04.2012). AML, ALL, APL patient samples at diagnosis and relapse were collected, prior to treatment, after getting written and informed consent.

Reagents and antibodies

ATO, a kind gift from Intas Pharmaceuticals Ltd, Ahmedabad, India, was used in the study. Daunorubicin, Cytarabine, Bafilomycin A1, Hydroxychloroquine, Bay11-7086 was procured from Sigma, St. Louis, USA. Antibodies used included those against Actin, ATG12, Beclin1, p62, p65 (Santa Cruz, CA, USA), LC3 (Cell Signaling Technology Inc, Massachusetts, USA), TLR2 (BD Pharmingen, New Jersey, USA) anti-mouse and anti-rabbit secondary antibodies conjugated with horseradish peroxidase (Cell Signaling Technology Inc., Massachusetts, USA) and with alexaflour 488 and 594 (Invitrogen, California, USA) were used for western blotting and immunofluorescence.

Assays for apoptosis

Leukemic cell-lines were added (1×10^5 cells/well) on a layer of primary stromal cells or HS-5 stromal cell-line in 24 well plates or seeded in transwells plates. The co-cultured cells were incubated overnight and then exposed to various chemotherapeutic agents along with appropriate controls. After 48 h incubation at 37 °C CO_2 incubator, the leukemic cells were carefully pipetted out and their viability was measured using Annexin V/7AAD apoptosis assay kit (BD Pharmingen, New Jersey, USA) as per manufacturer's protocol. CD105 staining was used to exclude stromal cells if present during acquisition and analysis. The flow data were analyzed using Cell Quest pro software (BD Biosciences, New Jersey, USA).

Small RNA library preparation and sequencing

Briefly, the NB4 cells were co-cultured with and without HS-5 cells for 24 and 48 h prior to this experiment. Three independent experiments were carried out to serve as biological triplicates. The NB4 cells (control) and the NB4 co-cultured (treated) were compared to generate statistically significant differentially expressed small RNAs. Small RNA libraries were prepared using the Illumina TruSeq small RNA kit as described by the manufacturer (Illumina). 1 microgram of total RNA were used from each sample for the library preparation. 5' and 3' Small RNA adaptors were ligated to the RNA and the ligated products were reverse transcribed using superscript II reverse transcriptase (Invitrogen, California, USA). The RT products were then amplified by PCR and resolved on an 8% polyacrylamide gel. Bands corresponding to 140–160 nucleotides nt were gel eluted. The size and integrity of each library was verified using the Bioanalyser. The libraries were sequenced on an Illumina Hiseq 1000 (Centre for cellular and Molecular Platforms (CCAMP), Bengaluru, India).

miRNA analysis

From the sequencing reads, we trimmed TruSeq small RNA adapters using customized perl script and cutadapt[44] program. We then mapped these reads to rRNA database and unaligned reads were taken for further analysis. We then segregated reads that are 18–24 nucleotides and mapped to GRCh38 Genome and miRNA databases[45] using bowtie v1.0.0[46] Customized perl script was used to obtain count data for all the miRNAs. The count data was normalized using DESeq[47] and the normalized data was used for further analysis. miRNAs which have adjusted p value < 0.05 were considered for further analysis. We plotted volcano plot using R ggplot2 package. For figure esthetic purpose, miRnas with adj.pvalue 1 are replaced with their p-values (if p value > 0.05). Targets for differentially expressed miRNAs were predicted using TargetScan v7.1[48] miRNA targets were overlapped with microarray data to identify targets that are upregulated/not changing. We did pathway and gene Ontology GO analysis of these genes using Gene Set Enrichment Analysis (GSEA)[49].

miRNA RT-PCR

Quantitative PCR was performed using miRNA-specific primers (MSPs). The primer for reverse transcription was designed with double-stranded stem–loop structure with universal reverse primer binding site at 5′ end and last eight nucleotides at the 3′-end complementary to the 3′-end of miRNA. cDNA generated using this Stem-loop-RT

primer was used to carried out real time PCR using miRNA-specific forward primers and universal primer with complementarity to the 'stem' sequence of the MSP. All primers used are listed in below. Reverse transcription was performed using SuperScript III RT (Invitrogen, California, USA), and the quantitative PCR was carried out using SYBR Green (Applied Biosystems, California, USA) as the fluorescent detector on an Applied Biosystems 7900HT machine. *miR-23a-5p* was analyzed for expression profiles at different conditions as mentioned in the respective experiments and levels where normalized to cellular U6snRNA levels. The primer sequences used were given below.

Primer Name	Sequence
U6snRNA RT-primer	CTCAACTGGTGTCGTGGAGTCGGCAATTCAGTTGAGAAAAATAT
U6snRNA Forward primer	ACACTCCAGCTGGGGTGCTCGCTTCGGCA
Universal reverse primer	TGGTGTCGTGGAGTCGCAATTCAGTTG
miR23a* RT-primer	CTCAACTGGTGTCGTGGAGTCGGCAATTCAGTTGAGAAATCCCA
miR23a* Forward primer	ACACTCCAGCTGGGGGGGTTCCTGGGGA

Cloning reporter constructs

Oligos containing three tandem repeat of the complementary sequence to *mir-23a-5p* or TLR-2 3′UTR region were commercially synthesized (Bioserve, Hyderabaed, India), phosphorylated using T4 PNK, annealed, and cloned in to EcoRI and XhoI site in pMXCRGb vector[50]. Positive clones were identified using colony PCR followed by sanger sequencing. Oligo sequences used are:

hsa-miR-23a-5p(forward)-AATTAAATCCCATCCCCAGGAACCCCAAATCCCATCCCCAGGAACCCCAAATCCCATCCCCAGGAACCCC;

hsa-miR-23a-5p(reverse)-5′TCGAGGGGTTCCTGGGGATGGGATTTGGGGTTCCTGGGGATGGGATTTGGGGTTCCTGGGGATGGGATTT3′

TLR2–3′UTR(forward)-5′AATTGACTTCATGGATGCAGAACCCATGACTTCATGGATGCAGAACCCATGACTTCATGGATGCAGAACCCAT3′,

TLR2–3′UTR(reverse)-5′TCGAATGGGTTCTGCATCCATGAAGTCATGGGTTCTGCATCCATGAAGTCATGGGTTCTGCATCCATGAAGTC3′.

TLR2–3′UTR mutant 1 (forward): AATTGACTTCATGGATGCAGATGCCATGACTTCATGGATGCAGATGCCATGACTTCATGGATGCAGATGCCAT

TLR2–3′UTR mutant 1 (reverse): TCGAATGGCATCTGCATCCATGAAGTCATGGCATCTGCATCCATGAAGTCATGGCATCTGCATCCATGAAGTC

TLR2–3′UTR mutant 2 (forward): AATTGACTTCTTGGATGCACATGCCATGACTTCTTGGATGCACATGCCATGACTTCTTGGATGCACATGCCAT

TLR2–3′UTR mutant 2 (reverse): TCGAATGGCATGTGCATCCAAGAAGTCATGGCATGTGCATCCAAGAAGTCATGGCATGTGCATCCAAGAAGTC

Semi-quantitative real time PCR

Total RNA was extracted using Trizol reagent (Invitrogen, California, USA). Five hundred nanogram of the extracted RNA was converted into cDNA using superscript II cDNA kit (Invitrogen, California, USA). The expression of genes was studied using SYBR green method (Finnzymes F410L, Thermo Scientific, Rockford, IL, USA). The Ct values were normalized with *ACTB* and the fold differences were calculated using $2^{-\Delta\Delta Ct}$ method. The NF-κB array (RT^2 profiler PCR array human NF-κB signaling target. Qiagen, Hilden, Germany, Catalogue No: PAHS-225z) was performed according to manufacturer's instructions.

Immunoblots

NB4 homogenates were obtained by cell lysis in RIPA buffer (Sigma, Missouri, USA), with complete protease inhibitors (Roche, Basel, Switzerland). Nuclear extracts were taken from cells using NE-PER kit (Thermo Scientific, Massachusetts, USA) according to the manufacturer's protocol. The lysates and elutes were analyzed in SDS–PAGE. After protein transfer to nitrocellulose membrane, membranes were blocked with non-fat dry milk (5%, 2 h) followed by incubation with primary antibodies overnight. The protein bands were detected by standard chemiluminescence method (ThermoScientific, Massachusetts, USA).

Electroporation

The electroporation of *miR-23a-5p* mimics (Exiqon, Denmark) into NB4 cells were performed using Amaxa electroporator unit (program NB4 X-01) and recovered in complete media for 24 h. Same kit was used to electroporate pMXCRGb and pMXCRGb-TLR2 vectors in NB4 cells. For analysis in vector electroporated experimental set up the cells were gated for RFP positive cells and looked for the expression of GFP upon re-introduction of *miR-23a-5p* mimics.

Immunofluorescence

The leukemic cells were co-cultured with stromal cells, the cells were carefully pipetted out and cytospin slides were made after 6 h of co-culture. The cells were fixed in 4% paraformaldehyde followed by blocking using 5% goat serum. It was further incubated with primary antibodies such as p65 (Santa Cruz, Dallas, USA) overnight at 4 °C. The slides were rinsed with PBS thrice and incubated with secondary antibodies (anti-mouse) conjugated with

alexaflour 594, (Invitrogen, California, USA) for 1 h. The slides were again washed, air dried and counterstained with DAPI containing mountant (Vectashield, California, USA). The images were acquired in fluorescence microscope (Axioimager M1, Carl Zeiss, Germany) at ×100 with oil immersion and images were analyzed using ISIS metasystem, (Metasystems GmbH, Altlussheim, Germany).

Flow cytometry analysis of TLR2 expression

For the expression of TLR2 (CD282) protein on the leukemic cells, phycoerythrin tagged antibody against TLR2 was purchased (PE Mouse Anti-Human CD282 Clone 11G7) from BD Pharmingen (New Jersey, USA). Briefly the cells were washed and incubated with the antibody in dark for 30 min at 4 °C. The cells were washed to remove unbound antibodies and the re-suspended in PBS-albumin (1%) solution. The cells were acquired in Beckman Coulter Gallios (California, USA) and the data were analyzed in FlowJo software V10.07 (Ashland, Orlando USA).

Mouse models and drug treatments

FVB/N mice were obtained from Jackson Laboratory (Maine, USA). Mice at 6 to 8 weeks of age were used in all the experiments. The animal study design and euthanasia protocols were approved by the Institutional animal ethics committee (IAEC approval number 17/2012). A well-established transplantable APL mouse model was used in this study[12,51]. Briefly, APL cells from the spleen of MRP8-PML-RAR transgenic mice (FVB/N) were harvested and cryopreserved (a kind gift from Dr. Christine Chomienne with permission from Dr. Scott Kogan). Mouse APL cells (5×10^4 cells/mouse) were injected intravenously via the tail vein into genetically compatible FVB/N recipients, without conditioning with either radiation or chemotherapy. ATO was given as intra-peritoneal at the concentration of 5 mg/kg of mice starting on day 7 post injection of malignant cells and continued for 28 days, while hydroxychloroquine was also given as intra-peritoneal at the concentration of 60 mg/kg of mice starting on day 7 post injection of malignant cells and continued for 28 days. Blood was collected on day 20 by retro-orbital method and the mice were monitored for their survival.

Acknowledgements

We acknowledge Intas Pharmaceutical Ltd, India and NATCO pharmaceutical Ltd, India for kindly providing us API of pharmaceutical drugs for this study. We thank Dr. Yoshio Kato, AIST, Japan for pMXCRGb plasmid and Angel Fernandes for help with molecular biology experiments. We also thank to Prof. Satyajit Mayor and Prof. Apurva Sarin for their critical inputs on the paper. This study is supported by a Wellcome DBT India Alliance research grant (IA/S/11/2500267) and DBT-COE grant (BT/COE/34/SP13432/2015), New Delhi, India. V.M. is supported by senior fellowship program of Wellcome DBT India Alliance (IA/S/11/2500267), New Delhi, India. N.V. lab is supported by DST-ECR award grant (Grant No. ECR/2016/ 000251), New Delhi, India and N.V. is supported by core funds from St. John's Research Institute, Bangalore, India. SG, HKP, SD were supported by senior research fellowship from Council for Scientific and Industrial Research (CSIR), New Delhi, India.

Author details

[1]Department of Haematology, Christian Medical College, Vellore, India. [2]Institute for Stem Cell Biology and Regenerative Medicine (InStem), Bengaluru, India. [3]Molecular Medicine Department, St. John's Research Institute, St. John's National Academy of Health Sciences, Bengaluru, India

Author's contributions

S.G. and H.K.P. performed research, involved in designing study, performed molecular tests, analyzed data, and wrote paper. V.L. performed research, performed bioinformatics analysis, and analyzed data NB: performed research, performed molecular tests, and analyzed data. A.A.A.: performed research, performed flow cytometry tests, and analyzed data. S.D. performed research, performed molecular tests, and analyzed data. A.V. and A.K. performed research, performed molecular tests, and analyzed data. B.G. performed research, clinical data accrual, and analyzed data. P.B. performed research, performed molecular tests, and analyzed data. D.P. performed research, RNASeq experiment design, and analyzed data. N.V. performed research, designed study, RNAseq data accrual, analyzed data, and wrote paper. V.M. performed research, designed study, clinical data accrual, analyzed data, and wrote paper.

Conflict of interest

The authors declare that they have no conflict of interest.

Ethics approval and consent to participate

The study was approved by the Institutional Review Board (IRB Min. No. 7826 dated 18.04.2012). AML, ALL, APL patient samples at diagnosis and relapse were collected, prior to treatment, after getting written and informed consent. The animal study design and euthanasia protocols were approved by the Institutional Animal Ethics Committee (IAEC approval number 17/2012).

Supplementary Information accompanies this paper at (https://doi.org/10.1038/s41419-019-1964-8).

Received: 3 April 2019 Revised: 8 August 2019 Accepted: 5 September 2019
Published online: 30 September 2019

References

1. Alderton, G. K. The tumour microenvironment drives metastasis. *Nat. Rev. Cancer* **16**, 199–199 (2016).
2. Medyouf, H. The microenvironment in human myeloid malignancies: emerging concepts and therapeutic implications. *Blood* **129**, 1617–1626 (2017).
3. Meads, M. B., Gatenby, R. A. & Dalton, W. S. Environment-mediated drug resistance: a major contributor to minimal residual disease. *Nat. Rev. Cancer* **9**, 665 (2009).
4. Bakker, E., Qattan, M., Mutti, L., Demonacos, C. & Krstic-Demonacos, M. The role of microenvironment and immunity in drug response in leukemia. *Biochimica et. Biophysica Acta* **1863**, 414–426 (2016).
5. Wang, W. et al. Aberrant levels of miRNAs in bone marrow microenvironment and peripheral blood of myeloma patients and disease progression. *J. Mol. Diagnostics* **17**, 669–678 (2015).
6. Chou, J., Shahi, P. & Werb, Z. microRNA-mediated regulation of the tumor microenvironment. *Cell cycle* **12**, 3262–3271 (2013).
7. Abdi, J., Qiu, L. & Chang, H. Micro-RNAs, New performers in multiple myeloma bone marrow microenvironment. *Biomark. Res.* **2**, 10 (2014).
8. Moses, B. S. et al. Bone marrow microenvironment niche regulates miR-221/222 in acute lymphoblastic leukemia. *Mol. Cancer Res.* **14**, 909–919 (2016).
9. Zhang, Y., Yang, P. & Wang, X.-F. Microenvironmental regulation of cancer metastasis by miRNAs. *Trends Cell Biol.* **24**, 153–160 (2014).

10. Mathews, V. et al. Single-agent arsenic trioxide in the treatment of newly diagnosed acute promyelocytic leukemia: long-term follow-up data. *J. Clin. Oncol.* **28**, 3866–3871 (2010).
11. Bai, D.-M. & Zheng, X.-F. PML-RARA mutations confer varying arsenic trioxide resistance. *Protein Cell* **8**, 296–301 (2017).
12. Ganesan, S. et al. Rationale and efficacy of proteasome inhibitor combined with arsenic trioxide in the treatment of acute promyelocytic leukemia. *Leukemia* **30**, 2169–2178 (2016).
13. Jacamo, R. et al. Reciprocal leukemia-stroma VCAM-1/VLA-4-dependent activation of NF-kappaB mediates chemoresistance. *Blood* **123**, 2691–2702 (2014).
14. Chendamarai, E. et al. Comparison of newly diagnosed and relapsed patients with acute promyelocytic leukemia treated with arsenic trioxide: insight into mechanisms of resistance. *PLoS ONE* **10**, e0121912 (2015).
15. Chhabra, R., Adlakha, Y. K., Hariharan, M., Scaria, V. & Saini, N. Upregulation of miR-23a∼27a∼24-2 cluster induces caspase-dependent and -independent apoptosis in human embryonic kidney cells. *PLoS ONE* **4**, e5848 (2009).
16. Wang, H. et al. Inhibition of miR-155 protects against lps-induced cardiac dysfunction and apoptosis in mice. *Mol. Therapy Nucleic Acids* **5**, https://doi.org/10.1038/mtna.2016.80 (2016).
17. Chen, L. et al. MiR-29b-3p promotes chondrocyte apoptosis and facilitates the occurrence and development of osteoarthritis by targeting PGRN. *J. Cell. Mol. Med.* **21**, 3347–3359 (2017).
18. Tian, Z. et al. Investigational agent MLN9708/2238 targets tumor suppressor microRNA-33b in MM cells. *Blood* https://doi.org/10.1182/blood-2012-01-401794 (2012).
19. Han, M.-S., Lee, J. M., Kim, S.-N., Kim, J.-H. & Kim, H.-S. Human papillomavirus 16 oncoproteins downregulate the expression of miR-148a-3p, miR-190a-5p, and miR-199b-5p in cervical. *Cancer BioMed. Res. Int.* **2018**, 1942867–1942867 (2018).
20. Zhou, F. et al. MiR-663a stimulates proliferation and suppresses early apoptosis of human spermatogonial stem cells by targeting NFIX and regulating cell cycle. *Mol. Therapy Nucleic Acids* **12**, 319–336 (2018).
21. Bai, H. et al. Involvement of miR-125a in resistance to daunorubicin by inhibiting apoptosis in leukemia cell lines. *Tumor Biol.* **39**, 1010428317695964 (2017).
22. Zhao, Y., Xu, K. & Liu, P. Post-transcriptional control of angiotensin II type 1 receptor regulates osteosarcoma cell death. *Cell. Physiol. Biochem.* **45**, 1581–1589, https://doi.org/10.1159/000487719 (2018).
23. Quan, J. et al. Oncogenic miR-23a-5p is associated with cellular function in RCC. **16**, 2309–2317 (2017).
24. Chen, B. et al. miR-23a suppresses pancreatic cancer cell progression by inhibiting PLK-1 expression. *Mol. Med. Rep.* **18**, 105–112 (2018).
25. Ntoufa, S., Vilia, M. G., Stamatopoulos, K., Ghia, P. & Muzio, M. Toll-like receptors signaling: A complex network for NF-kappaB activation in B-cell lymphoid malignancies. *Semin. Cancer Biol.* **39**, 15–25 (2016).
26. Kawai, T. & Akira, S. Signaling to NF-kappaB by toll-like receptors. *Trends Mol. Med.* **13**, 460–469 (2007).
27. Boelens, M. C. et al. Exosome transfer from stromal to breast cancer cells regulates therapy resistance pathways. *Cell* **159**, 499–513 (2014).
28. Vyas, N. & Dhawan, J. Exosomes: mobile platforms for targeted and synergistic signaling across cell boundaries. *Cell. Mol. Life Sci.* **74**, 1567–1576 (2017).
29. Mehmeti, M. et al. Wnt5a is a TLR2/4-ligand that induces tolerance in human myeloid cells. *Commun. Biol.* **2**, 176 (2019).
30. Parchure, A., Vyas, N. & Mayor, S. Wnt and hedgehog: secretion of lipid-modified morphogens. *Trends Cell Biol.* **28**, 157–170 (2018).
31. Lotterman, C. D., Kent, O. A. & Mendell, J. T. Functional integration of microRNAs into oncogenic and tumor suppressor pathways. *Cell Cycle* **7**, 2493–2499 (2008).
32. Rushworth, S. A. et al. Understanding the role of miRNA in regulating NF-κB in blood cancer. *Am. J. Cancer Res.* **2**, 65–74 (2012).
33. Rathore, M. G. et al. The NF-κB member p65 controls glutamine metabolism through miR-23a. *Int. J. Biochem. Cell Biol.* **44**, 1448–1456 (2012).
34. Zhang, Y.-C. et al. The NF-κB p65/miR-23a-27a-24 cluster is a target for leukemia treatment. *Oncotarget* **6**, 33554–33567 (2015).
35. Gu, X., Gao, Y., Mu, D.-G. & Fu, E.-Q. MiR-23a-5p modulates mycobacterial survival and autophagy during mycobacterium tuberculosis infection through TLR2/MyD88/NF-κB pathway by targeting TLR2. *Exp. Cell Res.* **354**, 71–77 (2017).
36. Rybka, J. et al. The expression of Toll-like receptors in patients with acute myeloid leukemia treated with induction chemotherapy. *Leuk. Res.* **39**, 318–322 (2015).
37. Bjørkøy, G. et al. Chapter 12 monitoring autophagic degradation of p62/SQSTM1. *Methods Enzymol.* **452**, 181–197 (2009).
38. Xie, Y. et al. Posttranslational modification of autophagy-related proteins in macroautophagy. *Autophagy* **11**, 28–45 (2015).
39. Borthakur, G. et al. High expression of autophagy related proteins negatively impacts clinical outcomes in acute myelogenous leukemia–time to target autophagy to improve therapy outcomes? *Blood* **118**, 2513–2513 (2011).
40. Lian, Y. et al. Clinical significance of BECLIN1 and ATG5 expression in acute myeloid leukemia patients. *Int J. Clin. Exp. Pathol.* **11**, 1529–1537 (2018).
41. Sui, X. et al. Autophagy and chemotherapy resistance: a promising therapeutic target for cancer treatment. *Cell Death Dis.* **4**, e838–e838 (2013).
42. Piya, S. et al. Atg7 suppression enhances chemotherapeutic agent sensitivity and overcomes stroma-mediated chemoresistance in acute myeloid leukemia. *Blood* **128**, 1260–1269 (2016).
43. Sumitomo, Y. et al. Cytoprotective autophagy maintains leukemia-initiating cells in murine myeloid leukemia. *Blood* **128**, 1614–1624 (2016).
44. Martin, M. Cutadapt removes adapter sequences high.-throughput sequencing reads. *EMBnet J.* **17**, 10–12 (2011).
45. Kozomara, A. & Griffiths-Jones, S. miRBase: annotating high confidence microRNAs using deep sequencing data. *Nucleic Acids Res.* **42**, D68–D73 (2014).
46. Langmead, B., Trapnell, C., Pop, M. & Salzberg, S. L. Ultrafast and memory-efficient alignment of short DNA sequences to the human genome. *Genome Biol.* **10**, R25 (2009).
47. Anders, S. & Huber, W. Differential expression analysis for sequence count data. *Genome Biol.* **11**, R106 (2010).
48. Agarwal, V., Bell, G. W., Nam, J. W. & Bartel, D. P. Predicting effective microRNA target sites in mammalian mRNAs. *eLife* **4**, https://doi.org/10.7554/eLife.05005 (2015).
49. Subramanian, A. et al. Gene set enrichment analysis: a knowledge-based approach for interpreting genome-wide expression profiles. *Proc. Natl Acad. Sci. USA* **102**, 15545–15550 (2005).
50. Kato, Y. et al. Real-time functional imaging for monitoring miR-133 during myogenic differentiation. *Int. J. Biochem. Cell Biol.* **41**, 2225–2231 (2009).
51. Brown, D. et al. A PMLRARalpha transgene initiates murine acute promyelocytic leukemia. *Proc. Natl Acad. Sci. USA* **94**, 2551–2556 (1997).

frontiers in Immunology

ORIGINAL RESEARCH
published: 14 June 2018
doi: 10.3389/fimmu.2018.01357

Arsenic Trioxide Enhances the NK Cell Cytotoxicity Against Acute Promyelocytic Leukemia While Simultaneously Inhibiting Its Bio-Genesis

*Ansu Abu Alex[1], Saravanan Ganesan[1], Hamenth Kumar Palani[1], Nithya Balasundaram[1], Sachin David[1], Kavitha M. Lakshmi[1], Uday P. Kulkarni[1], P. N. Nisham[1], Anu Korula[1], Anup J. Devasia[1], Nancy Beryl Janet[1], Aby Abraham[1], Alok Srivastava[1], Biju George[1], Rose Ann Padua[2,3], Christine Chomienne[2,3], Poonkuzhali Balasubramanian[1] and Vikram Mathews[1]**

[1] Department of Hematology, Christian Medical College, Vellore, India, [2] UMR-S1131, Hôpital Saint Louis, Paris, France, [3] Institut Universitaire d'Hématologie, Universite Paris Diderot, Paris, France

OPEN ACCESS

Edited by:
Chiara Romagnani, Deutsches Rheuma-Forschungszentrum (DRFZ), Germany

Reviewed by:
Jacques Zimmer, Luxembourg Institute of Health (LIH), Luxembourg
Catharina C. Gross, Universität Münster, Germany

***Correspondence:**
Vikram Mathews
vikram@cmcvellore.ac.in

Specialty section:
This article was submitted to NK and Innate Lymphoid Cell Biology, a section of the journal Frontiers in Immunology

Received: *25 October 2017*
Accepted: *31 May 2018*
Published: *14 June 2018*

Citation:
Alex AA, Ganesan S, Palani HK, Balasundaram N, David S, Lakshmi KM, Kulkarni UP, Nisham PN, Korula A, Devasia AJ, Janet NB, Abraham A, Srivastava A, George B, Padua RA, Chomienne C, Balasubramanian P and Mathews V (2018) Arsenic Trioxide Enhances the NK Cell Cytotoxicity Against Acute Promyelocytic Leukemia While Simultaneously Inhibiting Its Bio-Genesis. Front. Immunol. 9:1357. doi: 10.3389/fimmu.2018.01357

Natural killer cells (NK) contribute significantly to eradication of cancer cells, and there is increased interest in strategies to enhance it's efficacy. Therapeutic agents used in the treatment of cancer can impact the immune system in a quantitative and qualitative manner. In this study, we evaluated the impact of arsenic trioxide (ATO) used in the management of acute promyelocytic leukemia (APL) on NK cell reconstitution and function. In patients with APL treated with single agent ATO, there was a significant delay in the reconstitution of circulating NK cells to reach median normal levels from the time of diagnosis (655 days for NK cells vs 145 and 265 days for T cells and B cells, respectively). *In vitro* experiments demonstrated that ATO significantly reduced the CD34 hematopoietic stem cell (HSC) differentiation to NK cells. Additional experimental data demonstrate that $CD34^+$ sorted cells when exposed to ATO lead to a significant decrease in the expression of *IKZF2*, ETS1, and TOX transcription factors involved in NK cell differentiation and maturation. In contrast, exposure of NK cells and leukemic cells to low doses of ATO modulates NK cell receptors and malignant cell ligand profile in a direction that enhances NK cell mediated cytolytic activity. We have demonstrated that NK cytolytic activity toward NB4 cell line when exposed to ATO was significantly higher when compared with controls. We also validated this beneficial effect in a mouse model of APL were the median survival with ATO alone and ATO + NK was 44 days (range: 33–46) vs 54 days (range: 52–75). In conclusion, ATO has a differential quantitative and qualitative effect on NK cell activity. This information can potentially be exploited in the management of leukemia.

Keywords: natural killer cells, arsenic trioxide, immune response, acute promyelocytic leukemia, APL mouse model, NK cellular therapy

INTRODUCTION

There is increased evidence that the immune system plays a role in the prevention of cancer and also in the maintenance of durable remission post chemotherapy (1). Cells of both innate and adaptive arms of the immune system contribute to immune surveillance (2), and there are mechanisms by which malignant cells can escape from such surveillance (3). Anti-cancer drugs can be lymphodepleting,

immunostimulatory, or both (4, 5), and they also play a pivotal role in mediating anti-leukemic immune response (6, 7). Sensitization of malignant cells using chemotherapeutic agents helps in eliciting productive immune responses (8, 9).

Natural killer cells (NK) or innate lymphoid cells (ILCs) are a part of the innate immune system and are involved in the surveillance against malignant cells (10). Activated NK cells have been known to be effective in killing the tumor targets (11). The clinical efficacy of NK cell immunotherapy is well known in hematological malignancies (12). Various agents, such as all trans-retinoic acid and sodium valproate, were evaluated for their ability to induce NK ligands on leukemic cells and augmenting immune mediated anti-leukemic effect (13). Upregulation of functional activating receptors on NK cells by interleukin 15 (14), nicotinamide (15), or lenalidomide (16) to improve NK cell cytotoxicity has also been reported. Additional studies have shown the role of killer immunoglobulin-like receptor (KIR) gene haplotype as a predictor of disease outcome (17).

Acute promyelocytic leukemiaAPL is a subtype of acute myeloid leukemia (AML) characterized with distinct molecular and clinical features, and majority of cases characterized by the fusion between retinoic acid receptor alpha gene (RARα) on chromosome 17 and the partner gene promyelocytic leukemia (PML) on chromosome 15 as a result of reciprocal translocation t(15;17)(q24;q21), leading to the expression of a novel PML-RARα oncoprotein (18). Arsenic trioxide (ATO), as a single agent, is effective in the management of newly diagnosed cases of acute promyelocytic leukemia (APL). ATOArsenic trioxide, in a dose-dependent manner, exerts its therapeutic effect by promoting degradation of the oncoprotein that drives the growth of APL cells (19). Despite its efficacy in the treatment of APL, relapses occurs in 5–30% of cases mostly within the high-risk subset (20). It has been demonstrated that immune response is important in sustaining long-term molecular remission in a transplantable mouse model of APL (21, 22). There is are significant data which address the mechanisms of action of ATO on malignant promyelocytes (19, 23) and our own data looking at the extrinsic factors causing resistance to ATO (24), but limited data is are available on its effect on the innate and adaptive immune system. A few studies have shown the immunomodulatory property of ATO by up-regulating the NK ligands on tumor cells thereby increasing the susceptibility of cancer cells to NK cells (25).

Immune reconstitution following cessation of chemotherapy is one of the factors that have a potential impact on disease recurrence (26). Immune reconstitution has been studied extensively in hematological malignancies in context with hematopoietic stem cell transplantation (HSCT) in Ref. (27). NK cells were known to reconstitute rapidly post-transplant (28) while certain studies have shown impaired NK cell numbers and function (29, 30) post chemotherapy. There are limited data concerning long-term recovery of the immune subsets post chemotherapy in leukemia, and there are no data on the effect of ATO on immune reconstitution. Hence in this study we evaluated, the impact of ATO on the NK cell function and recovery and role of NK cellular therapy in combination with ATO.

MATERIALS AND METHODS

Cell Lines and Primary Cells

The human APL cell lines used in this study were NB4 (kind gift from Dr. Harry Iland, RPAH, Sydney, NSW, Australia with permission from Dr. Michel Lanotte), all-trans retinoic acid resistant cell line UF1 (kind gift from Dr. Christine Chomienne, Hôpital Saint-Louis, Paris) and an in-house generated ATO-resistant cell line NB4-EVAsR1 (detailed methodology in Supplementary Methods S1 in Supplementary Material). The myeloid cell lines K562, HL60, and U937, the lymphoid cell lines Jurkat E6.1 and SUP-B15, and NK cell line NK92MI were obtained from American Type Culture Collection (ATCC, Rockville, MD, USA). The cell lines were cultured at 37°C in a humidified atmosphere containing 5% CO_2 and were characterized phenotypically by flow cytometry and free of mycoplasma contamination (Universal Mycoplasma detection Kit, ATCC). Patients newly diagnosed with APL from March 2010 to May 2015 ($n = 112$) were prospectively enrolled in this study after getting written and informed consent. The patients were treated with single agent ATO as has been previously reported by us (31, 32) (detailed treatment protocol in Supplementary Methods S2). Peripheral blood samples were collected at different treatment time points as depicted in **Figure 1**. Samples were also collected from patients who have completed treatment for more than 2 years. The study was approved by the institutional review board, Christian Medical College, Vellore (IRB Min no: 7081 dated 17.02.2010) and have been performed in accordance with the ethical standards as laid down in the 1964 Declaration of Helsinki and its later amendments or comparable ethical standards.

In Vitro ATO Cytotoxicity Assay

The *in vitro* sensitivity of the malignant cell lines toward ATO was determined at 48 h using MTT assay (Biotium, Inc., CA, USA) as described previously (24). All experiments were done in triplicates and the half-maximal inhibitory concentration (IC50) values were generated using Graph Pad Prism V6 software (La Jolla, CA, USA).

NK Cell Cytotoxicity Assay

The cytotoxic activity of NK cell line NK92MI against malignant myeloid (K562, U937, HL60, UF1, NB4, and NB4-EVAsR1) and lymphoid cell lines (Jurkat E6.1, SUP-B15) was assessed using the CFSE/7AAD cytotoxicity assay kit (Cell Technology, Mountain view, CA, USA). Briefly the effector cells (NK cells) and CFSE (carboxyfluorescein diacetate succinimidyl ester) stained target cells (1×10^5 leukemic cells) were cocultured in different ratios 1:1, 2:1, 5:1, 10:1 in a 24-well plate with 500 µl 10% RPMI media. At the end of incubation at 37°C for 5 h, the cells were washed, and 2.5 µl of 7AAD was added to the samples and acquired in FACS Calibur (Becton Dickinson, Mansfield, MA, USA). The percentage of cytotoxicity was calculated, and the spontaneous death of the target cells was subtracted as background control. In a parallel set of experiments, the leukemic cell lines or NK cell line were exposed to 1 µM ATO overnight for 12 h and cytotoxicity was measured as described above.

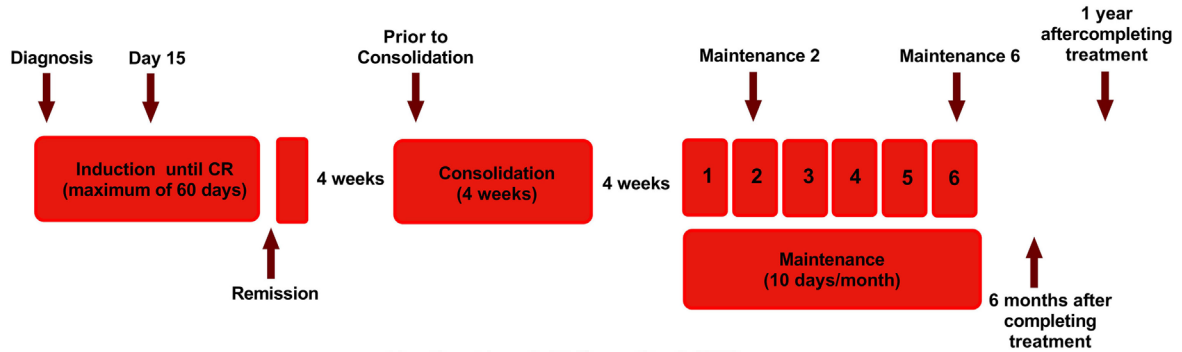

FIGURE 1 | Diagram showing the treatment protocol followed in our institution for newly diagnosed acute promyelocytic leukemia and time points of sample collection for this study. Arsenic trioxide (ATO) was administered intravenously at a dose of 10 mg for adults and 0.15 mg/kg for pediatric patients. Single-agent ATO was administered until complete hematologic remission (CR) for a maximum of 60 days. Following a 4-week interval, ATO was administered for another 4 weeks as a consolidation course, for those in CR. Again after a 4-week interval, for those continuing to remain in CR, single agent ATO was administered 10 days a month for 6 months (31). The arrow marks represent the time points in which samples were collected.

NK Cell Proliferation Assay

NK92MI (1×10^6 cells) were left untreated or treated with 1 μM ATO and seeded in 24-well plates in 500 μl minimal essential medium (MEM) supplemented with 10% FBS and checked for the proliferation. The intensity of CFSE was measured by flow cytometry using BD FACS Calibur at FL1 channel at 24, 48, and 72 h respectively.

NK Cell Degranulation Assay

NK92MI (5×10^5 cells/well) was plated in 96-well U-bottom plates at in the presence of CD107a (BD Pharmingen, San Diego, CA, USA) and was resuspended in 200 μl 10% RPMI media. Degranulation was induced by adding the leukemic target cells (5×10^5 per well, effector/target [E:T] ratio 2:1). At the end of incubation at 37°C for 5 h, CD56 was added and incubated for 20 min followed by PBS wash and were acquired in FACS Calibur (Becton Dickinson, Mansfield, MA, USA). The percentage of $CD107a^+CD56^+$ cells was measured. In another set of experiments, the target cells were treated with 1 μM ATO for 12 h, and NK cells were measured for degranulation. Similarly in APL patients who were on maintenance therapy with ATO, CD107a expression was measured by gating on $CD56^+CD3^-$ cells with and without adding target cells (NB4) ($n = 9$) and compared with healthy controls ($n = 7$).

Immunophenotyping Studies

To check for the expression of activating and inhibitory receptors on NK92MI cell line and NK ligands on leukemic cells, 1×10^6 cells were seeded in a 24-well plate and were left untreated or treated with 1 and 2 μM ATO for 6 and 24 h. The cells were then washed and stained with antibodies to NK cell receptors, and ligands along with the respective isotypic control antibodies (details of antibodies used are provided in Supplementary Methods S3) followed by incubation in the dark for 20 min. Unbound antibodies were removed by washing with phosphate buffer saline, and flow cytometric analysis was carried out in BD FACS Calibur (Becton Dickinson, Mansfield, MA, USA). The data were analyzed using BD CellQuest Pro software and plotted as histograms.

For immune reconstitution studies, peripheral blood samples were collected from newly diagnosed APL patients and stained with monoclonal antibodies and analyzed for the T cell subsets, B cells, NK cell subsets, and dendritic cells (Supplementary Methods S3). Following incubation with antibodies, a standard NH4Cl whole-blood lysing technique was done, and the washed cells were acquired and analyzed. Cell surface analysis was performed with a BD FACS Calibur flow cytometer (BD Biosciences, San Jose, CA, USA) using Cell quest pro software and absolute counts were calculated.

Genotyping of Human KIR Genes

Genomic DNA was extracted from the bone marrow or peripheral blood samples from APL patients by standard protocols, and KIR genotyping was performed by sequence-specific primers (SSP-PCR) using KIR typing kit (Miltenyi Biotech, Bergisch Gladbach, Germany), and the presence or absence of 15 human KIR genes plus two pseudo genes were analyzed.

NK Cell Therapy in APL Mouse Model

FVB/N mice were obtained from Jackson Laboratory (Bar Harbor, ME, USA). Mice at 6–8 weeks of age were used in all the experiments. The animal study design and euthanasia protocols were approved by the institutional animal ethics committee, Christian Medical College, Vellore (IAEC approval number 2/2012). Cells from the spleen of MRP8-PML-RARa transgenic FVB/N mice (33) were used to create APL transplantable model. APL blast cells were then harvested and cryopreserved (a kind gift from Dr. Christine Chomienne, Hôpital Saint-Louis with the permission from Dr. Scott Kogan and Dr. Michael Bishop). APL cells (5×10^4 cells/mouse) were injected intravenously *via* the tail vein into genetically compatible FVB/N recipients, without conditioning with either radiation or chemotherapy. Leukemic mice were then divided into following groups: ATO alone, NK cells alone, ATO + NK, ATO + IL-15, ATO + NK + IL-15,

and placebo group. ATO was given intraperitoneally at the concentration of 5 μg/g of mice starting on day 7 post injection of malignant cells and continued for 28 days. NK cells were isolated from the spleen of normal FVB/N and a total of 5×10^5 NK cells were injected intravenously *via* the tail vein for 3 doses with 10 days interval. 100 ng of recombinant mouse IL-15 was given intraperitoneally for a total of 5 doses with 5 days interval and survival was monitored (details of the methodology are provided in Supplementary Methods S4).

Stem Cell-Derived NK Cell Differentiation

$CD34^+$ cells were sorted from umbilical cord blood samples obtained after getting written and informed consent (approved by institutional review board (Ethics Committee) of Christian Medical College, Vellore, EC min no. IRB (EC) 16/08/2006) using EasySep Human CD34 positive selection Kit (Stem cell Technologies, Vancouver, Canada) and was cultured in NK differentiation medium (10%RPMI + 10 ng SCF + 30 ng FLT3 + 50 ng IL-15) (Supplementary Methods S5). They were assessed for NK differentiation on day 8 and day 14 with or without exposure to 0.5 μM ATO by flow cytometry.

Quantitative Real-Time PCR (RQ-PCR) for NK Cell Transcription Factors

RNA was extracted from CD34 cells in culture with or without exposure to 0.5 μM ATO on day 0 and day 14. The expression levels of NK transcription factors EOMES, IKZF2, PRDM1, KLF4, ETS1, TOX, and TBX21 were determined based on TaqMan® Gene Expression Assays (Supplementary Methods S6).

Statistical Analysis

Data were represented as mean of values ± SD or as median values with range as indicated in the figure legends. Student's *t*-test or Mann–Whitney *U* test was used to statistically compare the continuous variables. For reconstitution, graphs values were plotted as median with interquartile ranges. The relationships of clinical features to outcome were analyzed by Cox proportional hazard model. Logistic regression was used to compare the parameters with the end of induction RT-PCR values. The probability of survival was estimated with the use of the product-limit method of Kaplan–Meier for overall survival (OS) and event free survival (EFS), and the significance was assessed by the log-rank test. All survival estimates are reported as ±1SE. All *p*-values were 2-sided, with values of 0.05 or less indicating statistical significance. Statistical analysis used the SPSS 16.0 Software (Chicago, IL, USA). Non-linear regression curves and graphs were done with GraphPad Prism V6 software (California, USA) for calculating IC-50 values.

RESULTS

ATO Does Not Have Direct Cytotoxic Effect on NK Cells

In order to evaluate the cytotoxic effect of ATO on the malignant cell lines *in vitro*, MTT assay was done. The mean IC50 values of ATO was assessed at micromolar (μM) concentrations for all the cell lines used in this study (Table S1 in Supplementary Material). We observed that there was a wide variation in the IC50 values between different myeloid and lymphoid cell lines.

To evaluate the cytotoxic effect of ATO on NK cells at the concentrations, we used for the downstream experiments, MTT assay and a cell viability assay were done. The IC50 of NK92MI cell line was 3.84 ± 0.3μM ($n = 4$), and the 7-AAD positive cells were 1.48% when treated with 1 μM ATO for 24 h (Figure S1 in Supplementary Material). We have also checked the proliferation of NK cell line treated with 1 μM ATO for 24 h, 48 h, and 72 h. We have observed that the ATO concentration and duration of exposure used in our experiment was not cytotoxic to NK cells and did not alter the rate of proliferation (Figure S2 in Supplementary Material).

Differential Cytolytic Activity of NK Cells Toward Leukemic Cell Lines

Next, we evaluated the cytolytic activity of NK92MI toward different malignant myeloid and lymphoid cell lines. Toward this, we have performed CFSE 7AAD cytotoxicity assay. At the highest effector (NK cells), target (leukemic cell line) ratio of 10:1, significant cytolytic activity was noted against K562 cell line (65.15 ± 6.2%, $n = 3$). The mean cytolytic activity against NB4 was 21.5 ± 3.7% ($n = 3$), and HL-60 was 12.97 ± 1.7% ($n = 3$). The mean cytolytic activity of NK cells toward all the cell lines tested was summarized in **Table 1**. We observed that leukemic cell lines have a differential susceptibility to the cytolytic activity of NK cell line.

ATO Enhances the Cytolytic Activity of NK Cells

Since a significant NK cytolytic activity was observed against NB4, we next checked the effect of ATO on the NK cytotoxic activity toward these cell lines. We observed that NB4 cells when treated overnight with 1 μM ATO (>99% viability retained after this exposure) significantly increased the cytotoxic effect of NK92MI at all E:T ratios evaluated ($p = 0.002$) with a mean percentage cytolytic activity of 27.04 ± 7.3% ($n = 5$) at the highest E:T ratio of 10:1 (**Figure 2**). A similar cytolytic pattern was seen with other cell lines though it was not as prominent or significant as seen with NB4 cells (data not shown).

As CD107a is a functional marker for NK cell activity, we performed CD107a degranulation assay to evaluate the effect of ATO on NK cell activity toward these cell lines. At an E:T ratio

TABLE 1 | The percentage cytolytic activity of NK92MI cell line toward different leukemic cell lines at the E:T ratio of 10:1 assessed by CFSE/7AAD cytotoxicity assay.

Cell lines	% cytolytic activity (mean ± SD) ($n = 3$)
NB4	21.5 ± 3.7
NB4-EVAsR1	4.4 ± 0.65
UFI	16.32 ± 5.9
K562	65.15 ± 6.2
U937	10.9 ± 1.03
HL60	12.97 ± 1.7
SUP-B15	6.65 ± 2.7
Jurkat E6.1	16.7 ± 7.8

The data are represented as mean ± SD (n = 3).

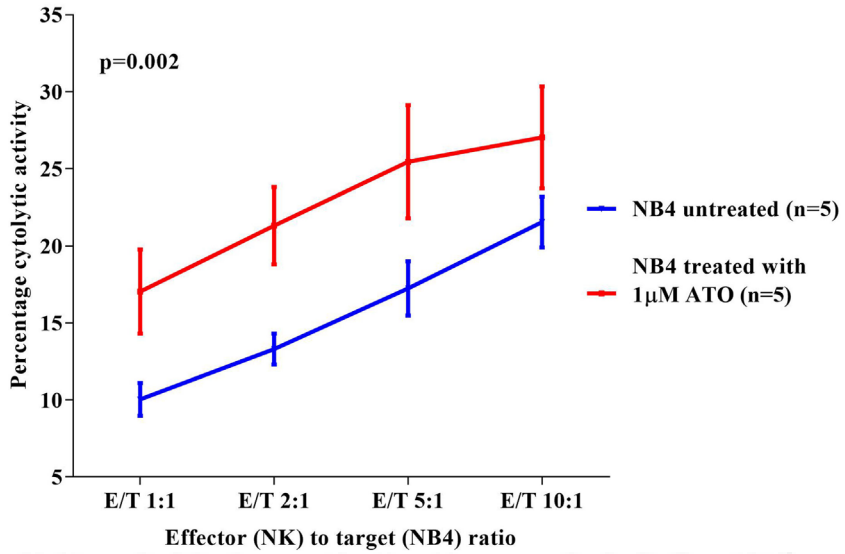

FIGURE 2 | Comparison of percentage cytolytic activity of NK92MI cell line toward NB4 untreated and treated with arsenic trioxide (ATO) (1 μM for 12 h). The CFSE labeled NB4 cells (1 × 10^5 cells untreated or treated with 1 μM ATO for 12 h) were co-cultured with effector cells (NK cell line) in different E:T ratios 1:1, 2:1, 5:1, 10:1 in a 24-well plate with 500 μl 10% RPMI media. At the end of incubation at 37°C for 5 h, the cells were washed, and 2.5 μl of 7AAD was added to the samples and acquired in FACS Calibur. The percentage cytolytic activity was calculated, and the values were plotted as mean with SEM (n = 5). p-value less than 0.05 was considered significant.

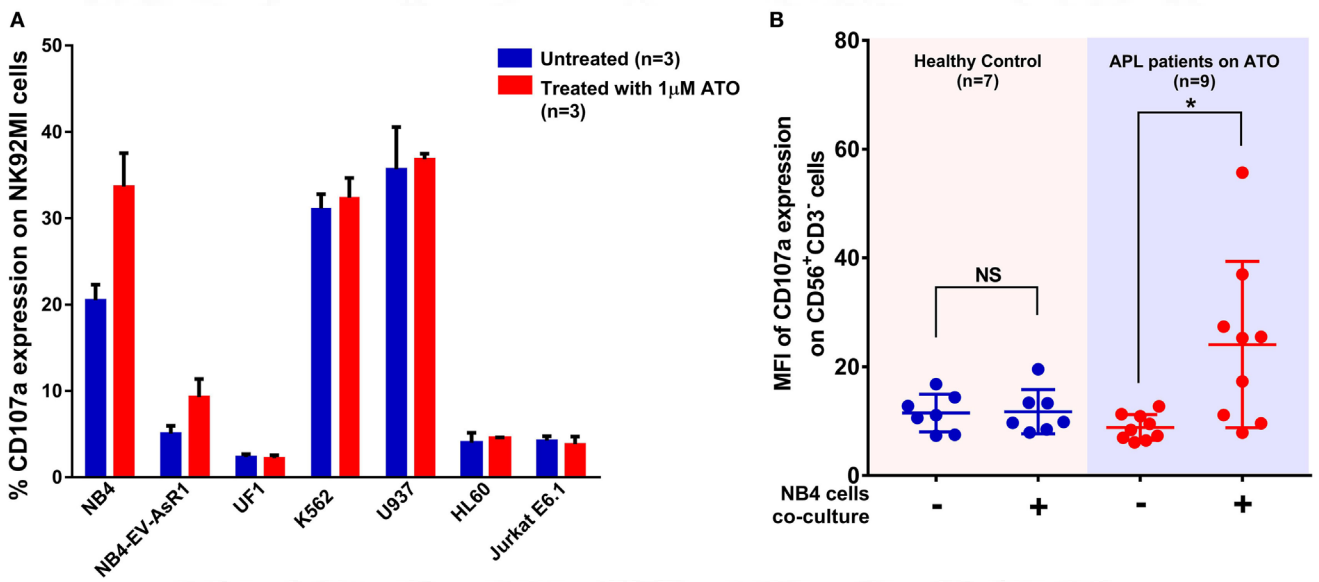

FIGURE 3 | Arsenic trioxide (ATO) enhances the cytolytic activity of NK cells. **(A)** Bar graphs showing the percentage expression of CD107a (a marker for degranulation of NK) when NK cell lines were cocultured with leukemic cell lines at the ratio of 2:1 for 5 h. The blue bars represent the experiment with untreated leukemic cell lines and the red bars represent the experiment after exposure of leukemic cell lines to 1 μM ATO for 12 h (n = 3). **(B)** Graph shows the mean fluorescence intensity (MFI) of CD107a expression gated on $CD56^+CD3^-$ cells obtained from PBMNCs of healthy controls (no ATO exposure; n = 7) and acute promyelocytic leukemia (APL) patients (under ATO treatment; n = 9) with and without co-culture of NB4 cells at the ratio of 2:1 for 5 h.

of 2:1 (n = 3), the mean percentage of CD107a with NB4 cell line without ATO treatment was 20.4 ± 1.8% at the end of 5 h. Whereas, when treated with 1 μM of ATO for 12 h there was a significant increase in the percentage of CD107a (33.6 ± 3.8%, n = 3) (**Figure 3A**). The mean percentages of CD107a of K562, U937, HL60, and Jurkat were 31.3 ± 1.6, 35.6 ± 4.8, 4 ± 1.13, and 4.2 ± 0.5%, respectively and of the resistant cell lines NB4-EVAsR1 and UF1 were 5.08 ± 0.8 and 2.33 ± 0.33%, respectively. Exposure

of these cell lines with 2 μM ATO did not significantly increase the CD107a expression (data not shown). We were also able to demonstrate this effect of ATO on NK cells ($CD56^+CD3^-$) *in vivo* by showing an increased expression of CD107a in APL patients (undergoing ATO treatment) when co-cultured with NB4 cells compared to healthy controls (no ATO exposure) (**Figure 3B**; Figure S3 in Supplementary Material).

ATO Alters NK Cell Receptor and Ligand Profile

In order to study the mechanism of increased cytolytic activity of NK cells in the presence of ATO, we checked the NK receptors and ligand profiles upon exposure to ATO by flow cytometry. We identified that NK92MI cell line upon 6 h of exposure 1 μM ATO resulted in increased expression of activating receptors NKG2D, NKP30, and KIR2DS4 and inhibitory receptor NKG2A and decrease in inhibitory receptors KIR3DL1/DL2 (**Figure 4A**). The cells also retained 99% viability at the end of 24 h by 7AAD assay. There were no changes in the expression of NKP46, KIR2DL1, KIR2DL2, and DNAM1 receptors (data not shown). Increased concentration of ATO (2 μM) or increased exposure time (24 h) did not further increase the expression of these markers. Similar increased expression of NKG2D receptor was observed in NK cells from APL patients on remission

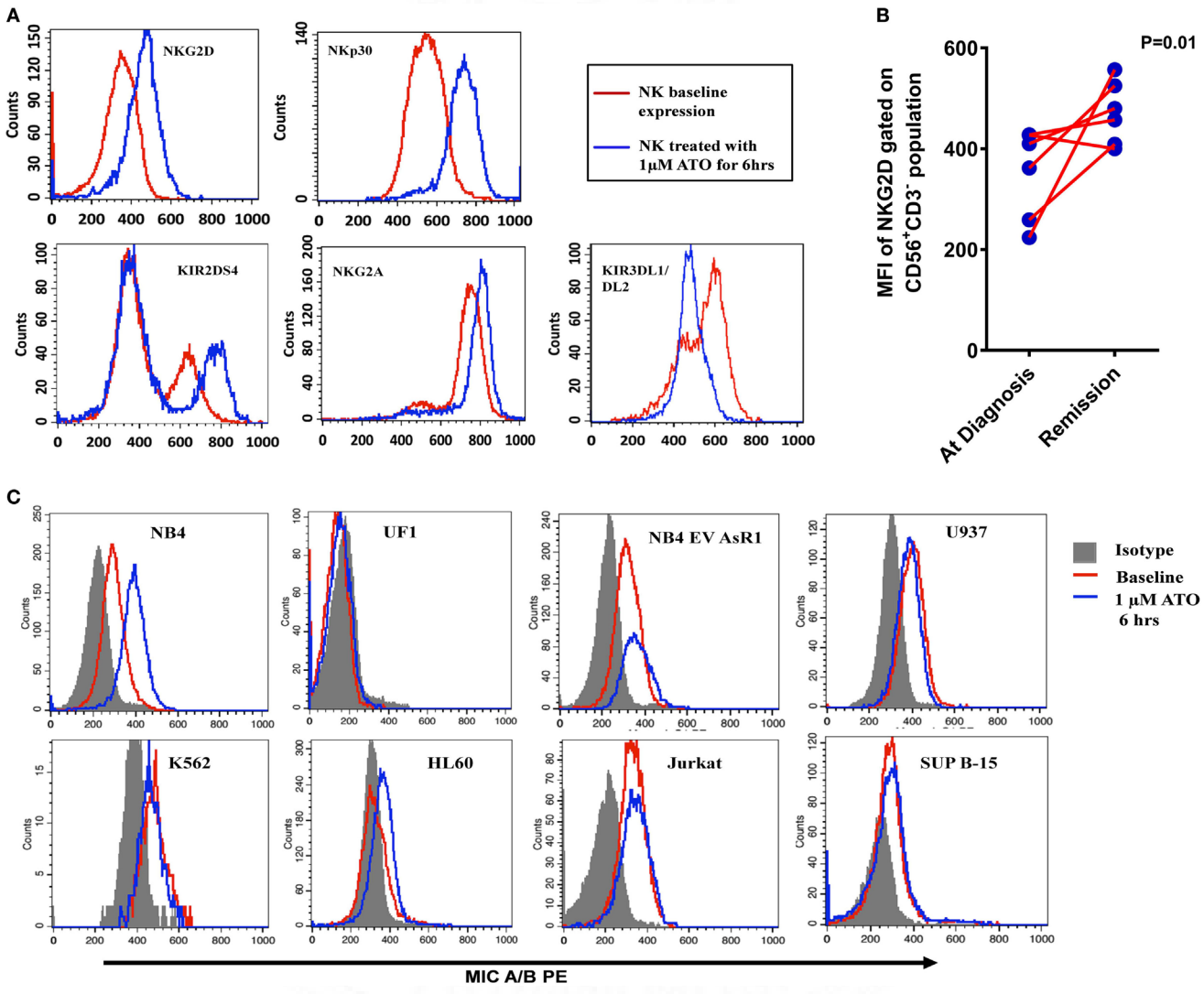

FIGURE 4 | Alteration of NK receptor and ligand profile by arsenic trioxide (ATO). **(A)** Representative histogram plots of NK activating receptors NKG2D, NKp30, and KIR2DS4 and NK inhibitory receptor NKG2A of NK cell line (NK92MI) treated with 1 μM ATO for 6 h ($n = 5$). The red lines represent the baseline expression and the blue lines which show a shift toward right indicated the increased expression with 1 μM ATO treatment for 6 h. **(B)** Mean fluorescence intensity (MFI) of NKG2D receptor expression (gated on $CD56^+CD3^-$ population) in PBMNCs of acute promyelocytic leukemia (APL) patients at diagnosis and on remission ($n = 6$). **(C)** Representative histogram plots of MICA/B expression in myeloid and lymphoid cell lines treated with 1 μM ATO for 6 h ($n = 3$). The shaded region represents the isotypic controls and the red line represents the baseline expression of ligands. The blue lines which show a shift toward the right in NB4 indicating increased expression of MICA/B after ATO treatment which was not observed in other cell lines.

when compared to their matched diagnosis samples following treatment with ATO. The median of NKG2D receptor's mean fluorescence intensity (MFI) was 386 (224–428) at diagnosis and on remission it increased to 468.6 (400–557) ($n = 6$, $p = 0.01$) (**Figure 4B**; Table S2 in Supplementary Material).

We also evaluated the effect of exposure of leukemic cell lines to 1 μM ATO for 6 h on NK ligand expression by flow cytometry. There is a significant increase in activating ligand MICA/B in NB4 cell line ($n = 3$; $p = 0.016$) and a marginal increase in HL60 when compared with other malignant cell lines (**Figure 4C**) on exposure to ATO. Similarly, there was a significant increase in the expression of CD112/Nectin-2 (DNAM-1 ligand) and HLA Class I in NB4 cell line on treatment with ATO (Figure S4 in Supplementary Material). There was no further increase in the expression of the above ligands when treated with increased concentrations or with increased exposure time.

NK Cellular Therapy With ATO Prolong the Survival in APL Mouse Model

Since we have observed the role of ATO in inducing the functional activity of NK cells, we then assessed the ability of NK cells in extending the survival in APL transplantable model (**Figure 5A**). Leukemic mice treated with NK cells alone did not show any improvement in survival when compared with the group treated with ATO (**Figure 5B**). Whereas, when ATO was given along with 3 doses of NK cells shows a significantly increased survival with a median survival of 54 days (range: 52–75 days) when compared with ATO group with a median survival of 44 days (range: 33–46 days) ($p = 0.0006$) (**Figure 5B**). Addition of IL-15 along with ATO and NK cells had an added survival advantage in comparison to the group treated with ATO + NK cells even though not statistically significant ($p = 0.328$) (Figure S5 in Supplementary Material).

Genotype Analysis of Activating and Inhibitory KIR Genes

To evaluate the expression of KIRs in APL patients who received treatment with single agent ATO based regimen, a standard KIR genotyping assay was done ($n = 55$). The median follow-up of this cohort was 46 months and 16 cases relapsed following initial therapy. All the 16 KIR genes (6 activating receptors KIR2DS1, KIR2DS2, KIR2DS3, KIR2DS4, KIR2DS5, KIR3DS1 and 8 inhibitory receptors KIR2DL1, KIR2DL2, KIR2DL3, KIR2DL4, KIR2DL5, KIR3DL1, KIR3DL2, KIR3DL3) and 2 pseudo genes (KIR2DP1, KIR3DP1) have been screened in all

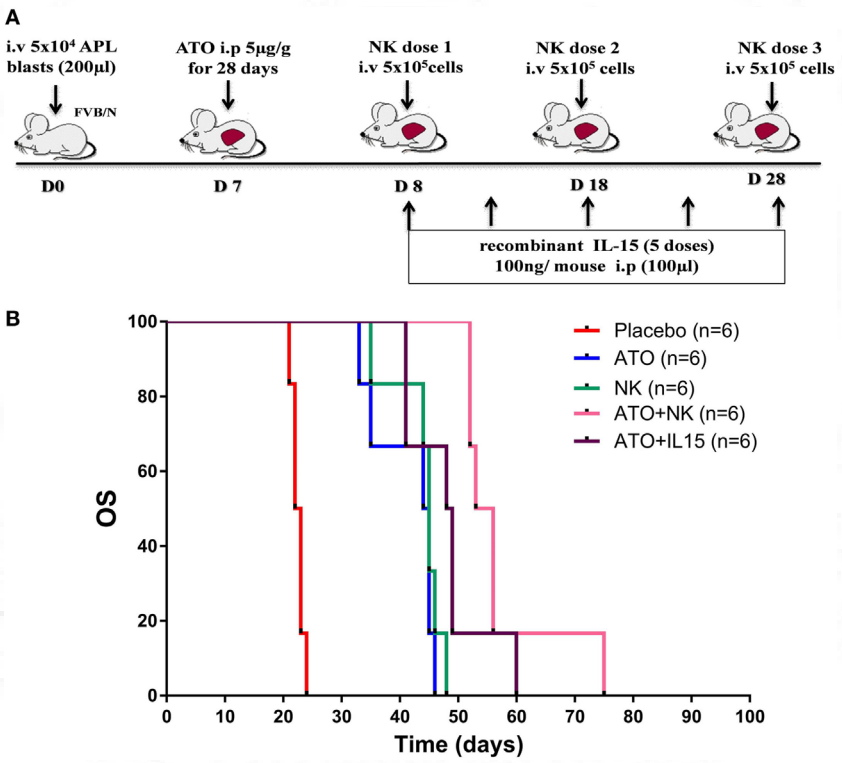

FIGURE 5 | NK cell therapy improved the overall survival in acute promyelocytic leukemia (APL) mice. **(A)** Schematic representation of NK cell therapy in APL mouse model. The time points and doses of administration of arsenic trioxide (ATO), NK cells, and IL-15 were mentioned. Mouse APL cells (5×10^4 cells/mouse) were injected intravenously *via* tail vein into wild-type FVB/N (Day 0). ATO (5 μg/g intra-peritoneal) was given from day 7 for 28 days. NK cells were sorted from the spleen of wild-type FVB/N and given intravenously (5×10^5 NK cells/mouse, 3 doses) from day 8 with 10 day intervals. Recombinant mouse IL-15 (100 ng/mouse, 5 doses) was administered intraperitoneally from day 8 with 5 day intervals. **(B)** Survival curve showing FVB/N treated with ATO, NK cells alone, ATO + NK cells, ATO + IL15, and placebo ($n = 6$/arm). Mice treated with ATO along with 3 doses of NK shows a significantly increased survival (median survival 54 days, range: 52–75 days) when compared with ATO alone (median survival 44 days, range: 33–46 days) ($p = 0.000$). *p*-value less than 0.05 was considered significant.

the patients (**Table 2**). Out of the 55 patients screened, 18.2% ($n = 10$) of the patients had A haplotype and 81.2% ($n = 45$) patients had B haplotype. On a univariate analysis, there was no specific association with any specific genotype or haplotype with the risk of relapse or any other clinical outcome parameter. However, there was a trend toward significance for KIR2DL2 inhibitory receptor in relapse patients (13 relapse patients out of 16 are positive for KIR2DL2) when compared to non-relapse group ($p = 0.069$) with a hazard ratio of 3.2 (95% CI: 0.91–11.26) (Table S3 in Supplementary Material).

Delayed Recovery of NK Cells in Newly Diagnosed APL Patients Treated With Single Agent ATO

We then looked at the immune reconstitution pattern of immune subsets in APL patients treated with single agent ATO at different time points of therapy (clinical details of the patients were given in Supplementary Results S1 in Supplementary Material and Table S4 in Supplementary Material). Following treatment with ATO, there was a differential pattern of immune reconstitution in different lymphocyte subsets (**Figure 6**; Figure S6–8 in Supplementary Material). The time span for circulating NK cells to achieve the median normal levels was beyond 655 days (1 year post treatment) when compared with T cells and B cells [145 days (at maintenance cycle 2) and 265 days (at maintenance cycle 6) respectively]. We observed a significant delay in the reconstitution of NK cells (median absolute counts at 6 months post treatment was 120.84 cells/μl, range: 27.85–484.22 cells/μl vs the long term follow-up samples median 177.85 cells/μl, range: 61.02–635.37 cells/μl) (Table S5 in Supplementary Material). We have also looked at the reconstitution pattern of two major subsets of NK cells, $CD56^{bright}$, and $CD56^{dim}$. The median absolute counts of $CD56^{dim}$ subset were lower throughout the course of treatment when compared with $CD56^{bri}$ subset (**Figure 6**). The $CD56^{+}CD3^{+}$ NKT subset lies almost in the normal limits till the end of maintenance.

Looking at the recovery pattern of other subsets, the earliest recovery to the normal range was seen in the $CD3^{+}CD8^{+}$ T cytotoxic cells, and the CD4/CD8 ratio remains inverted until the start of consolidation therapy. The absolute counts of the immune subsets at different time points of treatment were given in Tables S5 and S6 in Supplementary Material.

TABLE 2 | Table showing the presence or absence 16 KIR genes screened in APL patients ($n = 55$).

KIR genes	Number of APL patients ($n = 55$)	
	Positive	Negative
2DL1	55	0
2DL2	34	21
2DL3	44	11
2DL4	55	0
2DL5 A/B	40	15
2DS1	33	22
2DS2	32	23
2DS3	27	28
2DS4 Del	42	13
2DS4 Ins	19	36
2DS5	32	23
3DL1	45	10
3DL2	55	0
3DL3	55	0
3DS1	32	23
2DP1	55	0
3DP1	55	0

The framework genes KIR2DL4, KIR3DL2, KIR3DL3 and KIR3DP1, the pseudogenes KIR3DP1 and KIR2DP1 and KIR2DL1 is present in all the patients and controls. KIR, killer immunoglobulin-like receptor; APL, acute promyelocytic leukemia.

Impact of NK Cell Subset Reconstitution on Clinical Outcomes of Patients Treated With ATO

Since we observed a delayed NK cell recovery on treatment with ATO, we looked at the impact of this NK maturation pattern on clinical outcomes of APL patients. At the end of induction, the absolute counts of $CD56^{bright}$ $CD16^{-}$ immature subset were significantly lower in those patients who were RT-PCR positive ($n = 28$) with a median of 2.15 (range: 0.06–11.87) cells/μl compared with those who were RT-PCR negative ($n = 37$) with a median of 3.92 (range: 0.14–9.9) cells/μl ($p = 0.046$) (**Figure 7**). However, the NK reconstitution pattern did not correlate with EFS or OS. No other subsets evaluated at the end of induction were significant (data not shown).

Assessment of NK Differentiation From CD34 Cells With and Without ATO Treatment

Even though ATO was shown to have modulating the NK cell cytolytic activity, there was a defect in the NK cell recovery. Hence, we hypothesized that ATO may have an impact on normal hematopoietic stem cell (HSC) ability to differentiate and mature into NK cells accounting for this delay in reconstitution. Hence, we assessed the NK cell differentiation from CD34 cells *in vitro* with and without exposure to 0.5 μM ATO by flow cytometry. We observed that 5.1 ± 0.3% cells were positive for $CD56^{+}CD3^{-}$ NK on day 8 and it increased to 7.7 ± 0.4% on day 14 in the culture without ATO. Whereas, CD34 sorted cells seeded in media with ATO had only 2.3 ± 0.4% $CD56^{+}CD3^{-}$ cells on day 8 ($n = 3$, $p = 0.017$) and 5.2 ± 0.4% on day 14 ($n = 3$, $p = 0.038$) showing a delay in NK differentiation *in vitro*. There was a slight increase in the myeloid compartment on day 14 in culture whereas CD3 and CD19 remained the same (Figure S9 in Supplementary Material).

Role of Transcription Factors Involved in NK Cell Differentiation

In view of this quantitative defect in NK cells, we next evaluated the role of transcription factors contributing to NK differentiation and maturation. Even though the precise hierarchy of the transcription factors that control NK cell maturation is not known, we evaluated the expression of some of the major transcription factors like *EOMES, IKZF2, PRDM1, ETS1, TOX, KLF4*, and *TBX21* which are involved in the differentiation of CD34 cells to mature activated NK cells (34, 35). We observed a

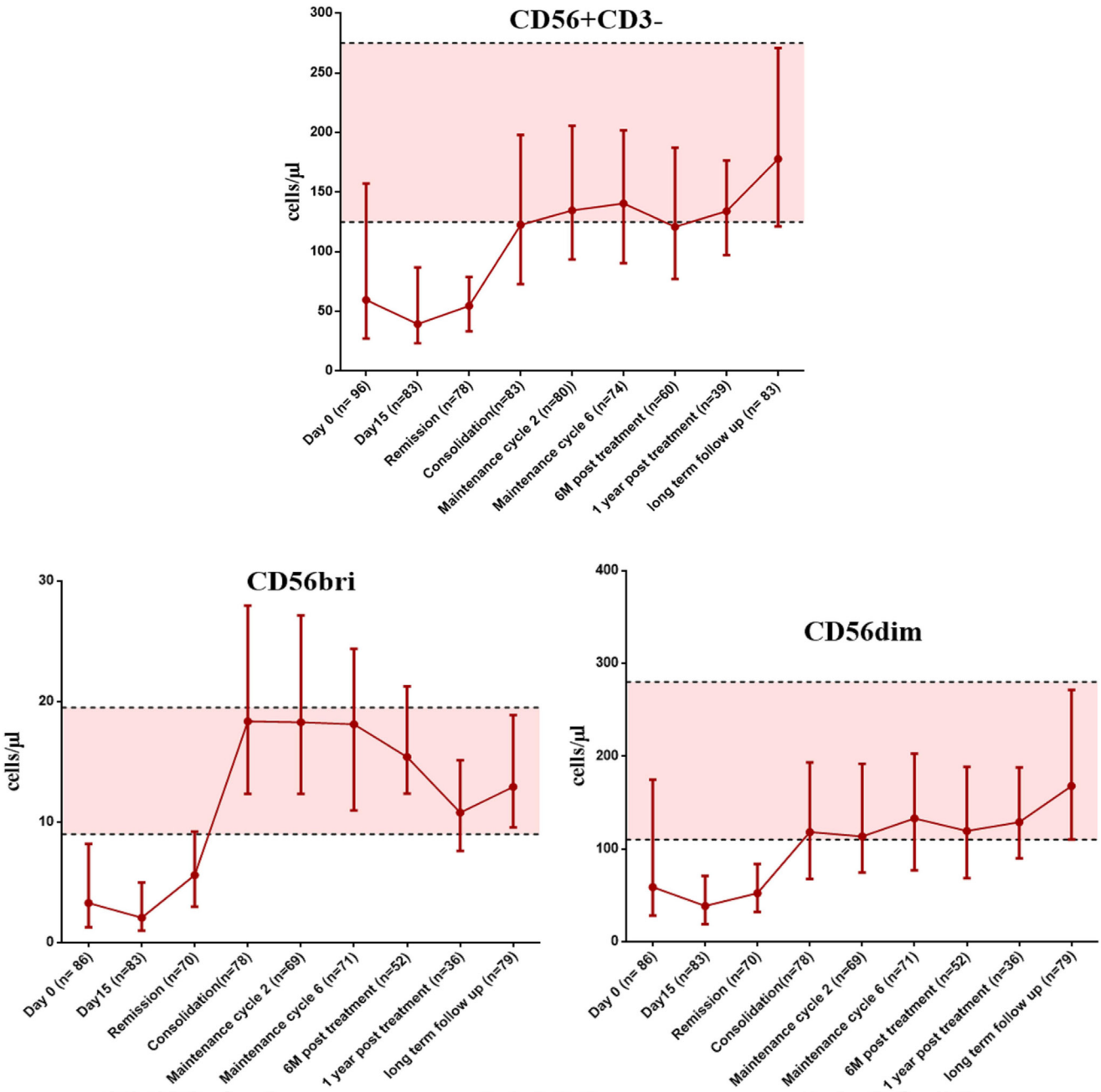

FIGURE 6 | The graphs showing the recovery of NK cells and it subsets (CD56^{bright} and CD56^{dim}) at appropriate time points post treatment with arsenic trioxide. The error bars indicate median with interquartile ranges. The shaded region represents the 25th to 75th percentile values of very long term follow-up samples serve as normal reference ranges. Number of samples available at each time points were mentioned in brackets. The time points of samples collected were mentioned on X axis. Absolute counts were given as cells per microliter on Y axis.

significant decrease in the expression of TFs *IKZF2, ETS 1*, and *TOX* in day 14 CD34 cells treated with ATO when compared to untreated ($p = 0.0005$, $p = 0.002$, and $p = 0.002$ respectively), which are shown to be involved in the transition from pre NK cells to immature NK (**Figure 8**). *TBX21* which is also involved in maturation of NK cells was not downregulated on treatment with ATO.

DISCUSSION

There is accumulating evidence of anti-cancer chemotherapy additionally being involved in augmentation of host immune reactivity (36). Earlier publications from our center showed the efficacy of single agent ATO in terms of durable remissions and minimal toxicity for the treatment of newly diagnosed APL

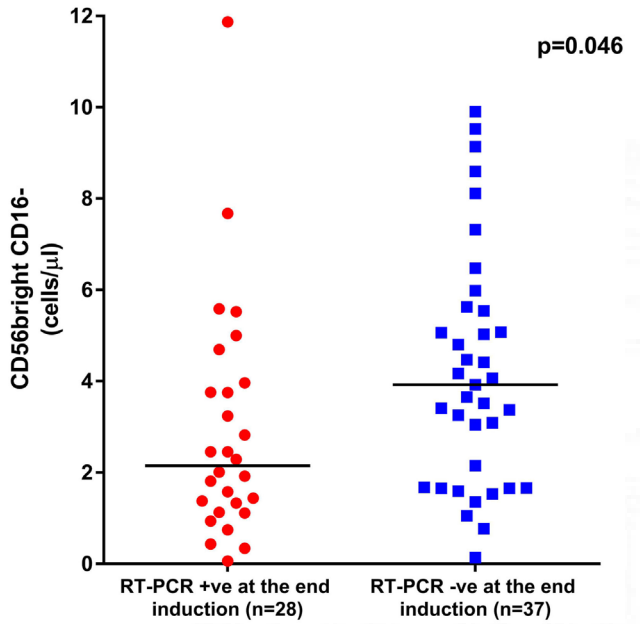

FIGURE 7 | Graphs showing the impact of CD56^{bright} CD16^{-} subset recovery on clinical outcome. The median absolute counts of CD56^{bright} CD16^{-} immature subset was significantly lower in those patients who were RT-PCR positive at the end of induction (n = 28) with a median of 2.15 cells/µl (range: 0.06–11.87 cells/µl) when compared with those who were RT-PCR negative (n = 37) with a median of 3.92 cells/µl (range: 0.14–9.9 cells/µl, p = 0.046).

patients (31). Studies were done looking at the ability of malignant promyelocytes to concentrate ATO intracellularly (37) and the role of ABC transporters involved in ATO efflux (38). Also, our group has looked at the innate environment mediated drug resistance to ATO in APL leukemic cells (24). Some studies have reported that ATO binds directly to cysteine residues and has shown direct interaction between ATO and the PML protein (39). Other than the known cellular mechanisms of ATO, its role in modulating immune system is less explored.

In this study, we tried to understand the effect of ATO, if any, in modulating the immune responses. Our initial work related to immune reconstitution following treatment of APL with single agent ATO illustrated an unusual pattern of delay in NK cell recovery post completion of treatment. This is contrast with our earlier reported data on NK cell recovery post-allogeneic stem cell transplantation where we noted that NK cells were the first subset to recover (28). Similarly, in many immune reconstitution studies post chemotherapy or post-allogeneic stem cell transplantation, it is usually the cells of the innate system that are the first to reconstitute (23, 30). In this study, the reconstitution pattern of NK cells was distinct and much delayed after exposure to ATO. To the best of our knowledge, this is the first time this observation has been made. This delay in reconstitution could not be explained by a direct cytolytic effect of ATO on NK cells as demonstrated by us. Additionally, as reported by us previously, the patients were treated with single agent ATO, and hence, this delay in reconstitution could not

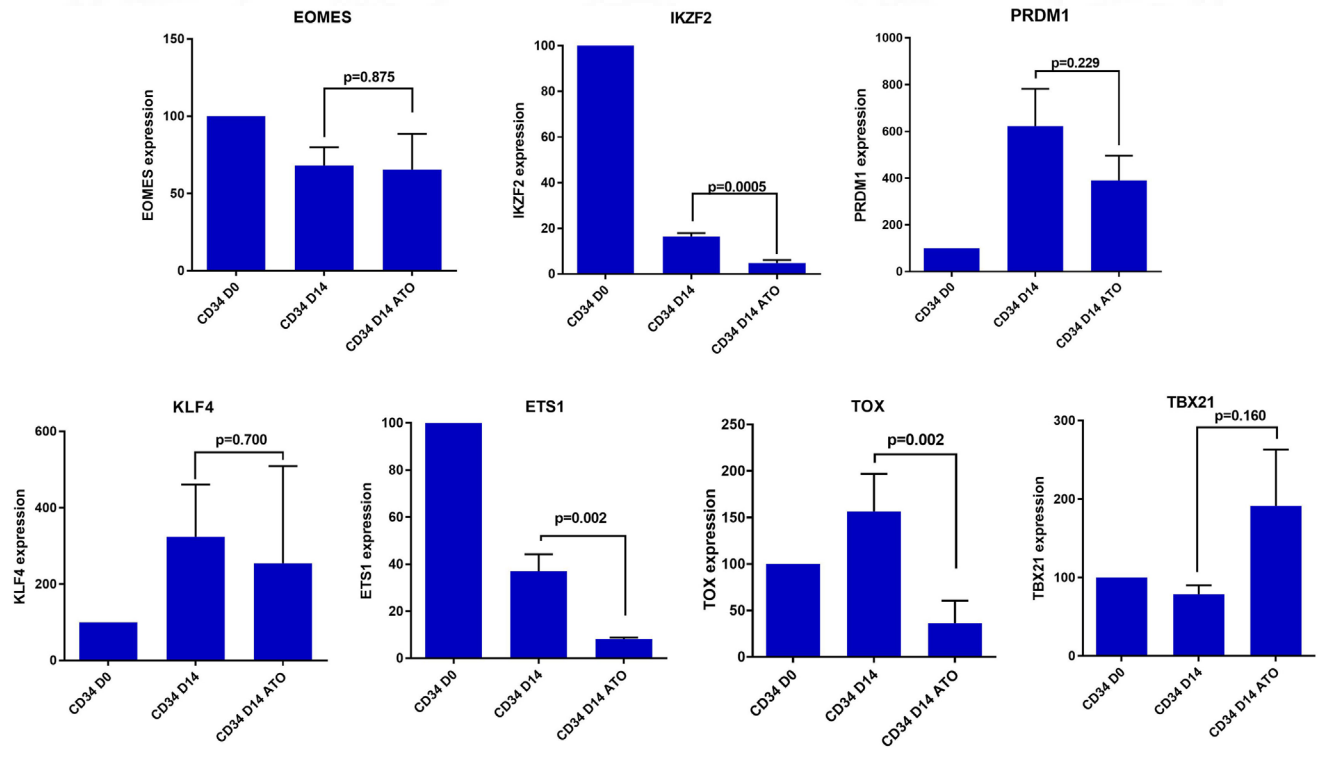

FIGURE 8 | Expression of differentially expressed transcription factors involved in NK cell differentiation and maturation by RQ-PCR. The expression of the genes were determined by $2^{\Delta\Delta CT}$ method. The expression of these genes were normalized to GAPDH and the relative expression of genes on CD34 on day 14 (±ATO) was calculated with CD34 day 0 sample (n = 3). p-value less than 0.05 was considered significant.

be attributed to any other chemotherapeutic agent. This delay in reconstitution persisted even after completing therapy and patient being in molecular remission with an otherwise normal bone marrow study. Immune reconstitution of other cellular subsets was as expected and consistent with previously reported studies. Further, our analysis has shown that among the CD56 subsets, the median absolute counts of $CD56^{dim}$ populations were lower and recovered slowly than the $CD56^{bright}$ population in our cohort. Since $CD56^{bright}$ are the immediate precursors of the CD56 dim subset, we think there is a delay in the differentiation of $CD56^{bright}$ to $CD56^{dim}$ population probably mediated by the exposure with ATO. Our data suggest the effect we observed is more likely to be an effect of ATO on normal differentiation and maturation of NK cells from HSC *in vivo*. Consistent with this hypothesis, we noted that ATO had no direct cytotoxic effect on NK cells *in vitro* nor did it alter the rate of proliferation of NK cells. We further evaluated the effect of ATO on normal $CD34^{+}$ HSC specifically looking at its effect of expression of transcription factors involved with NK cell development and differentiation (40, 41). We noted a significant decrease in the expression of *TOX* and *ETS-1* on day14 in CD34 cells treated with ATO when compared to untreated. These factors are critical for NK cell maturation and differentiation.

In contrast to the effect of ATO in delaying NK cell reconstitution post treatment, we also noted that ATO enhances NK cell-mediated cytolytic activity against leukemia cells. We confirmed this increased cytolytic activity of NK cells by performing CD107a degranulation assay (42). We also noted that this enhance NK cell cytolytic activity was predominantly seen with myeloid cell lines and very little to no effect with lymphoid cell lines.

The diversity of receptors and ligands of NK cells determine its ability to eliminate a defective target (43). We hypothesized that the cytolytic activity is mediated by the presence or absence of activating and inhibitory NK receptors and ligands which could potentially be modulated by ATO. Studies have shown reduction of MICA/B surface expression that may impair NKG2D-mediated immune surveillance of leukemia (44). Our experimental data suggest that ATO alters the NK cell receptor and malignant cell ligand profile in a direction that enhances NK cell mediated cytolytic activity. Similar observation was seen in one other study showing upregulation of NKG2D ligands by ATO in K562, NB4, and MCF7 breast cancer cell lines and increased susceptibility to NK-mediated cytotoxicity (25). Our data suggest that there is also additional modulation of the expression of the NK cell receptors by ATO and this effect could potentially be exploited to enhance NK cell anti-tumor effects. Additional experiments to further validate these observations that could potentially be done and were not done as part of this manuscript, could include blocking/activating of receptors and ligands using either small molecules, blocking antibodies, or activating agents.

Translating the observation from this study, we studied the effect of NK therapy in a mouse model of APL treated with ATO, previously established in our laboratory (10). We hypothesized that infusing mouse NK cells could increase the anti-leukemic activity and hence prolong the survival of mice treated with ATO. We observed that NK cells when infused along with ATO extended the survival in APL mice. NK cells pre-activated with IL-12, IL-15, and IL-18 were shown to induce functional responses against primary AML blasts (45). Our data suggest that addition of IL-15 along with NK cells had an added advantage on survival even though not statistically significant.

We have demonstrated for the first time the role of ATO in modulating the NK cell anti-tumor activity. Low dose ATO exposure to enhance NK cell activity could potentially be exploited in strategies that use NK cell *in vitro* expansion and optimization for treatment of cancer. Administration of ATO to patients prior to NK cell infusion could also be explored as a strategy to enhance NK cell activity especially, from this body of work, in AML.

ETHICS STATEMENT

All procedures performed in studies involving human participants were in accordance with the ethical standards of the institutional research committee and with the 1964 Helsinki declaration and its later amendments or comparable ethical standards.

AUTHOR CONTRIBUTIONS

AAA: performed research, designed study, performed flow cytometry, molecular tests, mouse experiments, analyzed data, and wrote paper. SG: performed research, performed molecular tests, flow cytometry, mouse experiments, and analyzed data. HP: performed research, performed flow cytometry, molecular tests, and analyzed data. NB, SD, and NJ: performed research and analyzed data. KL: performed statistical analysis. UK, PN, AK, AD, AA, AS, and BG: performed research, clinical data accrual, and analyzed data. RP and CC: performed research, mouse experiment design, and analyzed data. PB: performed research, performed molecular tests, and analyzed data. VM: performed research, designed study, clinical data accrual, analyzed data, and wrote paper.

ACKNOWLEDGMENTS

We acknowledge Intas Pharmaceutical Ltd., India and NATCO pharmaceutical Ltd., India for kindly providing us ATO for this study. We thank all the staffs in animal facility, Centre for Stem Cell Research (Unit of InStem–Bangalore), Vellore, India, for helping us with animal studies.

FUNDING

This study is supported by Indian Council of Medical research (ICMR) grant (INDO/FRC/645/2010-IHD) and CEFIPRA/Indo-French Centre for the Promotion of Advanced Research (IFCPAR) grant (IFC/4503-2/2012). VM is supported by senior fellowship program of Wellcome DBT India Alliance (IA/S/11/2500267), New Delhi, India. This study is funded in part by the Department of Biotechnology, New Delhi, India, grant to VM (DBT/COE/34/SP13432/2015). PB is supported by senior fellowship program of

Wellcome-DBT India Alliance (IA/S/15/1/501842), New Delhi. RAP and CC are funded by the Institut National de la Sante et de la Researche Medicale. SG, HKP, SD are supported by senior research fellowship from Council for Scientific and Industrial Research (CSIR), New Delhi, India.

SUPPLEMENTARY MATERIAL

The Supplementary Material for this article can be found online at https://www.frontiersin.org/articles/10.3389/fimmu.2018.01357/full#supplementary-material.

REFERENCES

1. Behl D, Porrata LF, Markovic SN, Letendre L, Pruthi RK, Hook CC, et al. Absolute lymphocyte count recovery after induction chemotherapy predicts superior survival in acute myelogenous leukemia. *Leukemia* (2006) 20(1):29–34. doi:10.1038/sj.leu.2404032
2. Disis ML. Immune regulation of cancer. *J Clin Oncol* (2010) 28(29):4531–8. doi:10.1200/JCO.2009.27.2146
3. Malmberg KJ, Ljunggren HG. Escape from immune- and nonimmune-mediated tumor surveillance. *Semin Cancer Biol* (2006) 16(1):16–31. doi:10.1016/j.semcancer.2005.07.007
4. Lacour S, Hammann A, Wotawa A, Corcos L, Solary E, Dimanche-Boitrel MT. Anticancer agents sensitize tumor cells to tumor necrosis factor-related apoptosis-inducing ligand-mediated caspase-8 activation and apoptosis. *Cancer Res* (2001) 61(4):1645–51.
5. Bracci L, Schiavoni G, Sistigu A, Belardelli F. Immune-based mechanisms of cytotoxic chemotherapy: implications for the design of novel and rationale-based combined treatments against cancer. *Cell Death Differ* (2014) 21(1): 15–25. doi:10.1038/cdd.2013.67
6. Zitvogel L, Apetoh L, Ghiringhelli F, Kroemer G. Immunological aspects of cancer chemotherapy. *Nat Rev Immunol* (2008) 8(1):59–73. doi:10.1038/nri2216
7. Markasz L, Stuber G, Vanherberghen B, Flaberg E, Olah E, Carbone E, et al. Effect of frequently used chemotherapeutic drugs on the cytotoxic activity of human natural killer cells. *Mol Cancer Ther* (2007) 6(2):644–54. doi:10.1158/1535-7163.MCT-06-0358
8. Davies FE, Raje N, Hideshima T, Lentzsch S, Young G, Tai YT, et al. Thalidomide and immunomodulatory derivatives augment natural killer cell cytotoxicity in multiple myeloma. *Blood* (2001) 98(1):210–6. doi:10.1182/blood.V98.1.210
9. Hallett WH, Ames E, Motarjemi M, Barao I, Shanker A, Tamang DL, et al. Sensitization of tumor cells to NK cell-mediated killing by proteasome inhibition. *J Immunol* (2008) 180(1):163–70. doi:10.4049/jimmunol.180.1.163
10. Waldhauer I, Steinle A. NK cells and cancer immunosurveillance. *Oncogene* (2008) 27(45):5932–43. doi:10.1038/onc.2008.267
11. Deng W, Gowen BG, Zhang L, Wang L, Lau S, Iannello A, et al. Antitumor immunity. A shed NKG2D ligand that promotes natural killer cell activation and tumor rejection. *Science* (2015) 348(6230):136–9. doi:10.1126/science.1258867
12. Miller JS, Soignier Y, Panoskaltsis-Mortari A, McNearney SA, Yun GH, Fautsch SK, et al. Successful adoptive transfer and in vivo expansion of human haploidentical NK cells in patients with cancer. *Blood* (2005) 105(8):3051–7. doi:10.1182/blood-2004-07-2974
13. Poggi A, Catellani S, Garuti A, Pierri I, Gobbi M, Zocchi MR. Effective in vivo induction of NKG2D ligands in acute myeloid leukaemias by all-trans-retinoic acid or sodium valproate. *Leukemia* (2009) 23(4):641–8. doi:10.1038/leu.2008.354
14. Boyiadzis M, Memon S, Carson J, Allen K, Szczepanski MJ, Vance BA, et al. Up-regulation of NK cell activating receptors following allogeneic hematopoietic stem cell transplantation under a lymphodepleting reduced intensity regimen is associated with elevated IL-15 levels. *Biol Blood Marrow Transplant* (2008) 14(3):290–300. doi:10.1016/j.bbmt.2007.12.490
15. Childs RW, Carlsten M. Therapeutic approaches to enhance natural killer cell cytotoxicity against cancer: the force awakens. *Nat Rev Drug Discov* (2015) 14(7):487–98. doi:10.1038/nrd4506
16. Jungkunz-Stier I, Zekl M, Stuhmer T, Einsele H, Seggewiss-Bernhardt R. Modulation of natural killer cell effector functions through lenalidomide/dasatinib and their combined effects against multiple myeloma cells. *Leuk Lymphoma* (2014) 55(1):168–76. doi:10.3109/10428194.2013.794270
17. Cooley S, Trachtenberg E, Bergemann TL, Saeteurn K, Klein J, Le CT, et al. Donors with group B KIR haplotypes improve relapse-free survival after unrelated hematopoietic cell transplantation for acute myelogenous leukemia. *Blood* (2009) 113(3):726–32. doi:10.1182/blood-2008-07-171926
18. Sirulnik A, Melnick A, Zelent A, Licht JD. Molecular pathogenesis of acute promyelocytic leukaemia and APL variants. *Best Pract Res Clin Haematol* (2003) 16(3):387–408. doi:10.1016/S1521-6926(03)00062-8
19. Chen GQ, Shi XG, Tang W, Xiong SM, Zhu J, Cai X, et al. Use of arsenic trioxide (As2O3) in the treatment of acute promyelocytic leukemia (APL): I. As2O3 exerts dose-dependent dual effects on APL cells. *Blood* (1997) 89(9): 3345–53.
20. Mathews V, Balasubramanian P, Shaji RV, George B, Chandy M, Srivastava A. Arsenic trioxide in the treatment of newly diagnosed acute promyelocytic leukemia: a single center experience. *Am J Hematol* (2002) 70(4):292–9. doi:10.1002/ajh.10138
21. Westervelt P, Pollock JL, Oldfather KM, Walter MJ, Ma MK, Williams A, et al. Adaptive immunity cooperates with liposomal all-trans-retinoic acid (ATRA) to facilitate long-term molecular remissions in mice with acute promyelocytic leukemia. *Proc Natl Acad Sci U S A* (2002) 99(14):9468–73. doi:10.1073/pnas.132657799
22. Padua RA, Larghero J, Robin M, le Pogam C, Schlageter MH, Muszlak S, et al. PML-RARA-targeted DNA vaccine induces protective immunity in a mouse model of leukemia. *Nat Med* (2003) 9(11):1413–7. doi:10.1038/nm949
23. Ablain J, Nasr R, Bazarbachi A, de The H. The drug-induced degradation of oncoproteins: an unexpected Achilles' heel of cancer cells? *Cancer Discov* (2011) 1(2):117–27. doi:10.1158/2159-8290.CD-11-0087
24. Chendamarai E, Ganesan S, Alex AA, Kamath V, Nair SC, Nellickal AJ, et al. Comparison of newly diagnosed and relapsed patients with acute promyelocytic leukemia treated with arsenic trioxide: insight into mechanisms of resistance. *PLoS One* (2015) 10(3):e0121912. doi:10.1371/journal.pone.0121912
25. Kim JY, Bae JH, Lee SH, Lee EY, Chung BS, Kim SH, et al. Induction of NKG2D ligands and subsequent enhancement of NK cell-mediated lysis of cancer cells by arsenic trioxide. *J Immunother* (2008) 31(5):475–86. doi:10.1097/CJI.0b013e3181755deb
26. van Tilburg CM, van Gent R, Bierings MB, Otto SA, Sanders EA, Nibbelke EE, et al. Immune reconstitution in children following chemotherapy for haematological malignancies: a long-term follow-up. *Br J Haematol* (2011) 152(2): 201–10. doi:10.1111/j.1365-2141.2010.08478.x
27. Savani BN, Mielke S, Rezvani K, Montero A, Yong AS, Wish L, et al. Absolute lymphocyte count on day 30 is a surrogate for robust hematopoietic recovery and strongly predicts outcome after T cell-depleted allogeneic stem cell transplantation. *Biol Blood Marrow Transplant* (2007) 13(10):1216–23. doi:10.1016/j.bbmt.2007.07.005
28. Rajasekar R, Mathews V, Lakshmi KM, George B, Viswabandya A, Chandy M, et al. Cellular immune reconstitution and its impact on clinical outcome in children with beta thalassemia major undergoing a matched related myeloablative allogeneic bone marrow transplant. *Biol Blood Marrow Transplant* (2009) 15(5):597–609. doi:10.1016/j.bbmt.2009.01.016
29. Talpaz M, Bielski M, Hersh EM. Studies of natural killer cell activity and antibody-dependent cell-mediated cytotoxicity among patients with acute leukemia in complete remission. *Cancer Immunol Immunother* (1982) 14(2):96–8. doi:10.1007/BF00200175
30. Alanko S, Salmi TT, Pelliniemi TT. Recovery of natural killer cells after chemotherapy for childhood acute lymphoblastic leukemia and solid tumors. *Med Pediatr Oncol* (1995) 24(6):373–8. doi:10.1002/mpo.2950240607
31. Mathews V, George B, Lakshmi KM, Viswabandya A, Bajel A, Balasubramanian P, et al. Single-agent arsenic trioxide in the treatment of newly diagnosed acute promyelocytic leukemia: durable remissions with minimal toxicity. *Blood* (2006) 107(7):2627–32. doi:10.1182/blood-2005-08-3532

32. Mathews V, George B, Chendamarai E, Lakshmi KM, Desire S, Balasubramanian P, et al. Single-agent arsenic trioxide in the treatment of newly diagnosed acute promyelocytic leukemia: long-term follow-up data. *J Clin Oncol* (2010) 28(24):3866–71. doi:10.1200/JCO.2010.28.5031
33. Brown D, Kogan S, Lagasse E, Weissman I, Alcalay M, Pelicci PG, et al. A PMLRARalpha transgene initiates murine acute promyelocytic leukemia. *Proc Natl Acad Sci U S A* (1997) 94(6):2551–6. doi:10.1073/pnas.94.6.2551
34. Gordon SM, Chaix J, Rupp LJ, Wu J, Madera S, Sun JC, et al. The transcription factors T-bet and Eomes control key checkpoints of natural killer cell maturation. *Immunity* (2012) 36(1):55–67. doi:10.1016/j.immuni.2011.11.016
35. Yun S, Lee SH, Yoon SR, Kim MS, Piao ZH, Myung PK, et al. TOX regulates the differentiation of human natural killer cells from hematopoietic stem cells in vitro. *Immunol Lett* (2011) 136(1):29–36. doi:10.1016/j.imlet.2010.11.008
36. Shurin MR, Naiditch H, Gutkin DW, Umansky V, Shurin GV. Chemo-ImmunoModulation: immune regulation by the antineoplastic chemotherapeutic agents. *Curr Med Chem* (2012) 19(12):1792–803. doi:10.2174/092986712800099785
37. Sahu GR, Jena RK. Significance of intracellular arsenic trioxide for therapeutic response in acute promyelocytic leukemia. *Am J Hematol* (2005) 78(2):113–6. doi:10.1002/ajh.20235
38. Leslie EM, Haimeur A, Waalkes MP. Arsenic transport by the human multidrug resistance protein 1 (MRP1/ABCC1). Evidence that a tri-glutathione conjugate is required. *J Biol Chem* (2004) 279(31):32700–8. doi:10.1074/jbc.M404912200
39. Zhang XW, Yan XJ, Zhou ZR, Yang FF, Wu ZY, Sun HB, et al. Arsenic trioxide controls the fate of the PML-RARalpha oncoprotein by directly binding PML. *Science* (2010) 328(5975):240–3. doi:10.1126/science.1183424
40. Luevano M, Madrigal A, Saudemont A. Transcription factors involved in the regulation of natural killer cell development and function: an update. *Front Immunol* (2012) 3:319. doi:10.3389/fimmu.2012.00319
41. Vong QP, Leung WH, Houston J, Li Y, Rooney B, Holladay M, et al. TOX2 regulates human natural killer cell development by controlling T-BET expression. *Blood* (2014) 124(26):3905–13. doi:10.1182/blood-2014-06-582965
42. Alter G, Malenfant JM, Altfeld M. CD107a as a functional marker for the identification of natural killer cell activity. *J Immunol Methods* (2004) 294(1–2):15–22. doi:10.1016/j.jim.2004.08.008
43. Pegram HJ, Andrews DM, Smyth MJ, Darcy PK, Kershaw MH. Activating and inhibitory receptors of natural killer cells. *Immunol Cell Biol* (2011) 89(2):216–24. doi:10.1038/icb.2010.78
44. Nowbakht P, Ionescu MC, Rohner A, Kalberer CP, Rossy E, Mori L, et al. Ligands for natural killer cell-activating receptors are expressed upon the maturation of normal myelomonocytic cells but at low levels in acute myeloid leukemias. *Blood* (2005) 105(9):3615–22. doi:10.1182/blood-2004-07-2585
45. Romee R, Rosario M, Berrien-Elliott MM, Wagner JA, Jewell BA, Schappe T, et al. Cytokine-induced memory-like natural killer cells exhibit enhanced responses against myeloid leukemia. *Sci Transl Med* (2016) 8(357):357ra123. doi:10.1126/scitranslmed.aaf2341

Conflict of Interest Statement: The authors declare that the research was conducted in the absence of any commercial or financial relationships that could be construed as a potential conflict of interest.

OPEN

Leukemia (2016) **30,** 2169–2178

www.nature.com/leu

ORIGINAL ARTICLE

Rationale and efficacy of proteasome inhibitor combined with arsenic trioxide in the treatment of acute promyelocytic leukemia

S Ganesan[1], AA Alex[1], E Chendamarai[1], N Balasundaram[1], HK Palani[1], S David[1], U Kulkarni[1], M Aiyaz[2], R Mugasimangalam[2], A Korula[1], A Abraham[1], A Srivastava[1], RA Padua[3,4], C Chomienne[3,4], B George[1], P Balasubramanian[1] and V Mathews[1]

Arsenic trioxide (ATO) mediates PML-RARA (promyelocytic leukemia–retinoic acid receptor-α) oncoprotein degradation via the proteasome pathway and this degradation appears to be critical for achieving cure in acute promyeloytic leukemia (APL). We have previously demonstrated significant micro-environment-mediated drug resistance (EMDR) to ATO in APL. Here we demonstrate that this EMDR could be effectively overcome by combining a proteasome inhibitor (bortezomib) with ATO. A synergistic effect on combining these two agents *in vitro* was noted in both ATO-sensitive and ATO-resistant APL cell lines. The mechanism of this synergy involved downregulation of the nuclear factor-κB pathway, increase in unfolded protein response (UPR) and an increase in reactive oxygen species generation in the malignant cell. We also noted that PML-RARA oncoprotein is effectively cleared with this combination in spite of proteasome inhibition by bortezomib, and that this clearance is mediated through a p62-dependent autophagy pathway. We further demonstrated that proteasome inhibition along with ATO had an additive effect in inducing autophagy. The beneficial effect of this combination was further validated in an animal model and in an on-going clinical trial. This study raises the potential of a non-myelotoxic proteasome inhibitor replacing anthracyclines in the management of high-risk and relapsed APL.

Leukemia (2016) **30,** 2169–2178; doi:10.1038/leu.2016.227

INTRODUCTION

Acute promyelocytic leukemia (APL) is characterized by a reciprocal translocation, t(15;17)(q22;q21), that results in a novel *PML-RARA* (*promyelocytic leukemia–retinoic acid receptor-α*) oncogene.[1] Arsenic trioxide (ATO) has proven efficacy as first-line therapy in the treatment of APL.[2] There has been a recent concern of ATO resistance in patients treated with upfront ATO.[3] The focus of ATO resistance has centered on mutations in *PML-RARA* gene,[3–5] specifically missense or point mutations in the B2 domain of the *PML* gene that results in the inability of ATO to directly bind to the PML and PML-RARA oncoprotein, leading to resistance.[5] Although additional mutations have been noted in up to a third of relapsed APL patients in the *PML-RARA* gene, it is not clear whether such mutations are associated with secondary ATO resistance as described for those in the PML B2 domain.[3] However, the published data suggest that patients with such mutations have an unfavorable clinical outcome.[3–5]

The relative specificity of ATO in the treatment of APL results from the ability of ATO to bind directly to the PML and chimeric PML-RARA protein that in turn leads to sumoylation of the PML portion followed by polyubiquitination and subsequent proteasomal degradation.[6,7] Based on the current understanding of the mechanism of action of ATO in APL, proteasomal inhibition would be antagonistic.[8] We had previously reported in an *in vitro* model that there was evidence of significant *de novo* micro-environment-mediated drug resistance (EMDR) to ATO.[9] Recently published data indirectly validate our preliminary observation by demonstrating that stromal cell and malignant promyelocyte interaction, mediated by VLA-4 (very late antigen-4) and VCAM-1)vascular cell adhesion molecule-1) interaction, upregulates the nuclear factor (NF)-κB pathway in both the stromal and malignant cell and in turn mediates chemoresistance.[10]

The direct cytotoxic effect of bortezomib on malignant promyelocytes has been previously reported.[11,12] Similarly, the synergistic effect of ATO and bortezomib on non-APL leukemic cells has been previously reported.[13] Preliminary *in vitro* observations from our laboratory suggest that proteasome inhibition can overcome EMDR to ATO. We also noted a possible synergistic cytotoxic effect of combining bortezomib (a proteasome inhibitor) and ATO on malignant promyelocyte in a stromal co-culture system. These preliminary observations were contradictory to existing dogma on the mechanism of action of ATO. The mechanism of such a synergy has not been previously evaluated and the theoretical antagonism of combining these two agents on PML and PML-RARA degradation, which is central to clearance of the leukemia-initiating compartment in APL and achieving cure,[5,8] has not been addressed. In this study we evaluated the mechanism of bortezomib (BTZ)-induced cytotoxicity against malignant promyelocytes, its potential mechanism of synergy with ATO and the fate of PML-RARA when ATO was combined with BTZ.

[1]Department of Haematology, Christian Medical College, Vellore, India; [2]Genotypic Technology, Bengaluru, India; [3]UMR-S1131, Hôpital Saint Louis, Paris, France and [4]Institut Universitaire d' Hématologie, Universite Paris Diderot, Paris, France. Correspondence: Dr V Mathews, Department of Haematology, Christian Medical College, Ida Scudder Road, Vellore 632004, India.
E-mail: vikram@cmcvellore.ac.in

Received 4 January 2016; revised 12 July 2016; accepted 3 August 2016; accepted article preview online 18 August 2016; advance online publication, 2 September 2016

MATERIALS AND METHODS

Cell lines and primary cells

The human APL cell line NB4[ref. 14] (kind gift from Dr Harry Iland, RPAH, Sydney, Australia, with permission from Dr Michel Lanotte) and an ATO-resistant NB4 cell line NB4 EVAsR1 (generated in-house and derived from NB4) was used for some of the experiments (detailed characterization of this cell line is provided in the Supplementary Methods section). Bone marrow samples from APL patients were collected during diagnosis before treatment and at hematological relapse after obtaining a written informed consent. Mesenchymal stromal cells were expanded *in vitro* using well-established protocols. HS-5 cell line was obtained from ATCC (Manassas, VA, USA). Additional details of cell culture techniques and other cell lines used are provided in the Supplementary Materials and methods. The study was approved by the institutional review board (IRB, Min. No. 7826 dated 18.04.2012).

In vitro cytotoxicity assay

The *in vitro* cytotoxicity of drugs were determined at 48 h using the MTT assay as described previously.[15] The half-maximal inhibitory concentration (IC_{50}) values were generated using Graph Pad Prism5 software (La Jolla, CA, USA). Combination index between drugs was calculated using Calcusyn software (Biosoft, Cambridge, UK).

Assays for apoptosis

Leukemic cell lines or primary APL cells were added (1×10^5 cells/well) on a layer of primary mesenchymal stromal cells or HS-5 stromal cell line in 24-well plates. The co-cultured cells were incubated overnight and then exposed to ATO (2 μM) with and without BTZ (200 nM) along with appropriate controls. After 48 h of incubation at 37 °C CO_2 incubator, the leukemic cells were carefully pipetted out and their viability was measured using Annexin V/7-aminoactinomycin D (7AAD) apoptosis assay kit (BD Pharmingen, San Diego, CA, USA) as per the manufacturer's protocol. CD105 staining was used to exclude stromal cells if present during acquisition and analysis. The flow data were analyzed using Cell Quest pro software (BD Biosciences, San Jose, CA, USA).

Measurement of ROS production

Levels of reactive oxygen species (ROS) were determined by dihydrorhodamine123 (DHR123; Life Technologies, Carlsbad, CA, USA) fluorescence as previously described.[16]

Mitochondrial membrane potential

The mitochondrial membrane potential (Δψm) of the cells treated with drugs was measured using JC-1 dye (Life Technologies, Carlsbad, CA, USA) as previously reported.[17] The fluorescence intensity was measured using Spectramax M4 (Molecular Devices, Sunnyvale, CA, USA) (green channel: excitation: 485 nm; emission: 530 nm; cutoff 515 nm; red channel: excitation: 485 nm; emission: 590 nm; cutoff 570 nm). The ratio of red to green fluorescence (590/530) was calculated and the Δψm of treated cells was compared with the untreated cells.

Proteasome activity assay

1×10^5 NB4 cells were lysed in RIPA buffer (containing protease inhibitor cocktail; Sigma, St Louis, MO, USA) on ice for 30 min. The cell lysates were collected by centrifugation and incubated with proteasome substrate, Z-Gly-Gly-Leu-7-amido-4-methylcoumarin (Z-Gly-Gly-Leu-AMC) (Sigma) for 60 min at 37 °C. After incubation, the fluorescence intensity was measured using Spectramax M4 (Molecular Devices) (excitation: 380 nm emission: 460 nm). The activity of untreated cells was normalized to 100% and the treated cell activity was compared with that of the untreated cells.

Co-immunoprecipitations and immunoblots

NB4 homogenates were obtained by cell lysis in RIPA buffer (Sigma), with complete protease inhibitors (Roche, Basel, Switzerland). Co-immunoprecipitation was performed using Co-IP kit (Thermo Pierce, Rockford, IL, USA) according to the manufacturer's protocol. Nuclear extracts were taken from cells using NE-PER kit (Thermo Pierce) according to the manufacturer's protocol. The lysates and elutes were analyzed in SDS–polyacrylamide gel electrophoresis. After protein transfer to nitrocellulose membrane, membranes were blocked with non-fat dry milk (5%, 2 h) followed by incubation with primary antibodies overnight. The details of antibodies used are given in the Supplementary Methods. The protein bands were detected by standard chemiluminescence method (Thermo Pierce Femto, Rockford, IL, USA).

Quantitative real-time PCR

Total RNA was extracted using Trizol reagent (Invitrogen, Carlsbad, CA, USA). Then, 500 ng of the extracted RNA was converted into cDNA using superscript II cDNA kit (Invitrogen). Quantification of the *PML-RARA* transcripts was done using EAC (Europe against Cancer) program protocols.[18] The reverse transcriptase-PCR and real-time quantitative PCR sensitivity was assessed in-house using methodology as reported previously by us.[19] The expression of other genes was studied using SYBR green method (Finnzymes F410L, Thermo Scientific, Rockford, IL, USA) (primer sequence given in Supplementary Table S1). The Ct values were normalized with *GAPDH* or *ACTB* and the fold differences were calculated using $2^{-\Delta\Delta Ct}$ method. The NF-κB array (RT^2 profiler PCR array human NF-κB signaling target; Qiagen, Hilden, Germany, Catalog no: PAHS-225z) was performed according to the manufacturer's instructions.

Knockdown experiment

The knockdown of p65 and p62 transcripts were performed by MISSION endoribonuclease-prepared short interfering RNA (esiRNA) purchased from Sigma (catalog numbers: p62- EHU027651, p65- EHU141461). Then, 30 nM of esiRNA was electroporated into NB4 cells using Amexa electroporator unit (Lonza Nucleofecto, Cologne, Germany; Program NB4 X-01) and recovered in complete media for 24 h.

Confocal microscopy analyses

NB4 cells were treated with ATO, BTZ or combination and cytospin slides were made after 24 h of treatment. The cells were fixed in 4% paraformaldehyde followed by blocking using 5% goat serum. It was further incubated with primary antibodies such as PML (Santa Cruz, Dallas, TX, USA), LC3, P62 and Ubiquitin (Abcam, Cambridge, UK) overnight at 4 °C. The slides were rinsed with phosphate-buffered saline three times and incubated with secondary antibodies (anti-mouse and/or anti-rabbit) conjugated with Alexaflour 594 and Alexaflour 488 (Invitrogen) for 1 h. The slides were again washed, air dried and counterstained with DAPI (4',6-diamidino-2-phenylindole) containing mountant (Vectashield, Burlingame, CA, USA). The images were acquired in confocal microscope (Olympus FV1000, Melville, NY, USA) at ×20 and ×100 with oil immersion and the images were analyzed using Fluoview software version 3.1b.

Mouse model and drug treatments

FVB/N mice were obtained from Jackson Laboratory (Bar Harbor, ME, USA). Mice at 6 to 8 weeks of age were used in all the experiments. The animal study design and euthanasia protocols were approved by the institutional animal ethics committee (IAEC approval number 17/2012). APL cells from the spleen of MRP8-PML-RAR transgenic mice[20] (FVB/N) were harvested and cryopreserved (a kind gift from Dr Scott Kogan). APL cells (5×10^4 cells/mouse) were injected intravenously via the tail vein into genetically compatible FVB/N recipients, without conditioning with either radiation or chemotherapy. ATO was given intraperitoneally at the concentration of 5 mg/kg of mice starting on day 7 post injection of malignant cells and continued for 28 days, whereas BTZ was given subcutaneously at a dose of 0.5 mg/kg of mice on days 8, 12, 16 and 20. Details of methodology used for secondary transplantation are provided in Supplementary Methods.

RESULTS

Malignant promyelocytes are protected from ATO-induced apoptosis by stromal cells through upregulation of NF-κB pathway

We had previously reported that NB4 cells (APL cell line) or the primary blasts from APL patients had a significant survival advantage against ATO when co-cultured with either primary stromal cells or stromal cell line.[9] A global gene expression array for differential gene expression in NB4 cells with and without HS-5 cell co-culture was performed. The Gene Set Enrichment Analysis (GSEA) revealed an enrichment of NF-κB pathway in the malignant cell line upon co-culture (Figure 1a and Supplementary Figure S1). This was further validated by real-time PCR array where an

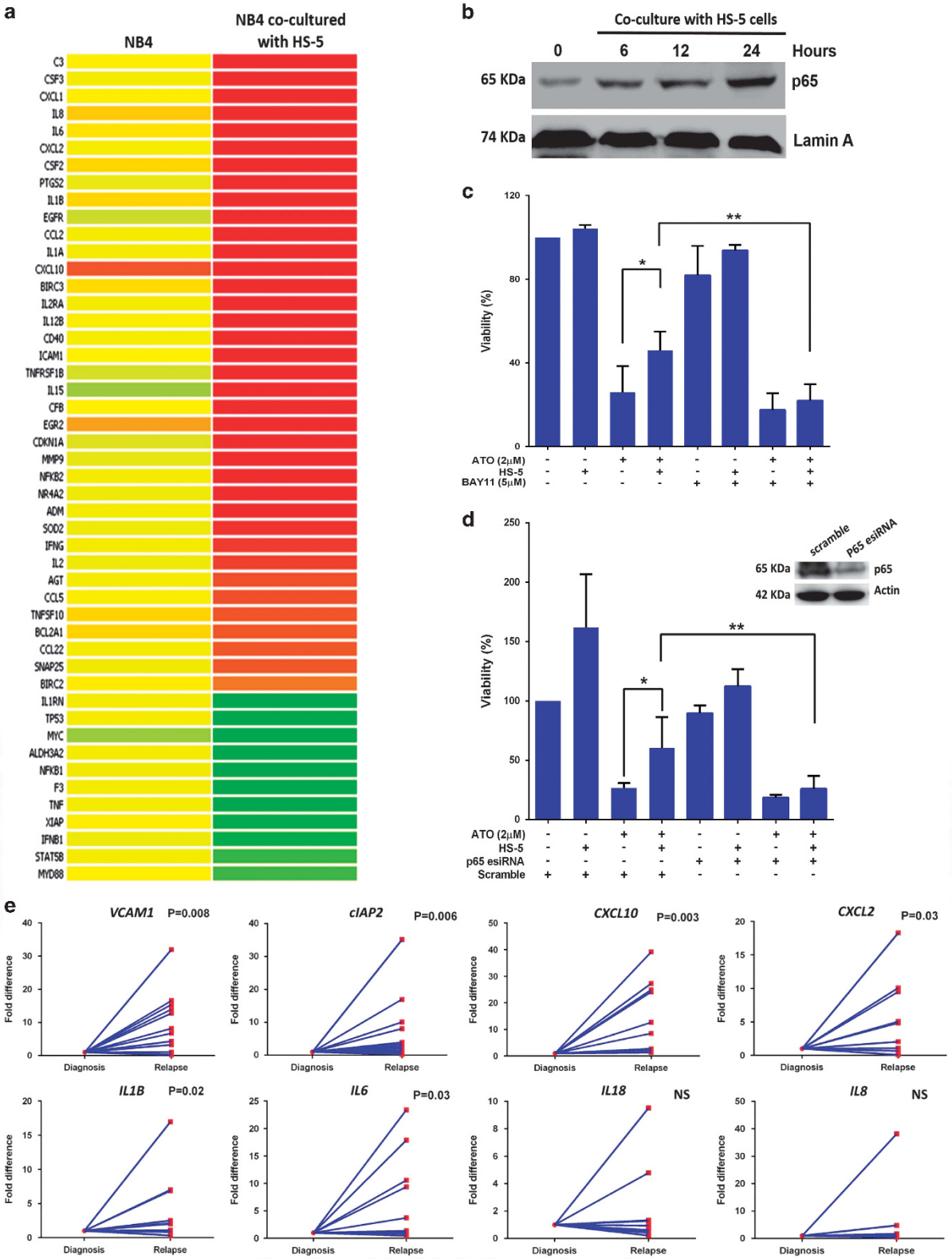

Figure 1. Stromal cells protect malignant promyelocytes against ATO *in vitro* through upregulation of NF-κB pathway. (**a**) Heat map showing differential regulation of NF-κB pathway in leukemic cells in co-culture in comparison with NB4 cells alone. (**b**) Activation of NF-κB pathway in the malignant promyelocytes (NB4 cells) co-cultured with HS-5 cells for 6, 12 and 24 h shows increased translocation of p65 subunit in the nuclear compartment over time ($n=3$) on co-culture. (**c**) NF-κB inhibitor (Bay11-7082–5 μM) was able to overcome the protective effect mediated by the HS-5 cells along with ATO (2 μM); assays were done using apoptosis assay (Annexin V/7AAD measured after 48 h of exposure; $n=5$). (**d**) Knockdown of p65 was able to overcome the protective effect against ATO (2 μM) mediated by the HS-5 cell co-culture (Annexin V/7AAD measured after 48 h of exposure; $n=5$). (**e**) Expression of NF-κB target genes *VCAM1*, *cIAP2*, *CXCL10*, *CXCL2*, *IL1B*, *IL6*, *IL18* and *IL8* in matched samples of newly diagnosed ($n=13$) and relapsed ($n=13$) APL blasts. Statistical significance was calculated using Wilcoxon matched pairs signed rank test (paired two tailed) and Student's *t*-test (two tailed *t*-test) and the *P*-values are denoted as $*P=0.02$ and $**P=0.001$.

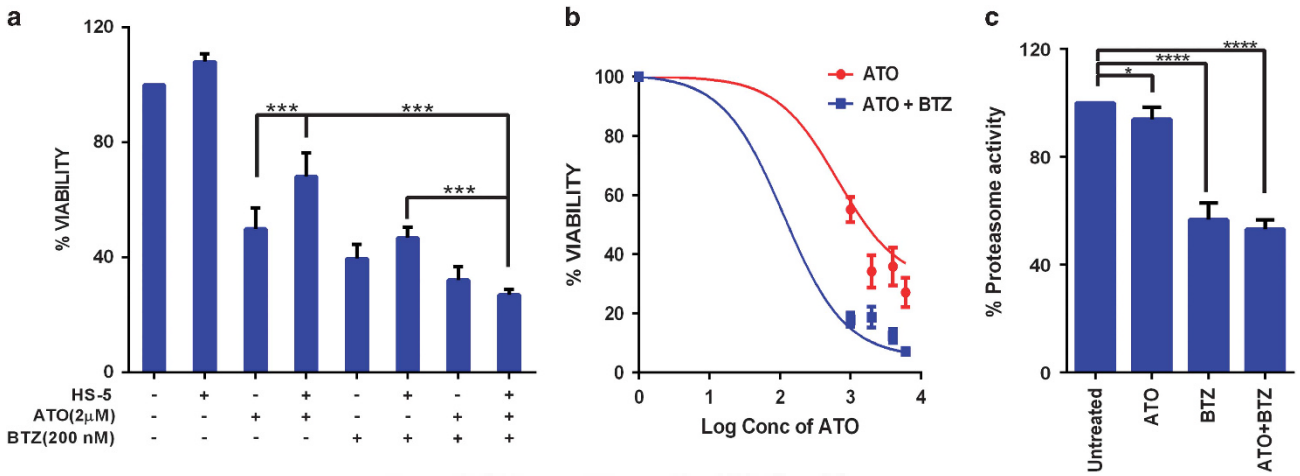

Figure 2. Bortezomib overcomes the stromal cell-mediated drug resistance and has a synergistic effect with ATO. (**a**) Bortezomib (BTZ) at pharmacologically relevant concentrations (200 nM) restores the sensitivity of malignant promyelocytes to ATO (2 μM) in NB4 cells (Annexin V/7AAD measured after 48 h of exposure; $n=8$) even in the presence of HS-5 cells; the viability of untreated cells was normalized to 100% and the treated cell viability was compared with normalized untreated cells. (**b**) The combination of ATO and BTZ had a combination index (CI) of 0.7 calculated using Calcusyn software ($n=12$), where at a dose of 200 nM BTZ significantly reduced the IC_{50} of ATO on NB4 cells (measured by an MTT assay after 48 h of drug exposure). (**c**) Proteasome activity of NB4 cell lysates 6 h after treatment with either ATO (2 μM), BTZ (200 nM) or both. The activity was measured by the ability of the lysate to hydrolyze Z-Gly-Gly-Leu-AMC peptide ($n=5$). Statistical significance was calculated using Student's *t*-test (two-tailed *t*-test) and the *P*-values are denoted as $^{*}P=0.02$, $^{***}P=0.0001$ and $^{****}P<0.0001$.

increase in NF-κB target genes was observed (Supplementary Figure S2). Western blotting analysis also showed an increased translocation of NF-κB subunit p65 into the nuclear compartment of NB4 cells co-cultured with HS-5 stromal cells (Figure 1b). Inhibiting this pathway using a chemical inhibitor (Bay11-7082) or knockdown of p65 subunit using esiRNA in NB4 cells resulted in reversion of resistance to ATO upon co-culture (Figures 1c and d).

We also observed an upregulation of this pathway target genes in relapsed compared with newly diagnosed (13 matched newly diagnosed and relapsed) APL patient blasts (Figure 1e) even in the absence of co-culture with stroma. This suggests that the NF-κB pathway can potentially play an important role in the mechanism of EMDR in APL, especially in relapsed APL.

Proteasome inhibitor overcomes the bone marrow micro-environment-mediated drug resistance through downregulation of NF-κB pathway

To overcome the ATO resistance of NB4 cells on co-culture we screened various molecules (data not shown). We observed that proteasome inhibitors (MG-132 and bortezomib) when combined with ATO were able to overcome the protective effect mediated by stromal cell (HS-5 and primary mesenchymal stromal cells) co-culture to NB4 cells (Figure 2a) and to primary APL cells (Supplementary Figure S3). Bortezomib, a well-known inhibitor of the NF-κB pathway, was able to reverse the effect of stromal culture-induced activation of the NF-κB pathway (validated by documenting downregulation of NF-κB target genes that had previously been upregulated on co-culture; Supplementary Figure S4).

Direct cytotoxicity of bortezomib on malignant promyelocytes and its synergy with ATO

The IC_{50} for BTZ on NB4 cell line was 14 nM (Supplementary Figure S5), whereas for in-house-generated ATO-resistant cell line (NB4 EV-AsR1) the IC_{50} value was 17 nM. For primary APL blasts the median IC_{50} was 12 nM. These values are comparable to its effect on myeloma cell lines.[21,22] BTZ was able to synergize with ATO (Figure 2b) as demonstrated by a combination index value (0.7). Combining ATO and BTZ does not alter the efficacy of BTZ in inhibiting proteasome complex (Figure 2c).

Mechanism of synergy of combining ATO with bortezomib in APL

Next, the potential mechanism of synergism between these two drugs was evaluated. As a result of proteasome complex inhibition a significant accumulation of ubiquitinated proteins at 24 h in NB4 cells treated with BTZ or a combination ATO and BTZ was observed (Figure 3a). A similar observation was noted *in-vivo* in mice treated with ATO and BTZ and *in vitro* in primary human APL cells; Supplementary Figure S6). As a result, this combination induced upregulation of the UPR pathway more than either ATO or BTZ could as single agents, as evidenced by significant upregulation of *CHOP* and *ATF4* (UPR pathway genes involved in apoptosis; Figures 3b and c and Supplementary Figure S7). The combination of ATO and BTZ also significantly induced ROS generation (Supplementary Figure S8) and decreased the mitochondrial membrane potential of NB4 cells when compared with ATO or BTZ alone (Figure 3d). Inhibiting ROS by *N*-acetyl cysteine followed by treatment with ATO and BTZ significantly rescued the cells from apoptosis induced by ATO and ATO+BTZ but not BTZ alone (Figure 3e). The net effect of the above changes led to a more effective induction of apoptosis by the combination of these drugs than either drug alone (Figure 3f). Although it has been previously reported that BTZ induces apoptosis in malignant promyelocytes through UPR pathway and endoplasmic reticulum stress,[12] these data demonstrate the additive effect of ATO on these effects along with an increased ROS activity and decreased mitochondrial membrane potential that accounts for the documented synergy of these two agents.

Proteasome inhibition is dispensable for the degradation of PML-RARA

Degradation of PML-RARA was observed through nuclear body reformation in the ATO+BTZ-treated NB4 cells that were similar to ATO-alone-treated cells, whereas a micro-speckled pattern was observed in the untreated cells (Supplementary Figure S10). This was further validated by immunoblot, where the degradation was seen at 48 h (Figure 4a). BTZ and the combination of ATO+BTZ

resulted in initial stabilization of PML-RARA but subsequent degradation beyond 24 h was observed; these data correlated with the clearance of ubiquitinated proteins at the same time points (Figure 3a and Supplementary Figure S11). As ATO is known to induce ubiquitination of PML-RARA, an immunofluorescence assay for ubiquitin and PML was performed. On combining ATO

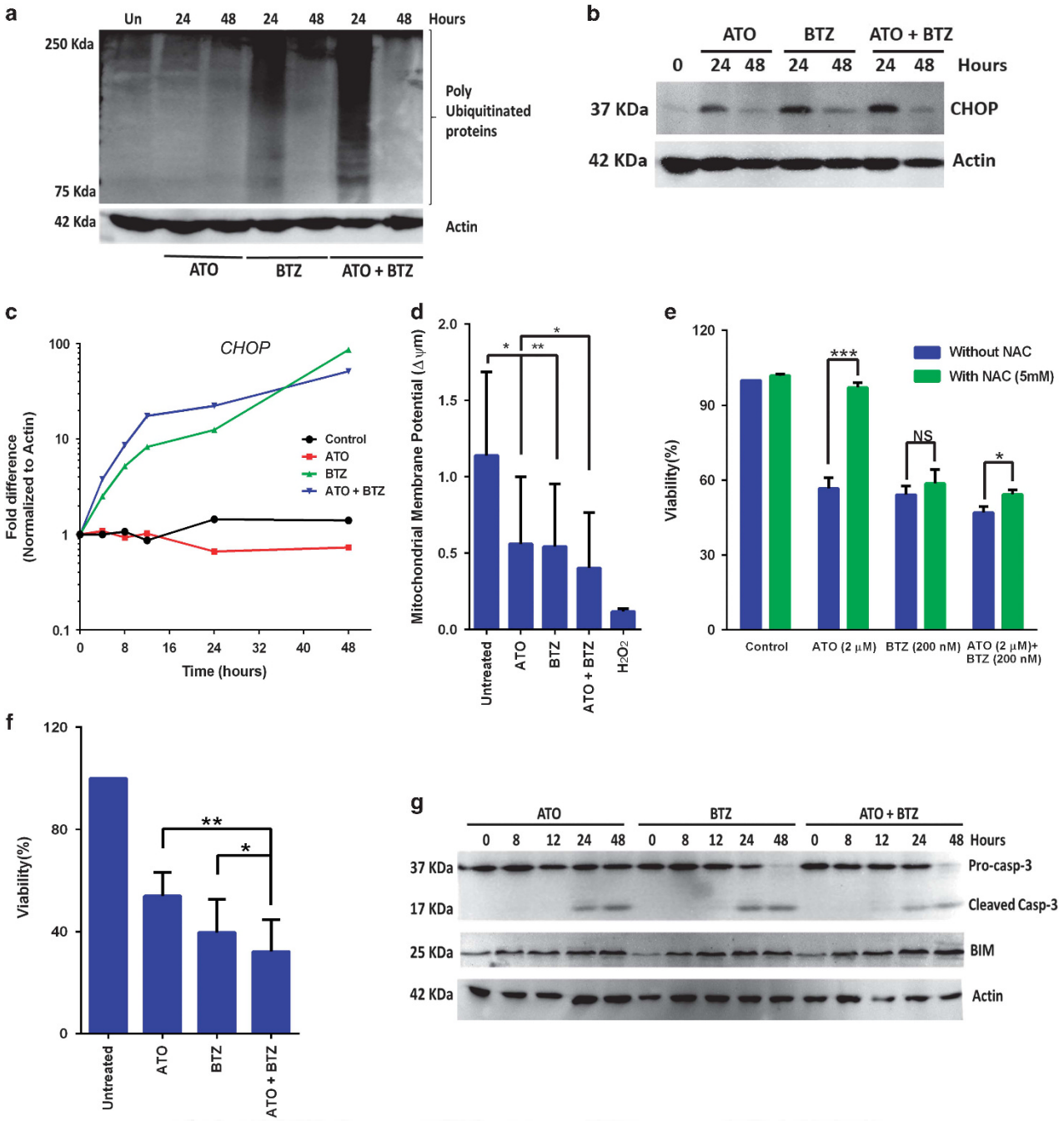

Figure 3. ATO and bortezomib synergizes by inducing apoptosis by UPR pathway. (**a**) Immunoblot shows accumulation of ubiquitinated proteins in ATO (2 μM) and BTZ (200 nM) combination-treated NB4 cells at 24 h and disappearance of the same by 48 h ($n=3$). (**b**) Immunoblot shows upregulation of UPR gene *CHOP* at 24 h and subsequent reduction at 48 h after drug exposure at same concentration as mentioned above in NB4 cells ($n=5$). (**c**) Upregulation of UPR gene *CHOP* was also observed by real-time PCR that increased over time to a maximum at 48 h after drug treatment, at the same concentrations as mentioned above ($n=3$) in NB4 cells. (**d**) The combination of ATO (2 μM) and BTZ (200 nM) decreased mitochondrial membrane potential (MMP) in NB4 cells (MMP was measured 6 h post drug treatment; $n=6$). (**e**) Pretreatment of NB4 cells with ROS inhibitor, *N*-acetyl cysteine (NAC, 5 mM) significantly rescued the NB4 cells from ATO (2 μM) and ATO (2 μM) plus BTZ (200 nM) induced apoptosis but not from BTZ-alone-treated cells (viability was assessed 48 h post drug treatment using Annexin V/7AAD measurement; $n=3$). (**f**) Viability assay demonstrating ATO (2 μM) and BTZ (200 nM) combination induces a significant greater cell kill than either drug alone (Annexin V/7AAD measured after 48 h of exposure; $n=6$). (**g**) Western blot demonstration of activation of caspase-3 and increased expression of pro-apoptotic protein BIM to induce apoptosis at different time points at drug concentrations as mentioned above. Statistical significance was calculated using Student's *t*-test (two-tailed *t*-test) and the *P*-values are denoted as NS, not significant, $^{*}P=0.02$, $^{**}P=0.001$ and $^{***}P=0.0001$.

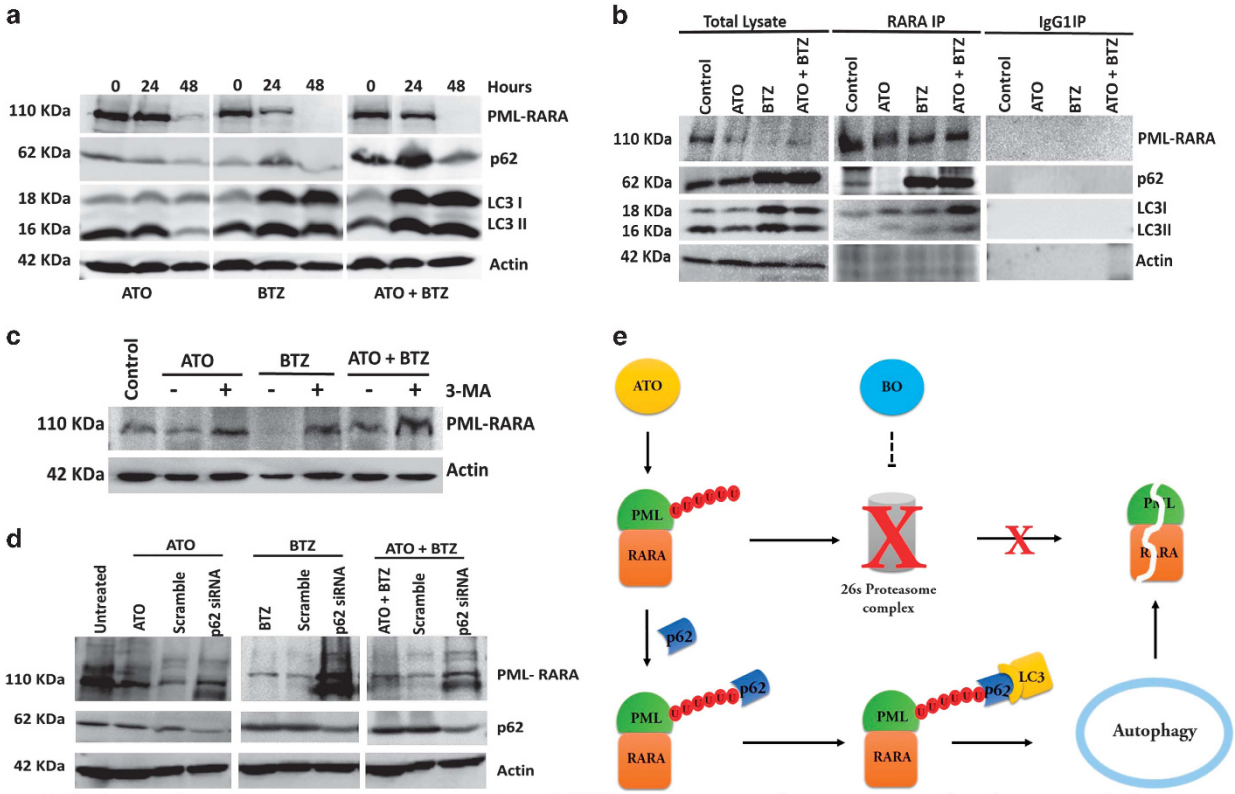

Figure 4. PML-RARA is degraded alternatively by autophagy pathway. (**a**) Immunoblot assay showing increased activation of autophagy pathway through increased conversion of LC3I to LC3II and p62 accumulation and degradation by 24 and 48 h corresponding to PML-RARA degradation (ATO (2 μM) and BTZ (200 nM)). (**b**) Co-immunoprecipitation assays showing interaction between P62, LC3 and PML-RARA at 24 h post drug treatment. (**c**) Inhibition of autophagy by pretreating the cells with 3 methyl adenine (3 MA; 5 mM) inhibited the degradation of PML-RARA in cells treated with ATO (2 μM) and BTZ (200 nM) for 24 h. (**d**) Knockdown of p62 by esiRNA inhibited the degradation of PML-RARA in cells treated with ATO (2 μM) and BTZ (200 nM) for 24 h, $n = 3$. (**e**) Schematic representation of PML-RARA degradation by a combination of ATO and BTZ with proteasome inhibition.

and BTZ, we demonstrated that PML colocalized with ubiquitin even with this combination (Supplementary Figure S12). Together, these data suggest that PML-RARA is ubiquitinated and degraded by a proteasome-independent pathway when ATO is combined with BTZ.

Proteasome inhibition results in the induction of autophagy that degraded PML-RARA oncoprotein

Existing data suggested that induction of autophagy upon proteasomal inhibition can degrade the accumulated ubiquitinated proteins.[23] We hypothesized that PML-RARA (ubiquitinated upon ATO+BTZ treatment) must be degraded via the autophagy pathway when proteasome was inhibited. The analysis of autophagy genes expression in the combination-treated NB4 cells showed an additive induction of autophagy genes (such as LC3II, *ATG5* and *BECN1*; Figure 4a and Supplementary Figure S13). With the combination of ATO+BTZ we also observed a time-dependent induction and subsequent degradation of p62 protein (adaptor protein involved in degradation of PML-RARA during myeloid differentiation[24] by all-*trans* retinoic acid (ATRA)) correlated with ubiquitinated protein and PML-RARA levels at these time points (Figure 4a and Supplementary Figure S14 with extended time points). On immunofluorescence analysis, PML proteins colocalized with LC3 and P62 upon treatment with this combination (Supplementary Figure S12), and this was further validated by co-immunoprecipitation assay (Figure 4b). However, the same combination treatment (ATO+BTZ) of NB4 cells along with inhibition of autophagy with a small-molecule inhibitor 3-methyl adenine (3MA) or transient knockdown of p62 by esiRNA resulted in the accumulation of PML-RARA (Figures 4c and d). Induction of autophagy in NB4 cells by starvation also degraded PML-RARA (data not shown). These results indicate that autophagy degrades PML-RARA, that this process involves the p62 cargo binding protein and that the combination of ATO and BTZ has an additive effect in inducing autophagy.

ATO and bortezomib combination is effective in ATO-resistant NB4 cells

We next assessed the efficacy of this combination on an in-house-generated ATO-resistant NB4 cell line (NB4-EVAsR1: harboring A216V mutation in PML B2 domain; data provided in Supplementary Methods). These resistant cell lines were sensitive to BTZ. Treating the resistant cells with ATO and bortezomib resulted in a synergistic effect (combination index = 0.02; Supplementary Figure S15). The mechanism of action of combination drugs was similar to NB4-naive cells (data not shown). Bortezomib was also able to synergize with other drugs such as ATRA and anthracyclines and this effect was seen in both naive NB4 cell line as well as resistant NB4 cell line. The effect of ATO with ATRA and BTZ on the viability was comparable with that of ATO with ATRA and anthracycline in both naive and ATO-resistant NB4 cells (Supplementary Figure S16).

ATO and bortezomib combination is effective in reducing leukemic burden and inducing long-term survival in an APL mouse model

We further evaluated the combination's efficacy *in vivo* using a transplantable APL mouse model (Figure 5a). The APL mice

treated with a combination of ATO and BTZ showed a significant reduction in the tumor burden on day 20, as evidenced by reduction in spleen size (Figure 5b), decreased PML-RARA copy numbers (Figure 5c) and decreased bone marrow blasts analyzed by flow cytometry (Figure 5d) and immunohistochemistry (hematoxylin and eosin staining; Figure 5e) compared with ATO- or BTZ-alone-treated mice. The combination therapy was also associated with a significantly superior survival compared with mice treated with either agent alone (Figure 5f).

Combination of ATO and bortezomib reduces leukemia-initiating cells in APL

We further evaluated the combination's effect on leukemia-initiating cells in APL. In the mouse model, secondary transplantation of bone marrow cells of leukemic mice harvested on day 20 after treatment with placebo, ATO alone or ATO+BTZ demonstrated a significantly superior survival of secondary recipients that received bone marrow cells from the ATO combined with BTZ-treated mice (Figures 5g and h). In the mice that had long-term survival (surviving >250 days; only seen in ATO+BTZ group) we failed to observe an expression of PML-RARA transcript in all the organs tested (data not shown). We also observed a prolonged survival of the mice that had been serially transplanted with the bone marrow cells from the long-term surviving mice (previously treated with ATO and BTZ; Supplementary Figure S17). Together, these data suggest that this combination is able to eliminate the leukemia-initiating cell compartment in a mouse model of APL.

Bortezomib and ATO combination is effective in relapsed APL patients

In 2011, based on preliminary *in vitro* laboratory data, two patients (RS and TK) with second relapse, both following an autologous stem cell transplant after their first relapse, were administered a combination of ATO (conventional doses as reported previously;[2] INTAS Pharmaceuticals, Ahmedabad, India) with bortezomib (1.4 mg/m^2/weekly $\times$ 4 doses; NATCO, Hyderabad, India) in induction and consolidation on a compassionate basis after getting written and informed consent. TK also received two doses of mitoxantrone (Neon Laboratories Ltd, Mumbai, India) in induction. RS subsequently received only maintenance therapy with ATO and ATRA (Roche Pharmaceuticals) as he did not have an allogeneic stem cell donor, whereas TK underwent a matched unrelated donor stem cell transplantation in molecular remission. The combination therapy was well tolerated with no significant Grade III/IV nonhematological toxicity. Both patients are currently in continuous molecular remission at 61 and 60 months since second relapse, respectively. An additional three patients received this combination on a compassionate basis after getting written and informed consent. One patient (SS) with multiple relapses had a transient hematological remission and relapsed and went on palliation, whereas two other patients in first relapse (BJ and AA) received a similar ATO and bortezomib combination in induction and consolidation. BJ had an autologous stem cell transplant, whereas AA received maintenance therapy with ATO and ATRA, and both remain in continuous molecular remission at 60 and 42 months (data summarized in Supplementary Table S2).

Based on this preliminary favorable experience, a phase II clinical trial for patients with APL in first relapse was initiated in 2013 after getting institutional IRB approval (IRB Min 8225 dated 27 February, 2013). The study was registered in the public domain (NCT01950611). The study continues to enroll patients at our center. Sixteen patients diagnosed to have relapsed APL have been enrolled in this study. All patients achieved hematological remission. The combination of ATO with bortezomib was well tolerated. There were no induction deaths. With the exception of one patient who developed grade III peripheral neuropathy requiring treatment, none of the other patients had any grade III/IV nonhematological toxicity. All patients remain in continuous molecular remission at a median follow-up of 447 days. Longer follow-up is required to validate the impact of this regimen on relapse-free and overall survival but one can conclude that the combination is safe and well tolerated.

DISCUSSION

Bone marrow microenvironment acts as a sanctuary for the leukemic cells to establish a niche and protect themselves from chemotherapeutic agents.[25] There are numerous reports on EMDR in leukemia.[26–31] We had previously reported, for the first time, that there was significant EMDR to ATO in APL.[9] We observed this protective effect with both primary stromal cells and stromal cell line but not with human umbilical vein endothelial cells, COS-7 or peripheral blood mononuclear cells (data not shown). We did not find any difference in the ATO concentration levels or in the intracellular ATO levels achieved in the malignant cells with and without co-culture, suggesting that the cross-talk with the stroma resulted in cell-intrinsic changes that mediated resistance. A global gene expression array was performed and the differentially regulated genes were subjected to GSEA where we could observe a significant enrichment of the NF-κB pathway. These findings were consistent with recently published data that demonstrated the important role of the NF-κB pathway in inducing this resistance to chemotherapy on stromal co-culture.[10] We screened a number of small molecules and antibodies based on the data we had for their ability to overcome EMDR to ATO. We were specifically interested in the beneficial effect of proteasome inhibitor bortezomib that is a known inhibitor of NF-κB, and also because it is an FDA (Food and Drug Administration)-approved drug that has been widely used in the clinic in the treatment of myeloma[32–34] and other hematological malignancies.[35–37]

We observed a significant cytotoxicity of bortezomib as a single agent on malignant promyelocytes (at concentrations evaluated there was no significant cytotoxicity on stromal cells, peripheral blood mononuclear cells or CD34$^+$ cells). In contrast to existing dogma that suggested that bortezomib and ATO were likely to be antagonistic, we demonstrated *in vitro* synergy between these two agents. The cytotoxicity on malignant promyelocytes was significantly superior to either agent alone. Although there was a trend to an increase in apoptotic proteins such as BIM on an immunoblot (Figure 3g) and a similar trend to an decrease in expression of anti-apoptotic genes such as *BCL2* and *cIAP2* on real-time PCR (Supplementary Figure S9), we could not demonstrate a similar increase in some apoptotic proteins such as Cleaved caspase 3 (Figure 3g).

We noted an induction of UPR on combining ATO and BTZ as demonstrated by significant increase in expression of *ATF4* and *CHOP*. For CHOP proteins, this was seen only until 24 h and at 48 h that there was a reduction in levels as seen on an immunoblot (Figure 3b). However, the real-time PCR values continued to be significantly increased even at 48 h (Figure 3c). We suspect that this is because of CHOP being a target of the ubiquitin proteasome system as has been reported previously[38] and subsequent clearance of CHOP along with other ubiquitinated proteins by autophagy as seen in Figure 3a.

Bortezomib has multiple mechanisms of action in cancer cells, and in combination with ATO we demonstrated the importance of multiple cellular processes in mediating the cytotoxicity in APL, in addition to NF-κB inhibition. A concern remained about the fate of the PML-RARA oncoprotein when this combination was used. Published data suggest that an intact proteasome was critical for ATO to mediate PML-RARA degradation and, in addition, clearance of the leukemia-initiating compartment in APL was dependent on degradation of this oncoprotein.[6,8,39] In this study we demonstrated that even with very effective proteasome blockade using a

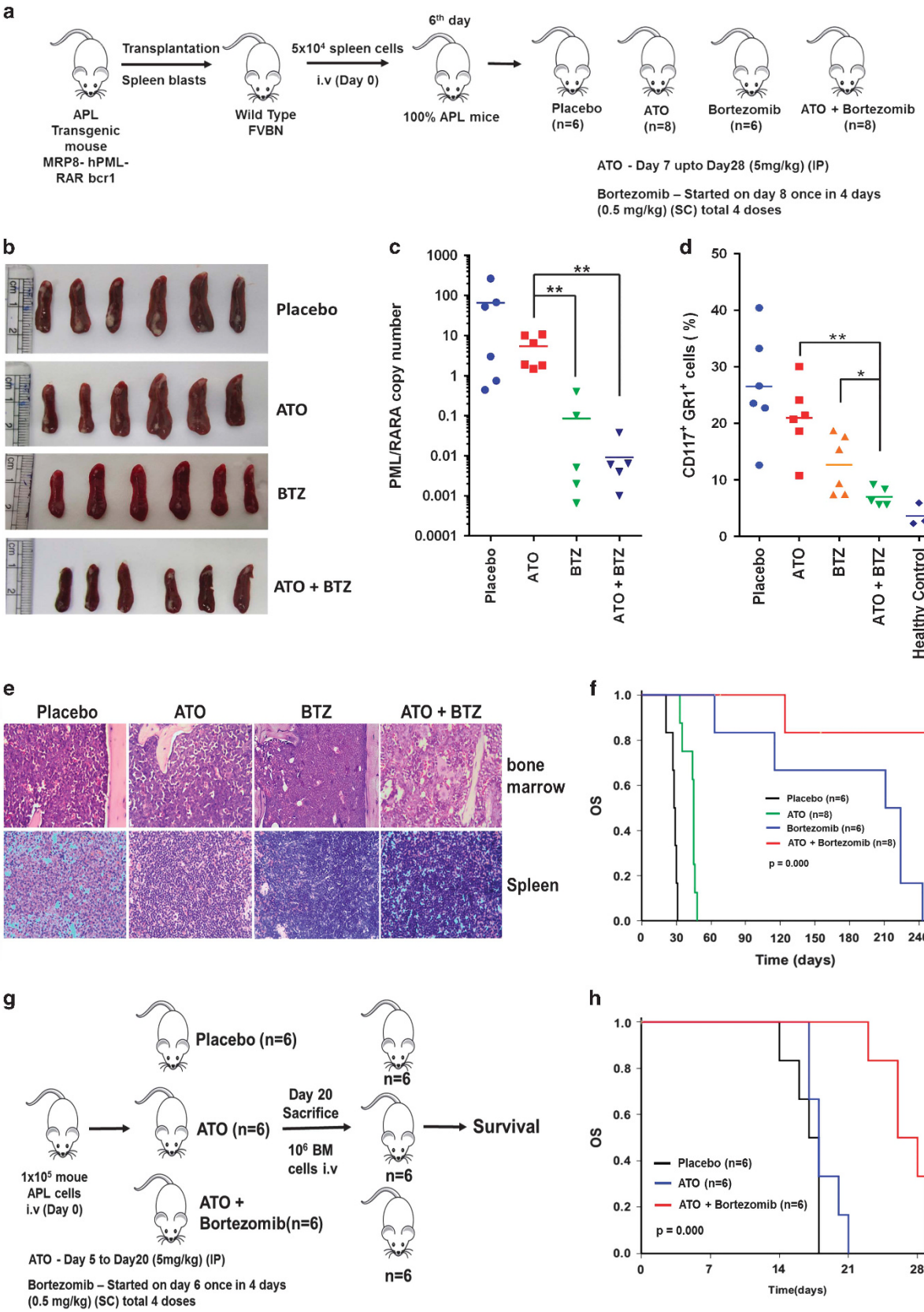
a
Transplantation
Spleen blasts
APL Transgenic mouse MRP8- hPML-RAR bcr1
Wild Type FVBN
5x10⁴ spleen cells
i.v (Day 0)
6th day
100% APL mice
Placebo (n=6)
ATO (n=8)
Bortezomib (n=6)
ATO + Bortezomib (n=8)
ATO - Day 7 upto Day28 (5mg/kg) (IP)
Bortezomib – Started on day 8 once in 4 days (0.5 mg/kg) (SC) total 4 doses
b
Placebo
ATO
BTZ
ATO + BTZ
c
PML/RARA copy number
Placebo
ATO
BTZ
ATO + BTZ
d
CD117+ GR1+ cells (%)
Placebo
ATO
BTZ
ATO + BTZ
Healthy Control
e
Placebo
ATO
BTZ
ATO + BTZ
bone marrow
Spleen
f
OS
Time (days)
Placebo (n=6)
ATO (n=8)
Bortezomib (n=6)
ATO + Bortezomib (n=8)
p = 0.000
g
Placebo (n=6)
ATO (n=6)
ATO + Bortezomib(n=6)
1x10⁵ moue APL cells i.v (Day 0)
Day 20 Sacrifice
10⁶ BM cells i.v
n=6
n=6
n=6
Survival
ATO - Day 5 to Day20 (5mg/kg) (IP)
Bortezomib – Started on day 6 once in 4 days (0.5 mg/kg) (SC) total 4 doses
h
OS
Time(days)
Placebo (n=6)
ATO (n=6)
ATO + Bortezomib (n=6)
p = 0.000

Figure 5. ATO and bortezomib combination reduces leukemia burden and leukemia-initiating compartment in an APL mouse model. (**a**) Schematic representation of transplantable APL mouse model and treatment plans. Demonstration of leukemic burden reduction in the combination treated arm through (**b**) reduced spleen size. (**c**) Reduced expression of PML-RARA transcript on day 20 in ATO- and bortezomib (BTZ)-treated group. (**d**) Flow cytometry analysis for tumor burden shown reduced leukemic cells (CD117+ and Gr1+ cells) in bone marrow of APL mice upon treatment with ATO and BTZ (**e**) Hematoxylin and eosin (H&E) staining of bone marrow and spleen from mice treated with Placebo, ATO alone, BTZ alone or ATO in combination with BTZ. Mice were killed on day 20 and examined for the presence of leukemic cells. In mice treated with placebo, there was a diffuse infiltrate of immature cells replacing the marrow and the spleen. In ATO-alone and BTZ-alone-treated mice, there was a reduction in the immature cell infiltrate in the bone marrow and the spleen. In mice treated with ATO+BTZ, scattered atypical cells were noted (less than with ATO or BTZ alone) and normal hematopoietic elements were seen in the marrow, and splenic architecture was preserved. (**f**) ATO and BTZ combination prolonged the median survival of APL mice (Placebo: 28 days; ATO: 45 days; BTZ: 211 days; ATO+BTZ, not reached). (**g**) Schematic representation of secondary transplantation experiment (not treated post transplantation) and followed them up to their death. (**h**) The survival curve of the secondary transplantation experiment shows that ATO and BTZ combined treated mice bone marrow cells upon secondary transplantation had a significant prolonged median survival (26 days) compared with placebo (17 days) or ATO-alone (18 days)-treated mice. Statistical significance was calculated using log rank test and nonparametric, unpaired, two-tailed, Mann–Whitney test. The *P*-values are denoted as $*P = 0.02$ and $**P = 0.004$.

combination of ATO and bortezomib we could still demonstrate effective PML-RARA degradation and that this degradation was independent of the proteasome pathway. Previously reported data suggest that proteasome inhibition can induce the autophagy pathway for the degradation of ubiquitinated proteins[23,40,41] and that PML-RARA can be degraded by the autophagy pathway during differentiation of NB4 cells treated with ATRA or ATO.[24,42,43] Our data demonstrate that degradation of PML-RARA oncoprotein on combining bortezomib and ATO was mediated by autophagy that was additively induced with this combination. Reported data suggest that cargo-binding proteins such as P62, ALFY and NBR1 are involved in degrading ubiquitinated proteins.[44–47] Previous reports suggest that p62 is involved in the degradation of PML-RARA by autophagy during myeloid differentiation[24] and ATO treatment.[42] Consistent with these observations we have demonstrated that a combination of bortezomib and ATO induces autophagy and the PML-RARA oncoprotein is degraded by a p62-dependent autophagy pathway.

The efficacy of the combination of bortezomib and ATO was further validated by us in a transplantable mouse model of APL and in preliminary data from the clinic. Based on these encouraging results a phase II clinical trial was initiated and continues to recruit patients with relapsed APL. The preliminary phase II study data that are reported here suggest that this combination is well tolerated. In addition, we also demonstrate that this combination is effective in ATO-resistant cell lines.

We have also demonstrated (*in vitro* data) that the combination of bortezomib with ATO and ATRA is comparable to the effect of anthracyline with ATRA and ATO on malignant promyelocytes. In the evolving strategy of de-escalation of therapy in APL,[48] the addition of bortezomib with ATO along with ATRA has the potential to further de-escalate the therapy in high-risk and relapsed APL by replacing the myelotoxic anthracycline with a relatively non-myelotoxic proteasome inhibitor.

The microarray data discussed in this manuscript have been deposited in the NCBI Gene Expression Omnibus (GEO) under the GEO series accession number GSE73157.

CONFLICT OF INTEREST

The authors declare no conflict of interest.

ACKNOWLEDGEMENTS

This study is supported by a Wellcome-DBT India Alliance research grant (IA/S/11/2500267). VM is supported by senior fellowship program of Wellcome-DBT India Alliance (IA/S/11/2500267), New Delhi, India. This study is funded in part by the Department of Biotechnology, New Delhi, India, grant to VM (DBT/COE/34/SP13432/2015). SG, HKP and SD are supported by senior research fellowship from Council for Scientific and Industrial Research, New Delhi, India. PB is supported by senior fellowship program of Wellcome-DBT India Alliance (IA/S/15/1/501842), New Delhi, India. RAP and CC are funded by the Institut National de la Sante et de la Researche Medicale. We acknowledge Intas Pharmaceutical Ltd, India, and NATCO pharmaceutical Ltd, India, for kindly providing us ATO and bortezomib, respectively, for this study. We thank Dr Jayandharan Giridhara Rao, Associate Professor, Department of Biological Sciences and Bioengineering, Indian Institute of Technology, Kanpur, India, for helping us with reagents. Dr Pratheesh Mankuzhy MVSc, PhD, Scientific Officer, Centre for Stem Cell Research (Unit of InStem–Bangalore), Vellore, India, for helping us with animal studies. Mr Vaidyanathan Subramaniam, Officer Incharge Core Facilities, Centre for Stem Cell Research (Unit of InStem–Bangalore), Vellore, India, for technical help.

AUTHOR CONTRIBUTIONS

SG: performed research, designed study, performed molecular tests, analyzed data and wrote paper; AAA: performed research, performed molecular tests, flow cytometry tests and analyzed data; EC, NB, HKP and SD: performed research, performed molecular tests and analyzed data; UK: performed research, clinical data accrual and analysis; MA and RM: performed microarray experiment and analyzed data; AK: performed research, clinical data accrual and analysis and histopathology analysis; AA: performed research, clinical data accrual and analysis; AS: performed research and administrative support; RAP and CC: performed research, mouse experiment design and analyzed data; BG: performed research, clinical data accrual, analysis and wrote paper; PB: performed research, performed molecular tests and analyzed data; VM: performed research, designed study, clinical data accrual, analyzed data and wrote paper.

REFERENCES

1 de The H, Chomienne C, Lanotte M, Degos L, Dejean A. The t(15;17) translocation of acute promyelocytic leukaemia fuses the retinoic acid receptor alpha gene to a novel transcribed locus. *Nature* 1990; **347**: 558–561.
2 Mathews V, George B, Chendamarai E, Lakshmi KM, Desire S, Balasubramanian P *et al.* Single-agent arsenic trioxide in the treatment of newly diagnosed acute promyelocytic leukemia: long-term follow-up data. *J Clin Oncol* 2010; **28**: 3866–3871.
3 Zhu HH, Qin YZ, Huang XJ. Resistance to arsenic therapy in acute promyelocytic leukemia. *N Engl J Med* 2014; **370**: 1864–1866.
4 Goto E, Tomita A, Hayakawa F, Atsumi A, Kiyoi H, Naoe T. Missense mutations in PML-RARA are critical for the lack of responsiveness to arsenic trioxide treatment. *Blood* 2011; **118**: 1600–1609.
5 Lehmann-Che J, Bally C, de The H. Resistance to therapy in acute promyelocytic leukemia. *N Engl J Med* 2014; **371**: 1170–1172.
6 Lallemand-Breitenbach V, Jeanne M, Benhenda S, Nasr R, Lei M, Peres L *et al.* Arsenic degrades PML or PML-RARalpha through a SUMO-triggered RNF4/ubiquitin-mediated pathway. *Nat Cell Biol* 2008; **10**: 547–555.
7 Zhang XW, Yan XJ, Zhou ZR, Yang FF, Wu ZY, Sun HB *et al.* Arsenic trioxide controls the fate of the PML-RARalpha oncoprotein by directly binding PML. *Science* 2010; **328**: 240–243.
8 Nasr R, Guillemin MC, Ferhi O, Soilihi H, Peres L, Berthier C *et al.* Eradication of acute promyelocytic leukemia-initiating cells through PML-RARA degradation. *Nat Med* 2008; **14**: 1333–1342.
9 Chendamarai E, Ganesan S, Alex AA, Kamath V, Nair SC, Nellickal AJ *et al.* Comparison of newly diagnosed and relapsed patients with acute promyelocytic

leukemia treated with arsenic trioxide: insight into mechanisms of resistance. *PLoS One* 2015; **10**: e0121912.
10 Jacamo R, Chen Y, Wang Z, Ma W, Zhang M, Spaeth EL *et al.* Reciprocal leukemia-stroma VCAM-1/VLA-4-dependent activation of NF-kappaB mediates chemoresistance. *Blood* 2014; **123**: 2691–2702.
11 Canestraro M, Galimberti S, Savli H, Palumbo GA, Tibullo D, Nagy B *et al.* Synergistic antiproliferative effect of arsenic trioxide combined with bortezomib in HL60 cell line and primary blasts from patients affected by myeloproliferative disorders. *Cancer Genet Cytogenet* 2010; **199**: 110–120.
12 Takenokuchi M, Miyamoto K, Saigo K, Taniguchi T. Bortezomib causes ER stress-related death of acute promyelocytic leukemia cells through excessive accumulation of PML-RARA. *Anticancer Res* 2015; **35**: 3307–3316.
13 Yan H, Wang YC, Li D, Wang Y, Liu W, Wu YL *et al.* Arsenic trioxide and proteasome inhibitor bortezomib synergistically induce apoptosis in leukemic cells: the role of protein kinase Cdelta. *Leukemia* 2007; **21**: 1488–1495.
14 Lanotte M, Martin-Thouvenin V, Najman S, Balerini P, Valensi F, Berger R. NB4, a maturation inducible cell line with t(15;17) marker isolated from a human acute promyelocytic leukemia (M3). *Blood* 1991; **77**: 1080–1086.
15 Pieters R, Loonen AH, Huismans DR, Broekema GJ, Dirven MW, Heyenbrok MW *et al.* In vitro drug sensitivity of cells from children with leukemia using the MTT assay with improved culture conditions. *Blood* 1990; **76**: 2327–2336.
16 Nemoto S, Takeda K, Yu ZX, Ferrans VJ, Finkel T. Role for mitochondrial oxidants as regulators of cellular metabolism. *Mol Cell Biol* 2000; **20**: 7311–7318.
17 Roy A, Ganguly A, BoseDasgupta S, Das BB, Pal C, Jaisankar P *et al.* Mitochondria-dependent reactive oxygen species-mediated programmed cell death induced by 3,3'-diindolylmethane through inhibition of F0F1-ATP synthase in unicellular protozoan parasite Leishmania donovani. *Mol Pharmacol* 2008; **74**: 1292–1307.
18 van der Velden VH, Boeckx N, Gonzalez M, Malec M, Barbany G, Lion T *et al.* Differential stability of control gene and fusion gene transcripts over time may hamper accurate quantification of minimal residual disease--a study within the Europe Against Cancer Program. *Leukemia* 2004; **18**: 884–886.
19 Chendamarai E, Balasubramanian P, George B, Viswabandya A, Abraham A, Ahmed R *et al.* Role of minimal residual disease monitoring in acute promyelocytic leukemia treated with arsenic trioxide in frontline therapy. *Blood* 2012; **119**: 3413–3419.
20 Brown D, Kogan S, Lagasse E, Weissman I, Alcalay M, Pelicci PG *et al.* A PMLRARalpha transgene initiates murine acute promyelocytic leukemia. *Proc Natl Acad Sci USA* 1997; **94**: 2551–2556.
21 Wang L, Liu Q, Li H, Lizhen L, Wang X. The establishment of bortezomib resistant myeloma cell line KM3/BTZ and explore the resistance mechanism. *Blood* 2014; **124**: 5226.
22 Chauhan D, Singh A, Brahmandam M, Podar K, Hideshima T, Richardson P *et al.* Combination of proteasome inhibitors bortezomib and NPI-0052 trigger in vivo synergistic cytotoxicity in multiple myeloma. *Blood* 2008; **111**: 1654–1664.
23 Laussmann MA, Passante E, Dussmann H, Rauen JA, Wurstle ML, Delgado ME *et al.* Proteasome inhibition can induce an autophagy-dependent apical activation of caspase-8. *Cell Death Differ* 2011; **18**: 1584–1597.
24 Wang Z, Cao L, Kang R, Yang M, Liu L, Zhao Y *et al.* Autophagy regulates myeloid cell differentiation by p62/SQSTM1-mediated degradation of PML-RARalpha oncoprotein. *Autophagy* 2011; **7**: 401–411.
25 Meads MB, Gatenby RA, Dalton WS. Environment-mediated drug resistance: a major contributor to minimal residual disease. *Nat Rev Cancer* 2009; **9**: 665–674.
26 Ben-Batalla I, Schultze A, Wroblewski M, Erdmann R, Heuser M, Waizenegger JS *et al.* Axl, a prognostic and therapeutic target in acute myeloid leukemia mediates paracrine crosstalk of leukemia cells with bone marrow stroma. *Blood* 2013; **122**: 2443–2452.
27 Dosen-Dahl G, Munthe E, Nygren MK, Stubberud H, Hystad ME, Rian E. Bone marrow stroma cells regulate TIEG1 expression in acute lymphoblastic leukemia cells: role of TGFbeta/BMP-6 and TIEG1 in chemotherapy escape. *Int J Cancer* 2008; **123**: 2759–2766.
28 Zeng Z, Shi YX, Samudio IJ, Wang RY, Ling X, Frolova O *et al.* Targeting the leukemia microenvironment by CXCR4 inhibition overcomes resistance to kinase inhibitors and chemotherapy in AML. *Blood* 2009; **113**: 6215–6224.
29 Tabe Y, Jin L, Tsutsumi-Ishii Y, Xu Y, McQueen T, Priebe W *et al.* Activation of integrin-linked kinase is a critical prosurvival pathway induced in leukemic cells by bone marrow-derived stromal cells. *Cancer Res* 2007; **67**: 684–694.
30 Tabe Y, Konopleva M, Munsell MF, Marini FC, Zompetta C, McQueen T *et al.* PML-RARalpha is associated with leptin-receptor induction: the role of mesenchymal stem cell-derived adipocytes in APL cell survival. *Blood* 2004; **103**: 1815–1822.
31 Konopleva M, Konoplev S, Hu W, Zaritskey AY, Afanasiev BV, Andreeff M. Stromal cells prevent apoptosis of AML cells by up-regulation of anti-apoptotic proteins. *Leukemia* 2002; **16**: 1713–1724.
32 Moreau P, Pylypenko H, Grosicki S, Karamanesht I, Leleu X, Grishunina M *et al.* Subcutaneous versus intravenous administration of bortezomib in patients with relapsed multiple myeloma: a randomised, phase 3, non-inferiority study. *Lancet Oncol* 2011; **12**: 431–440.
33 Sonneveld P, Schmidt-Wolf IG, van der Holt B, El Jarari L, Bertsch U, Salwender H *et al.* Bortezomib induction and maintenance treatment in patients with newly diagnosed multiple myeloma: results of the randomized phase III HOVON-65/GMMG-HD4 trial. *J Clin Oncol* 2012; **30**: 2946–2955.
34 Moreau P, Richardson PG, Cavo M, Orlowski RZ, San Miguel JF, Palumbo A *et al.* Proteasome inhibitors in multiple myeloma: 10 years later. *Blood* 2012; **120**: 947–959.
35 Robak T. Bortezomib in the treatment of mantle cell lymphoma. *Future Oncol* 2015; **11**: 2807–2818.
36 Robak T, Huang H, Jin J, Zhu J, Liu T, Samoilova O *et al.* Bortezomib-based therapy for newly diagnosed mantle-cell lymphoma. *N Engl J Med* 2015; **372**: 944–953.
37 Attar EC, Johnson JL, Amrein PC, Lozanski G, Wadleigh M, DeAngelo DJ *et al.* Bortezomib added to daunorubicin and cytarabine during induction therapy and to intermediate-dose cytarabine for consolidation in patients with previously untreated acute myeloid leukemia age 60 to 75 years: CALGB (Alliance) study 10502. *J Clin Oncol* 2013; **31**: 923–929.
38 Zhang P, Gao K, Tang Y, Jin X, An J, Yu H *et al.* Destruction of DDIT3/CHOP protein by wild-type SPOP but not prostate cancer-associated mutants. *Hum Mutat* 2014; **35**: 1142–1151.
39 Nasr R, Lallemand-Breitenbach V, Zhu J, Guillemin MC, de The H. Therapy-induced PML/RARA proteolysis and acute promyelocytic leukemia cure. *Clin Cancer Res* 2009; **15**: 6321–6326.
40 Bonfili L, Cuccioloni M, Cecarini V, Mozzicafreddo M, Palermo FA, Cocci P *et al.* Ghrelin induces apoptosis in colon adenocarcinoma cells via proteasome inhibition and autophagy induction. *Apoptosis* 2013; **18**: 1188–1200.
41 Casarejos MJ, Solano RM, Gomez A, Perucho J, de Yebenes JG, Mena MA. The accumulation of neurotoxic proteins, induced by proteasome inhibition, is reverted by trehalose, an enhancer of autophagy, in human neuroblastoma cells. *Neurochem Int* 2011; **58**: 512–520.
42 Isakson P, Bjoras M, Boe SO, Simonsen A. Autophagy contributes to therapy-induced degradation of the PML/RARA oncoprotein. *Blood* 2010; **116**: 2324–2331.
43 Zeng CW, Chen ZH, Zhang XJ, Han BW, Lin KY, Li XJ *et al.* MIR125B1 represses the degradation of the PML-RARA oncoprotein by an autophagy-lysosomal pathway in acute promyelocytic leukemia. *Autophagy* 2014; **10**: 1726–1737.
44 Shaid S, Brandts CH, Serve H, Dikic I. Ubiquitination and selective autophagy. *Cell Death Differ* 2013; **20**: 21–30.
45 Pankiv S, Clausen TH, Lamark T, Brech A, Bruun JA, Outzen H *et al.* p62/SQSTM1 binds directly to Atg8/LC3 to facilitate degradation of ubiquitinated protein aggregates by autophagy. *J Biol Chem* 2007; **282**: 24131–24145.
46 Clausen TH, Lamark T, Isakson P, Finley K, Larsen KB, Brech A *et al.* p62/SQSTM1 and ALFY interact to facilitate the formation of p62 bodies/ALIS and their degradation by autophagy. *Autophagy* 2010; **6**: 330–344.
47 Kirkin V, Lamark T, Johansen T, Dikic I. NBR1 cooperates with p62 in selective autophagy of ubiquitinated targets. *Autophagy* 2009; **5**: 732–733.
48 Mathews V. De-escalation of treatment for acute promyelocytic leukaemia? *Lancet Haematol* 2015; **2**: e348–e349.

Supplementary Information accompanies this paper on the Leukemia website (http://www.nature.com/leu)

Received: 28 July 2018 | Revised: 20 September 2018 | Accepted: 16 October 2018

DOI: 10.1111/hae.13633

ORIGINAL ARTICLE

WILEY Haemophilia

Prevalence of FVIII inhibitors in severe haemophilia A patients: Effect of treatment and genetic factors in an Indian population

Sachin David[1] | Sukesh C. Nair[2] | G. Surender Singh[2] | Ansu Abu Alex[1] | Saravanan Ganesan[1] | Hamenth Kumar Palani[1] | Nithya Balasundaram[1] | Kavitha M. Lakshmi[1] | Aditi Joshi[3] | S. Kannan[3] | Anu Korula[1] | Fouzia Nambiatheyil Aboobacker[1] | Aby Abraham[1] | Biju George[1] | Shashikant Janardan Apte[3] | Alok Srivastava[1] | Vikram Mathews[1]

[1]Department of Haematology, Christian Medical College, Vellore, India

[2]Department of Immunohaematology and Transfusion Medicine, Christian Medical College, Vellore, India

[3]Sahyadri Speciality Hospital, Pune, India

Correspondence
Vikram Mathews, Department of Haematology, Christian Medical College, Vellore, India.
Email: vikram@cmcvellore.ac.in

Funding information
The study was initially supported through Bayer Haemophilia Awards Program-2006 awarded to VM. This study is majorly funded by the Department of Biotechnology, New Delhi, India (BT/PR14423/MED/12/477/2010). VM is supported by senior fellowship program of Wellcome-DBT India Alliance (IA/S/11/2500267), New Delhi, India. SD is supported by senior research fellowship from Council of Scientific and Industrial Research (CSIR-8/16 (48)/2012-EMR-I), New Delhi, India.

Introduction: Factor replacement therapy in treatment of haemophilia A is complicated by the production of neutralising antibodies known as inhibitors. The formation of inhibitors is multifactorial being associated with both genetic and environmental factors.

Aim: To document the prevalence of inhibitors in severe haemophilia in the community where most patients receive only infrequent episodic replacement therapy and evaluate the factors which could be contributing to it.

Methods: Community based camps were conducted in different parts of the country. Patients were assessed through a structured questionnaire and blood samples were obtained for laboratory evaluation of inhibitors and defined immunological parameters.

Results: Inhibitors were present in 87/447 (19.5%) of the evaluated patients. High-titre inhibitor (>5 Bethesda Units [BU]) was identified in 31 (35.6%) patients. HLA DRB1-13-positive cases (RR = 2.04; 95% CI 1.06-3.911; $P = 0.033$) had an increased risk of inhibitor formation which was retained in the high-titre subset. A decreased risk of inhibitor formation was noted with heterozygous *IL4-590 C/T* allele (RR = 0.22; 95% CI 0.108-0.442: $P = 0.000$). There were no significant correlations between any of the evaluated environmental factors and the development of inhibitors in this study.

Conclusion: The overall prevalence of inhibitors in patients with severe haemophilia A is similar to that reported among patients receiving regular replacement therapy. The data from this study, limited by its retrospective and cross-sectional study design, would suggest that genetic rather than environmental are more likely to impact the development of inhibitors.

KEYWORDS
environmental, genetic, haemophilia, inhibitors, risk factors

1 | INTRODUCTION

Haemophilia A, an X-linked bleeding disorder is characterized by reduced levels of coagulation factor VIII.[1] The treatment of haemophilia A involves replacement of FVIII with factor concentrates. The replacement therapy is hindered by the development of neutralising antibodies against the infused FVIII. Antibodies which neutralize the replaced factors are called as inhibitors. These inhibitors have been identified to be predominantly immunoglobulin IgG1 and IgG4 subtype.[2] The prevalence of inhibitors in patients with severe haemophilia vary from 25%-30%[3] and has been identified as the major complication in the treatment of haemophilia. The reason why inhibitors develop only in a subset of patients remains a pertinent question. Biological components like *F8* gene mutation and haplotypes,[4] immunophenotype of Treg population,[5,6] ethnicity,[7] positive family history[8] and patient-related modifiers like age of the first exposure to FVIII products, intensity of treatment or type of clotting factor used have been implicated to the development of inhibitors.[9,10]

These causative factors have been studied in different populations with varying conclusions. Mutations in the *F8* gene have been identified to be closely associated with the development of inhibitors in haemophilia A.[10,11] HLA polymorphisms have also been identified to be involved in the formation of inhibitors.[12] Polymorphisms in immune-regulatory genes (*CTLA-4*, *IL-10*, *TNF-α*) have been studied in different populations, and their associations with inhibitor formation have been identified.[13-15] Exposures to different types of FVIII products have led to varying implications on inhibitor development, ranging from definitive risk to no evidence of any correlation.[16] Most of the available data on incidence, prevalence and predisposing factors for inhibitor development are from developed countries with adequate access to factor concentrate replacement with the majority of patients being of Caucasian descent.

There is a paucity of data regarding the prevalence of inhibitors in severe haemophilia A from low and middle income countries (LMIC) and from different races and ethnicities. A previous study that published data in this regard from India showed an overall prevalence of 6.07% with a varying distribution of 4.17%, 4.89%, 5.45% and 13.04% of inhibitors from Western, Eastern, Northern and Southern regions.[17] Several of these studies were not comprehensively designed and have a tertiary centre referral bias. In this study, we undertook a comprehensive community-based evaluation of severe haemophilia A patients to study the prevalence of inhibitors and its predisposing factors.

2 | MATERIALS AND METHODS

2.1 | Patient recruitment and sample collection

Patients were recruited from haemophilia treatment centres by physicians involved in haemophilia care through haemophilia chapters and from the haemophilia clinic of Department of Haematology, Christian Medical College, Vellore, India (Figure S1; Table S1). Informed patient consent was obtained as approved by the Institutional Review Board of Christian Medical College, Vellore, India (IRB approval number IRB Min. No. 7281 dated 22.09.2010). We included patients who had FVIII: C activity ≤1% and who had ≥5 exposure days of FVIII in their lifetime for evaluation of factors that predisposes to the development of inhibitors. The patients were assessed with a detailed questionnaire for history of factor consumption; type of factor used as well as cumulative lifetime factor utilization. Extended details of family history and particulars which were considered to be potential determinants of inhibitor formation were collected through the comprehensive questionnaire (Table S2). All the data in this study were collected from these questionnaires administered by trained staff supplemented where possible by chart reviews.

2.2 | Sample collection and DNA extraction

Plasma was separated from peripheral blood samples collected in citrated tubes (BD Biosciences, Franklin Lakes, NJ, USA) and transferred in dry ice to the laboratory at the Christian Medical College, Vellore. DNA was extracted from the K_3EDTA tubes (Greiner Bio-One, Kremsmünster, Austria), through standard phenol-chloroform method. Samples were collected in heparin tubes (Greiner Bio-One) for flow cytometric analysis. Peripheral blood was collected from healthy volunteers and genomic DNA was used as controls for determining the allelic frequency.

2.3 | Coagulation factor and inhibitor assays

Prothrombin time (PT) and activated partial thromboplastin time (APTT) was assessed by photo-optical method in ACL TOP 700 (IL, Milan, Italy) and CA 1500 automated coagulation analyzer (Sysmex, Kobe, Japan) with reagent Recombiplastin 2G (IL) and Innovin (Siemens, Marburg, Germany), respectively, along with Synthesil (IL). One-stage APTT-based FVIII assay was performed in the same instruments in the presence of immune depleted FVIII-deficient plasma (Siemens) and IL calibrator (IL).

Mixing studies, correction of APTT was performed as screening test for inhibitors. Nijmegen-Bethesda assay (NBA) was performed on all the samples for the presence of inhibitors. A level of ≥0.6 Bethesda Units (BU) per mL was considered as positive for inhibitor status.

2.4 | Polymorphisms in immunoregulatory genes and HLA class typing

A subset of 60 inhibitor-positive patients was studied for polymorphisms. The polymorphisms were studied in the ratio of 1:2 of inhibitor-positive against inhibitor patients. Genomic DNA was used for PCR-RFLP's to identify the polymorphism in *IL4Rα Ile50Val; Arg551Gln*, *IL4 -590C/T*, *IL5 746T>C*, *CTLA4 49G/A*. Allele-specific PCRs for identifying cytokine polymorphisms in *TNF α -308G/A*, *TGF β 1 codon 10T/C*; *codon 25C/G*, *IL6 -174C/G*, *IL10 -592A/C*; *-819C/T*; *1082A/G*, *IFNγ +874T/A* were done using a CYTGEN cytokine genotyping trays from One Lambda (Canoga Park, CA, USA). VNTRs in

IL5Rα 3′UTR were screened by fluorescent PCR and capillary electrophoresis and the alleles characterized by GeneScan and Genotyper analysis in an ABI 310 genetic analyser (Applied Biosystems, Foster City, CA, USA). HLA Class II typing was done in the 60 inhibitor-positive cases and in 252 inhibitor-negative cases using AllSet^{+SSP} PCR kits (Dynal, Merseyside, UK).

2.5 | Assessment of T-cell subsets

The immunophenotype of the Treg population was analysed by flow cytometry in 60 inhibitor-positive cases and in 252 inhibitor-negative cases. Briefly, 1×10^6 cells were suspended in 100 µL of PBS and incubated with $CD4^+$ and $CD25^+$ markers (Becton Dickinson, Franklin Lakes, NJ, USA) conjugated with FITC and PE, respectively. The cells were then washed and re-suspended in 500 µL of PBS and analysed immediately on a BD FACSCalibur flow cytometer (Becton Dickinson). An appropriate isotypic control was used to define positivity.

2.6 | FVIII gene mutations—intron 22 and intron 1 inversions

Intron 22 and intron 1 inversions were screened in a set of 60 inhibitor-positive patients. Intron 22 inversion was screened by long PCR/inverse PCR as per published protocols.[18,19] Samples negative for intron 22 inversion was analysed for intron 1 inversion as per previous published modified protocol from our lab.[18]

2.7 | Haplotype assessment

The haplotypes reported previously in exon 10 (G1679A), exon 14 (A2554G and C3951G) and exon 25 (A6940G)[20] were identified by sequencing. DNA sequencing was performed in the exons harbouring the variants. DNA sequencing was performed with fluorescently labelled di-deoxy nucleotide triphosphates using Big Dye Terminator cycle sequencing kit ver1.1 (Applied Biosystems). The PCR products were cleaned post wash using a magnetic bead-based method. High Prep™ DTR (Magbio Genomics, Gaithersburg, MD, USA), a paramagnetic bead system was used to remove the unincorporated dye terminators after the sequencing PCR. The sequencing was performed in an automated sequencer; ABI—Hitachi 3130 Genetic Analyser (Applied Biosystems).

2.8 | Statistical analysis

Comparisons between inhibitor-positive and inhibitor-negative patients were performed using Mann-Whitney *U* test/chi-square test

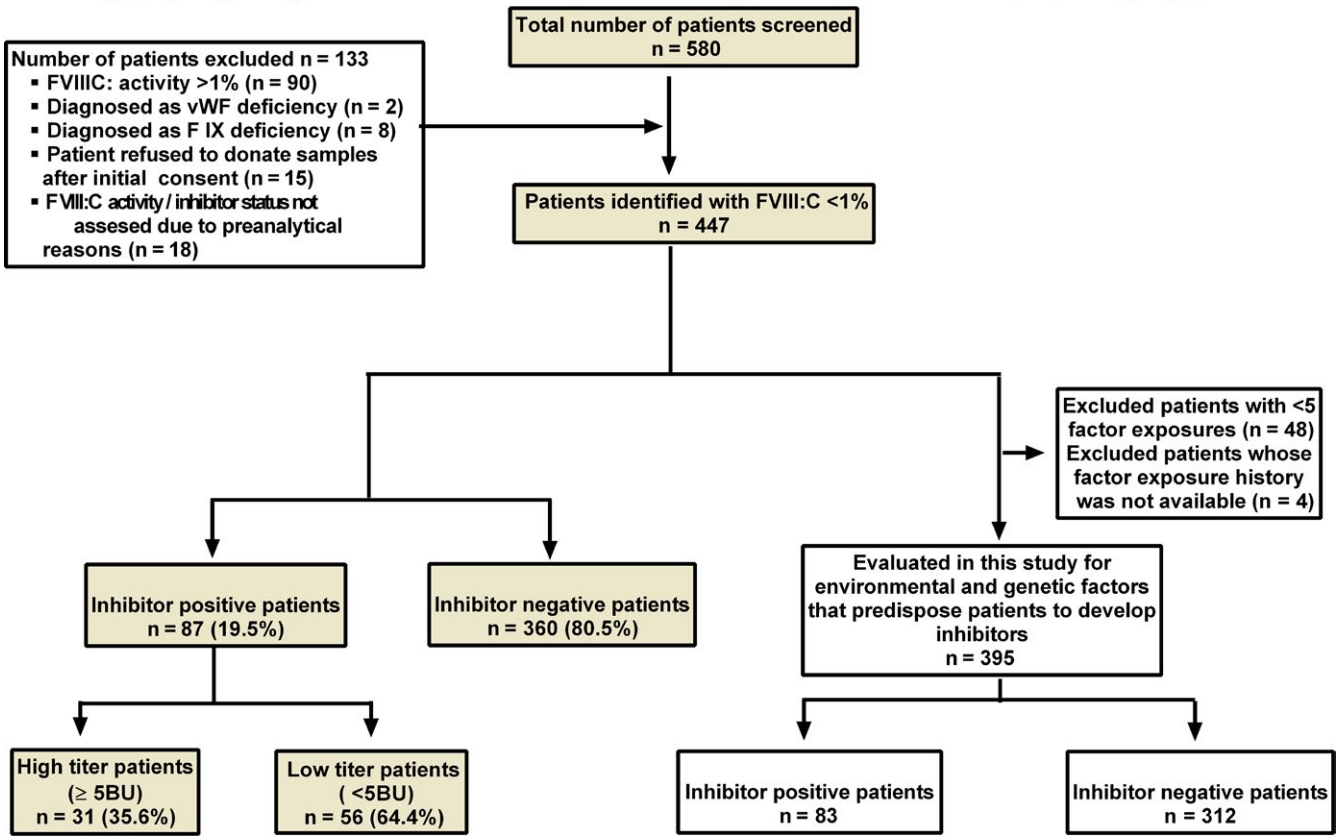

FIGURE 1 Patient recruitment profile in the study. Patients were recruited by conducting medical camps with the help of local haemophilia chapters. Out of the 580 patients recruited, 133 patients were excluded from the study as detailed in the figure. We could identify 447 patients of which 87 (19.5%) was positive for inhibitors. When the inclusion criteria for the study (FVIII: C < 1% and ≥5 exposures of FVIII replacement products) were applied, 395 patients were identified to be eligible for further analysis. There were 83 (21%) patients who were inhibitor positive and 312 (78.9%) patients who were inhibitor negative in this subgroup

as applicable. Relative risks were calculated together with their 95% confidence intervals. For all tests, a 2-sided *P* value of 0.05 or less was considered statistically significant. SPSS 24.0 software (IBM Corp, Armonk, NY, USA) was used to perform statistical analysis.

3 | RESULTS

3.1 | Patient characteristics

Among 580 patients that were screened for this study, 447 were enrolled (Figure 1). The presence of inhibitors in 87 patients in this group suggests an overall prevalence of inhibitors of 19.5%. Of the 87 patients, 31 patients (35.6%) were high titre (≥5 BU) and 56 patients (64.4%) were low titre (<5 BU). A total of 360 patients (80.5%) were negative for the presence of inhibitors in this group. When the study criteria of patients identified with severe haemophilia A and ≥5 exposures to factor replacement were applied, 395 patients were identified to be eligible to be included for further evaluation of predisposing factors. A total of 83 (21%) patients of the 395 were identified to be inhibitor positive and 312 patients (79%) were inhibitor negative. A further subset analysis of cases with severe haemophilia A of these 395 patients 128 (32.4%) had ≥50 exposures and of these 128 cases 28 (22%) had inhibitors. The inhibitor-positive patients had a median age of 18 years (range: 3-59 years), and for inhibitor-negative patients, it was 18 years with a range of 2-75 years (*P* = 0.80). Of the 83 patients, 29 (34.9%) patients had a high titre of antibodies (≥5 BU) and 54 (65%) patients had a low titre (<5 BU).The assay identified antibodies showing an inhibitory activity ranging from 0.6 to 220 BU (median: 2 BU). The inhibitory antibodies ranged from 6 to 220 BU in high-titre patients with a median of 20 BU. The baseline demographic characteristic of the patients in the study is summarized in Table 1.

TABLE 1 Demographic characteristics of the patients involved in the study

Patient demographics (n = 395)	Median (range)/n (%)	*P* value
Age (y)	18 (2-75)	0.801
Inhibitor positive	18 (3-59)	
Inhibitor negative	18 (2-75)	
Age of diagnosis (y)	1.5 (0-55)	0.164
Inhibitor positive	1 (0-55)	
Inhibitor negative	1.5 (0-35)	
Inhibitor positive (≥ 0.6 BU)	83 (21)	-
High-titre patients (≥5 BU)	29 (34.9)	
Low-titre patients (<5 BU)	54 (65)	
Inhibitor negative (<0.6 BU)	312 (79)	-
Number of families involved in the study	387	-
Number of patients who had siblings with inhibitors	9 (2.3)	-
Parental consanguinity	91 (23)	0.561
Inhibitor positive	18 (30)	
Inhibitor negative	56 (22.2)	
Number of factor exposures in first year of life	0 (0-25)	0.606
Inhibitor positive	0 (0-7)	
Inhibitor negative	0 (0-25)	

3.2 | Clinical and environmental factors in inhibitor development

The familial history including parental consanguinity was collected. Familial haemophilia was observed in 53 (63.9%) patients in inhibitor-positive group and 188(60.3%) patients in the inhibitor-negative group (*P* = 0.613). Parental consanguinity was seen in 21 patients (25.3%) with inhibitors against 70 patients (22.4%; *P* = 0.561) whose inhibitor status was negative.

The number of exposure to factors was negligible in the first year of life (median: 0; range: 0-25 times) for the entire cohort. The number of exposures for the inhibitor-positive patients (median 0; range: 0-7) and inhibitor-negative patients (median 0; range: 0-25; *P* = 0.606) was similar in first year of life. The factor replacement support and the various types of factors used (FFP/cryoprecipitate, rFVIII/pdFVIII and other blood products) in the first year of life were also not significantly different in the two groups (Table S3).

Bleeding events in the first year of life and for lifetime in inhibitor-positive and inhibitor-negative patients were analysed and is detailed in Table S3. Besides a significant difference of history of intracranial bleeds observed between inhibitor-positive and inhibitor-negative patients (*P* = 0.008), there was no significant difference in the history of bleeding at any other anatomical site (Table S3).

3.3 | T- cell subsets and genetic markers in inhibitor development

Total $CD4^+$ (*P* = 0.241) and $CD4^+$ $CD25^+$ (*P* = 0.593) in inhibitor-positive and inhibitor-negative patients when analysed through flow cytometry confirmed no quantitative and qualitative differences between the two groups. Fourteen selected polymorphisms associated with inflammatory responses or autoimmune conditions which were analysed have been detailed in Table 2. In *IL4 -590C/T* (rs 2243250) polymorphism prevalence of heterozygous CT was statistically lower in inhibitor-positive patients (RR = 0.22; 95% CI 0.108-0.442; *P* = 0.000). The protective effect of the heterozygous condition was retained in the high-titre inhibitor patients when low-titre–positive cases were excluded from the analysis. Allelic frequency of *IL4 -590C/T* analysed with normal control (n = 50) maintained Hardy-Weinberg equilibrium in the general population.

There was a significant increased risk of inhibitor formation among cases that were HLA DRB1*13 positive (RR = 2.04; 95% CI 1.06-3.911; *P* = 0.033) and this significance was retained in the high-titre subset. There was also a trend to decreased risk of inhibitor formation among those that were HLA-DRB1*07 positive and this

TABLE 2 Polymorphisms of immune-regulatory genes analysed in the study

Polymorphism	Allele	Inhibitor positive n (%)	Inhibitor negative n (%)	*P*-value
TNFα -308GA	GG	44 (81.5)	100 (84)	0.832
	GA	9 (16.7)	16 (13.4)	
	AA	1 (1.9)	3 (2.5)	
TGFβ 10CT	CC	6 (11.3)	13 (10.1)	0.658
	CT	33 (62.3)	73 (56.6)	
	TT	14 (26.4)	43 (33.3)	
TGFβ 25GC	GG	25 (53.2)	66 (51.6)	0.472
	GC	22 (46.8)	58 (45.3)	
	CC	0 (0)	4 (3.1)	
IL 10 -1082 AG	AA	27 (58.7)	64 (48.1)	0.244
	AG	19 (41.3)	64 (48.1)	
	GG	0 (0)	5 (3.8)	
IL10 -819 CT	CC	10 (19.2)	41 (30.8)	0.243
	CT	32 (61.5)	66 (49.6)	
	TT	10 (19.2)	26 (19.2)	
IL10 -592 AC	AA	14 (28)	31 (24.6)	0.868
	AC	23 (46)	63 (50)	
	CC	13 (26)	32 (25.4)	
IL 6 -174CG	CC	5 (10)	7 (5.3)	0.448
	CG	11 (22)	26 (19.5)	
	GG	34 (68)	100 (75.2)	
IFN b +874 AT	AA	21 (42.9)	40 (32)	0.398
	AT	20 (40.8)	62 (49.6)	
	TT	8 (16.3)	23 (18.4)	
CTLA 4 +49A/G	AA	23 (40.4)	75 (50.7)	0.356
	AG	31 (54.4)	64 (43.2)	
	GG	3 (5.3)	9 (6.1)	
IL 4 -590 C/T	CC	21 (41.2)	21 (16.2)	0.001
	CT	28 (54.9)	104 (80)	
	TT	2 (3.9)	5 (3.8)	
IL 4 RA Ile 50 Val	*Ile 50 Ile*	12 (26.1)	48 (33.1)	0.665
	Ile 50 Val	27 (58.7)	76 (52.4)	
	Val 50 Val	7 (15.2)	21 (14.5)	
IL 5 746T/C	TT	6 (11.1)	19 (13.5)	0.880
	TC	23 (42.6)	61 (43.3)	
	CC	25 (46.3)	61 (43.3)	
IL RA Q 551 R	Q551 Q	32 (57.1)	65 (57)	0.840
	Q 551R	21 (37.5)	45 (39.5)	
	R 551 R	3 (5.4)	4 (3.5)	
IL 5 3′UTR	Wild type	12 (21.1)	31 (20.3)	1.000
	Mutant	45 (78.9)	122 (79.7)	

achieved statistical significance among the inhibitor cases that were high titre positive (RR = 0.24; 95% CI 0.055-1.05: *P* = 0.047).

Of the 60 inhibitor-positive patients analysed for intron 22 inversion, 28 patients (46.6%) were identified to have intron 22 inversion. When the mutations were stratified between high titre and low titre, 12 (54.5%) of high titre and 16 (47%) of low titre had intron 22 inversion as causative mutation. Only one patient was identified for intron 1 inversion from the patients analysed from patients who were negative for intron 22 inversions (n = 32). Sequencing for haplotype (n = 20, randomly selected) in the inhibitor-positive (n = 10)

and inhibitor-negative (n = 10) patients confirmed all the patients were of H1 haplotype.

4 | DISCUSSION

The study identifies the prevalence of inhibitors in Indian population. The per capita use of clotting factor concentrate in India in 2016 according to World Federation of Haemophilia Annual Global Survey, 2016 was 0.105 IU, which is much less than the global per capita FVIII usage of 2.29 IU.[21] Considering the fact that the factor consumption is much less compared to the developed countries, we hypothesized that the prevalence of inhibitors in our population was likely to be significantly lower as was also suggested by some of the published data from other LMIC's. Additionally, we made an effort to comprehensively evaluate for known genetic and environmental factors that could potentially be predisposing our patients to develop inhibitors.

This study involved evaluation of 395 severe haemophilia A patients for factors that could predispose them to develop inhibitors. The median age of patients recruited into the study was 18 years and the median age of diagnosis was around 1.5 years of age. The late age of diagnosis in our study group can be attributed to difference in the medical infrastructure as well as the general lack of information and awareness regarding bleeding disorders in the general public.[22] The number of patients whose parents were consanguineous was 91 (23%) in the study cohort. The percentage of high familial haemophilia can be due to the fact that consanguineous marriages are common (20%-40%) in the south of India from where most of our patients were recruited.[23]

There is a paucity of data in the literature regarding the incidence and prevalence of inhibitors in developing countries and a perception that the incidence and prevalence may be lower than estimated in the developed world.[24] The overall prevalence of inhibitors in our study population was 19.5% (87/447), which is consistent with figures reported in many developed countries.[16] It may be noted that nearly two thirds of the inhibitor patients had low-titre inhibitors (64.4% low titre; 35.6% high titre), it is possible that some of these could be transient in nature. Furthermore, our study included patients from a population where no one underwent immune tolerance induction. The recent SIPPET study has reported a cumulative incidence of 35.4% of inhibitors in both plasma-derived FVIII and recombinant factor VIII treatment arms.[25] India has the largest number of identified patients with haemophilia accounting for about 7% global number of patients with haemophilia.[21] The high rate of prevalence in India is especially significant in the context of the fact that the factor consumption in India is significantly lower than in the developed countries.[26] A study in the patients with Hispanic origin had reported a high prevalence (24.5%) of high-titre inhibitors when controlled for possible confounders such as age and use of prophylaxis.[27] Studies have also reported that the prevalence of inhibitors in black patients was twice than that in the white patients in the United States of America[8,28] suggesting the possible influence of race on the risk of development of inhibitors. Association of age and first exposure has been identified in several studies as a risk factor for inhibitor development. Lorenzo et al[29] have identified that age of start of therapy can be a predictor of inhibitor risk although contradictory results have also been reported.[30] We have identified that even though the exposure was negligible in the first year of life in our country the prevalence of the inhibitor was high and there was no evidence of an association with exposures to factor concentrates in the first year of life and inhibitor formation. We observed a significant difference in the number of intracranial bleeds between inhibitor-positive and inhibitor-negative patients ($P = 0.008$). As the study was retrospective in nature, we could not asses the direct link between this particular event and inhibitor formation.

In our study, we surveyed the consumption of FFP/cryoprecipitate, plasma-derived or recombinant FVIII, and CFC's. The study was limited by its retrospective natures and absence of well-maintained records and reliance on memory in some cases. We could not find a correlation with either the type of factor concentrate replacement that was used or the quantity used and inhibitor formation in contrast to previously reported studies.[16,31-33]

We have analysed fourteen polymorphisms associated with autoimmune conditions. To the best of our knowledge, this is the largest series from any LMIC to study polymorphisms of immune-regulatory genes with respect to inhibitor formation in severe haemophilia A *IL4 -590C/T* (rs 2243250) was identified to have a significant protective association against inhibitor formation, this type I cytokine is produced predominantly by $CD4^+$-Th2 cells, NK cells, basophils and mast cells.[34] The function of IL-4 is pleiotropic in nature, and plays a major role in differentiation of antigen-stimulated naïve T cells. IL-4 has also has been identified to play major role immunoglobulin class switching of IgE and IgG4 from B cells.[35] IgG4 is considered as the major IgG population against FVIII.[36] B cells stimulated with IL-4 increase their cell surface expression of major histocompatibility complex (MHC) class II molecules.[37] Previous studies on *IL-4 -590C/T* in autoimmune thyroid diseases, hypothyroidism (AIH) and Graves' disease (GD) have shown the variant has a protective effect against the autoimmune disease especially GD,[38] though there was no reported association with inhibitor formation in haemophilia in prior studies.[14,39]

A previously reported study from India in severe haemophilia A (n = 119) did not find any association with any of the HLA alleles and risk of inhibitor formation.[40] In contrast, our data suggest and increased risk of inhibitor formation with HLA DRB1*13 and this significance was retained in the high-titre subset. There was also a trend to decreased risk of inhibitor formation among those that were HLA-DRB1*07 positive. It is recognized that there is significant heterogeneity in allele distribution of DRB1*07 and DRB1-13 in the Indian population.[41] The DRB1*07 have an allele frequency ranging from 0.088 to 0.265 and DRB1*13 has an allele frequency ranging from 0.116 to 0.231 in the Indian population as per Allele Frequency Net Database. The allele frequency of DRB1*07 in the Caucasoid population ranged from 0.025 to 0.246, and in the population of Black origins it was 0.0017-0.2100. DRB1*13 allele frequency in the Caucasoid population was 0.009-0.197, and in Black origins it was 0.0130-0.290.[42]

A previous study from India has shown a higher incidence of H1 in the population.[43] When we sequenced randomly inhibitor-positive

(n = 10) and inhibitor-negative (n = 10) patients, all the patients were of H1 haplotype and hence we feel that the haplotype may not be a deciding factor in the Indian population in concurrence with the previous published that the haplotype mismatch of the FVIII sequence between the product and the patient may not be a contributing factor for inhibitor formation.[44,45] In conclusion, we have identified that the overall prevalence of inhibitors in severe haemophilia is similar to that reported in the developed countries. The involvement of transient inhibitors would have also played a role, the analysis being cross-sectional in nature; an additional limitation of this study was that it relied predominantly on patient and family recall, especially when the data were collected from peripheral camps with limited record keeping facilities. From our data, it appears that genetic factors predominate in the development of inhibitors with less, if any, impact of environmental factors. Additional and detailed genetic studies are required to dissect out the possible mechanism of inhibitor formation in some patients.

ACKNOWLEDGEMENTS

We thank all the haemophilia chapters (Angamaly, Bengaluru, Chennai, Coimbatore, Puducherry, Tirunelveli-India) involved in the recruitment and organization of the community camps.

DISCLOSURES

The authors declare no conflict of interest.

AUTHOR CONTRIBUTIONS

SD performed research, designed the study, performed molecular tests, analysed the data and wrote the manuscript. SCN performed coagulation assays and clinical data accrual and analysed the data. GSS performed coagulation assays. AAA performed flow cytometry and analysed data. SG, HKP and NB performed research and analysed the data. KML performed statistical analysis. AJ, SK, SJA, AK and AA performed research and clinical data accrual and analysed the data. AS designed the study, performed research and clinical data accrual, analysed the data and reviewed the manuscript. VM designed the study, performed research and clinical data accrual, analysed the data and wrote the manuscript.

ORCID

Sachin David http://orcid.org/0000-0002-9433-9624
Alok Srivastava http://orcid.org/0000-0001-5032-5020
Vikram Mathews http://orcid.org/0000-0001-9417-2353

REFERENCES

1. Graw J, Brackmann H, Oldenburg J, et al. Haemophilia A: from mutation analysis to new therapies. *Nat Rev Genet*. 2005;6(6):488-501.
2. Whelan SF, Hofbauer CJ, Horling FM, et al. Distinct characteristics of antibody responses against factor VIII in healthy individuals and in different cohorts of hemophilia A patients. *Blood*. 2013;121(6):1039-1048.
3. Lillicrap D, Fijnvandraat K, Santagostino E. Inhibitors - genetic and environmental factors. *Haemophilia*. 2014;20(Suppl 4):87-93.
4. Viel KR,Ameri A, Abshire TC, et al. Inhibitors of factor VIII in black patients with hemophilia. *N Engl J Med*. 2009;360(16):1618-1627.
5. Bray GL, Kroner BI, Arkin S, et al. Loss of high-responder inhibitors in patients with severe hemophilia A and human immunodeficiency virus type 1 infection: a report from the Multi-Center Hemophilia Cohort Study. *Am J Hematol*. 1993;42(4):375-379.
6. El-Asrar MA, Hamed AE-S, Darwish YW, et al. Assessment of the frequency of regulatory T cells (CD4+CD25+CD127-) in children with hemophilia A: relation to factor VIII inhibitors and disease severity. *Blood Coagul Fibrinolysis*. 2016;27(1):42-46.
7. Bardi E, Astermark J. Genetic risk factors for inhibitors in haemophilia A. *Eur J Haematol*. 2015;94(Suppl 77):7-10.
8. Astermark J, Berntorp E, White GC, Kroner BI. The Malmo International Brother Study (MIBS): further support for genetic predisposition to inhibitor development in hemophilia patients. *Haemophilia*. 2001;7(3):267-272.
9. Chambost H. Assessing risk factors: prevention of inhibitors in haemophilia. *Haemophilia*. 2010;16(Suppl 2):10-15.
10. Gouw SC, van den Berg HM. The multifactorial etiology of inhibitor development in hemophilia: genetics and environment. *Semin Thromb Hemost*. 2009;35(8):723-734.
11. Boekhorst J, Lari GR, Doiron R, et al. Factor VIII genotype and inhibitor development in patients with haemophilia A: highest risk in patients with splice site mutations. *Haemophilia*. 2008;14(4):729-735.
12. Pergantou H, Varela I, Moraloglou O, et al. Impact of HLA alleles and cytokine polymorphisms on inhibitors development in children with severe haemophilia A. *Haemophilia*. 2013;19(5):706-710.
13. Astermark J, Wang X, Oldenburg J, Berntorp E, Lefvert A-K. Polymorphisms in the CTLA-4 gene and inhibitor development in patients with severe hemophilia A. *J Thromb Haemost*. 2007;5(2):263-265.
14. Astermark J, Oldenburg J, Pavlova A, Berntorp E, Lefvert AK, MIBS Study Group. Polymorphisms in the IL10 but not in the IL1beta and IL4 genes are associated with inhibitor development in patients with hemophilia A. *Blood*. 2006;107(8):3167-3172.
15. Pavlova A, Delev D, Lacroix-Desmazes S, et al. Impact of polymorphisms of the major histocompatibility complex class II, interleukin-10, tumor necrosis factor-alpha and cytotoxic T-lymphocyte antigen-4 genes on inhibitor development in severe hemophilia A. *J Thromb Haemost*. 2009;7(12):2006-2015.
16. Wight J, Paisley S. The epidemiology of inhibitors in haemophilia A: a systematic review. *Haemophilia*. 2003;9(4):418-435.
17. Pinto P, Shelar T, Nawadkar V, et al. The Epidemiology of FVIII Inhibitors in Indian Haemophilia A Patients. *Indian J Hematol Blood Transfus*. 2014;30(4):356-363.
18. Jayandharan G, Shaji RV, Baidya S, Nair SC, Chandy M, Srivastava A. Identification of factor VIII gene mutations in 101 patients with haemophilia A: mutation analysis by inversion screening and multiplex PCR and CSGE and molecular modelling of 10 novel missense substitutions. *Haemophilia*. 2005;11(5):481-491.
19. Rossetti LC, Radic CP, Larripa IB, De Brasi CD. Genotyping the hemophilia inversion hotspot by use of inverse PCR. *Clin Chem*. 2005;51(7):1154-1158.
20. Viel KR, Machiah DK, Warren DM, et al. A sequence variation scan of the coagulation factor VIII (FVIII) structural gene and associations with plasma FVIII activity levels. *Blood*. 2007;109(9):3713-3724.
21. https://www1.wfh.org/publication/files/pdf-1669.pdf. Accessed February 21, 2018.
22. Ghosh K, Ghosh K. Management of haemophilia in developing countries: challenges and options. *Indian J Hematol Blood Transfus*. 2016;32(3):347-355.

23. Hamamy H. Consanguineous marriages: Preconception consultation in primary health care settings. *J Community Genet*. 2012;3(3):185-192.
24. Mathews V, Nair S, David S, Viswabandya A, Srivastava A. Management of hemophilia in patients with inhibitors: the perspective from developing countries. *Semin Thromb Hemost*. 2009;35(8):820-826.
25. Peyvandi F, Mannucci PM, Garagiola I, et al. A randomized trial of factor VIII and neutralizing antibodies in hemophilia A. *N Engl J Med*. 2016;374(21):2054-2064.
26. Stonebraker JS, Brooker M, Amand RE, Farrugia A, Srivastava A. A study of reported factor VIII use around the world. *Haemophilia*. 2010;16(1):33-46.
27. Carpenter SL, Michael Soucie J, Sterner S, Presley R. Increased prevalence of inhibitors in Hispanic patients with severe haemophilia A enrolled in the Universal Data Collection database. *Haemophilia*. 2012;18(3):e260–e265.
28. Bray GL, Gomperts ED, Courter S, et al. A multicenter study of recombinant factor VIII (recombinate): safety, efficacy, and inhibitor risk in previously untreated patients with hemophilia A. The Recombinate Study Group. *Blood*. 1994;83(9):2428-2435.
29. Lorenzo JI, Lopez A, Altisent C, Aznar JA. Incidence of factor VIII inhibitors in severe haemophilia: the importance of patient age. *Br J Haematol*. 2001;113(3):600-603.
30. Chalmers EA, Brown SA, Keeling D, et al. Early factor VIII exposure and subsequent inhibitor development in children with severe haemophilia A. *Haemophilia*. 2007;13(2):149-155.
31. Witmer C, Young G. Factor VIII inhibitors in hemophilia A: rationale and latest evidence. *Ther Adv Hematol*. 2013;4(1):59-72.
32. Gouw SC, van der Bom JG, Ljung R et al. Factor VIII products and inhibitor development in severe hemophilia A. *N Engl J Med*. 2013;368(3):231-239.
33. Calvez T, Chambost H, Claeyssens-Donadel S, et al. Recombinant factor VIII products and inhibitor development in previously untreated boys with severe hemophilia A. *Blood*. 2014;124(23):3398-3408.
34. Nelms K, Keegan AD, Zamorano J, Ryan JJ, Paul WE. The IL-4 receptor: signaling mechanisms and biologic functions. *Annu Rev Immunol*. 1999;17:701-738.
35. Gascan H, Gauchat JF, Roncarolo MG, Yssel H, Spits H, de Vries JE. Human B cell clones can be induced to proliferate and to switch to IgE and IgG4 synthesis by interleukin 4 and a signal provided by activated CD4+ T cell clones. *J Exp Med*. 1991;173(3):747-750.
36. Lollar P. Pathogenic antibodies to coagulation factors. Part one: factor VIII and factor IX. *J Thromb Haemost*. 2004;2(7):1082-1095.
37. Noelle R, Krammer PH, Ohara J, Uhr JW, Vitetta ES. Increased expression of Ia antigens on resting B cells: an additional role for B-cell growth factor. *Proc Natl Acad Sci USA*. 1984;81(19):6149-6153.
38. Hunt PJ, Marshall SE, Weetman AP, Bell JI, Wass J, Welsh KI. Cytokine gene polymorphisms in autoimmune thyroid disease. *J Clin Endocrinol Metab*. 2000;85(5):1984-1988.
39. Pinto P, Ghosh K, Shetty S. Immune regulatory gene polymorphisms as predisposing risk factors for the development of factor VIII inhibitors in Indian severe haemophilia A patients. *Haemophilia*. 2012;18(5):794-797.
40. Pinto P, Parasannanavar D, Ghosh K, Shetty S. The association of HLA-DRB1 and HLA-DQB1 alleles with the development of factor VIII inhibitors in severe haemophilia A patients in India. *Tissue Antigens*. 2014;84(2):235-237.
41. Robinson J, Halliwell JA, McWilliam H, Lopez R, Marsh SG. IPD–the immuno polymorphism database. *Nucleic Acids Res*. 2013;41(Database issue):D1234–D1240.
42. Gonzalez-Galarza FF, Takeshita LY, Santos EJ, et al. Allele frequency net 2015 update: new features for HLA epitopes, KIR and disease and HLA adverse drug reaction associations. *Nucleic Acids Res*. 2015;43(Database issue):D784-D788.
43. Pinto P, Ghosh K, Shetty S. Factor VIII haplotypes in severe hemophilia A patients in India. *Ann Hematol*. 2012.
44. Schwarz J, Astermark J, Menius ED, et al. F8 haplotype and inhibitor risk: results from the Hemophilia Inhibitor Genetics Study (HIGS) Combined Cohort. *Haemophilia*. 2013;19(1):113-118.
45. Gunasekera D, Ettinger RA, Nakaya Fletcher S, et al. Factor VIII gene variants and inhibitor risk in African American hemophilia A patients. *Blood*. 2015;126(7):895-904.

SUPPORTING INFORMATION

Additional supporting information may be found online in the Supporting Information section at the end of the article.

How to cite this article: David S, Nair SC, Surender Singh G, et al. Prevalence of FVIII inhibitors in severe haemophilia A patients: Effect of treatment and genetic factors in an Indian population. *Haemophilia*. 2018;00:1–8. https://doi.org/10.1111/hae.13633